

307216

34/1991

Acta Geologica Hungarica



VOLUME 34 NUMBERS 1—2, 1991

EDITOR
J. FÜLÖP

EDITORIAL BOARD

F. BENKŐ, G. CSÁSZÁR, J. HAAS, G. HÁMOR,
T. KECSKEMÉTI, GY. PANTÓ, T. SZEDERKÉNYI,
É. PÉCSI-DONÁTH (Co-ordinating Editor)



Akadémiai Kiadó, Budapest

ACTA GEOL. HUNG. 34(1—2) 1—157 (1991) HU ISSN 0236—5278

ACTA GEOLOGICA

A QUARTERLY OF THE HUNGARIAN ACADEMY OF SCIENCES

Acta Geologica publishes original reports of studies in geology, crystallography, mineralogy, petrography, geochemistry and paleontology.

Acta Geologica is published in yearly volumes of four issues by

AKADÉMIAI KIADÓ

Publishing House of the Hungarian Academy of Sciences
H-1117 Budapest, Prielle Kornélia u. 19–35.

Manuscripts and editorial correspondence should be addressed to

Acta Geologica

H-1363 Budapest P.O. Box 24

Subscription information

Orders should be addressed to

AKADÉMIAI KIADÓ

H-1519 Budapest P.O. Box 245

or to its representatives abroad

Acta Geologica Hungarica is abstracted/indexed in Bibliographie des Sciences de la Terre, Biological Abstracts, Chemical Abstracts, Chemie-Information, Hydro-Index, Mineralogical Abstracts

Contents

Triassic paleogeography and Cimmerian orogeny in SE Bulgaria and on the adjacent territories. <i>Petar M. Goche</i>	3
Triassic carbonate platform of the Drina–Ivajnica element (Dinarides). <i>Mara M. Dimitrijević, Milorad D. Dimitrijević</i>	15
Middle Miocene mangrove vegetation in Hungary. <i>Esther Nagy, József Kókay</i>	45
Lithostratigraphical and sedimentological framework of the Pannonian (s. l.) sedimentary sequence in the Hungarian Plain (Alföld), Eastern Hungary. <i>Györgyi Juhász</i>	53
Biostratigraphic revision of the Middle Pontian (Late Neogene) Battonya Sequence, Pannonian basin (Hungary). <i>Imre Magyar</i>	73
Diagenesis and low-temperature metamorphism in a tectonic link between the Dinarides and the Western Carpathians: the basement of the Igal (Central Hungarian) Unit. <i>P. Árkai, Cs. Lantai, I. Fórizs, Gy. Lelkes-Felvári</i>	81
K–Ar dating of the Perelik volcanic massif (Central Rhodopes, Bulgaria). <i>Zoltán Pécskay, Kadosa Balogh, Alexandra Harkovska</i>	101
Studies on chromite and its significance in the Lower and Middle Cretaceous of the Tatabánya Basin and Vértes Foreground. <i>Klára Vaskó-Dávid</i>	111
The heavy mineral content and mineralogical maturity of the Cenozoic psammites in Hungary. <i>Edit Tamó-Bozsó</i>	127
Genetics of garnets from andesites of the Karancs Mountains. <i>Csaba Lantai</i>	133
<i>Book reviews</i>	
Chaline, J.: Paleontology of Vertebrates. <i>Miklós Monostori</i>	155
Hellmut Grabert: Der Amazonas – Geschichte und Probleme eines Strombietes zwischen Pazifik und Atlantik. <i>Ottó Tomschey</i>	156
Hartmut Heinrichs – Albert Günter Hermann: Praktikum der Analytischen Geochemie. <i>Ildikó Vidra</i>	157

Triassic paleogeography and Cimmerian orogeny in SE Bulgaria and on the adjacent territories

Petar M. Gochev

Geological Institute, Bulgarian Academy of Sciences, Sofia

Paleogeography of the Triassic basins in the north margin of Paleotethys with Mesoeurope is analysed. The Strandzhides structure in SE Bulgaria and in Turkey and the evolution of the Cimmerian–Austrian collision orogen lying between the Moesian shelf and the Cimmerian continent of West Anatolian are presented.

Keywords: Variscian peneplain, Triassic, Balkanides, Strandzhides, Paleotethys, tectofacies, thrusts

Introduction

The Alpine tectonic units of SE Bulgaria and European Turkey – the Strandzhides orogen (Gochev 1986) and the deep Tertiary depression of Ergene (Lower Thrace) at its back – in many respects are similar to the recent ensemble of the southernmost part of the West Carpathian (Slovakia and Hungary) – namely the nappes of: Meliata, Silice, Bódva, Torna, Bükk, etc., and the Pannonian depression that starts at their back.

With respect to the structural history the Strandzhides in the SE part of the Balkan Peninsula are parts of the innermost zones of the Alpidic branch (Alpian–Carpathian–Balkan collisional orogenic belt), polyphase collage associated in the form of several nappes systems, formed during the Cimmerian or Austrian tectogenesis towards the deformed southern margin of Eurasia (the Mesoeuropean continent), and overlapped during the Young Alpine stage (Subhercynian and Pyrenean phases) by a collisional (Upper Cretaceous–Paleogene) or postcollisional (Neogene) neoautochthone – the latter more or less belonging to the last Mediterranean stage of the western part of the Alpine–Himalayan intercontinental orogenic fold belt (Gochev 1991).

The orogenic segment of the Strandzhides in SE Bulgaria, Greece, and Turkey – the Paleoalpides (Gochev 1991/a) are a strongly shortened suture zone between the European and African development (Fig. 1). They consist of ultrametamorphic Variscian "basement" (Ksiazkiewicz 1930) and of regionally metamorphized (schistes lustres, etc.), during the Mesocretaceous tectogenesis, Mesozoic continental and oceanic complexes (Dimitrov 1958, Chatalov 1988). They are partially overlapped by a second disharmonious orogenic stage – the Mesoalpides, presented by a non-metamorphized neoautochthone. In the Alps and the Carpathians they are presented by the pre–Gosau and Gosau development and in the Strandzhides by the Subhercynian–Laramian island–arc orogenic development of the Balkan

Address: Petar M. Gochev: Acad, G. Bonchev Str. 1b.24. Sofia, 1113, Bulgaria

Received: February 3, 1991

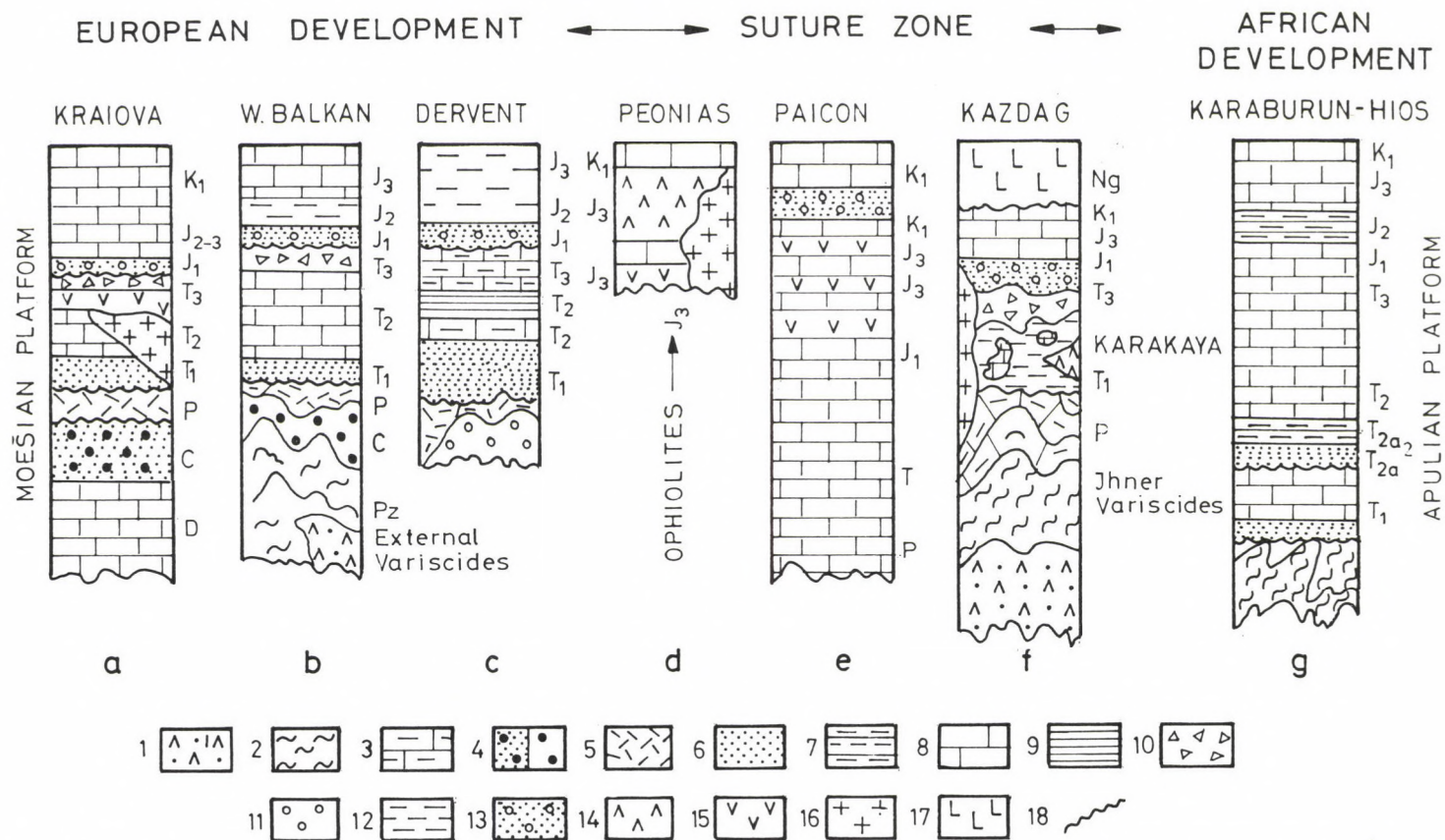


Fig. 1. Structural assemblage of the tectotope of European, Paleotethysian and African development in the Balkan-Aegean Region (after Gochev, 1991/ b): 1. amphibolites, metagabbros, metadunites, serpentinites, etc.; 2. gneisses and schists; 3. marbles; 4. Variscan molasses – detrital (a) and intraorogenic (b); 5. detrital-evaporite type of Permian (Verucano, Zechstein, etc.); 6. epicontinental type of Triassic (Buntsandstein, Werfen, sandstone and conglomerate of North Chios, etc.); 7. marly limestone, etc.; 8. massive limestones and dolomites; 9. black shales and marly limestones; 10. Rhaetian and calcareous breccia (breches de flanc, etc); 11. metamorphosed molasses (Klocotniza complex, etc); 12. Jurassic black shales, quartzites, etc. (Etrapole and Zvezdez Formations); 13. detrital-calcareous Lower Jurassic (Gresten, Hlerlatz, and Adnet type); 14. Triassic and Jurassic metavolcanites; 15. continental rift volcanites (basic, etc.); 16. Triassic intrusives (granitic, etc.); 17. Neogene basalts (Aegean island-arc orogen); 18. transgressive limit

Peninsula, including the so-called Sredna Gora volcanogenic-sedimentary marginal basin and the Rhodope-Strandzha archipelago and Vardar-Pontide Trench (Gochev 1988).

The Hercynian orogen of the Balkans had a very clearly expressed complete geotectonic development (Haydoutov 1989). It was an intercontinental collision orogen situated in the margin between Gondwana and Laurasia. At the end of Permian a large part of this orogen was already a peneplain, destroyed and covered by the Tethys waters of the southern margin of Eurasia (Gochev 1976) – the Mesoeurope and the North Tethys, the Paleotethys "ocean" (Sengör et al. 1980) or by the Apulian carbonate platform in the Aegean region (Afro-Arabia), which were formed as early as Carboniferous (Brunn 1967).

On the territory of Bulgaria the denudated Variscan orogen presented both by different paleogeographic environment – the deformed margin of the Russian platform and by the Berkovitsa island-arc association (Cambrian) including the Balkan Mountains ophiolites, etc. (Precambrian). At the latest studies have shown they are tightly pressed "one over the other" by a staged allochthone (Thracian suture), whose uppermost elements consists of old orogenic crystalline rocks – Thracian continental fragment. The so-called Thracian-Hercynian suture (Haydoutov 1989) nowadays can be traced in Bulgaria in a number of places under the Cimmerian-Austrian Alpine orogen (W. Bulgaria).

Early Triassic paleogeography

At the beginning of Triassic almost on the whole territory of Bulgaria was formed the southern margin of continental Mesoeurope (Gochev 1976). It was flooded by the waters of the European continental basin (Germanic basin), while its slope area in Thrace – by the waters of the so-called North Tethys. The general paleogeographic environment of the Balkans at that time, however, was rather differentiated and complex (Fig. 2). The Moesian periplatform carbonate "wedge" (Gochev 1972) lay in the extreme north. It was a fragment torn off from Mesoeurope by the Cimmerian suture zone of the Tethydes, respectively from the Scythian platform. The Moesian "wedge", besides Moesia (the Danube valley) also comprises a large part of the Fore-Balkan and the West Balkan Mountains (Fig. 3). Its north part is characterized by the Moesian group of Triassic rocks, where the evaporatives are numerous. South of the Moesian group follow elements of the differentiated continental slope zone of the North Tethys where the isopic European groups of the "Balkanide" and "Sub-Balkanide" Triassic, as well as groups lying further to the south of them – the Sakar, Dervent, Istanbul, Vardar and other region successions of Triassic – were successively separated from the north to the south (Fig. 4). The southernmost element of the latter is the Perieuropean island-arc system Karakaya (Fig. 5) which has formed an active contact with the frontal "plate" of the Apulian platform (Gochev 1991), obviously separating the North Tethys from the South Tethys – the so-called "Cimmerian microcontinent Sakarya" (Sengör et al. 1984). Probably the different Triassic-Jurassic flysch troughs of Ko-

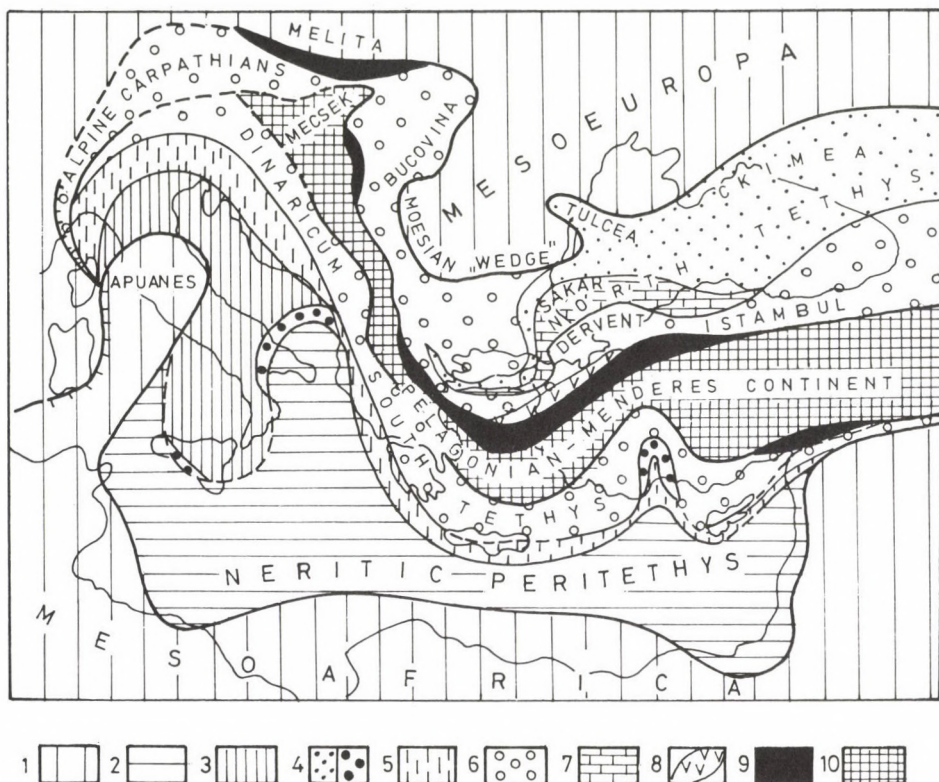


Fig.2. Triassic Paleo-Tethys palinspastic model: 1. Continental postvariscan plates; 2. Apulian neritic Peritethys; 3. Dalmatian shelf; 4. Flysch trench in North Tethys (a) and in South Tethys (b); 5. Inner carbonate platform of the High Karst-Gavrovo and Tripolitza; 6. shelf zone of the North and South Tethys (North Alpine-Carpathian-Balkan-Dervent and Dinaro-Tauricum); 7. Inner carbonate platform of Sakar; 8. Perieuropean volcanic island-arc - Karakaya; 9. Oceanic and accretional troughs of the Paleotethys; 10. Pelagonian-Menderes Cimmerian continent ("Sakarya")

tel-Nalbant (without volcanism) and of Makri-Melisohori (with volcanism?), etc., should be regarded as regional elements formed in several back-arc troughs of the Old Cimmerian embryonic island-arc orogenic system Karakaya (NW Anatolia). At present the place of the Perieuropean as well as of the back-arc carbonate Triassic platforms of Sakar Mountain in Bulgaria and of the so-called "Paikon zone" (Mercier 1966) in the southern part of the Vardar zone, etc., is still debatable, notwithstanding that some authors consider both to be fragments of the large "Cimmerian microcontinent Sakarya" (Sengör et al. 1984, Fig. 2). The Triassic carbonate platform of Sakar Mountain is an element of the North Tethys and it probably lay between the basin of the so-called "Sub-Balkanide" (Intrabalkanide) Triassic in the north and the basins of the "Istanbul", "Dervent", and "Serbian-Macedonian" (the band Deve-Koran in North Greece) Triassic in the south which are

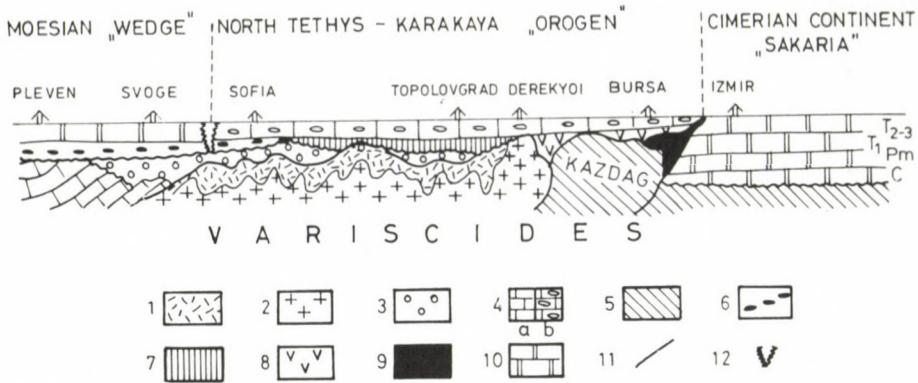


Fig. 3. Palinspastic section across the North Tethys (after Gochev, 1991 b): 1. Variscan pre-molasse complex (Cambrian-Devonian); 2. Variscan granitoids; 3. Variscan molasses (Carboniferous-Permian); 4. Variscan carbonate platform (a), carbonate platform of the North Tethys in Middle-Upper Triassic (b); 5. Variscan basement of the Apulian platform and Karakaya trough; 6. Lower Triassic of Mesoeurope - Bunsandstein; 7. Lower Triassic of the North Tethys (Verfen, etc.); 8. island-arc Karakaya (Lower Triassic); 9. Paleo-Tethys oceanic crust; 10. Moesian and Apulian continental platform (Carboniferous-Triassic); 11. suture zone; 12. transgressive limit

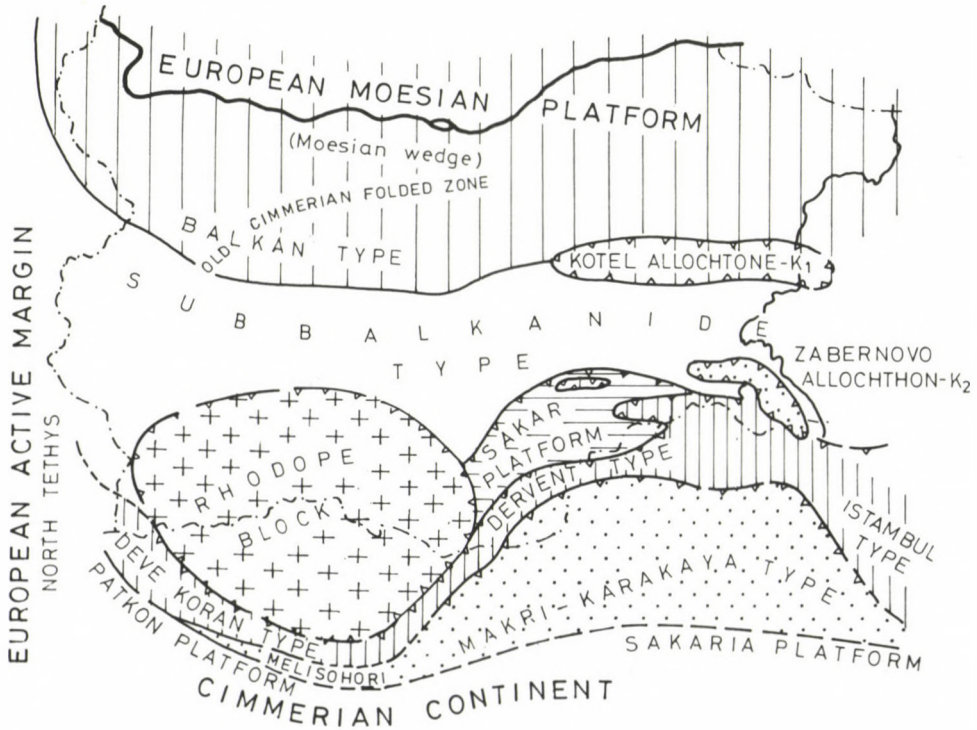


Fig. 4. Cimmerian-Austrian European margin and orogenic collage

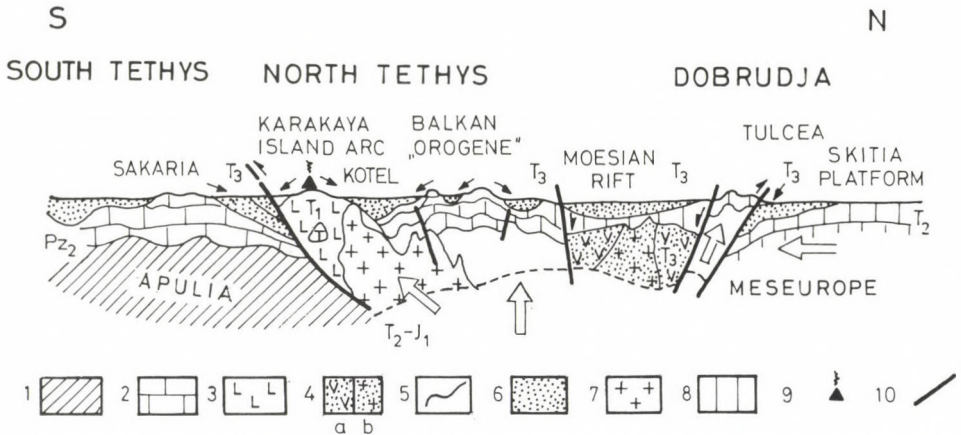


Fig. 5. North Tethys Old Cimmerian - Mesocimmerian collisional block-rogen (after Gochev, 1990 b): 1. Variscan platform basement; 2. Cimmerian continental platform - Sakarya; 3. volcanic island-arc complex of Karakaya; 4. rift volcanite (a) and plutonite (b) of Triassic age; 5. Old Cimmerian - Mesocimmerian fold mirror; 6. Old Cimmerian troughs with complexes of type Keuper, etc. (Koslodui complex); 7. synorogenic plutonite (Old Cimmerian and Mesocimmerian) - granites, aplites and other; 8. (Mesoeuropean platform (Scythia)); 9. volcanoes; 10. faults and obduction zone

generally similar, together with the Triassic sequences in the North Alps, the Internal Carpathians and West Serbia. At the same time the "Paikon zone" in North Greece is probably a lateral fragment of the "Sakariya microcontinent" (Sengör et al. 1984), whereas the new string deforming the carbonate Triassic platform of West Serbia (Goliya) and South Hungary (Villány-Mecsek) most probably was extended to the south in the real "Pelagone zone" of Macedonia and North Greece and then in Thessalia, Cyclades and Menderes, south of the Izmir-Aukara-Ezzincan suture (Okay 1989). It is this zone that should be considered to be at the recent main tectonic relic of the Early Alpine "Sakarya Microcontinent" (Fig. 1). South of it lies the ocean basin of the South Tethys obviously not comprising the area of the so-called "Tavrian thrusts" (Antalia, etc.) and the deep-water Triassic of Crete, Budva and South Italy, north from the Apulian margin.

The Moesian periplatform carbonate wedge started destroying in the Middle and Upper Triassic. Probably as a result of the active bilateral collision (Isker and Old Cimmerian phases) of the area of the North Tethys (Fig. 5). In the larger part of the Moesian platform a continental rift system was formed - the South Moesian rift (Gochev 1991), which is characterized by a specific set of sediments (Kozlodui Formation?) and by widely spread events of basal and acid volcanism (Gochev 1976, Fig. 4; Sandulescu et al. 1984).

A large embryonic "block-rogen" (Gochev 1972) was formed at the end of Triassic as a result of the general compensation of the whole area of the North Tethys, between Sakarya and the Scythian platform in the eastern part of the Balkan Peninsula and in NW Anatolia (Fig. 6/a). This orogen, emerging in the relief

and being defined at the beginning of Jurassic (Mesocimmerian time) as a wide archipelago chain of mountains, was almost of an autochthonous structure and was a vast megaanticlinorium by nature (Fig. 6/b) with sporadic demonstrations and mainly of acid magmatism (Marble Sea, Kiranlar, etc.). Elements of this Old Cimmerian earliest orogen of the Alpides can be established today almost in the whole area from Tulcha (Romania) to NW Anatolia.

Cimmerian orogen in SE Bulgaria and the Aegean area

The Cimmerian orogen of SE Bulgaria is thrust over the strongly deformed active Palealpine margin of Mesoeurope—the Balkanides. It is included in the Cimmerian–Austrian tectonic system of the Strandzhides (Gochev 1985) in the form of several basal charrriages (Fig. 3). The tectonic evolution of the collage orogen of the Strandzhides starts from the Lower Triassic with the deformation of the Moesian margin and the formation of the island-arc system Karakaya (Fig. 4) and with the successive metamorphism of the Karakaya formation (Bingöl 1976). It continues further on during Young Cimmerian and Austrian to end as a two-

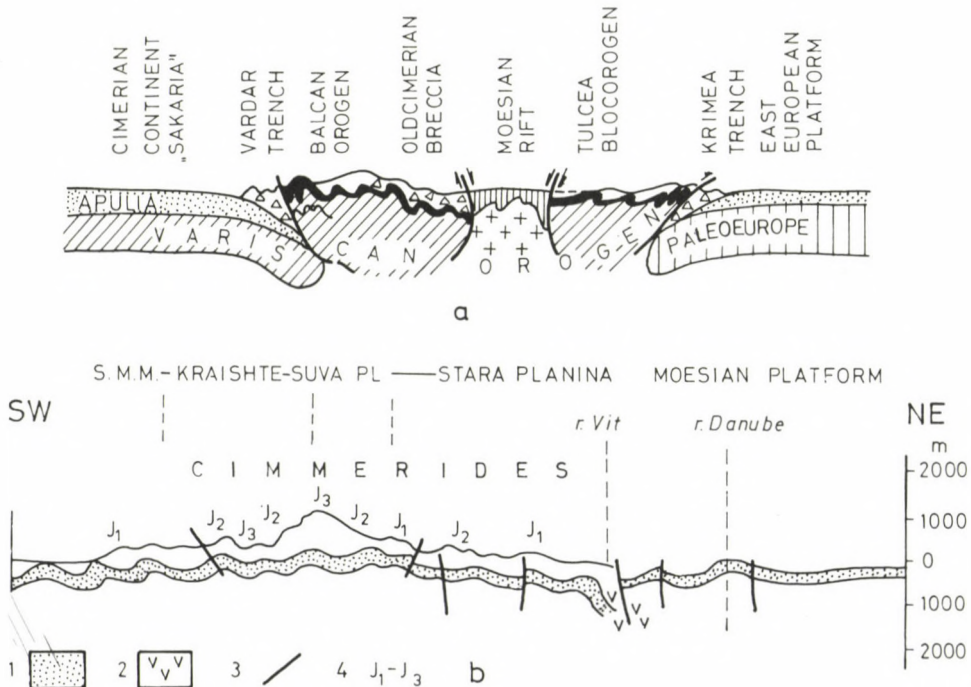


Fig. 6. a) Cimmerian embryonic block-orogen (after Gochev, 1990 b); b) Cimmerian Orogen relief in the Balkan realm after the level of Jurassic transgression. 1. Old Cimmerian fold mirror; 2. rift volcanites; 3. faults; 4. age of transgression

stage (Paleo-Alpine) orogen prior Upper Cretaceous, when over it the Morava-Rhodope-Strandzha island-arc started building. A back-arc riftbasin of the latter is the Sredna Gora, system in Bulgaria while a fore-arc trench is the Vardar-North-Aegean one (Gochev 1991).

The charriage tectonics of Strandzha and Sakar was first advanced by Ksiazki-ewicz (1930) as a superposed allochthone consisting of 4 Variscian thrusts, the highest of which is the Sakar one.

Later Tollman (1965) motivated Strandzha and Sakar Mountain as an Austrian tectonic window (type "Parning") in the northern branch of the Alpides. North of it lies the East Balkan charriage (Kotel zone?) while south of it lies the Istanbul thrust comprising Paleozoic and Triassic of Bosphorus (Fig. 4).

The region considered was first motivated by Gochev (1979) as an Early Alpine orogenic complex or Strandzhides consisting of several superposed nappes of clearly expressed northern vergency. Three main charriage units were first defined – the Sakar, Dervent, and Strandzha nappes (Fig. 7). Later External and Internal or Southern Strandzhides were distinguished (Gochev 1986) – the first ones probably being a lateral correlate of Moravicum and the Serbian-Macedonian Massif, while the second ones – an exotic element (collage) of the "Karakaya orogen" and the Vardar zone (s. l.).

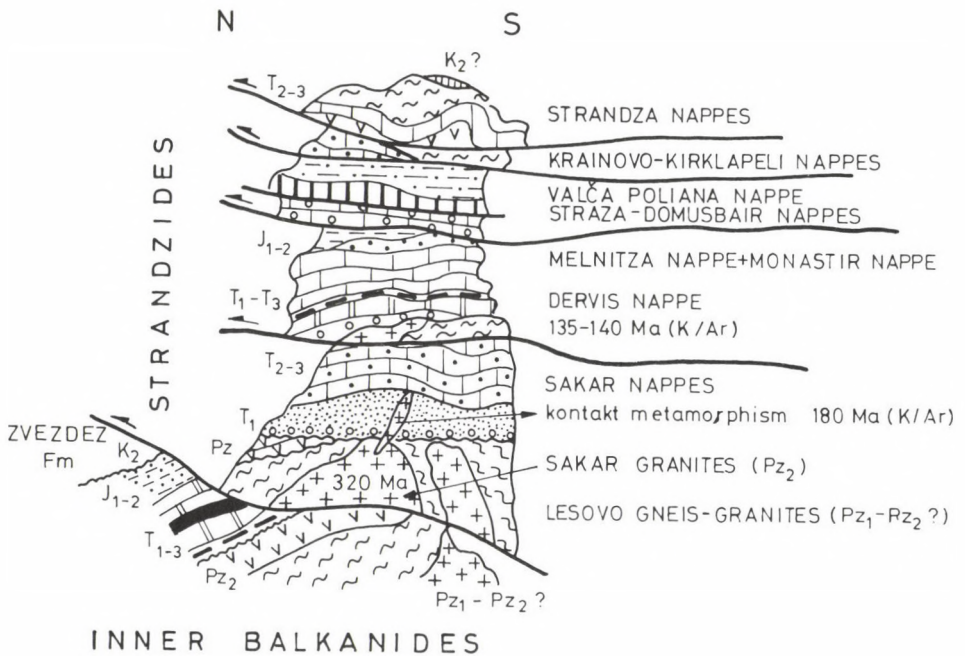


Fig. 7. Tectonic superposition model of the Strandzhides in the SE Thrace

Shortly after that also the "model of the Strandzha–Cimmerides" (Chatalov 1980) was created. This model was first constructed of an autochthone and an allochthone, which lately was developed by Chatalov (1988) and by Dabovski et al. (1989). Nowadays the model is a three-component one from the bottom upwards: Moesian allochthone (Balkanides) and lower and upper allochthone (or Zubernovo thrust) entirely built of the so-called "Strandzha type" of Triassic (Chatalov 1980).

On the other hand a three-stage thrust "sandwich" of the Strandzhides has been also proposed by Sengör et al. (1981, 1984). It is constructed of three allochthonous plates lying north-vergently over the Moesian shelf, the lowermost being the "Küre nappe" (Pontides) which also comprises the oceanic lithosphere of Paleotethys. This thrust is considered by Sengör et al. (1984) to be outcropping also under the "Kirkklareli nappe" in NE Strandzha, and the Zubernovo thrust (Chatalov 1988) corresponds to this thrust. The uppermost thrust in the system is the "Istanbul nappe" which is considered to be lying over the Karklarelili nappe near Chataldzha.

Recently the author carried out new structural studies on the territory of Sakar and Dervent and partly in Strandzha (Gochev 1991).

As a result it has been established that in the Strandzhides, thrust over elements of the Internal Balkanides (Moesian shelf and active margin) the allochthone comprises not three but six nappes (Fig. 7.), not counting the Istanbul thrust (Sengör et al. 1984). Five of these thrusts belong to Cimmerian–Austrian age while the Zubernovo thrust (or the "Strandzha thrust" according to other authors) is considerably younger and appeared at its location in NE Strandzha during Sub–Hercynian (Fig. 8).

The Paleo–Alpine allochthone is built of highly crystalline rocks – Prepaleozoic and Paleozoic (?), where Hercynian magmatites (the so-called "South Bulgarian granites") metamorphic and strongly deformed deep-water Paleozoic rocks (Silurian–Lower Devonian) (Latcheva et al. 1988), "Sakar" and "Dervent" metamorphic Triassic rocks, and metamorphic Lower and Middle Jurassic (in different tectofacies) rocks were intruded (Fig. 9). There are data available on magmatic activity (granitoids, apatites, etc.) during Triassic (Sakar) or Lower Jurassic (Istanbul, NW Anatolia, etc.).

Obviously allochthonous plates, genetically belonging to "the Sakarya microcontinent" cannot be found in SE Bulgaria (the Strandzhides). The Sakar carbonate Triassic platform as well as Dervent thrusts visibly belong to the southern deformed margin of Eurasia and the North Tethys (Fig. 3). The Istanbul nappe of the Bosphorus Region (Tollman 1965) is superposed over them. The island-arc association of the deep-water Triassic rocks constructing the Zubernovo thrust visibly comes from even more southern regions – NW Anatolia and "Karakaya orogen" (Gochev 1985).

Being the deepest one the Sakar allochthone (comprising the Sakar nappes and several rabotage plates) is also the strongest metamorphized one (up to an amphibolitic facies inclusive the Triassic rocks). It is also affected by retrometamorphism. In the other Dervent and Strandzha thrusts the metamorphism is within the limits of metamorphism of schists lustres and antimetamorphism. The degree of the Triassic sequence in the Subhercynian Zubernovo thrust (Strandzha nappes) increases again (Chatalov 1988).

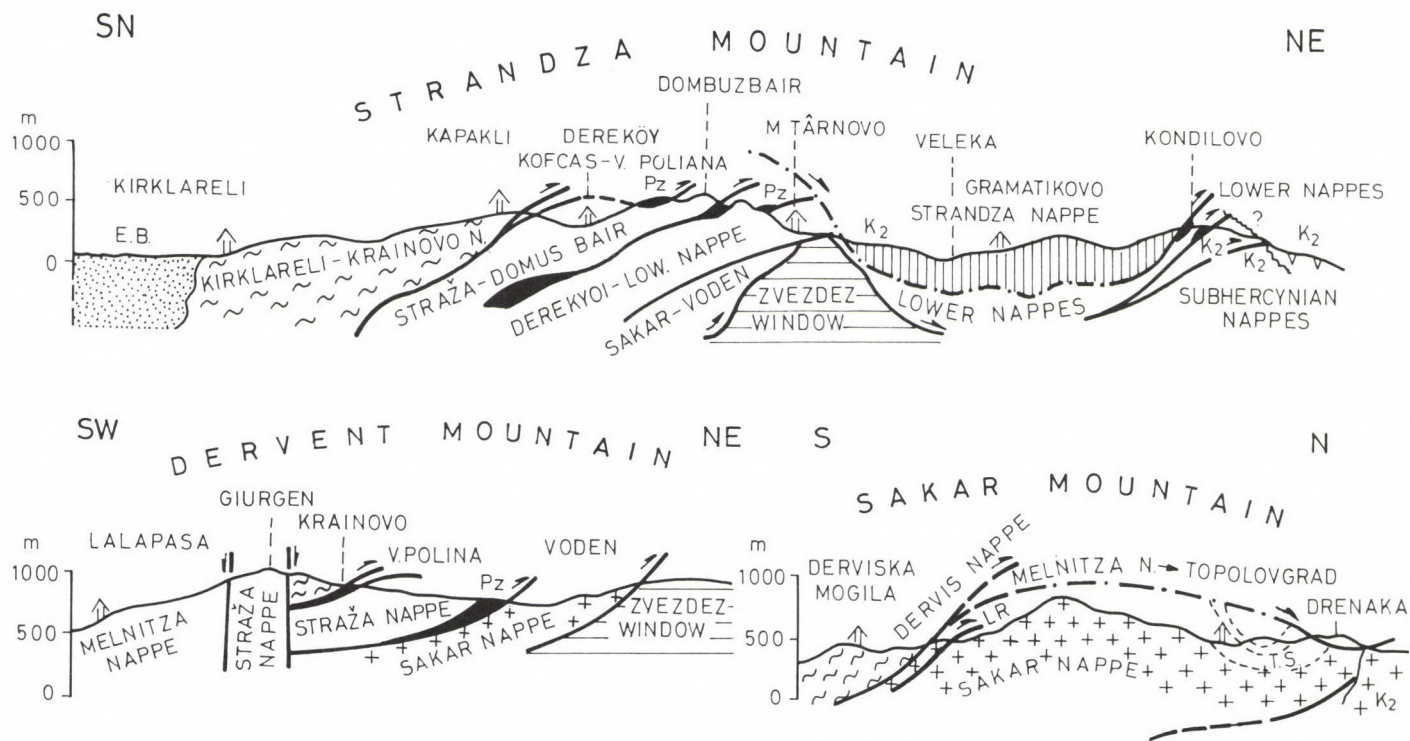


Fig. 8. Sakar, Derwent and Strandzha nappe systems in SE Bulgaria and Turkey (after Gochev, 1990 a). In black the metamorphic Paleozoic complexes in Derwent nappe system

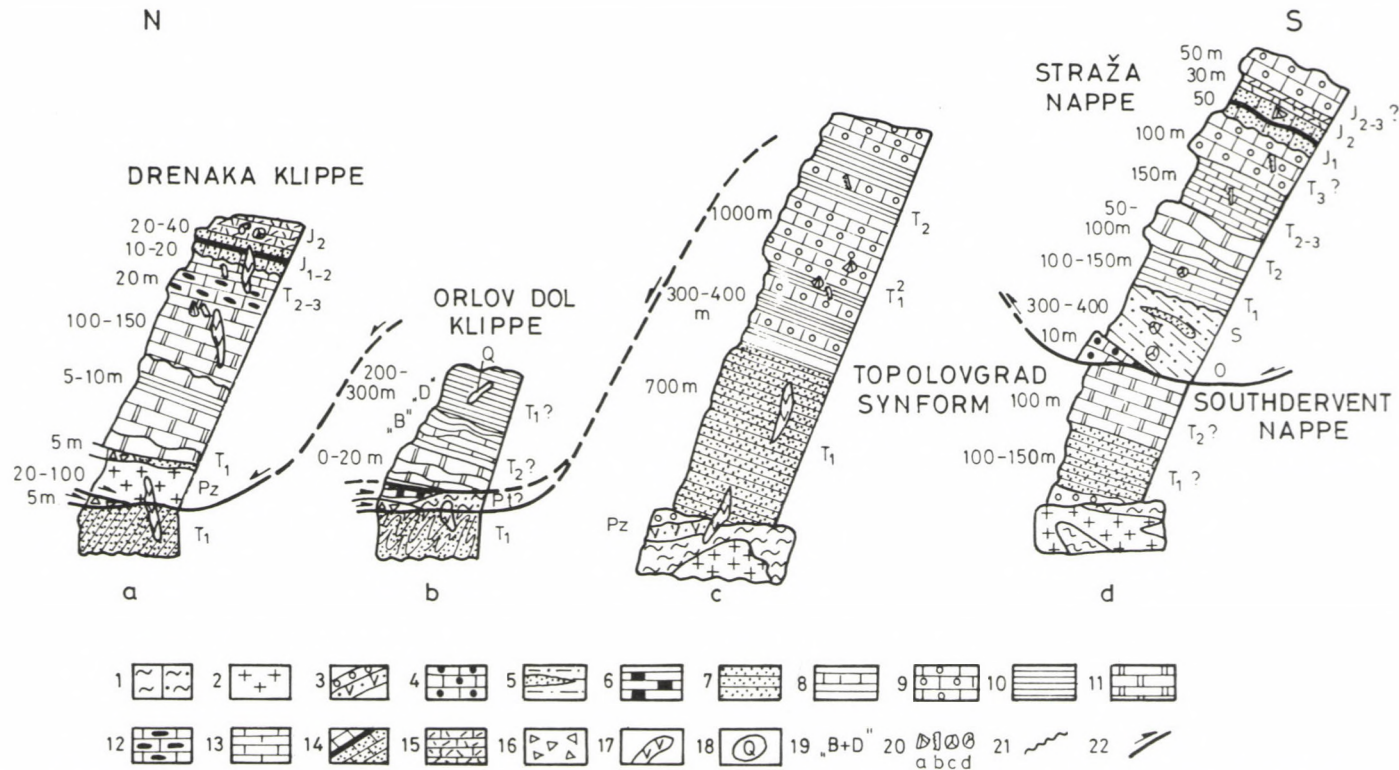


Fig. 9. Schematic Sakar- and Derwent- sequences of the allochthones (after Gochev, 1990 a): a. Drenak klippe (Monastir nappe); b. Orlovdol (Kavrakovo) klippe; c. Sakar nappe; d. Derwent Heights (Strandzha and South Derwent nappes); 1. high crystalline: a. gneisses and mica schists, b. migmatites; 2. schistous, porphyric and aplitoidal granitoids (South Bulgarian granites); 3. Klokotnitsa and Chernogorovo Formation, etc. (Young Paleozoic?); 4. metaquartzites (Old Paleozoic?); 5. complex of the green iron-chloritic schists with metasandstones and metaconglomerates (Ordovician?), complex of black phillites and quartzites (Ordovician-Silurian?) and a complex of gray-greenish and gray graywackes, green and grey phillites and calc-schists and marbles (Silurian-Devonian?); 6. gray-blackish shale-schists and phillites; 7. metaconglomerates, arkoses, calc-schists; 8. calc-schists, sandstones and marblized limestones, etc.; 9. marbles and marblized limestones and limestone breccia; 10. shale-schists and calc-schists; 11. metamorphosed dolomites; 12. marblized limestones; with chert; 13. gray-dove coloured limestones; 14. quartzites and phillites; 15. dark argillites and argillaceous limestones; 16. tectonic breccia; 17. dykes of microdiorites, diorite-porphyrates, etc. (Upper Cretaceous?); 18. quartz veins; 19. flysch rhythms (according to A.H. Bouma); 20. flora and fauna established up to now: a. bivalves, etc., b. conodonts, c. palynomorphs, d. ammonites; 21. transgressive and wash-out boundary; 22. thrust boundary

References

- Bingöl, E. 1976: Évolution géotectonique de l'Anatolie de l'Ouest. – *Bull. Soc. Geol. Fr.* (7), 18, 2, pp. 431–450.
- Boyantov, I., C. Dabovski, P. Gochev, A. Harkovska, V. Kostadinov, Tz. Tzankov, I. Zagorcev 1989: A new view of the Alpine Tectonic evolution of Bulgaria. – *Geologica Rhodopica*, 1, pp. 107–121.
- Brunn, I. 1967: Recherche des éléments majeurs du système Alpin. – *Rev. Géograph. phys. Géol. Dyn.*, 9, 1, pp. 17–34.
- Chatalov, G. 1980: Two facies types of Triassic in Strandzha Mountain, SE Bulgaria. – *Riv. Ital. Paleont.*, 85, 3–4 pp. 1029–1046.
- Chatalov, G. 1988: Recent developments in the Geology of the Strandzha zone in Bulgaria. – *Bull. Tech. Univer. Istanbul*, 41, 3, pp. 433–465.
- Dabovski, C., G. Chatalov, S. Savov 1989: The Strandzha Cimmerides and some Problems of the Paleotethys. – XIV Congress CBGA, Sofia, Extended abstracts II, pp. 503–506.
- Dimitrov, S. 1958: Über die alpidische Regional-metamorphose und ihre Beziehungen zu der Tektonik und dem Magmatismus in Südostbulgarien. – *Geologie*, Berlin, 7, 3–6, pp. 560–568.
- Gochev, P.M. 1972: On the evolution of the "Kimmerides" on the Balkan Peninsula. – *Rev. Bulg. Geol. Soc.*, 38, 1, pp. 1–12 (in Bulgarian).
- Gochev, P.M. 1976: L' evolution géotectonique du megabloc bulgare pendant le Trias et le Jurassique. – *Bull. Soc. geol. Fr.* (7), 18, 2, pp. 203–216.
- Gochev, P.M. 1979: The place of Strandzha in the alpine structure of the Balkan Peninsula. – *Rev. Bulg. Geol. Soc.*, 40, 1, pp. 27–46 (in Bulgarian).
- Gochev, P.M. 1985: Strandzhides. – *Geotect., Tectonophys. and Geodyn.*, Sofia, 18, pp. 28–54 (in Bulgarian).
- Gochev, P.M. 1986: Modèle pour une nouvelle Synthèse tectonique de la Bulgarie. – *D. S. Inst. Geol. Geofiz.*, 70–71, 5 (1983;1984), pp. 97–107.
- Gochev, P.M. 1988: On the age of Vitosa Pluton and some Problems of the Srednogie – a discussion. – *Geol. Balc.*, 18, 5, pp. 85–93.
- Gochev, P.M. 1991 a: Some Problems of the Nappe Tectonics of the Strandzhides in Bulgaria and Turkey. – *Bull. Technic. Univ. Istanbul* (in Press).
- Gochev, P.M. 1991 b: The Alpine orogen of the Balkans – a polyphasic collisional structure. – *Geotectonics, Tectonophysics, and Geodynamics*, 22, Sofia (in press).
- Haydoutov, I. 1989: Precambrian ophiolites, Cambrian island-arc and Variscan suture in the South Carpatian-Balkan region. – *Geology*, 17, pp. 905–908.
- Ksiazkiewicz, M. 1930: Sur la Géologie de l'Strandja et des territoires voisins. – *Orris* 3, Cracovie, pp. 1–28.
- Latcheva, I., P. Gochev, I. Lakova 1989: Data on the Paleozoic age of some lowgrade metamorphic rocks in the Derwent Heights (Southeast Bulgaria) and part of Strandzha (Turkey). – *Geol. Balc.*, 19, 3, pp. 1–96.
- Mercier, I. 1966: Mouvements orogéniques et magmatisme d'âge Jurassique Supérieur-éocretacé dans les Zones internes des Hellénides, (Macedoine, Grece), *Rev. geogr. phys. geol. Dynam.*, 8, 4, pp. 265–278.
- Okay, A.I. 1989: Tectonic units and sutures in the Pontides, Northern Turkey. – *Tectonic Evolution of the Tethyan Region*, Kenwer Academ. Publ., pp. 109–116.
- Tollmann, A. 1965: Das Strandscha – Fenster, ein neurs Fenster der Metamorphiden in alpinen Nordstamm des Balkan. – *N. Jb. Geol. Paleont. Mh.*, 4, pp. 234–248.
- Sengör, A., M., C., Y. Yilmaz, I. Ketin 1980: Remnants of a pre-late Jurassic ocean in Northern Turkey: fragments of Permian-Triassic Paleo-Tethys. – *Geol. Soc. Am. Bull.* 91, 10, pp. 599–609.
- Sengör, A., M.C.Y. Yilmaz, O. Sungurlu 1984: Tectonics of the Mediterranean Cimmerides: nature and evolution of the western termination of Paleo-Tethys. – *Geol. Evolution of the Eastern Mediterranean*. *Geol. Soc., England, Sp. Publ.* 17, pp. 77–112.

Triassic carbonate platform of the Drina-Ivanjica element (Dinarides)

Mara N. Dimitrijević

Milorad D. Dimitrijević

Serbian Academy of Sciences and Arts, Geological Research Group, Beograd

The Drina-Ivanjica element (NE part of the Dinarides) has been covered with Triassic deposits. After the Lower Triassic, when shallow water clastics and the Bioturbate Formation were deposited, beginning of evolution of carbonate platform is marked by the Ravni Formation. Follows the Bulog Limestone, here presented as product of very shallow sea, synchronous with rifting from the Europe (present S France) and typical platform facies – Wetterstein and Dachstein, Ilidza F. and Lofer. Deposits of the SW platform flank represents the Grivska F. In the Upper Jurassic platform deposits slid toward SW into the Ophiolitic Melange and over it, forming large olistoplake.

Keywords: Triassic, Dinarides, carbonate platform

Introduction

Triassic platform carbonates overlie the south-western border of the Drina-Ivanjica Paleozoic, as the north-eastern part of the Dinarides, as well as parts of the Ophiolitic Belt. These were originally deposited over the Paleozoic base, but during the Upper Jurassic closing of the subduction trough they slumped into it in form of huge olistoplake, olistoliths and blocks. Original relationship have been thus highly obliterated and only some formations can be observed as a whole in some olistoplake.

This paper deals with the part of the Triassic platform, situated at the Zlatibor Mt, south of Titovo Uzice. Correlation with Northern and Southern Calcareous Alps pointed to such similarities, that names from classical localities have been employed for some of formations observed here. Where correlation was not sufficiently clear, or where the differences in description of the same Alpine formation lead to ambiguities, local names for formations have been established.

Triassic succession of Zlatibor consists of the following formations:

Pre-platform units

Kladnica Clastics

Seis Clastics

(Sirogojno Formation)

Bioturbate Formation

Platform units

Ravni Formation with three members – Utrina Micrite, Dedovici Biosparite and Lucici Onkosparite

Bulog Limestone

Addresses: Mara N. Dimitrijević, Milorad D. Dimitrijević:

11000 Beograd, H. Melentijeva 82. Yugoslavia

Received: February 14, 1991

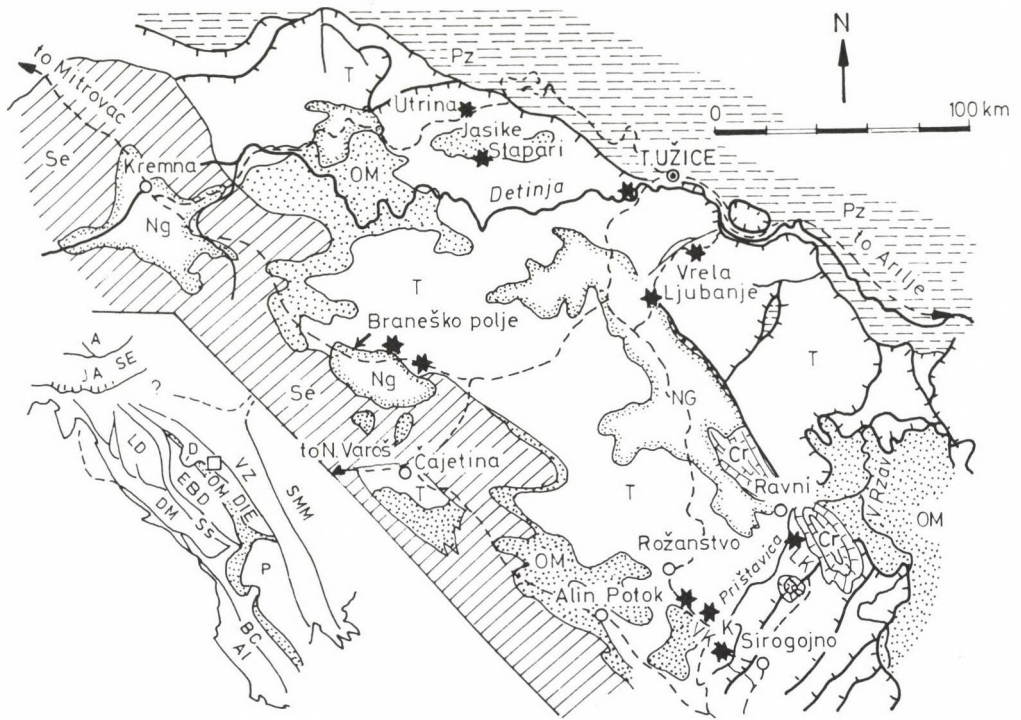


Fig. 1. General distribution of Paleozoic (Pz), Triassic (T), Jurassic Ophiolitic Melange (OM), ultramafics (Se), Cretaceous (Cr) and Neogene rocks. Asterisks show sections mentioned in text: I – Ilidža, VK – Veliki Krš, K – Klisura quarry, LK Lucica Krš. Insert shows subdivision of the Dinarides: AI – Adriatic–Ionian, B – Budva–Cukali, DH – Dalmatian–Herzegovinian, Ss – Sarajevo Sigmoid, LD – Likara–Dinara, EBD – East Bosnian–Durmitor, Om – Ophiolite Melange Belt, DIE – Drina Ivanjica element (D – Devetak nappes), and associated areas (A – Alps, JA–SF – Julian Alps and Sava Folds, VZ – Vardar Zone, SMM – Serbo–Macedonian, P – Pelagonian (Hellenides), after M.D. Dimitrijević, 1974. Square shows the area described

Wetterstein Formation with the Klisura Member

Dachstein Formation with Reef complex, Ilidža Formation and Lofer Formation.

Flank of the platform

Grivska Formation

Kladnica Clastics

These strata have been named after a locality some 25 km south of Arilje. They are preserved in a limited area, transgressive over the Paleozoic, being elsewhere tectonically reduced during the gravity transport into the Ophiolite Trough.

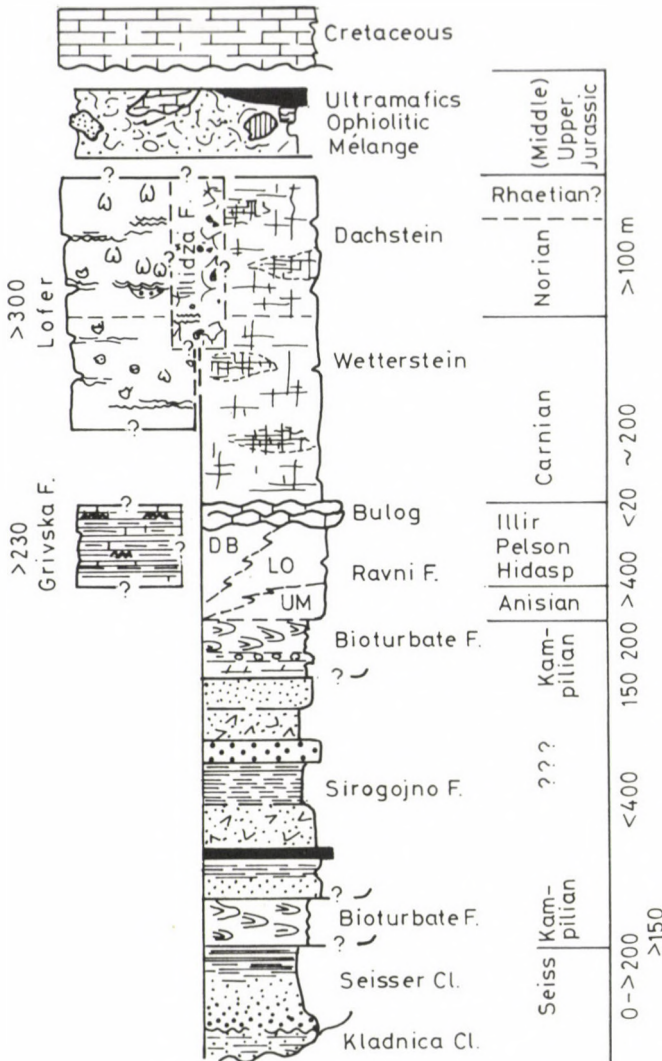


Fig. 2. Formations of north-eastern Zlatibor

Seiss Clastics

Rocks of this unit are only partly preserved, due to tectonic reduction. These are composed of medium-grained greywackes with an only weakly expressed stratification, a few meters thick horizons of conglomerates, sandstones with dm-sets of cross-laminae (type Pi), centimetric alternation of fine- and medium-grained subgreywackes with thin sets of horizontal, cross and wavy lamination and an alternation of sandstones and siltstones. Maximum measured thickness amount

to 177 m. According to previous investigations (Mojsilović et al., 1978) the formation bears also limestones in the upper parts.

Sirogojno Formation

These strata build a specific olistopla with completely unknown original position. This is a volcanic–sedimentary formation, composed of pink tuffose sandstone, with interlayers of fine-grained and lapillitic tuffs, volcanic breccia, andesite flows and coarse-grained quartz sandstone. Maximum measured thickness is 337 m. The age is questionable, the formation bearing no fossils – it has been regarded as Lower Triassic, the floor and the roof being made of the Bioturbate Formation. Both contacts are clearly tectonic (decollement surfaces). The formation appears over only some 40 km² and in the whole Triassic succession over the Drina–Ivanjica Paleozoic there are no volcanics; these are characteristics of the SW border of the Ophiolite Belt.

Bioturbate Formation

This formation has been named (Dimitrijević M.N. et al., 1980) after its most striking characteristic predominance of filled traces of unknown moving organisms named *Rhizocorallium* (Miller, 1962). This formation corresponds to the lowermost parts of the Alpine Muschelkalk (Flügel 1962; Kubanek 1969; Sarntheim 1965). Kubanek described "Wurstelkalkbänke" as laminated dolomites, dolomiticrites, dolosparites, marly limestone rich in bioturbations, micrites, pelmicrites and arenitic micrites. Sarntheim (1965) described a rhythmic alternation of "Wurstelkalkbänke" and layers of grey calcarenites built of pseudooids and bioturbations with a strong dolomitization in places. The age is in Alps ascribed to Hidasp. In Hungary these "vermicular limestones" have been described in several papers (for references see Kovács et al. 1989, and other papers).

In the Zlatibor area these deposits have been described as "recrystallized limestones with Campilian fauna" by several authors (Mojsilović et al. Brković et al. 1978). Only Rampnoux (1974) mentioned bioturbations as their important characteristic.

Typical sections of this formation occur along several roads around Sirogojno (Rozanstvo–Sirogojno, Sirogojno–Ljubanje) and in the Detinja river near Titovo Uziče. In the Sirogojno region the floor toward the Sirogojno Formation is marked by a decollement plane. In the Stapani locality (west of Titovo Užice) the formation develops gradually from Seis Clastics, beginning with 35 m of laminated sandy micrite with bioturbations. These are overlain by massive dark grey recrystallized micrite, sandy in places, with bioturbations in various degrees. The thickness of the unit amounts there up to 60 m, with possible ambiguities due to intraformational sliding. The roof represents the Utrina Micrite. Along the road Sirogojno–Rozanstvo the floor is not open, and the measured thickness of the formation is 76 m up to Utrina Micrite as the roof. There, as well as in numerous other sections, in the upper part of the formation occur metric horizons of limestone, Utrine Micrite type.

The best section of the formation crops out along the road Sirogojno–Dedovići. Its lower contact is tectonic (decollement) and the thickness is over 190 m. The lowermost part shows 7 m of light grey to reddish intrasparite with signs of rhythmical subaerial exposure (plasticlasts, oxidation of upper parts of beds, rare desiccation cracks). Follow 63 m of alternation of dolomite (primary in places), oolite, and very subordinate micrite, with secondary dolomitization expressed in various degrees. In the middle part of the unit there are thin sabkha horizons, with partly transported clasts of dolomite in a red cement. Follow 67 m of characteristic limestones with varied share of bioturbations, bearing several horizons of *Utrina* Micrite type. The section ends with some 50 m of typical bioturbate limestone of *Utrina* Micrite type.

Main microfacies of the formation are WS, ooide bioclastic GS, and dolomite.

WS (*micrites*) with bioturbations are the most frequent, giving the most conspicuous characteristic to the formation. These are greyish, well-bedded limestones (beds 5–25 cm thick), laminated in places with a nodular appearance due to horizontal bioturbations; when weathered, they look thus as calcirudites. "*Rhysocorallium*" channels are filled with sediment of the same composition as the groundmass of richer in sand, darker in color. The size of channels varies (length from 2 to more than visible 20 cm; width 2–20 mm), frequently rhythmically in layers. Channels are often coated with an argillaceous–ferruginous film, or bounded by stilolitic sutures of small amplitude. The groundmass is of carbonate mud, in places argillaceous or sandy, with frequent lenses of argillaceous–ferruginous matter. Organic detritus is represented by rare fragments of crinoids, pelecipods and gastropods. Rather frequent are ostracods and Campilian forams (determined by S. Pantić–Prodanović). This MF corresponds to a shallow carbonate subtidal of low energy up to watt, with a very slow deposition and sufficiently oxygenated. It is conspicuous that the same type of rocks occurs over the whole area.

Oobiosparites (*ooide bioclastic GS*) form a metric body of dark grey, poorly bedded to massive oolite inside WS with bioturbations, with lenses and irregular concentrations of large ooids, in places forming channels. The rock is built up of ooids, different in size, and coated grains (mostly algal bioclasts), in places densely packed and well sorted. Cement is sparite to microsparite.

These deposits are found over a very small area, pointing to a dekametric width; length is not known. They are explained as tidal delta, where tidal streams transported intertidal ooids and bioclasts, with a rapid deposition

Dolomite, dolomitized micrite (WS) and bioclastic oobiosparite (GS) are greyish-pink massive rocks, in places with a discontinuous lamination. Dolomite is often spotty and breccia-like. In places are seen also dolomite breccias with green cement and angular fragments of red dolomite, or with red cement and white fragments (subaerial discoloration). Dolomite is composed of very fine dolomite grains with still visible contours of ooids and bioclasts. Dolomite grains are sometimes coated with a fine argillaceous or micritic film. Very frequent are also zonal crystals of late-diagenetic dolomite. Process of dolomitization influenced there rocks in different

stages of diagenesis, in periods of subaerial exposition in the intertidal to supratidal domain.

The Bioturbate Formation has been deposited in a shallow, quiet, aerated subtidal area with rare tidal channels of high energy. Large areas with uniform facies point to a very large flat shelf or pericontinental sea.

Ravni Formation

The name of this formation has been derived from the Ravni settlement, some 11 km south of Titovo Uzice (M.N. Dimitrijević et al., 1986).

In the Calcareous Alps as Alpine Muschelkalk (A. v. Morlat 1848, Gümbel 1860) was described a group of Middle Triassic shallow marine deposits, which ends with filamentous nodular limestones. The development differs in various parts of the Alps (Kubanek 1963, Müller 1965, Bistricky 1982). The part between "Wurstelkalk" and filamentous limestones corresponds facially to the Ravni Formation, and thus we used earlier this name (M. N. Dimitrijević et al. 1982). This name is presently abandoned, comprising a larger time span than the Ravni Formation and being rather differently used in different parts of the Alps.

Brković et al. (1978, as "probably") and Sudar (1985) compare one part of this formation with the Gutenstein limestone, introduced by Hauer (1835). This author describes a succession of thin bedded limestone, appearing first as some ten centimetres thick interlayers with "*Ceratites cassianus*" in the "Werfener Schichten", and continuing farther as the roof of these strata. Upwards the limestones show interlayers of yellow Rauhwaacke, being dolomitized in places themselves. Chert appears in nests, nodules and thin beds. Subsequent authors describe in this formation rather different lithologies and microfacies (e.g. Flügel 1963, 1972, Flügel and Kirchmayer 1963, Summersberger 1966, Tollmann 1976, Bistricky 1982). These differences make the correlation rather ambiguous and allow the choice of characteristics according to various authors, and thus make possible various stand-points concerning the correlation of the Ravni Formation and Gutenstein. According to lithologic features and MF, the Ravni Formation does not correspond to the Gutenstein strata in the original definition.

The Ravni Formation is in the whole divided into three members with different vertical and lateral relations. These are Utrina Micrite, Dedovići Biosparite and Lucić Oncosparite.

Utrina Micrite

The name of this member has been derived from the Utrina settlement at the Titovo Uziče-Kremna road (M.N. Dimitrijević et al., 1980). Typical sections are in Utrine, along the Detinja river upstream of Titovo Uziče and below the Lučića Krš along the Sirogojno-Ravni road.

The member develops gradually from the Bioturbate Formation and the most frequently represents the lowermost part of the Ravni Formation. In places it was followed up to the very roof of the formation, having lateral relations with other two members. Its thickness amounts from a few tens of meters up to 110 m.

The Utrina Micrite shows a full section in the Utrina locality, where it develops gradually from the Bioturbate Formation, and is topped by the Bulog Formation. First 60 m of the unit build dark grey, less frequently medium grey breccia-like micrite, often recrystallized, massive or with weak discontinuous stratification, in places with a reddish binder between clasts. Follow 6 m of strongly recrystallized pink rocks, 31 m of dark grey breccia-like micrite with a few reddish interlayers of cm-thicknesses in the middle part, and 13 m of irregularly nodular dark grey microsparite with yellowish and reddish interlayers of Bulog-type limestone in the upper part.

In the Vrela-Čitići section (road Titovo Uziče-Rožanstvo) the lower part of the unit shows in places inside the dark grey micrite a well expressed planar lumpy bedding, with nodules which are in places before the consolidation stretched into flasers and discontinuous laminae, beside horizons of light massive limestone. Along the road Mitrovac-HE Perućac, west of Titovo Uziče, the Bioturbate Formation is overlain with 114 m of the Ravni Formation, 73 m of which belong to dark grey microsparite and breccia of the Utrina Micrite. These are followed upwards by the Lučići Oncosparite.

Main MF are as follows:

Micrite and microsparite (MS-WS) are the most frequent. These are massive or thick-bedded limestones, homogeneous in composition. The groundmass is micrite or microsparite, with scattered tiny dark micrite intraclasts. Organic component is built up mostly of crinoid bioclasts with syntaxial calcite, rare fragments of pelecypod shells and echinoid spines, with some benthic forams and ostracodes, cyanophyceans and dasycladaceans.

Two-component breccias are thick-bedded or massive. These are composed of pink and grey micrite plasticlasts, with a micrite matrix, of reddish, less frequently grey color. Plasticlasts are mostly large (5–20 cm), differing from the matrix only in color. Quite rare are intrabiosparite clasts, identical in composition with the next described MF. These breccias originated by syndiagenetic mixing of two muds accompanied by process of contraction.

Intrabiosparites (intraclastic GS) with infrequent ooids are mostly thick-bedded, dark grey in color. Together with ooids with one envelope these contain bioclasts of crinoids and pelecypods, gastropods, some green algae and infrequent ostracods and forams. Cement is sparitic, in places microsparitic.

Microfacies of the Utrina Micrite point to a shallow subtidal of a restricted lagoon with a low, in places variable energy. In the early diagenetic stage contraction lead to formation of in situ breccias, without subaerial exposition, with partial enrichment of one of muds with Fe from the land. Intrasparites with ooids are bound to local barrier reefs with a higher energy of environment.

Dedovići Biosparite

The member has its name from the Dedovici creek (M.N. Dimitrijević 1980) where these rocks occur in the Klisura quarry directly below the Bulog Limestone. The member occurs mostly in the middle and the upper parts of the Ravni For-

mation. It develops most frequently from the Utrina Micrite; upwards it gradually passes into the Lučići member, or is topped by Bulog Limestone with a sharp contact. The thickness of the unit is over 40 m.

Sudar (1985) correlates these strata with Steinalm limestone. Pia (1930) defined "Steinalmkalk" as white, light grey and drab, partly dolomitic, in places dark grey Anisian limestone, with beds a few centimetres to 2 m thick, built up of algal sparite with micritic domains. The notion has been later enlarged to thick-bedded to massive light colored limestone of the lower part of the Middle Triassic, rich in dasycladaceans. As with some other alpine strata, correlation depends on choice of author and domain. The Dedovići section, very monotonous in composition, shows a gradual metric alternation of biosparite and intrabiomicrite. In this section have been measured 37 m of the unit below the Bulog Limestone; the lower part of the member is covered. The lowermost visible 20 m is consist of weakly stratified mixture of greyish to drab micrite with nests of bioclasts, and biosparite. Follow 5 m of white, completely recrystallized limestone, and 12 m of light to medium grey weakly stratified sparite and biosparite, with a lenticular lamination in places. Toward the Bulog roof, which has a very sharp limit, a several metres thick horizon is characteristic, with numerous neptunic dykes of dm–m length and cm–dm width, filled by reddish limestone of Bulog-type, and with irregular nests of Bulog Limestone.

Main MF are as follows:

Biosparites (bioclastic GS) are grey, bedded, in places massive rocks. They consist of coated bioclasts (0.1–1 mm), bound by sparite cement. In places they bear oncoids and ooids, and very infrequently they represents oolite. Grains are mostly filled with mosaic calcite, but in grains with a better preserved form and structure can be recognized fragment of green algae (mostly dasycladaceans), echinoderms, gastropods and forams. Some ooids have only one envelope, but there are found even double ooids forming one coated grain. Pellets are infrequent. In lower parts of the unit rocks are finer in grain, more densely packed and with many micritized grains; the grain size of sparite increases upwards as well as the share of sparite cement, and oncoids and large coated grains are bound only to highest horizons of the member.

Intrabiomicrites (bioclastic WS–PS) are sparse, occurring mostly in lower horizons. These are light grey, bedded or less frequently massive rocks, with bioclasts, the same as in the previously described MF, mostly with micrite coatings or fully micritized. Pelloids are frequent and densely packed. Groundmass is micrite to microsparite, with bioturbations here and there. S. Pantić–Prodanović found in the Dedovići Biosparite numerous types of forams, mostly benthic, as well as other fauna of Pelson age.

Depositional environment of biosparite corresponds to a shallow subtidal–intertidal of a shelf with free circulation and a rather high energy. Bioclasts and other carbonate fragments are transported from the coastal belt, forming concentrations over an instable bottom. Coated grains with sparite cement are characteristic of areas with constant water agitation, and their larger concentrations

represent washed sands of the platform edge. Intrabiosparites point to somewhat more quiet domains directly below the local wave base, with an open circulation. Their composition shows a structural inversion, where components from high-energy shoals were transported into more quiet shallow domains.

Lučići Onkosparite

Name of the unit was derived from the settlement Lučići and the locality Lucica Krš, some 4 km north of Sirogojno at the road to Ravni (M.N. Dimitrijević et al. 1981). The member develops gradually upward from the Utrina Micrite or Dedovići Biosparite, and in type locality gradually passes into the Bulog Limestone. Very good outcrops are found also at the Sirogojno water collector and along the road Mitrovac-HE Perucac. Some horizons of the member have characteristics close to Dedovići Biosparite, toward which the member shows lateral transition. According to lithologic character, this member may correspond to Steinalm limestone in the original definition of Pia (1930) in a somewhat greater degree than the Dedovići Biosparite.

In the type locality at Lučića Krš, the unit develops gradually upwards from the Utrina Micrite, passing also gradually upwards into the Bulog Limestone. Measured thickness is 240 m, with possible uncertainties due to local faults. First 40 m built slightly breccia-like to homogeneous fine grained sparites, intramicrosparites and pelsparites. These grade upwards into massive to weakly bedded light grey onkoide sparitic types, which in the upper part show alternation with subordinate reddish pelletoidal micrite and microsparites.

The main part of the column is characterized by very well expressed corrosion cavities with conspicuous traces of the vadose history (A and B cement, reddish internal sediment, continuation of crystallization up to the stage of "tectonic" calcite veins, vadose etching and rounding of clasts), moldic cavities, numerous fenestrae and impressive strings and horizons of densely packed oncoids, frequently accompanied by pellets and bioclasts. Two-component breccia-type rocks are sparse, as well as thin algal laminae. An important characteristic is the occurrence of irregular dm-lumps of Bulog Limestone in the uppermost parts of the unit.

Main MF are:

Intrabiosparites with oncoids (oncoide bioclastic GS) are the most frequent rocks, although not in all domains and in all parts of the column. These are bedded light grey rocks, composed mostly of numerous aggregate grains of algal pellets (type grapestone). Aggregate grains are irregular in form, frequently micritized and coated with a micritic film of cyanophyceans, in form which suggest oncoids. They are accompanied by numerous rounded pelmicrite intraclasts, and in upper parts of the section there is a higher share of "algal ball" -type oncoids in a sparry cement, the rocks showing transitions into oncobiosparites. Birds-eyes, as well as corrosion cavities with A and B cement and internal sediment are frequent. Bio-components are represented by recrystallized fragments of dasycladaceans, benthic forams, ostracods, cyanophyceans and tiny gastropods.

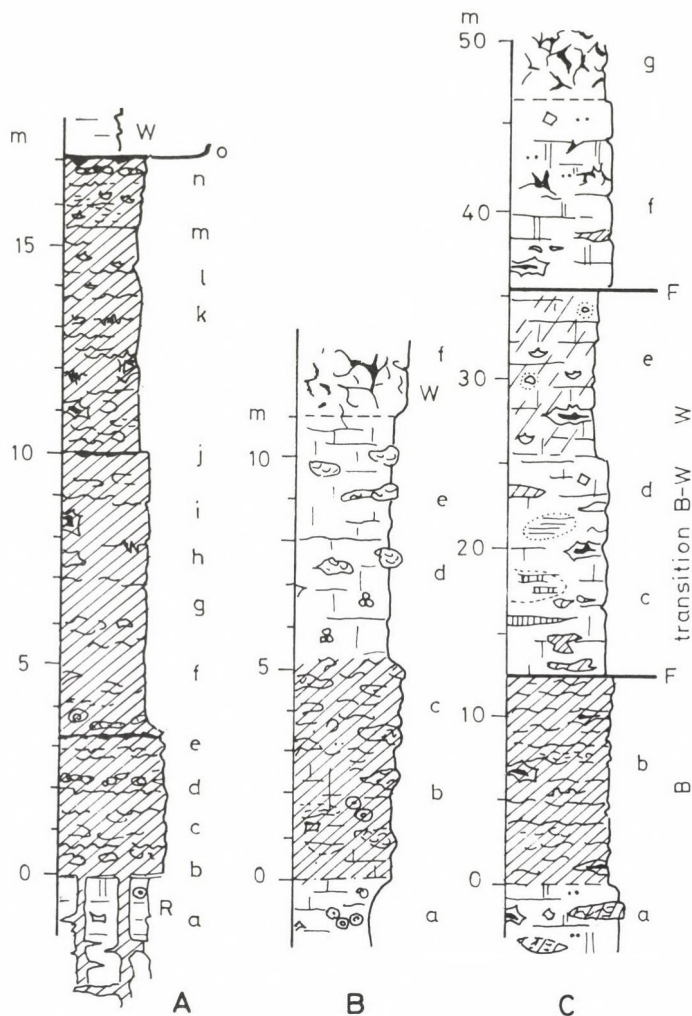


Fig. 3. Characteristic sections of the Bulog Formation. A – KLISURA QUARRY: a – Ravni Formation, Dedovica Biosparite, grey, with irregular cm–dm lumps of Bulog limestone. Bioclasts, micritized fragments of green algae and echinoderms; peloids, "algal-ball" oncooids, Neptunian dykes; b – micritre layer with laminar accumulations of filaments; c – grey micrite and biosparite with irregular red strata, nests lenses and lumps; discontinuous red or brown micrite laminae; d – "desiccation cracks" followed by ammonite lumachelle; e – red nodular micrite, corrosional surfaces, ammonite nests; f – grey nodules, oncooids, echinid spines and ammonite shells with algal borings, some filaments, detritus of blue-green algae; g – pellets, ostracods (frequently with geopetal fabric), agglutinate forams, some bioturbation, fenestrae (mostly filled, in places geopetal); h – solution cavities (A + red calcisiltite with filaments); i – red nodular pelmicrite and microsparite with breaks every few dm–m, in places showing accumulations of calcareous sand and small Neptunian dykes; j – erosional surface with calcarenite pockets k – mechanical accumulations of filaments, frequently cross-laminated; l – irregular micritic laminae marking breaks in deposition; m – nodular micrite, stylolites with Fe-films, solution cavities; numerous fenestrae, geopetal in part; n – red nodular micrite with ammonites, filaments and red laminae

Oncobiosparites (oncoide GS) are found mostly in the upper parts of the unit. They bear numerous algal oncoids, different in size, frequently in strings. Cores are mostly of crinoids, as well as of echinoid spines, cyanophyceans, rarely also forams, and envelopes are of blue-green algae. Oncoids are mostly of the group R, but C and I types are also found (classification according to Logan et al. 1964), from the group of ss-stromatolites. Thin horizons of stromatolites are rarely seen.

Breccia-like intrapelsparite with oncoids (oncoide breccia-like GS) represent contraction–desiccation breccia, with fragments connected most frequently with A, and only in places also with cement B. The voids between fragments show both the subaquatic and the vadose phase. Fragments are angular, moved and rotated in a very small degree, most probably by tidal movements. In the voids reddish internal sediment is seen.

Biopelmicrites–microsparites (pelletal WS) occur mostly in the lowermost horizons. These are composed of micrite–microsparite groundmass with scattered large intraclasts and numerous pellets (frequently in nests), and with some bioturbations. Biocomponent is very sparse (small forams and fragments of crinoids; only in places are seen concentrations of fragments of tiny ammonoids, molluscs and other forms).

Depositional environment of these rocks shows very fine variations inside a shallow lagoon with an only slightly differentiated bottom. Lowermost parts of the unit represent transitions from a quiet shallow subtidal where currents transported pellets and intraclasts into micritic mud, and somewhat higher subtidal followed by the intertidal with higher energy. In local deeps of the shallow subtidal and during stagnation of movement a micritic mud was deposited, with local accumulation of bivalvae, crinoids, gastropods, cyanophyceans and small ammonites, most probably transported along narrow connections with the open sea. In short periods of intertidal deposition was formed desiccation breccia, with infrequent stromatolitic laminae. Higher parts of the unit, with very conspicuous nests and strings of oncoids, point to restricted shallows and slow deposition with a relative low energy, followed by locally higher energy. Currents transported oncoids, concentrating them into nests.

o – red laminated sandy calcarenite. Decollement surface. W – Wetterstein, algal micrite with tuffitic stringers. B – LUCICA KRŠ: a – Ravni formation. Biopelsparite with pellets, oncoids, ostracods, echinoid spines, fragments of crinoids; b – red filamentous micrite in flasers, in biomicrite with oncoids and bioclasts, cyanophyceans, fragments of bivalvae and gastropods, echinoids; e – mixture of red and grey micrite in flasers and lenses; d – grey micrite with lumps of Bulog limestone, ostracods, filaments; e – grey micrite with tiny microfauna; some lenses, discontinuous inserts and lumps of Bulog limestone; f – Wetterstein, grey and pink two-component breccia. C – TARA–PERUCAC: a – Ravni Formation – Intrapellsparite with lumps of Bulog-type filamentous micrite; b – massive light red Bulog, slightly nodular, solution cavities; c – light grey recrystallized massive limestone with cm–dm algal nests, sheet cracks, solution cavities; d – recrystallized pellsparite with some red Bulog-type inserts and small intraclasts; e – Bulog-type micrite with pellets, fenestrae, micrite coatings. Recrystallized pellsparite with tiny ooids. Dasycladacea, Cyanophyceans; f – massive light-grey intrasparite and intrabiosparite, recrystallized. Red internal sediment in contraction fissures and small Neptunian dykes. Irregular lenses of red micrite. g – two-component mixture of red micrite and grey sparite

In the Perucac–Tara domain well sheltered intertidal was extraordinary favorable for rapid development of green algae (dasycladaceans), in later low energy phases being coated by blue-green algae, which led to densely packed, fascinatingly beautiful oncolites.

Bulog Limestone

This formation has been introduced by Hauer in 1887 (Kalke von Han Bulog), the type locality being at Bulozi near Sarajevo (presently destroyed by road construction). This is a nodular limestone of the type known from the Silurian "Orthoceras Kalke" up to Jurassic Ammonitico Rosso. In the Alps it may correspond to the Schreyeralmkalk (E.V. Mojsisovič, 1882). In the Zlatibor area it was first described by Živković (1907).

The formation is best developed in the Klisura quarry near Sirogojno, where it is exploited under the commercial name of "Red Sirogojno". For understanding of its deposition and environment very important are also sections at Lucica Krš and in Stapari. In all sections it is clearly recognized by its reddish to dark red color and nodular fabric; most frequently with a hand lens filaments visible, and in places some horizons are rich in ammonites.

In the Klisura quarry the formation begins very sharply, with a laminated horizon of reddish micrite, about 10 cm thick, over the Dedovici Biosparite invaded by neptunian dykes up to 4 m long. First 5 m of the formation are made of grey limestone with red nodular layers, lenses and nests, bearing filaments, microfauna and infrequent intraclasts. Over distances of a few decimetres occur lensoid red or drab micritic laminae, a few centimetres thick, with soles showing desiccation cracks in places. Ammonite shells (whole or fragments, frequently with Fe–Mn coatings) occur in laterally discontinuous horizons several decimetres thick, often above such laminae. Follow 6 m of red nodular limestone, with stylolites which in places border the nodules. Characteristic are large corrosion cavities, irregular in form, frequently with contours which follow the boundaries of nodules. These do not show a typical geopetal fabric, because the white blocky calcite is mostly in the lower part of the cavities, below the red internal sediment. It points to calcite crystallization from a saturated connate solution, before the subsequent mechanical filling of the cavity (vadose history!). Following 5.5 m consist of red nodular limestone with scattered ammonites. Continuous red laminae mark breaks in deposition at every few decimetres. The uppermost part of this horizon abound in small fenestrae, frequently with geopetal fabric, together with well developed corrosion cavities. The unit ends with a conspicuous 0.8 m thick red layer with profuse ammonites, frequently showing geopetal fabric. The sole and the roof of the layer are marked by red Fe–Mn films. The upper boundary is very sharp, with concentration of red residuum in pockets, covered by a 3–4 cm thick bed rich in filaments. The relation toward the Ladinian roof is tectonic – decollement surface with characteristic folding in the immediate roof.

At Lucica Krš the formation has no sharp contacts neither with the floor nor with the roof. The Bulog Limestones develop gradually from the Lucici Oncospa-

rite, with an irregular alternation of grey intertidal to shallow subtidal rocks of the Lucici member and typical filamentous Bulog micrite. Bulog is there composed of some 14 m of red and grey micrite in nodules, frequently stretched into flasers. It passes upwards gradually grey biopelmicrosparite (pelletoidal MS) with irregular lumps of Bulog Limestone.

In other localities the floor of Bulog Limestone is built up of any member of Ravni Formation, with boundaries of various type. The formation itself differs in color, faunal content and compactness; the upper contact is gradual or sharp (in this case mostly tectonic-decollement plane).

Main MF are as follows:

Grey biomicrite (WS) contain some oncoids scattered or in nests, fragments of crinoids and echinoid spines with algal coatings, sparse filaments, ostracods, plasticlasts of oosparite with oncoids, radiolarians and forams.

Red biopelmicrite, pelmicrite and microsparite (PS) bears profuse small peloids. In places these are laminated, with laminae marked by concentrations of peloids, microfauna and filaments. Ostracodes are frequent, in places with geopetal fabric, as well as small forams (agglutinate in situ), sphaerae (radiolarians), ammonoids transported and deposited in strings, microgastropods and bivalvae. Corrosion cavities are frequent, in places filled with filamentous red internal sediment. Fenestrae are infrequent and only rarely show geopetal fabric.

Intrasparudite-intraformational breccia is infrequent. It is composed of angular fragments of biomicrite, without traces of transport, within a micritic matrix.

In these strata S. Pantić-Prodanović determined Illyrian microfauna.

Toward north and northwest, the formation loses its compactness, sharp boundaries and mostly also its rich color. At Lucica Krš it is reduced to patches and irregular thin beds mixed with strata of the Ravni Formation, and at Stapani it is a hardly recognizable thin pink horizon, consisting of several thin beds inside greyish lagoonal limestone, without ammonites and with sparse filaments.

Such nodular limestones are traditionally regarded as deep marine (for references see e.g. Aubouin 1964), deposited over a deep bank surrounded by even deeper sea. Field relation and sedimentological characteristics of rocks clearly speak against this model. The floor and the roof are shallow subtidal to intertidal, showing in places intimate intermixing with Bulog Limestone. If peloids, solution cavities with A and B cement and internal sediment, fenestrae, geopetal filling and rare stromatolitic laminae (found in the vicinity of Sarajevo in the same formation) are normally seen in shallow marine sediments and regarded as proof of their depositional environment, it seems strange that these features have been in the red nodular limestones placed even in the depths of several kilometres by some authors. It seems that the main culprit for such a supposition were concentrations of ammonites. Such rich cemeteries of nekton can hardly be expected in deep waters, especially not over banks with rather strong currents (hardground without deposition in the traditional model). As typical necroplankton, ammonite shells can be expected to accumulate only in shallows influenced by an open basin. Such domains are the most probable in large coastal lagoons and beaches.

As well as the ammonite shells, filaments represent ingredients mechanically transported from the open sea, representing thus a typical thanatocoenosis in a shallow coastal environment.

Next important genetic problem is the formation of lumps. This has been ascribed by various authors to algal nodules (Schmidt 1939), lithoclasts (Garrison and Fischer 1969), unmixing of a primarily homogeneous mixture (Gründel and Rosler 1963, Hallam 1964, Jenkyns 1974), pull-apart (McCarsson 1958), desiccation (Matter 1967), differential compaction (Wilson 1969), overburden compression (Wanless 1973), pressure solution (Tucker 1974), secondary (Pettijoh, 1975), subsolution (Heim 1958, Hollmann 1962, 1964, Bandel 1974). It seems that the process can be explained through two phases:

(1) rhythmical deposition of two muds – one grey, as the autochthonous sediment of the shallow subtidal, and one red with filaments, with transport from the open sea; the red coloration of this mud remains an open question;

(2) lumpy mixing of these two muds, with changes from very early ones to all stages of development. Products of this evolution can be seen in all stages – from still visible, almost continuous beds to complete dismembering into nodules, and with flasering up to late diagenesis (A-cement, stylolites). An important process could be differential compaction of these two muds, accompanied by the tectonic unrest of the area, brought about by movements in western Mediterranean and breaking off of this part of the Dinarides from this part of Europe which is now the southern France. These movements are responsible also for opening neptunian dykes.

Wetterstein Limestone

This formation has been introduced by Gümbel (1861) for Ladinian–Cordevolian reef complex of carbonate platform in western Calcareous Alps of Bavaria and Tyrol. The name has been adopted also for the Drina–Ivanjica platform (M.N. Dimitrijević et al., 1980), basic sedimentological characteristics being the same.

At the Zlatibor Mt. a wholesome section of the formation is not seen. The better part of it, with the lower contact but without the roof, appears along the road Mitrovac–HE Perucac (over 304 m thick). A good section, also without roof (88 m) is found in the Dedovica creek up to the Klisura quarry, where the upper contact is tectonic (decollement). At Greda locality, east of Rožanstvo, a 124 m thick part of the section shows well the characteristics of the unit, but without the lower and upper contacts.

The formations consists of several basic facies, with variable horizontal relations. These are deposits of patch reefs with backreef sands, reef flat, reef framework and reef talus and of subordinate interreef lagoons. In some places in the lower part of the patch reef complex are found discontinuous and diffuse bodies of reddish rocks close appearance to Bulog as seen in atypical development north of Sirogojno. A specific part of the unit is the Klisura Member, seen over a very small area.

Patch reefs

These deposits compose the largest part of the formation. Along with observations during mapping, the best insight into the internal organization of such reefs has been obtained by a very detailed mapping of a domain at Veliki Krš (road Rožanstvo–Sirogojno). Reefs are thin (up to a few tens of metres) and small (mostly up to a few hundreds square metres). The reef framework is conserved to a very small degree, and deposits are mostly composed of products of reef destruction – backreef sands, reef flat and reef debris. Deposits of interreef lagoons are highly subordinate, and reef debris are intermixed with the reef framework, showing various degrees of movements of the material developed from mechanical disintegration of the reef body. In vertical succession frequent are the contacts between reef flat-reef framework toward reef debris, with a transition upwards into reef sands or lagoon. This points to a quick lateral migration of dekametric reefs which did nowhere reach the organization maturity characteristic of large, regional reefs, but were rapidly disintegrated into reef sands. The zone of reefs represented a platform margin of higher energy, but not as sharply developed as in the Wilson model.

Backreef sands

This, most widespread facies, consists of two main MF: *bio- to oopelsparite*, and *intrabiopelsparite* (both corresponding to oolite and pelletal bioclastic GS), differing only in the quantitative variations of allochems. These are thick to weakly bedded rocks, light to medium grey in color. Constituents are intraclasts and profuse bioclasts, introduced from the intertidal or shallow subtidal, mostly of micritized fragments of green algae (dasycladaceans, less frequently codiaceans), cyanophytes, crinoids, tubiphytes, pelecypods and gastropods, forams, echinoid spines and other forms; to the connection with the open sea point tiny ammonites. Pellet form agglomerations, being most probably algal in origin. Oncoids are sparse. Sorting is poor, in places moderate, and only exceptionally good, in the span from coarse to medium grained sand. The most part of grains has a micrite coating, or rather thick algal crusts of the A and B type. Cement is sparite, type B, and voids are somewhere filled also with micrite. These facies correspond to a mixture of MF 3, MF 4, partly also MF 5 in Wurm's classification (1982, Schutkalke) and to Wilson's SMF 11.

Bioclastic GS with profuse dasycladaceans were deposited in an environment of a slightly higher energy, with stronger currents and very frequent (storm?) shocks. That is the reason for their sorting, poorer than usual in backreef sands of mature reefs; it seems probable that such rocks are more frequent in patch reefs.

A specific feature of this facies and the reef flat facies represent intense flasering, seen in several places (very good examples are along the road Rožanstvo–Sirogojno, above the Klisura quarry). Rock components were in early stage of diagenesis stretched in flasers in various degrees – from stages where the original form of allochems may be reconstructed, up to a full "flame" – forms in the rock, which is then composed of completely stretched and vague lenses. The orientation of flasers

varies from parallel with bedding to oblique to it at various angles. The process can most probably be connected with sliding of nonlithified to semilithified mud and allochems under pressure of overlying rocks.

Reef flat

This facies is relatively frequent, represented by intrabiosparudite and intrabiosparite (bioclastic RS–GS). These are light grey, mostly massive rocks, only in places bedded, with very sparse graded laminae or lensoid strings of bioclasts. Very characteristic are irregular corrosion cavities, filled with coarse-grained drusy calcite growing inwards, or a multiple A and B cement with red internal sediment or without it. In the center of the cavity a fragment of the surrounding sediment is frequently seen, which is not seen in Dachstein Limestone. Both types of rocks consist mostly of intraclasts and bioclasts, aggregates of pelloids, coated grains and oncoids. Sorting is variable. Among intraclasts most frequent are weakly rounded fragments of pelmicrite–microsparite, and fine-grained bioclastic GS. Bioclasts are profuse, representing organisms from various depositional environments. These are fragments of crinoids with micritic rim, small dasycladaceans and codiaceans, rather frequent solenoporeans, as well as fragments of reef organisms mostly calcispongia and corals, accompanying organisms (tubiphytes, cyanophytes), and fragments of pelecypods and gastropods. Among forams the most frequent are benthic types (according to S. Pantić–Prodanović), which most probably were taken in from sea-grass meadows, from where originated also pellets and their aggregates. Bioclasts from the reef framework make about 10% of the mass.

Reef flat is the domain of transition between reef framework and narrow back-reef sands, only some 1–2 m deep. In this outstandingly photic environment, the seagrass forms a biotope very favourable for forams and boring organisms (especially molluscs), as well as for production of peloids. Relatively high energy of this domain is suitable for mixing of organisms from various facial environments.

Reef framework

Facies of this environment are found very frequently, but only as small preserved bodies. These consist for the most part of BS (framestone with transitions toward floatstone). For one part those are autochthonous limestones deposited in a very shallow domain of high energy (waves, storms, tidal movements) with constant turbulence. Rocks are light grey, massive, with reef organisms accentuated by weathering. They are mostly reef builders (calcispongia, dendroid corals, hydrozoa), binding organisms (stromatoporoids, cyanophyta, tubiphytes) and other forms. Bioclast of these organisms are frequently coated by algae and tubiphytes. In places there are also green algae (solely *Thaumatoporella parvovesiculifera*, according to S. Pantić–Prodanović), as well as solenoporaceans. Cavities in the reef, sheltered from movements, bear also concentrations of *Baccanalla* in a micritic mud. Fragments of corals and calcispongia frequently show traces of boring organisms activity. Micritized skeleton fragments are mostly disintegrated

in pellets, the aggregations of which reveal contours of the original organism (e.g. large dasycladaceans). In fine-grained varieties of these rocks profuse pellets, fragments of molluscs and forams can also be seen, with ample mud cement. Such intermixing of small or large reef organism, tiny bioclasts and small biomorpha is characteristic of relatively restricted part of the reef. Corrosion cavities are frequent also here, with fragments of organism or pellet aggregates in the central part. These cavities are in places frequent in such a measure that the rocks look like a collapse breccia.

First products of the reef destruction are represented by FS-breccia formed of fragments of reef organisms and rocks. Intraclasts and bioclasts are tied by early diagenetic calcite cement, and voids are frequently filled with a drusy A calcite. Intraclasts of biosparite, oncobiopelmicrite and biospelsparite are angular, differing in size. These are highly subordinate in relation to bioclasts – fragments of spongia, dendroide corals, hydrozoa, cyanophyceae, tubiphytes (which envelops whole shells and bioclasts), codiaceans and less frequently solenoporaceans, crinoids, together with small foram biomorpha.

Interreef lagoons

These deposits are not typical lagoonal MS, characteristic of large lagoonal areas. Lagoons were here of a small size, and rocks abound in small detritus transported from domains of permanent degradation of patch reefs.

The most frequent MF are pelmicrites, pelmicrite–microsparite and biomicrite with frequent bioturbations (WS–PS, WS). Rocks bear fragments of biosparite, oosparite and pelsparite, plenty of fragments of crinoids and echinid spines, as well as small foram biomorpha and ostracodes. Clasts show micrite coatings, most probably of encrusting algae, as well as traces of borings. Small forams are frequently micritized. Exceptionally are found also tiny ammonoids and concentrations of large filaments. These features point to very shallow subtidal of interreef domains, where the material of reef degradation was transported in shocks. Periodical streams introduced also the open sea elements.

Klisura Member

Rock of this member occur only in the Klisura quarry in the Dedovića creek, at a length of some hundred metres, and in Stamati, a few kilometres to the north. These form the roof of the Bulog Limestone, separated from these by a decollement plane. It could be assumed that the tectonic reduction of the succession is relatively small. The unit is some 20 m thick, with an upward transition into Wetterstein reef limestone.

Lower part of the unit, several metres thick, consists of well bedded grey pelmicrite with lenses and irregular interlayers of Bulog pelmicrite. These beds are separated by thin green beds of pietra verde type. Upwards follow well bedded biosparites (fine-grained GS) and the main part of the unit, with an alternation of well bedded pelmicrite (pelletoidal WS–PS) and thicker beds of intrasparite. Pelmicrites and pelmicrosparites (pelletoidal WS–PS) represent transitions from

Bulog biomicrite to biopelsparite. These consist of micritic to microsparitic groundmass with sphaere and filaments, tiny algae (cyanophyceans and dasycladaceans) and forams, with many peloids which are very small and hard to recognize. In the grey PS lamination is very frequent, in places lenticular, and in GS in places is seen also graded bedding. WS frequently contain thin interlayers or nodules of secondary chert.

The Wetterstein Formation was deposited over a broad and shallow open shelf, with scattered patch reefs separated by domains of backreef sands and infrequent larger lagoons. Reefs were small, shortlived, without possibilities of structural maturation, with a quick growth and a quick destruction. Internal reef facies can be recognized, but do not show neither a sharp separation from other facies, nor well differentiated and wholly adapted biocoenoses. Dendroide corals are very frequent, with branching tendency, growing in a partly turbulent environment.

The Klisura Member represents a lagoonal deposit of a quiet subtidal to intertidal. It is specific for interlayers of possible volcanic origin, which do not occur over the whole area, and for secondary silicification, which may be connected with local introduction of tuffaceous matter from faraway places.

According to S. Pantić-Prodanović, deposition of the Wetterstein Limestone embraces the whole Ladinian, and probably also the lower part of the Carnian.

Grivska Formation

This formation is named after the Grivska village in the Arilje area (M.N. Dimitrijević et al. 1981). These beds seem to be synchronous with lower part of Wetterstein Formation (Ladinian).

Only two section are known presently: one in Grivska, in the valley of V. Rzav, and another in the village Zbojštica, 6 km south of Titovo Užice. Relations around the first section have still not been investigated. The second section appears in a tectonic window below decollement sheets of the platform Triassic, about 1 km long and some 100 m wide. The floor is not visible, and the roof at Zbojštica are shallow marine facies close to Wetterstein Formations.

In the Grivska locality the formation consists of thin beds of grey to drab micrite and biomicrite (WS), with frequent thin interlayers of argillaceous matter, slaty in appearance. Micrites alternate with subordinate fine- to coarse-grained intrasparite (GS), which are upwards richer in bioclasts. In all these rocks occur lenses, nodules and irregular interbeds of chert, as product of an early diagenetic silicification.

Micrite and biomicrite (WS, Bioclastic WS) form over 70% of the formation. These are composed of a micritic groundmass, with biocomponents scattered or concentrated into lenses or irregular laminae. It is represented by calcispheres, radiolarians and filaments, thin and tiny, but profuse in places.

Intrasparites (GS) form beds 3–15 cm thick. Here and there thicker beds are graded. In these beds the lower part is frequently graded and the upper parts show a horizontal or cross-lamination, pointing to a turbiditic character, but without sole markings. Grain diameter of these rocks varies from 0.1 to 2 mm.

Detritus consists of fragments of micrite, pelmicrite, and microsparite, as well as pellets. In higher parts of the column these rocks grade into intrabiosparites with fragments of oosparite, oncomicrite and algal micrite, together with tiny bioclasts of reef organism.

In the Zbojštica section an alternation of (pel-, intrapel-, bio-) micrite (WS) and (biointra-, oobiopel-, oncoide biopel-) sparite (GS), dark to light grey in color, is also visible. In lower parts of the column beds are thinner, with interlayers and nodules of chert, while in upper parts thick-bedded carbonate sands dominate. Terrigenous siliciclastic ingredients are almost absent. Also in lower part of the column small-scale organic detritus dominate: upwards an intermixing of pelagic and shallow marine forms can be seen, transported from the shelf area (*Cyanophyceans*, *dasycladaceans*, encrusting organisms, benthic forams), indicating a transition toward shallow marine areas.

Grivska Formation shows a number of features sharply differing from the platform deposits. These are, first of all, homogeneous micrites with laminated beds and thin argillaceous interlayers, fine-grained sparites with horizontal and cross lamination, graded intrasparite, early diagenetic chert, distal carbonate turbidites, autochthonous pelagic microplankton and allochthonous shallow marine organic detritus, as well as slump phenomena. According to these features the Grivska Formation corresponds to the transitional (clinotherm–fondochem of the carbonate platform margin (Wilson's belt 4). The Zbojštica column shows upward a transition toward the carbonate platform with patch reefs, that points to lateral migration of the platform.

The largest part of olistoplake in the Zlatibor area consists of Upper Triassic rocks, with mutual relations preserved in such a degree that the original distribution of depositional environments can be at least partly reconstructed.

Dachstein Limestone Formation

From NE to SW three main areas of deposition can be seen within the Upper Triassic carbonate platform system

- area of patch reefs (Dachstein Formation)¹
- backreef area (Ilidža Formation)
- shallow sea (Lofer Formation)

"Dachsteinkalk" is a name given by F. Simony (1847) for Norian and Rhaetian limestones in Loferer Steinberge. Carnian part of these beds is known as "Tisovec-Kalk" (V. Kollárová–Andrusosová 1960). For deposits of (Upper?) Carnian to Rhaetian age we adopted a common name of "Dachstein Reef Complex" because of impossibility to make any geologically significant vertical subdivision.

1 In the Alpine Triassic these three facies types have traditionally been considered as a single formation (Dachstein Limestone Formation). However, in the author's opinion their distinction at a rank lower than formation (e.g. as members) is too low to express their differences

Dachstein reef complex has been recorded only in the broader domain of Rožanstvo, where good outcrops are seen along the road from Rožanstvo up to Ilidza as well as east of Alin Potok village. This complex develops gradually from Wetterstein without important differences. Practically the same depositional conditions were thus preserved in the area from Ladinian up to Rhaetian, speaking for the stability of conditions, not frequently seen in carbonate platforms.

The complex consists of patch reefs, divided by shallow marine belts covered with products of reef destruction. Reefs are somewhat larger and better defined than in the Wetterstein Fm. A detailed analysis of a section east of Ilidza showed that the most frequent are contacts reef sands/reef debris (29%), reef sands/reef framework (25%), and reef flat/reef framework (21%); less frequent are contacts reef flat/reef debris (13%), reef framework/reef debris (12%) and reef framework/interreef lagoon (4%). Direct contacts reef flat/lagoon and reef sands/reef flat have not been observed. These data show that the whole domain represents an area of permanent growth and destruction of small reefs, which did not nowhere reach neither a constructional organization nor ecological maturity. Reefs are mostly of dekametric dimensions; they were growing in a belt composed mostly of reef sands. Small lagoons with typical sediments are rare. The fauna is mixed without regularity characteristic of mature regional reefs: there are found together reef-building corals, bryozoans, lumachelle of bivalvae, and algae. In such a complex some reef facies can be recognized, with incompletely developed characteristics.

The main facies are:

Interreef lagoons

These deposits are sparse. These are products of a shallow subtidal, below the local wave base, where material from the reef sands was introduced intermittently. Most frequent are pelmicrites (peloide WS). In their composition enter pellets and oncoids (mostly densely packed in laminae), sparse grapestone, as well as fragments of crinoids, small forams, and rare fragments of green algae and forams.

Reef sands

These sands are very widespread (the term fits better than "backreef sands", which are connected with the topography of mature, constructionally well organized reefs). The water energy was here higher than in lagoons, but lower than at the reefs, and water depth was most probably 1–5 m. Width of local bodies of sands amounts frequently to only several metres. Coarse-grained intrabiosparite and intrabiopelsparite of this unit (bioclastic GS) are light grey thick-bedded rocks, with the grain diameter 0.1–7 mm. These are composed of intraclasts (biosparite, biomicrite, biopelsparite), grapestone, sparse oncoids and peloids. Bioclasts are of corals, tubiphytes, bryozoans and porostromata, a large share of these clasts being enveloped by thick algal crusts of the type A, rarely B. There were found also fragments of crinoids and bivalvae, with profuse forams and less frequent echinoid spines and ostracods. These rocks show transition toward MF of the reef flat.

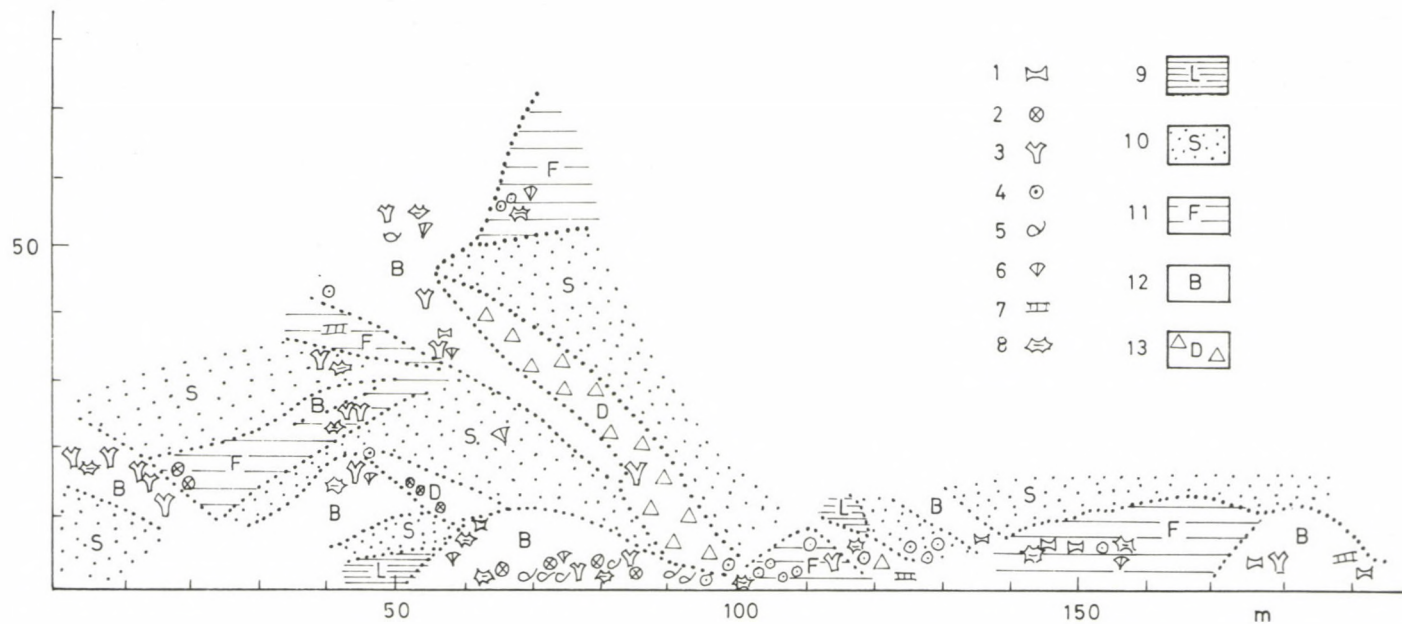


Fig. 4. Reconstruction of a patch-reef area, Dachstein, some 150 m from Ilidza (bridge over Prištavica) toward Sirogojno. The section is made after a very detailed mapping and analyses of specimens 1 – bioclasts, 2 – monocorals, 3 – colonial corals, 4 – crinoids, 5 – bivalvae, 6 – bryozoans, 7 – algae, 8 – corrosion vugs, 9 – lagoon, 10 – back-reef sands, 11 – reef flat, 12 – reef body, 13 – reef debris

Medium-grained intrabiosparites (bioclastic GS) are light grey bedded rocks with grain 0.1–2 mm in diameter. These differ from the former MF by content of oncoids, pellets and sparse ooids. Instead of algal crusts, grains are mostly coated by a micritic film. The largest part of organic detritus constitute dasycladaceans, reef-organisms being less frequent. Detritus is loosely packed, and interstices are filled with blocky calcite. Shells of molluscs show in places a geopetal fabric, formed before the final deposition. These rocks are typical representants of reef sand from areas with constant agitation.

Peletoidal biopelsparite–microsparite (peletoidal PS) are sparse. These are thin-bedded rocks, only in places laminated, composed of profuse tiny peloids and small micritized organic detritus, where only fragments of crinoids escaped micritization. Forams are sparse. Detritus is densely packed and well sorted. Rocks are deposited in somewhat less agitated areas, transitional between reef sands and interreef lagoons.

Fine-grained peletoidal intrabiosparite (fine-grained bioclastic GS) are well bedded with corrosion cavities. They bear a large quantity of carbonate detritus with predominant peloids, small ooids and tiny micritic intraclasts, accompanied by some small grapestones and fine fragments of dasycladaceans, filamentous algae, crinoids and echinoid spines, as well as by very small mollusc shells. Grain size shows that these rocks were deposited in a low energy domain, into which only the most fine-grained material was transported.

Reef flat

This facies is very widespread. Rocks are light coloured, massive or thick bedded, rich in corrosion cavities, with large fragments of reef organisms. Most frequent MF are biointrasparites and biointrasparrudites (bioclastic GS and RS), which differ only in the grain size and sorting (weaker in GS). Rocks consist of rich and very diverse organic detritus. Intraclasts are less frequent (pelsparites and biopelmicrites) as well as oncoids and ooids occur only exceptionally. Pellets are in groups, forming large blankets, originating most probably by disintegration of green algae and algal crusts. Grapestones are frequent, in places coated with micrite. Biodeposit is composed of fragments of corals, hydrozoans and spongia (mostly with algal crusts), as well as dasycladaceans, rare coralline algae, crinoids and echinoid spines, with profuse and different forams. Pelecypods form in places lumachelle nests (*Monotis?*).

In mature reefs the reef flat is situated between reef sands and reef framework. In our area it is composed of rocks which show mixing of these two facies, contracting the most frequently with the reef framework.

Reef framework

These rocks are composed of BS or biolithites. These are light grey massive, intensively recrystallized rocks with colonies of corals and infrequent but conspicuous hydrozoan *Heterastridium* (determination D. Turnšek). Among the reef association D. Turnšek separated two: (1) colonial corals and *Alpinophragmium*,

with coral algae (internal part of the reef framework) and (2) hydrozoans and spongia, with dasycladaceans and *Lamellitubus* (external part of the reef). The third, non-reef association is composed of hydrozoans (*Heterastridium*), ahermatypic corals and spongia, along with solenopora, microproblematica and, fragments of ammonites.

Reef slope

This facies is weakly expressed and hardly discernible in the field: such small reefs had not a well developed reef slope, and products of reef disintegration are mixed with the reef deposits. Rocks are RS-FS with angular fragments 0.1–6 cm in size, poorly sorted. Clasts are of pelsparite, biopelsparite, profuse fragments of reef and accompanying organism – corals, calcispongia, algal crusts, hydrozoans, crinoids and other forms. Forams are sparse, and pellets profuse. Groundmass is micrite or sparite, depending on energy of the domain in which the fragments came to a stand.

Ilidza Formation

This formation represents Carnian–Norian (–Rhaetian?) backreef deposits. The name comes from the locality Ilidza (Turkish for "spa") on the Prištavica rivulet (road Rožanstvo–Sirogojno).

The floor of the formation is not visible in the type locality, as well as in splendid outcrops along the road Arilje–Krušica, east of the type area.

The most conspicuous feature of this member represent fine to coarse-grained carbonate breccia, in vague lenses and pockets dm–m in size. Characteristic of this breccia is the presence of numerous grey to black bioclasts and intraclasts ("black pebbles") of green and coralline algae, fragments of corals, spongia, bryozoans and hydrozoans; intraclasts are of PS and GS. Fragments originated by destruction of rocks from the high-energy zone of the patch reefs area (first phase), being by waves and/or tidal movements transported into depressions with relatively anaerobic conditions, where these obtained their dark colour (probably by algal action; second phase). In the third phase black fragments have been transported by storms, tidal and other streams into the intertidal to subtidal domain of deposition of Ilidza Formation, where these have been deposited together with other fragments. With this breccia occur also the following MF:

Intrabiomicrite with peletoids (WS–PS) are bedded rocks, forming horizons of metric thickness. These are composed of numerous densely packed peloids, lensoidal concentrations of intraclasts and bioclasts (partially black), brecciated in appearance, fragments of micrite and biosparite (frequently coated by a micrite envelope), coated grains and oncoids. Biodetritus is composed of fragments of dasycladaceans, codiaceae (less frequently biomorpha), solenoporacea, molluscs and reef organisms, as well as forams and ostracodes. In places were found nests of megalodonts. Corrosion cavities are frequent, filled with A and B cement, occasionally also with red internal sediment. These are deposits of the lower intertidal to shallow subtidal, with a mostly low energetic potential, into which clasts were introduced intermittently.

Intrabiosparite (bioclastic GS), fine to coarse-grained and very poorly sorted, are very frequent. These are bedded to only slightly stratified rocks, with conspicuous breccias, bearing nests and pockets with dark clasts. Differently packed detritus of these rocks is composed of subangular to angular clasts or even plasticlasts of micrite and biosparite, sparse ooids with one envelope, pellets, less frequently oncoids (grouped) and grapestone. The most part of the detritus represent bioclast of cyanophyceae, dasycladacea, solenoporacea, sponges, hydrozoa, bryozoa, corals, bivalvae, gastropods, rare crinoids and echinoid spines. Grains are mostly coated with a micrite envelope. Cement is blocky calcite, and around some grains encrusting calcite cement can be seen.

In places these rocks contain concentration of large smooth bivalvae with thick shells. Corrosion cavities are frequent and almost wholly filled with red internal sediment. Depositional environment of these rocks correspond to a specific back-reef area with good circulation and conspicuously diversified energy, with subtidal domains where micritic mud accumulated. The water depth amounted to only a few metres.

In the formation also Lofer deposits have been recorded somewhat atypical but with recognizable member B (fenestral micrite) and C (fine-grained bioclastic GS). Thickness of Lofer interlayers is only a few decimetres, and their occurrence point to a connection with adjacent Lofer areas.

Lofer Formation

The name has been given by B. Sander (1936) for well bedded and laminated limestones of Dachstein Fm. in the Loferer Steinberge. In the alpine literature they are known under various names (Loferer Schichten, Loferer facies, Loferer Dachsteinkalk, Loferer typus des Dachsteinkalkes). This formation occurs over a very large area west of the zone of the Ravni Formation and Dachstein, through the whole Carnian, Norian and most probably also Rhaetian stages. The floor was not found, and the unconformable roof represent marly and sandy micrites of Liassic (–Dogger) age, or directly the Ophiolitic Melange. Excellent sections of the formation can be seen along the road Titovo Užice–Nova Varoš. The unit was earlier described in detail (M.N. Dimitrijević et al. 1982, Nastic and Zupancic 1986), and only a short summary is given here.

The most conspicuous characteristic of the formation is a rhythmic dm/m exchange of "Lofer cyclothems", consisting of three members: A – infrequent reddish or greenish horizons of marly MS or WS up to few centimetres thick, with irregular lower boundary, pockets and lenses and filling of mud crack and small neptunian dykes, bearing witness of subaerial exposure and erosion. B – Loferite breccia, fenestral micrite and algal stromatolite = intertidal with algal mats. C – Massive biomicrite and biosparite with megalodonts, corrosion and moldic cavities and contraction breccia = shallow subtidal. In the ideal case cyclothems have sharp C/A or C/B boundaries, but gradual BCB transitions as well as sharp contacts B/C have been observed. Thin cyclothems continue only a few metres laterally.

The Carnian part of the unit differs from the Norian (–Rhaetian) one by presence of oncoids, smaller megalodonts that are also less frequent, and more frequent C/BC/B... or BCBC cyclothemes.

Characteristics of Lofer point to a shallow sea with constant local rhythmic emergence, without permanent streams but with a rather well expressed water agitation in the intertidal.

Tentative Reconstruction of the History

Triassic strata at the Zlatibor area are nowhere preserved in the original position, building up several olistoplake (decolllement sheets) of highly different, mostly kilometeric size. These sheets slipped down from the Paleozoic into the Melange trough, mostly at the end of Jurassic. Basal parts of these sheets have been during this sliding tectonically reduced in different amounts, in such a manner that present decolllement surfaces cut the Triassic column at various places. As a consequence, different parts of the Triassic column directly overlie the Paleozoic base. Original relations are mostly seen inside large olistoplake. This situation very seriously impede the reconstruction of the platform geometry and development, relations between units, and toward adjacent deposits.

One of serious problems represents the boundary between Paleozoic and Ophiolitic Melange in the floor of the Triassic. Inside the area Paleozoic appears as the immediate floor along present boundary of olistoplake near Titovo Uzice, and in the Bukovac brook a few kilometres SW of this town. Already 3 km to the south the tectonic floor of the Triassic (here represented by Wetterstein Limestone) is the Grivska Formation, and one kilometre farther south as the base appears the Ophiolitic Melange. These relations suggest that only a narrow belt exists where Triassic strata still overlie the Paleozoic, whereas all other Triassic bodies lie inside the melange or over it. This assumes decolllement movements of at least 10–15 km, with platform strata overriding the clinotheme deposits of the SW flank of the ramp.

During the pre-platform stage (Lower Triassic) fine-grained clastics covered folded, emerged and planated Paleozoic strata. Sedimentology of these clastics has not been studied in detail, but deposits of possible braided rivers and shallow sea with migrating bottom forms have been recorded. The scenery did not change very much also in the upper part of the Lower Triassic, but without transport of siliciclastics from the land. The environment corresponds to a broad, shallow continental shelf. It seems that the Drina–Ivanjica element was up to the Campilian connected with its Provençal neighbourhood in the western corner of the Mediterranean (Dimitrijević and Dokovic 1989). Volcanic products of this rafting are not seen NE from the Melange trough – the Sirogojno Formation is not a normal member of the local Triassic column, but an olistoplaka of unknown origin.

Regional data place the Ravni Formation in the times of rifting, with beginning of formation of the carbonate ramp. From Pelson up, the platform phase is clear: the area represented an offshore bank flanked along both sides by oceanic basins

– at the northeast by a branch of Tethys, and from southwest by the oceanic tract of the Ophiolite Belt. Bulog corresponds to a stage of basin influenced shallow shelf or beach, with intensified breaking at the beginning of its deposition. Basin influences are weaker toward present NW, and the formation fade up into other shallow marine deposits.

Relations in Ladinian are at least partly elucidated by disposition of deposits pertaining to different environments. Wetterstein Fm belongs to the high energy zone, close to the NE margin of the bank, and the Grivska Formation marks the original clinothem/fondothem of its southwestern margin. It is not clear how to paleogeographically interpret the Klisura Member; it can be relatively close to the SW platform margin, with traces of a rather far-off volcanic activity.

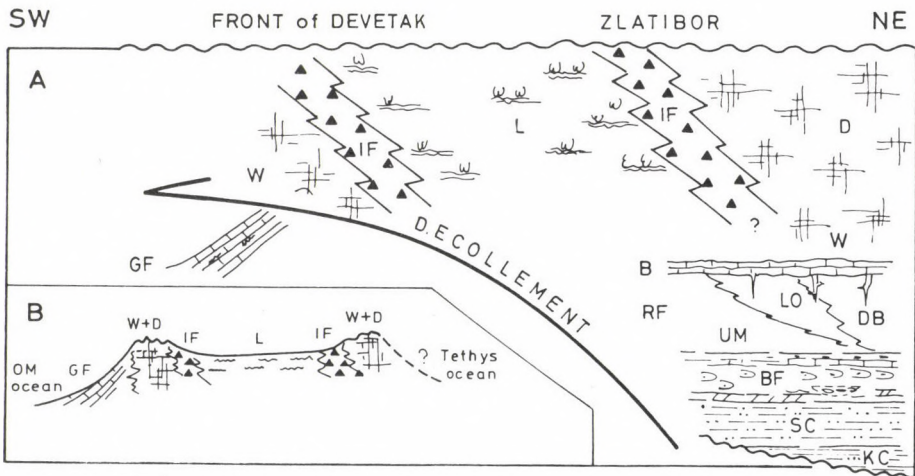


Fig. 5. A – Distribution of Triassic formations in the Zlatibor area (right) and front of the Devetak olistoplake. B – Reconstruction of the platform

Relative positions of Upper Triassic units are much clearer: at the east was a rather narrow high energy belt (Dachstein reef complex); follows the very narrow and poorly preserved back-reef belt (Ilidža Formation) and a large shallow marine area with constant local exchange of intertidal and shallow subtidal.

Farther west and southwest data are missing. Toward northwest, in Devetak (Vujnović, 1983) along the southwestern border of the platform occur Ladinian–Carnian reef limestones, overlain by Norian–Rhaetian Lofer that in its lower parts bear "black fragments of limestone and small megalodonts" (=Ilidža). This makes possible the reconstruction of the off-shore bank in the Upper Triassic, with large Carnian high energy belt at the southwest, a narrow zone of the Ilidža Formation, a large area of Lofer in the main part, followed toward NE by a narrow zone of

the Ilidža Formation, and eventually the high energy zone along the NE border (Wetterstein Fm, Dachstein Fm). During the Norian and Rhaetian the platform migrated toward SW, with the Ilidža Formation, which at the front of the Devetak group of olistoplake appeared in the Carnian–Norian, and with Norian–Rhaetian Lofer. At Devetak, the front of nappe pile from the NE overlies the Triassic of the East Bosnian–Durmitor area (Vujnović et al. 1981), with Lower Triassic similar to the Devetak development, but with strikingly different younger units – Anisian is composed of thick-bedded and massive limestones with crinoids, brachiopods and ammonites, with some dolomite. In the Ladinian prevail thin-bedded marly and sandy limestones with chert lenses, lumps and thin beds, together with profuse pyroclastic rocks. Upper Triassic is poorly exposed. It consists of thin-bedded limestone with chert nodules and alternations of such limestones, silicious rocks and marl.

The roof of the platform visible very rarely is represented by a Melange or shallow marine Cretaceous.

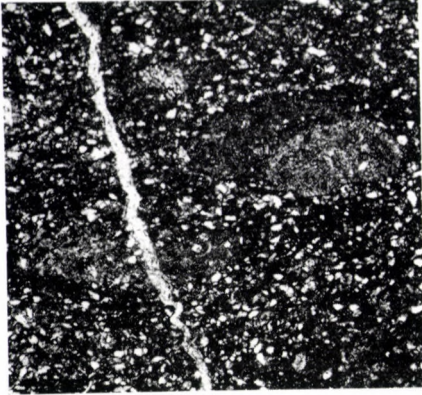
Facies almost identical with the Drina–Ivanjica area occur toward northwest and west (e.g. Dolomites and Julian Alps, Eastern Transdanubian Midmountains, Tyrol, Northern Calcareous Alps, Tirolikum, Sicilia) and even to the south (Črna Gora). This opens the question of the mutual relations of these areas in the Middle–Upper Triassic times, solved by various authors in most different ways. We explain the Drina–Ivanjica area as part of the European continent up to the Anisian. Contrary to many authors, who see the Drina–Ivanjica element turned toward the Mediterranean ocean, we place this boundary turned toward the Southern France, because of its Paleozoic base, pertaining to a very large depositional basin. Mutual relations with other areas of similar deposition are still open.

References

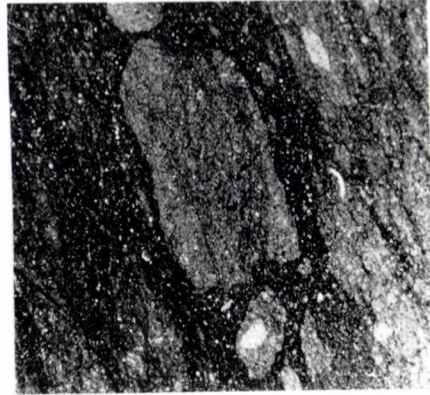
- Aubouin, J. 1964: Réflexions sur le faciès "Ammonitico rosso". – Bull. Soc. geol. France, 7, 6, pp. 475–501.
- Bandel, K. 1974: Deep-water limestones from the Devonian–Carboniferous of the Carnic Alps, Austria. – IAS I, Pelagic Sediments on Land and under the Sea, pp. 93–116.
- Bistrický, J. 1982: The Middle and Upper Triassic of the Stratsenska Hornatina Mts and its Relation to the Triassic of the Slovak Karst Silica Nappe (the West Carpathian Mts, Slovakia). – Geol. Zbornik – Geol. Carpathica, 33, 4, pp. 437–462.
- Brković, T., M. Malešević, M. Urošević, S. Trifunović, Z. Radonovanić, M. Rakić 1970: Explanation for the Cacak Sheet. – SGZ, Beograd.
- Dimitrijević, M.D., I. Doković 1981: Pre-Triassic Position of the Eastern Dinarides. – LMGK Bulletin 3, pp. 37–50.
- Dimitrijević, Mara N., M.D. Dimitrijević 1986: Sedimentology of the Triassic of SW Serbia (Abstract). – V. Skup sedimentologa Jugoslavije, Brioni, pp. 7–10.
- Dimitrijević, Mara N., M.D. Dimitrijević 1987: Trijaska karbonatna platforma Drinsko-Ivanjickog elementa. – Geol. glasnik, 12, pp. 5–34, Titograd.
- Dimitrijević, Mara N., M.D. Dimitrijević, S. Pantić–Prodanović, Z. Radovanović 1981: Field Guide. – 4. Plenum sedimentologa Jugoslavije LMGK Bulletin, 4, pp. 1–44.
- Dimitrijević, Mara N., M.D. Dimitrijević 1982: Lofer-facia severnog Zlatibora. – 10. jubilarni Kongres geologa Jugoslavije, Zbornik radova, 1, pp. 455–471, Budva.
- Dimitrijević, Mara N., M.D. Dimitrijević, J. Tišljar, S. Pantić–Prodanović 1983: Bulog Formation – Nodular Ammonitic Limestone. – 4th IAS Reg. Meeting, Split, Zagreb, Abstracts, pp. 51–52.
- Flügel, E. 1962: Untersuchungen im Obertriadischen Riff des Gosaukammes (Dachstein Gebiet, Oberösterreich) – Verh. Geol. A. Wien, A. H., 1, pp. 138–145.
- Flügel, E. 1963: Mikrofazies der alpinen Trias. – Jb. Geol. –A., Wien, 106, pp. 205–228.
- Flügel, E. 1972: Mikrofazielle Untersuchungen in der alpinen Trias. – Methoden und Probleme. Mitt. Ges. Geol., 21, pp. 9–64.
- Flügel, E., M. Kirchmayer 1963: Typokalität und Mikrofazies des Gutensteiner Kalkes (Anis) der nordalpinen Trias. – Mitt. Nat. Ver. Steiermark, pp. 93–136.
- Garrison, R.E., A.G. Fischer 1969: Deep-water Limestones and Radiolarites of the Alpine Jurassic. – In: G.M. Friedmann (Hrsg.) Depositional Environments in Carbonate Rocks. SEPM Spec. Publ., 14, pp. 20–56.
- Gründel, J., H.J. Rosler 1963: Zur Entstehung der Oberdevonischen Kalkknollengesteine. – Thüringens Geologie, 12, pp. 1009–1038.
- Gümbel, C.W. 1861: Geognostische Beschreibung des bayerischen Alpengebirges und seines Vorlandes. – Gotha Pertes.
- Hallam, A. 1964: Origin of the Limestone–Shale Rhythm in the Blue Lias of England: a Composite Theory. – J. Geology, 72, pp. 157–169.
- Hollmann, R. 1962: Ueber Subsolution und die "Knollenkalk" des Calcarea Ammonitico Rosso Superiore in Monte Baldo. – N. Jb. Geol. Pal., Mn., pp. 163–179.
- Hollmann, R. 1964: Subsolutions–Fragmente (Zur Biostratinomie der Ammonoidea im Malm des Monte Baldo/ Norditalien). – N. Jb. Geol. Pal., Abh. 119, pp. 22–82.
- Hauer, F.V. 1853: Ueber die Gliederung der Trias, Lias und Juragebilde in den nordöstlichen Alpen. – Jb. Geol. R. A., 4, pp. 715–784, Wien.
- Hauer, F.V. 1887: Die Cephalopoden des bosnischen Muschelkalkes von Han Bulog bei Sarajevo. – Denkschr. K. Akad. Wiss., math. –nat. Kl., 54, pp. 1–50.
- Heim, A. 1958: Oceanic Sedimentation and Submarine Discontinuities. – Ecol. Geol. Helv., 51, pp. 642–649.
- Jenkins, H.C. 1974: Origin of Red Nodular Limestone (Amm. rosso, Knollenkalk) in the Mediterranean Jurassic: a Diagenetic model. – IAS Spec. Publ., 1, pp. 249–272.
- Kaldi, J. 1980: Origin of Nodular Structures in the Lower Magnesian Limestone of Yorkshire, England. – Contr. Sedimentology, Stuttgart, 9, pp. 45–60.

- Kollárová-Andrusová, W. 1960: Recentes trouvailles d'Ammonoides dans le Trias des Karpates Occidentales. – Geol. Sbornik Slov. Akad. Vied, Bratislava, 11, pp. 105–110.
- Kovács, S., Gy. Less, O. Piros, Zs. Réti., L. Róth 1989: Triassic Formations of the Aggtelek–Rudabánya Mountains (northeastern Hungary). – Acta Geol. Hung., 32/1–2, pp. 31–63.
- Kubanek, F. 1969: Sedimentologie des Alpenen Muschelkalkes (Mitteltrias) am Kalkapensüdrand zwischen Kufstein (Tirol) und Saalfelden (Salzburg). – Univ. Diss., TU, Berlin.
- Logan, B., E. Rezak, R.N. Ginsburg 1964: Classification and Environmental Significance of Algal Stromatolites. – J. Geol., 72, pp. 68–83.
- Matter, A. 1967: Tidal Flat Deposits in the Ordovician of Western Maryland. – J. Sed. Petr., 37, pp. 601–609.
- McCrossan, R.G. 1958: Sedimentary "Boudinage" Structures in the Upper Devonian Inetion Formation of Alberta. – J. Sed. Petrol., 28, pp. 316–320.
- Miller, H.v. 1962: Der Bau des westlichen Wettersteingebirges. – Z. Geol. Ges. 113, (1961), pp. 409–425. Hannover.
- Mojsilovic, S., D. Bakljajic, I. Dokovic, V. Avramovic 1978: Expanation for the Titovo Uzice sheet. SGZ, Beograd.
- Mojsisovics, E.v. 1882: Die Hallstätter Entwicklung des Trias. – Sitzber. Akad. Wiss. math.– natw. Kl. 1, 101, pp. 769–780.
- Nastic, V., N. Zupancic 1986: The Section "Jelova Gora" of the Lofer–Facies, Zlatibor (Abstract). –5. Skup sedimentologa Jugoslavije, Brioni.
- Pettijohn, J.P. 1975: Sedimentary Rocks. – Harper intern. Edition. New York – London.
- Pia, J. 1930: Grundbegriffe der Stratigraphie. – Leipzig – Wien.
- Rampoux, J.P. 1974: Contribution a l'étude géologique des Dinarides: Un secteur de la Serbie méridionale et du Monténégro orientale (Yougoslavie). – Mem. Soc. géol. France, N. S., 52, pp.16–272; Mem., 119, pp. 1–100.
- Sander, B. 1936: Beitrage zur Kenntniss der Anlagerungsgefuge (Rhythmische Kalke und Dolomite aus der Trias). – Min. Petr. Mitt., 48.
- Sarnthein, M. 1965: Sedimentologische Profilreichen aus den mitteltriadischen Karbonatgesteinen der Kalkalpen nördlich und südlich von Innsbruck. Ver. Geol. –A. Wien, A.H., 1–2 u. 3, pp. 119–162.
- Simony, F. 1847: 2. Winteraufenthalt im Hallstätter Schneegebirge und 3. Ersteigung der hoher Dachsteinspitze. – Ber. Mitt. Freunde Naturwiss., 2, pp. 207–221.
- Sudar, M. 1985: Mikrofosili i biostratigrafija trijasa unutrašnjih Dinarida između Gučeva i Ljubišnje. – Dr disertacija RGF, Beograd, and Geol. An. Balk. Pol., 50, Beograd.
- Summesberger H. 1966: Zum Typusprofil des Gutensteiner Kalken Stellungnahme zu Flügel E. und Kircmayer, 1962. – Mitt. Ges. Geol. Bergbaustud., Wien, 16, pp. 85–88.
- Summeschberger, H., L. Wagner 1972: Der Stratotypus des Anis (Trias). – Ann. Naturhist. Mus., Wien, 76, pp. 515–538.
- Tucker, M.E. 1974: Sedimentology of Paleozoic Limestones: The Devonian Griotte and Cephalopodenkalk. – IAS Spec. Publ., pp. 71–92.
- Vujnovic, L. 1983: Explanation for the Praca sheet. – SGZ, Beograd.
- Vanless, H.R. 1973: Microstylolites, Bedding and Dolomitization. – Abstract of Papers, Ann. Meeting SEPM, Anaheim, and AAPG Bull., 57, 811.
- Wilson, J.L. 1969: Microfacies and Sedimentary Structures in "Deep Water" Lime Mudstones. – SEPM Spec. Publ., 14, pp. 4–19.
- Wurm, D. 1982: Mikrofazies, Paläontologie und Paläoökologie der Dachsteinriffkalke (Nor) des Gosaukammes. Österreich. – Fazies, 6, pp. 203–246.
- Zivkovic, M. 1907/8: Geologija uzicke okoline. – Izd Uzicke gimnazije, Uzice.

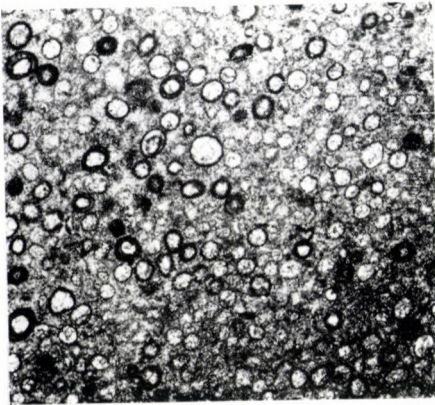
Plate 1



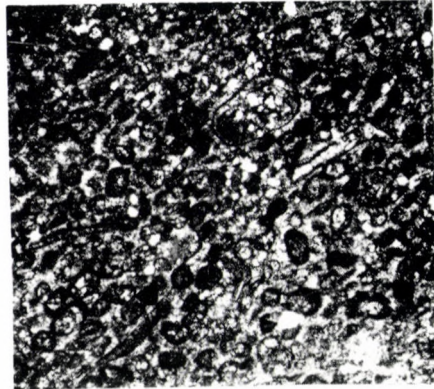
1



2



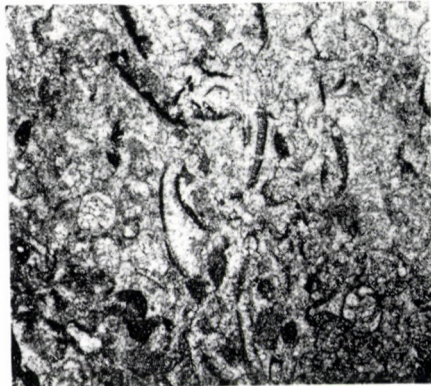
3



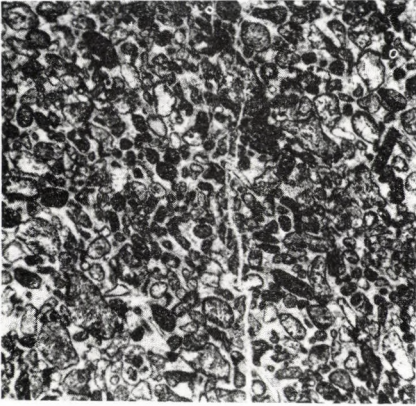
4



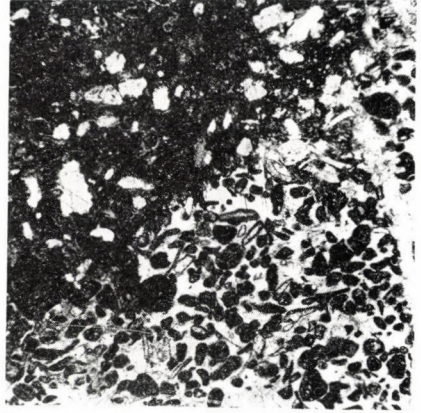
5



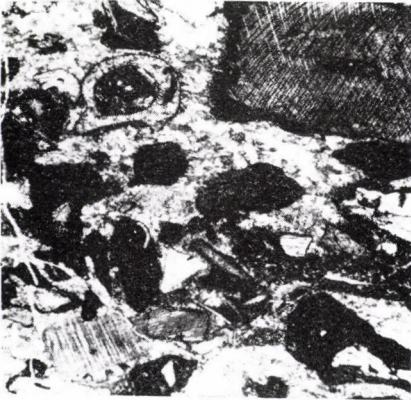
6



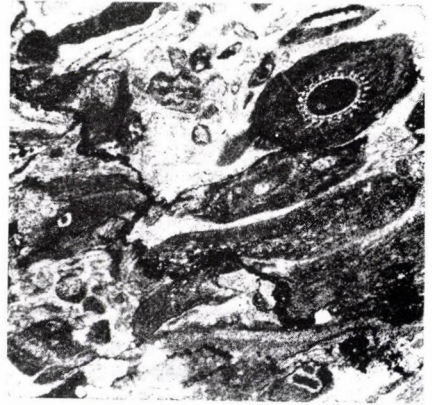
1



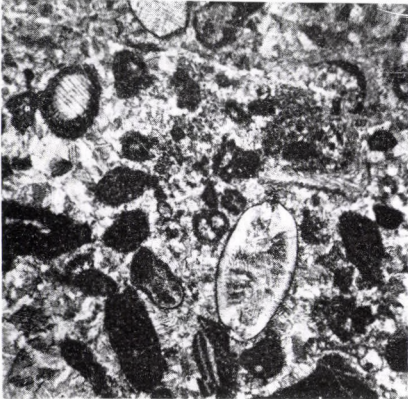
2



3



4

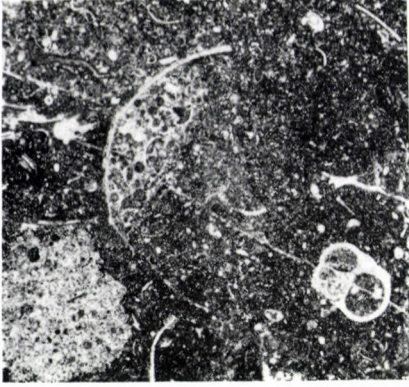


5



6

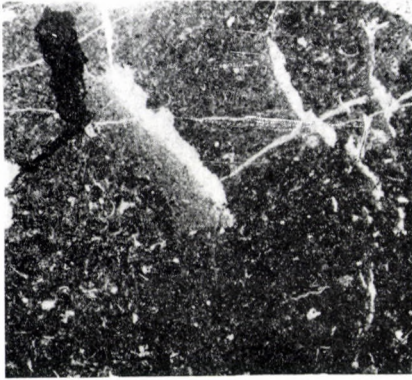
Plate 3



1



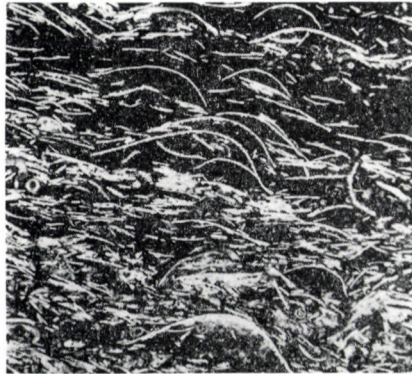
2



3



4

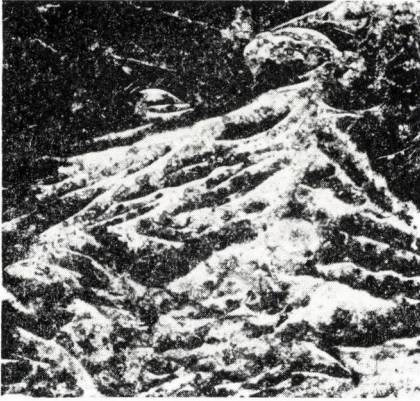


5

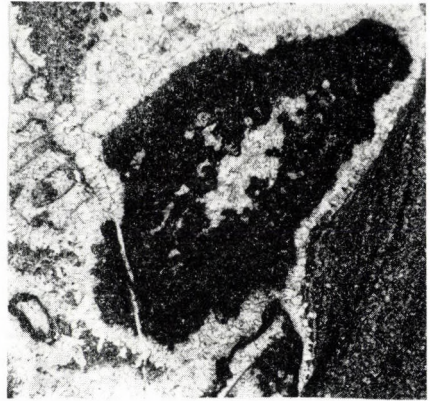


6

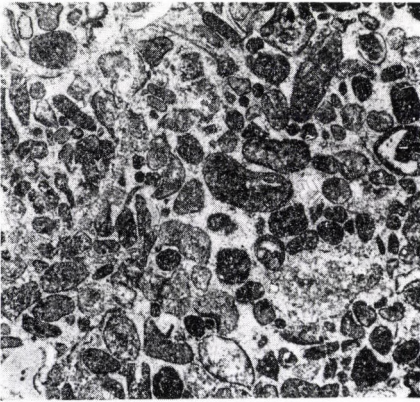
Plate 4



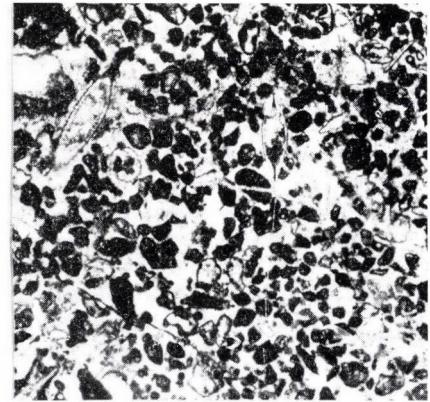
1



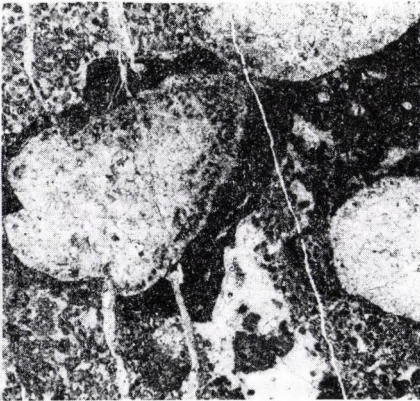
2



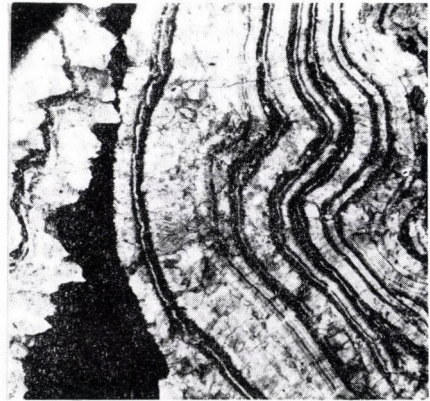
3



4



5

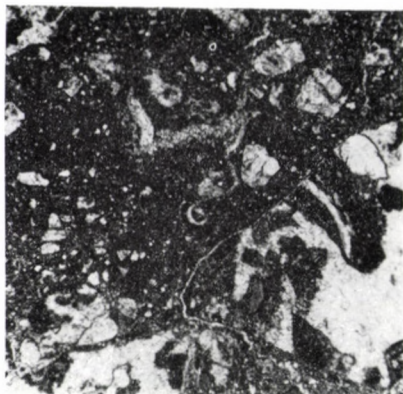


6

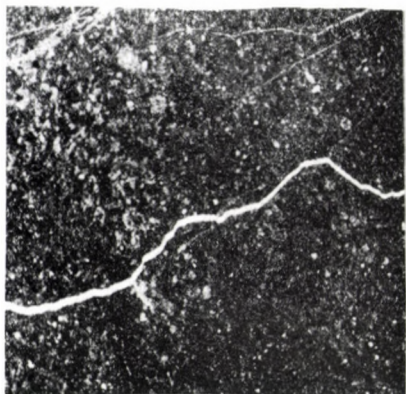
Plate 5



1



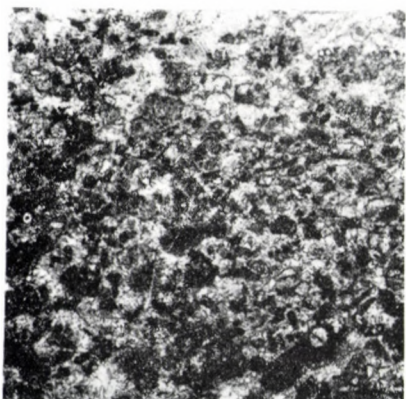
2



3



4

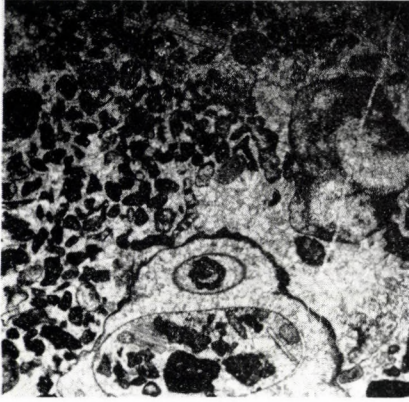


5



6

Plate 6



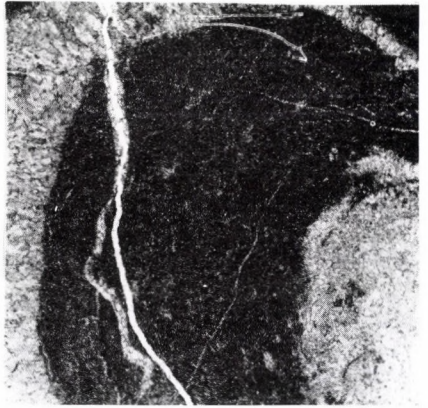
1



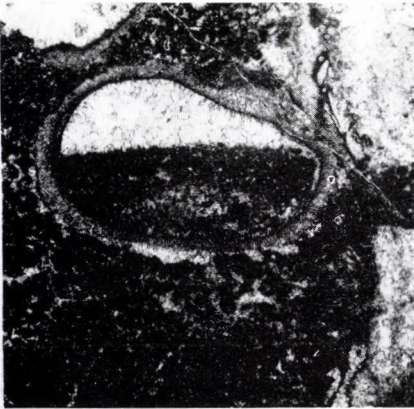
2



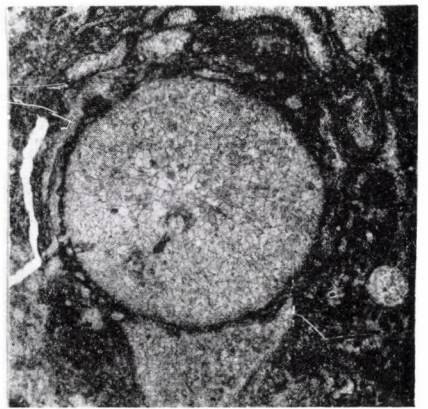
3



4

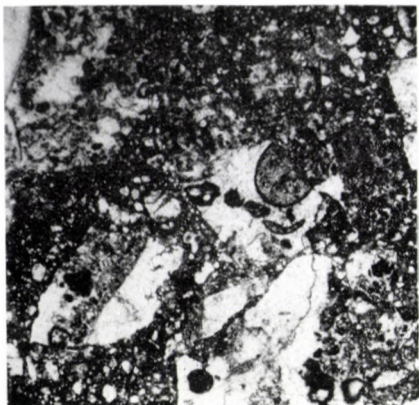


5



6

Plate 7



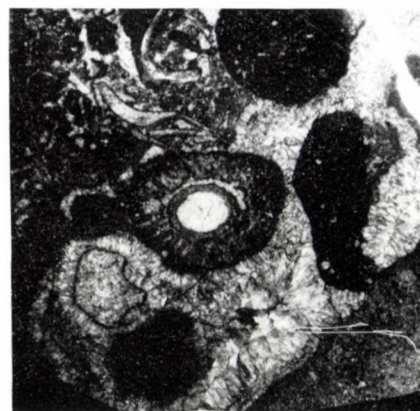
1



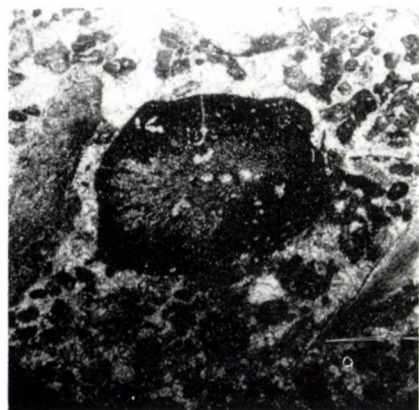
2



3



4

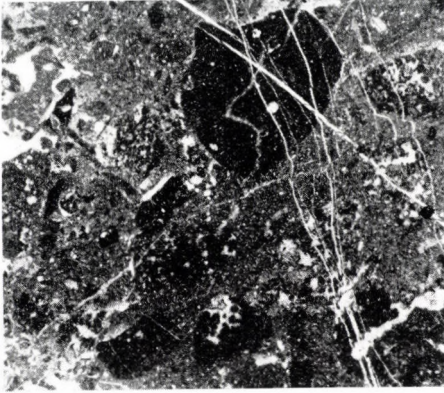


5

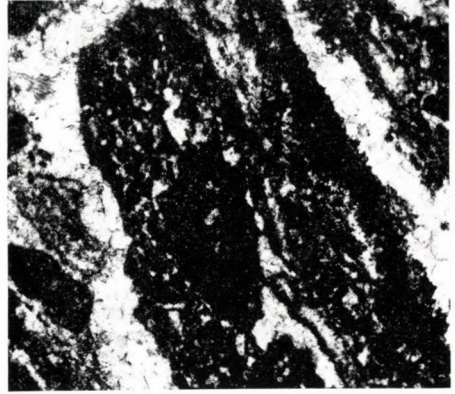


6

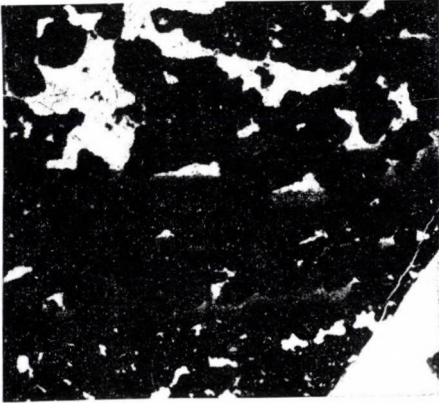
Plate 8



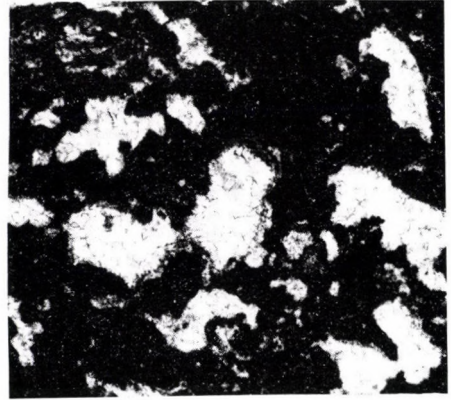
1



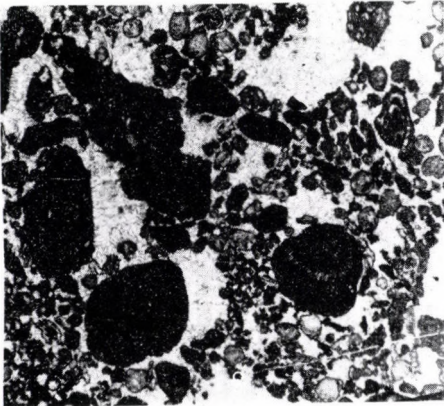
2



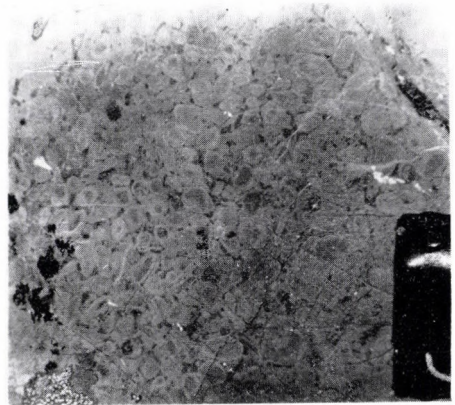
3



4

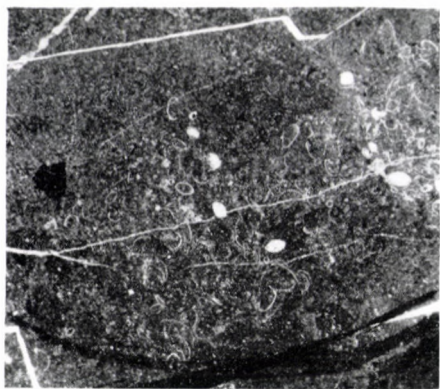


5



6

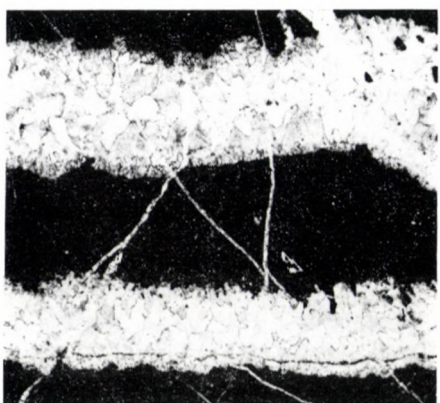
Plate 9



1



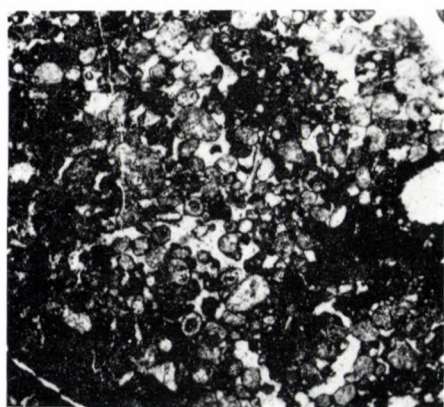
2



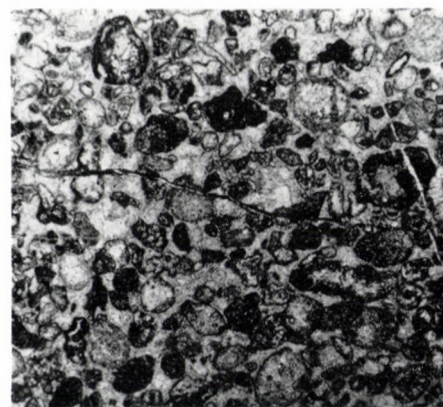
3



4



5



6

Plate 1

1. — *Bioturbate Formation*, lowermost horizons. Sandy WS rich in burrows, rather large, filled with microsparite, These are coated with a ferruginous and argillaceous film. Sample 1868. The side of the photograph is 6 mm.
2. — *Bioturbate Formation*. Sandy micrite with bioturbations. Sample 560. The side of the photograph is 6 mm.
3. — *Bioturbate Formation*. Oolite with rather well sorted recrystallized ooids with micritic coating. Sample 1785. The side of the photograph is 6 mm.
4. — *Bioturbate Formation*. Algal bioclastic GS with large dolomitized ooids and algae (mostly cyanophyceae). Sample 1867. The side of the photograph is 6 mm.
5. — *Bioturbate Formation*. Oolite with ooids partly micritized or coated with micritic film. Some algal detritus. Sample 1879. The side of the photograph is 6 mm.
6. — *Bioturbate Formation*. Bioclastic GS with micritized or recrystallized ooids, forams, fragments of filamentous algae etc. Sample 1775. The side of the photograph is 6 mm.

Plate 2

1. — *Ravni Formation, Dedovići Member*. Bioclastic GS with small ooids and profuse biotritus. The most part of grains show a micritic coating, and some grains are completely micritized. Sample 1420a. The side of the photograph is 5.5 mm.
2. — *Ravni Formation, Dedovići Member*. Bioclastic GS with partly micritized cement. Sparite domains contain profuse tiny detritus (cyanophyceans, green algae), and the micrite bears small fragments of crinoids, forams etc. Sample 1419. The side of the photograph is 5.5 mm.
3. — *Ravni Formation, Lučići Member*. GS composed of oncoids and bioclasts wrapped in a micritic film. Voids are filled with blocky calcite, and around some oncoids grows A-calcite. Sample 1263a. The side of the photograph is 5 mm.
4. — *Ravni Formation, Lučići Member*. GS with deformed oncoids and bioclasts coated by micrite. Sample 1234a. The side of the photograph is 6 mm.
5. — *Ravni Formation, Lučići Member*. Bioclastic GS with oncoids and various bioclasts and intraclasts, frequently coated with micritic film or completely micritized. Sample 522. The side of the photograph is 6 mm.
6. — *Ravni Formation, Utrina Member*. Biomicrite with profuse tiny pellets, fragments of crinoids, echinid spines, and other biotritus. Sample 1418b. The side of the photograph is 6 mm.

Plate 3

1. — *Bulog Formation*. WS—PS with ample pellets and tiny organic detritus (filaments, algae, ostracods, etc.). In the mollusc fragments concentrations of pellets and biotritus. Sample 1425. The side of the photograph is 5.5 mm.
2. — *Bulog Formation*. Nodular MS—WS with lumps of MS containing some tiny bioclasts, WS rich in filaments, and PS with bioclasts. Sample 1429. The side of the photograph is 5.5 mm.
3. — *Bulog Formation*. MS—WS with large geopetal fenestrae and profuse tiny organic detritus in the micritic groundmass. Sample 1428a. The side of the photograph is 5.5 mm.
4. — *Bulog Formation*. MS—WS with large filaments showing the “umbrella structure”, and tiny recrystallized biotritus. Sample 571. The side of the photograph is 5.5 mm.
5. — *Bulog Formation*. WS—PS, characteristic of the upper part of the unit. Concentrations of filaments, some of which show the “umbrella structure”. Sample 577. The side of the photograph is 6 mm.

6. — *Bulog Formation*. MS—PS with bioclasts and small filaments. One shell with geopetal structure is inverse in regard to the orientation of fenestrae (transported). Sample 1425a. The side of the photograph is 6 mm.

Plate 4

1. — *Wetterstein*. Lagoonal MS—WS with concentrations of large filaments. Sample 1827a. The side of the photograph is 5.5 mm.
2. — *Wetterstein*, interreef lagoon. Algal bioclastic GS with large dasycladacea and oncoids of algal origin, the external parts of which are transformed into densely packed algal pellets. In the corrosional cavities (only one part is visible in the photograph) cross-lamination in the reddish internal sediment. Sample V—40. The side of the photograph is 5.5 mm.
3. — *Wetterstein*. Bioclastic GS with biodetritus frequently showing thin micritic coatings. Cement is sparite. Sample 1108a. The side of the photograph is 6 mm.
4. — *Wetterstein*, back-reef sands. Bioclastic GS with large pellets, some small ooids, biodetritus (mostly algal) and micritized bioclasts. The side of the photograph is 5.5 mm.
5. — *Wetterstein*, reef flat. Bioclastic GS (FS—BS) composed of bioclastic detritus with large fragments of reef-forming organisms — monocorals, sponges etc. The sparitic groundmass bears profuse pellets of algal origin. Some larger bioclasts are coated with tubifites or blue-green algae. Sample 1058a. The side of the photograph is 5.5 mm.
6. — *Wetterstein*, reef flat. Corrosion cavity with several generations of A-cement, separated by dust films. Sample 5254. The side of the photograph is 5.5 mm.

Plate 5

1. — *Wetterstein*, reef facies, FS with largely recrystallized reef organisms, frequently coated with blue-green algae. Interspaces are filled with micrite, bearing tiny organic detritus (small filaments originating from filamentous algae, algal pellets). Sample 1276. The side of the photograph is 5.5 mm.
2. — *Wetterstein*, reef breccia, composed of angular fragments of reef rocks and fine-grained detritus. Sample 1272. The side of the photograph is 5.5 mm.
3. — *Grivska Formation*. WS—PS built up of densely packed pellets in a micritic to microsparitic mass. Sample 1828. The side the photograph is 6 mm.
4. — *Grivska Formation*. MS—WS with radiolarians tiny filaments and pellets, with domains of sparitic cement and intraclast. Sample 1831a. The side of the photograph is 6 mm.
5. — *Grivska Formation*. Fine-grained GS with pellets and profuse tiny rounded micritic intraclasts and micritized bioclasts. Sample 1831b. The side of the photograph is 6 mm.
6. — *Grivska Formation*, par of the type section. Mali Ostrėš, Grivska village.

Plate 6

1. — *Dachstein*, back-reef sands. Bioclastic GS with small micritized intraclasts, and bioclasts, and larger biodetritus (algae, etc.). Chambers of the gastropod are filled with the same biodetritus and sparry cement. The most part of fragments represents black-pebbles (not visible in the thin section). Sample 1934a. The side of the photograph is 6 mm.
2. — *Dachstein*, back-reef sands. Peletoide bioclastic GS; tiny detritus of pellets and biota, large mollusc fragments. Sample 63—K. The side of the photograph is 7 mm.
3. — *Dachstein*, reef flat. Bioclastic GS with biodetritus, pellets, algae with geopetal fabric. Grains are mostly surrounded by drusy calcite. Sample K—32. The side of the photograph is 7 mm.

4. — *Dachstein*, reef flat. Thick algal crust of the A-type around a recrystallized coral. Voids of the crust filled with calcite. Around the crust perpendicular drusy calcite. Sample K-21. Side of the photograph is 7 mm.
5. — *Dachstein*, reef body. BS with recrystallized reef organisms with geopetal fabric; voids are filled with densely packed algal pellets. Sample K-120. The side of the photograph is 7 mm.
6. — *Dachstein*, reef frame. Coral with completely recrystallized internal fabric and with coating of enveloping organisms. Sample K-114. The side of the photograph is 7 mm.

Plate 7

1. — *Dachstein*, reef slope. GS-RS with angular fragments transported from the reef; sample tiny detritus, poorly sorted. Sample K-13. The side of the photograph is 7 mm.
2. — *Dachstein* reef. Heterastridium. Road Sirogojno-Rožanstvo, Ilidža locality.
3. — *Dachstein*, reef frame. Coral colony. Road Sirogojno-Rožanstvo, Ilidža locality.
4. — *Ilidža Formation*. Bioclastic GS with pellets, plasticlasts and biodebitris (mostly fragments of molluscs, algae, etc.) as black pebbles. Almost every grain bears an aureole of incrusting calcite. Sample 1932. The side of the photograph is 6 mm.
5. — *Ilidža Formation*. Bioclastic GS with biodebitris mostly micritized or coated with blue-green algae. Bioclasts mostly represent black pebbles. Sample 1932b. The side of the photograph is 6 mm.
6. — *Ilidža Formation*. Interlayer of Lofer B-member. MS-WS with fenestrae and geopetal fabric. Sample 1936c. The side of the photograph is 6 mm.

Plate 8

1. — *Carnian Lofer*, member B. Loferite breccia composed of angular fragments and plasticlasts of micrite, pelmicrite and pelsparite. Cement is of microsparite with rare fenestrae. Sample 1016. The side of the photograph is 5.5 mm.
2. — *Carnian Lofer*, member B. Loferite with laminae of micrite, pellets and characteristic "sheet cracks"; one oncoid. Sample 1733. The side of the photograph is 6 mm.
3. — *Carnian Lofer*, member B. Fenestral peletal WS-PS with oncoids. Fenestrae are mostly parallel with bedding, showing geopetal fabric. Sample 1669. The side of the photograph is 6 mm.
4. — *Carnian Lofer*, member B. Fenestral PS-GS with pellets, oncoids and numerous fenestrae. A — cement of fenestrae is composed of dolomite and B — cements of calcite. Sample 1593b. The side of the photograph is 6 mm.
5. — *Carnian Lofer*, member C. GS with pellets, and bioclasts. Pellets are of various size, mostly grouped in lenses. Large oncoids, in places micritized, with cores mostly of algal clasts. Large algae are coated with a micrite film. Voids are filled with mosaic calcite, with profuse biodebitris. Sample 1010. The side of the photograph is 5.5 mm.
6. — *Carnian Lofer*, member C. Concentrations of oncoids. Point TU 489. Sušica river.

Plate 9

1. — *Norian Lofer*, member B. MS-WS with tiny ostracods. Sample 1167. The side of the photograph is 5.5 mm.
2. — *Norian Lofer*, member B. Algal stromatolites with geopetal fabric. Sample 1151c. The side of the photograph is 5.5 mm.
3. — *Norian Lofer*, member B. Micrite ortochem. Sheet cracks filled with A and B cement (Fisher's "Zerra Limestone"). Sample 1670. The side of the photograph is 6 mm.
4. — *Norian Lofer*, member B. Loferite breccia. Sušica river.

5. — *Norian Lofen*, member C. Rounded grains filled with calcite, most probably corresponding to algae, forams, infrequent ostracods and micritized bioclasts, some pellets and micritized ooids. Groundmass is of fine-grained sparite. Sample 1667. The side of the photograph is 6 mm.
6. — *Norian Lofen*, member C. Bioclastic GS. Sample 1093b. The side of the photograph is 5.5 mm.

Middle Miocene mangrove vegetation in Hungary

Esther Nagy

Hungarian Geological Institute, Budapest

József Kókay

Hungarian Geological Institute, Budapest

This palynological study confirmed the presence of mangrove vegetation in the Hungarian Middle Miocene. In the Miocene layers of the Paratethyan realm till now was not known this vegetation type. The geological study of the territory and the collecting of the material was made by J. Kókay and the palynological study was made by Esther Nagy.

Keywords: Middle Miocene, mangrove vegetation, Central Paratethyan

Geological results

The Miocene layers of the Herend Basin were part of the Bakony Mountains in Middle Hungary. The area was long time known in the geological literature. The geological, paleontological character of this basin has been described previously by Kókay (1966).

The Herend Basin in the Early Badenian was a long bay extending westwardly from the Bakony Mountains (Kókay 1966). The maximum thickness of the sequence in Herend Basin is approximately 200 m. The lowest sediment was described as brown coal from early studies on boreholes. Successively higher strata include brackish-water deposits, marine clays, clay marl layers, and sandy limestones. Numerous taxa of molluscs, corals have been described from these materials (Kókay 1966, Hegedüs 1970) from the eastern and south eastern regions of the basin. Hegedüs (1970) described the original coral fauna from the southern part of the basin. The coral-reefs were present in a warm environment and included the mangrove as shown from pollen grains composition of the sediments. The geological analysis showed a southernly inclination of the basin area and thickening of the sedimentary series (Kókay 1966). The shoreline toward the north, described as a low plain, may have been the site of mangrove vegetation.

Palynological results

The palynological and paleontological description of the Herend Basin (Kókay 1966, Hegedüs 1970) has given the supposition of mangrove and has been verified from palynological studies.

The presence of mangrove has reported from the Hungarian Eocene by L. Rákosi (1979).

Addresses: Esther Nagy, József Kókay
H-1143 Budapest, Népstadion út 14. Hungary
Received: January 5, 1991

Mangrove also was found from Miocene in Catalonia (Spain), Languedoc and Provence (France) by Bessedik (1981, 1985). His material was gathered in Catalonia from the Late Burdigalian till the Langhian (NN₄–NN₅), respectively from the Middle Tortonian (NN₁₀–NN₁₁), in the territory of Languedoc from the Aquitanian–Burdigalian–Langhian–Serravallian and Tortonian, in Provence, respectively in Rhone valley from Aquitanian – till the Messinian. Mangrove was mostly from the Aquitanian till the Early Serravallian together with a warm, dry climate associated with formations of coral-reefs and gypsum. In the upper part of the Serravallian mangrove vegetation was absent (Bessedik, 1985, p. 84).

The mangrove – a tropical "salt forest" – is distributed in both hemisphere and includes both subtropical and temperate climates (Chapman 1976). Mangrove distribution is limited in the northern hemisphere at latitude 24–32° and in the southern hemisphere at latitude 37° in Australia and New-Zealand. The distribution is associated with the direction of the ocean drifts currents (Chapman's map, 1976, p.18).

In Bessedik work (1981, p. 29) – after reference of Elhai (1968) – the mangrove occurs on the Chatam-island on the south latitude 44°.

The genus *Avicennia* can be found in all mangrove vegetation (Chapman 1976, p. 20–21, Tissot, 1980, p. 121). There are some areas where the species of *Avicennia* are represent the single woody plants of the mangrove (Bessedik, 1985, p. 109). In some region alone *Avicennia* are forming the mangrove (Bessedik, 1981, p. 290). The fossil mangrove is represented by the presence of *Avicennia* pollen grains (Bessedik, 1981).

Relatively few fossil *Avicennia* pollen grains are reported in studies of Hungarian deposits and the same were written by Bessedik (1981), Vishnu-Mittre and Guzder (1975). In the same work Vishnu-Mittre and Guzder (l.c.) also reported on the lack of the *Rhizopora* genus in recent and nearrecent mangrove by Bombay.

In our palynological study of the Hungarian Middle Miocene we studied the following samples :

Herend 13 (He-13)	61.4 – 64.4 m	Herend 47 (He-47)	80.8 – 81.8 m
	75.6 – 76.2 m		87.0 – 87.3 m
	103.6 – 106.6 m	Bánd 2	72.0 m
	119.1 – 126.3 m	Bánd 4	12.0 – 14.6 m
	130.4 – 134.6 m		18.0 – 20.4 m
	137.6 – 140.4 m		23.2 – 24.9 m
	142.2 – 143.0 m		48.4 – 50.4 m
	143.3 – 144.4 m		62.7 – 68.1 m
	161.1 – 165.5 m		65.8 – 67.2 m
Herend 38 (He-38)	25.2 – 26.5 m		67.2 – 68.1 m
	53.4 – 55.0 m	Márkó 2	27.4–30.0 m
Herend 46 (He-46)	78.0 – 79.0 m		40.6 m

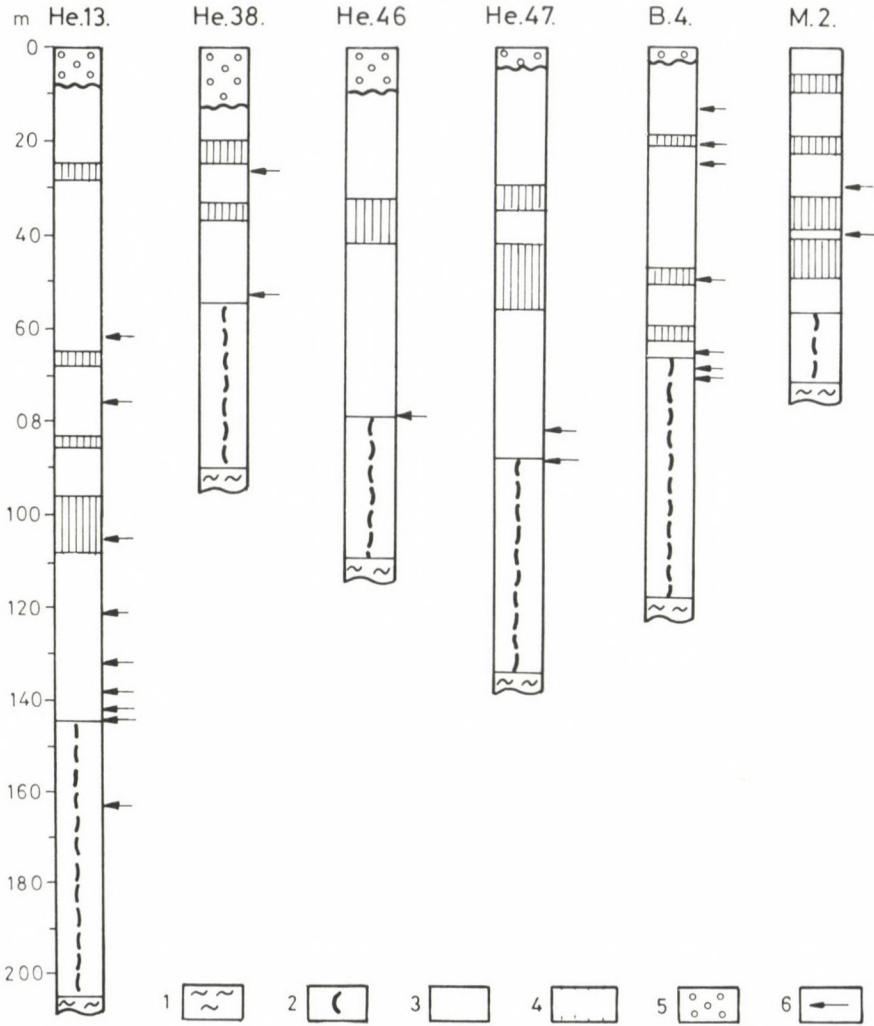


Table 1. The sequences of the Early Badenian in Herend Basin 1. multicolored clay, 2. brown coal, 3. corbula clay, 4. brachyhalin clay marl, 5. Quaternary (clay with gravel, 100ss), 6. the examined samples

The samples except two – are very rich in palynomorphs. The data from the samples were presented in ecological diagrams in absolute numbers. They showed the following biotops from the seaside: the marine plankton, the mangrove vegetation, the freshwater plants, the swamp-forest, the riparian forest, the mixeddeciduous forest and the hillside forest.

The evaluation

The nine samples from borehole Herend 13 were very rich in palynomorphs. No plankton were detected in the brown coal layer (161.1–165.1 m). The embedding place of the material was in the shallow freshwater swamp, the other vegetation types were also present. In the riverside forest included some tree and a rich fern assemblage. In the drier places were joined the not very dense mixed deciduous forest and farther the hillside forest with conifers.

The microforams were a sign of transgression in samples from 142.2–144.4 m. The swamp and the fernery disappeared. The mangrove was presented by *Rhizophoraceae* pollen grains. The spectra of the mixed deciduous forest was rich, with tropical, subtropical and temperate elements. The hillside forest also was widespread. In the sample from 137.6–140.4 m the microforams were few, while *Botryococcus braunii* became high in number, *Cymatiosphaera* salinwater and *Spirogyra* freshwater algae refer to a brachihaline environment. Mangrove pollen also was present in this and in the next sample (130.4–134.6 m). We found only 1 – 2 pollen grains of *Rhizophoraceae* and *Avicennia* together microforams with *Botryococcus* in the samples 61.4–126.5 m from the upper part of the sequence (Corbula clay). In these clay-marl samples also were embedded the pollen grains of riparian, mixed deciduous and hillside forest.

The sporomorph of two samples from the borehole Herend 38 provided an interesting comparison. The lower sample 53.4–55.0 m contained many microforams, *Pleurozonaria concinna*, *Hystrichosphaeride* and few *Botryococcus*, whereas the sample from 25.2–26.5m contained only *Botryococcus braunii*.

The lower sample represented a mangrove, and a salty marsh. The upper sample was from a freshwater swamp-forest and contained the pollenspectra of the other forest types, too.

The sample from 78.0–79.0 m borehole Herend 46 contained many microforams and some *Botryococcus braunii* alga colonies. They relate to seaside environment. Some *Avicennia* and *Rhizophoraceae* pollen grains indicate the presence of mangrove. A salty marsh can be supposed from the assemblages of *Chenopodiaceae*, *Salicornia*, *Artemisia*, *Polygonum persicaria* pollen grains. Pollen from riparian, mixed deciduous and hillside forest along with many subtropical and temperate elements also were present.

Two samples were examined from borehole Herend 47. Sample 87.0–87.3 m contains microforams, hystrichosphers, some *Botryococcus specimens* indicate brackish water. *Rhizophoraceae* mangrove pollen grains also were present. Near the shoreline was a salty marsh containing *Artemisia*, *Chenopodiaceae* and *Graminea* pollen grains.

Freshwater also was present in the area as indicated from pollen of *Stratiotes*, *Utricularia* and a riparian forest containing *Carya*, *Salix*, *Betula*, *Liquidambar*. Subtropical, tropical ferns also were present. Farther from the shoreline in a drier place was a deciduous forest with chiefly subtropical elements, and a hillside forest very rich in subtropical and temperate elements.

The other component of the sample 80.8–82.3 m contained some forams and *Botryococcus*, *Rhizophoraceae* of the mangrove, some elements of salty marsh, farther freshwater *Taxodium* swamp-forest and riparian forest. The mixed deciduous forest with many *Sapotaceae* pollen grains, and hillside forest were present with pollen grains, too.

One sample from (72.5 m) the borehole Bánd 2 was examined. It was very rich in palynomorphs. The *Botryococcus braunii* was dominant. The riverside forest was rich in species and specimens. The mixed deciduous forest was rich in tropical (palms, *Sapotaceae*, *Pentapollenites*), subtropical (*Symplocos*, *Momipites*) and temperate (*Platycarya*, *Zelkova*, *Elaeagnus*, *Celtis* etc.) species. Tropical species were found (*Cycas*, *Dacrydium*), but the subtropical elements were dominant among the temperate taxa in the hillside forest.

Seven samples were examined from the borehole Bánd 4 (12.0–67.2 m). Microforams and *Botryococcus* were present. Pollen grains of *Avicennia*, and *Rhizophoraceae* were in the lower samples as well. They were only in the samples of 18.0–20.7 m, and 23.2–24.9 m indicated a swamp-forest. The more developed forest type was the riparian forest with many *Carya* and several fern species. In the mixed deciduous forest were tropical elements (*Sapotaceae*, *Buxus*, palms), and subtropical and temperate elements (*Ostrya*, *Carpinus* etc.). In the hillside forest were many subtropical (*Podocarpus*, *Keteleeria*) and some tropical species (*Dacrydium*, *Cycas*), but mostly temperate elements.

The two samples of the borehole Márko 2 are very rich in sporomorphs. In the lower sample (40.6 m) there were *Botryococcus* and *Spirogyra* freshwater algae and pollen grains related to a swamp forest. There were some pollen grains of freshwater (*Utricularia*). The riparian forest was also not very rich in remnants. After the sporomorph were many species in the mixed deciduous forest, and also in the middle mountain hillside forest.

The upper layer (27.4–30.4 m) contained very few algal colonies of *Botryococcus*, but the remnants of seawater plankton (microforams, *Cymatiosphaera*) also were present. *Avicennia* pollen grains indicated a mangrove environment. The other forest types indicated a subtropical environment.

The spectral remains from the boreholes show a connection between the presence of the marine plankton organism and the pollen grains of the mangrove. There is also a connection between the freshwater plants and the *Taxodium* swamp-forest (see Table 2 a., b.).

Summarising the results the paleoenvironment was a flat shoreline of the sea in some places with mangrove vegetation, more distant from the shoreline different forest type with very rich vegetation and warm, subtropical climate. The picture be suitable for the statement, that in the whole Neogene was the richest

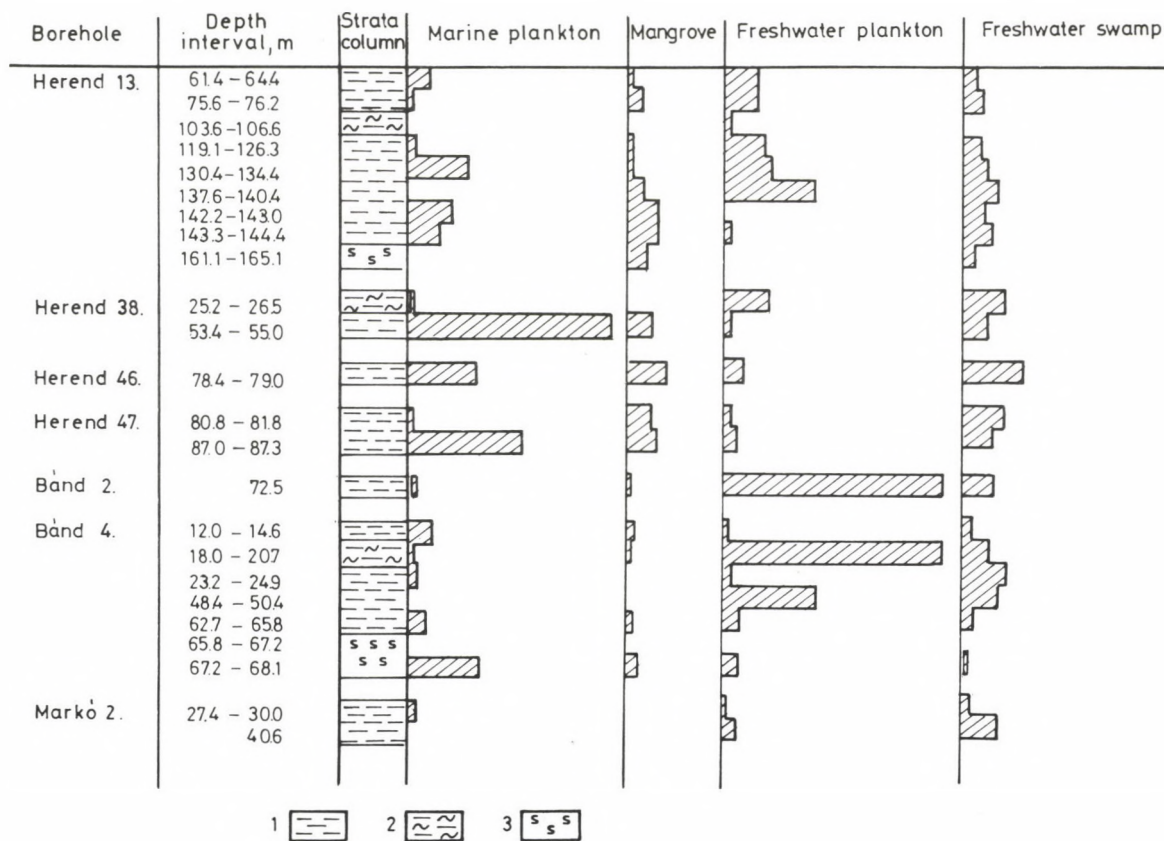


Table 2/a. The ecological distribution of the palynomorphs
 1. clay, 2. clay marl, 3. brown coal, 0.5 cm = 10 pieces

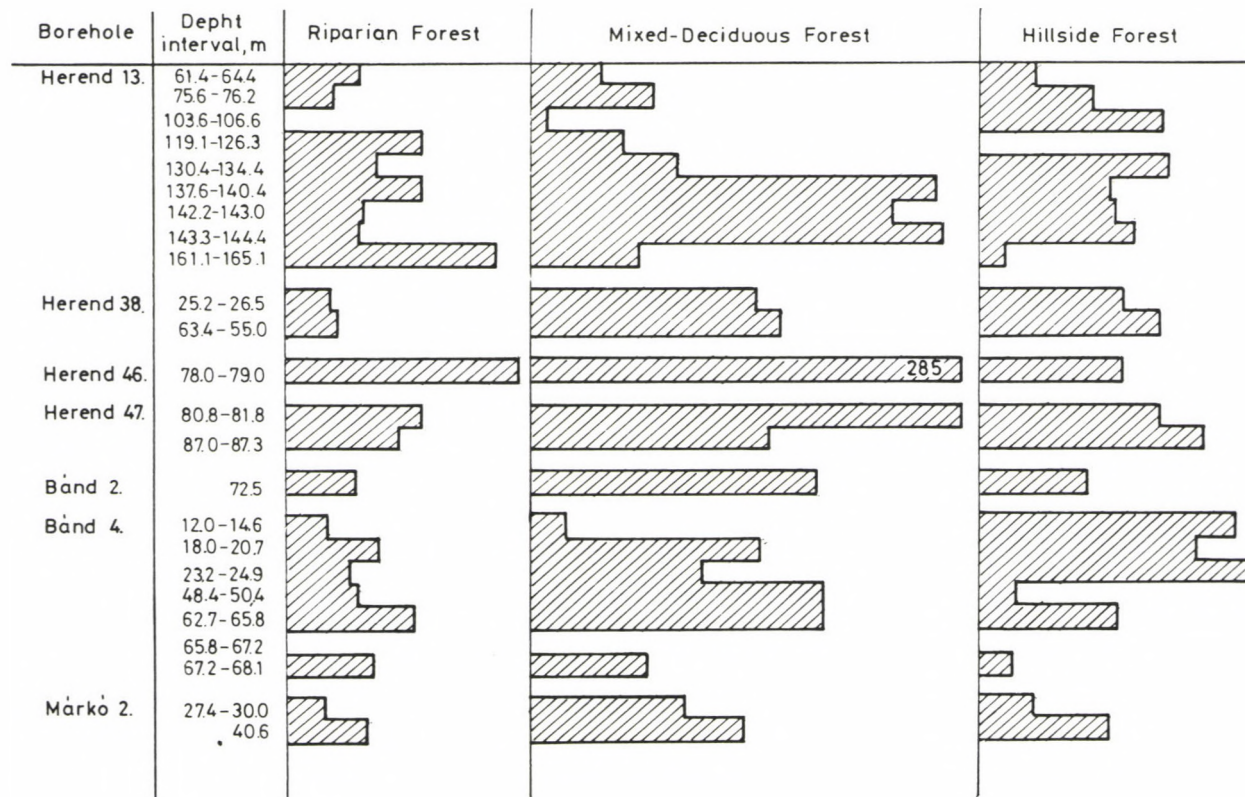


Table 2/ b. The ecological distribution of the palynomorphs
 1. clay, 2. clay marl, 3. browncoal, 0.5 cm=10 pieces

vegetation in the Early Badenian (see Plates I–V) in our research field in the Central Paratethyan realm.

References

- Bessedik, M. 1981: Recherches palynologiques sur quelques sites du Burdigalien du midi de la France. – Acad. Montpellier, Univ. Sci. Tech. du Languedoc. These 1–43, VI–VIII.
- Bessedik, M. 1985: Reconstitution des environnements miocène des régions Nord–Ouest méditerranéennes à partir de la palynologie. – Acad. Montpellier, Univ. Sci. Tech. Languedoc. These 1–162.
- Bessedik, M., L. Cabrera 1985: Le couple récif–mangrove à Sant Pau d’Ordal (Vallés – Pénédès, Espagne), témoin du maximum transgressif en Méditerranée nord occidentale (Burdigalien supérieur – Langhien inférieur). – *Newsl. Stratigr.*, 14 /1/, 20–35, Berlin–Stuttgart.
- Chapman, V.J. 1976: Mangrove vegetation. 1–447. – Cramer, Vaduz.
- Hegedüs, Gy. 1970: Tortonai korallok Herendről (Coralliaires tortoniens de Herend). – *Bull. of the Hungarian Geol. Soc.*, 100, 2, 185–191, Budapest.
- Kókay, J. 1966: A Herend–Márkói barnakőszéntérület földtani és őslénytani vizsgálata (Geologische und Paläontologische Untersuchung des Braunkohlengebietes von Herend–Márkó /Bakony–Gebirge Ungarn/). – *Geol. Hung. Ser. Palaeont.*, 36, 1–149, I–XV, Budapest.
- Rákosi, L. 1979: A magyarországi eocén mangrove palynologiai adatai (Données palynologiques de la mangrove Eocene de Hongrie). – *MÁFI Évi Jel.* 1976. évről 357–374, Budapest.
- Tissot, C. 1980: Palynologie et évolution récente de deux mangroves du Tamil Nadu /Inde/, – in "Mangroves d’Afrique et l’Asie". C.E.G.E.T. 109–214, fig. 29, 17. pl., Bordeaux.
- Vishnu-Mittre et Statira Guzder 1975: Stratigraphy and palynology of the mangrove swamps of Bombay. – *The Palaeobotanist.*, Vol. 22, No. 2, 111–117, Lucknow.

Plate I

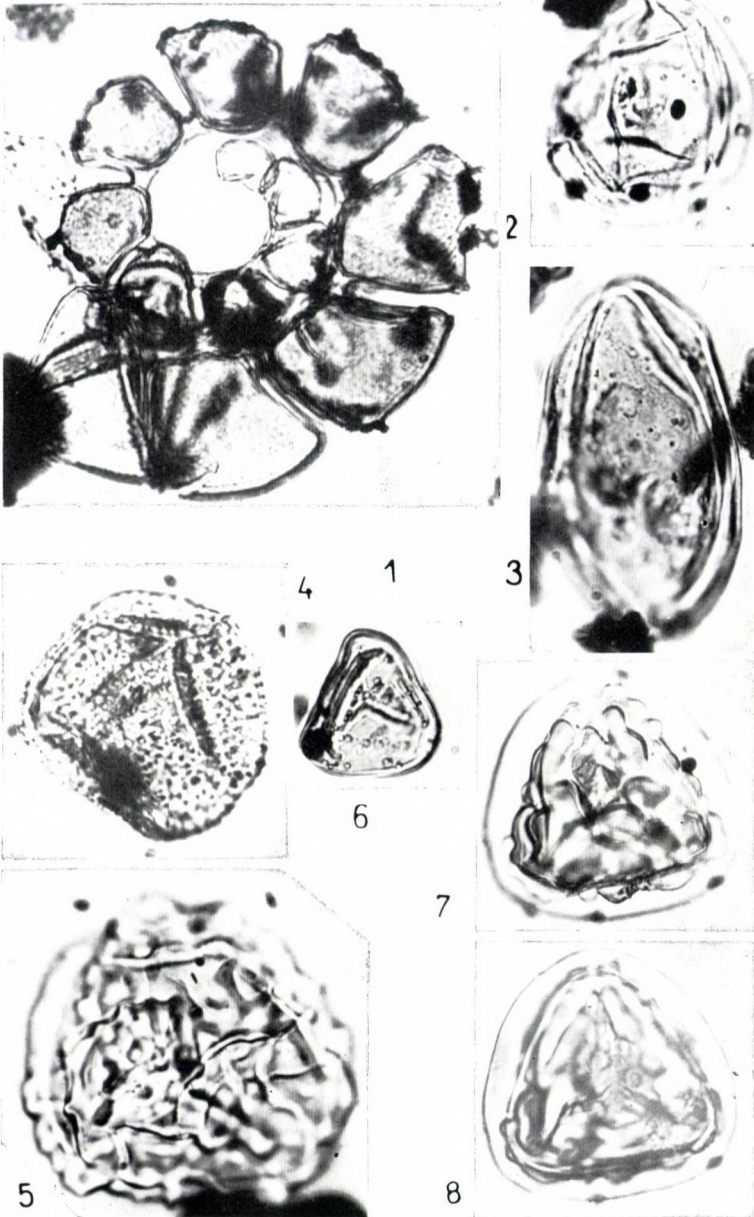
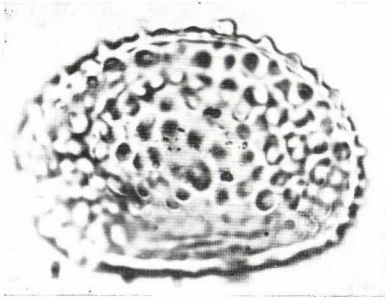
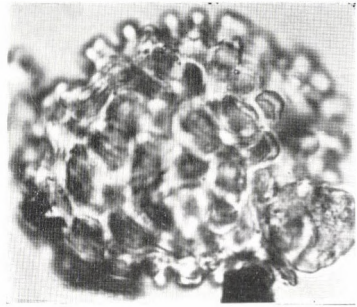


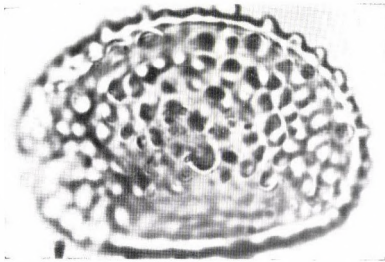
Plate II



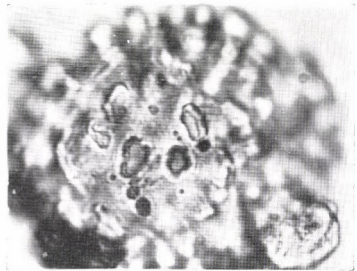
1



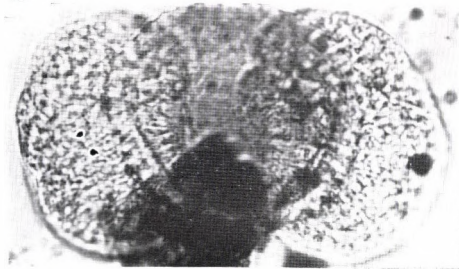
3



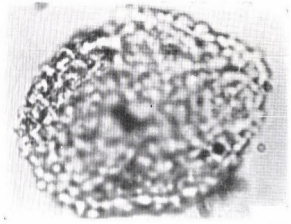
2



4



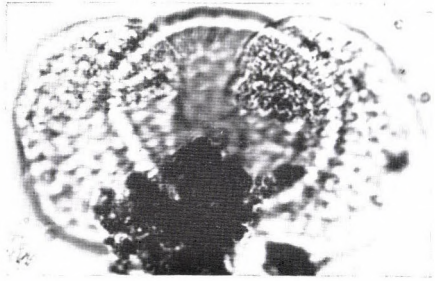
5



7



8



6

Plate III

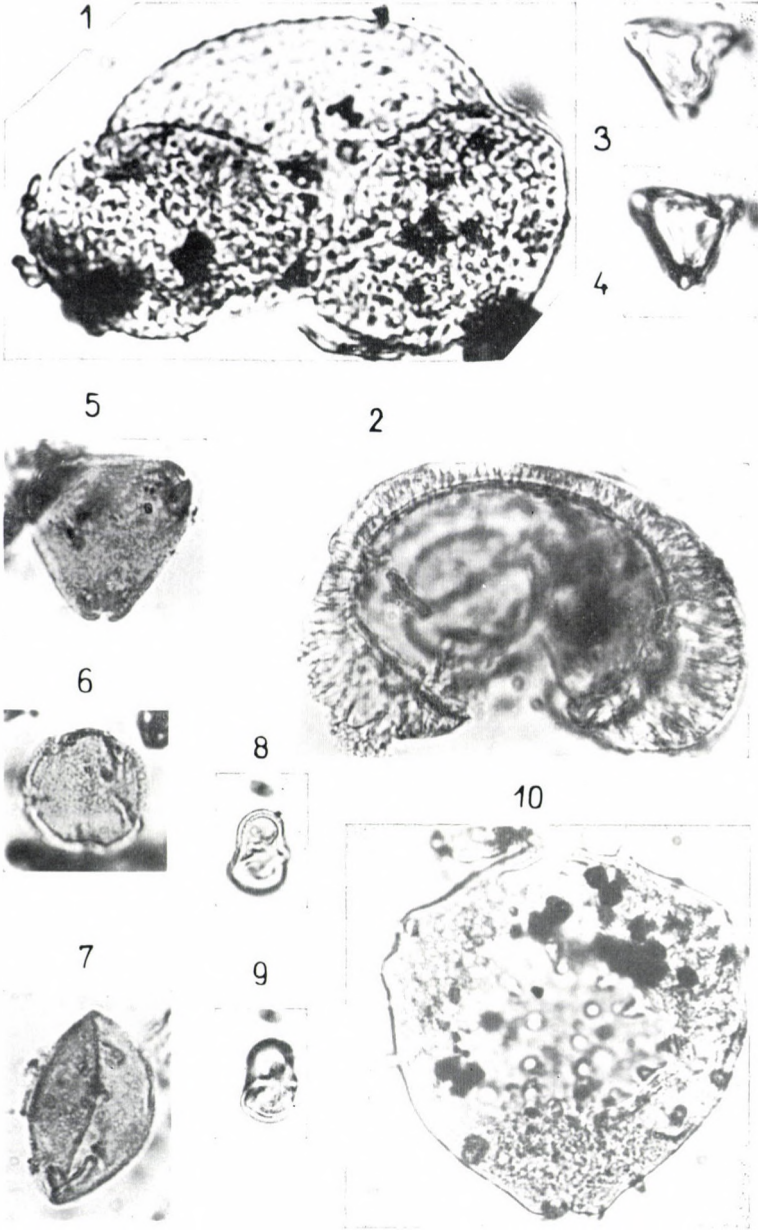


Plate IV



1



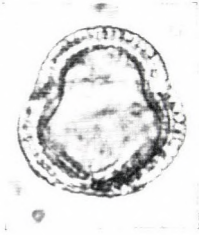
2



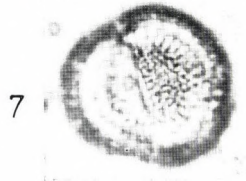
3



4



6



7



5



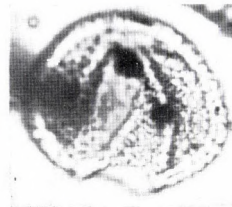
12



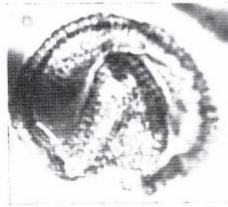
8



9



10



13



11



14



15

Plate V

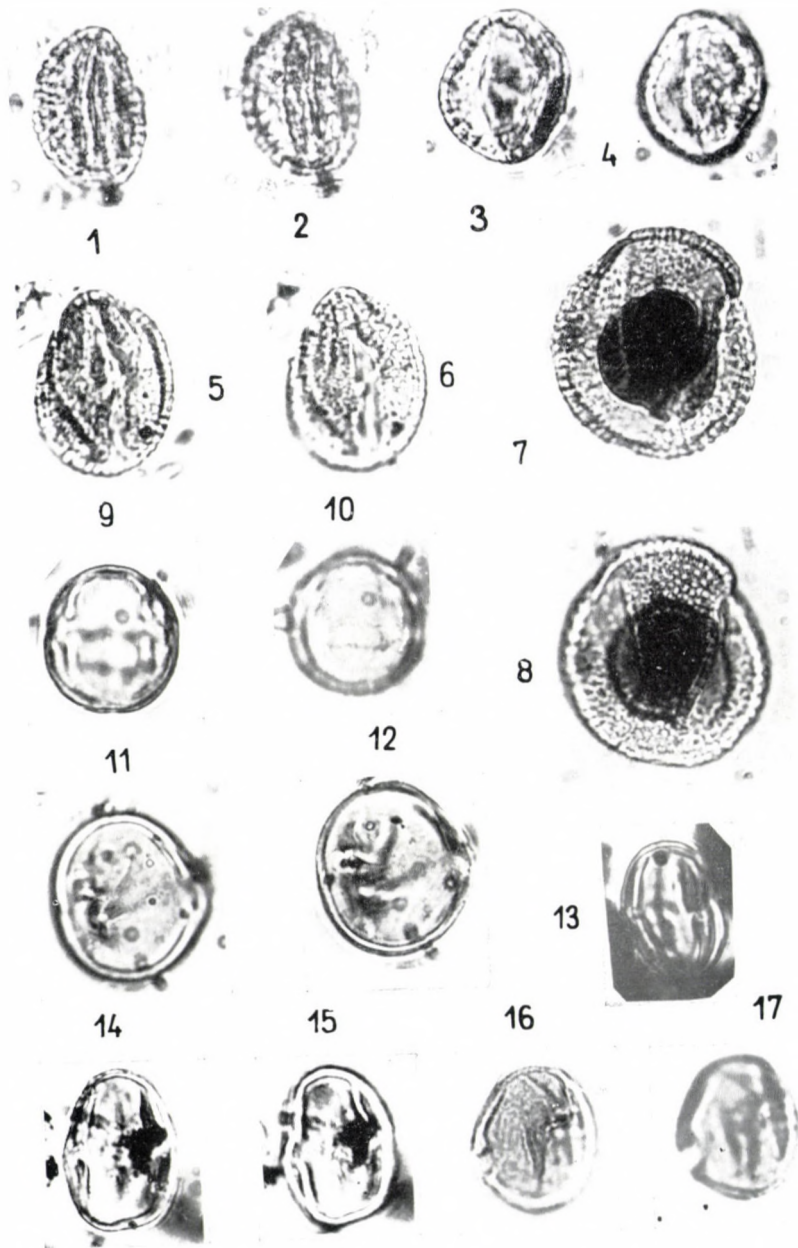


Plate I

1. Mikroforaminifera Herend 47, 87.0–87.3 m 500×
 2. *Hidasia* sp. Bánd 4, 62.7–64.8 m
 3. *Spirogyra* sp. Herend 46, 78.0–79.0 m
 4. *Osmundacidites primarius* (Wolff 1934) Nagy 1985 ssp. *primarius*, Bánd 4, 62.7–64.8 m
 5. *Bifacialisporites nogradensis* Nagy 1985, Herend 13, 61.4–64.4 m
 6. *Leiotriletes microlepidoidites* W. Kr. 1962, Herend 46, 78.0–79.0 m
 - 7–8. *Polypodiaceae* sporites *mecsekensis* Nagy 1985, Márkó 2, 40.6 m
- The photos are magnified by 1000×, only scales differing from this are indicated.

Plate II

- 1–2. *Polypodiisporites potonieí* Nagy 1969 Herend 13, 61.4–64.4 m
- 3–4. *Polypodiisporites histiopteroides* (W. Kr. 1962) Nagy 1973 ssp. *histiopteroides* Herend 47, 87.0–87.3 m
- 5–6. *Podocarpidites macrophylliformis* Nagy 1969 Bánd 2, 72.5 m
7. *Sciadopityspollenites serratus* (R. Pot. et Ven 1934) Raatz 1937 Herend 47, 87.0–87.3 m
8. *Ephedripites* sg. *Ephedripites landenensis* W. Kr. 1977 Herend 13, 75.6–76.2 m

Plate III

1. *Pinuspollenites latisaccatus* (Trev. 1967) Nagy 1985 ssp. *medius* Trev. 1967, Herend 38, 53.4–55.0 m
2. *Cedripites balansaeformis* (Nagy 1969) Nagy 1985, Bánd 2, 72.5 m
- 3–4. *Pentapollenites pentangulus* (Pf. 1953) W. Kr. 1958, ssp. *pentangulus*, Bánd 4, 48.4–50.4 m
5. *Porocolpopollenites hidasensis* Nagy 1963, Bánd 2, 72.5 m
6. *Rutacearumpollenites komloensis* Nagy 1969, Herend 47, 80.0–82.3 m
7. *Sabalpollenites areolatus* (R. Pot. 1934) n. c. (*Basionym Monocolpopollenites areolatus* R. Pot. n. c. in Thomson-Pflug 1953, p. 63), Bánd 2, 72.5 m
- 8–9. *Umbelliferoipollenites tenuis* Nagy 1985, Herend 46, 78.0–79.0 m
10. *Diervillapollenites megaspinus* Dokt.-Hreb. 1957, Bánd 4, 48.4–50.4 m

Plate IV

- 1–3. *Avicennia intermedia* Griff.
- 4–5. *Avicennia* sp.; Bánd 4, 67.2–68.1 m
- 6–7. *Avicennia intermedia* Griff.
- 8–9. *Avicennia* sp.; Herend 47, 80.0–82.3 m
- 10–11. *Avicennia* sp.; Herend 47, 80.0–82.3 m
- 12–13. *Avicennia intermedia* Griff.
- 14–15. *Avicennia* sp.; Bánd 4, 67.2–68.1 m

Plate V

- 1–2. *Avicennia marina* (Forsk.) Vierh.
- 3–4. *Avicennia marina* (Forsk.) Vierh.
- 5–6. *Avicennia* sp., Herend 13, 75.6–76.2 m
- 7–8. *Avicennia* sp., Herend 47, 80.0–82.3 m
- 9–10. *Kandelia candel* (L.) Druce, *Rhizophoraceae*
- 11–12. *Rhizophoraceae* sp., Bánd H, 62.2–68.1 m
13. *Rhizophoraceae* sp., Herend 13, 61.4–64.4 m
- 14–15. *Rhizophoraceae* sp., Herend 13, 143.9–144.4 m
- 16–17. *Rhizophoraceae* sp., Herend 47, 87.0–87.3 m

Lithostratigraphical and sedimentological framework of the Pannonian (s. l.) sedimentary sequence in the Hungarian Plain (Alföld), Eastern Hungary

Györgyi Juhász

Hungarian Hydrocarbon Institute, Százhalombatta

Depositional sequences of the Pannonian (s. l.) in the Hungarian Plain were accumulated in an extensional basin forming an individual sedimentary cycle.

Sedimentation began with the deposition of shallow water basinal marls and coastal sandy conglomerates around preexisting islands. As a consequence of increased subsidence, turbidites accumulated in the deepest zones. The upper part of these turbidites were probably connected to high constructional fluvial dominated delta systems, the main ones prograding from the NW and NE directions towards the basin.

This resulted the accumulation of the vertical assemblages of the characteristic lithofacies above one another: prodelta, delta slope, delta front, delta plain units. The deposits of the two main delta systems form complicated intertonguing in space and time in some areas of the basin.

The principal regularities of sedimentation were obtained in the southeastern part of the basin. Now regional correlation and interpretation were carried out in all the area of the basin. On the basis of paleogeographic reconstruction a lot of problems could be solved and mapping of the different lithofacies units became possible. The structural and isopach maps are based on the data of about 900 wells.

Keywords: Pannonian (s. l.), sedimentology, basin analysis, lithostratigraphy, turbidites, deltaic environment, mapping

1. Introduction

The Hungarian Plain (Alföld) lies in the central part of the Carpathian Basin, in SE Hungary. Its area is about 40.000 km², having the largest areal extension among the subbasins. It is surrounded by the North Hungarian Range on the north, the river Danube on the west and it passes the Hungarian borders towards the south and east. Our investigations are focused on the Hungarian part of it (Fig. 1).

The aim of this paper is to give an overview about the sedimentological and lithostratigraphical framework of the Hungarian Plain, and to present the structural and isopach maps of the different lithofacial units, drawn up by the data of about more than 900 wells.

2. Paleogeographical framework

The basement was formed by the Nealpine evolutionary stage during Miocene and Pliocene times, when extension occurred, characterized by normal faults and

Address: Györgyi Juhász: 1063 Budapest, Munkácsy M. u.12

Received: January 27, 1991



Fig. 1. Location and structural map of the Pannonian (s. l.) basement (after A. Jámor et al., MÁFI, 1986)

stike-slip faults (Horváth, 1984). In the northern part of the basin, however, sedimentation seems to be uninterrupted since the Oligocene. In the meantime a differential subsidence occurred. The Neogene depression is filled with a thick sedimentary sequence which thickness is highly variable. On the margins it is a few hundred meter thick, in the deepest troughs, however, it can reach 7–8000 m totally. The contour map of the Pannonian (s. l.) basement illustrates the present geometry of the basin as well as the main depocenters. They are the Makó–Hódmezővásárhely trough (1), the Békés-subbasin (2), the Derecske trough (3), and Jászság subbasin (4), (Fig. 1).

After a rapid transgression, brackish water and marine sedimentation occurred. By the end of the Badenian marine connections had been lost, and the salinity of the inland sea reduced gradually. After a short regression and shallowing at the end of the Sarmatian, the last sedimentary cycle began about twelve million years ago. Deposition took place from the end of Sarmatian to Quaternary times. Since the Sarmatian sedimentation was not continuous, in some places erosion occurred, and Badenian sediments or pre-Neogene formations underlie the Pannonian (s. l.) succession.

3. Previous investigations

Hydrocarbon exploration provided a lot of information for developing depositional models in the last twenty–thirty years.

The first conclusions on the geological setting of the basin were made by Körössy (1971). Concerning the lithostratigraphic aspects of the well-known areas, Gajdos et al. (1983) summarized the preliminary results. The model itself was applied in two dimensional scale. The sediments of the marginal areas were investigated by Á. Jámbo

The principal sedimentological regularities were drawn up by I. Bérczi, I. Bérczi – R.L. Phillips, I. Révész, R. Mattick et al., Á. Szalay–K. Szentgyörgyi, C.M. Molenaar and others in the last few years, based on sedimentological and seismic stratigraphic investigations in the southeastern part of the basin.

In these days investigations of the other areas of the basin and correlation is being made. The broader perspectives and new aspects of interpretation gave a new impulse for further investigations. On the basis of paleogeographic reconstruction a lot of problems could be solved, and finally mapping of the different lithofacies units became possible.

4. Geological setting up of the Pannonian (s. l.) sequence–lithostratigraphical framework

A rapid subsidence began at the beginning of the Pannonian (s. l.) and a morphologically strongly subdivided basin was formed gradually with a series of crests and subbasins (pull-apart basins). At the first period only the area of the deepest zones was inundated by the sea. The marginal areas and the basement highs became flooded gradually much later. In the marginal zones sedimentation took place in a wave-dominated coastal environment. In the nearshore area,

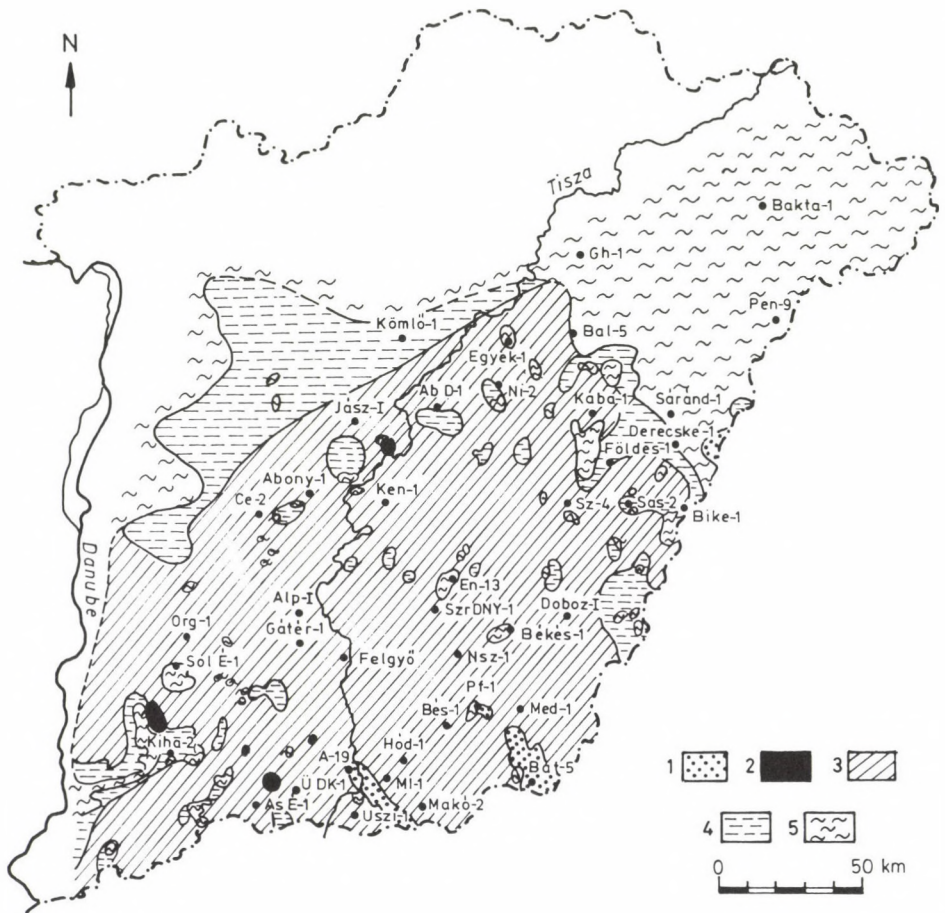


Fig. 2. The initial members of the Pannonian (s. l.) sequence. 1. Basal conglomerates and sandstones; 2. volcanics; 3. calcareous marl; 4. marl; 5. argillaceous marl

depending on the rate of infilling, locally thinner or thicker sandstone strata were formed intercalating with the shaly-silty sequence.

4.1. The initial members of the Pannonian (s. l.)

The initial members of the sequence are basal marls settled in brackish water in most of the examined area, except some basement highs. Around pre-existing Miocene islands and shorelines, abrasional coastal sandy conglomerates and coarse grained sandstones were formed (Fig. 2).

The coastal *conglomerates* can be found on the Algyó, Pusztaföldvár, Battonya and Kismarja highs or crests in the southern part of the Hungarian Plain. Its thickness never exceeds 100 m anywhere, and thins towards the highest points of

the crests and towards the deeper zones. The examined rock samples are usually poorly sorted, unbedded oligomict conglomerates or sandstones, sometimes with plant fragments and gradational patterns. This succession is called *Békés Formation*. They are overlain by calcareous marls and marls (I. Bérczi 1970, Gy.K. Juhász 1985).

Due to tectonic events, on a very few places *volcanics* can be found at the base of the Pannonian (s.l.) sequence, intercalated with the marls. This unit, called *Kecel Formation*, can be found near Ruzsa, Kecel, Sándorfalva and Nagykörü (S. Papp 1986; A. Nusszer –E. Balázs 1987)

At the base of the Pannonian (s.l.) sequence *basal marls* can be found which are widespread all over the basin, and reflect calm water, balanced depositional conditions. This unit is diachronous, its formation took place as transgression continued, in consequence of differential subsidence. The basal marls are probably the youngest in the southeastern part of the basin, where e.g. above the Battonya high, the fauna content is of Pontian age (I. Magyar, this volume).

Its thickness varies between 20 and a few hundred meter. In the northern part of the Hungarian Plain, in the Jászság subbasin, where the bay was probably formed very early, argillaceous marls of a huge thickness accumulated. Its thickness can reach 7–800 meter here (Fig. 7).

The basal marls can have different internal structures depending on the pre-existing morphology of the basin floor. Where the relief was steep, pebbles from the basement can occur in the lowermost part of the sequence, (earlier called *Dorozsma Formation*). In the upper parts locally thin sandstone intercalations can appear, interpreted as distal turbidites, (earlier *Vásárhely Formation*).

The basal marl sequence has two main types, (Fig. 3). The succession usually starts with calcareous marl or marl called *Tótkomlós Formation*, and grades upward into argillaceous marl, which is called *Nagykörü Formation*. The areal distribution and isopach map of the calcareous marl unit can be seen on Fig. 4. On the margins, mainly to the north, only the argillaceous marl unit is developed.

The *Tótkomlós Formation* has different appearance depending on the depth. On basement highs its colour is pale yellow, and contains pyritic plant fragments. It was settled in calm, shallow water conditions. Laterally this unit shows a gradual transition into a moderately deep facies with brown colour, and further to the deepest zones it changes to black, and is strongly pyritic, indicating a reducing environment.

4.2. Sandy turbidite sequence – Szolnok Formation

The basal marl unit is overlain by a thick *turbidite* sequence in the deep basinal areas, called *Szolnok Formation*. The thickness of this lithofacial unit can exceed 1000 m in the deepest zones (1090 m in Hód-1, 1020 m in Derecske-1 well, and can be more according to seismics), while pinches out towards the margins and also on some basement highs (Fig. 5). The upper surface of this unit rises to the N and W to 1500–1000 m and dips to the deeper zones to 3500 m (Fig. 6.). It consists of the cyclic alternation of dark grey argillaceous marls, siltstone and light grey sandstone beds. The thicker sandstone beds are composed of small rhythms.

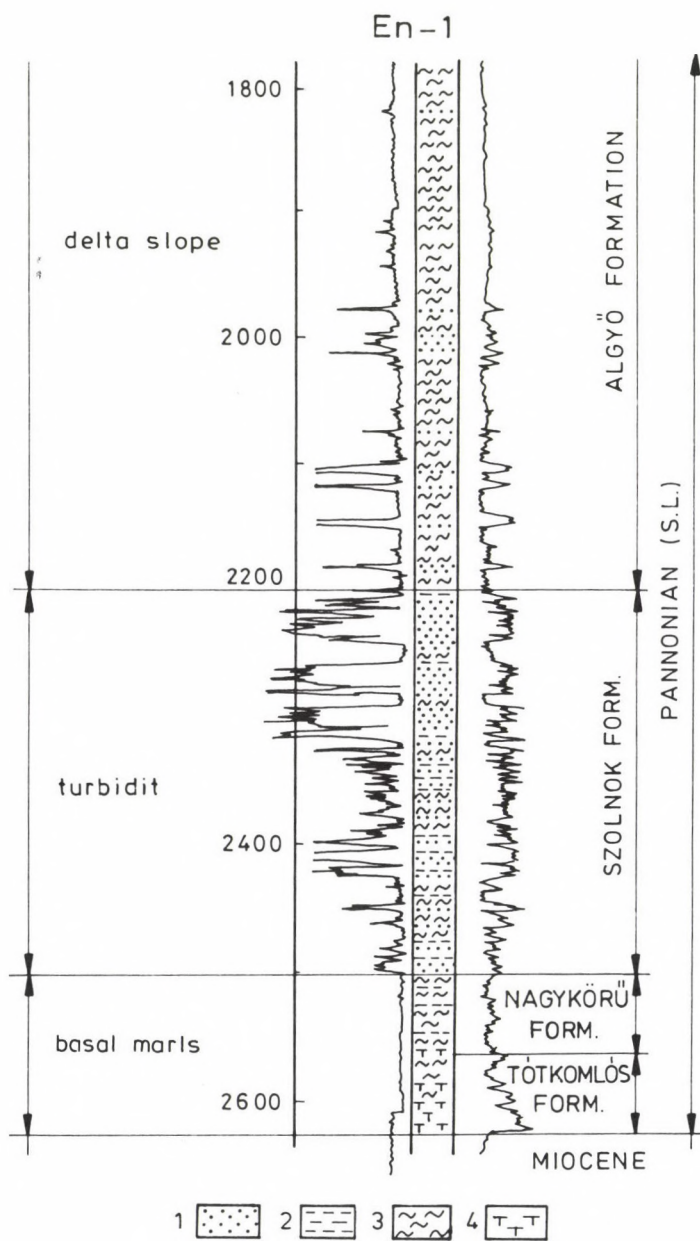


Fig. 3. Lithology, lithostratigraphy and lithofacies in the lower part of the Pannonian (s. l.) sequence in Endrőd-1 well. 1. sandstone; 2. siltstone; 3. argillaceous marl; 4. calcareous marl

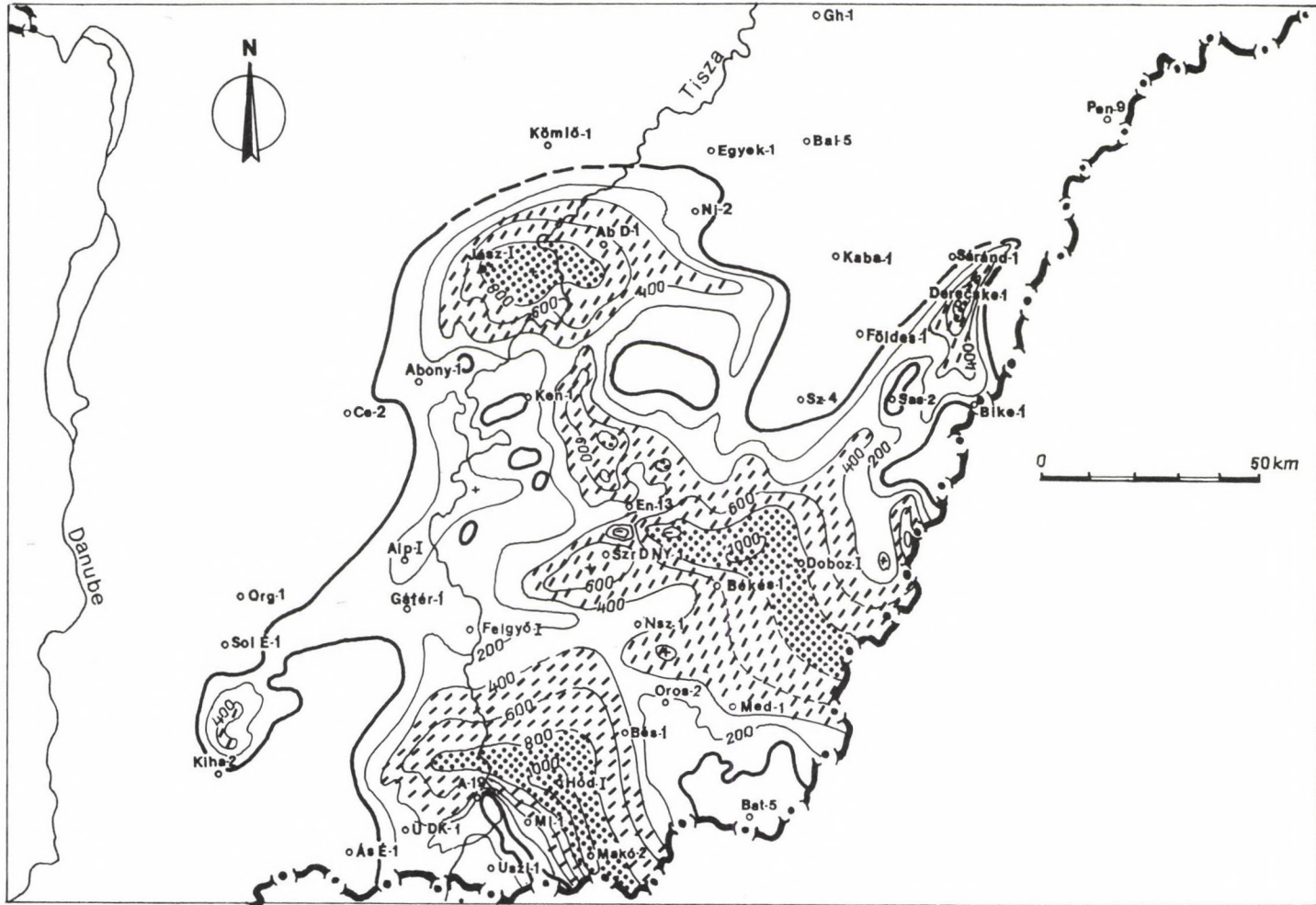


Fig. 5. Isopach map of the sand-rich turbidite sequence (Szolnok Formation)

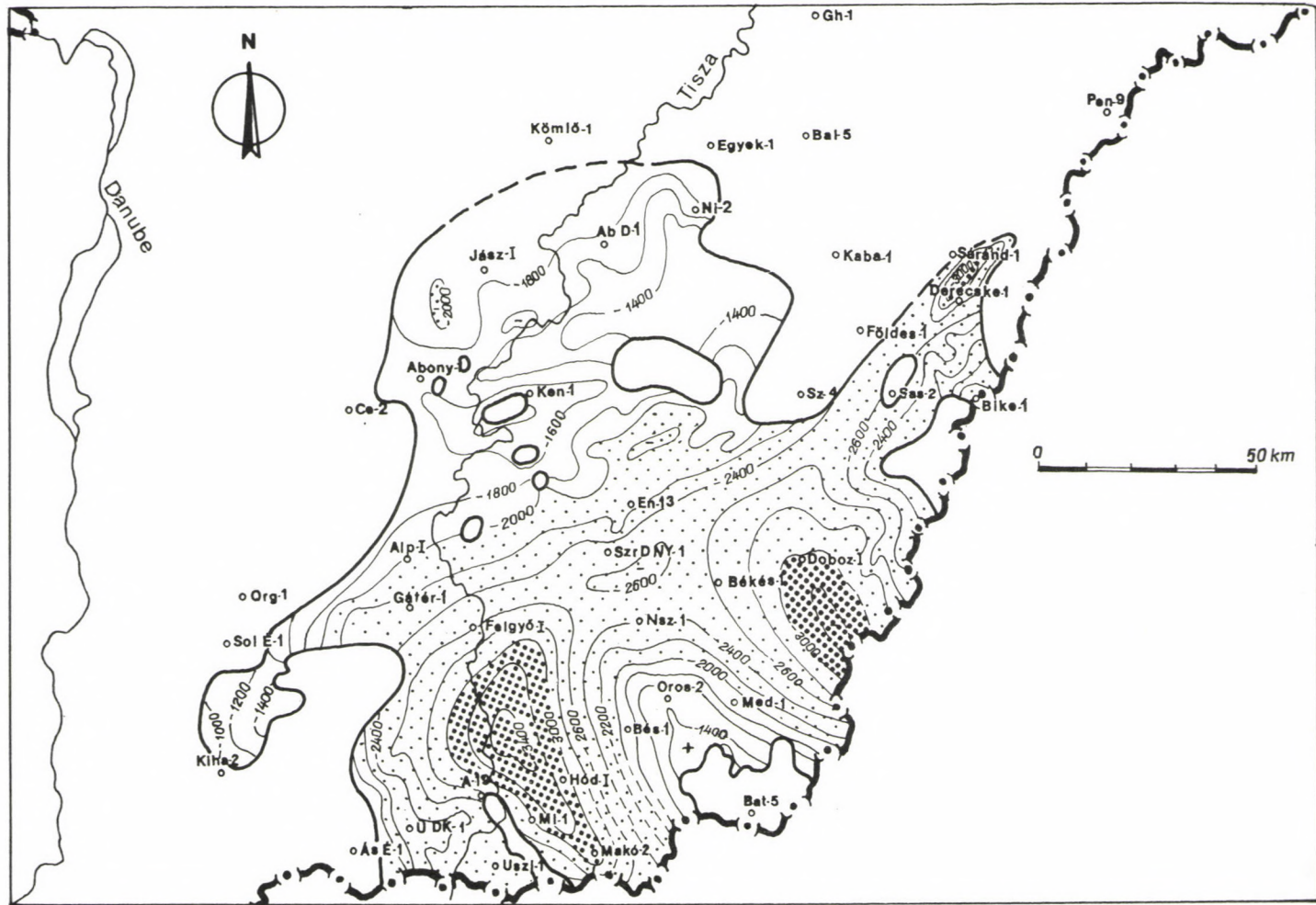


Fig. 6. Structural map at the top of Szolnok Formation ("S" marker)

The lower part of the sequence represents distal turbidites, whereas the upper part contains the sandstone bodies of proximal turbidites. On top and sometimes inside the sequence slump deposits can be found, deriving from the slope. The thickness of the marl strata, settled in calm periods, varies between 4 and 30 m.

Most of the turbidite sequence, except the deepest zones, are supposed to be connected to the delta system, prograding from the NW direction, and partly to those, arriving from E–NE direction. The sediments of this latter delta system seems to be rather fine-grained or shaly according to the core samples and well-logs except in the middle of the trough (Derecske–1 well), where supposedly sandy turbidites were transported in a fan channel through the Derecske trough into the Békés basin. In the Békés basin there is an interface of these two turbidite systems.

Sedimentary structures in this sequence show characteristic features of turbidites, massive to laminated fine-grained sandstones with convolution, dish and flame structures, Bouma sequences, clay marl intraclasts, etc. in the sandstone strata.

On the sedimentological profile, crossing the basin of approximately NW–SE direction, the location, distribution of the turbidite sequences as well as the other lithofacies units are shown (Fig. 7). The turbidite bodies are continuous over long distances as a package, but individually the extension of the sandstone bodies is limited.

A few examples of the characteristic well-log shapes are shown on Fig. 8, identified by the analysis of the well-log response.

4.3 Deltaic sedimentation – Algyő and Törtel Formation

The *Algyő Formation* overlaps the turbidite sequence, and is wide-spread all over the basin. On the margins it overlies the basal marls. It represents the sediments of the *delta slope* and on the margins the nearshore environments. It consists mainly of mudstones, e.g. siltstone and argillaceous marl strata, interbedded with a very few sandstone bodies. These sandstone bodies can be of turbidite origin at the lower part, containing slumps, grain flows and mud flows. At the top of the succession they can be mouth-bar and delta-marine fringe sedimentary rhythms. In some places they occur as underwater channel fills (Fig. 8).

Sedimentary structures scarcely can be identified, possibly in the fine-grained sandstone or siltstone strata. These are massive or often cross-laminated, with coalified plant fragments or leaf prints on the joint surfaces. Dipping of strata are very common, varies between 5–7 degree, and can reach 18–20 degree on some places.

In a few areas, where the delta progradation reached the basement highs, before overlapping the high, sandstones were settled in the foreground and almost all of the sequence is fairly sandy (to the NW of Szarvas, Üllés and Orosháza areas).

In the NE part of the basin the succession is very shaly, there cannot be observed sandy turbidites. The *Algyő Formation* contains here not only the *delta slope* facies but also the pelitic *prodelta* sequence and the *basal marls* as they are practically

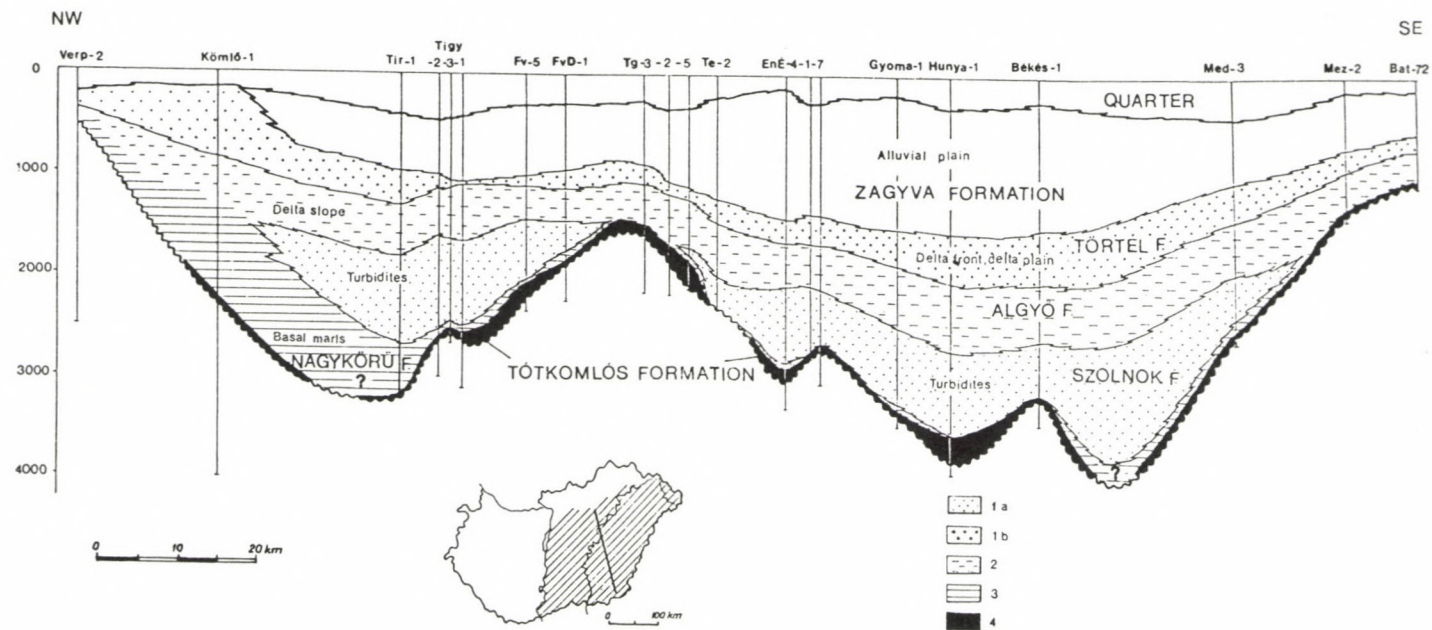


Fig. 7. Sedimentological and stratigraphic profile across the Hungarian Plain in NW-SE direction. The prevailing rock types: 1. a, b sandstone; 2. siltstone; 3. argillaceous marl; 4. calcareous marl

undistinguishable (Fig. 9). Sandy turbidites probably were carried along towards the Békés basin in a fan channel in the middle and deepest part of the Derecske–trough.

This lithofacial unit is overlain by the sediments of the sandy *delta front, delta plain* environments (Fig. 10). This sandy unit is called *Törtel Formation*. The contact between the Törtel and Algyő Formations are mostly abrupt in the Hungarian Plain, but it can be gradual, too. Generally a coarsening–upward mouth-bar rhythm starts the succession (Figs 8, 9, 10).

Previously this boundary was considered to be a time boundary, i.e. top of the Pannonian (s. str.) or Miocene (earlier Lower-Pannonian). Today in the Pannonian Basin, however, it is considered to be a facies boundary, which is time–transgressive (Fig. 11). In the SE part of the basin rocks are much younger than in the northeastern and northwestern part since accumulation occurred much later.

In the Törtel Formation sandstone bodies occur as distributary mouth bars (generally superimposed) and distributary channel fill rhythms of about 20–50 m thickness, according to the analysis of the well–log response and core investigations (Figs 8, 9, 10). The extension and continuity of these sandstone bodies are rather restricted, but they can merge laterally with one another.

Coalified plant fragments, limonitic concretions are common as well as lignite intercalations in the upper part of the sequence. Sandstones are massive, stratified, laminated or cross-laminated, medium to fine-grained, and siltstone intercalations are frequent.

There is an *interface* area on the NE part of the basin, in the Nagyunság sub-basin. Here we can find probably the joining area of the two delta systems arriving from the NW and NE directions, bringing about a very complicated intertonguing both in space and time. In a well limited area two (or sometimes three) delta front and delta slope successions can be traced above each other (Fig. 12).

The sedimentological profile in SW–NE direction touches the northern edge of this area (Fig. 13), where these delta front successions fuse, causing the extreme thickening of the Törtel Formation in this region (in wells Egyek–2,1 – approx. 900 m), forming a series of superimposed mouth bar sequences. Not far from here to the NW direction, however, the Törtel Formation is almost missing. Its thickness is about 15–20 m, caused probably by erosion.

4.4. Alluvial plain sedimentation – Zagyva Formation

The uppermost part of the Pannonian (s. l.) sequence is consisted of a thin-bedded siltstone, claystone and sandstone succession, with the dominance of the fine grained fraction, called *Zagyva Formation*. In the lower part of it paludal and lignite intercalations are frequent, and generally the sediments of a fluvial-lacustrine environment are common. In the uppermost part of it the sequence contains variegated clays and fluvial-terrestrial fauna. Channel fill and point bar sandstone sedimentary rhythms can be observed in it. Sediments are loose or friable here, horizontally bedded, with brown and red patches, and with lignite intercalations.

Towards the margins this thin-bedded unit gradually thins and a sandy sequence can be observed. It cannot be differentiated from the delta front, delta

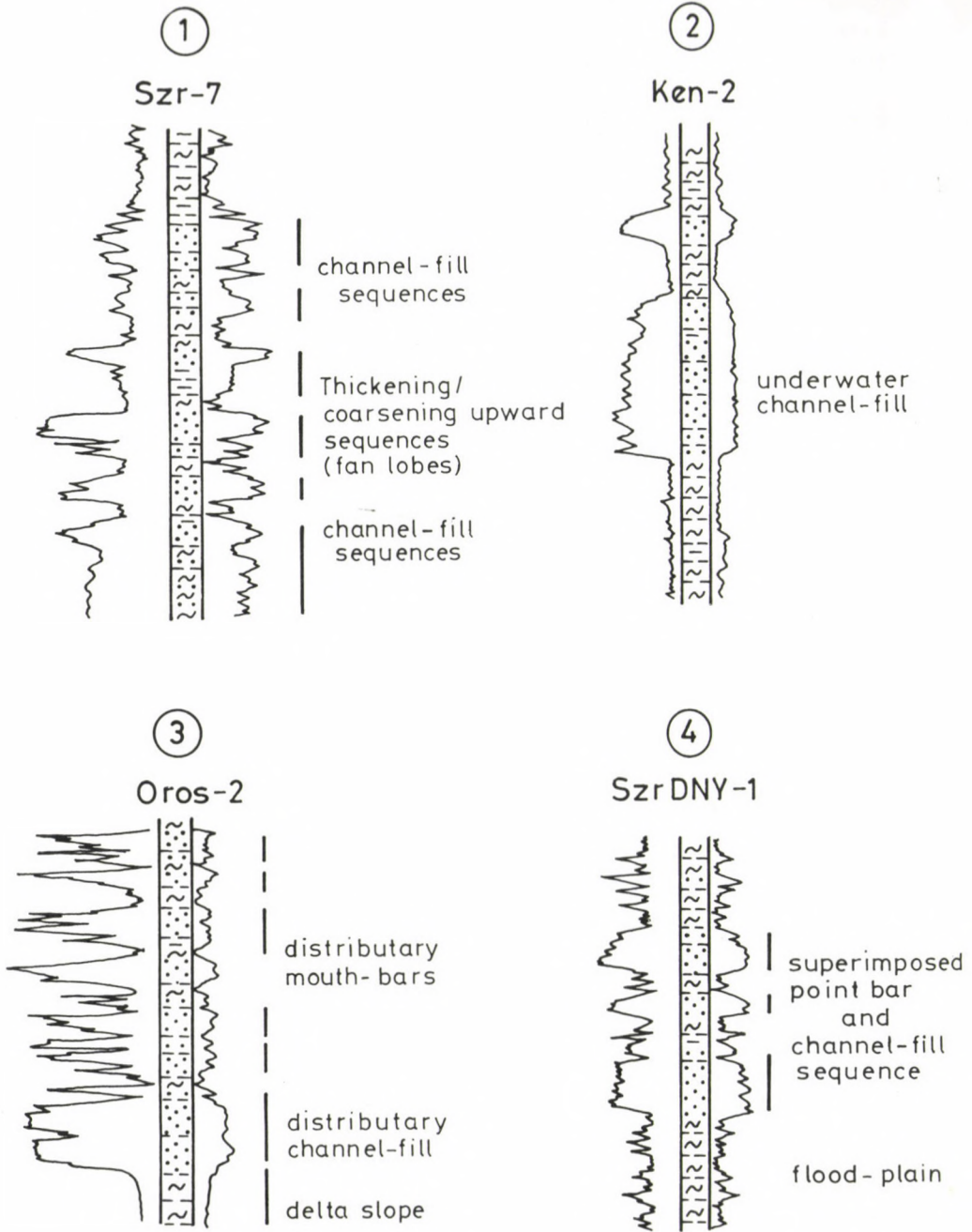


Fig. 8. Characteristic well-log shapes in the different lithofacial units. 1. turbidites; 2. delta slope; 3. delta front, delta plain; 4. alluvial plain

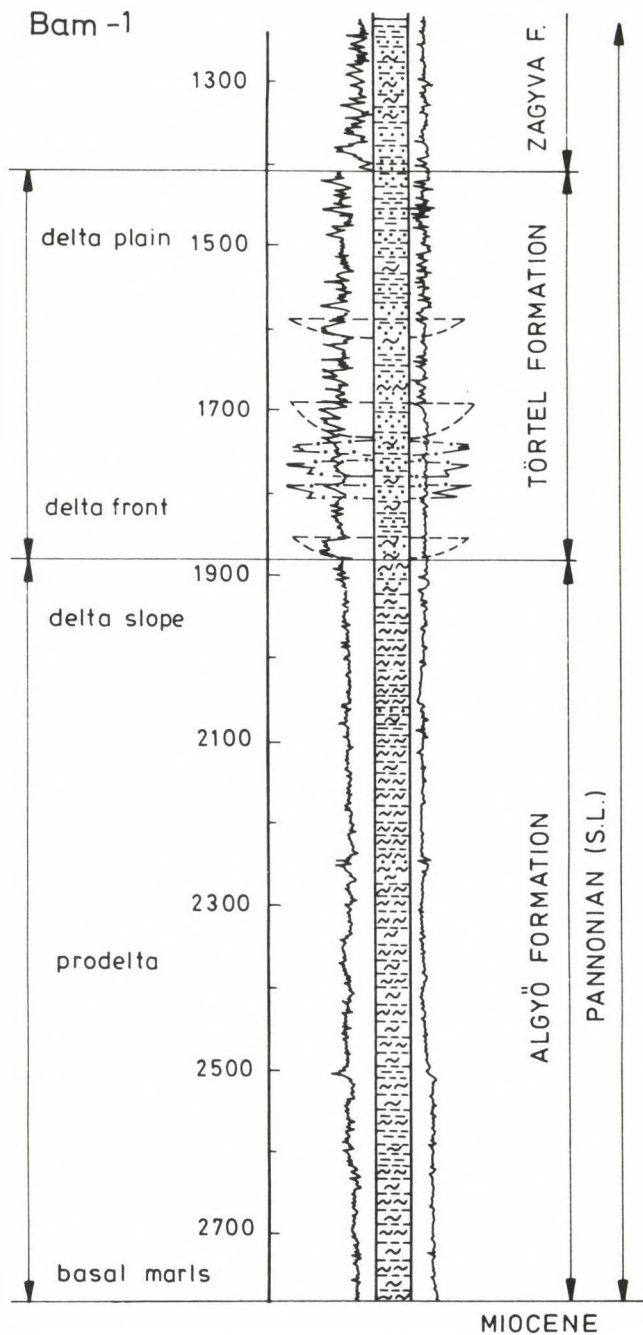


Fig. 9. Lithofacial units in Bam-1 well in the NE part of the basin in the Derecske trough

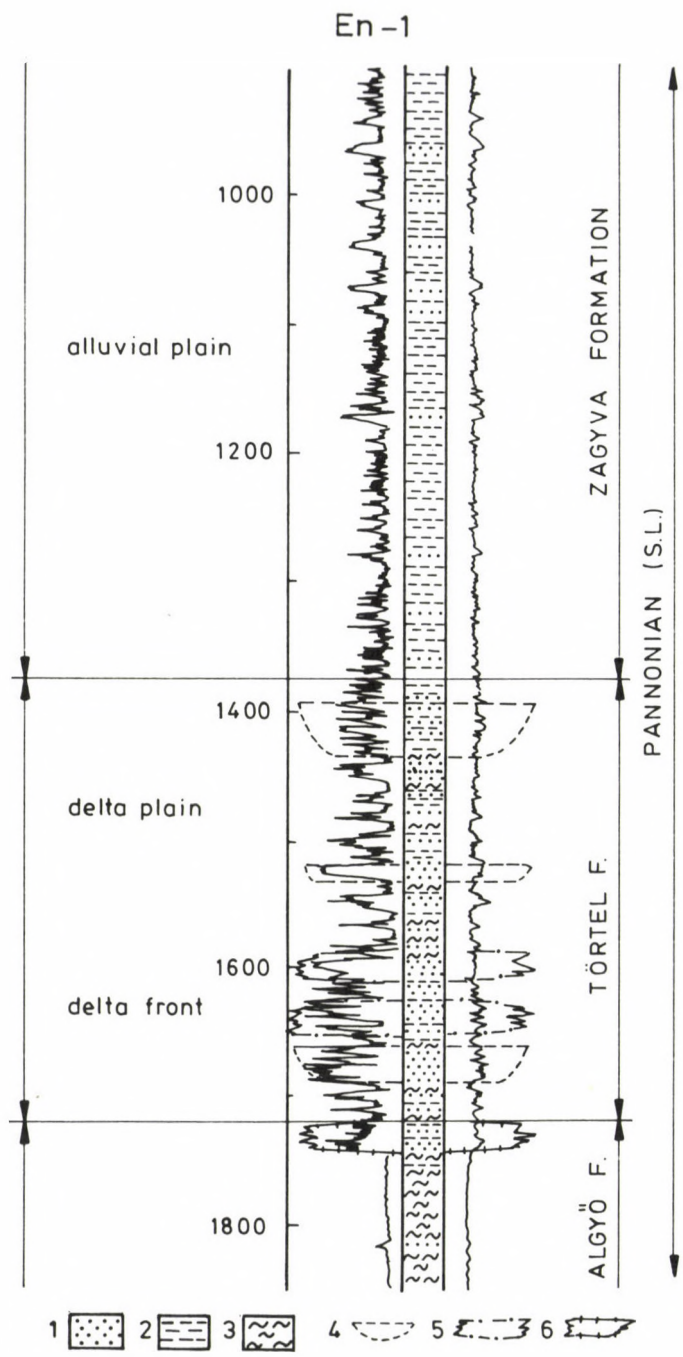


Fig. 10. Lithology, lithostratigraphy and lithofacies in the upper part of the Pannonian (s. l.) sequence in Endrőd-1 well. 1. sandstone; 2. siltstone; 3. argillaceous marl; 4. distributary channel fill; 5. mouth bar; 6. reworked sandstone body

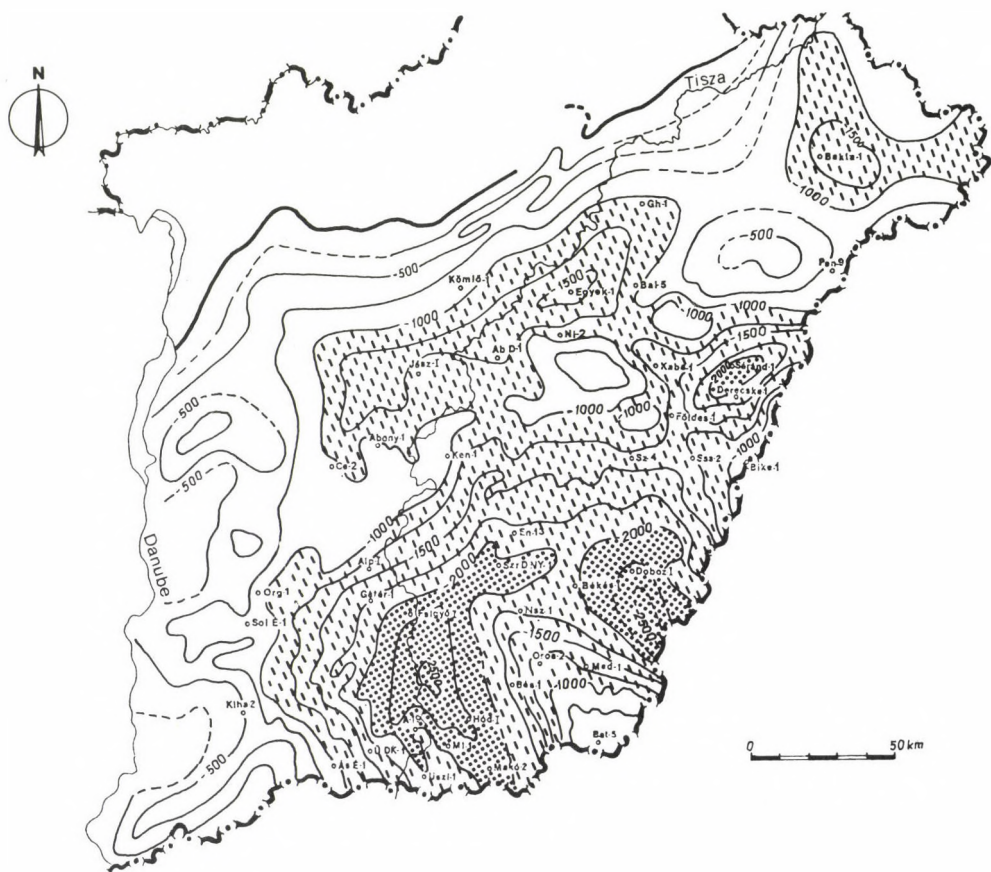


Fig. 11. Structural contour map at the top of Algyő Formation ("L" marker), (previously top of Lower-Pannonian

plain lithofacial unit on the basis of the available data, e.g. mostly well logs, in the lack of core samples. Sometimes it overlaps the Zagyva Formation. This is why the upper boundary of the Törtel Formation cannot be correlated on the margins, only where the Zagyva Formation exists (Fig. 12).

5. Conclusions

The Pannonian (s. l.) sedimentary cycle in the Hungarian Plain began with the deposition of calcareous marl and marl after the Sarmatian approximately twelve million years ago (Fig. 14). Around the pre-existing islands coastal sandy

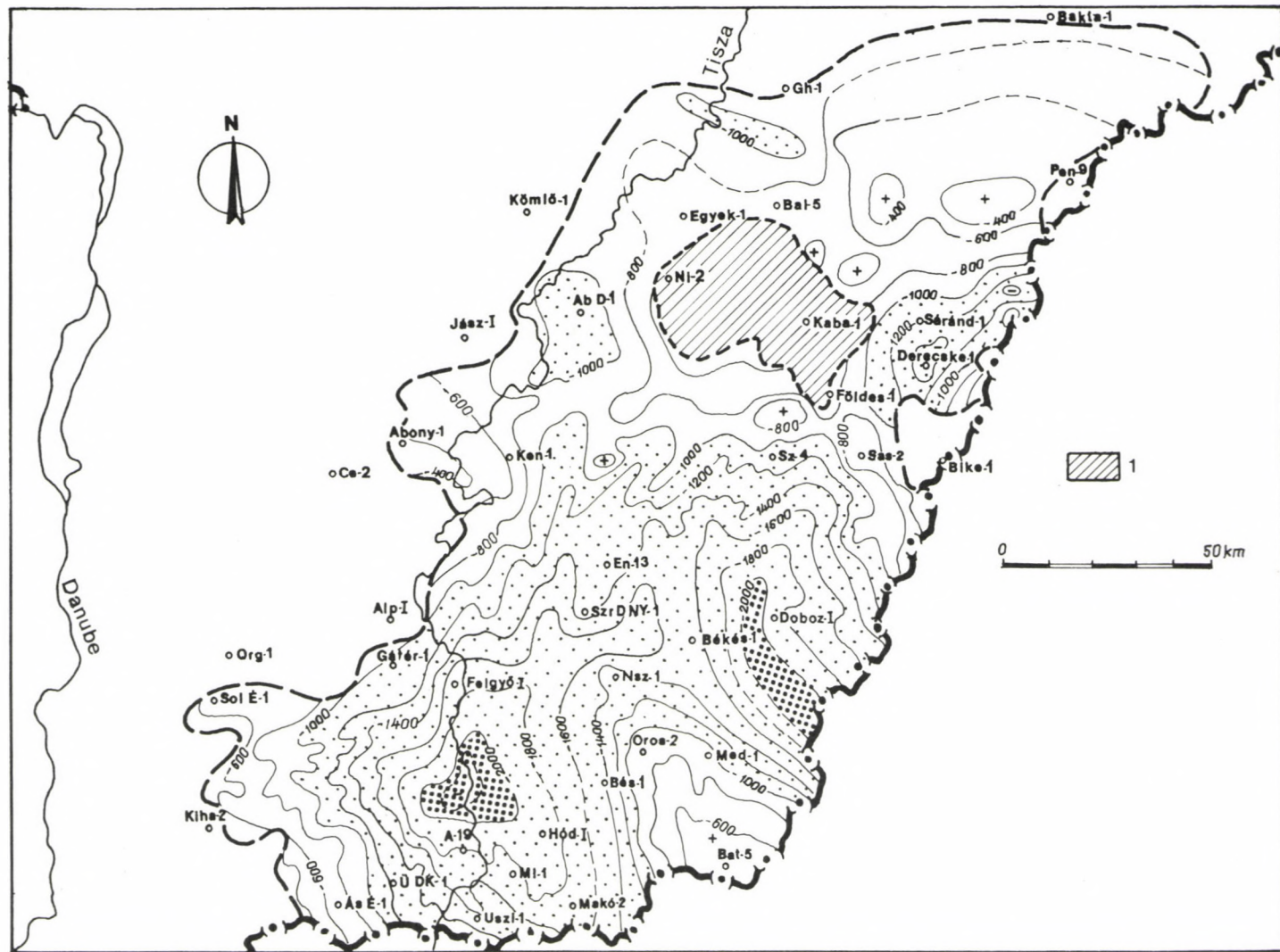


Fig. 12. Areal distribution and bottom of Zagyva Formation ("D" marker, Top of Törtel Formation, where it can be correlated)

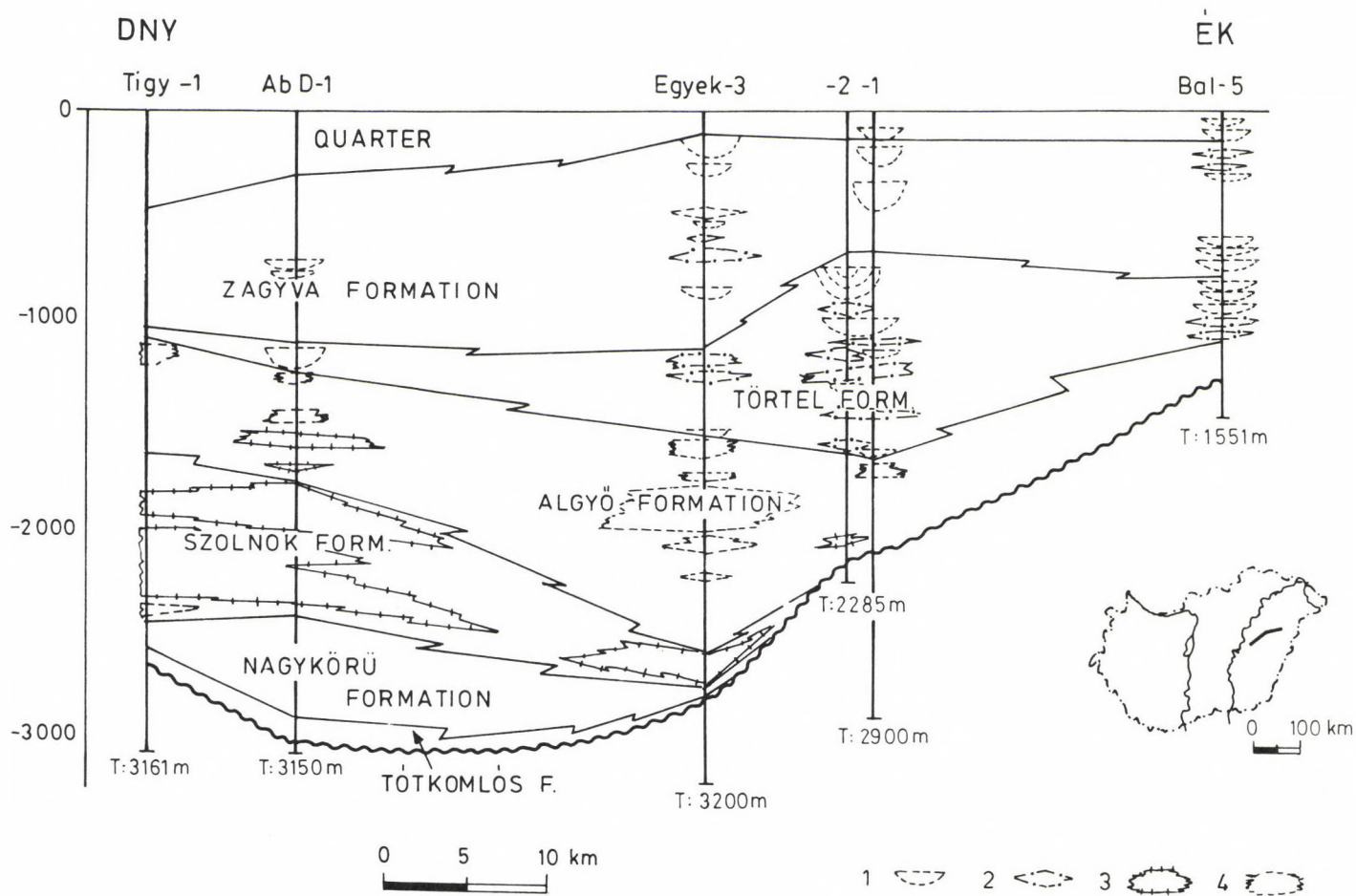


Fig. 13. Sedimentological and stratigraphic profile in the northern part of the basin, next to the interface area. 1. channel fill and point bar; 2. mouth bar; 3. turbidite bodies; 4. underwater channel fill

conglomerates and sandstones were settled. In a very few places volcanics were found.

As subsidence became stronger, turbidites accumulated in the deepest zones. After this two high constructional fluvial dominated delta systems prograded from the NW and NE directions towards the basin, while other fluvial systems of much less importance reached the basin, from SE, S, SW directions, with much less sediment influx. This resulted the accumulation of the vertical assemblages of the characteristic lithofacies above each other: the prodelta turbidites, delta slope, delta front and delta plain lithofacial units. Their distribution, depths and thickness are shown on the previous figures. The last stage of the Pannonian (s. l.) sedimentation is represented by alluvial plain deposits.

The delta system, prograding from the NW direction, carried along sand-rich sediments. Most of the sediments, however, having arrived from the NE direction, are fairly shaly as for the prodelta and delta slope units. Sandstones were carried by a fan system along the deepest part of the Derecske trough. The Szolnok Formation in the Békés basin form an interface of these turbidite units.

Another interface can be found in the area of the Nagykunság, where the two delta systems met, bringing about a very complicated intertonguing both in space and time in the delta front and delta slope lithofacial units.

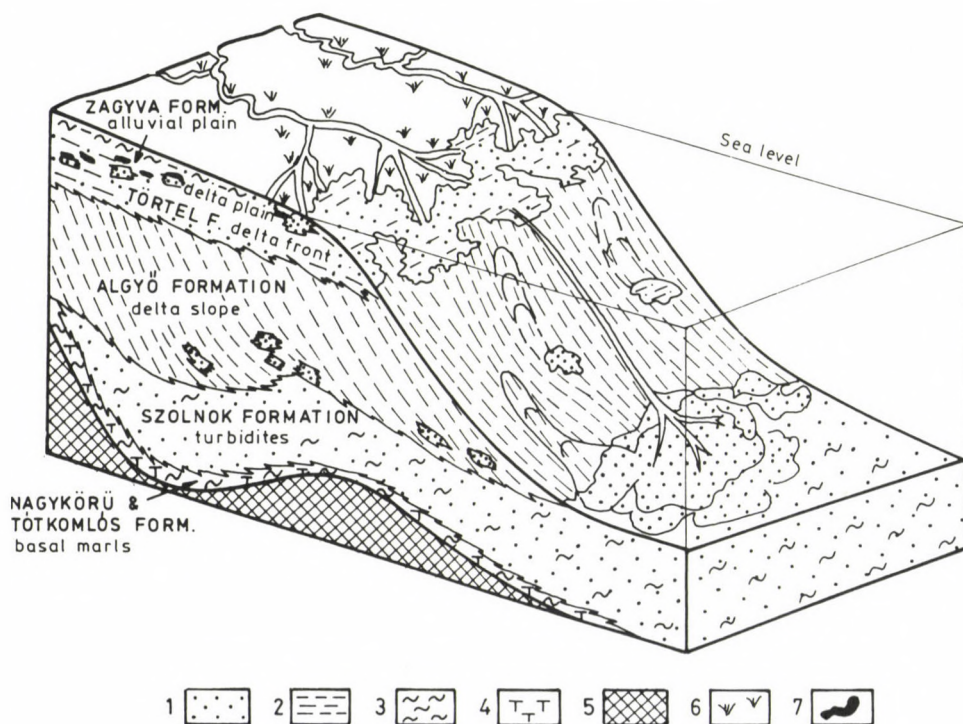


Fig. 14. Block diagram, showing the depositional environments, lithofacies and lithostratigraphic units of the Pannonian (s. l.) sequence in the Hungarian Plain. 1. sandstone; 2. siltstone; 3. argillaceous marl; 4. calcareous marl; 5. Pre-Pannonian basement; 6. swamp; 7. peat (lignite)

References

- Balázs, E., A. Nusszer 1987: Volcanism in the Kunság stage in the basinal areas of Hungary. – MÁFI Annales of the Hungarian Geol. Institute, LXIX, pp. 95–115.
- Bérczi, I. 1970: Sedimentological investigation of the coarse-grained clastic sequence of the Algyő hydrocarbon holding structure. – Acta Geol. Acad., 14, pp. 287–300.
- Bérczi, I. 1988: Preliminary sedimentological investigation of a Neogene depression in the Great Hungarian Plain. – In: The Pannonian Basin, AAPG Memoir, 45, pp. 107–114.
- Bérczi, I., R.L. Phillips 1985: Processes and depositional environments within Neogene deltaic-lacustrine sediments, Pannonian Basin, Southeastern Hungary. – In: Geophysical Transactions, special edition, pp. 71–87.
- Bérczi, I. et al. 1986: Preliminary report on play selections in the Békés Basin. – Sedimentology. OKGT – USGS Project, Internal report p. 73.
- Bérczi, I. et al. 1987: Formations of the Kunság stage (Pannonian s. str.) in the Hungarian Plain. – MÁFI Annales of the Hungarian Geol. Institute, LXIX, pp. 179–198. (in Hungarian).
- Gajdos, I. et al. 1983: Lithostratigraphic units of the Pannonian (s. l.) formations in the Hungarian Plain. – MÁFI special edition (in Hungarian), p. 70.
- Jámbor, Á. et al. 1987: General characteristics of the Pannonian (s. l.) deposits in Hungary. – MÁFI Annual Report, LXX, pp. 155–167 (in Hungarian).
- Jámbor, Á. 1988: Geology of the Pannonian (s. l.) formations in Hungary. – Academic doctoral theses (in Hungarian).
- Juhász, Gy.K. 1985: The deposition of shoreline conglomerates in the southern part of the Great Hungarian Plain at the beginning of the Pannonian (s. l.). – XIII Congress of Carpatho-Balkan Association, Krakow, Abstracts, pp. 182.
- Juhász, Gy.K. et al. 1986, 1987, 1988: Lithological and sedimentological investigations on seismic research areas. – SZKFI Internal Reports, Budapest (in Hungarian).
- Juhász, Gy.K. 1989: Lithostratigraphy of the Pannonian (s. l.) sequence in the Hungarian Plain. – SZKFI Internal Report, Budapest, (in Hungarian), p.44.
- Körössy, L. 1971: Subsurface geological and evolution historical outline of the Pannonian in Hungary. – In: Researches in the Hungarian Pannonian formations. pp. 199–221, Budapest, Akadémiai Kiadó (in Hungarian).
- Mattick, R.E. et al. 1988: Seismic stratigraphy and depositional framework of sedimentary rocks in the Pannonian Basin, SE Hungary. – In: The Pannonian Basin, AAPG Memoir, 45, pp. 117–146.
- Molenaar, C.M. et al. 1988: Stratigraphic framework of the Pannonian (s. l.) sequence, Békés Basin, Hungary. – USGS Researches on energy resources, Denver, Abstract, p. 16.
- Mucsi, M., I. Révész 1975: Neogene evolution of the southeastern part of the Great Hungarian Plain on the basis of sedimentological investigations. – Acta Min.-Petr. Szeged, 22 (1), pp. 29–49.
- Papp, S. 1986: Lower-Pannonian basalt volcanism in the Hungarian Plain. – Spec. Issue of the Research Team on the Great Plain, H.A.S., pp. 7–34 (in Hungarian with English abstract).
- Pogácsás, Gy., I. Révész 1987: Seismic stratigraphic and sedimentological analysis of Neogene deltaic features in the Pannonian Basin. – MÁFI Annual Report LXX, pp. 267–273.
- Reading, H.G. 1981: Sedimentary environments and facies. – Blackwell Scientific Publications, Oxford, p. 269.
- Reineck, H.E., I.B. Singh 1973: Depositional sedimentary environments. – Springer Verlag, Berlin.
- Révész, I. 1980: Geological setting, sedimentological heterogeneity and paleogeography of the Algyő –2 pool. – Földt. Közl., 110, (3–4) pp. 512–539 (in Hungarian).
- Szalay, Á., K. Szentgyörgyi 1988: A method for lithogenetic subdivision of Pannonian (s. l.) sedimentary rocks. – In: The Pannonian Basin. AAPG Memoir, 45, pp. 89–96.

Biostratigraphic revision of the Middle Pontian (Late Neogene) Battonya Sequence, Pannonian basin (Hungary)

Imre Magyar

Hungarian Hydrocarbon Institute, Százhalombatta

Revision of core sample fossils (Mollusca) from the Battonya sequence, SE Hungary, offered a new stratigraphic interpretation: the "Pannonian-Pontian" sequence proved to be Middle Pontian (Portaferrian) sensu Stevanovic (1951). Occurrence of *Congeria banatica* R. Hörnes *Dreissenomya digitifera* (Andrusov) and *Paradacna abichi* (R. Hörnes) together with, or above typical Portaferrian species, such as *Lymnocardium* (Budmania) *crisitagalli* (Roth), *Lymnocardium schmidti* (M. Hörnes) and *Lymnocardium hungaricum* (M. Hörnes) can be explained by their slow evolutionary rate in a stable, relatively deep and quiet lacustrine environment. Consequently, their biostratigraphic role should be reconsidered. A summary of the Pontian sedimentary history of the Battonya area is also given.

Keywords: Mollusca, biostratigraphy, chronostratigraphy, sedimentary history, Pontian, Pannonian basin

Introduction

In the first half of our century, the Pannonian-Pontian (Late Neogene) mollusc biostratigraphy of the Pannonian basin was based on collections coming from surface exposures (Halaváts 1903, Lörenthey 1906, Strausz 1942, Papp 1951, Stevanovic 1951). Different interpretations of facies variety led to different stratigraphic frameworks. Reconciliation of contradictions and better understanding of deep basin facies were expected from the increasing hydrocarbon exploring drilling activity. Sporadic coring and poor preservation of the fossils, however, made the interpretations difficult.

Drilling activity in the Battonya area (southern margin of Békés basin, SE Hungary) (Fig. 1) was started in 1957. Between 1957 and 1964 40 boreholes, between 1970 and 1974 further 9 ones provided cores containing mollusc assemblages. Part of data were published and interpreted by M. Széles (Hungarian Hydrocarbon Institute) in 1971; unfortunately, this volume was published only in Hungarian. The Battonya fossil record is a key to understanding the relation of some biofacies, thus it has an outstanding significance in biostratigraphy. It gave M. Széles much trouble to fit the Battonya data into her routine biostratigraphic framework; in fact, she could not perform that. In the bottom of the sequence she found Pontian (Upper Pannonian s. l.) forms together with, or under "Pannonian" (Lower Pannonian s. l.) ones. Geological structure of the area precluded any possibility of tectonic inversion.

Address: Magyar Imre: Hungarian Hydrocarbon Institute, H-2443 Százhalombatta, Pf.32

Received: January 12, 1991

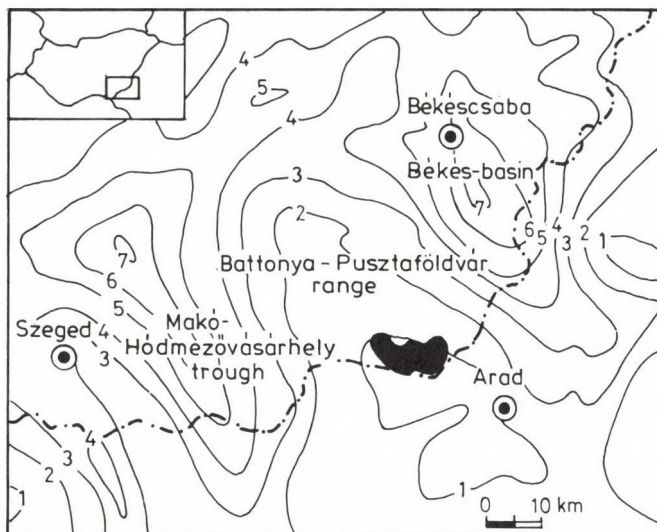


Fig. 1. Location of Battonya area (shaded) on the preneogene Battonya–Pusztaföldvár range. Thickness of the Neogene–Quaternary basin fill in kms, according to Horváth (1988)

Revision of the Battonya fossil record was carried out in 1989 as a part of the comparative examination of seismic and biostratigraphy in the Békés basin. We came to the conclusion that the deposition of the Battonya Neogene sequence started in the Middle Pontian (Portaferrian) (that is, Upper Pannonian s. l.). This young age interpretation is supported by sedimentological, magnetostratigraphic and seismic evidences as well.

Sedimentary sequence

The Battonya area is situated at the southern margin of the Neogene Békés basin – a subunit of the Pannonian basin – in SE Hungary, 25 km NW of Arad (Fig. 1). Seismic and gravimetric exploration of the area was started in 1940, and the first well was drilled in 1957. In the very base of the Neogene sequence, at about 1000 m depth, a considerable hydrocarbon reservoir was discovered. Having performed several dozens of drillings, a rather complete picture could be obtained about the Neogene sedimentary sequence and the basement formations (Dank 1962, Kovács 1965).

The sedimentary history of the Battonya area in the Pontian can be subdivided into two periods. First one is characterized by sediment starvation, while the second one is characterized by rapid infilling.

In the beginning, sedimentation was controlled by morphological conditions. The Battonya area is situated on a subsurface preneogene ridge between the Békés basin and the Makó–Hódmezővásárhely trough (Battonya–Pusztaföldvár range)

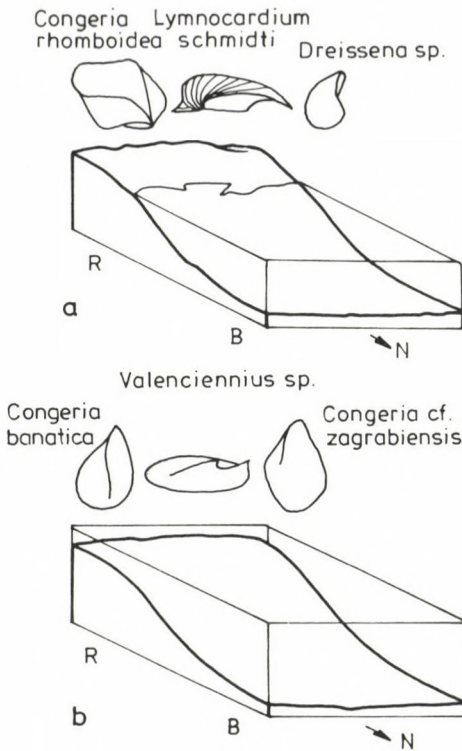


Fig. 2. First period in the Pontian evolution of the Battonya area (sediment starvation) and the characteristic fossils. Prevailing sedimentary processes are: a) clastic sedimentation, b) carbonate precipitation (R: Battonya-Pusztaföldvár range, B: Békés basin)

(Fig. 1). The southward transgression reached the area in the Middle Pontian. As the main sediment transport direction was north to south, fine-grained prodelta sediments were trapped by the deep parts of the Békés basin, north of the Battonya area (Fig. 2). Thus, in the first period, autochthonous sedimentation took place. The Pontian sequence starts with conglomerates and pebbly sandstones, formed by weathering and abrasion of the underlying Palaeozoic granite and quartz-porphry. Thick-shelled molluscs of rather great size, such as *Lymnocardium hungaricum*, *L. schmidti*, *L. majeri*, *L. cristagalli*, *Dreissena* sp., *Phyllocardium planum*, *Melanopsis* sp., and *Congeria rhomboidea* lived in the agitated, well aerated, nearshore and shallow water (Fig. 2/a).

As a consequence of the subsidence of the Battonya-Pusztaföldvár range, carbonate precipitation started to prevail against clastic sedimentation. The coarse-grained clastic sediments are covered, and sometimes interbedded with light grey, yellow or white calcareous marl or limestone. Thin-shelled molluscs lived in the quiet environment: *Congeria* cf. *zagrabiensis*, *Valenciennius* sp., *Lymnocardium* cf. *araceum*. *Congeria banatica* was especially common (Fig. 2/b).

These two formations together, with a thickness of usually less than 100 m, form the "basal" hydrocarbon reservoir.

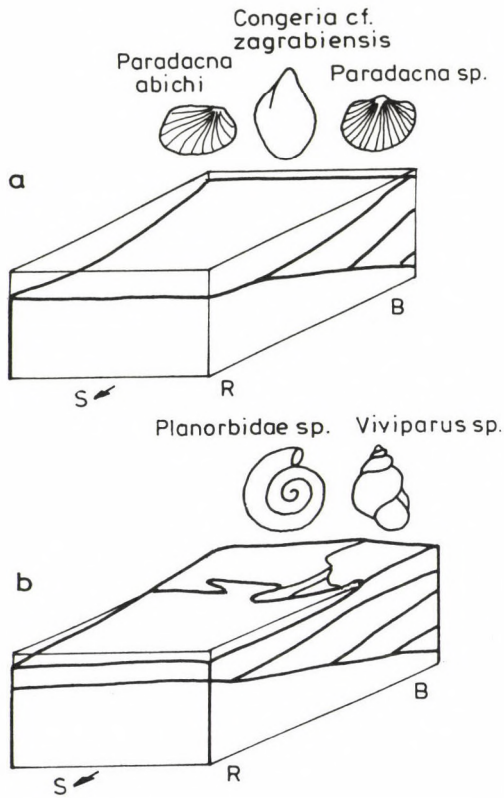


Fig.3. Second period in the Pontian evolution of the Battonya area (rapid infilling) and the characteristic fossils. Prevailing sedimentary processes are: a) delta slope sedimentation, b) delta plain and alluvial sedimentation (R: Battonya-Pusztaföldvár range, B: Békés basin)

During the second period, sedimentation was controlled by a southward prograding delta system (Mattick-Phillips-Rumpler 1988, Pogácsás et al. 1989). Deep parts of the Békés basin were filled by this time, and an increasing amount of fine-grained sediment was transported and deposited within the Battonya area (Fig. 3). Marl, argillaceous marl and siltstone were formed with an upward decreasing carbonate content. The average thickness of this fine-grained sequence is about 350 m. Thin-shelled and small-sized molluscs, mainly inbenthonic forms, such as *Paradacna abichi*, *Paradacna sp.*, *Lymnocardium riegei*, *Dreissenomya digitifera* and *Congeria cf. zagrabiensis* lived in the relatively deep water (Fig. 3/a).

With subsequent shoaling sediments of great variety were deposited (submerged delta plain environment). The alternating beds of sand, silt, clay and lignite has an average thickness of 250 m. Sand beds contain considerable amount of natural gas. According to the often changing water depth and shore distance, the mollusc fauna is also varying. Forms characteristic for strongly reduced salinity and fresh water, such as *Prosodacnomya sp.*, *Viviparus sp.*, *Lymnocardium cf. ochetophorum* and *Planorbidae sp.* appeared (Fig. 3/b).

After the filling of the basin, lacustrine, fluvial and terrestrial sedimentation took place during the Pliocene and Pleistocene. The non-cored beds of clay, sand and gravel were penetrated in a thickness of about 400 m (Fig. 4).

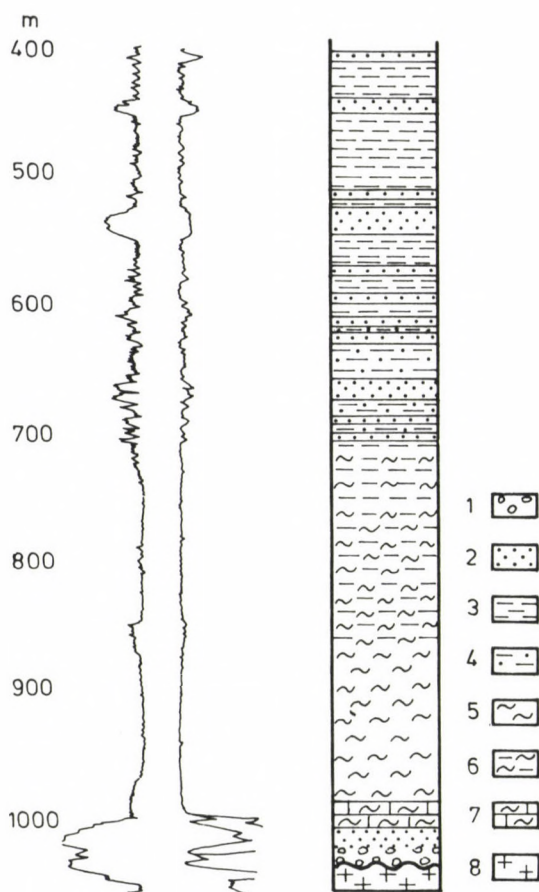


Fig. 4. Lithology, SP and resistivity logs of the Pontian of Battyanya-14 borehole. 1. Conglomerate, 2. sandstone, 3. clay, 4. silt, siltstone, 5. marl, 6. argillaceous marl, 7. calcareous marl, 8. granite

Biostratigraphic interpretation

Cores of Battyanya drillings provided a rather rich fauna of molluscs. Specimens coming from the basal conglomerate and calcareous marl are poorly preserved moulds. Most of the fossils were determined by the late M. Széles. She published and evaluated part of these data in 1971. Cores of drillings Battyanya-K-7 to Battyanya-K-20 were investigated by M. Mucsi and L. Magyar.

The revision of the material became necessary in 1989 for the comparative ex-

amination of seismic and biostratigraphy in the Békés basin. Part of the material has been lost by this time, on the other hand, some unidentified samples turned up. New specimens of molluscs were found also by further preparation of the cores.

The interpretation of the data gave M. Széles much trouble, as species like *Congeria banatica* and *Paradacna abichi* had been considered to be older (Pannonian s. str. and, in the case of *P. abichi*, even Lower Pontian) than *Lymnocardium schmidtii*, *L. hungaricum*, *L. cristagalli* (= *Budmania meisi* Brusina), *Phyllocardium planum* and so on (Middle Pontian). Széles (1971) thought that the latter ones evolved just here in the Late Pannonian, but their spreading over the shallow water environments of the Pannonian basin was prohibited by the surrounding deep water basins until the Pontian. In her interpretation, this fauna belongs to the Upper Pannonian "transitional zone", where younger forms often appear. These assumptions, however, seem to be rather unfounded. A deep, but only several km wide basin can not be a barrier for planctotroph larvae of shallow water molluscs. In addition, any deep basin is surrounded by shallow water environments.

I think that the mollusc fauna of the basal formation does not display any transitional character and unambiguously indicates its Middle Pontian (Portaferrian) age. It is the appearance of *Congeria banatica* and *Paradacna abichi* that will take some explaining, rather than that of the younger forms. These thin-shelled, relatively deep water species survived until the Middle Pontian. They appeared wherever favourable circumstances were formed (relatively deep, quiet water, fine-grained sedimentation). Due to the stable environment, their evolutionary rate was relatively slow. Consequently, the age of any formation, that was dated by the presence of these species, should be revised.

The young-age interpretation of the Battonya sedimentary sequence was supported by seismic methods (Pogácsás et al. 1988). Magnetostratigraphic datum levels were tracked along the Békés basin by regional seismic sections. According to these data, the Pontian sequence of the Battonya area was deposited about 5

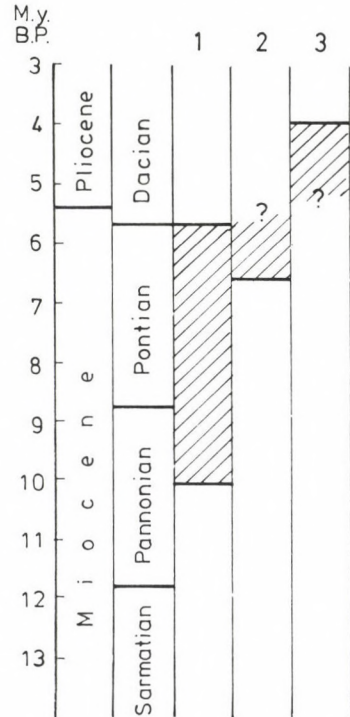


Fig. 5. Chronostratigraphic interpretations of the Battonya Neogene sequence. 1. Széles (1971), 2. Magyar (this paper), 3. Pogácsás et al. (1988)

to 4.2 mys B.P. These data show too young age, i.e. post-Pontian instead of Pontian. However, Pogácsás (pers. comm.) thinks that the condensed basal formation can be considerably older than 5 my, as its thickness is comparable with the resolution of the seismic profiles (Fig. 5).

Conclusions

1. The Battonya sequence is the first place where the occurrence of *Congeria banatica*, *Dreissenomya digitifera* and *Paradacna abichi* in the Middle Pontian (Portaferrian) is proved. *Congeria banatica* was held Pannonian, *Paradacna abichi* was held Pannonian and Lower Pontian, *Dreissenomya digitifera* was held Lower Pontian. Their persistency is probably due to their stable environment habitat. Consequently, the mollusc biostratigraphy of the Pannonian and Pontian should be based on shallow water forms of relatively fast evolutionary rate.

2. As a consequence of delta sedimentation, sedimentary sequences of considerable thickness could be formed in the Pannonian basin during relatively short time intervals. According to the Battonya area, the Pannonian and Lower Pontian may be absent under even a thick Pontian sequence starting with clastic sedimentary beds. Thus, the biostratigraphic revision of some other areas in the Pannonian Basin (e. g. Algyó) can be expected to result similar ages (Pontian, instead of Pannonian-Pontian).

References

- Dank, V. 1962: Geological structure of the new Hungarian natural gas deposits. – Hungarian Mining Journal (Bányászati Lapok), 95, pp. 756–768.
- Halaváts, Gy. 1903: Die Fauna der pontischen Schichten der Umgebung des Balatonsees. – In: Resultate der wissenschaftlichen Erforschung des Balatonsees 1/1 Pal. Anh. 4/2, pp. 1–80.
- Kovács, G. 1965: Geology of the Battonya region. – Bull. Hung. Geol. Soc. (Földtani Közlöny), 95, pp. 183–189.
- Lőrenthey, I. 1906: Beiträge zur Fauna und stratigraphischen Lage des pannonischen Schichten in der Umgebung des Balatonsees. – In: Resultate der wissenschaftlichen Erforschung des Balatonsees 1/1 Pal. Anh. 4/3, pp. 1–215.
- Mattick, R.E., R.L. Phillips, J. Rumpler 1988: Seismic stratigraphy and depositional framework of sedimentary rocks in the Pannonian Basin in southeastern Hungary. – In: L.H. Royden, F. Horváth eds.: The Pannonian Basin. A study in basin evolution, AAPG Memoir, 45, pp. 117–145.
- Papp, A. 1951: Das Pannon des Wiener Beckens. – Mitt. geol. Ges. Wien, pp. 39–41, 99–103.
- Pogácsás, Gy. et al. 1988: Seismic facies, electro facies and Neogene sequence chronology of the Pannonian Basin. – Acta Geologica Hungarica, 31, pp. 175–207.
- Pogácsás, Gy. et al. 1989: A nagyalföldi neogén képződmények kronosztratigrafiái viszonyai szeizmikus és paleomágneses adatok összevetése alapján. – Magyar Geofizika, 30, pp. 41–62.
- Stevanovic, P.M. 1951: Pontische Stufe im engeren Sinne – Obere Congerienschichten Serbiens und der angrenzenden Gebiete. – Serb. Akad. Wiss., Math. – naturw. Kl., Beograd, 187.
- Strausz, L. 1942: Das Pannon des mittleren Westungarns. – Ann. Hist. – Nat. Mus. Nat. Hung., 35, pp. 1–102.
- Széles, M. 1971: A Nagyalföld medencebeli pannon képződményei. – In: Góczán F., Benkő J. eds.: A magyarországi pannonkori képződmények kutatásai, Akadémiai Kiadó, Budapest, pp. 253–344.

Diagenesis and low-temperature metamorphism in a tectonic link between the Dinarides and the Western Carpathians: the basement of the Igal (Central Hungarian) Unit

P. Árkai, Cs. Lantai, I. Fórizs

Laboratory for Geochemical Research
Hungarian Academy of Sciences, Budapest

Gy. Lelkes-Felvári

Hungarian Geological Institute, Budapest

The Igal (Central Hungarian) Unit represents a complicated tectonic zone connecting the Internal Dinarides and the Bükk Unit which forms the innermost part of the Western Carpathians at present, and which was dislocated by Meso-Alpine, large scale horizontal crustal block ("microplate") movements from its original position, from the Dinarides. The basements of the Igal Unit is built up by Late Paleozoic, and predominantly, by Mesozoic (Triassic) formations. Microstructural, mineral paragenetic, illite "crystallinity", white mica b_0 geobarometric, vitrinite reflectance and carbonate geothermometric methods were applied in order to determine the grades of diagenesis and metamorphism of the basement rocks deriving from hydrocarbon exploratory bores. For geologic interpretation of the petrologic data, the lithostratigraphic and facies classification of Bérczi-Makk (1988) served as a base.

In the Northern Zone of the Igal Unit, the Transdanubian Midmountains type Mesozoic (near village Sávo) shows only the signs of diagenesis. The grades of regional alterations in the Dinaric type formations of the Northern Zone are varying: diagenetic (village Nikla), dynamothermal anchizonal (village Öreglak), and low-T contact metamorphic (villages Buzsák and Újfal). In the Dinaric type Mesozoic of the Southern Zone epizonal (villages Semjénháza, Pat), anchizonal (villages Inke, Iharosberény and Bajcsa), and diagenetically altered rocks (villages Pátró, Liszó, Murakeresztúr) were distinguished. Low- to intermediate fluid (H_2O) pressure ranges (high to intermediate metamorphic thermic gradients) are characteristic of the Eo-Alpine (Cretaceous) regional metamorphism. Polyphase retrograde metamorphism connected to cataclastic deformation, contact metamorphism, low-T hydrothermal alterations are the signs of younger (Meso-Alpine) tectogenesis.

Keywords: Low-T metamorphism, diagenesis, anchizone, epizone, illite "crystallinity", vitrinite reflectance, b_0 geobarometry, carbonate geothermometry, Igal Unit, Mesozoic, Dinarides, Western Carpathians

Introduction

The geologic and tectonic position of the Igal (Central Hungarian) Unit is demonstrated in Fig. 1. The south-alpine and dinaric affinities of the stratigraphic, lithologic and paleontological features of the Paleozoic and Mesozoic formations in the Bükkium (NE-Hungary) were recognised by Balogh (1964), and have been confirmed by several authors since then. At present, the internal dinaric type Bükkium forms the innermost part of the Western Carpathians. Wein (1969) supposed paleogeographic connection between Bükkium and the Internal Dinarides

Addresses: Péter Árkai, Csaba Lantai, István Fórizs: H-1112, Budapest, Budaörsi út 45, Hungary,
Gyöngyi Lelkes-Felvári: H-1143 Népstadion út 14, Hungary
Received: February 11, 1991

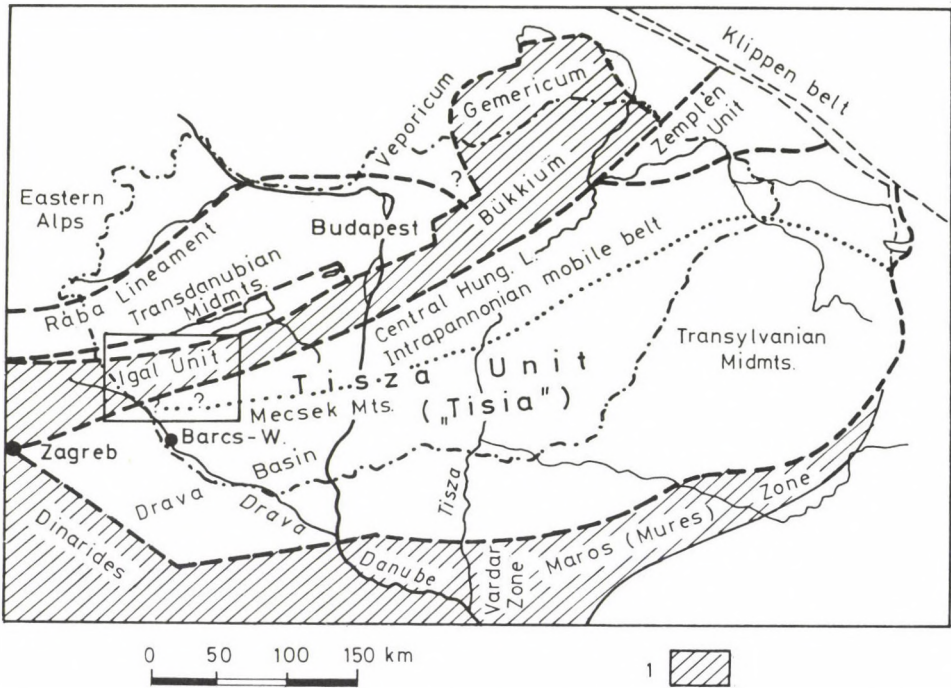


Fig. 1. Tectonic sketch map of Hungary after Kovács (1984), with the location of the investigated area. 1. Alpine mobile zones

("Igal-Bükk eugeosyncline"). Further investigations have not proved the existence of such a small-scale, separate paleogeographic, paleotectonic unit, and the present, exotic position of the Bükkium has been interpreted by large-scale, horizontal block ("microplate") movements. Thus, the Igal (Central Hungarian) Unit represents a complicated tectonic zone, along which the Bükkium was shifted several hundred kilometres to ENE from its original position corresponding to the north-western part of the Dinarides, during the Meso-Alpine tectonophases (Kovács 1982 Kázmér and Kovács 1985, Haas 1987, Balla 1988).

In the Bükkium Alpine (Cretaceous, pre-Senonian) regional metamorphism was evidenced. The metamorphic grade varies from deep diagenesis through the anchizone up to the epizone (chlorite, maximally biotite isograds). In metavolcanites mineral associations corresponding to the prehnite-pumpellyite, pumpellyite-actinolite and greenschist facies were determined. Low and low-intermediate pressure (high to high-intermediate metamorphic thermal gradient) conditions are characteristic of the Bükkium (Árkai 1983a).

On the contrary, the Late Paleozoic formations explored by boreholes in the Igal Unit have been considered as non metamorphic in general (Kázmér 1986), notwithstanding that only sporadic petrographic data have been published so far.

Tomor (1957) postulated the presence of metamorphosed Mesozoic – by means of lithostratigraphic analogies – in the bore Inke-9, describing serpentinite and contact dolomitic limestone. Árkai (1983b) determined anchi- and epizonal regional metamorphism in the core samples of bores Inke-I, Iharosberény Ib-2 and Semjénháza Sem-3. The bore Inke-I supplied first time Mesozoic biostratigraphic data (Middle Carnian radiolarians) recognised as metamorphic from this unit (Chikán et al. 1985, Haas et al. 1988).

The present paper aims at the metamorphic petrogenetic characterization of the basement rocks of this unit.

Geology

The geologic-tectonic map of the pre-Neogene basement of the Transdanubian part of the Pannonian Basin was constructed and improved by Bardócz (1973–1986). A part of this map served as a base for Fig. 2.

The Igal Unit is separated by the Paleogene Balaton Lineament from the Transdanubian Midmountains Unit in NW and by the Central Hungarian (Zagreb-Zemplén) Lineament from the Tisza Unit in SE. For metamorphic petrological characterization of the northwestern surroundings see Lelkes-Felvári (1978, 1987, the latter in Árkai and Lelkes-Felvári, 1987) and Árkai (1987), for that of the Tisza Unit see Lelkes-Felvári and Sassi (1981), Árkai (1984), Árkai et al. (1985). The pre-Neogene formations of the Igal Unit continue towards WSW in the Sava folds of the Dinarides and towards ENE in the Bükkium, although the details of the connections are not known (Fülöp 1989).

Recently, Kázmér (1986) summarized the (mostly not published) stratigraphic, lithologic and paleontologic data of Bérczi-Makk, Haas, Jámbor, Juhász and Vass, Szabó, Sztrákos and Vető-Ákos (for references see the cited work of Kázmér). The strongly hypothetical stratigraphic column of the given zone consists of Upper Carboniferous limestone, Lower and Middle Permian marine sandstone, slate, dolomite and limestone (Újfalu Limestone Formation), Upper Permian calcareous silt, dolomite and limestone, Lower Triassic dolomitic marl, Middle Triassic tuffitic Buchenstein beds and algal dolomite, Upper Triassic (Norian) dolomite, Mesozoic ophiolitic rocks (basalt, spilite, gabbro, radiolarite) of unknown tectonic and stratigraphic position, and Cretaceous (?) red claystone, silt and conglomerate. This sequence is unconformably overlain by Eocene, Oligocene and younger sediments. Magmatic activity is characterized by Triassic (?) ophiolitic magmatism and Paleogene calc-alkaline volcanism. Melange type rocks formed by folds, overthrusts and transcurrent faults are common. It is worth to mention that presumed Paleozoic (Silurian, Devonian?) formations indicated by Bardócz near the southern border of the Igal Unit (villages Inke, Iharosberény), the anchizonal regional metamorphism of which were determined formerly by Árkai (1983b), have not been interpreted in the summary of Kázmér.

Detailed lithostratigraphic and partly biostratigraphic reambulation of the area by Bérczi-Makk (1988) and Bérczi-Makk et al. (1990) proved the former statements of Kovács (1982) and Kázmér (1986), emphasizing that the Igal Unit is a compres-

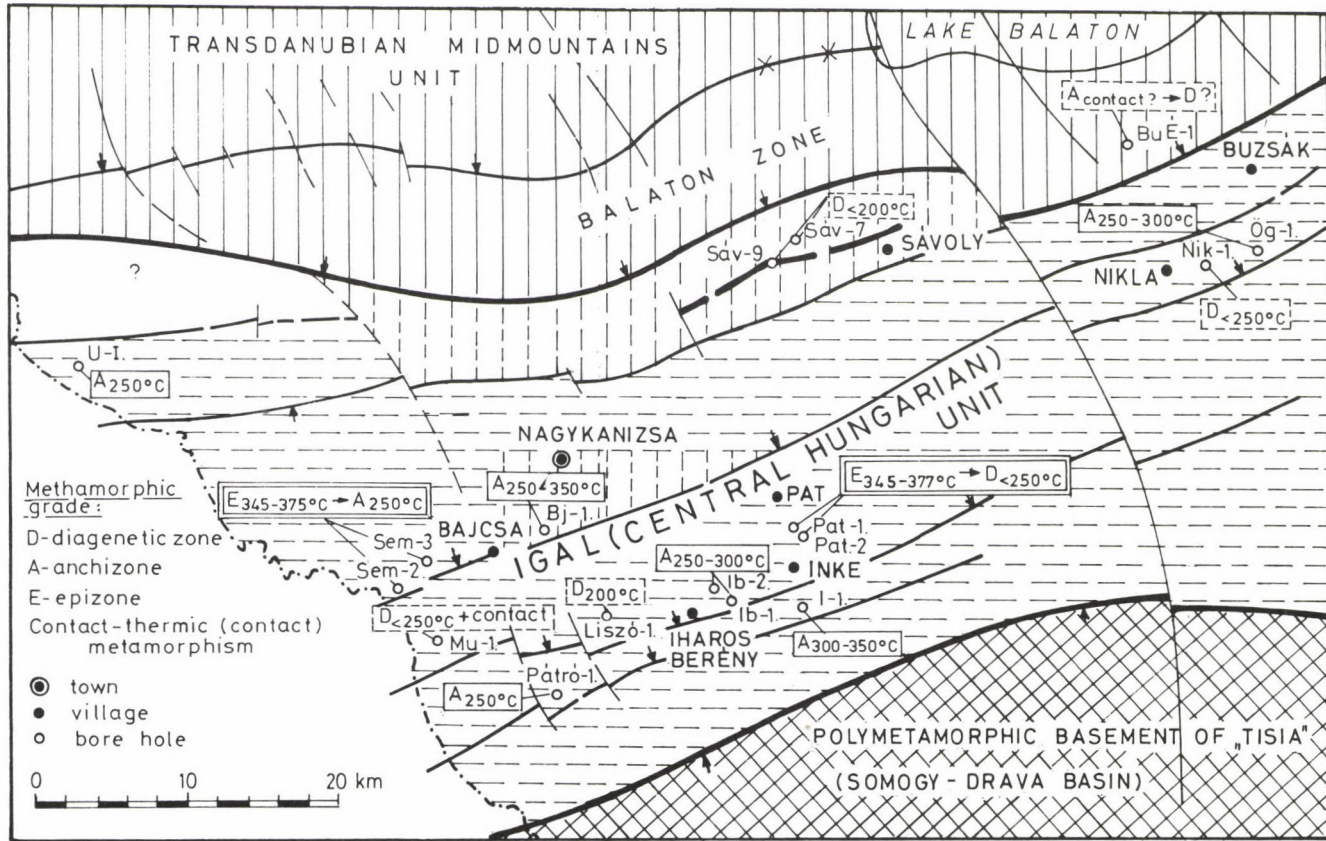


Fig. 2. Tectonic sketch map of the Igal Unit after Bardócz (1973–1986) with the distribution of the Investigated borehole materials. Diagenetic and metamorphic zones and the approximated temperatures of alterations are also indicated

sive, strongly tectonized zone, in which various parts of different geologic units were juxta- or superposed. Evaluating the Mesozoic facies types, the following four subunits were distinguished by Bérczi-Makk:

I. Dinaric type Mesozoic (based on the Ladinian carbonate platform facies): zone between villages Somogyásmon – Táska – Buzsák;

II. Transdanubian Midmountains type Mesozoic (based on the Ladinian radiolarian, tuffitic limestones and Upper Triassic platform facies carbonates): Nagybonak – Újudvar – Sávoly;

III. Triassic formations of uncertain (possibly Transdanubian Midmountains type) affinities: Bajcsa – Bagolasánc – Nagyrécse;

IV. Dinaric (presumably Bükk) type Mesozoic: non-metamorphic neritic carbonates and anchizonal metamorphic fine-detritic facies units, having irregular contacts along younger tectonic faults and overthrust surfaces.

Neither Jurassic nor Cretaceous formations were proved by Bérczi-Makk.

Methods

In addition to the mesoscopic and light microscopic observations, which included also the measurement of vitrinite reflectance, X-ray diffractometric (XRD), and electron microprobe investigations were carried out on selected core materials.

The XRD investigations aimed at the determination of qualitative and semi-quantitative mineral composition of rocks, their acid insoluble residue samples (using 3% HCl) and <2 μm grain size fractions. Illite "crystallinity" (IC) indices after Kübler (1968, 1975) for metamorphic zone determinations and white mica b_0 parameters for geobarometric purposes (Sassi 1972, Guidotti and Sassi 1976, 1986) were also measured on different mounts.

XRD recording conditions were: $\text{CuK}\alpha$ radiation, 45 kV/35 mA, graphite monochromator proportional counter, divergency and detector slits: 1° , goniometer speeds of $2^\circ/\text{min}$ and $1/2^\circ/\text{min}$, time constant: 2 s, chart speed: 2 cm/min.

All the details of sample preparations, mounting, and IC calibration were given earlier (Árkai 1983a, 1987, 1990). The correlation of IC zones with coal rank and meta-basite mineral facies is given here only for rough orientation (Fig. 3). In the following diagenetic, anchi- and epizones are used as they are interpreted in Fig. 3 with the remark "present work". Using this figure, the original zone classification of Kübler can be easily applied for our IC data, thus the corresponding IC zones (in the sense of Kübler) can be determined. The problems of delimitation of the anchizone based solely on IC values or on the complex application of different parameters were discussed in detail earlier (Árkai 1987, 1991).

Chemical compositions of carbonate minerals were determined by a JEOL Superprobe 733 electron microprobe equipped with an energy dispersive spectrometer (EDS) device, under the following conditions: 15 kV, 2.8 nA, electron beam diameter of 10 μm , counting time: 40 s. Carbonate standards from Smithsonian Institution were used, namely calcite-136321 for Ca, dolomite-10057 for Mg, and siderite-R2460 for Mn and Fe measurements (Jarosewich and Macintyre 1983).

Results, discussion

Rock samples of the basement of the Igal Unit selected for metamorphic studies are listed in Table 1. All the cores derive from hydrocarbon exploratory boreholes. Table 2 contains the mineral compositions of the samples determined by XRD technique. The metamorphic grade (zone) and pressure indicating illite-muscovite parameters can be found in Table 3, the vitrinite reflectance data in Table 4.

Taking into consideration the relatively large area covered by this study, the sporadic distribution of the samples (Fig. 2) as well as the big variety of rock types (Table 1) and the large scattering of metamorphic grade indicating parameters, it seems to be obvious that only a mosaic-like picture can be constructed about the metamorphic conditions of the basement.

From the *Transdanubian Midmountains type part of the Northern Zone* (Zone II of Bérczi-Makk (1988)) Triassic (?) rock types of the bores *Sávoly Sáv-7* and *Sáv-9* were investigated (Table 1). The varying clay mineral assemblages and the also varying, dominantly large IC values (Table 2 and 3) refer to diagenetic alterations. The rock type of the metavolcanite can not be determined exactly due to the strong weathering (carbonate and clay mineral formation). Based on the small (secondary) quartz and the significant feldspar contents, intermediate character can be supposed.

Contrasting the *Transdanubian Midmountains type* basement rocks, the grade of regional alteration of the *Dinaric type basement* of the Northern Zone is rather varying.

Based on the chlorite+sericite assemblage, IC and R data as well as on microstructural characteristics, the Permian dolomite and metasandstone from the bore *Újfalu U-1* represent low-T anchizonal (about 250°C) conditions. The granoblastic texture of the dolomite indicates recrystallization conditions without oriented pressure. The available data do not allow to make conclusions about the contact (static) or dynamothermal nature of the alteration (the former one seems to be more probable).

Also anchizonal, but – judging from slaty cleavage, preferred sericite orientation – dynamothermal type metamorphism was proved by IC data in case of slates from bore *Óreglak Óg-1*. The phyllosilicates of slates are illite-muscovite and chlorite, the b_0 parameter of illite-muscovite refers to low pressure range (Table 3). Formerly, these rocks were hypothetically interpreted as dismembered parts of the Early Paleozoic complex of the *Transdanubian Midmountains*, which was affected by low-T/low-P Hercynian regional metamorphism (Balázs and Juhász 1969). The age of the regional metamorphism proved to be 96.7 ± 12.3 Ma (determined by K–Ar isotopic method by Kadosa Balogh on the $<2 \mu\text{m}$ sericite fractions of the slates, pers. communication), contradicting to the lithostratigraphic correlation mentioned above. As in other cases, the Mesozoic (Triassic) sedimentation age seems to be the more probable at present.

The matamorphic grade of the Triassic (?) limestone with claystone intercalations, fissure fillings (core No. 4), brecciated, ankeritic limestone (core No. 5) and banded, slaty, ankeritic marl and sandy dolomite (core No. 6) of the bore *Buzsák*

Table 1. List of rock samples from the basement of the Igal Unit selected for metamorphic petrological research

location village	bore	core	depth (m)	rock type	age
Újfalu	U-I.	1.	3369.0–3372.0	dolomite ("crystalline")	P
Újfalu	U-I.	4.	3700.5–3702.5	metasandstone	P
Sávoly	Sáv-7.	5.	1467.0–1471.0	dolomitic clay-marl	T
Sávoly	Sáv-9.	3.	1406.5–1410.0	ankeritic limestone breccia	T
Sávoly	Sáv-9.	4.	1584.0–1587.0	intermediate–basic(?) metavolcanite	T
Sávoly	Sáv-9.	5.	1650.0–1655.0	carbonatic, brecciated metavolcanite	T
Sávoly	Sáv-9.	6.	1765.5–1768.5	carbonatic metavolcanite	T
Nikla	Nik-1.	17.	1858.0–1862.0	banded pelitic limestone/marl	T
Buzsák	Bu-K-1.	4.	1065.0–1069.0	I: limestone, II: claystone (metatuffite?)	T
Buzsák	Bu-K-1.	5.	1125.0–1128.5	I: ankeritic limestone, II: brecciated limestone	T
Buzsák	Bu-K-1.	6.	1195.0–1199.0	a) ankeritic marl intercalated with b) sandy dolomite	T
Öreglak	Ög-1.	29.	2487.5–2489.5	Calcareous slate (pelitic/silty)	T
Öreglak	Ög-1.	30.	2528.0–2531.0	brecciated, carbonatic slate (pelitic/silty)	T
Semjénháza	Sem-2.	13.	3241.5–3247.0	a) limestone; b) dolomitic limestone (I) and cipolino (II, III)	T
Semjénháza	Sem-2.	14.	3300.0–3302.5	slate (silty, with metasandstone lenses)	T
Semjénháza	Sem-2.	15.	3334.0–3336.0	slate (silty, carbonatic)	T
Semjénháza	Sem-2.	16.	3377.0–3381.5	dolomite (brecciated)	T
Semjénháza	Sem-2.	17.	3432.5–3435.0	brecciated slate (pelitic–silty: Ia and IIa, silty–psammitic: Ib and IIb), metasandstone (III)	T
Semjénháza	Sem-3.	7.	3154.0–3156.5	metarhyolite–tuff	T
Semjénháza	Sem-3.	11.	3313.0–33.14.5	carbonatic metasandstone (schistose)	T
Semjénháza	Sem-3.	14.	3545.5–3548.0	magnesian anhydrite rock with slate fragments	T
Semjénháza	Sem-3.	18.	3767.0–3775.0	brecciated dolomite with anhydritic fissure filling	T
Murakeresztúr	Mu-1.	4.	3304.0–3308.0	limestone, partly brecciated	T
Murakeresztúr	Mu-1.	5.	3345.0–3350.0	shale (a) and metarhyolite tuffite contacts (b and c)	T
Bajcsa	Bajcsa-M-1.	2.	3076.0–3078.0	banded chert/slate	T
Liszó	Liszó-1.	18.	2363.5–2365.0	shale (marly)	T
Liszó	Liszó-1.	19.	2415.5–2416.5	shale (with carbonate+quartz bands, lenses)	T
Liszó	Liszó-1.	20.	2467.0–2468.0	laminated dolomite	T
Pátró	Pátró-1.	10.	1692.0–1692.6	banded, carbonatic, psammitic siltstone	T
Pátró	Pátró-1.	12.	1851.0–1854.0	banded slate (silty/pelitic)	T
Pátró	Pátró-1.	14.	1964.0–1969.5	limestone ("crystalline")	T
Iharosberény	Ib-1.		1838.0	slate (siliceous)	T
Iharosberény	Ib-1.		1839.0	slate (siliceous)	T
Iharosberény	Ib-1.		1842.4	slate (siliceous)	T
Iharosberény	Ib-1.		1848.0–1849.4	slate (siliceous)	T
Iharosberény	Ib-1.		1944.7	slate (siliceous)	T
Iharosberény	Ib-2.	20.	2248.0–2249.0	slate (siliceous, carbonatic)	T
Inke	Inke-I.	10.	4551.0–4553.0	intermediate metavolcanite (tuff?)	T
Inke		11.	4657.0–4659.0	metarhyolite tuff	T
Inke		12.	4790.0–4791.0	serpentinite	T
Inke		13.	4870.0–4871.0	limestone ("crystalline")	T
Inke		14.	4880.5–4881.5	carbonatic metatuffite (rhyolitic?)	T
Inke		15.	4946.0–4947.0	slate	T
Inke		16.	4999.0–5000.0	carbonatic slate (pelitic, siliceous)	T
Inke	Inke-9.	12.	1715.5–1721.5	spilite (metabasalt)	T
Inke	Inke-9.	13.	1727.0–1729.0	spilite (metabasalt)	T
Pat	Pat-1.	20.	2002.5–2005.5	a) silty sandstone (M); b) brecciated dolomite marble	T
Pat	Pat-1.	21.	2005.5–2007.5	brecciated dolomite marble	T
Pat	Pat-1.	22.	2094.0–2097.0	brecciated dolomite	T
Pat	Pat-1.	23.	2107.0–2109.0	brecciated dolomite and dolomite marble	T
Pat	Pat-2.	8.	2056.5–2058.0	brecciated calcite–dolomite marble	T
Pat	Pat-2.	10.	2108.0–2110.5	brecciated calcite–dolomite marble	T
Pat	Pat-2.	16.	2262.5–2264.5	dolomitic limestone ("crystalline")	T
Pat	Pat-2.	17.	2300.0–2301.0	dolomitic limestone ("crystalline")	T
Pat	Pat-2.	18.	2333.0–2334.0	dolomite ("crystalline", partly brecciated)	T

P – Permian, T – Triassic, M – Miocene

Table 2. Mineral composition of basement rocks, Igal Unit (XRD data)

sample	quartz	plagioclase (albite)	kalifeldspar	illite-muscovite	pyrophyllite	chlorite	vermikulite	kaolinite	illite/smectite	mixed layer	smectite	calcite	dolomite	ankerite	siderite	magnesite	pyrite	hematite	goethite	rutil	gypsum	anhydrite	baryte	chrysotile
U-11.	x	x	o	x								o	+				o	tr						
U-14.	x	o	x	o		x						x	x				o	tr		tr				
Sáv-7/5/a	x	o	x	x				o		x		x	x				o	o		tr				
Sáv-7/5/l	x	tr	x	x				o				o	x				tr			tr				
Sáv-9.3.	o	x	x	tr	x			tr				+		x			tr							
Sáv-9.4.	x	x	x	x				tr				+					tr							
Sáv-9.5.	x	x	x	x				tr				+		x			o							o
Sáv-9.6.	x	x	x	x				tr				o	tr											
Nik-1.17/a	x	o	tr	x	o			o		o		+	tr				tr			tr				
Nik-1.17/b	o	tr	o	tr	o			o		o		+					tr			tr				
Bu-K-1.4/l.	tr	o	tr	x	tr			x		o		+					tr							
Bu-K-1.4/ll.	tr	o	tr	x	x			x		o		+					tr							
Bu-K-1.5/l.	o	tr	o	tr	tr			tr		tr		+					tr							
Bu-K-1.5/ll.	tr	x	o	tr	o			tr		tr		+					tr							
Bu-K-1.6/a	x	x	o	tr	o			o		+		o	+				tr							
O ₅ -1.29.	x	x	x	x	x			x		x		x	o				tr			tr				
O ₅ -1.30.	x	x	x	x	x			o		o		x	o				tr			tr				
Sem-2.13/a	o	o	o	o	o			o		+		tr	x				tr			tr				tr
Sem-2.13/bI.	o	o	o	o	o			o		x		tr	x				tr			tr				
Sem-2.13/bII.	o	o	o	o	o			o		x		+	x				tr			tr				
Sem-2.13/bIII.	o	o	o	o	o			tr		o		+	x				tr			tr				
Sem-2.14.	x	x	x	x	x			o		+		o	+				tr			tr				
Sem-2.15.	x	x	x	x	x			tr		o		+	x				tr			tr				
Sem-2.16.	o	o	o	o	o			tr		+		o	+				tr			tr				
Sem-2.17/1a.	o	x	o	x	o			o		tr		o	+	x			tr			tr				
Sem-2.17/b.	+	+	+	+	+			+		+		+	+				+			+				
Sem-2.17/IIa	x	x	x	x	x			x		o		x	o				o			o				tr
Sem-2.17/IIb	x	x	x	x	x			x		o		x	o				o			o				tr
Sem-2.17/III	x	x	x	x	x			o		+		+	+				+			+				+
Sem-3.7	+	+	+	+	+			+		+		+	+				+			+				+
Sem-3.11.	o	x	o	x	o			tr		o		o	x				tr			tr				o
Sem-3.14.	o	o	o	o	o			tr		+		+	+				tr			tr				+
Sem-3.18.	o	o	o	o	o			tr		+		+	+				tr			tr				+
Mu-1.4.	tr	x	tr	tr	o			o		+		+	o				tr			tr				+
Mu-1.5/b-c	x	x	tr	tr	o			o		+		+	+				tr			tr				+
Bajcsa-M-1.2	x	x	x	tr	o			o		x		tr	x				tr			tr				
Liszó-1.18.	x	x	tr	x	x			o		tr		tr	tr				tr			tr				
Liszó-1.19.	+	+	tr	tr	tr			o		tr		tr	tr				tr			tr				
Liszó-1.20.	tr	tr	tr	tr	tr			tr		+		+	+				tr			tr				
Pátró-1.10.	x	x	x	o	x			x		o		o	o				tr			tr				
Pátró-1.12	x	x	x	x	tr			tr		+		+	+				tr			tr				
Pátró-1.14.	tr	tr	tr	tr	tr			tr		+		+	+				tr			tr				
Ib-1./aII'	+	+	+	x	x			x		o		o	o				o			tr				tr
Ib-2.20.	+	+	+	x	x			x		o		o	o				o			tr				tr
Inke-1.10.	x	x	o	x	x			o		tr		x	x				o			o				+
Inke-1.11.	x	o	x	x	o			o		tr		tr	x				tr			tr				
Inke-1.12.	x	x	o	x	x			o		tr		tr	x				tr			tr				
Inke-1.13.	tr	tr	tr	tr	tr			tr		+		+	+				tr			tr				
Inke-1.14.	x	x	o	x	x			tr		+		+	+				tr			tr				
Inke-1.15.	x	x	o	x	x			tr		+		+	+				tr			tr				
Inke-1.16.	x	x	tr	x	x			tr		x		x	x				tr			tr				
Inke-9.12-13.	o	+	+	x	x			o		+		+	+				tr			tr				
Pat-1.20/a	x	x	tr	x	tr			o		x		tr	tr				tr			tr				
Pat-1.20/b	tr	tr	tr	tr	tr			tr		+		+	+				tr			tr				
Pat-1.21-23.	o	o	o	o	o			tr		+		+	+				tr			tr				
Pat-2.8.	o	tr	o	tr	tr			tr		+		+	+				tr			tr				
Pat-2.10.	o	tr	o	tr	tr			tr		+		+	+				tr			tr				
Pat-2.16-17.	o	tr	o	tr	tr			tr		+		+	+				tr			tr				
Pat-2.18.	o	tr	o	tr	tr			tr		+		+	+				tr			tr				

Legend: + dominant (>50%), x abundant (10-50%), o subordinate (1-10%), tr traces (<1%)

Table 3. "Crystallinity" and b_0 data of illite–muscovite

sample or sample group	whole rock and acid insoluble residue samples									<2 μ m fraction samples					
	2 $^\circ$ /min			IC ($\Delta^\circ 2\theta$)			b^0 (Å)			2 $^\circ$ /min			IC ($\Delta^\circ 2\theta$)		
				1/2 $^\circ$ /min									1/2 $^\circ$ /min		
\bar{x}	s	n	\bar{x}	s	n	\bar{x}	s	n	\bar{x}	s	n	\bar{x}	s	n	
U-1.4.	0.255	-	1	0.186	-	1	8.992	-	1	-	-	-	-	-	-
Sáv-7.5/a	0.536	-	2	0.449	-	2	8.993	-	2	0.535	-	1	0.507	-	1
Sáv-7.5/I	0.403	-	2	0.351	-	2	9.006	-	2	0.471	-	2	0.419	-	2
Sáv-9.3	-	-	-	-	-	-	-	-	-	0.936	-	1	-	-	-
Sáv-9.4,6	-	-	-	-	-	-	-	-	-	1.329	-	2	0.837	-	1
Nik-1.17/a-b	0.504	-	2	0.495	-	2	9.013	-	1	0.906	-	2	0.807	-	1
Bu-K-1.4/I.	-	-	-	-	-	-	-	-	-	1.161	-	1	-	-	-
Bu-K-1.4/II.	-	-	-	-	-	-	-	-	-	2.507	-	2	-	-	-
Bu-K-1.5/I.	-	-	-	-	-	-	-	-	-	1.318	-	2	-	-	-
Bu-K-1.5/II.	-	-	-	-	-	-	-	-	-	1.286	-	2	1.231	-	1
Bu-K-1.6.	0.468	-	1	-	-	-	8.990	-	1	0.680	-	1	0.548	-	1
Ög-1. 29-30	0.286	0.048	6	0.241	0.027	4	8.996*	-	3	0.327	-	2	0.280	-	1
Sem-2 and -3 carbonatic rocks incl. cipollino (Sem-2.13, 16):	0.241	0.031	5	0.177	0.053	5	9.010	0.010	5	0.242	-	3	0.191	-	3
slates (Sem-2.14, 15):	0.256	0.024	4	0.177	0.025	4	9.024*	0.008	4	-	-	-	-	-	-
brecciated slate, metasandstone (Sem-2.17., Sem-3.11.):	0.355	0.037	6	0.292	0.054	6	9.017	0.007	6	0.362	0.042	6	0.303	0.049	6
metarhyolite-tuff (Sem-3.7.):	0.442	-	1	0.312	-	1	-	-	-	0.671	-	1	0.663	-	1
Mu-1.4/a-b	-	-	-	-	-	-	-	-	-	1.040	-	2	-	-	-
Mu-1.5/b (metarhyolite tuffite):	0.614	-	2	-	-	-	9.006	-	1	1.268	-	1	-	-	-
Mu-1.5/c (shale):	0.666	-	-	-	-	-	8.995	-	1	0.652	-	1	0.555	-	1
Bajcsa -M-1.2	0.345	-	1	0.258	-	1	-	-	-	0.290	-	1	0.205	-	1
Liszó-1.18.	0.374	-	3	0.319	-	3	9.028	-	2	0.383	-	2	0.339	-	2
Liszó-1.20.	0.527	-	1	0.412	-	1	9.008	-	1	0.342	-	1	-	-	-
Pátró-1.10.	-	-	-	-	-	-	-	-	-	0.329	-	1	0.286	-	1
Pátró-1.12.	0.460	-	1	0.413	-	1	9.005	-	1	0.601	-	1	0.551	-	1
Pátró-1.14.	-	-	-	-	-	-	-	-	-	0.271	-	1	0.172	-	1
Ib-1. 1839.0-1944.7 m	0.360	0.036	6	0.322	0.024	6	9.000	0.004	6	0.371	0.048	6	0.308	0.052	6
Inke-I.10.	0.297	0.054	4	0.210	-	2	9.025	0.010	4	0.391	-	3	0.263	-	1
Inke-I.11.	0.262	0.029	7	0.186	0.010	5	9.028	0.005	7	0.287	0.087	5	0.242	0.087	6
Inke-I.14.	0.357	-	2	0.312	-	2	9.017	-	2	0.358	-	2	0.325	-	2
Inke-I.15.	0.238	-	1	0.178	-	1	8.994	-	1	0.266	-	1	0.231	-	1
Inke-I.16.	0.227	-	3	0.194	-	3	9.025	-	3	0.272	-	3	0.196	-	3
Pat-1 and -2, silty sandstone (Pat-1.20/a)	0.303	-	1	-	-	-	9.008	-	1	0.380	-	1	0.282	-	1
brecciated dol. marble and dolomite (Pat-1.21, 22, 23; Pat-2.8, 19.):	0.365	-	3	0.308	-	3	9.008	-	3	0.583	-	4	0.543	-	4
dolomitic limestone (Pat-2.16, 17):	0.280	-	2	0.261	-	2	9.012	-	2	0.217	-	2	0.167	-	1
dolomite (Pat-2.18):	0.353	-	1	-	-	-	9.020	-	1	0.234	-	1	0.147	-	1

\bar{x} – average; s – standard deviation; n – number of samples; * – b_0 value, applied for pressure estimation

Table 4. Coal petrographic characterization and vitrinite reflectance values

sample	coalified particles	n	Rrandom	Rmax	Rmin	ΔR (bireflectance)
U-I.4	autochthonous anthracite	50	$\frac{3.05}{(0.25)}$	$\frac{3.43}{(0.26)}$	$\frac{2.47}{(0.40)}$	$\frac{0.96}{(0.46)}$
Nik-1.17.	bituminous coal + allochthonous graphite flakes	3	1.74	1.82	1.53	0.29
Sem-2.17/I a, b	graphite		not measurable			
Mu-1.5/b	metaanthracite	30	$\frac{4.05}{(0.48)}$	$\frac{5.45}{(0.59)}$	$\frac{2.68}{(0.67)}$	$\frac{2.77}{(1.01)}$
Mu-1.5/c	metaanthracite	35	$\frac{4.61}{(0.62)}$	$\frac{5.66}{(0.83)}$	$\frac{3.46}{(0.56)}$	$\frac{2.20}{(0.87)}$
Pátró-1.12.	autochthonous anthracite	20	$\frac{3.06}{(0.68)}$	$\frac{3.50}{(0.66)}$	$\frac{2.22}{(0.47)}$	$\frac{1.28}{(0.68)}$
Ib-2.20.	fine-grained anthracite		not measurable			
Inke-1.16.	fine-grained anthracite		not measurable			

n = number of measurements

$$\frac{\text{average}}{\text{(standard deviation)}}$$

Bu-K-1 is rather uncertain. Clay mineral assemblages of the pelites and the acid insoluble residues of carbonatic rock types consist of illite, illite/smectite irregular mixed-layer clay mineral, kaolinite and chlorite, characteristic of only slight, diagenetic alteration. On the contrary, strong, static recrystallization of the carbonatic rock types implies considerable thermic (contact metamorphic) effect. To explain this contradiction, two hypotheses were set up:

(i) contact metamorphism of pure carbonatic rocks followed by fracturing. The open fissures were filled later on by non-metamorphic pelitic-marly material;

(ii) the carbonatic rocks together with their (syngenetic) pelitic-marly intercalations suffered contact (thermal) metamorphism. The observed clay mineral assemblages are younger than the contact metamorphism, and may reflect the degradational effects of circulating younger, low-T hydrothermal fluids.

The clay mineral assemblage (illite, illite/smectite, kaolinite and chlorite), IC and R data refer to diagenetic (middle diagenetic, wet gas zone) alteration of the Triassic (?) banded, pelitic limestone and marl of the bore *Nikla Nik-1*.

In the *Southern Zone* strongly varying diagenetic - metamorphic grades were determined. No systematic differences were found between the presumed Transdanubian Midmountains and Dinaric-Bükk type parts of Bérczi-Makk (1988), or between the carbonatic and clastic lithofacies. In metamorphic grade no regular spatial changes were found either.

From the bores *Semjénháza Sem-2* and *-3* Lower Triassic (?) metasedimentary rocks (limestone, dolomitic limestone, cipollino-like limestone with sericite–chlorite bands, networks, dolomite, slate (pelitic, silty, carbonatic, subordinately psammitic) and metarhyolite tuff was described (Table 1)). Microstructural features (penetrative continuous cleavage in slates, weak crenulation, rough cleavage in clastics, preferred orientation of phyllosilicates, slight pressure shadow, and recrystallization of carbonate minerals) refer to regional (dynamothermal) effect. IC averages suggest epizonal (greenschist facies chlorite zone) alteration. b_0 data of slate with adequate mineral composition (quartz, albite, sericite, pyrite) indicate intermediate fluid (H_2O pressure range ($b_0=9.014–9.034$, in average, 9.024 \AA). Carbonate geothermometric calculations (Table 6) based on chemical composition of coexisting calcite and dolomite (Table 5) proved the low-T greenschist facies conditions presumed by IC data ($345–375^\circ\text{C}$, in average, $362 \pm 13^\circ\text{C}$).

This event was followed by cataclastic deformation connected with a new phase of illite-muscovite neof ormation or recrystallization. IC data of the brecciated slate and dolomite suggest temperature corresponding to the boundary between diagenetic and anchizones (cca 250°C). Thus, a retrograde overprint could be demonstrated by combined application of microstructural observations, IC and carbonate geothermometric data.

Table 5: Average chemical composition of coexisting calcite and dolomite in carbonatic metamorphic rocks EDS electron microprobe analyses

sample	Sem-2.13/b/II				Pat-2.10			
	7 calcite		6 dolomite		5 calcite		5 dolomite	
number of measurement mineral	\bar{x}	s	\bar{x}	s	\bar{x}	s	\bar{x}	s
	weight %							
MgCO ₃	1.47	0.64	41.82	1.84	1.55	0.26	45.12	0.47
CaCO ₃	96.41	1.35	54.82	1.01	97.99	1.56	55.76	1.03
MnCO ₃	0.04	0.04	0.02	0.04	0.11	0.16	0.12	0.09
FeCO ₃	0.36	0.21	3.18	0.20	0.28	0.41	0.17	0.22
total	98.33		99.50		99.93		101.17	
	mole %							
MgCO ₃	1.77	0.77	46.44	1.44	1.83	0.32	48.88	0.28
CaCO ₃	97.87	0.93	50.98	1.47	97.83	0.48	50.89	0.43
MnCO ₃	0.04	0.04	0.02	0.04	0.10	0.14	0.10	0.07
FeCO ₃	0.32	0.19	2.57	0.16	0.24	0.35	0.13	0.17

\bar{x} – average, s – standard deviation

In case of metarhyolite tuff, microstructural features refer to anchizonal conditions, whereas IC corresponds only to the diagenetic zone. As no signs of retrograde (cataclastic) effects could be observed, chemical weathering may be the cause of this discrepancy.

Also epizonal (greenschist facies, chlorite zone) metamorphism was demonstrated by IC and carbonate geothermometric data (Tables 3, 5 and 6) for non-brecciated, recrystallized carbonatic rocks of the bores *Pat-1* and *-2* (345–377°C, in average, $361 \pm 14^\circ\text{C}$). Brecciated parts of the carbonatic rocks were cemented by pelitic-marly material. Judging from the clay mineral associations containing illite-muscovite, kaolinite, illite/smectite irregular mixed-layer clay mineral and chlorite and from the strongly scattering IC data of the brecciated variants, the pelitic-marly material was only diagenetically altered, following the cataclastic deformation.

In the melange type Triassic profile of the bore *Inke-1* intermediate (?) metavolcanite, metarhyolite tuff, serpentinite, limestone, intermediate (?) metatuffite, pelitic slate and siliceous, carbonatic slate were distinguished going downwards in the bore profile.

Table 6. Metamorphic temperatures of carbonatic rocks in °C calculated by carbonate geothermometric methods

Sample	T ₁	T ₂	T ₃	T ₄	T ₅	T ₆
Sem-2.13/B/II	365	375	347	345	365	375
Pat-2.10	364	–	345	(350)	371	377

T₁ and T₂: calculated by equations (3) and (4) of Bickle and Powell (1977)

T₃ and T₄: calculated by equations (1) and (2) of Powell et al. (1984)

T₅ and T₆: calculated by equations (23) and (31) of Anovitz and Essene (1987)

No primary magmatic minerals were found in the intermediate metavolcanite composed of quartz, albite, sericite, dolomite-ankerite, siderite, hematite ± calcite. Slaty cleavage, foliation (preferred orientation of sericite), and weak crenulation are the characteristic microstructural features of this rock type as well as those of the metarhyolite tuff. In volcanics and volcanoclastics relic textures are present, they include trachitic – pilotaxitic or blastoporphyr textures. Flattening and pressure shadows are present. Mylonitic deformation is witnessed by layers with perfect dimensional and optical orientation of white mica, containing minor, rounded, dispersed clasts. In metarhyolite tuff "spiny-like" quartz-sericite overgrowth and quartzitic textures were also observed around the relic quartz phenocrysts (blastoporphyr or crystalloclasts). Biotite phenocrysts are pseudomorphosed by serici-

te + hematite. The foliated, recrystallized matrix consists of quartz, sericite, albite, chlorite and hematite, and in bands, small amounts of carbonate minerals. Serpentine is built up predominantly by chrysotile. Chlorite is subordinate. Traces of clinopyroxene refer to lherzolitic character of the ultrabasite. The volcanic part of the presumed Dinaric type, dismembered ophiolite complex is represented by the spilite (metabasalt) explored by bore *Inke-9*. The intermediate (?) metatuffite is characterized by its high potash feldspar content. Penetrative continuous cleavage (S_1), subordinately anastomosing cleavage defined by concentration of organic material and crenulation are characteristic of slates associated with acidic volcanoclastics. Branching and anastomosing microfaults and minor shear define the S_2 together with microkinks. Pressure fringes around pyrite composed of quartz + mica are widespread in the black, pelitic, siliceous slates, the phyllosilicates of which are represented by sericite and chlorite. Post-metamorphic fracturing with quartz + carbonate fillings are also found. Both the IC averages and the microstructural features suggest medium-, high-temperature (cca 300–350°C) anchizonal dynamothermal metamorphism. Because of the inadequate mineral composition, most of the b_0 data can not be used for pressure determination. Based on b_0 value of one sample (*Inke-I. 15*) low H_2O pressure regime can be supposed.

The siliceous, pelitic, subordinately silty slate samples of the bores *Iharosberény Ib-1 and -2* are characterized by the main mineral phases of quartz and sericite. All of the investigated samples contain kaolinite and pyrite, while feldspars and chlorite are lacking. Carbonate minerals proved to be mostly of post-metamorphic (fissure filling) origin. Slates are composed of very fine-grained, preferentially oriented sericite preserving a faint detritic texture with sporadic coarser muscovite flakes. Slates are intercalated with radiolarian cherts. Transitional slaty cherts also occur. In these rocks sericite makes up disseminated flakes, cleavage films or thin laminae. In the pure sericite slate very thin anastomosing cleavages can be seen. Siliceous slates (cherts) show a millimetric – submillimetric alternation of fine-grained laminae having a high quantity of disseminated opacitic pigment, and coarser-grained laminae with a low content of them. The laminae are composed of aggregates of microcrystalline quartz with a high quantity of radiolarians and infrequent sponge spiculae. Beside rough and anastomosing cleavage, stylolites developed, bearing sericite and accumulated opaque material.

A succession of replacement fabrics are present in this sequence generated by diagenetic, metamorphic and hydrothermal processes. They include: chert and chalcedony replacement of carbonate and vice versa, kaolinite and carbonate replacement of pyrite, kaolinite replacement of sericite.

The main deformational characteristics of this sequence are: anastomosing and rough cleavage, penetrative continuous cleavage in slates and in slaty cherts, faint orientation of cherts and carbonate rocks, displayed by the elongation of clastic components (carbonates) and radiolarians. In few cases weak rotation is mirrored by bent coaxial quartz fibers from pressure fringes around euhedral pyrite crystals. Micro-crenulation is present in slates at the chert-slate interface, with a discrete cleavage defined by phyllosilicates. Buckled quartzite veins are also present. These

rocks suffered a post-metamorphic fracturing and brecciation with a variety of fracture filling minerals.

Based on the mineral composition, IC data and microstructural features, low-T (cca 250–300°C) anchizonal regional metamorphism followed by a younger, lower T (hydrothermal (?)) alteration producing carbonate minerals and kaolinite can be deduced.

The regional metamorphism of the banded, siliceous, pelitic slate sample of bore *Bajcsa-M-1* corresponds to anchizonal conditions (slaty cleavage, strong foliation indicated by sericite preferred orientation, kaolinite→pyrophyllite transformation and IC data).

Samples from the upper (clastic) and lower (carbonatic) sequences of the bore *Pátró-1* were also investigated. The weak penetrative continuous cleavage, the preferred sericite orientation in slate, and regenerated cement in metasandstone, the sericite-chlorite assemblage as well as the IC and R data prove low-T (cca 250°C) anchizonal dynamothermal metamorphism. This was followed by cataclastic deformation, circulation of lower T fluids producing kaolinite, poorly "crystallized" illite and siderite in the brecciated variants. Similar metamorphic–postmetamorphic history can be deduced also for the carbonatic sequence. Differences in metamorphic grade between the clastic and carbonatic sequences supposed formerly by Bérczi-Makk (1988) could not be proved by petrographic parameters.

The shale samples of bore *Liszó-1* show fracture cleavage with intense sericite neoformation or recrystallization along the planes of microfractures. In the more siliceous (cherty) types continuous cleavage, slight orientation of microcrystalline quartz aggregates were found. Varying carbonate content (calcite >> dolomite), "matured" detritus (quartz, sericite, kaolinite) and IC values corresponding to the deep diagenetic zone are the characteristic features of these samples. The matrix of the underlying dolomite is recrystallized. The metamorphic zone indicating parameters of its acid insoluble residue are in accordance with those of the shales.

From the bore *Murakeresztúr Mu-1* limestone, metarhyolite tuffite containing black, psammitic shale were investigated. The texture of limestone with relic organic remnants was recrystallized. In shales alternating with acidic volcanoclastics crenulation, pressure fringes around pyrite with rotation, as well as pressure shadows around quartz and feldspar clasts were observed, implying strong deformation. On the contrary, their clay mineral assemblages contain illite-muscovite, illite/smectite irregular mixed-layer clay mineral, kaolinite and vermiculite. These clay minerals, as well as the high IC values suggest only diagenetic alterations. No signs of post-metamorphic alterations (weathering) could be seen. The anomalously high vitrinite reflectance values of shale can be explained by short-term thermic effect of the acidic volcanism, as textural observations deny the eventual allochthonous nature of the dispersed coalified material. The controversial textural, caly mineralogical and vitrinite reflectance data refer to complicated geologic evolution, the correct interpretation of which needs further research.

Conclusion

Summarizing the new petrographic results and comparing them to the available geologic and tectonic models (Bardócz 1973–1986, Kázmér 1986, Bérczi-Makk 1988), the following conclusions can be drawn.

1. The Igal (Central Hungarian) Unit represents a tectonically strongly disturbed, composite zone, in the basement of which the metamorphic grade of the Late Paleozoic and mostly Mesozoic (Triassic) fragments belonging to different paleotectonic realms and lithofacies, are strongly varying from the middle diagenetic stage (cca 100–200°C) through the anchizone up the epizone (chlorite zone of the greenschist facies, cca 350–400°C).

2. Short-term thermic effects (low-T contact metamorphism), cataclastic deformation (breccia formation) followed by retrograded (low-T) anchizonal metamorphism or degradation (chemical weathering) caused by the circulating low-T hydrothermal (?) fluids made the interpretation of the metamorphic history very complicated in many cases. To solve these problems, the complex application of illite "crystallinity", vitrinite reflectance and carbonate geothermometric methods was attempted.

3. The spatial distribution of diagenetic – metamorphic grades proved to be more complicated than that which was supposed in the model of Bérczi-Makk (1988) based on litho- and biostratigraphic data and analogies: the Northern Zone of the Igal Unit also contains metamorphic rocks, and the Southern Zone, which was considered as "anchimetamorphic" by Bérczi-Makk, contains non-metamorphic anchizonal and epizonal formations as well. Considering the large area in question, as well as the sporadic, irregular distribution of samples, there is no real possibility at present to delineate the boundaries of the zones characterized by distinct lithologies and metamorphic grades.

4. Particular attention must be paid to the widespread cataclastic deformation detected in several bores, which in some cases can be related to low-T metamorphic conditions, in others only to diagenetic circumstances. Our data are not sufficient to decide whether we are dealing with the different levels of a telescoping phenomenon or with clearly differing phases. More radiometric data are needed to unravel this problem.

5. In the Northern Zone, the Transdanubian Midmountains type Mesozoic basement proved to be only diagenetically altered (Sávoly), in accordance with the grade of alteration observed in the outcrops and boreholes of Transdanubian Midmountains (Viczián 1976, 1987).

6. On the contrary, the grade of regional alterations in the Dinaric type formations of the Northern Zone strongly varies: diagenetic (Nikla), anchizonal dynamothermal (Öreglak), and low-T contact metamorphism (Buzsák, Újfalú) were detected.

7. In the Dinaric type Mesozoic of the Southern Zone epizonal (Semjénháza, Pat), anchizonal (Inke, Iharosberény, Bajcsa, Pátró) and diagenetic (Liszó, Mura-keresztúr) rock types were distinguished.

8. Very few data were obtained on the baric type of regional metamorphism, the mineral associations being inadequate for white mica b_0 geobarometric purposes. Low-pressure (Öreglak, Inke) and intermediate fluid (H_2O) pressure (Semjénháza) regimes could be evidenced.

9. Based on the Late-Paleozoic and Triassic ages of sedimentation, the unconformably overlaying character of the non-metamorphic Tertiary formations as well as the tectonic evolution of the given area, the age of the low-T regional metamorphism is most probably Alpine, Cretaceous. Contact metamorphism, cataclastic deformation, retrograde metamorphism and low-T hydrothermal (?) alterations, weathering are connected to Meso-Alpine tectonophases characterised by calc-alkaline volcanic activity and large-scale horizontal displacements along the Central Hungarian Lineament.

The sporadic radiometric data support this chronologic model (Kad. Balogh, Á. Kovách, É. Singor, personal communications; Balogh et al., in preparation). K-Ar measurements were done by Kad. Balogh, using sericite-rich $<2 \mu\text{m}$ grain size fractions, while the Rb-Sr model ages were obtained using whole rock samples with presumed initial $^{87}\text{Sr}/^{86}\text{Sr}$ ratio of 0.708, which was supposed to be characteristic of acidic magmatic rocks.

The sericite K-Ar age ($187 \pm 7.1 \text{ Ma}$) of metasandstone from bore Újfalú U-I can be interpreted as mixed age without any geologic meaning between the ages of sedimentation (Permian) and metamorphism (Cretaceous), while that of the slate from bore Öreglak Ög-1 ($96.7 \pm 12.3 \text{ Ma}$) clearly indicates Cretaceous regional metamorphism. Also Cretaceous metamorphic age was obtained by K-Ar method on the $<2 \mu\text{m}$ sericite fraction of the metarhyolite tuff from bore Inke-I (sample Inke-I.11): $92.9 \pm 3.7 \text{ Ma}$. The Rb-Sr age of the whole rock sample from the same core ($184 \pm 52 \text{ Ma}$) is between the presumed age of volcanism (Upper Triassic) and that of the metamorphism. In case of intermediate(?) metavolcanite sample (Inke-I.10) the lower sericite K-Ar age ($61.7 \pm 2.4 \text{ Ma}$) refers to postmetamorphic Tertiary effects. The very low sericite K-Ar and whole rock Rb-Sr model ages (21.1 ± 1.2 and $46 \pm 25 \text{ Ma}$, respectively) of the metarhyolite tuff from the bore Semjénháza Sem-3 may be interpreted either by the low-T retrograde (cataclastic) event or/and by the chemical weathering of the sample.

10. Both the lithotypes and the metamorphic feature (microstructures, grades and pressure types) of certain anchi-, epizonal occurrences in the Southern Zone of the Igal Unit (Semjénháza, Iharosberény, Pat, partly Inke and Pátró) are very similar to those of the Mesozoic formations of the Barcs-West area (Drava Basin, S-Transdanubia), located South of the Igal Unit, presumably forming an allochthonous fragment of the Dinaric type Mesozoic transported on or within the fragments of the Southwestern edge of the Tisza Unit (see Árkai 1990, Balogh et al. 1990).

Acknowledgements

The authors are grateful to the Oil and Gas Mining Enterprise (Nagykanizsa), personally to B. Bardócz, chief-geologist, I. Tormássy, head of department, and the

late L. Mészáros, head of section for initiating and supporting a great part of the research. Thanks are due to Drs Kadosa Balogh, Ádám Kovách and Éva Svingor (Nuclear Research Institute of the Hungarian Academy of Sciences, Debrecen) for K–Ar and Rb–Sr isotope geochronologic measurements. One of the authors (I. Fórizs) is indebted to the National Museum of Natural History – Smithsonian Institution, Washington, personally to E. Jarosewich, for providing the carbonate reference materials for electron microprobe analyses. This work forms also a part of the authors' metamorphic petrogenetic research program No. 284/1987–1991 sponsored by the Hungarian National Research Foundation (OTKA).

References

- Árkai, P. 1983a: Very low- and low-grade Alpine regional metamorphism of the Paleozoic and Mesozoic formations of the Bükkium, NE-Hungary. – *Acta Geol. Hung.*, 26, pp. 83–101.
- Árkai, P. 1983b: Mineralogic–petrologic and geochemical investigation of the metamorphic basement of the Drava Basin. – Research report, National Oil and Gas Industrial Trust, Budapest (in Hung.).
- Árkai, P. 1984: Polymetamorphism of the crystalline basement of the Somogy–Drava Basin (Southwestern Transdanubia, Hungary). – *Acta Miner. Petr.*, Szeged, 26, pp. 129–153.
- Árkai, P. 1987: New data on the petrogenesis of metamorphic rocks along the Balaton Lineament, Transdanubia, W-Hungary. – *Acta Geol. Hung.*, 30, pp. 319–338.
- Árkai, P. 1988: Report on the metamorphic petrological investigations of the basement of the Central Hungarian (Igal) Unit. – Oil and Gas Mining Enterprise, Nagykanizsa (in Hung.).
- Árkai, P. 1990: Very low- and low-grade metamorphic rocks in the pre-Tertiary basement of the Drava Basin, SW-Hungary, I.: mineral assemblages, illite "crystallinity", b_0 data, and problems of geological correlation. – *Acta Geol. Hung.*, 33, pp. 43–66.
- Árkai, P. 1991: Chlorite "crystallinity": an empirical approach and correlation with illite "crystallinity", coal rank and mineral facies as exemplified by Paleozoic and Mesozoic rocks of NE-Hungary. – *Journal of Metamorphic Geology*, 9 (in press).
- Árkai, P., Gy. Lelkes-Felvári 1987: Very low- and low-grade metamorphic terrains in Hungary. – In: Flügel, H.W.; Sassi, F.P.; Grecula, P. (eds): Pre-Variscan events in the Alpine – Mediterranean mountain belts. *Mineralia Slovaca – Monography*, Alfa, Bratislava, pp. 51–68.
- Árkai, P., G. Nagy, G. Dobosi 1985: Polymetamorphic evolution of the South-Hungarian crystalline basement, Pannonian Basin: geothermometric and geobarometric data. – *Acta Geol. Hung.*, 28, pp. 165–190.
- Balázs, E. 1969: Explanatory text of the basement map of the Hungary in scale of 1:500.000. Part II. Transdanubia. – Manuscript, National Oil and Gas Industrial Trust, Budapest (in Hung.).
- Balla, Z. 1988: On the origin of the structural pattern of Hungary. – *Acta Geol. Hung.*, 31, pp. 53–63.
- Balogh, K. 1964: Geological formations of the Bükk Mountains. – *Földt. Int. Évk.*, 48, pp. 243–719.
- Balogh, Kad., Á. Kovách, Z. Pécskay, É. Svingor, P. Árkai 1990: Very low- and low-grade metamorphic rocks in the pre-Tertiary basement of the Drava Basin, SW-Hungary, II: K–Ar and Rb–Sr isotope geochronologic data. – *Acta Geol. Hung.*, 33, pp. 67–76.
- Bardócz, B. 1973–1986: Tectonic and geological map of the basement of the Transdanubian Neogene basins. – Manuscript, Oil and Gas Mining Enterprise, Nagykanizsa.
- Bérczi-Makk, A. 1988: Re-investigation of the Mesozoic sedimentary formations from the Transdanubian basement, South of the Balaton Lineament. – Research report, Hydrocarbon Research and Developing Institute, Százhalombatta (in Hung.).
- Bérczi-Makk, A. J. Haas, E. Rálich-Felgenhauer, A. Oravecz-Scheffer 1990: Late Paleozoic and Mesozoic formations of the Central Transdanubian Unit and their connections. – Manuscript, Hungarian Geological Institute, Budapest (in Hung.).
- Chikán, G. et al. 1985: Geological evaluation of the results of the Inke–I borehole. – Manuscript, Hungarian Geological Institute, Budapest (in Hung.).
- Frey, M. 1986: Very low-grade metamorphism of the Alps: an introduction. – *Schweiz. Mineral. Petrogr. Mitt.*, 66, pp. 13–27.
- Fery, M., M. Teichmüller et al. 1980: Very low-grade metamorphism in the external parts of the Central Alps: illite crystallinity, vitrinite reflectance and fluid inclusion data. – *Eclogae geol. Helv.*, 73, pp. 173–203.
- Fülöp, J. 1989: Bevezetés Magyarország geológiájába (Introduction to the geology of Hungary). – Akadémiai Kiadó, Budapest (in Hung.).
- Guidotti, C.V., F.P. Sassi 1976: Muscovite as a petrogenetic indicator mineral in pelitic schists. – *N. Jb. Mineral., Abh.*, 127, pp. 97–142.
- Guidotti, C.V., F.P. Sassi 1986: Classification and correlation of metamorphic facies series by means of muscovite b_0 data from low-grade metapelites. – *N. Jb. Miner., Abh.*, 153, pp. 363–380.

- Haas, J. 1987: Position of the Transdanubian Central Range structural unit in the Alpine evolution phase. – *Acta Geol. Hung.*, 30, pp. 243–256.
- Haas, J., H. Kozur, Gy. Lelkes-Felvári 1988: Alpine very low-grade metamorphic Upper Triassic formations from the bore Inke-I (SW-Transdanubia). – Manuscript, Hungarian Geological Institute, Budapest (in Hung.).
- Haas, J., E. Rálish-Felgenhauer, A. Oravecz-Scheffer, A. Bérczi-Makk 1988: Triassic key sections in the Mid-Transdanubian (Igal) structural zone. – *Acta Geol. Hung.*, 31, pp. 3–17.
- Jarosewich, E., I.G. Macintyre 1983: Carbonate reference samples for electron microprobe and scanning electron microscope analyses. – *J. Sediment. Petrol.*, 53, pp. 677–678.
- Kázmér, M. 1986: Tectonic units of Hungary: their boundaries and stratigraphy (a bibliographic guide). – *Annales Univ. Sci. Budapest.*, 26, pp. 45–120.
- Kázmér, M., S. Kovács 1985: Permian–Paleogene paleogeography along the eastern part of the Insubric–Periadriatic Lineament system: evidence for continental escape of the Bakony–Drauzug Unit. – *Acta Geol. Hung.*, 28, pp. 71–84.
- Kovács, S. 1982: Problems of the "Pannonian Median Massif" and the plate tectonic concept. Contributions based on the distribution of Late Paleozoic – Early Mesozoic isopic zones. – *Geol. Rundschau* 71, pp. 617–640.
- Kübler, B. 1968: Evaluation quantitative du métamorphisme par la cristallinité de l'illite. – *Bull. Centre Rech Pau – S.N.P.A.*, 2, pp. 385–397.
- Kübler, B. 1975: Diagenese – anchimetamorphisme et métamorphisme. – *Institute national de la recherche sci. Petrole. Manuscript, Quebec.*
- Kübler, B., J. Pitton et al. 1979: Sur le pouvoir réflecteur de la vitrinite dans quelques roches du Jura, de la Molasse et des Nappes préalpines, helvétiques et penniques. – *Eclogae geol. Helv.*, 72, pp. 343–373.
- Lelkes-Felvári, Gy. 1978: Petrographische Untersuchung einiger präpermischen Bildungen der Balaton Linie. – *Geologica Hungarica, ser Geologica*, 18, pp. 193–295.
- Lelkes-Felvári, Gy., F.P. Sassi: Outlines of the pre-Alpine metamorphism in Hungary. – *IGCP project No. 5 Newsletter*, 3, pp. 89–99.
- Sassi, F.P. 1972: The petrologic and geologic significance of the b_0 value of the potassic white micas in low-grade metamorphic rocks. An application to the Eastern Alps. – *Tschermaks Mineral. Petrogr. Mitt.*, 18, pp. 105–113.
- Teichmüller, M., R. Teichmüller, K. Weber 1979: Inkohlung und Illit-Kristallinität vergleichende Untersuchungen im Mesozoikum und Paläozoikum von Westfalen. – *Fortsch. Geol. Rheinl. u. Westf.*, 27, pp. 201–276.
- Tomor, J. 1957: Research for oil and gas in Transdanubia. – In: *Methods of oil research and exploration in Hungary*, pp. 157–201. National Oil and Gas Industrial Trust, Budapest (in Hung.).
- Viczián, I. 1975: A review of the clay mineralogy of Hungarian sedimentary rocks (with special regard to the distribution of diagenetic zones). – *Acta Geol. Acad. Sci. Hung.*, 2, pp. 243–256.
- Viczián, I. 1987: Clay minerals in sedimentary rocks of Hungary. – *D.Sc. Thesis, Budapest (in Hung.)*.
- Weber, K. 1972: Kristallinität des Illits in Tonschiefern und andere Kriterien schwacher Metamorphose im nordöstlichen Rheinischen Schiefergebirge. – *N. Jb. Geol. Paläont., Abh.*, 141, pp. 333–363.
- Wein, Gy. 1969: Tectonic review of the Neogene covered areas of Hungary. – *Acta Geol. Acad. Sci. Hung.*, 13, pp. 399–436.
- Wolf, M. 1972: Beziehung zwischen Inkohlung und Geotektonik im nördlichen Rheinischen Schiefergebirge. – *N. Jb. Geol. Paläont., Abh.*, 141, pp. 222–275.

K–Ar dating of the Perelik volcanic massif (Central Rhodopes, Bulgaria)

Zoltán Pécskay, Kadosa Balogh

*Institute of Nuclear Research,
Hungarian Academy of Sciences,
Debrecen*

Alexandra Harkovska

*Geological Institute of Bulgarian Academy of Sciences
Sofia*

The Perelik volcanic massif belongs to the Central Rhodope volcanic area (CRVA) of the Macedonian–Rhodope North Aegean Volcanic Zone (MRNAVZ). The volcanics are interpreted as High Aspect Ratio Ignimbrites. According to the $\text{Na}_2\text{O} + \text{K}_2\text{O}/\text{SiO}_2$ ratio the Perelik volcanics have rhyolitic to rhyodacitic composition and on the basis of the $\text{K}_2\text{O}/\text{SiO}_2$ ratio they belong to calc-alkaline and high K–calcalkaline series.

K–Ar dating was performed on whole rock samples and biotite and feldspar. The age pattern shows a very short interval of 30.9 ± 0.92 Ma for the volcanic activity. It agrees very well with the age of the Kotily–Vitina volcanic massif (Central Rhodopes) which has the same petrologic feature and an age of 30.3 ± 0.7 Ma (Innocenti et al. 1984) or 30 ± 1 Ma (Eleftheriadis and Lippolt, 1984).

Keywords: Perelik, Central Rhodopes, Bulgaria, ignimbrites, K–Ar dating, Lower Oligocene

Introduction

The Perelik volcanic massif (Bahneva, Stephanov 1975) belongs to the Central Rhodope volcanic area (CRVA) of the Paleogene Macedonian – Rhodope North Aegean Volcanic Zone (MRNAVZ – Harkovska et al. 1986). It is situated in the central parts of the Rhodope Mountains, immediately to the north–west of the town of Smolyan (Fig. 1–inset). The massif covers more than 200 sq. km. It is built up of acid volcanics described as nevaditic rhyolites (Ivanov 1964), "ignimbrite – like complex" of rhyolites and ignimbrites (Bahneva, Stefanov 1975), pseudo-ignimbrites (Ivanov 1984) porphyroclastic rhyolites (Bahneva 1983). Recently the volcanics were interpreted (Harkovska, Sirakov 1986) as High Aspect Ratio Ignimbrites (according to the Walker's morphological classification – 1980).

The age of the Perelik volcanics is considered to be Upper Oligocene–Lower Miocene (Bahneva, Stefanov 1975, Bahneva 1983; Bahneva et al. 1984, Ivanov 1984) or Lower Oligocene (Harkovska et al. 1986). These suggestions are based on some regional geological relationships. In 1989 Lilov and Bahneva reported, that according to geochronological (K–Ar) data the Perelik massif ("the Perelik structure") had been built up in a time–interval between 32.5 and 30 Ma (Lilov and Bahneva 1989). Using for a comparison Harland's et al. (1985) time table they referred this age to the Upper Oligocene. The first K–Ar age determinations of the Perelik

Addresses: Zoltán Pécskay, Kadosa Balogh: H–4001, Debrecen, Bem tér 18/c, Hungary

Alexandra Harkovska: 1505, Sofia, Bul. Hristo Kabakchiev 23, Bulgaria

Received: Januar 23, 1991

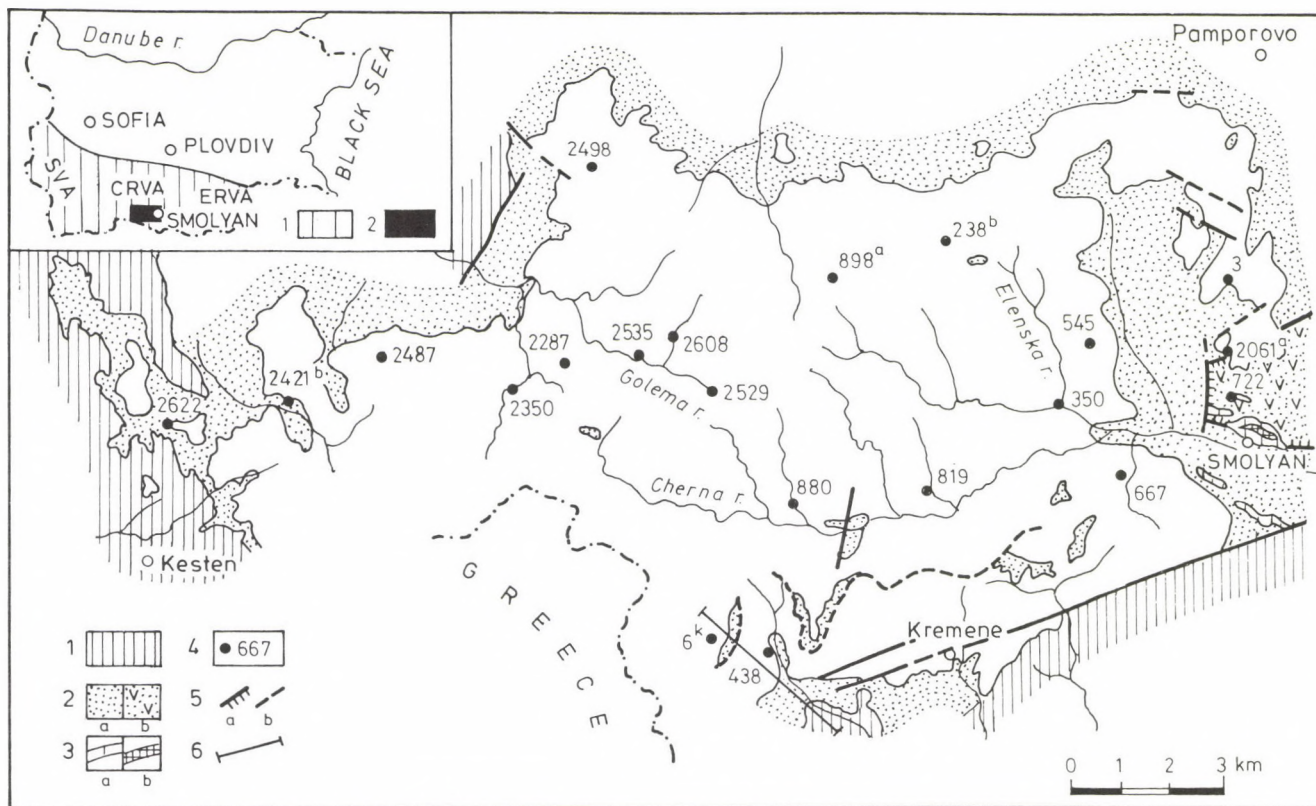


Fig. 1. Geological sketch of the Perelik volcanic massif (Bulgarian part) and location of the samples used for K–Ar age determination. 1. crystalline metamorphic rocks of the Pre–Paleogene basement; 2. Paleogene stratified deposits: a) sedimentary and volcano-sedimentary deposits, 2 b) pyroclastic sequence; 3 a. latites; 3 b. felsitic rhyolites; 4. Perelik massif with the numbers of the measured samples (see Table I, column 2); 5. fault; 6. section N° 5 on Fig. 2. Inset: confines of the Macedonian – Rhodope North Aegean Volcanic Zone – MRNAVZ (1) and location of the studied region (2); SVA – Struma Volcanic Area; CRVA – Central Rhodope Volcanic Area; ERVA – East Rhodope Volcanic Area

volcanics obtained by the authors of this paper (Harkovska et al. 1990) gave similar data (30.8 ± 1.2 to 31.9 ± 1.2 Ma).

Here we discuss all K–Ar datings we have obtained as a result of systematical sampling and age determinations of the Perelik volcanics. The investigations is based on 22 samples collected from different parts (Fig. 1) and different levels (Fig. 2) of the volcanic massif. The sampling was made by A. Harkovska. The dating was performed by Z. Pécskay and K. Balogh.

Brief description of the Perelik volcanic massif

The Perelic volcanics (thick up to 500–600 m) bury a very pronounced relief in the underlying high-grade metamorphics and the Paleogene (Eocene–Lower Oligocene) continental terrigenous sedimentary and volcano-sedimentary sequence. The locations of their feeding channels are under discussion. The double recurrence of the Paleogene section in the south–western part of the massif is due either to a normal stratification relationships (Vacev, Hristov 1984) or to a possible thrusting (Harkovska 1987) (Fig. 3, column 5).

The petrological features of the Perelik volcanics are very uniform. They contain (Bahneva et al. 1984) abundant (43–70%) phenocrysts with protoclastic joints and their fragments: quartz, K-feldspar (sanidine and/or orthoclase), andesine, deformed biotite, hornblende, sphene, apatite; the accessories are titan-magnetite, zircon and rare monazite. The volcanics also include numerous irregularly distributed xenoliths of the underlying metamorphics and Paleogene sedimentary rocks and a lot of acid cognate inclusions (e.g. 898 a – Table I; Fig. 1) of different petrographic features. The groundmass textures are very variable (microallotriomorphic, felsitic and microfelsitic, glassy, microspherulitic etc.; the structures are fluidal, massive, taxitic, eutaxitic. According to the $\text{Na}_2\text{O} + \text{K}_2\text{O}/\text{SiO}_2$ ratio the Perelik volcanics have rhyolitic to rhyodacitic composition. According to the $\text{K}_2\text{O}/\text{SiO}_2$ ratio they belong to calc-alkaline and high K–calc-alkaline series. There are no petrological differences between the rocks from different levels of the massif.

The lowermost parts of sections nearly always contain a number of small irregular vitrophyric bodies (Fig. 2) and more xenogenic and cognate volcanogenic inclusions. A rough vertical zonality in the distribution of the joining types is established (Fig. 2).

Analytical techniques

All samples were first crushed and sieved and the fractions of 250–500 μm have been used when whole rock samples were dated. Feldspars were separated from the 250–315 μm fraction and biotites from the 315–500 μm one. Heavy liquids and magnetic separation were used for obtaining mineral concentrates; the biotite was additionally cleaned by handpicking.

Pulverized samples (0.1 g) were digested in HF with the addition of some sulphuric and nitric acids. The digested sample was dissolved in 100 ml 0.25 n HCl and after a five-fold dilution 100 ppm Na and Li were added as buffer and internal

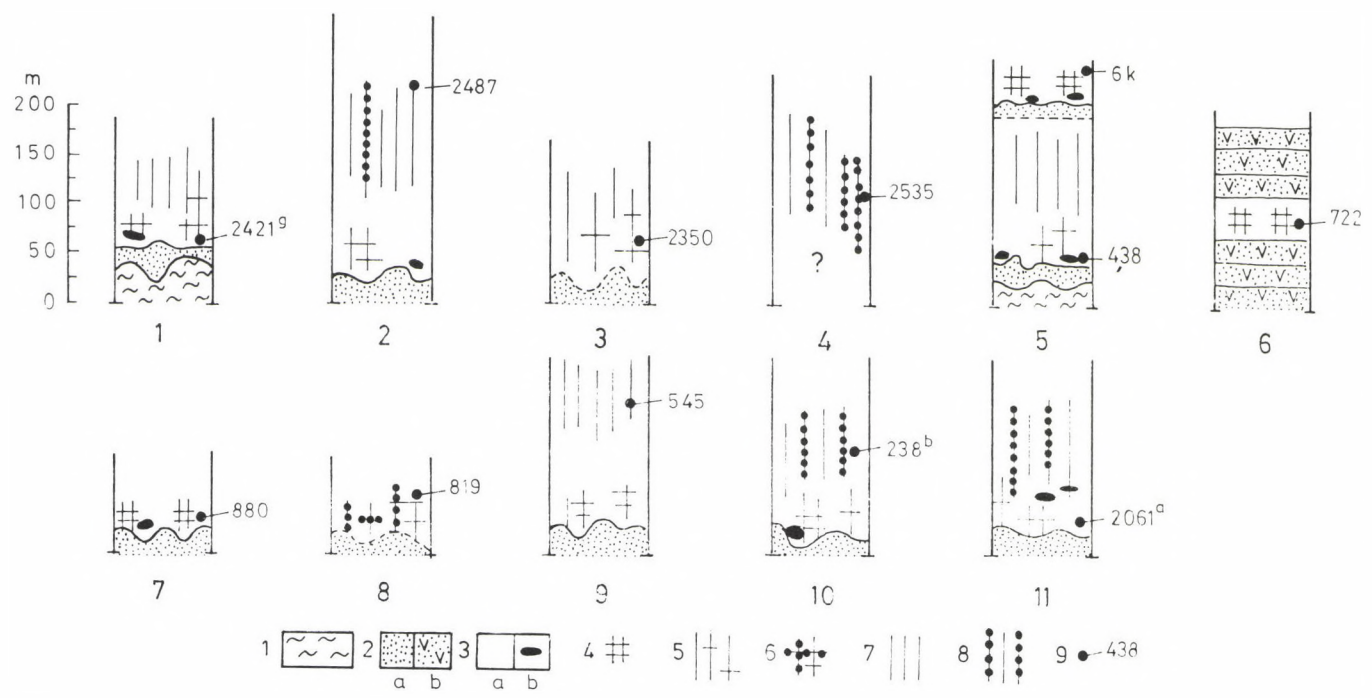


Fig. 2. Simplified sections (1–11) of the Perelik volcanics with the location of samples; the scale is approximated 1. crystalline metamorphic rocks of the basement; 2–3. same legend as on Fig. 1; 4–8. types of jointing; 4. block type; 5. block to coarse columnar; 6. block and plate; 7. columnar; 8. columnar to platy

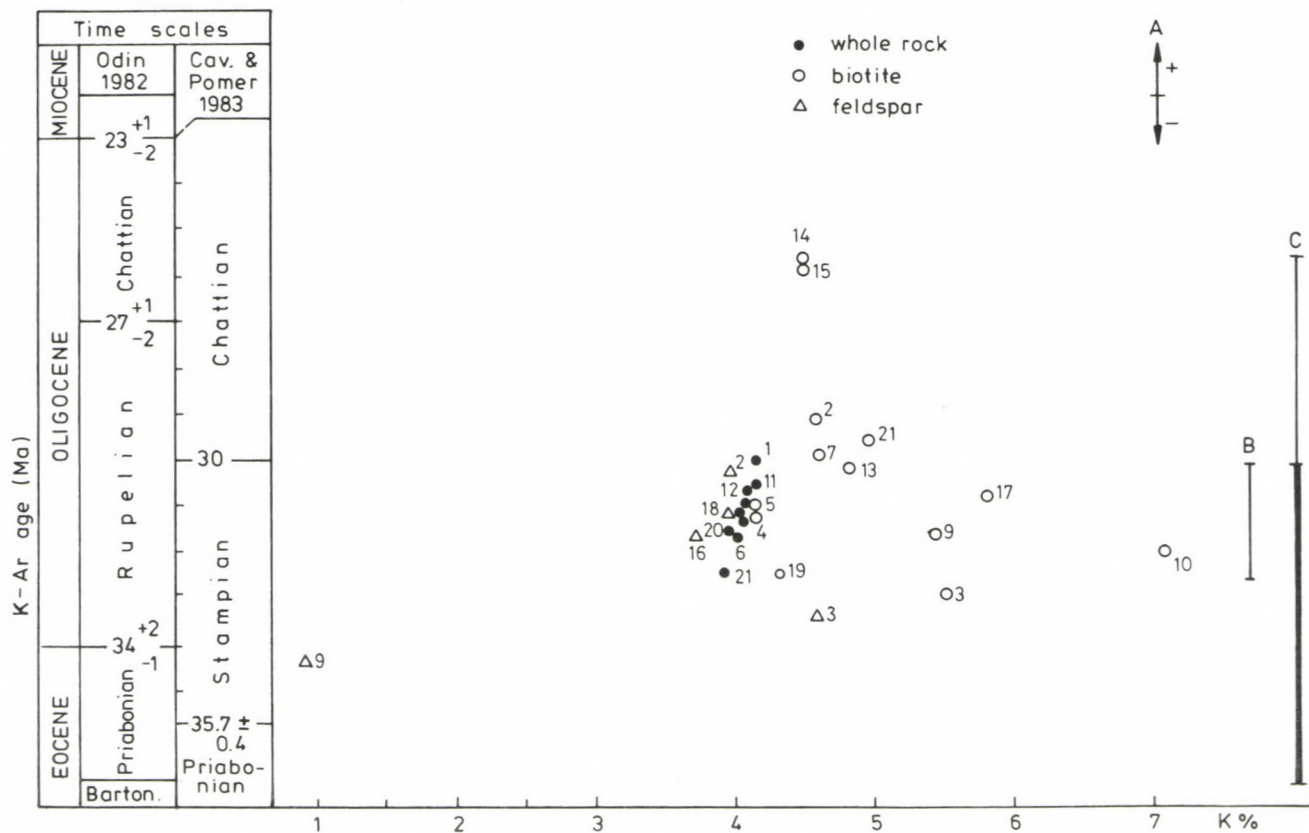


Fig. 3. The K-Ar age of the Perelik volcanics versus their K-content. The numbers of the samples are given in column 1, Table I. A - scale of experimental error; B - formation time-span for Perelik volcanic massif (Lilov and Bahneva, 1989); C - time-span of the Paleogene volcanism in the East Rhodope Volcanic Area (ERVA - Fig. 1); the heavy line indicates the interval of the paroxysmal events (according to Eleftheriadis and Lippolt, 1984; Lilov et al. 1987)

standards. Potassium concentration was measured with a digitalized OE-85 type flame photometer (made in Hungary).

Argon was extracted via high frequency induction heating in a molybdenum crucible, the liberated Ar was spiked with ^{38}Ar , and after cleaning, it was introduced directly into the mass-spectrometer (magnetic sector type of 150 mm radius and 90° deflection, constructed in ATOMKI, Debrecen and used in a static regime). Recording and evaluation of Ar spectrum were controlled by a microcomputer. The mass discrimination was checked each day by analysing atmospheric Ar. K- and Ar- determinations were controlled regularly by interlaboratory standards Asia/65 (made in SU) and GL-0 (made in France). Atomic constants suggested by Steiger, - Jäger (1977) were used for calculating age. The experimental errors were calculated according to Cox, - Dalrymple (1967) and were given at 1σ levels. Details of the experimental methods have been published elsewhere (Balogh 1985).

Results and discussions

The measured K/Ar data are presented in Table I. The majority of samples give similar ages in spite of their different position in the cross-sections (Fig. 2). Nearly all of them agree with each other within the limits of the experimental error (Table I, Fig. 3). This suggests that K/Ar data marked with an asterisk in Table I indicate the real age of the major part of the Perelik volcanic massif. What is more, all these ages are closer to each other than it would follow from the given experimental error. This implies (as it has been discussed elsewhere by Balogh 1985), that the experimental error is overestimated and that only a maximum time-span can be given for the duration of the volcanic activity. It has to be emphasized also, that the duration of the volcanic activity is overestimated here since some dubious results were included in the calculations too and the given errors allow to observe the scattering of K/Ar ages even in case of an extremely short volcanic activity. May be some geological errors can not be fully excluded for these ages, but they cannot be greater than the value of the analytical error. E.g. it is known that biotites with a high K-concentration cannot produce (as a consequence of a hydrothermal alteration) K/Ar ages older than geological ages.

From the biotite data which are geologically reliable, the oldest value has been measured in sample N^o 2487 (that biotite is with a highest K-concentration, Table I). On this ground it cannot be excluded that the younger biotite ages from other parts and levels of the Perelik massif are a result of a little loss of Ar due to alteration, but in view of the given error and of the microscopic mineralogical features of those biotites, this assumption cannot be supported.

Nearly all whole rock and biotite ages mark the same age interval (Fig. 3), but the whole rock age of sample N^o 722 differs from its biotite age (in the limits of the experimental error), the latter being younger. At the present stage of our study the whole rock value of this sample is more acceptable especially taking into account the geological position of the body from which the sample was collected (Fig. 2, column 6). That sheet-like body is built up of the Perelik type volcanics

but is interbedded into the pyroclastic sequence filling the Levochevo caldera (Figs 1, 2) which had been formed before the Perelik massif.

The major part of the feldspar determinations do not differ from the whole rock and biotites ages (Fig. 3). The single exception is feldspar N° 2622 which has an unusually low K-content (Table I, Fig. 3). This content could be explained by an assumption, that the feldspar under question is mainly of a xenogenic origin. As it is observed e.g. by McDougall et al. (1969) and Gillespie et al. (1982) lava and pyroclastic xenoliths may reserve a part of their preexisting radiogenic argon content and may give older ages. Such a statement e.g. can explain the relatively old value of sample N° 898 which represents a cognate volcanogenic inclusion. An argument against the reliability of the N° 2622 - feldspar value is the 31.6 ± 1.3 Ma age of the biotite from the same N° 2622 sample.

An ambiguous interpretation can be given for sample 2061^a. Its biotite and feldspar have given 32.9 ± 1.2 Ma and 33.4 ± 1.3 Ma respectively. The agreement between these two ages suggests that they reflect a real geological age of the rock. The feldspar age N° 2061^a is the oldest value measured in the Perelik massif sample collection. An incomplete degassing cannot be ruled out as a possible explanation of that relatively oldest age, but it has to be noted also that the sample N° 2061^a was collected from the lowermost parts of the section - (Fig. 2, column 11) even under the level, containing vitrophyric bodies. More detailed investigations appear to be necessary to answer the question if sample N° 2061^a reflects one of the earliest volcanic event within the Perelik massif, or its relatively older age is caused by a presence of excess Ar.

The youngest and similar biotite ages are obtained for the three biotites collected from the north-western parts of the Perelik massif (N° 2535, 2608 and 2498 - Fig. 1, Table I). Such young ages (25.6 ± 1.0 - 24.4 ± 1.0) can be interpreted as a result of Ar loss caused by secondary effects likely by hydrothermal processes. On one hand these younger ages cannot be attributed to postvolcanic hydrothermal processes, because the biotites are not hydrothermally altered. On the other hand we have no geological data (including petrological ones) to state that the north-western part of the Perelik massif is built up of products of a different and younger volcanic phase.

Conclusions

1. The age of the Perelik volcanic massif (Central Rhodopes, Bulgaria) obtained by a systematical sampling and K-Ar age determination is an Oligocene one (Fig. 3):

a) The massif has been formed mainly in the Early Oligocene (Rupelian - Odin, 1982; Stampian - Cavelier, Pomerol, 1983). At the present stage of our studies the most likely age of the volcanism can be obtained by averaging of the ages, marked with asterisk (*) in Table 1. This age is 30.9 ± 0.92 Ma, where the error characterizes the joint effects of the duration of the volcanic processes and analytical uncertainties. It has to be emphasized that the duration is overestimated here, since some dubious results were averaged too and the given analytical errors allow the

Table 1. K/Ar ages of the Perelik volcanics

No. on Fig.3	No. on Fig.1	No. of K/Ar laboratory	Dated fraction	K content (%)	$^{40}\text{Ar}_{\text{rad}}$ (%)	$^{40}\text{Ar}_{\text{rad}} - 6 \times 10(\text{cc STP/g})$	Apparent age (M a)
1	6k	1716.	w.r.	4.128	69	4.856	$30.0 \pm 1.2^*$
2	438	1718.	biotite	4.584	64	5.209	$29.0 \pm 1.2^*$
3	2061 ^a	1850.	felspar	3.940	83	4.659	$30.2 \pm 1.1^*$
			biotite	5.530	76	7.128	32.9 ± 1.2
			feldspar	4.623	89	6.046	33.4 ± 1.3
4	350	1726.	w.r.	4.087	60	5.022	$33.4 \pm 1.3^*$
5	238 ^b	1724.	w.r.	4.077	92	4.893	$30.6 \pm 1.1^*$
6	3	1694.	w.r.	4.001	87	4.971	$31.7 \pm 1.2^*$
7	880	1717.	biotite	4.622	74	5.387	$29.8 \pm 1.2^*$
8	2421 ⁹	1721.	w.r.	4.155	82	5.031	$30.9 \pm 1.2^*$
9	2622	1971.	biotite	5.485	58	6.804	$31.6 \pm 1.3^*$
			feldspar	0.911	83	1.228	34.3 ± 1.3
10	2487	1720.	biotite	7.026	69	8.779	$31.9 \pm 1.2^*$
11	2350	1723.	w.r.	4.153	91	4.979	$30.6 \pm 1.1^*$
12	819	1719	w.r.	4.120	92	5.062	$31.2 \pm 1.1^*$
13	667	1722.	biotite	4.766	74	5.613	$30.1 \pm 1.2^*$
14	2608	1846.	biotite	4.499	62	4.520	25.6 ± 1.0
			biotite	4.489	75	4.435	25.3 ± 0.9
15	2535	1844.	biotite	4.498	53	4.289	24.4 ± 1.0
			biotite	4.501	48	4.525	25.7 ± 1.1
16	2498	2062.	feldspar	3.693	80	4.569	$31.6 \pm 1.2^*$
17	2287	1713.	biotite	5.824	85	7.035	$30.8 \pm 1.2^*$
18	2529	1987.	feldspar	3.957	68	4.819	$31.0 \pm 1.2^*$
19	898 ^a	1714.	w.r.	4.368	78	5.567	$32.5 \pm 1.2^*$
20	545	1849.	w.r.	4.024	83	4.725	$30.6 \pm 1.1^*$
21	722	1849.	w.r.	3.978	89	5.052	$32.4 \pm 1.2^*$
			biotite	4.925	75	5.688	$29.5 \pm 1.2^*$

observed scattering of K–Ar ages in case of extremely short volcanic activity. The obtained age is in a good agreement with the data of Lilov, Bahneva (1989) and Harkovska et al. (1990). It agrees also very well with the age of the Kotily–Vitina volcanic massif (Central Rhodopes) which has the same petrologic features and an age of 30.3 ± 0.7 Ma – Lippolt 1984, (respectively – 30 ± 1) Elephteriadis – Innocenti et al. 1984).

b) A relatively younger – 25.7 ± 1.1 – 24.4 ± 1.0 Ma (Chattian, Fig. 3) age is established for the North–Western part of the Perelik massif, this age being given by three samples (Table I). We need more detailed radiometric chronological investigations to answer the question whether these data reflect a real younger age of these rocks, because up to now we have neither geological relationships, nor petrological data, supporting such younger age.

2. The relatively older whole rock age of the sample 722 is an agreement with the geological position of the sampled body, which is the oldest body of the Perelik petrological type (Fig. 1, Fig. 3, column 6). This age and the geological interrelations north to the town of Smolyan indicates that there is no long period between the processes of the deposition of the pyroclastics from the Levochevo caldera and the formation of the Perelik massif.

3. The time–span of the formation of the Perelik massif corresponds as a whole to the time–span of the paroxysmal volcanic events in the East Rhodope Volcanic Area (ERVA, Fig 1. – inset, Fig. 3).

4. In the limits of the given experimental errors it is impossible to comprehend whether the samples N^o 438 and N^o 6 (Fig. 3, column 5) belong to one and the same thrust body or to different but very close phases.

Acknowledgements

This investigation was performed according to the program of the bilateral scientific cooperation between the Hungarian and Bulgarian Academies of Sciences. K/Ar dating was sponsored by the Hungarian National Scientific Research Found (OTKA), Project N^o 1180. The authors thank the authorities of both Academies, of ATOMKI and Geological Institute (Sofia) for the organizing financial support.

References

- Bahneva-Stefanova, D. 1981: On the genesis of the West-Rhodope porphyroclastic rhyolitic complex. – 12th Congress CBGA, Abstracts, pp. 215–216.
- Bahneva, D., N. Stefanov 1975: Facies and volcano-structural predestination of the volcanism in the Central Rhodope (on the example of the Perelik structure). – *Geol. Balcanica*, 5, 4, pp. 29–43.
- Bahneva, D., M. Stoinov, N. Stefanov, T. Poyak, F. Eggerer, K. Nomeskanski 1984: Comparative characteristic of the Tertiary acid volcanism in the Central Rhodope (Bulgaria) and in the North-Eastern Hungary. – *Ann. High. Inst. of Min. and Geol., Sofia; Part II, Geol.*, 30, pp. 73–88.
- Balogh, Kad., 1985: K/Ar dating of Neogene volcanic activity in Hungary: Experimental technique, experiences and methods of chronological studies. – *ATOMKI report D/1.*, pp. 277–288.
- Cavelier, C., Ch. Pomerol 1983: Stratigraphy of Paleogene. – *Bull. Soc. geol., France*, 8, 2, pp. 255–265.
- Cox, A., G.B. Dalrymple 1967: Statistical analysis of geomagnetic reversal data and the precision of potassium-argon dating. – *Jour. Geophys. Research*, 72, pp. 2603–2614.
- Eleftheriadis, G., H.J. Lippolt 1984: Age determinations on Oligocene volcanites from the Southern Rhodope massif (Northern Greece). – *Jb. Geol. Paläont. Mh. Stuttgart*, H. 3, pp. 179–191.
- Evernden, J.F., G.T. James 1964: Potassium-argon dates and the Tertiary floras of North American. – *Am. Jour. Sci.*, 262, pp. 945–974.
- Gillespie, A.R., J.C. Huneke, G.J. Wasserburg 1982: An assessment of ^{40}Ar - ^{39}Ar dating of incompletely degassed xenoliths. – *J. Geophys. Res.*, 87, pp. 9247–9257.
- Harland, W.B., A.V. Cox, P.G. Lewillyn, C.A. Hecton, A.G. Smith, R. Walters 1982: Geological Time Scale. – Cambridge University Press, p. 131.
- Harkovska, A. 1987: Injection clastic dykes in the eastern part of the Perelik volcanic massif (Central Rhodopes). – *Geotect., Tectonophys. and Geodinam.*, 20, pp. 46–61. (in Bulg. Engl. abstr.)
- Harkovska, A., N. Sirakov 1986: Morphological types of jointing and fracture surface marks in Paleogene volcanics west of Smolyan (South Bulgaria). – *Geotect., Tectonophys., Geodinam.*, 19, pp. 23–38.
- Harkovska, A., Y. Yanev, P. Marchev 1989: General features of the Paleogene orogenic magmatism in Bulgaria. – *Geol. Balcanica*, 19, 1, pp. 37–72.
- Innocenti, F., N. Kolios, P. Manetti, R. Mazzuoli, A. Peccerillo., F. Rita, L. Villari 1984: Evolution and Geodynamic of the Tertiary Orogenic Volcanism in Northeastern Greece. – *Bull. Volcanol.*, 47, 1, pp. 26–37.
- Ivanov, R. 1984: Main Tectonomagmatic and Ore-Generating Structures in the Rhodope Massif. – *Travaux de l'Institut d'exploration des gîtes métallifères et nonmétallifères. Sofia*, pp. 135–157. (in Bulg.)
- Lilov P., D. Bahneva 1989: K/Ar dating of the acidic volcanism in the Central Rhodopes. – 14th Congress CBGA Extended Abstracts, pp. 1190–1194.
- McDougall, I., H.A. Polach, J.J. Stipp 1969: Excess radiogenic argon in young subaerial basalts from Auckland volcanic field, New Zealand. – *Geochim. Cosmochim. Acta*, 33, pp. 1485–1520.
- Odin, G. 1982: The Phanerozoic time scale revised. – *Episodes*, 3, pp. 3–9.
- Steiger, R.H., E. Jäger 1977: Subcommission on Geochronology; Convention on the use of decay constants in Geo- and Cosmochronology. – *Earth Planet. Sci. Lett.*, 36, pp. 359–362.
- Vacev, M., I. Christov 1983: Lithostratigraphy of the Tertiary sedimentary- volcanic complex in the Smolyan depression. – *Ann. of Min. and Geol., Sofia, Part II; Geology*, XXX, 28, 2, pp. 105–120. (in Bulg. Eng. abstr.)
- Walker, G.P.L. 1983: Ignimbrite types and ignimbrite problem. – *Volcanol. Geotherm., Res.*, 17, pp. 65–88.

Studies on chromite and its significance in the Lower and Middle Cretaceous of the Tatabánya Basin and Vértes Foreground

Klára Vaskó-Dávid

*Geological Research Team,
Hungarian Academy of Sciences, Budapest*

Al-chromite is the most characteristic detrital heavy mineral in the Neszmély Formation and in the Vértessomló Aleurolite Formation, and occurs also in the Tés Clay-Marl Formation. The accumulation of Cr is 18-fold in the Neszmély Sandstone Formation and 10-fold in the Vértessomló Aleurolite (concerning the samples studied). In the Tés Clay-Marl Formation studied in detail the accumulation is only 4-fold. This accumulation is bound to the transgressive phases of basin sediments with changing salinity. In addition the well-known Cr-accumulation of Cretaceous bauxites, in the Fenyőfő bauxite small fragments of Al-chromite could be identified. The ilmenite grains of the Iszcaszentgyörgy bauxite contain Cr in varying quantities. Data obtained by laser microspectral analyses show Cr-free to high-Cr ilmenites.

Based on the mineralogical features, X-ray diffractometric data (wavelength and intensity) the Al-chromite falls between the Cr-picotite and Cr-hercynite. By means of activation analysis a molar Cr/Al ratio of 43:1 was determined. The occurrence of detrital Al-chromite in these formations proves that the sedimentary basins of these formations were situated in a region into which the material of ophiolitic rocks generated in eugeosyncline zone was also transported.

Keywords: Lower-Cretaceous sandstone, Middle-Cretaceous aleurolite and clay-marl, Al-chromite ophiolites, bauxite, ilmenite

Introduction

The mineralogical-geochemical investigation of clastic sedimentary rocks provides a fair possibility to the petrological identification of the primary rock bodies and to the areal determination of their extension. By means of the minerals of indicator value from the genetic point of view key data can be obtained concerning the existence and evolution of different geological structures.

As a first approximation microscopic studies were carried out. The modern instrumental analysis can be used in the second stage after the required preparation and enrichment.

The application of the mineralogical-geochemical method is especially significant in case of the Cretaceous formations of the Transdanubian Midmountains since subsequently to the Triassic and Jurassic predominantly carbonate rock species of chemical and biogenic origin, the Cretaceous formations contain remarkable clastic material of terrestrial origin. This method could not play important role in

Address: Klára Vaskó-Dávid: H-1088. Budapest, Múzeum krt. 4/a
Received: February 12, 1991

the research of Cretaceous formation so far since only sporadic data were available from certain formations and sequences. The serial analyses seemed to be promising. Some preliminary analyses were carried out by E. Csánk on several Middle Cretaceous variegated clays from the Vértes Foreground. In addition to some igneous and metamorphic heavy minerals, no chromite is mentioned. In the course of my studies it succeeded to determine chromite in several Lower and Middle Cretaceous sequences of the Transdanubian Midmountains.

Since chromite is primarily found mostly in peridotitic rocks, in abyssal ultramafic differentiates (Szádeczky-Kardoss 1955) and due its genetic significance as a guide in geological conclusions concerning the temporal and spatial relationships, detailed studies were carried out on the chemical composition and crystal structure.

Based on the investigations performed so far some specific mineralogical information were gained concerning the provenance areas of sediments of the Lower and Middle Cretaceous basins that may be of great importance from the tectonic and bauxite genetic points of view in Hungary.

Materials

This work was done in the frame of elaborating the geological key sections of Cretaceous formations in the Transdanubian Midmountains initiated by J. Fülöp.

The instrumental analytical investigations were carried out at the Department for Mineralogy, for Petrology and Geochemistry of the Eötvös University, and the Laboratory for Geochemical Research of the Hungarian Academy of Sciences granted by full professors J. Kiss and I. Kubovics and by Gy. Pantó, scientific director. Analyses were done by J. Kiss, J. Nagy-Balogh., J. Bérczi and M.N. Tóth.

I. By each meter micromineralogical investigations were made:

1. from the Tés Clay-Marl Formation of lagoonal kind of the Vértes Foreground (Fig. 1), from the Albian sequences of

- Pusztavám–980 borehole, 216 m;
- Mór–15 borehole, 178.3 m;
- Bokod–1828 borehole, 94 m;
- Oroszlány–1981 borehole 92 m.

2. From the marine Vértessomló Aleurolite Formation of the Tatabánya basin (Fig. 1), from the Albian strata of

- Tatabánya–1462 borehole 84 m;
- TVG–59 borehole, 35.5m (metres denote the sampled intervals).

II. Sporadic samples:

1. Neszmély Formation (Fig. 1)

- from the Lower Cretaceous sandstone to aleurolite sequence of the Tatabánya–1329 borehole (19 pieces) and Tatabánya–1481 borehole (22 pieces)

2. Some bauxite samples

- pisolithic variety from Iszkaszentgyörgy;
- spotty-veined variety from Gánt;
- from the Fenyőfő–683 borehole (87.4–112.1 m)

3. Tata, Kálvária Hill, from Jurassic rock samples (5 pieces).

Investigations were carried out after the treatment with hydrochloric acid of 10 %, from the fraction of 0.1–0.2 mm diameter, in nitrobenzol–Canada balsam preperates.

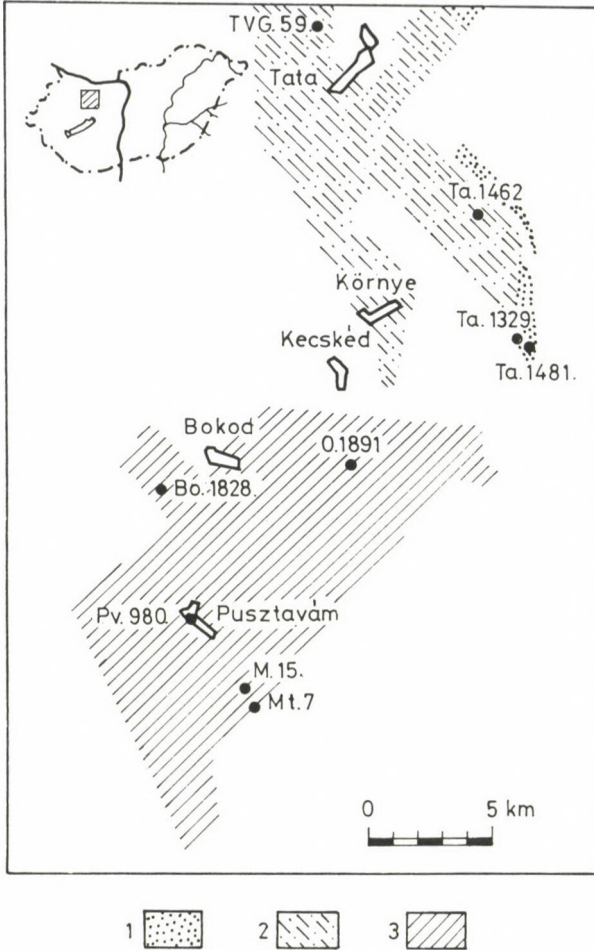


Fig. 1. Geographical position of the studied Lower and Middle Cretaceous formations and the boreholes in the Tata-bánya Basin and in the Vértessomló Foreground. 1. Neszmély Formation; 2. Vértessomló Aleurolite Formation; 3. Tés Clay-Marl Formation

Al-chromite in the clastic material of the studied borehole profiles

Throughout the Neszmély and the Vértessomló Aleurolite Formation (Figs 3, 4) and in certain horizons of the Tés Clay-Marl Formation (Fig. 2) a dark-brown-to-black population of conchoidal fracture with deep-purple transparency in the margins could be determined, this opaque mineral proved to be chromite (Plates 1., 2.).

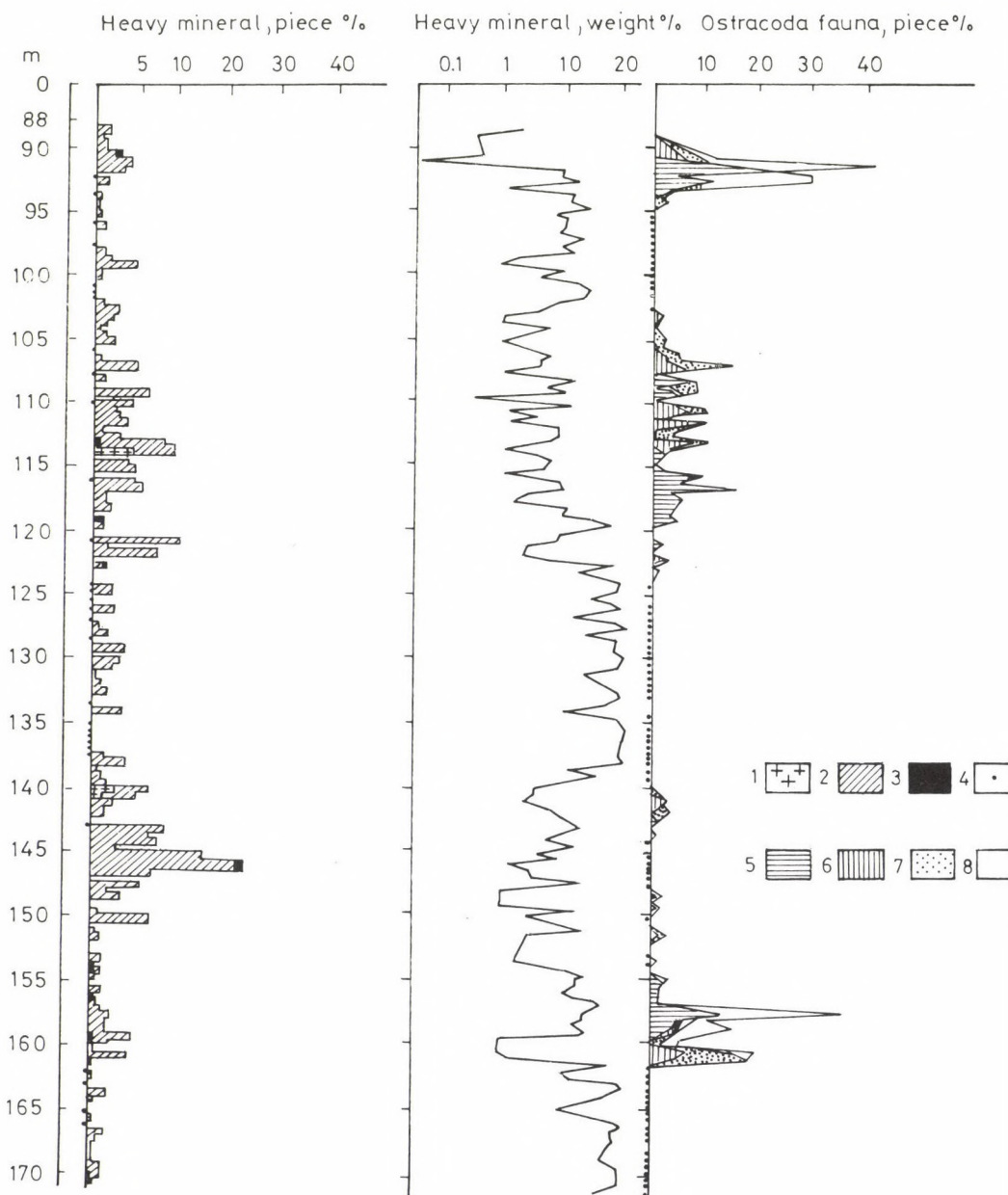


Fig. 2/a. Relation between the heavy minerals and biofacies of the Tés Clay-Marl Formation, in the borehole Mór-15 (Vaskó-Dávid, K. 1988). 1. Igneous heavy minerals; 3. Al-chromite; 4. no detrital heavy minerals can be determined, fauna-free; 5. freshwater biofacies; 6. brackish biofacies; 7. marine biofacies; 8. fauna fragments

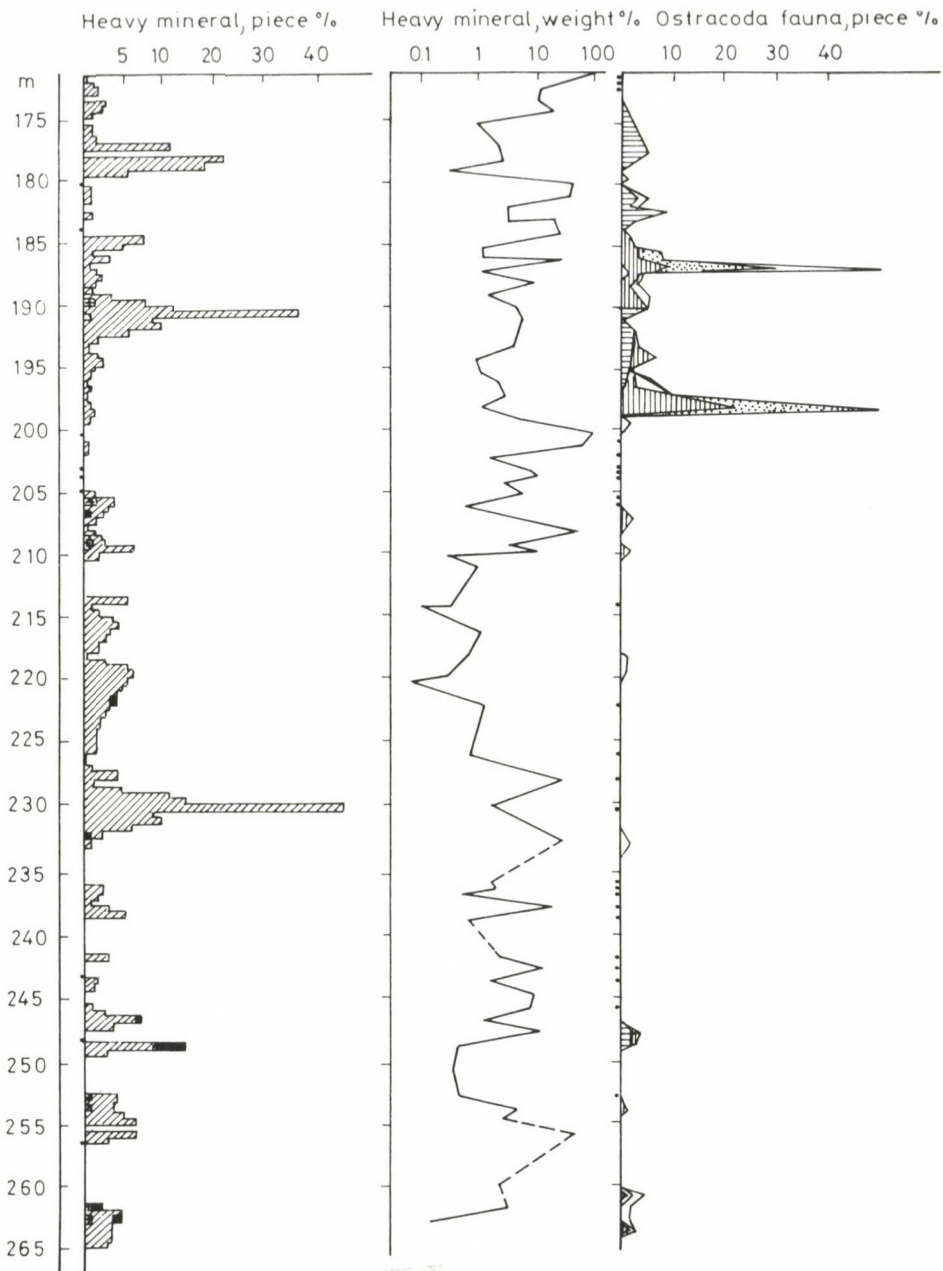


Fig. 2/b. legend: see Fig. 2/a.

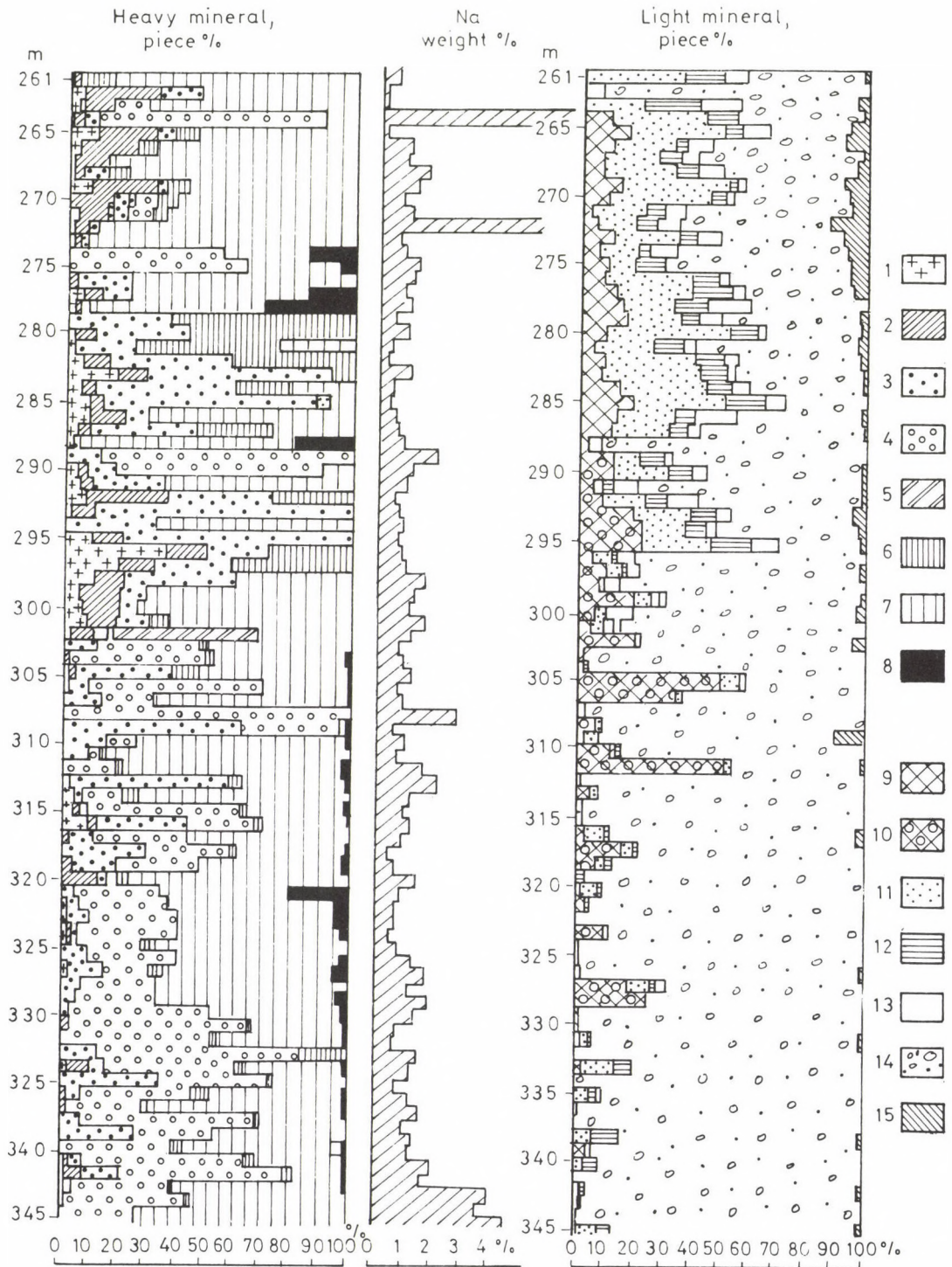


Fig. 3. Micromineralogical data of the Vértessomló Aleuolite Formation in the Tatabánya-1462 borehole. 1. Heavy minerals of mixed and metamorphic origin; 3. Al-chromite in the detritus; 4. detritus; 5. barite; 6. limonite; 7. pyrite; 8. plant remnants; 9. siliceous groundmass; 10. chalcedony spherulite; 11. quartz; 12. quartzite; 13. muscovite; 14. detritus; 15. feldspars

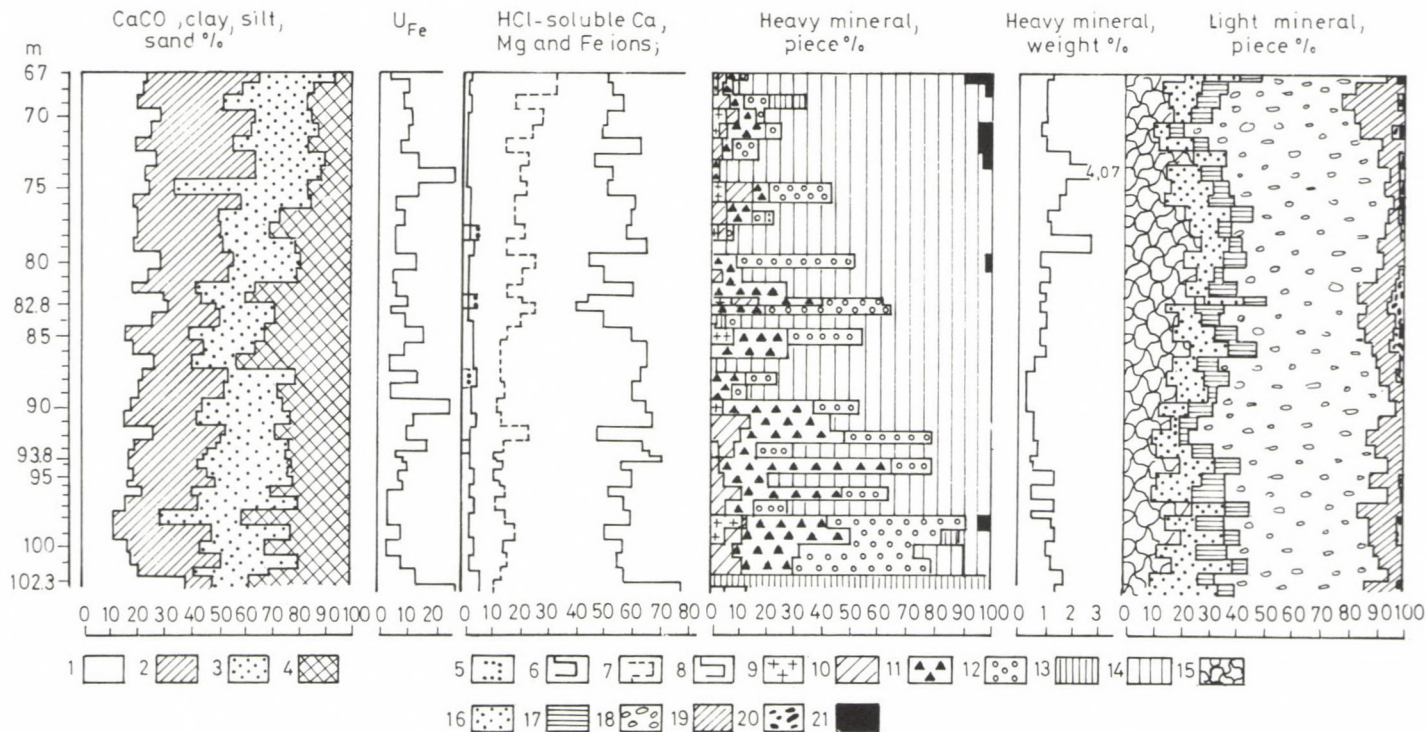


Fig. 4. Profile of the Vértessomló Aleurolite Formation in the TVG-59 borehole (Vaskó-Dávid, K. 1988) 1. CaCO₃; 2. clay; 3. silt; 4. sand; 5. MgO; 6. FeO+Fe₂O₃; 7. CaO; 8. solution residue; 9. minerals of igneous origin; 10. minerals of mixed and metamorphic origin; 11. Al-chromite; 12. leucoxene; 13. limonite; 14. pyrite, chalcopyrite; 15. microcrystalline rock detritus; 16. quartz; 17. quartzite; 18. weathered rock detritus; 19. plagioclase; 20. feldspars; 21. organic plant remnants

Components determined by laser microspectral analysator

Records were made of seven presumably chromite grains (borehole Ta-1329, depth: 488.2 m). All the grains produced the same spectrum.

Main components: Fe, Cr

Main or subordinate components: Al

Minor components: Si, Ca, Mn

Trace components: Ti, Co, Zn?, Pb?

Analyses were carried out by J. Nagy-Balogh, Eötvös University, Department for Petrology and Geochemistry.

X-ray diffractometry

The X-ray diffractometric records were made by M.N. Tóth (Laboratory for Geochemical Research, Hungarian Academy of Sciences), from chromite enriched by magnetic separator from the heavy mineral fraction. Table 1 contains the wavelengths of the mineral and the closest ASTM values.

Table 1.

Chromite (ASTM)		Chromite (ASTM)		Borehole Ta-1481, Chromite diffraction record		Debye-Scherrer record		Cr-hercynite (ASTM)	
dA	I	dAo	I	dA°		dA°	I	dA°	I
4.65	8 111	4.800	5 111	4.762	111	4.7450	ms	4.70	8 111
2.84	9 220	2.930	6 220	2.917	220	2.9029	ms	2.91	7 220
2.42	10 311	2.499	10 311	2.491	311	2.4880	ms-w	2.48	10 311
2.32	1 222	2.390	1 222						
2.01	9 400	2.070	7 400	2.058	400	2.05979	ms-s	2.05	7 400
1.85	8 311						ms		
1.64	9 422	1.690	4 422	1.673	422	1.6865	s	1.67	2 422
1.55	9 511	1.592	9 511	1.588	511-333	1.5876	s	1.58	9 511
	-333		-333						-333
1.42	10 440	1.461	9 440	1.461	440	1.4609		1.455	10 440
		1.398	1 534						
		1.310	2 620						
1.22	6 533	1.261	5 533				s	1.212	3 533
		1.196	3 444			1.1919	w-vw	1.186	1 444
1.14	4 711	1.158	3 711						
	-551		-551						
		1.107	3 642						
1.05	2 731	1.079	3 731			1.0753	ms	1.072	4 731
	-553		-553						-553

Debye-Scherrer powder record

Record was made from the heavy mineral separated of the material from the borehole Ta-1329. Results are as follows:

	I	d (Å)	Mineral
1.	ms	4.7450	Cr
2.	ms	3.3143	Le
3.	ms	2.9029	Cr
4.	ms-w	2.6984	He
5.	vs	2.4880	Cr
6.	ms-s	2.0579	Cr
7.	vw	1.8554	He
8.	(ms) w	1.7333	Le
9.	ms	1.6865	Cr
10.	s	1.5876	Cr
11.	s	1.4609	Cr
12.	ms	1.2606	Cr
13.	w-vw	1.1919	Cr
14.	w	1.1067	He
15.	ms	1.0753	Cr
16.	ms	0.9591	He

Abbreviations: I = line intensity; vs = very strong; ms = medium strong; w = weak; vw = very weak; s = strong; Cr = Al-chromite, Fe (Cr, Al)₂O₄; He = hematite, Fe₂O₃; Le = lepidocrocite, FeOOH (record: É. Györe, evaluated: J. Kiss)

Based on its reflexion lines the mineral is qualified as Al-chromite or Cr-hercynite.

Neutron activation analysis

As to the results of neutron activation analyses the measure of Al-substitution in the mineral is 43/1 MolCr/MolAl. Measurements were carried out by J. Bérczy (Eötvös University, Department of Mineralogy, with the aid of the nuclear reactor of the university).

In Table 2 the detrital heavy mineral content of the sequences are summarized. As it is seen from the table the main part of the group of mafic-ultramafic origin is constituted by Al-chromite. In addition to chromite, magnetite and hematite are also frequent, and metamorphic chlorite, tremolite-actinolite, antophyllite are also found (Table 2). In the thin section of the rock it is seen that serpentine and chlorite are main components of the Lower Cretaceous sedimentary facies (K. Vaskó-Dávid 1988). In the electron micrograph of chromite fine-dispersed hematite and antophyllite lamellae are seen. In the electron diffraction picture, in addition to the main lines of chromite, some lines of hematite and antophyllite also occur (K. Vaskó-Dávid 1988).

Temporal and spatial changes of Cr-contents and chromite contents of the studied formations

The semi-quantitative trace element analytical data obtained from emission spectrographic records (Q-24 Zeiss) are comprehended in Table 3. The accumulation is 18-fold in the Lower Cretaceous sandstone and 10-fold in the Albian Vértessomló Aleurolite Formation. The average enrichment factor in the borehole M-15 drilled in the Albian Tés Clay-Marl Formation is only 0.59. The maximal enrichment factor is only 4. In the borehole lying northeast of this borehole, No. 0.1981 the average Cr-enrichment is 1.77-fold. The enrichment of Cr is accompanied to certain extent by that of Ni and Co. No remarkable enrichment was experienced in case of Ti. Trace element analyses were carried out at the Department for Ge-

ochemistry of the Hungarian Geological Survey and partly at the Department for Petrology and Geochemistry of the Eötvös University, Budapest.

Table 2. Percentual distribution of detrital heavy minerals among each other in the studied Lower and Middle Cretaceous borehole profiles Vaskó-Dávid, K. 1988, modified version.

Fraction of 0.1–0.2 mm of the solution residue after treatment with HCl of 10%		Lower Cretaceous				Middle Cretaceous					
		Neszmély Formation		Vértessomló Aleurolite Formation		Tés Clay–Marl Formation					
number of samples taken into account in average calculation		22	19	84	41	120	245	214	176	59	
borehole number		Ta–1481	Ta–1329	Ta–1462	TVG–59	Mt–7	M–15	PV–980	Bo–1828	O–1891	
limonitic–hematitic grains (piece %)		84.81	79.62	84.54	67.90	>90%	>90%	>90%	>90%	94.54	
average detrital minerals (piece %)		15.19	20.38	15.46	32.10	6.48 db/e	6.51 db/e	2.41 db/e	13.60 db/e	5.46	
heavy minerals of igneous origin	mafic–ultra mafic	chromite	32.60	43.09	1.25	49.52	7.72	2.00	0.19	1.16	2.35
		chromite–containing detritus	1.90	2.76	65.98	23.13	–	–	–	–	–
		magnetite	25.56	17.04	1.85	2.43	1.8	5.20	0.39	3.08	2.09
		ilmenite	–	–	–	–	–	–	–	–	6.72
		augite	0.29	–	0.03	–	–	0.06	4.27	1.20	–
		hypersthene	1.02	1.24	1.12	0.78	0.39	1.19	0.97	0.62	1.49
		enstatite	0.14	–	0.07	–	–	–	–	–	0.14
		rutile	–	–	0.48	0.04	1.29	0.94	0.78	0.16	0.41
		anatase	–	–	–	0.01	–	–	–	–	–
		brookite	0.29	–	–	–	0.26	–	–	0.04	0.14
	hematite	19.71	22.19	–	–	–	–	–	–	–	
	total:		81.51	86.32	70.78	75.91	11.46	9.39	6.60	6.26	13.34
	acid	zircon	0.87	0.38	1.88	1.13	10.81	1.75	1.75	2.37	3.63
		apatite	–	–	0.03	–	1.93	0.56	0.78	–	0.27
		titanite	0.14	–	–	–	1.42	–	–	–	0.27
		biotite	–	–	4.77	3.39	–	0.88	9.71	1.41	12.60
	vein min.	fluorite	–	–	–	–	–	–	–	–	18.19
barite		–	–	4.88	–	–	–	–	1.19	12.60	
total		1.01	0.38	11.56	4.52	14.16	3.19	12.24	4.97	47.56	
heavy minerals of mixed and metamorphic origin	mixed	garnet	3.80	0.85	6.62	2.43	17.37	45.90	24.08	9.91	17.64
		tourmaline	3.07	0.76	1.37	6.52	27.41	13.34	10.10	12.58	12.35
		chlorite	0.43	1.00	6.90	9.95	16.60	11.21	28.74	63.20	3.91
	epi-	alkali amphibole	1.31	0.55	0.94	0.93	1.29	3.88	0.58	1.01	0.63
		tremolite–actinolite	2.92	3.52	0.18	0.17	4.51	1.31	7.77	0.10	0.27
		antophyllite	6.28	6.00	–	–	–	0.69	–	0.20	0.27
		epidote	0.14	–	0.41	0.21	3.60	6.39	4.85	1.37	2.09
		zoisite	0.43	0.14	0.45	0.04	2.19	4.00	4.47	0.95	0.69
	meso-	staurolite	0.14	0.38	0.04	–	0.13	–	–	0.12	–
		andalusite	–	–	–	–	–	–	–	–	0.14
		blue amphibole	–	–	–	–	0.51	0.44	0.19	0.40	0.32
		kyanite	–	–	0.05	–	0.77	0.25	0.39	0.12	0.41
	total		18.52	13.30	16.96	20.25	74.38	87.51	81.17	89.36	38.72

The occurrence of chromite (Fig. 5 and Table 2) as well as the Cr-contents (Fig. 6 and Table 3) show an increasing tendency northeastwards.

The Neszmély Formation displays most remarkably the traces of deposition of the ultramafic detrital material. Al-chromite is found mainly in form of individual grains and the highest Cr-enrichment can be assigned to these fractions. Al-chromite can be throughout determined in the Vértessomló Aleurolite.

Based on the locally enriched Cr-values and on the chromite occurrence in some samples only a several times repeating indirect effect can be determined in the Albian variegated clay.

Out of the two profiles of the Vértessomló Aleurolite in the borehole TVG-59 lying in the north the piece percentage of detrital heavy minerals is much higher and the chromite grains are mainly individual grains (in the borehole Ta-1462 chromite is found mainly in the detrital material of lower specific weight).

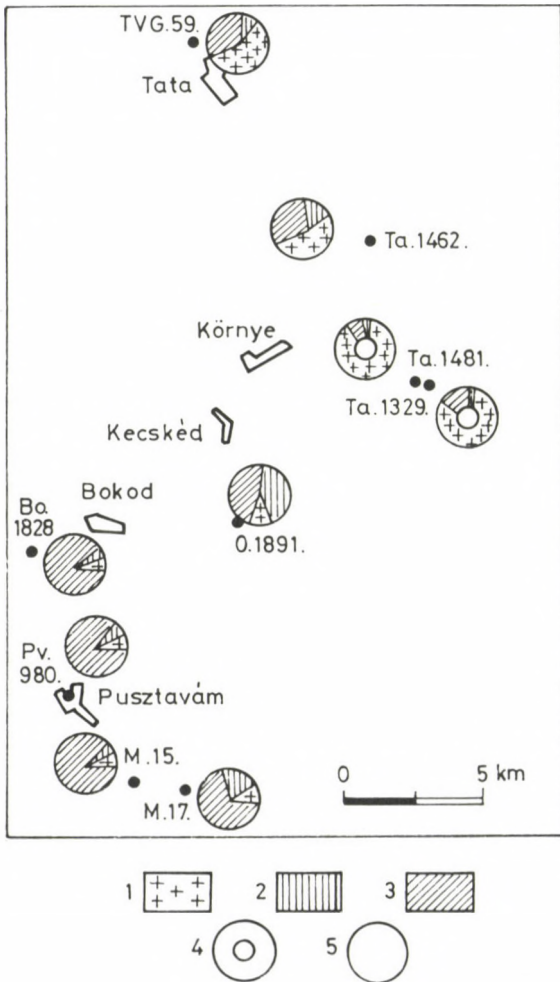


Fig.5. Proportion of occurrence of the detrital heavy minerals of different genetics in the studied Lower and Middle Cretaceous sequences (Vaskó-Dávid, K. 1988). 1. Basic igneous; 2. acid igneous; 3. heavy minerals of mixed and metamorphic origin; 4. Lower Cretaceous; 5. Middle Cretaceous

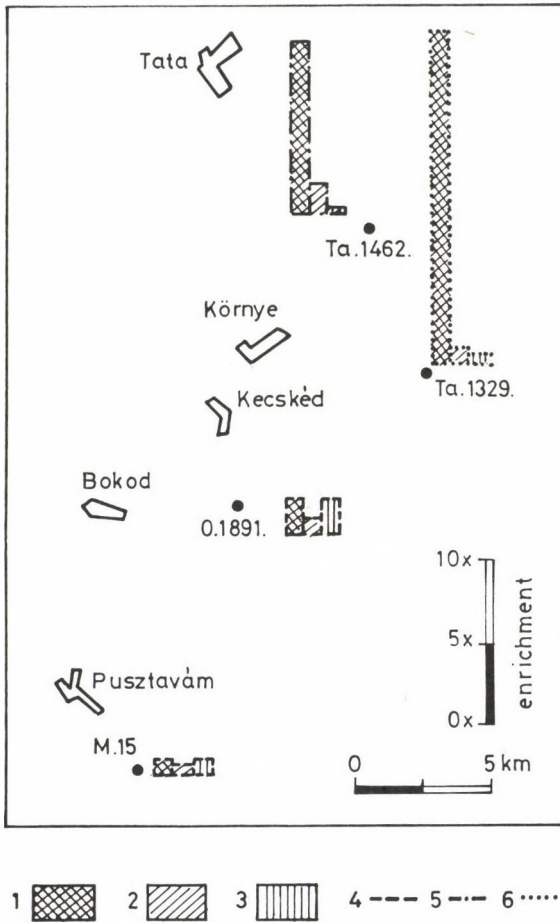


Fig. 6. Enrichment ratios of Cr, Ni and Pb in the studied Lower and Middle Cretaceous sequences (Vaskó-Dávid, K. 1988). 1. Cr; 2. Ni; 3. Pb; 4. Tés Clay-Marl Formation; 5. Vértes-somló Aleurolite Formation; 6. Neszmély Formation

The ultramafic provenance area supplying Al-chromite

In the Jurassic limestone varieties containing very small amounts of detrital material (Lower Liassic and Lower Dogger of the Tata Kálvária Hill) the Al-chromite could also be determined. The rock supplying Al-chromite was probably exposed in the source area during the Jurassic, too. The presence of acid soluble Mg-bearing minerals of the Lower Cretaceous sandstone refers to short distance of the rock from the site of deposition.

In the Rossfeld strata being stratigraphically akin to the Neszmély Formation also large amounts of Cr-spinel were determined (Decker et al. 1987; Pober and Faupl 1988). The determinability of Al-chromite deriving from ophiolites relating to the former position of eugeosynclines proves in the studied formations that the sediment collectors of these formations were situated in a region into which also the detrital material of these ophiolites was transported

Table 3. Trace element concentrations in the studied Lower and Middle Cretaceous formations (Vaskó-Dávid, K. 1988, modified version)

	studied trace elements	sedimentary average of Vinogradov	Lower Cretaceous	Middle Cretaceous													
			Neszmély Formation Ta-1481, Ta-1329 6 pieces	Vértessomló Aleurolite Formation Ta-1462, 3 pieces	Tés Clay-Marl Formation												
					O-1891 10 pieces	M-15 borehole 268 samples											
						Complete profile				marine strata		brackish strata		freshwater strata		fauna-free strata	
D	D	D	a	Da	Max.	D. max	a	D	a	D	a	D	a	D			
elements relating to mafic rocks	Cr	100	18.00	10.10	1.77	53.46	0.53	400	4.00	84.86	0.84	60.25	0.60	69.00	0.69	46.50	0.46
	Ni	95	1.55	1.68	0.80	48.29	0.50	100	1.05	56.45	0.59	55.44	0.58	61.79	0.65	46.54	0.47
	Co	20	1.29	1.35	0.40	14.59	0.72	40	2.00	15.84	0.79	14.25	0.71	18.00	0.90	12.26	0.61
	Ti	4500	0.69	0.13	0.58	2888.00	0.64	10000	2.22	2589.00	0.57	3545.00	0.78	3791.000	0.84	2816.00	0.65
	V	130	0.43	0.19	1.00	55.12	0.42	250	1.92	50.71	0.39	70.62	0.54	73.000	0.56	55.00	0.42
elements relating to acid rocks	Li	30	2.60	3.33		88.16	2.93	250	8.33	88.61	2.95	94.80	3.16	121.70	4.05	86.57	2.88
	Pb	20	0.43	0.20	1.87	12.22	0.61	100	5.00	6.60	0.33	11.81	0.59	17.44	0.87	11.31	0.56
	Ba	800	0.32	0.31	0.44	263.50	0.33	1600	2.00	269.0	0.33	328.30	0.41	370.80	0.46	266.00	0.33
	Ga	30	0.30	0.13	0.55	9.85	0.32	40	1.33	8.82	0.29	1.69	0.38	14.81	0.49	10.14	0.333
	B	100	0.18	0.25	0.44	61.56	0.61	250	2.50	48.78	0.48	60.20	0.60	73.29	0.73	60.61	0.60
	Sr	450	0.95	1.33	0.53	186.20	0.41	1000	2.22	280.00	0.62	359.00	0.79	257.00	0.57	92.00	0.20
	Cu	57	0.66	0.70	1.40	39.00	0.68	100	1.75	37.15	0.65	41.91	0.73	52.93	0.92	35.21	0.61
	Mn	670	1.64	2.39	2.63	1168.00	1.74	6000	8.96	1609.00	2.40	1810.00	2.70	1663.00	2.48	715.1	1.12

D – enrichment as compared to the sedimentary averages of Vinogradov; a – average trace element concentration (ppm); Da – enrichment calculated from the averages; Max – maximal trace element concentration (ppm); D. max – enrichment calculated from the maximal trace element concentrations

Cr being accumulated usually in terrestrial sediments occurs in the marine strata of the Tés Clay-Marl Formation with somewhat higher enrichment factor than in the brackish, freshwater or fauna-free strata (Table 3).

The average piece percentage of detrital heavy minerals (5.46 piece %) is much lower in the O-1891 borehole lying closest to the borehole Ta-1462 in the northern part of the profile, than in the only marine Vértessomló Aleurolite in the borehole Ta-1462 (15.46 piece %).

All these seem to support the fact that the increase of Cr-content can be related to the temporarily repeating marine effects and if there were some Cr-containing material transport between the two regions of different facies, this could exist only from the direction of the aleuritic formations.

Relations to the bauxite genesis

Among the microminerological and geochemical data concerning the Iszka-szentgyörgy bauxite reference is made to the unexplainable Cr-accumulation (Vörös 1958), but no chromite could there be determined. Based on this data the overwhelming majority of the bauxite heavy minerals is represented by ilmenite.

In the course of our investigations, in the fraction of 0.1–0.063 mm of the Fenyőfő sample chromite was found showing sharp edges similarly to those mentioned above and which cannot be considered to be autochthonous. Its quantity, however, was subordinated: besides several hundred ilmenite grains only a few chromite grains were found.

When looking for the reason of Cr-accumulation in the Iszka-szentgyörgy bauxite, the bind of Cr to different grain size fractions of the bauxite was also studied. The lowest amount of Cr (60 ppm) was found in the filtrate after boiling with hydrochloric acid of 10% and in the clay fraction of 0.063 mm. The Cr quantity increases with the Ti-contents: the proportion of Cr increases as compared to Ti in the coarsest fraction (0.2–0.5 mm) that contains large resorbed ilmenite grains, too. In the Fenyőfő sample being the poorest in Ti, in the fraction of 0.2–0.5 mm relatively Ti-lack and slight Cr-surplus are found.

Laser spectrographic study of ilmenites

It was our presumption that mafic rocks also occur among the source rocks of bauxites. To prove this assumption the laser spectrographic analyses of ilmenites of greater possibilities in origin than chromites were performed. Results are summarized in Table 4. Analyses were carried out by J. Nagy-Balogh (Eötvös University, Department of Petrology and Geochemistry).

The studied 11 grains seem to represent three types:

1. High Cr-content (with slight V, Co, Si and Zr contents);
2. Idiomorphic grains of corroded surface and of coloured reflection with Zr and Si contents (with slight Cr-content), as well as ilmenite fragments of conchoidal fracture, brownish-black colour and of sharp margin.

Plate 1

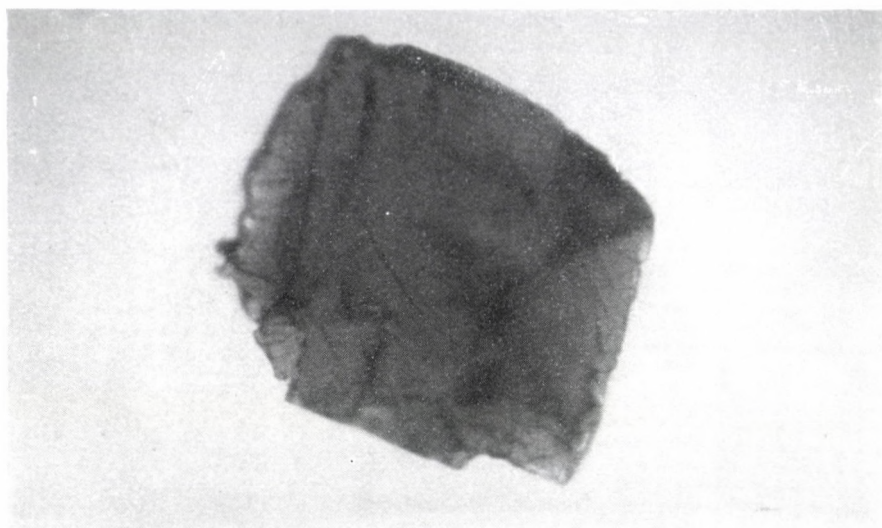
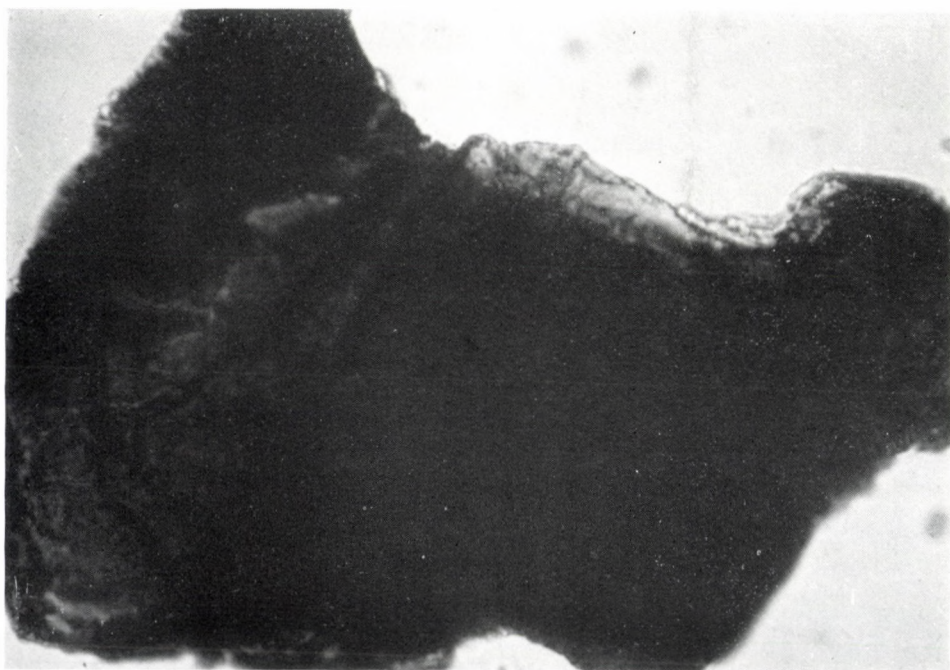


Plate 2



1 - 2. Micromineralogical prepare. Al-chromite grain imbedded in Canada balsam, from heavy mineral fraction of the studied samples, IN, M = 560X, IN 960X (Vaskó-Dávid, K. 1988).

3. Practically Cr-free, Si-free and Zr-free idiomorphic grains with complete faces and edges, with white reflection colour.

As a conclusion it can be stated that Cr accumulating in the coarse fraction of bauxite, is found in ilmenite of definite type in addition to chromite, and these may derive from mafic rocks.

Table 4. LMA spectra of ilmenite grains from bauxite (Vaskó-Dávid, K. 1988)

	Ti	Cr	Ni	Co	V	Mg	Al	Zr	Si	Mn	Ca	Fe	Cu	It
1	many	s	0	0	s	s	t	0	vw	s	vw	many	t	0
2	many	st	0	0	s	s	s	0	t	s	s	many	t	w
3	many	st	0	0	s	s	s	0	0	s	s	many	st	w
4	many	st	0	0	st	s	t	0	0	st	st	many	st	vw
5	many	t	0	0	s	s	st	vw	0	s	s	many	st	w
6	many	vw	0	0	s	s	t	t	st	s	vw	many	t	0
7	many	t	0	0	s	s	st	vw	st	s	s	many	st	0
8	many	w	0	0	s	s	st	vw	0	st	s	many	st	vw
9	many	vw	0	vw	t	st	t	0	0	st	st	many	st	0
10	many	vw	0	0	t	t	st	t	vw	st	st	many	st	vw
11	many	0	0	0	t	t	t	0	0	st	st	many	t	0

s= strong; st= strong trace; t=trace; w=weak; vw=very weak; vvw=very-very weak

Conclusions

1. In the erosion surface an ultramafic rock existed already in the Jurassic and commenced to be eroded in the Lower Cretaceous. The Al-chromite bearing material of this rock can be traced in the Lower Cretaceous of the Tatabánya Basin and the Albian of the Vértes Foreground. This proves that the sediment collectors of these formations were situated in a region into which ophiolites generated in eugeosyncline zone could be transported.

2. Out of the studied formations, Cr-shows the highest accumulation in the Neszmély Formation, the Al-chromite is most frequent here, too.

3. Al-chromite can be continuously determined only in the marine Albian Vértessomló Aleurolite Formation.

4. Al-chromite is rarely found in the Tés Clay-Marl Formation of Albian age deposited in the basin of changing salinity. The relatively higher Cr-contents can be determined only in the marine formations of this sequence.

5. In the two Middle Cretaceous Formations the chromite quantities show a trend of increase northwards.

6. It is improbable that one has to deduce the known trace element associations of the Hungarian bauxite beds only from acid igneous, metamorphic and sedimentary source rocks, but the role of basic igneous rocks has to be considered, as well.

References

- Decker, K., P. Faupl, A. Müller 1987: Synorogenic sedimentation on the Northern Calcareous Alps during the Early Cretaceous. – *Geodynamics of the Eastern Alps*, Wien, pp. 126–142.
- Fülöp, J. 1958: A Gerecse hegység kréta időszaki képződményei (Cretaceous formations of the Gerecse Mountains). – *Geol. Hung. ser. Geol.*, 11, p. 122.
- Fülöp, J. 1964: A Bakony hegység alsókréta képződményei (Lower Cretaceous formations of the Bakony Mountains). – *Geol. Hung. ser. Geol.*, 13, p. 193.
- Pober, E., P. Faupl 1988: The chemistry of detrital chromian spinels and its implications for the geodynamic evolution of the Eastern Alps. – *Geol. Rundschau*, 77, 3, pp. 641–670.
- Szádeczky-Kardoss, E. 1955: *Geokémia* (Geochemistry). – Akad. Kiadó, Budapest, p. 680.
- Vaskó-Dávid, K. 1988: Krómit vizsgálatok és azok jelentősége a Tatabányai medence és a Vértes előterének alsó- és középsőkrétájában (Chromite investigations and their significance in the Lower and Middle Cretaceous of the Tatabánya Basin and Vértes foreground). – *MÁFI Annual Report on 1986*, pp. 241–261.
- Vörös, I. 1958: Iszkaszentgyörgyi bauxit-szelvények mikromineralógiai és nyomelemvizsgálata (Micromineralogical and trace elements analyses in the bauxite profiles of Iszkaszentgyörgy). – *Földt. Közl.*, 88, 1, pp. 48–56.

The heavy mineral content and mineralogical maturity of the Cenozoic psammites in Hungary

Edit Thamó-Bozsó

Hungarian Geological Institute, Budapest

The data obtained from the micromineralogical examination of about 5500 Hungarian Cenozoic psammite samples, the fraction of 0.1–0.2 mm, published before 1983, was processed by computer. The heavy mineral content and the maturity of different epoches were compared with frequency histograms and statistical characteristics (mean, standard deviation, median).

Eocene psammites have the lowest heavy mineral content and are the most mature in Cenozoic. Holocene sands have the highest heavy mineral content and are the most immature. Apart from a few exceptions, the older the psammites are, the less heavy mineral content they have and the more mature they are. So probably the most important aspect of heavy mineral content and maturity is that it is a measure of time in connection with the intrastratal solution of the less resistant minerals.

Relative maturity of epoches of Paleogene and Neogene data varies according to the changes in climate, relief, sedimentary environment, volcanism and recycling of older sedimentary rocks.

Keywords: Heavy minerals, mineralogical maturity, Cenozoic, statistical distribution

Introduction

It is since 1910 that regular micromineralogical studies have been performed in Hungary. Since that time a great number of results of analysis have been yielded.

Micromineralogical data relating to a total of about 20.000 Cenozoic sedimentary rock samples from the Carpathian-Basin, and published before 1983 or stored in the Data Base of the Institute have been collected in the Hungarian Geological Institute.

Of data relating to nearly 8.000 sand or sandstone samples predominantly taken from shallow boreholes, a total of 5.500 samples obtained from the analysis of the 0.1 to 0.2 mm fraction of psammite, are included in this study. Data were processed by using computer (IBM PC).

The psammite fraction ranging from 0.1 to 0.2 mm was separated by sieving, whereas their heavy mineral content was determined by separation with bromoform. The mineralogical maturity of the samples – in other words the ratio of the stable and the unstable minerals – was calculated in different ways from the heavy or the light mineral composition obtained by point counting (after F.J. Pettijohn 1949, and A. Callison 1964):

1. ZTR – index:
$$\frac{\text{zircon} + \text{tourmaline} + \text{rutile grains}}{\text{all mineral grains}}$$
2. Quartz : Feldspar ratio

Address: Edit Thamó-Bozsó: H – 1443 Budapest, Népstadion út 14, Hungary

Received: January 15, 1991

3. (Quartz + Chert) : (Feldspar + Rock fragments) ratio
4. Feldspar %

The heavy minerals and mineralogical maturity

The heavy mineral content and mineralogical maturity of psammites depend on their mineralogical composition influenced by a number of parameters, which are as follows:

- for the source area:
 - lithology
 - climate
 - relief
- for the source rocks minerals:
 - grain size
 - chemical and physical stability during weathering, transport and after the sedimentation
 - specific weight and shape of grains, determining their hydro- or aerodynamical behaviour during the transport and deposition
- the conditions during transport, sedimentation and diagenesis, the geological time passed after the sedimentation

Under dry and cool climatic conditions the chemical weathering is not so intensive and the unstable minerals remain too, so psammites are expected to have more heavy minerals and are less mature than those developed under wet and warm climatic conditions.

If the relief is high, the erosion and the sedimentation are fast, the period of weathering will be shorter and the sediments will be less mature than those found in areas where the relief is low.

The sedimentary environment also is of importance. For example, fluvial sediments are less mature than shore sediments, transported away from the source area and reworked by wave action from time to time.

Recycling of older sedimentary rocks will result in more mature sediments.

The intrastatal solution of unstable minerals causes heavy mineral content to decrease and the sedimentary rocks to become more mature.

The heavy mineral content and maturity of psammites developed in different epoches are compared on the basis of frequency histograms and statistical characteristics of distribution: mean, standard deviation, median (Table 1).

Conclusion

The heavy mineral content of the 0.1–0.2 mm fraction of the Cenozoic psammites found in Hungary are usually less than 4 weight %. The distribution of data of the heavy mineral content of samples is asymmetric, and the older the samples

are the more the distribution is shifted toward lower weight percents. This tendency is reflected mainly by medians, except for the Oligocene psammites, where break is observed due to their relatively too high heavy mineral content. Consequently, the older the psammites are – except for Oligocene – the lower the heavy mineral content is.

Table 1: Statistics of distributions

	number of samples	mean	standard deviation	median
<i>Heavy mineral content</i>				
Holocene	105	4.93	5.42	3.55
Pleistocene	1002	2.94	3.10	2.10
Pannonian	1708	2.39	3.63	1.34
Miocene	720	2.75	4.91	1.20
Oligocene	1287	4.04	8.17	1.45
Eocene	382	2.76	5.72	0.70
<i>ZTR-index</i>				
Holocene	127	2.30	2.00	2.00
Pleistocene	1051	3.84	3.97	3.00
Pannonian	1827	4.52	5.90	3.00
Miocene	770	7.26	8.30	4.00
Oligocene	1367	5.80	7.40	4.00
Eocene	413	11.54	19.12	5.00
<i>Quartz : Feldspar</i>				
Holocene	96	8.20	8.77	4.36
Pleistocene	865	10.67	14.80	6.56
Pannonian	1633	14.33	23.01	6.20
Miocene	727	14.09	27.72	3.00
Oligocene	1177	20.74	31.74	6.25
Eocene	336	39.44	40.07	16.10
<i>(Quartz + Chert) : (Feldspar + Rock fragments)</i>				
Holocene	96	6.92	8.15	3.34
Pleistocene	865	7.10	11.46	3.91
Pannonian	1633	10.83	20.19	3.89
Miocene	727	9.02	22.42	1.50
Oligocene	1177	10.71	21.43	2.68
Eocene	336	30.71	38.19	9.89
<i>Feldspar %</i>				
Holocene	96	14.41	6.68	15.50
Pleistocene	865	12.71	9.06	11.00
Pannonian	1633	12.03	9.52	10.00
Miocene	727	20.10	17.47	15.00
Oligocene	1177	13.58	12.57	9.00
Eocene	336	6.96	8.47	4.00

The comparison of distribution of maturity values calculated in several different ways for sands and sandstones of different age has shown that the Holocene sands found in the Carpathian Basin are the most immature ones in the Cenozoic,

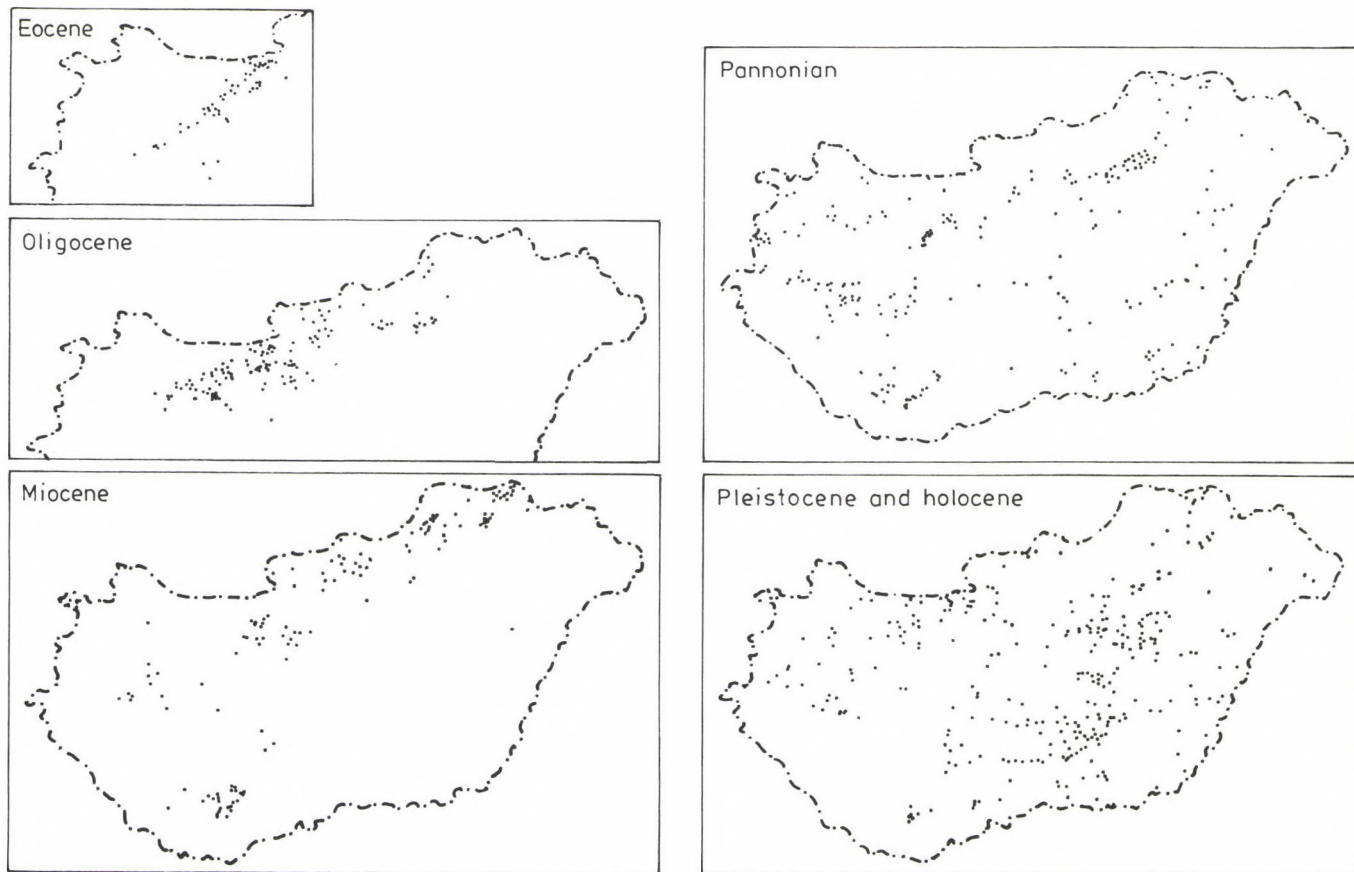


Fig. 1. Location of Cenozoic psammite samples in Hungary

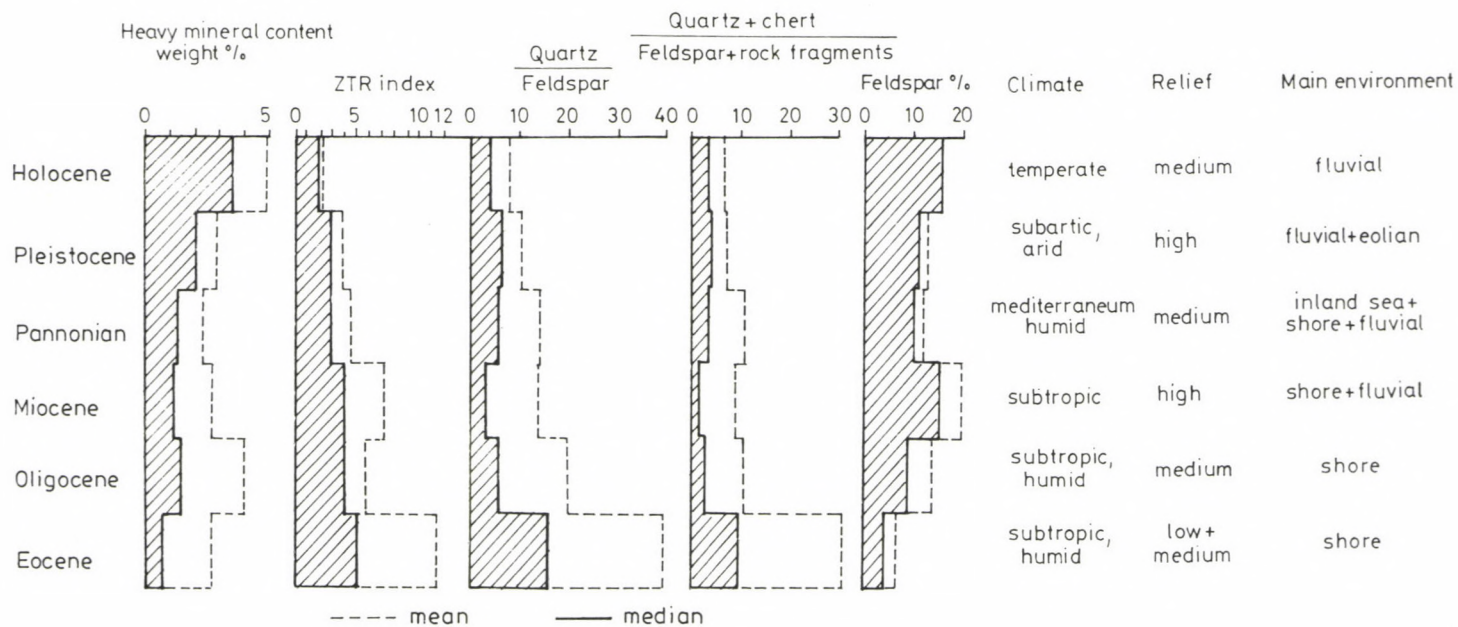


Fig. 2. The heavy mineral content and maturity of Cenozoic psammites in Hungary and their relationships with climate, relief and environment

and have the lowest median of ZTR-index, the lowest (Quartz+Chert) : (Feldspar+Rock fragments) and Quartz : Feldspar ratios, and the highest median of Feldspar %. For Eocene samples these values show an opposed tendency, thus Eocene psammites are the most mature ones in the Cenozoic. Except for some cases the medians of ZTR-index and Feldspar % and the means of Quartz : Feldspar and (Quartz + Chert) : (Feldspar + Rock fragments) ratio for psammites of different epoches show that the older the psammites are, the more mature they are.

Eocene psammites have the lowest heavy mineral content and are the most mature ones in the Cenozoic (Fig. 2). This is mainly caused by the long-lasting intrastratal or diagenetical solution of unstable minerals, the humid, subtropic climate prevailing in the Eocene, the low or medium relief and mainly the shore sedimentation.

Oligocene psammites have higher heavy mineral content than Eocene ones have, and are more immature. It may be caused by the increased relief energy and the altered source areas.

Miocene sands and sandstones have less heavy mineral content than Oligocene ones have, and on the basis of the light mineral composition they are more immature than the older psammites, which may be due to the higher relief energy and to the occurrence of fluvial sediments too. The very high feldspar % points to an increasing intermedier and acidic vulcanism.

Pannonian (Upper-Miocene–Pliocene) psammites have lower heavy mineral content and ZTR-index than Miocene ones have, but on the basis of the light mineral composition they are more mature, which may be due to the decrease in relief energy, reworking and the cessation of intermedier or acidic vulcanism.

Pleistocene sands and sandstones have higher heavy mineral content than Pannonian ones have slightly more immature, according to the means, because climate turned colder and the relief energy became higher.

Holocene sands have the highest heavy mineral content and are the most immature in the Cenozoic. It may be caused by the lack of any diagenetic processes and the major part of theirs are fluvial sediments.

References

- Bárdossy, Gy. 1967: Statisztikai módszerek alkalmazása a földtanban (Application of statistical methods in geology). – *Földt. Közl.*, 87, pp. 325–342.
- Cailleux, A. 1964: Petrographische Eigenschaften der Gerölle und Sandkörner als Klimazeugen. – *Geol. Rundsch.*, 54, 1. pp. 5–15.
- Griffiths, J.C. 1967: Scientific method in analysis of sediments. – New York, p. 508.
- Pettijohn, F.J. 1949: *Sedimentary Rocks.*, – New York, p. 625.
- Sallay, M. 1984: A magyarországi harmad- és negyedidőszaki üledékes képződmények mikromineralógiai adatai I.–VI. (Micromineralogical data of the Tertiary and Quaternary formations of Hungary). – Manuscript, Hungarian Geol. Survey, Documentation Centre.

Genetics of garnets from andesites of the Karancs Mountains

Csaba Lantai

*Laboratory for Geochemical Research
Hungarian Academy of Sciences, Budapest*

The tholeiitic calc-alkali andesite of Miocene age of the Karancs Mountains contains almandine rich garnet phenocrysts that were analyzed by electron probe, their Ree and trace element contents were determined. Garnets are doubtlessly of igneous origin, the core and rim zones are of different composition. The cores crystallized from the tholeiitic melt while the rims precipitated during the processing crustal contamination from the calc-alkali melt.

Keywords: Calc-alkali andesite, garnet phenocrysts, igneous origin, inverse zoning

Introduction

Garnets are common accessories almost in all igneous rocks (Irving and Frey 1978). To determine the genesis of garnets of the calc-alkali volcanics bears a lot of problems. Among the theories the two most frequent ones are as follows: 1) garnet is the residual phase of the partial melting of high grade metamorphic rocks of the crust (Hensen and Green 1973); 2) the garnet crystallized from the magma at high pressures as a near-liquidus phase (Fitton 1972; Brousse et al. 1972).

Based on the high pressure experiments (as most important tools of modelling the mineral phases) Green and Ringwood (1968a, b) found that between 9 and 18 kbar garnet is formed from the rhyodacitic melt, its composition corresponds to that of natural garnets. Stern et al. (1973, 1975, 1978) stated that with the increase of water content of the calc-alkali magma, the liquidus temperature of garnet formation decreases. In case of acid melts Green (1976, 1977) stated that the grossularite and spessartite content of garnets increase with decreasing pressure of formation. The work of Green (1980) aiming at the investigation of crystallization of melts of basalt-andesite composition can be regarded as the compilation of the high pressure experiments. Fitton (1972) believed that the crystallization and preservation of garnets need the condition that the magma should be stored provisionally in a deep-seated magma chamber (at the mantle-crust boundary) and subsequently ascend rapidly to the surface. When this rising is slow, the garnet may resolve. Hentschke (1987) stated three main conditions as bases of garnet formation:

- 1) the melt should be of calc-alkali character;

Address: Csaba Lantai: Laboratory for Geochemical Research Hungarian Academy of Sciences,
H-1112 Budapest, Budaörsi út 45

Received: March 10, 1991

2) the melt should have enough time in the subvolcanic magma chamber to produce the crystallization of garnets;

3) crystallization should proceed under hydrous conditions.

Based on the results of high pressure experiments the theory concerning the igneous origin of garnets can be accepted though some researchers (e.g. Birch Gleadow 1974; Embey-Isztin et al. 1985) observed the igneous growth of metamorphic garnets.

The following can be said in general on the garnets of calc-alkali rocks:

1) their shape is euhedral to subhedral;

2) at the rims cordierite + hypersthene, cordierite + plagioclase or biotite can be observed, that can be interpreted as reaction products of garnets formed at high pressures and got lower pressures;

3) garnets contain the same inclusion minerals as the other phenocryst;

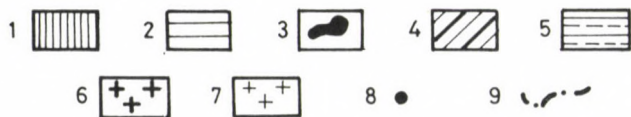
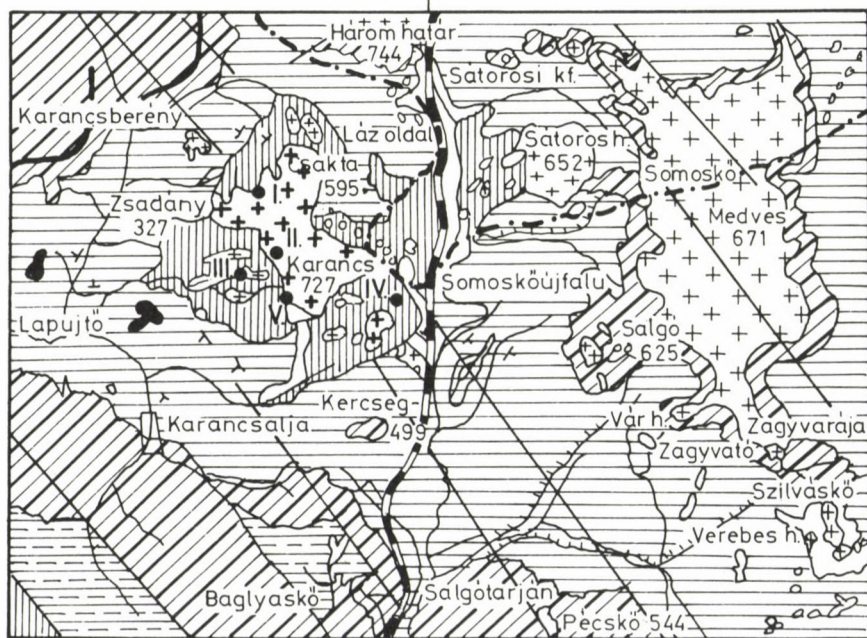
4) the chemical composition of the source rock may of decisive role as regards the garnet composition. As to Hentschke (1987) the Mg-value of the rock (100 MgO / FeO+MgO) and the PY-value of the garnet (100 pyrope / pyrope+almandine) show positive correlation.

As regards the garnets of Miocene andesites of Hungary, several researchers dealt with the problem. Szabó (1977) stated that the garnets of the Karancs Mountains are of igneous origin and denied the opinion of Odor (1962) who believed the garnets as products of transvaporization of the surrounding schlier. Having studied the garnets of the Börzsöny Mountains Z. Balla and E. Csillag (1980) stated that the depth of their initial crystallization could be as deep as 40 to 50 km, excluded the effect of crustal contamination and did not accept the theory of Nagy (1975), i.e. the garnets were formed at temperatures of 530–550 °C. Embey-Isztin et al. (1985) believed the garnets of andesites of the Börzsöny Mountains to be of high pressure, those of granite of the Bükk Mountains that can be interpreted as differentiate of gabbro, to be of low pressure formations.

Geological setting

The geological setting of the studied area is shown in Fig. 1 after Noszky et al. (1952). The basement of the mountains consists of Proterozoic rocks of Veporids type that became revealed as xenoliths in andesite (Scholtz 1917; Szabó 1977). Oligocene clayey sandstone is the oldest formation on the surface, this is overlain by glauconitic sandstone and rhyolite tuff. The characteristic regressive sequence is overlain by a transgressive formation: Miocene brown coal. The andesite constituting the main mass of the Karancs Mountains is of Miocene age, this is proved also by the 15.1 Ma K/Ar age. The andesitic magma either penetrated the Oligocene strata or uplifted these as laccolith. The recent shape of the Karancs-type laccolith (about 25 km² area and 500 m thickness) was formed by faults of NE–SW and NW–SE direction (Noszky, et al. 1915).

Fig. 1. Geological map of the Karancs Mountains after Noszky (1952) 1. O₃ marl (schlier); 2. O₃ Glauconitic sandstone; 3. M₁ rhyolite tuff; 4. M₁ coal sequence; 5. M₃ marl (schlier) 6. M₃ garnetiferous amphibole andesite; 7. P₁ basalt. 8. sampling locality; 9. frontier; I. Karancsberény quarry; II. Talp quarry; III. Lepke exposure; IV. Farkasnyak quarry; V. Karancsalja quarry



Sampling and analytical methods

In addition to the petrological–geochemical qualification of the rocks of the Karancs Mountains our investigations aimed at the determination of genesis and chemical composition of the accessory garnet. Due to the poor outcrops only five localities, i.e. quarries were sampled. Two quarries were sampled in particular (Farkasnyak, Karancsberény).

To determine the mineral composition of the samples microscopic studies, electron probe analyses, as well as complete chemical and neutron activation analyses were carried out. The electron probe measurements were made by a JEOL SUPERPROBE 733 microprobe in the Laboratory for Geochemical Research, with the aid of the program elaborated by Nagy (1984). The accelerating voltage was 25 kV in case of garnet and 20 kV in that of plagioclase. Beam current was 35 to 40 nA, the beam diameter always 10 μm . The correction procedure applied: ZAF. Neutron activation analyses were carried out in the students' reactor of the Technical University of Budapest with ORTEG Ge detector and CANBERRA 80 analysator of 8000 channel. The chondrite normalization of the results was made after the data of Hermann (1970).

Petrological–geochemical investigation of the Karancs andesite

Based on the analytical results it can be stated that the rock material is uniformly garnetiferous amphibole andesite. Main components are: plagioclase, hornblende-type amphibole, quartz; accessories are: garnet, opaque minerals and calcite. In the western part of the mountains the rock texture is microholocrystalline porphyritic, in the eastern part (Farkasnyak) holocrystalline porphyritic. It can be presumed that the eastern part represents the deeper horizon of the laccolith. In addition to the textural differences, there is difference in the garnet quantities between the two parts. Eight samples were analyzed for complete chemical analysis (Table 1) and in harmony with these data and with the data of Table 2 comprehending the characteristic features of the neighbouring volcanic mountains the following statements can be made:

- 1) The average silica content does not differ from that of the neighbouring mountains.
- 2) The K_2O values, i.e. the absolute and that related to the Na_2O and SiO_2 are considerably lower and this relates to crustal contamination of smaller extent.
- 3) When demonstrating the results in the SiO_2 – K_2O diagram (Fig. 2), showing also the andesite categories and magma generation depths of Taylor, it can be stated that rocks can be assigned to calc-alkali andesites.
- 4) In the Fm–diagram of Simpson (1954) (Fig. 3) the samples display Fe-enrichment as compared to the normal calc-alkali trend.
- 5) In the AFM–diagram (Fig. 4) when drawing the calc-alkali – tholeiite boundaries of Hutchinson (1975) and Irwing, Baragar (1971), the rocks fall for the most part to the tholeiite field.
- 6) In the FeO_{tot} /MgO– SiO_2 diagram of Miyashiro (1974) the data fall predominantly to the tholeiite field (Fig. 5).

The REE and other trace element contents of seven samples were determined by neutron activation analysis (Table 3). The shape of the chondrite normalized curves of the Karancs samples (Fig. 6) show only small dispersion, within the

Table 1. Chemical analyses

	1	2	3	4	5	6	7	8
SiO ₂	56.03	61.04	59.34	57.94	57.49	57.96	54.94	60.11
TiO ₂	0.61	0.86	0.43	0.52	0.43	0.61	0.50	0.43
Al ₂ O ₃	16.44	16.03	17.84	16.22	17.30	16.44	16.45	17.82
Fe ₂ O ₃	0.78	1.13	2.15	1.66	1.53	1.28	4.39	3.36
FeO	5.63	5.22	4.40	4.31	4.67	5.10	1.41	2.64
MnO	0.06	0.12	0.14	0.07	0.15	0.06	0.09	0.10
MgO	2.85	1.49	1.73	3.12	1.69	2.79	1.34	1.43
CaO	7.52	5.00	7.91	7.21	6.92	7.50	5.77	6.91
K ₂ O	1.49	1.68	1.27	1.44	1.60	1.54	1.64	1.64
Na ₂ O	3.01	2.66	2.90	3.17	2.71	2.80	1.27	3.11
⁻ H ₂ O	0.23	0.18	0.67	0.65	0.60	0.60	4.48	1.07
⁺ H ₂ O	2.69	4.08	1.53	2.71	2.63	1.65	4.98	1.39
CO ₂	1.60	1.25	0.51	0	1.75	0.78	1.95	0.23
P ₂ O ₅	0.16	0.14	0.12	0.13	0.12	0.15	0.13	0.14
Σ	99.10	100.88	100.94	99.15	99.59	99.22	99.34	100.38
C.I.P.W.								
q	13.87	27.25	16.65	13.17	20.20	20.70	28.00	17.07
c	0.28	4.21	0	0	2.97	4.07	3.34	0
or	9.21	10.33	7.65	8.94	9.87	9.22	11.10	9.97
ab	26.57	23.37	24.97	28.12	23.89	23.94	12.28	27.03
ns	0	0	0	0	0	0	0	0
an	27.34	16.64	32.46	27.01	23.48	16.93	30.14	30.62
di	0	0	2.94	8.01	0	0	0	1.89
di Ca	0	0	1.44	4.03	0	0	0	0.93
di Mg	0	0	0.47	1.93	0	0	0	0.29
di Fe	0	0	1.02	2.04	0	0	0	0.67
Wo	0	0	0	0	0	0	0	0
hip.	16.64	12.57	12.35	12.77	13.63	15.84	12.47	11.10
hip. Mg	7.40	3.85	3.91	6.22	4.39	7.02	3.82	3.37
hip. Fe	9.24	8.72	8.44	6.55	9.24	8.82	8.66	7.73
ac.	0	0	0	0	0	0	0	0
il.	1.21	1.69	0.83	1.04	0.85	1.17	1.09	0.84
mt.	0.69	0.68	0.68	0.64	0.66	0.66	0.64	0.61
hm.	0	0	0	0	0	0	0	0
cc	3.80	2.95	1.18	0	4.14	7.10	0.59	0.54
ap.	0.39	0.33	0.29	0.32	0.29	0.35	0.35	0.34
D.I.	49.65	60.95	49.28	50.22	53.96	53.87	51.38	54.07
S.I.	20.71	12.23	13.90	22.77	13.85	20.60	13.33	11.74
Mg-val.	44.52	28.87	32.74	48.93	33.25	44.30	30.82	31.04

1 - Karancsalja,

3 - Karancsberény, lower mining level,

5 - Karancsberény, upper mining level,

7 - Talp exposure, weathered andesite,

Mg-val - Mg-value

2 - Farkasnyak,

4 - Karancsberény, middle mining level,

6 - Talp exposure, fresh andesite,

8 - Lepke exposure,

mountains no remarkable igneous differentiation can be mentioned though the La/Yb ratio is lower in the eastern than in the western part of the mountains (7.6 to 8.2 and 9 to 11, respectively).

Table 2.

	Börzsöny			Cserhát	Mátra			Karancs
	I.	II.	III.		I.	II.	III.	
SiO ₂	56.03	55.88	58.18	54.67	54.61	56.33	56.17	57.92
K ₂ O	2.22	2.16	2.26	2.01	2.16	1.98	2.03	1.58
Na ₂ O	3.18	3.04	3.33	2.88	2.59	2.49	2.28	2.90
D.I.	59.1	52.3	52.6	48.0	48.9	67.0	46.8	53.0
S.I.	14.7	14.6	11.9	18.2	13.1	19.5	20.9	16.2
Sz (km)	184.0	178.6	187.5	165.2	178.6	165.2	166.9	126.8
C (km)	40.8	39.7	41.6	37.0	39.7	36.5	37.4	29.4

C – calculated crust thickness after Condie (1973);

Sz – magma generation depth after Hatherton and Dickinson (1969)

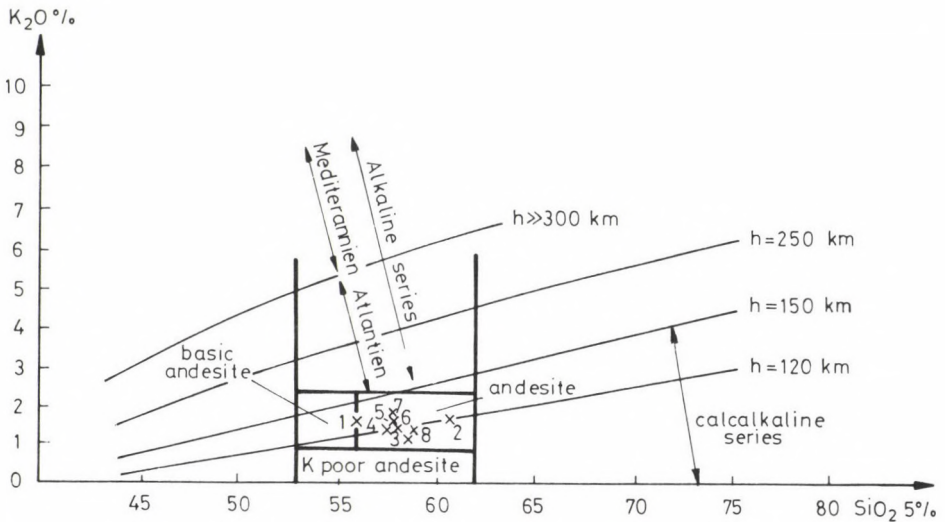


Fig. 2. K₂O vs SiO₂ diagram with the andesite categories and magma generation depths of Taylor

Table 3. Neutron activation analyses

ppm	1	2	3	4	5	6	7	8	9
La	2.5 ± 0.1	15.0 ± 0.3	17.0 ± 0.3	15.0 ± 0.2	3.31 ± 0.2	14.5 ± 0.2	2.3 ± 0.2	14.2 ± 0.3	14.0 ± 0.3
Ce	69.3 ± 2.5	31.0 ± 1.2	30.0 ± 1.0	32.0 ± 1.1	51.8 ± 2.2	29.6 ± 1.0	30.0 ± 1.2	29.6 ± 1.2	30.6 ± 1.2
Nd	-	-	-	-	-	-	-	-	-
Sm	4.5 ± 0.1	3.8 ± 0.1	4.42 ± 0.05	3.8 ± 0.02	3.8 ± 0.1	3.5 ± 0.1	4.0 ± 0.10	3.50 ± 0.10	3.6 ± 0.10
Eu	1.3 ± 0.1	1.0 ± 0.1	0.91 ± 0.05	1.01 ± 0.05	1.20 ± 0.07	0.88 ± 0.05	1.01 ± 0.06	0.85 ± 0.06	0.79 ± 0.05
Tb	1.73 ± 0.19	0.27 ± 0.23	-	0.3 ± 0.23	1.43 ± 0.19	-	0.36 ± 0.22	0.31 ± 0.22	0.34 ± 0.20
Tm	-	-	-	-	-	-	-	-	-
Yb	43.0 ± 0.2	1.96 ± 0.12	2.06 ± 0.13	1.94 ± 0.12	34.9 ± 0.2	1.3 ± 0.10	1.50 ± 0.10	1.48 ± 0.10	1.49 ± 0.10
Lu	7.00 ± 0.20	0.24 ± 0.0	0.20 ± 0.03	0.26 ± 0.02	5.6 ± 0.2	0.18 ± 0.02	0.24 ± 0.02	0.20 ± 0.02	0.20 ± 0.02
U	-	1.6 ± 0.3	1.5 ± 0.3	1.5 ± 0.3	-	0.9 ± 0.2	1.5 ± 0.03	1.3 ± 0.2	1.6 ± 1.2
Th	-	6.0 ± 0.2	5.9 ± 0.2	5.5 ± 0.2	-	5.9 ± 0.2	5.7 ± 0.2	6.2 ± 0.2	6.4 ± 0.2
Cr	43.7 ± 3.5	17.0 ± 2.4	-	18.4 ± 2.4	38.4 ± 3.2	22.3 ± 2.2	30.0 ± 2.3	32.9 ± 2.2	33.2 ± 2.1
Fe%	18.5 ± 0.1	4.87 ± 0.3	3.22 ± 0.03	4.85 ± 0.04	14.71 ± 0.07	4.4 ± 0.24	4.83 ± 0.04	4.23 ± 0.04	4.47 ± 0.04
Hf	2.2 ± 0.2	2.4 ± 0.2	2.6 ± 0.2	2.7 ± 0.2	1.6 ± 0.69	2.5 ± 0.2	2.3 ± 0.2	2.6 ± 0.2	2.43 ± 0.10
Sc	36.2 ± 0.1	14.0 ± 0.1	15.0 ± 0.1	13.4 ± 0.1	29.1 ± 0.1	13.6 ± 0.1	14.0 ± 0.1	12.3 ± 0.1	12.4 ± 0.1
Rb	-	-	73 ± 12	-	-	53 ± 12	-	61 ± 13	72 ± 12
Co	20.1 ± 0.3	13.5 ± 0.3	14.4 ± 0.3	14.0 ± 0.3	21.0 ± 0.4	13.1 ± 0.3	17.0 ± 0.5	13.2 ± 0.3	17.8 ± 0.3
Ta	-	0.56 ± 0.22	0.4 ± 0.23	0.64 ± 0.11	0.32 ± 0.23	0.40 ± 0.17	0.78 ± 0.11	0.64 ± 0.10	0.62 ± 0.10
Cr	-	3.3 ± 0.3	3.5 ± 0.3	2.5 ± 0.3	-	3.5 ± 0.3	6.7 ± 0.4	2.8 ± 0.3	7.0 ± 0.3
Zn	-	102 ± 11	106 ± 7	116 ± 13	-	100 ± 10	94 ± 11	83 ± 9	92 ± 10
La/Lu	0.38	62.50	85.00	57.70	0.59	80.56	56.25	71.00	70.00
La/Yb	0.06	7.65	8.25	7.73	0.09	11.15	9.0	9.59	9.40

1 = Farkasnyak garnet separate, 2 = Farkasnyak, fresh andesite, 3 = Karancsalja, fresh andesite, 4 = Talp exposure, fresh andesite, 5 = Talp-II exposure, garnet separate, 6 = Lepke exposure, fresh andesite, 7 = Karancsberény, lower mining level, fresh andesite 8 = Karancsberény, middle mining level, fresh andesite, 9 = Karancsberény, upper mining level, fresh andesite

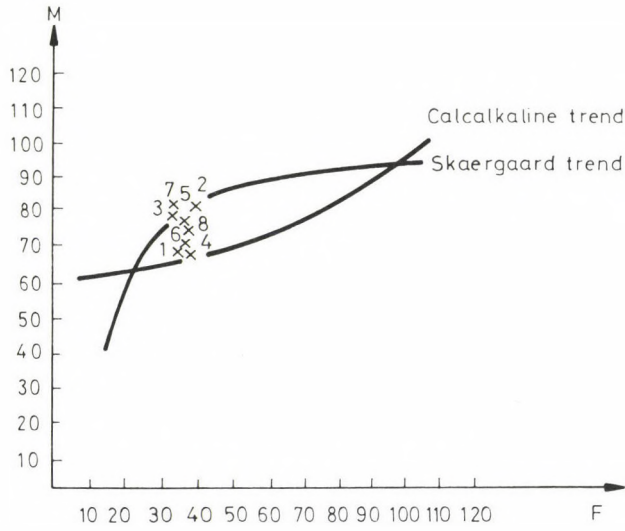


Fig. 3. The FM-diagram of Simpson

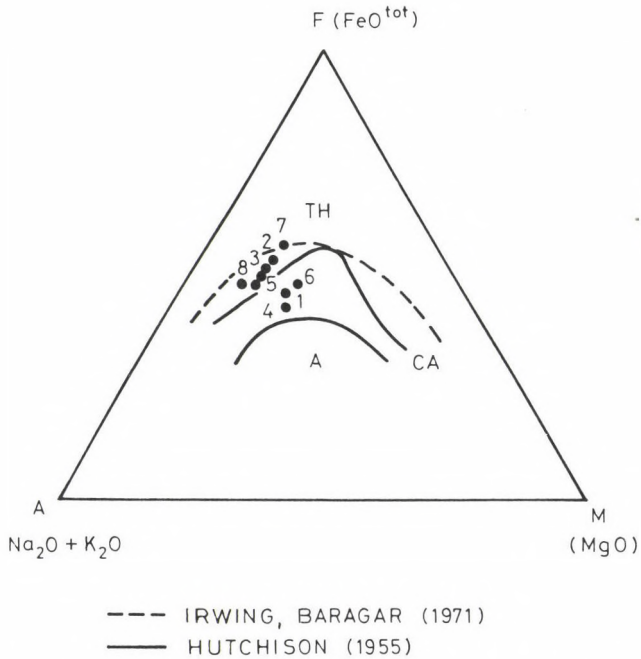


Fig. 4. The AFM-diagram, with the calc-alkali boundaries of Irving Baragar, 1971, and Hutchinson, 1975

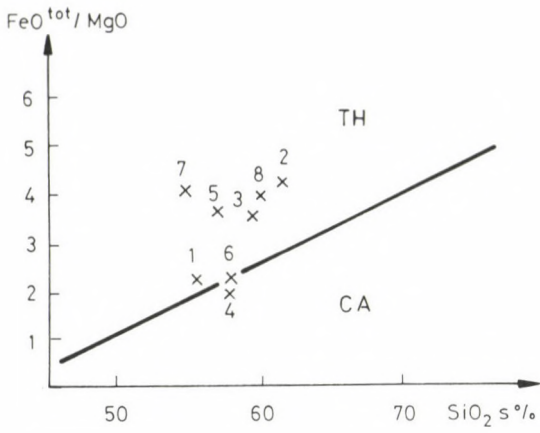


Fig. 5. The $FeO_{tot} / MgO-SiO_2$ diagram of Miyashiro (1974)

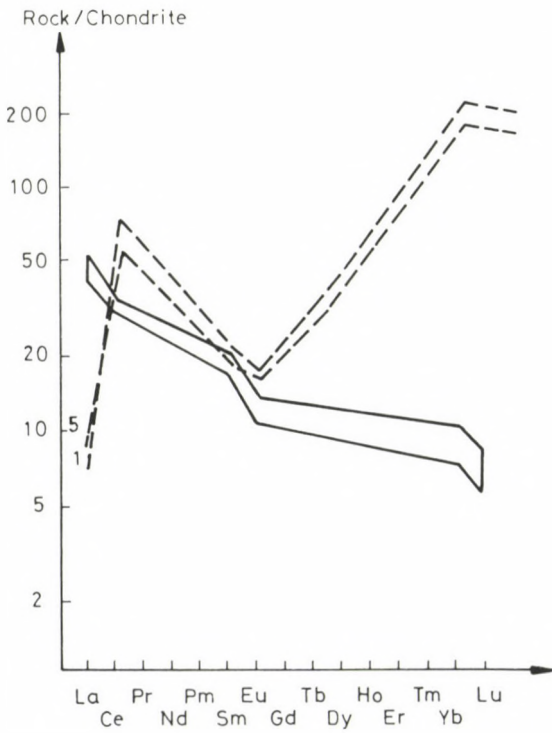


Fig. 6. Chondrite normalized REE-distribution curves

The Karancs garnets

Dimensions, appearance and inclusions

The garnets of the eastern and western parts of the mountains differ from each other taking either frequency or their size. The size of garnets from the Farkasnyak quarry (eastern part) varies between 5 and 20 mm. An inclusion-free strong pink core and an inclusion-bearing rim zone can be distinguished both macro- and microscopically. In the northwestern part (Karancsberény, Lepke) the size (0.1–0.4 mm) and frequency of garnets are lower and the lack of the inclusion-bearing rim zone is characteristic, while in case of garnets from the Talp exposure the lack of the core can be observed. Resorption holes are characteristic of the garnet surfaces in both areas. The most frequent inclusion minerals are plagioclase, opaque minerals and apatite. The circular, ring-shaped arrangement of plagioclases prove indirectly the igneous origin of garnets (Plate I). It is characteristic that around the garnet core as crystallization centre started the precipitation of plagioclase from the melt while the plagioclase phenocrysts crystallized only later. This is proved by the detailed microprobe study of plagioclase inclusions (Table 4) of garnets from the Farkasnyak quarry (Plate I), and of the plagioclase phenocrysts (Table 5 and Plate II) of the whole rock. The average An-content of the plagioclase inclusion garlands in garnets decreases towards the rims (67.5–65.3–53.2 %) while the An-content of plagioclase phenocrysts is 56.8 % (Fig. 7).

Main element composition, zoning

The garnet of the eastern exposure of Karancs (Farkasnyak) was analyzed by microprobe in two directions, i.e. N–S and E–W (Plate I, Table 6). Having plotted the measurement results in the Alm + Spess – Gorss + And – Pyr triangle (Fig. 8), as well as the on-line distribution of the elements (Fig. 9) it can be stated that the core of garnet can be sharply distinguished after its Mg inverse zoning and Fe-enrichment from the rim where these anomalies do not occur. The garnets of exposures from the western part of the mountains (Karancsberény, Plate II; Table 7 a–c; Lepke, Plate II, Table 8) are homogenous, their composition corresponds to the core composition of the Farkasnyak garnets in the Alm + Spess – Gross + And – Pyr triangle (Fig. 10). In the southwestern part the garnet of the Talp exposure (Plate III, Table 9) is homogeneous, the points of analyses fall solely on the rim zone values of the Farkasnyak garnet (Fig. 10), this fact relates to the lack of core.

Trace element composition

The chondrite normalized REE distribution curve of garnet separates of two samples (Farkasnyak, Talp) shows that these are enriched in heavy lanthanides (Fig. 6), which, in harmony with the statement of Irving, Frey (1978) due to the strong incompatible character of the heavy lanthanides relates unambiguously to the fact that garnets were formed close to the solidus. Nevertheless, the REE-determinations were of several uncertainty factors.

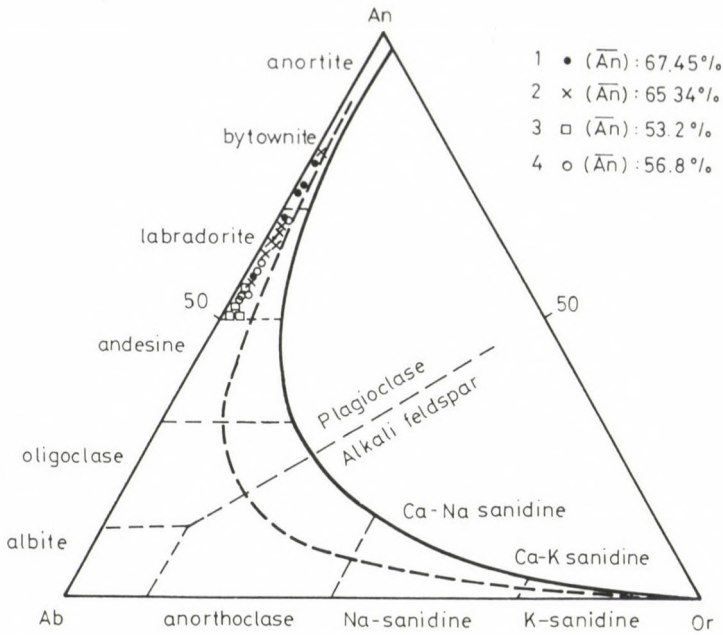


Fig. 7. Plotting of microprobe analytical results of the Farkasnyak feldspar inclusions and feldspar phenocrysts in the Ab-An-Or triangle Innermost inclusion ring (An=67.45%); middle inclusion ring (An= 53.2%); feldspar phenocryst in the rock (An=56.8%)

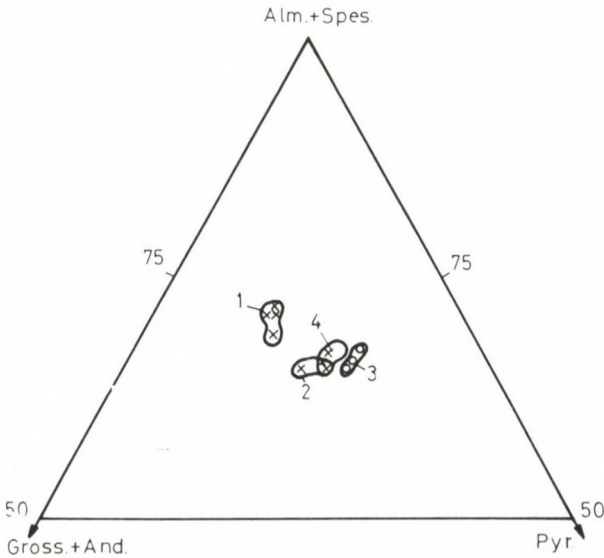


Fig. 8. Plotting of microprobe analytical data of the Farkasnyak garnet in the Alm+Spes - Gross+And - Pyr triangle 1. core; 2. innermost rim; 3. inner rim; 4. outer rim

Table 4. Farkasnyak, feldspar inclusions of garnet, microprobe analyses

	1	3	4*	5**	6	7	8	9*	10**	11*	12**	13	14	15	16
SiO ₂	48.76	49.42	51.32	49.76	56.08	53.65	53.10	52.03	52.11	52.92	47.87	52.53	53.49	56.03	54.46
Al ₂ O ₃	32.69	32.62	31.59	32.77	28.11	29.86	30.26	31.31	31.35	31.30	34.22	31.63	30.70	28.13	29.88
CaO	15.43	14.97	13.70	14.85	9.66	12.01	12.11	13.63	13.44	12.91	16.09	13.74	12.65	10.30	12.13
Na ₂ O	2.33	2.70	3.51	2.82	5.08	4.41	4.65	3.81	3.96	4.03	2.32	4.32	4.05	5.54	5.05
K ₂ O	0.08	0.09	0.17	0.14	0.22	0.16	0.17	0.13	0.14	0.16	0.06	0.16	0.13	0.21	0.26
Σ	99.29	99.80	100.29	100.34	99.15	100.09	100.29	100.91	101.00	101.32	100.56	102.38	101.02	100.21	101.78
ion numbers for 8 O															
Si	2.240	2.257	2.324	2.260	2.531	2.420	2.396	2.341	2.432	2.365	2.179	2.335	2.393	2.514	2.423
Al	1.770	1.755	1.686	1.754	1.495	1.588	1.609	1.660	1.661	1.649	1.835	1.657	1.619	1.487	1.567
Ca	0.759	0.732	0.665	0.722	0.467	0.580	0.586	0.657	0.647	0.618	0.785	0.654	0.606	0.495	0.578
Na	0.208	0.239	0.308	0.248	0.445	0.386	0.407	0.333	0.345	0.349	0.204	0.372	0.351	0.482	0.436
K	0.005	0.005	0.10	0.008	0.013	0.009	0.010	0.007	0.008	0.009	0.004	0.009	0.008	0.012	0.015
An+Ab+Or=100%															
An	78.1	75.0	67.7	73.8	50.5	59.5	58.4	65.9	64.7	63.3	79.1	63.2	62.8	50.1	56.2
Ab	21.4	24.5	31.3	25.4	48.1	39.6	40.6	33.4	34.5	35.8	20.5	35.9	36.4	48.7	42.4
Or	0.5	0.5	1.0	0.8	1.4	0.9	1.0	0.7	0.8	0.9	0.4	0.9	0.8	1.2	1.4

1-7: inner inclusion ring, 8-14: outer inclusion ring, 15-16: plagioclase beside the garnet; *: grain centre; **: grain rim

Table 5. Farkasnyak, feldspar phenocryst, microprobe analyses

	1	2	3	4	5	6	7	8	9
SiO ₂	55.46	55.36	53.34	54.69	51.26	55.23	52.85	54.55	55.29
Al ₂ O ₃	28.64	28.56	30.44	28.78	31.48	28.82	30.36	29.42	29.12
CaO	10.89	10.51	12.44	11.00	13.81	10.71	12.53	11.27	11.12
Na ₂ O	4.92	5.02	4.69	4.82	3.69	5.20	4.26	4.93	4.97
K ₂ O	0.20	0.19	0.17	0.29	0.13	0.22	0.16	0.25	0.22
Σ	100.11	99.64	101.08	99.58	100.37	100.18	100.16	100.42	100.72
ion numbers for 8 O.									
Si	2.491	2.496	2.391	2.473	2.322	2.481	2.388	2.450	2.472
Al	1.516	1.517	1.608	1.534	1.680	1.526	1.617	1.558	1.535
Ca	0.524	0.508	0.597	0.533	0.670	0.515	0.607	0.542	0.533
Na	0.428	0.439	0.408	0.423	0.324	0.453	0.373	0.429	0.431
K	0.011	0.011	0.010	0.017	0.007	0.012	0.009	0.014	0.013
An+Ab+Or = 100%									
An	54.4	53.0	58.8	54.8	66.9	52.6	61.4	55.0	54.6
Ab	44.4	45.8	40.2	43.5	32.4	46.2	37.7	43.6	44.1
Or	1.2	1.2	1.0	1.7	0.7	1.2	0.9	1.4	1.3

1-9: measurement points

Table 6. Karancs–Farkasnyak mine, garnet, microprobe analyses

	1	2	3	4	5	6	7	8	9	11	12	15	16	18	19	20
SiO ₂	37.63	37.67	38.30	38.30	38.34	38.45	38.47	38.23	38.33	37.95	37.70	38.32	38.38	38.20	38.59	38.25
TiO ₂	0.37	0.47	0.42	0.18	0.29	0.38	0.27	0.34	0.34	0.39	0.42	0.30	0.33	0.29	0.26	0.27
Al ₂ O ₃	19.77	20.50	21.09	20.97	20.35	20.45	20.51	20.86	20.32	20.63	20.03	20.62	20.66	20.72	20.69	20.60
FeO	30.31	30.41	29.03	29.06	28.58	28.63	28.96	29.29	28.82	30.61	30.35	28.31	28.64	28.85	28.59	28.68
MnO	2.10	2.47	2.24	2.50	2.43	2.32	2.38	2.46	2.38	2.34	2.58	2.31	2.29	2.14	2.38	2.39
MgO	3.19	2.88	4.33	5.09	5.19	5.12	5.06	5.02	4.85	2.97	2.74	5.23	5.27	5.23	4.85	4.73
CaO	6.39	5.91	5.75	4.59	4.96	5.12	4.59	4.56	5.32	6.06	6.26	5.12	5.15	4.74	5.44	5.32
Σ	99.76	100.31	101.16	100.69	100.14	100.47	100.24	100.76	100.36	100.95	100.08	100.21	100.82	100.17	100.80	100.24
ion numbers for 24 O																
Si	6.024	6.007	5.991	6.005	6.042	6.039	6.039	5.996	6.037	6.008	6.031	6.024	5.999	6.012	6.044	6.030
Ti	0.045	0.057	0.049	0.022	0.035	0.045	0.045	0.041	0.040	0.046	0.051	0.036	0.032	0.034	0.030	0.032
Al ^{IV}	–	–	0.009	–	–	–	–	0.004	–	–	–	–	0.001	–	–	–
Al ^{VI}	3.731	3.852	3.881	3.875	3.779	3.785	3.785	3.851	3.772	3.850	3.778	3.820	3.803	3.844	3.821	3.827
Fe ³⁺	0.131	0.020	0.030	0.071	0.067	0.046	0.046	0.071	0.075	0.043	0.057	0.059	0.120	0.064	0.031	0.049
Fe ²⁺	3.927	4.035	3.768	3.738	3.699	3.716	3.716	3.770	3.721	4.009	4.004	3.664	3.623	3.734	3.714	3.732
Mn	0.285	0.334	0.297	0.333	0.324	0.308	0.308	0.328	0.319	0.315	0.351	0.308	0.302	0.285	0.316	0.320
Mg	0.762	0.685	1.011	1.190	1.218	1.200	1.200	1.173	1.139	0.701	0.654	1.226	1.251	1.227	1.132	1.111
Ca	1.095	1.010	0.964	0.766	0.837	0.861	0.861	0.766	0.898	1.028	1.074	0.862	0.862	0.800	0.912	0.899
Alm+Spes+Pyrope+Andr+Gross = 100%																
Alm	64.7	66.5	62.4	62.0	60.9	61.1	62.6	62.4	61.2	66.2	66.0	60.5	60.0	61.8	61.1	61.6
Spes	4.7	5.5	4.9	5.5	5.3	5.1	5.2	5.4	5.4	5.2	5.7	5.1	5.0	4.7	5.2	5.3
Pyrope	12.6	11.3	16.7	19.8	20.0	19.7	19.5	19.5	18.7	11.6	10.7	20.2	20.7	20.3	18.7	18.3
Andr	3.2	0.5	0.7	1.8	1.7	1.1	0.1	1.8	1.8	1.1	1.4	1.5	3.0	1.6	0.8	1.2
Gross	14.8	16.2	15.3	10.9	12.1	13.0	12.6	10.9	12.9	15.9	16.2	12.7	11.3	11.6	14.2	13.6
Py	16.3	14.5	21.2	24.1	24.8	24.4	23.8	23.7	23.0	14.9	14.0	25.1	25.7	24.7	23.4	22.9

1–20: measurement points

Table 7/a. Karancsberény quarry, lower mining level, garnet, microprobe analyses

	1	2	3	4	5
SiO ₂	37.25	37.58	38.12	37.243	37.28
TiO ₂	0.44	0.45	0.44	0.45	0.43
Al ₂ O ₃	20.45	20.47	20.45	20.73	20.66
FeO	31.12	30.83	31.03	31.58	30.63
MnO	1.88	1.86	1.92	2.15	1.86
MgO	3.20	3.10	3.26	3.13	3.13
CaO	5.62	5.98	5.48	5.14	6.22
M	99.96	100.27	100.70	100.42	100.21
ion numbers (for 24 O)					
Si	5.971	5.966	6.044	5.950	5.955
Ti	0.053	0.054	0.052	0.054	0.052
AlIV	0.029	0.004	0	0.050	0.045
AlVI	3.834	3.846	3.822	3.855	3.844
Fe ³⁺	0.132	0.075	0	0.130	0.146
Fe ²⁺	4.040	4.038	4.114	4.090	3.946
Mn	0.255	0.251	0.258	0.290	0.251
Mg	0.763	0.738	0.772	0.744	0.745
Ca	0.966	1.023	0.931	0.880	1.065
Alm + Spess + Pyrope + Andr + Gross = 100%					
Alm	67.1	66.7	67.7	68.1	65.7
Spess	4.2	4.2	4.2	4.8	4.2
Pyrope	12.7	12.2	12.7	12.4	12.4
Andr	3.2	1.9	0	3.3	3.6
Gross	12.8	15.0	15.4	11.4	14.1
Py	15.9	15.5	15.8	15.4	15.9

1-5: measurement points

1) We have no possibility to correct the REE contents of garnets with the REE contents of the inclusion minerals (plagioclase, opaque mineral, apatite).

2) We had no possibility to determine separately the REE contents of the cores and rims in case of the Farkasnyak garnet, though this would have serious genetic significance. Since the volume of the core is negligible as compared to that of the rims (Fig. 7), it can be stated that the REE content obtained concerns the rim zones of the garnet.

Garnet-source rock relationships

According to Hentschke (1987) the PY-value of garnets (see the microprobe analyses in the Tables) and the Mg-values of the rock (Table 1) were determined. Between the PY-values of the rim zones and the Mg-values of the rock the correlation is good ($r = + 0.79$), while between the PY-values of the core and the Mg-values of the rock this is less ($r = + 0.4$). This shows that the rim zones are in stronger relationship with the recent chemistry of the rock than the core parts.

Table 7/b. Karancsberény quarry, middle mining level, garnet microprobe analyses

	1	2	3	4	5
SiO ₂	37.43	37.69	37.86	37.75	37.88
TiO ₂	0.36	0.53	0.39	0.55	0.45
Al ₂ O ₃	20.87	20.53	20.69	20.59	20.77
FeO	28.59	30.32	29.79	29.77	30.07
MnO	1.61	2.08	2.15	2.26	1.97
MgO	3.73	3.57	3.61	3.39	3.32
CaO	7.26	5.72	5.95	6.25	6.35
Σ	99.85	100.44	100.44	100.56	100.81
ion numbers for 24 O					
Si	5.953	5.989	6.002	5.989	5.992
Ti	0.043	0.063	0.046	0.065	0.054
Al ^{IV}	0.047	0.011	0	0.011	0.008
Al ^{VI}	3.865	3.834	3.866	3.838	3.864
Fe ³⁺	0.144	0.077	0.055	0.063	0.054
Fe ²⁺	3.658	3.952	3.894	3.887	3.923
Mn	0.217	0.280	0.289	0.303	0.264
Mg	0.884	0.846	0.854	0.802	0.782
Ca	1.237	0.974	1.011	1.062	1.077
Alm+Spes+Pyrope+Andr+Gross = 100%					
Alm	61.0	65.3	64.4	64.2	64.9
Spes	3.6	4.6	4.8	5.0	4.4
Pyrope	14.7	14.0	14.1	13.3	12.9
Andr	3.6	1.9	1.4	1.6	1.3
Gross	17.1	14.2	15.3	15.9	16.5
Py	19.5	17.6	18.0	17.1	16.6

1–5: measurement points

Presumed process of garnet formation

The garnets studied can be assigned to three groups.

1) Garnets with core of inverse Mg-zoning and free of inclusions, and of rims enriched in inclusions (Farkasnyak);

2) Inclusion-free garnets with homogenous main element distribution, with "core-composition" (Karancsberény, Lepke);

3) Inclusion-rich garnets with homogenous main element distribution, with "rim-composition" (Tálp).

Garnet formation can be reconstructed as follows. The core was formed in the abyssal magma chamber (in harmony with the high pressure experiments at the mantle-crust boundary, in a depth of about 30 to 40 km), as a near-liquidus phase, from the tholeiite-like melt. The calc-alkali character has gradually developed as a result of gradual crustal contamination, its temperature decreased. Around the garnet cores, as crystallization centres the precipitation of plagioclase started, this

Table 7/c Karancsberény quarry, upper mining level, garnet, microprobe analyses

	1	2	3	4	5	6	7
SiO ₂	38.23	38.11	38.13	37.81	38.58	38.39	38.22
TiO ₂	0.48	0.42	0.42	0.34	0.40	0.40	0.35
Al ₂ O ₃	20.39	20.45	20.61	20.50	20.26	20.22	20.51
FeO	30.49	30.55	30.52	30.63	30.02	30.35	30.43
MnO	1.89	1.97	1.90	1.90	1.99	2.07	1.91
MgO	3.71	3.66	3.65	3.61	3.52	3.67	3.77
CaO	5.75	5.69	5.69	5.65	6.33	5.67	5.63
Σ	100.94	100.85	100.91	100.44	101.10	100.77	100.82

ion numbers for 8 O.

Si	6.035	6.027	6.021	6.009	6.075	6.070	6.036
Ti	0.057	0.050	0.049	0.041	0.047	0.047	0.041
Al ^{IV}	0	0	0	0	0	0	0
Al ^{VI}	3.793	3.811	3.836	3.839	3.760	3.768	3.819
Fe ³⁺	0.033	0.053	0.037	0.092	0	0	0.040
Fe ²⁺	3.992	3.987	3.994	3.978	3.954	4.013	3.979
Mn	0.253	0.263	0.254	0.256	0.266	0.277	0.256
Mg	0.874	0.864	0.859	0.854	0.827	0.865	0.889
Ca	0.973	0.963	0.963	0.962	1.068	0.960	0.953

Alm + Spes + Pyrope + Andr + Gross = 100%

Alm	65.5	65.6	65.8	65.8	64.7	65.6	65.5
Spes	4.2	4.3	4.2	4.2	4.3	4.5	4.2
Pyrope	14.3	14.2	14.2	14.1	13.5	14.2	14.6
Andr	0.8	1.3	0.9	2.3	0	0	1.0
Gross	15.2	14.6	14.9	13.6	17.5	15.7	14.7
Py	18.0	17.8	17.7	17.7	17.3	17.7	18.3

1-7: measurement points

process being parallel to the precipitation of garnet rims under constant pressure (Fitton 1972). During gradual cooling the other phenocryst phases also precipitate. The ascension of magma to higher levels is of decisive importance from the aspect of garnet preservation. If the secondary magma chamber lies deep, the garnets are able to resorb due to the changed P-T conditions. If the magma sticks in higher crustal parts, the garnet have no time to resorb due to the rapid cooling. The formation of garnet of only "core-composition" can be reconstructed so that the core crystallized in the abyssal magma chamber has no time to overgrow or the precipitated rim zones were resorbed in a secondary magma chamber of deeper level. The garnets of the third group started to precipitate around the crystal germs of the calc-alkali melt and not the garnet core overgrew.

Table 8. Lepke exposure, garnet, microprobe analyses

	1	2	3	4	5
SiO ₂	38.45	38.16	37.85	37.94	38.07
TiO ₂	0.43	0.40	0.43	0.43	0.40
Al ₂ O ₃	20.56	20.52	20.65	20.59	20.72
FeO	30.04	30.16	30.33	29.84	29/64
MnO	2.23	2.19	2.06	1.96	2.23
MgO	3.64	3.61	3.72	3.53	3.65
CaO	5.77	5.89	5.59	6.29	6.25
Σ	101.12	100.93	100.63	100.58	100.96
ion numbers for 24 O					
Si	6.051	6.027	5.996	6.009	6.004
Ti	0.051	0.047	0.051	0.051	0.047
Al ^{IV}	0	0	0.004	0	0
Al ^{VI}	3.813	3.820	3.852	3.844	3.851
Fe ³⁺	0	0.048	0.075	0.055	0.071
Fe ²⁺	3.953	3.935	3.944	3.897	3.838
Mn	0.298	0.292	0.276	0.262	0.298
Mg	0.853	0.850	0.879	0.834	0.859
Ca	0.973	0.997	0.948	1.067	1.056
Alm+Spess+Pyrope+Andr+Gros = 100%					
Alm	65.0	64.8	65.2	64.3	63.4
Spes	4.9	4.8	4.6	4.3	4.9
Pyrope	14.0	14.0	14.5	13.8	14.2
Andr	0	1.2	1.9	1.4	1.8
Gros	16.1	15.2	13.8	16.2	15.7
Py	17.8	17.8	18.2	17.6	18.3

1-5: measurement points

their formation neither the metamorphic origin nor the assimilation theory can be accepted.

C) The fact that the rocks of numerous volcanic mountains do not have garnets indicates that the reason of their presence or missing can be traced back to the manner of magma ascend:

1) Long enough time is needed in the abyssal magma chamber to the garnet formation;

2) It is also required that the magma should not be stored for longer times in a secondary magma chamber since due to the changed P-T conditions the garnet may resolve.

D) Only the rims of garnet crystallized from the melt the composition of which corresponds to recent rock chemistry, the core parts derive from tholeiitic melt. The crystallization of rims and the developing calc-alkali character due to crustal contamination are simultaneous processes. The process of crustal contamination was proved by main and trace element, as well as isotope studies by several authors (Pantó 1981, 1987; Póka 1988).

Table 9. Talp-II exposure, garnet, microprobe analyses

	1	2	3	4	5	6	7	8	9	10	11	12	13	14	15	17	19	
SiO ₂	38.38	38.87	38.15	38.45	38.23	38.67	38.64	38.61	38.79	38.84	38.40	38.13	38.63	38.64	38.71	38.87	38.78	
TiO ₂	0.21	0.18	0.20	0.28	0.18	0.28	0.34	0.34	0.16	0.35	0.44	0.41	0.33	0.15	0.26	0.41	0.32	
Al ₂ O ₃	21.12	21.16	20.85	20.99	21.01	20.95	21.08	21.03	21.09	21.10	20.77	20.79	20.90	21.29	21.09	21.11	21.02	
FeO	28.76	28.83	28.87	28.96	29.34	29.46	28.89	28.99	28.93	28.90	29.77	29.23	29.00	29.30	29.42	28.98	29.15	
MnO	2.09	2.10	2.06	2.06	1.94	1.90	1.89	1.91	1.74	1.56	2.11	2.02	1.96	1.90	1.88	1.93	1.57	
MgO	4.81	4.84	4.58	4.61	4.47	4.56	4.66	4.67	5.03	5.04	4.45	4.60	4.81	4.67	4.58	4.76	4.93	
CaO	5.41	5.57	5.56	5.65	5.64	5.56	5.78	5.77	5.52	5.70	5.49	5.38	5.53	5.45	5.76	5.84	5.70	
Σ	100.78	101.55	100.27	101.00	100.81	101.38	101.28	101.32	101.25	101.49	101.43	100.56	101.16	101.40	101.70	101.90	101.47	
ion numbers for 24 O																		
Si	6.007	6.038	6.011	6.015	5.996	6.003	6.023	6.017	6.035	6.029	6.000	5.998	6.029	6.017	6.016	6.023	6.026	
Ti ^{IV}	0.025	0.021	0.024	0.032	0.022	0.033	0.040	0.040	0.019	0.041	0.052	0.048	0.039	0.018	0.031	0.048	0.038	
Al ^{VI}	-	-	-	-	0.004	-	-	-	-	-	-	0.002	-	-	-	-	-	
Al ^{VI}	3.896	3.873	3.871	3.870	3.879	3.853	3.872	3.862	3.868	3.860	3.824	3.853	3.843	3.906	3.862	3.854	3.850	
Fe ³⁺	0.040	0.009	0.058	0.036	0.082	0.017	-	0.024	0.023	0.001	0.072	0.054	0.021	0.025	0.043	0.005	0.022	
Fe ²⁺	3.725	0.736	3.746	3.752	3.766	3.827	3.766	3.755	3.741	3.750	3.818	3.791	3.764	3.791	3.780	3.750	3.766	
Mn	0.277	0.276	0.275	0.273	0.259	0.251	0.249	0.252	0.229	0.205	0.279	0.269	0.259	0.251	0.248	0.253	0.206	
Mg	1.123	1.120	1.076	1.075	1.044	1.060	1.084	1.085	1.165	1.167	1.036	1.079	1.119	1.083	1.060	1.098	1.142	
Ca	0.907	0.927	0.939	0.946	0.948	0.929	0.966	0.965	0.919	0.948	0.919	0.907	0.926	0.909	0.959	0.970	0.950	
Alm+Sps+Pyrope+Andr+Gross = 100%																		
Alm	61.8	61.7	62.1	62.1	62.6	63.1	62.1	62.0	61.8	61.8	63.1	62.7	62.0	62.8	62.5	61.8	62.1	
Spes	4.6	4.6	4.6	4.5	4.3	4.1	4.1	4.2	3.8	3.4	4.6	4.4	4.3	4.2	4.1	4.2	3.4	
Pyrope	18.6	18.5	17.8	17.8	17.4	17.5	17.9	17.9	19.2	19.2	17.1	17.8	18.5	17.9	17.5	18.1	18.8	
Andr	1.0	0.2	1.4	0.9	2.0	0.4	0	0.6	0.6	0	1.8	1.4	0.5	0.6	1.1	0.1	0.6	
Gross	14.0	15.0	14.1	14.7	13.7	14.9	15.9	15.3	14.6	15.6	13.4	13.7	14.7	14.5	14.8	15.8	15.1	
PY	23.2	23.4	22.4	22.3	21.7	21.7	22.3	22.4	23.7	23.7	21.3	22.2	22.9	22.2	21.9	22.7	23.3	

1-19: measurement points

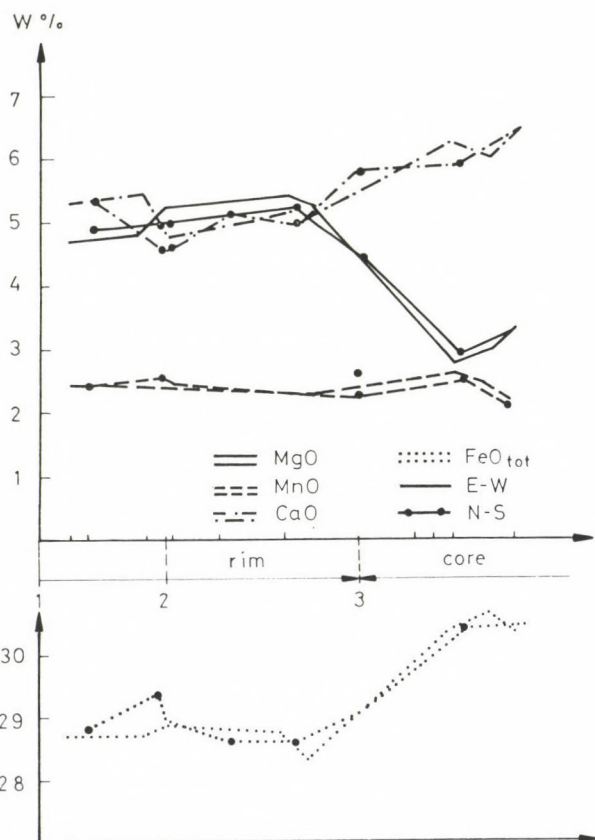


Fig. 9. On - line distribution of elements in the Farkasnyak garnet. 1. grain rim; 2. first inclusion ring; 3. second inclusion ring

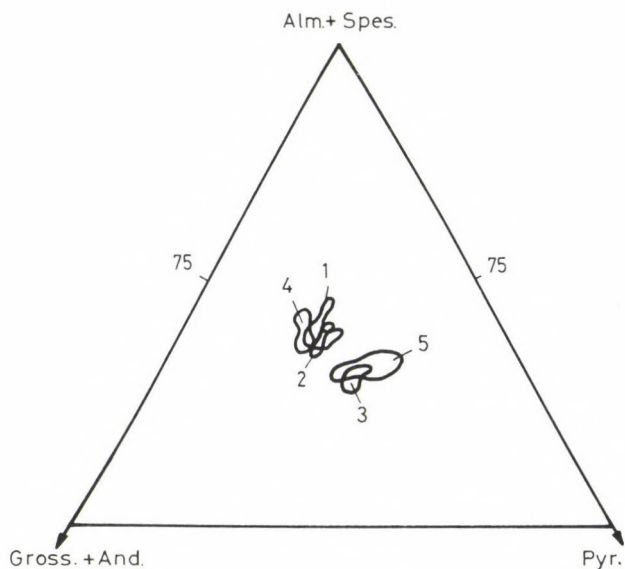
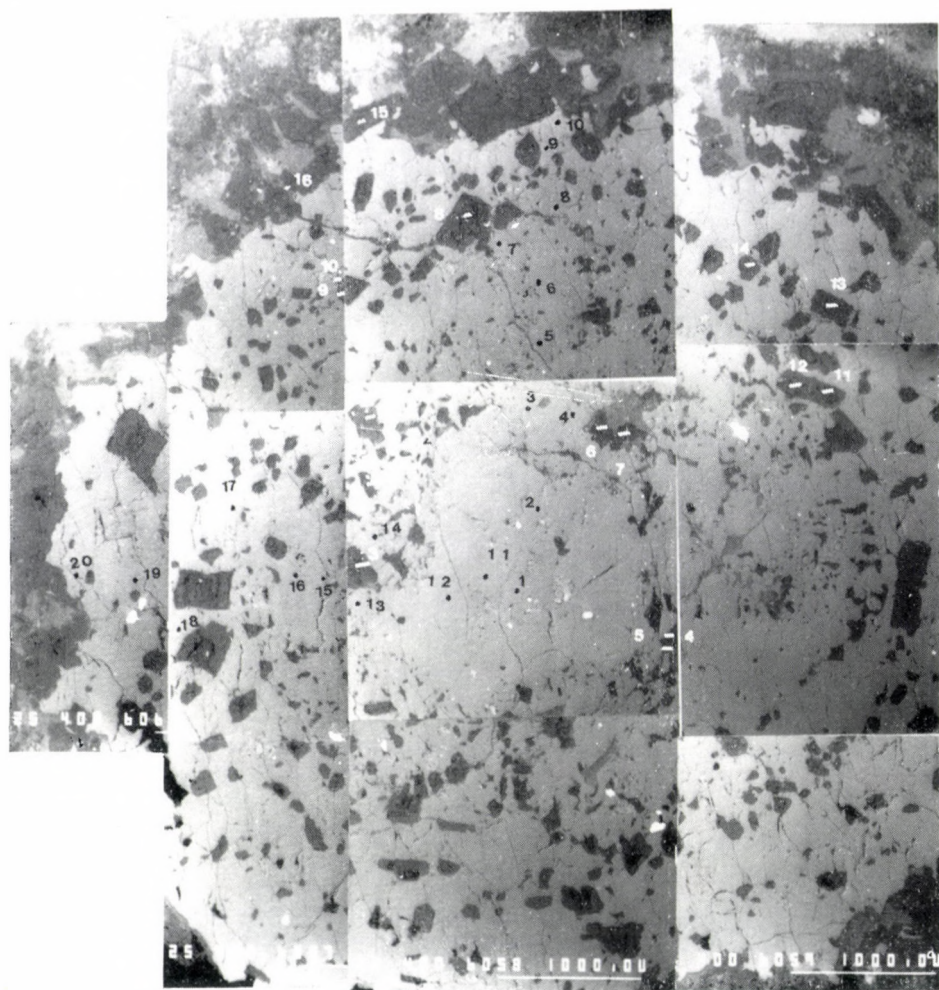


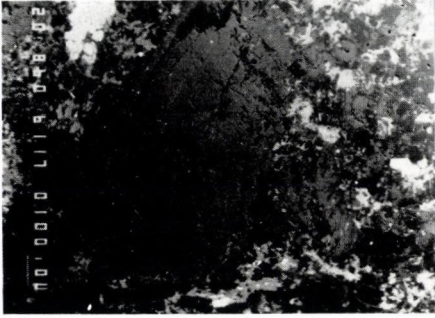
Fig. 10. The Alm + Spess - Gross + And - Pyr triangle 1. Karancsberény; 2. Lepke; 3. Talp; 4. Farkasnyak core; 5. Farkasnyak rim

Plate I

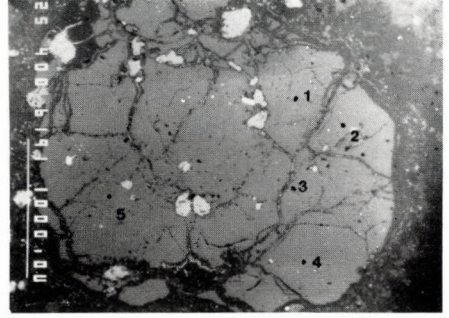


Farkasnyak garnet, composition electron picture. — Black numbers: measurement points in garnet; white numbers: measurement points in plagioclase

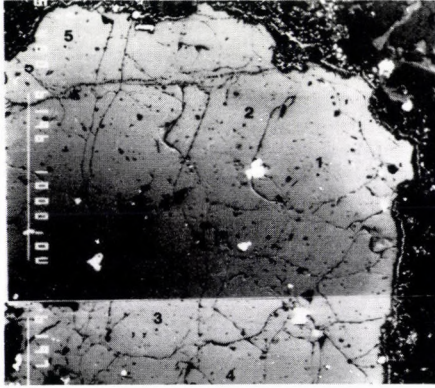
Plate II



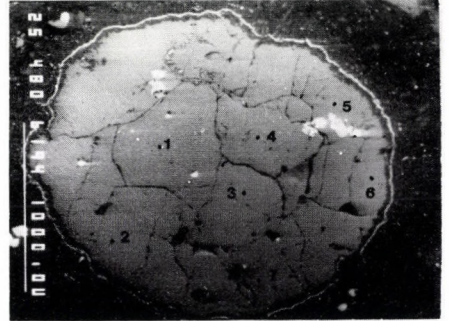
1



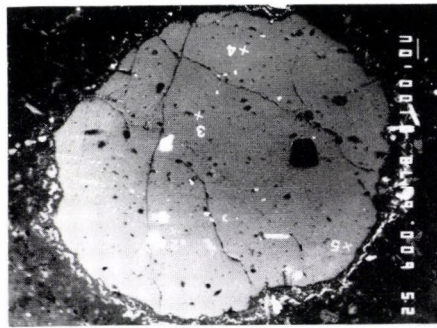
2



3



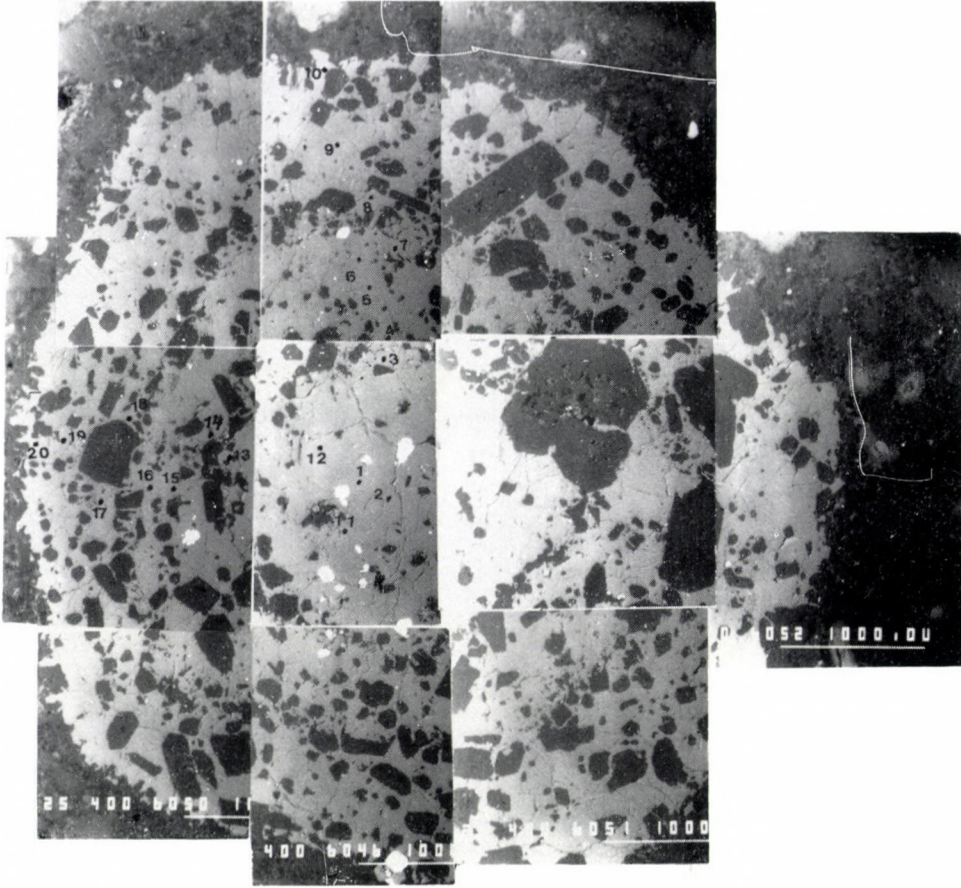
4



5

1. — Farkasnyak feldspar phenocryst, composition electron picture, with the measurement points,
2. — Karancsberény, lower mining level, garnet, composition electron picture, with the measurement points,
3. — Karancsberény, middle mining level, garnet, composition electron picture, with the measurement points,
4. — Karancsberény, upper mining level, garnet, composition electron picture, with the measurement points,
5. — Lepke garnet, composition electron picture with measurement points.

Plate III



Talp garnet, composition electron picture with measurement points

Acknowledgements

Author is highly indebted to Gy. Pantó and T. Póka for having the possibility to study this topic, to G. Dobosi and I. Fórizs for the microprobe analyses, to the late J. Bérczy and M. Balla (Technical University, Budapest) for the neutron activation analyses, to J. Lefler (Laboratory for Geochemical Research) for the chemical analyses, and to P. Árkai and V. Széky-Fux for the possibility of consultations and for their valuable advices.

References

- Balla, Z., T.E. Csillag 1980: A börszönyi gránát eredete és petrogenetikai jelentősége (Origin and petrogenetic significance of garnets of the Börzsöny Mountains). – *Gen. Geol. Review*, 13, pp. 163–189.
- Birch, W.D., A.J.W. Gleadow 1974: The genesis of garnet and cordierite in acid volcanic rocks: evidence from the Cerberean Caldera, Central Victoria, Australia. – *Contr. Miner. Petr.*, 45, pp. 1–3.
- Brousse, R., H. Bizouard, J. Salát 1972: Grenats des andesites et des rhyolites de Slovaquie, origine des grenats dans les séries andésitiques. – *Contr. Miner. Petr.*, 35, pp. 201–213.
- Condie, K.C. 1973: Archean magmatism and crustal thickening. – *Geol. Soc. Am. Bull.*, 84, pp. 2981–2992.
- Embey-Isztin, A., G. Noske-Fazekas, G. Kurat, F. Brandstätter 1985: Genesis of garnets in some magmatic rocks from Hungary. – *Tschermaks Min. Petr. Mitt.*, 34, pp. 49–66.
- Fitton, J.G. 1972: The genetic significance of almandine–pyrope phenocrysts in the Borrowdale Volcanic Group, Northern England. – *Contr. Miner. Petr.*, 36, pp. 231–248.
- Green, T.H. 1976: Experimental generation of cordierite- or garnet-bearing granitic liquids a pelitic composition. – *Geology*, 4, pp. 85–88.
- Green, T.H. 1977: Garnet in silicic liquids and its possible use as a P–T indicator. – *Contr. Miner. Petr.*, 65, pp. 59–67.
- Green, T.H. 1980: Anatexis of mafic crust and high pressure crystallization of andesite. – In: *Andesites*, ed. Thorpe, R.S. pp. 468–487.
- Green, T.H., A.E. Ringwood 1968 a: Genesis of the calc-alkaline igneous rock suite. – *Contr. Miner. Petr.*, 18, pp. 105–162.
- Green, T.H., A.E. Ringwood 1968 b: Origin of garnet phenocrysts in calc-alkaline rocks. – *Contr. Miner. Petr.*, 18, pp. 163–171 A.
- Hensen, B.J., T.H. Green 1973: Experimental study of the stability of cordierite and garnet in pelitic compositions at high pressures and temperatures. III. Synthesis of experimental data and geological applications. – *Contr. Miner. Petr.*, 38, pp. 151–166.
- Hermann, 1970: Yttrium and lanthanides in Handbook of Geochemistry, II/5. – Wedepohl, K. H. Springer.
- Hentschke, U. 1987: The genetic significance of garnets in the plutonic complexes of the Harz Mountains. – *N. Jb. Miner. Abh.*, 156, 2, pp. 141–153.
- Hutchinson, C.S. 1975: The norm, its variations, their calculation and relationships. – *Schweiz. Min. Petrograph. Mitt.*, 55, pp. 243–256.
- Irving, A.J., F.A. Frey 1978: Distribution of trace elements between garnet megacrysts and host volcanic liquids of kimberlitic to rhyolitic composition. – *Geochim. Cosmochim. Acta*, 43, pp. 770–787.
- Irving, T.N., W.R.A. Baragar 1971: A guide to the chemical classification of the common volcanic rocks – *Can. J. Earth Science*, *, pp. 523–548.
- Miyashiro, A. 1974: Volcanic rocks series in island arcs and active continental margins. – *Am. J. Sci.*, 274, pp. 321–355.

- Nagy, G. 1975: Temperature determination of igneous processes on the basis of the decomposition of coexistent mineral pairs. – *Acta Geol. Acad. Sci. Hung.*, 19, 1–2, pp. 16.–25.
- Nagy, G. 1984: Computer programs for quantitative electron microprobe analyses for geological applications. – *Electron Microscopy*, 2, pp. 1041–1042.
- Noszky, J. sen. 1915: A Mátrától É-ra levő dombos vidék földtani viszonyai (Geology of the hilly region north of Mátra Mountains). – *MÁFI Évi Jel.* pp. 115–160.
- Noszky, J., M. Hermann, V.S. Nemes 1952: Keletnógrádi andezitek (Andesites from east Nógrád country). – *Földt. Közl.*, 82, pp.8–36.
- Odor, L. 1962: A Karancs-hegység kőzettani és földtani viszonyai (Geology and petrology of the Karancsd Mountains). – *Földt. Közl.*, 92, pp. 387–399.
- Pantó, Gy. 1981: Rare earth elements geochemical patterns of the Cenozoic volcanism in Hungary. – *Earth Evol. Sci.*, 21 3–4, pp. 249–256.
- Pantó, Gy., V.J.M. Salters, S.R. Hart 1988: Origin of Late Cenozoic volcanic rocks of the Carpathian Arc, Hungary. – *AAPG memoir 45. The Pannonian Basin*, Chapter 19, pp. 269–292.
- Póka, T. 1988: Neogene and Quaternary volcanism of the Carpathian–Pannonian region: Changes in chemical composition and its relationship to Basin formation. – *AAPG Memoir 45. The Pannonian Basin*, Chapter 18. 257–277.
- Scholtz, M. 1917: A Karancs-hegység andezitjei (Andesites of the Karancs Mountains). – *Földt. Közl.*, 47, pp. 224–237.
- Simpson, E.S.W. 1954: On the graphical representation of differentiation trends in igneous rocks. – *Geol. Mag.*, 91, pp. 238–244.
- Stern, C.R., P.J. Wyllie 1973: Melting relations of basalt–andesite–rhyolite–H₂O and pelagic red clay at 30 kb. – *Contr. Miner. Petr.*, 42, pp. 313–323.
- Stern, R.C., W.L. Huang, P.J. Wyllie 1975: Basalt–andesite–rhyolite–H₂O: Crystallization intervals with excess H₂O and H₂O–undersaturated liquids surfaces to 35 kilobars, with implications for magma genesis. – *Earth Planet. Sci. Lett.*, 28, pp. 189–196.
- Stern, R.C., P.J. Wyllie 1978: Phase composition through crystallization intervals in basalt–andesite–H₂O at 30 kilobars with implication for subduction zone magmas. – *Amer. Miner.*, 63, pp.641–663.
- Szabó, Cs. 1977: A karancsi gránát (The garnet of Karancs). – *Eötvös University*, manuscript.

Book review

Chaline, J.: *Paleontology of Vertebrates*

Springer Verl., Berlin, Heidelberg, New York, 1990. pp. 1–186

The book serves first of all for students and represents an introduction into the paleontology of Vertebrates.

The first part includes the indispensable knowledges: what is a fossil, what means fossilization, in what environs the vertebrate fossils are preserved and in what state, finally how these fossils can be prepared and studied. The history of the concept up to the concept of species in space and time. It is emphasized that paleontology is able to apply the morphological features that can be made exactly by biometric methods.

The history of classification is also summarized, among others the evolutionary and the cladistic classification are dealt with. Problems are also discussed that derive partly from the different interpretation of the morphological features and partly from the fact that how the results of paleontology are used.

At the end of the chapter the types of changes of the ontogeny that are responsible for the evolutionary changing during geological times are shortly reviewed.

The second chapter deals with the common anatomical characteristics of vertebrates, with the theories concerning their origin with their many-sidedness and with their earth-historic (temporal) and paleogeographical (spatial) extension. As a clue of this chapter author makes an attempt to create a new classification that tries to synthesize the former classification concepts.

Chapters 4–6 the vertebrate fossil material is discussed in a phylogenetic system with more or less systematics. The discussion follows the line: occupation of the aquatic environment – occupation of the continents – occupation of the atmosphere – development of mammals and of the man. Within this sequence the adaptive significance of the changes in the fundamental organic structures are

emphasized. When discussing the primitive tetrapods (Chapter 4) a special section is devoted to the ontogenetic changes in phylogeny (neotaxia, progenesis), with examples referring to the theoretical part of the preceding chapter. When discussing the mammals (Chapter 7) the debated problems of species formation are lightened by the evolution of rodents.

In possession of the vertebral material, and supplementing this material with modern evolutionary genetic data, author explains his new theory on species evolution (Chapter 9). He tries to synthesize the gradualist and punctuated equilibria theories set against each other so far.

The last chapter outlines the possibility of application of vertebrate paleontological results in geology (biostratigraphy, paleoecology, paleoclimatology, paleogeography, plate tectonics).

When evaluating this work as a text-book, there are some problems. The basic elements of morphology and biology of vertebrates are incompletely discussed, the parts dealing with the theories of evolution presumes fundamental knowledges in this field. As to the aim of the book, i.e. it was prepared as a text-book for students in the fields of geology, the last chapter dealing with the application of these data represents only some indications. As a whole, for the reader this book seems not to be an introduction into the paleontology of vertebrates but rather to be a comprehension of evolutionary concepts in the field of vertebrate paleontology.

Since in the book mainly the evolutionary problems of vertebrate paleontology are discussed, it can be useful for teachers of biology and for everybody being interested biology.

Miklós Monostori

Hellmut Grabert: *Der Amazonas – Geschichte und Probleme eines Stromgebietes zwischen Pazifik und Atlantik.*

Springer Verlag, Berlin, Heidelberg, New York, 1991 pp. 1–235

The river Amazonas, its environment, the marvellous fauna and flora of the huge territory of South America – these are things that have been always interesting to the European people. This book comprises all the facts about this "unknown" continental-sized land that may be and by all means are important when one wants to be get acquainted with "Amazonia".

The structure of the book serves the aims of the author: to take the chronological sequence both in natural scientific and in human historic points of view. The first introductory part gives short review on the discovery of Amazonia from the times of the Spanish conquistadors through the world-famous French expedition of de la Condamine to the expeditions and discoveries of the last and of our centuries.

Fortunately, in the first chapter the Paleozoic–Mesozoic evolution of South America is outlined but in the frame of the modern plate tectonic concepts. Subsequently, the break off of the ancient Gondwana continent, i.e. the formation of the independent South America and Africa is discussed and the geodynamic reasons and consequences of this continental separation are emphasized.

In chapters 3 and 4 the development and evolution of the South American continent from the Tertiary to our days are summarized including the emphasis of significance of the Andean orogeny as well as the subsequently developed river network

In chapter 5 subdivided into four parts the geomorphology and recent geodynamics are discussed. The special significance of the river network of Amazonas is emphasized and in this respect for me it is the first occasion to be acquainted with the water types of Amazonia, i.e. with the limnology and hydrography in particular.

Being "green" in mid, the chapter 5.4 is most interesting for me. There are a lot of talking in telecommunication media about the significance of the tropic forests, on their role in the oxygen supply of our atmosphere, so I judge this last chapter to be very important from the environmental points of view. "Deua é grande, mas o mato é maior (God is mighty but the forest is more!) say the caboclos and Prof. Grabert's last sentence should be cited: Hat das heute noch Geltung, oder zerstört der Mensch in seiner Aggressivität das so empfindliche Ökosystem Amazonien?

This last sentence cries for help, to keep the natural equilibrium there.

If Springer aimed at the publication of an interesting and popular book, it has full success. Unfortunately, the photos are of rather bad condition, maybe the original ones were not the best. This fact, however, does not reduce the value of the book that is highly suggested to read both for scientist and for the public.

Ottó Tomschey

Hartmut Heinrichs – Albert Günter Hermann: Praktikum der Analytischen Geochemie

Springer Verlag, Berlin, Heidelberg, New York 1990

The unbroken evolution of the research fields and analytical methods of geochemistry needs the publication of manuals that summarize the new results. This is why researchers look forward to the publication of the *Praktikum der Analytischen Geochemie*. This book is the revised edition of the "Praktikum der Gesteinsanalyse" by Paula Schneiderhöhn (Springer Verlag) "in die Analysenvorschriften für die Methoden der Gravimetrie und Spektralphotometrie sind viele praktische Erfahrungen übernommen worden" and it contains novelties that have been awaited by the researchers.

The book consists of two parts. In Part I the concepts related to the rock analysis are found from the discussion of the analytical problems of determining the main, micro and trace elements to the sample processing, analytical and measurement methods, so practically all details are dealt with. In this part the units of measurement used most frequently by analysts and the recalculation factors are presented in tables. The modes of calculation and presentation of results are demonstrated, the error calculations are dealt with and exemplified.

In Part II the concrete analytical methods are described. The different methods of attack are discussed and it is shown how to choose the suitable method of attack for analyzing the required component. Subsequently, the determination of the main and trace components by means of gravimetry, titrimetry, spectrophotometry etc. is presented. A special chapter is devoted to the separation of the rare earth elements for ICP–AES analy-

tical purposes. In the next chapter the modes of determination of different elements by means of the Perkin Elmer 4000, Perkin Elmer HGA 500 atomabsorption spectrophotometer and of ARL 35000C ICP–AES instruments are discussed. The enclosed tables are very useful since these contain the measurement parameters (e.g. gas flow etc.) more particularly than the Perkin Elmer manuals. In the subsequent parts the general laboratory, cleaning, health and safety problems are dealt with that provide remarkable aid to the practicing analysts and can be rarely found in manuals of this type. Finally, a valuable list of references follows.

The shape and edition of the book follows the traditions of the Springer. Tables are clear, understandable, cross-references are unambiguous.

In the field of the earth sciences (petrology, mineralogy, geochemistry etc.) the quantitative determination of the main and trace elements is not only of the most important documentation of the researches themselves but may be occasionally of primordial significance. The ever more exact performance of chemical analyses and the joint determination of trace and main elements need precise and complicated analytical methods. To realize these requirements, this book serves as a good basis for mineralogy and petrology.

This highly awaited manual is not only a useful book for students but serves as a guide for researchers and technicians, as well.

Ildikó Vidra

PRINTED IN HUNGARY

Akadémiai Kiadó és Nyomda Vállalat, Budapest

GUIDELINES FOR AUTHORS

Acta Geologica Hungarica is an English-language quarterly publishing papers on geological topics (geochemistry, mineralogy, petrology, paleontology, stratigraphy, tectonics, economic geology, regional geology, applied geology). Along with papers on outstanding scientific achievements and on the main lines of geological research in Hungary, reports on workshops of geological research, on major scientific meetings, and on contributions to international research projects will be accepted.

Manuscripts are to be sent to the Editorial Office for refereeing, editing, and translation into English.

A clear, careful and unequivocal formulation of the papers, lucidity of style and the use of uniform nomenclature adopted in Hungary are basic requirements. It is convenient to subdivide the text of the papers into sections under subheadings.

Form of manuscript

The paper complete with abstract, figures, captions, tables and bibliography should not exceed 25 pages (25 double-spaced lines with a 3 cm margin on both sides).

The first page should include:

- the title of the paper
- the name of the author(s)
- the name of the institution and city where the work was done
- an abstract of not more than 200 words
- a list of five to ten keywords
- a footnote with the name and postal address of the author(s)

The SI (System International) should be used for all units of measurements.

References

In text citations the author's name and the year of publication should be given. The reference list, which follows the text, should be typed double-spaced, arranged alphabetically, and should not be numbered. For the preferred sequence and punctuation of authors' names see the examples below.

The author's name is followed by the year of publication in parentheses, the title of the paper or book (individual words in English titles of papers should have lower case initials, those of books upper case ones). Paper titles are followed by periodical titles, a comma, volume number, and inclusive page numbers. For books the publisher and the place of publication should be given.

Examples:

Bruckle, L. H. (1982): Late Cenozoic planktonic diatom zones from the eastern equatorial Pacific. *Nova Hedwigia, Belh.*, **39**, 217–246.

Surdam, R. C., H. P. Eugster (1976): Mineral reaction in the sedimentary deposits of the Lake Magadi region, Kenya. *Geol. Soc. Amer. Bull.*, **87**, 1739–1752.

Perelman, A. J. (1976): *Geochemistry of Epigenesis*. Plenum Press, New York, Amsterdam.

Figures and tables

Figures and tables should be referred to in the text and their approximate place indicated on the margin.

Figures should be clear line drawings (suitable for being redrawn without consulting the author) or good-quality black-and-white photographic prints. The author's name, title of the paper, and figure number (arabic) should be indicated with a soft pencil on the back of each figure. Figure captions should be listed at the end of the manuscript. They should be as concise as possible.

Tables should be typed on separate sheets with the number (roman) and a brief title at the top. Horizontal lines should be omitted.

Proofs and reprints

The authors will be sent a set of galley and page proofs each. These should be proofread and returned to the Editorial Office within a week of receipt. Hundred reprints are supplied free of charge, additional reprints may be ordered.

307216

Acta Geologica Hungarica

VOLUME 34 NUMBER 3, 1991

EDITOR

J. FÜLÖP

EDITOR-IN-CHIEF

J. HAAS

EDITORIAL BOARD

**G. CSÁSZÁR, G. HÁMOR, F. HORVÁTH,
T. KECSKEMÉTI, GY. PANTÓ, T. SZEDERKÉNYI,
Á. KRIVÁN-HORVÁTH (Co-ordinating Editor)**



Akadémiai Kiadó, Budapest

ACTA GEOL. HUNG. 34(3) 159-270 (1991) HU ISSN 0236-5278

ACTA GEOLOGICA

A QUARTERLY OF THE HUNGARIAN ACADEMY OF SCIENCES

Acta Geologica publishes original reports of studies in geology, crystallography, mineralogy, petrography, geochemistry and paleontology.

Acta Geologica is published in yearly volumes of four issues by

AKADÉMIAI KIADÓ

Publishing House of the Hungarian Academy of Sciences
H-1117 Budapest, Prielle Kornélia u. 19–35.

Manuscripts and editorial correspondence should be addressed to

Acta Geologica

H-1363 Budapest, P.O. Box 24

Subscription information

Orders should be addressed to

AKADÉMIAI KIADÓ

H-1519 Budapest, P.O. Box 245

Acta Geologica Hungarica is abstracted/indexed in Bibliographie des Sciences de la Terre, Biological Abstracts, Chemical Abstracts, Chemie-Information, Hydro-Index, Mineralogical Abstracts



TETHYAN BAUXITES

IGCP 287

Part I

Contents

Tethyan Bauxites. <i>The state of the Art</i>	161
Jurassic karst bauxites in the Subbetic, Betic Cordillera, Southern Spain. <i>J. M. Molina, P. A. Ruiz-Ortiz, J. A. Vera</i>	163
A review of karst bauxites and related paleokarsts in Spain. <i>J. M. Molina</i> ..	179
Les principaux types de gisement et modèles génétiques des bauxites karstiques en France et en Sardaigne. <i>P. J. Combes</i>	195
Bauxite exploring methods and their results in the Strázovské vrchy Mts., NW Slovakia. <i>F. Beleš</i>	215
The geological setting and facies of bauxite deposits in Hungary, including the conditions of their development. <i>J. Knauer, A. Fekete, K. Tóth</i>	221
Application of sedimentological methods to karst bauxites evaluation: the Halimba-Szőc area, Hungary. <i>Gy. Bárdossy, E. Juhász</i>	241
Tectonic and eustatic control of bauxite formation in the Transdanubian Central Range (Hungary). <i>J. Haas</i>	253
Geoexplorer – the development of a knowledge-based consultation system for supergene deposits. <i>M. Wagner, K. Fischer, K. Germann, J. Luo, W. Skala</i>	263

PRINTED IN HUNGARY
Akadémiai Kiadó és Nyomda Vállalat,
Budapest

Tethyan Bauxites

The state of the Art

IGCP-287 was launched in 1989 with the objectives of critically summarize the accumulated knowledge on bauxites and related paleokarst occurrences of the West Central Mediterranean section of Tethys and to correlate major bauxite/paleokarst horizons with orogenic/eustatic/climatic events already recognized within the studied region. It is assumed, that this approach may help to understand better not only the genesis of bauxites (and thus promote the prediction and exploration of further bauxite reserves) but also it may reveal some hitherto obscured details of the tectonic evolution of the region.

From the Triassic through the Tertiary karst bauxites occur in several stratigraphic horizons all over the carbonate terrains of the Tethyan realm. They are related to subaerial exposure phases brought about apparently either by orogenic/epeirogenic movements or by eustatic sea-level drops. There are places and times, however, within the same region, where these processes resulted in non-bauxitic paleokarst fillings rather than in bauxite deposits. Whether the two things are mutually exclusive either in space or in time, is one of the questions which may be answered only after having attempted a correlation between "bauxitic" and "non-bauxitic" episodes of karstification and other major events recognized in the study area in Mesozoic–Tertiary times.

Mainly due to the inspiring activity of ICSOBA (International Committee of Studies on Bauxite, Alumina and Aluminium) large amounts of relevant information on bauxite have been accumulated during the past 25 years. Research on paleokarst was greatly stimulated partly by the recognition of the karst-related nature of Bleiberg-type Pb–Zn deposits and partly by detailed studies on carbonate platform evolution. Research in these two sectors evolved more or less independently: scientists though occasionally making use of each others results, rarely treat the subject with an integrated approach. The amount of the accumulated knowledge, however, strongly calls for correlation.

In the field of bauxite geology latest research revealed that karst bauxites could conveniently be described as fine grained clastic sediments, and that the lithofacies concept can be applied when carrying out regional studies on them. The first attempts to relate bauxite lithofacies to the enclosing (and underlying) karst morphology seem to be promising enough to provide the common basis for an integrated treatment of bauxites and paleokarst.

The generally accepted fact karst phenomena (and karst evolution in general) is strongly dependent on the position of the site of karstification as related to the karstic watertable gives

the opportunity to use bauxites and related paleokarst in reconstructing paleorelief on the small-scale and also to contribute to large-scale paleogeographic reconstructions (they may help to delineate tectonically uplifted areas; give an idea about the degree of relative uplift; their material may give a hint about the geology of contemporaneously exposed non-carbonatic terranes, etc.).

Work has begun in 1989 with the inaugural meeting held in Sümeg/Hungary, where participants agreed upon the principles of correlation, formed National Working Groups and set out to prepare a review of the available data on bauxites and paleokarst phenomena in each of the countries represented, with the final aims of correlation in mind. These reviews are presented here together with a collection of research papers presented at the second working meeting of the project in Itea-Delphi, Greece 1990.

The Meeting was jointly organized by Parnass Bauxite Mining Co. and the National Technical University of Athens with Prof. A. Vgenopoulos as chief organizer. Financial support was provided by UNESCO/IUGS and the Group of Greek Bauxite Mining Companies (including the Bauxite Mines of Parnass, Helicon, Delphi-Distomon and Eleusis).

Thanks to Parnass' superb facilities and efficient crew it was a professionally organized Meeting which provided a perfect environment for scientific discussions seasoned with the proverbial hospitality of the Greek

colleagues and with the natural beauties and historical heritage of the Parnass-Ghiona area.

IGCP-287 is greatly indebted to all the sponsors and organizers, particularly to Dr. Ulysess Kyriacopoulos (Director, Parnass Bauxite Mining Co.) and Prof. A. Vgenopoulos (Athens Technical University) who did their best to make the Meeting as successful as it was. Particular thanks are due to the late Prof. Walther Petrascheck for his invaluable help in the organization of the Meeting. It was his personal attachment to Greece and to Parnass Bauxite and his devotion to bauxite geology which had undoubtedly the greatest influence on both the professional and the human merits of the Meeting.

J. Haas, Gy. Bárdossy, A. Mindszenty (eds)

18. December 1991, Budapest

-Note: Most of the papers in this volume are printed as submitted by the authors, only a few of them had to be changed for editorial reasons. Corrections and changes were restricted to those paragraphs which were difficult to understand because of obvious linguistic problems. We know very well that even the corrected text is not perfect but we had to find a compromise between completely rewriting papers and this way perhaps losing their essence or publishing a volume the wording of which would hamper the proper understanding of what was meant by the authors. We truly hope that the alterations did not affect the original ideas expressed and even though clumsy the language still may be at places it does convey the "message".

The number of papers submitted in Itea-Delphi did not allow publish all the collection in one single volume. Thanks to the generosity of the Editorial Board of *Acta Geologica*, however, we are granted to fill another volume with the rest of the papers to be printed not later than October of 1992.

Jurassic karst bauxites in the Subbetic, Betic Cordillera, Southern Spain

José M. Molina, Pedro A. Ruiz-Ortiz

*Dept. of Stratigraphy and Paleontology
Univ. of Granada, Jaén*

Juan A. Vera

*Dept. of Stratigraphy and Paleontology
Univ. of Granada, Granada*

The studied bauxite orebodies are hosted in Jurassic limestones of the Internal Subbetic. This paleogeographic domain of the Southern Iberian Margin was during the Middle and Upper Jurassic a sedimentary pelagic swell in which emersion and karstification periods occurred. The bauxites fill karstic caves in the Lower Liassic limestones, below a main stratigraphic discontinuity over which Oxfordian pelagic limestones (Ammonitico Rosso facies) are disposed. The bauxites and the overlying unconformity were generated subaerially between the Carixian and the Oxfordian. The analyzed bauxites are analogous to those described in other Alpine realms (Appennines, Alps, Dinarides) which are also in relation with disconformities generated in a carbonate island of the continental margin.

Key words: Bauxite, paleokarst, unconformities, Jurassic, Subbetic Zone, Betic Cordillera, Spain

Introduction, geological setting

The Southern Iberian Continental margin was structured during the Mesozoic in different paleogeographic realms. Among them, the Subbetic, was characterized by sedimentation generally of pelagic nature from the Middle Liassic. During the Middle and Late Jurassic a through realm (Middle Subbetic) bounded by the north and south by swell domains (External and Internal Subbetic, respectively) were differentiated into the Subbetic. In one of these swells (Internal Subbetic), far from any significant terrigenous contribution, different stages of emergence and karstification (Carixian, Aalenian-Lower Bajocian, Bathonian and Kimmeridgian) took place (Vera et al. 1988). After this, the paleokarsts were buried by pelagic sediments. The following criteria has been used to recognize paleokarst:

- 1) surface morphologies,
- 2) speleothems,
- 3) collapse breccias,
- 4) laminated continental cavern sediments,
- 5) freshwater phreatic and vadose cements in cavity host rocks,
- 6) some meteoric diagenetic features of the wallrocks,
- 7) geochemical analysis,
- 8) age of pelagic sediments in Neptunian dikes and
- 9) karst bauxites and paleosols

Addresses: J. M. Molina, P. A. Ruiz-Ortiz: 23071 Jaén, Universidad de Granada, Facultad de Ciencias, Experimental de Jaén, Spain

J. A. Vera: 18071 Granada, Universidad de Granada, Facultad de Ciencias Granada, Spain

Received: 16 August, 1991

Bauxites are one of the most convincing evidences of subaerial exposure and karstification. In the Subbetic Zone of the Betic Cordillera (Southern Spain), small bodies of bauxites related to Jurassic paleokarst occur (Vera et al. 1986–87; Molina et al. 1989). The purpose of this report is to review the occurrence, stratigraphic attributes, origin and paleogeographic significance of these karst bauxites.

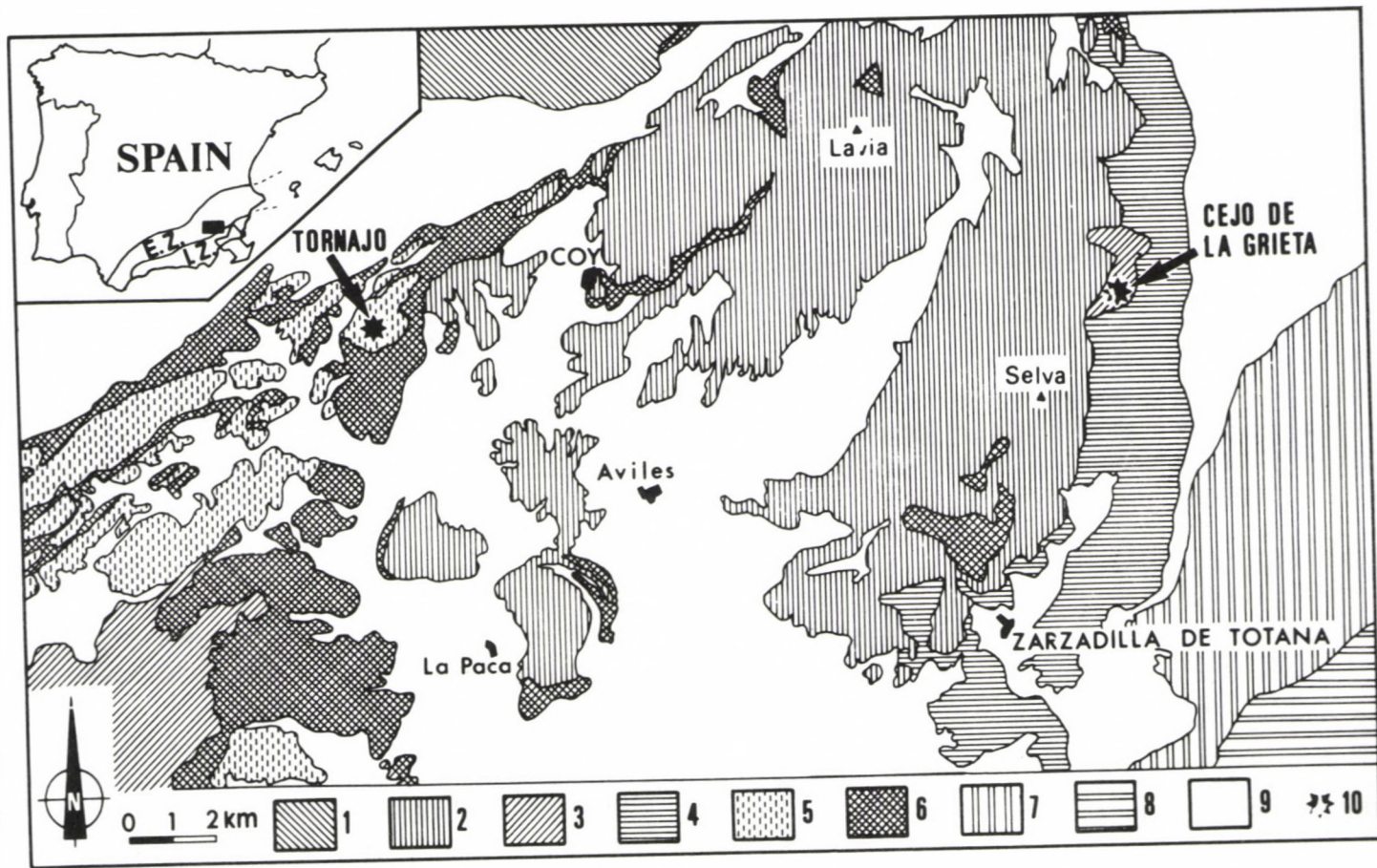
The main bauxite orebodies are found north (about 7 km) of Zarzadilla de Totasna in the Murica region (Figs 1 and 2). Geologically they are located in a small tectonic unit (Canteras Unit, number 3 in Figure 1) overthrust by other more extensive unit (Sierra de Ponce Unit, number 2 in Figure 1) which have a different Jurassic stratigraphy.

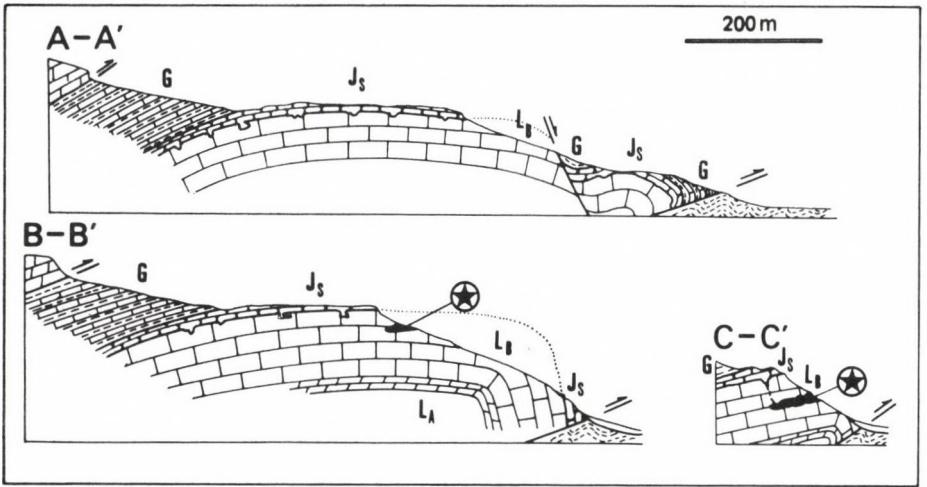
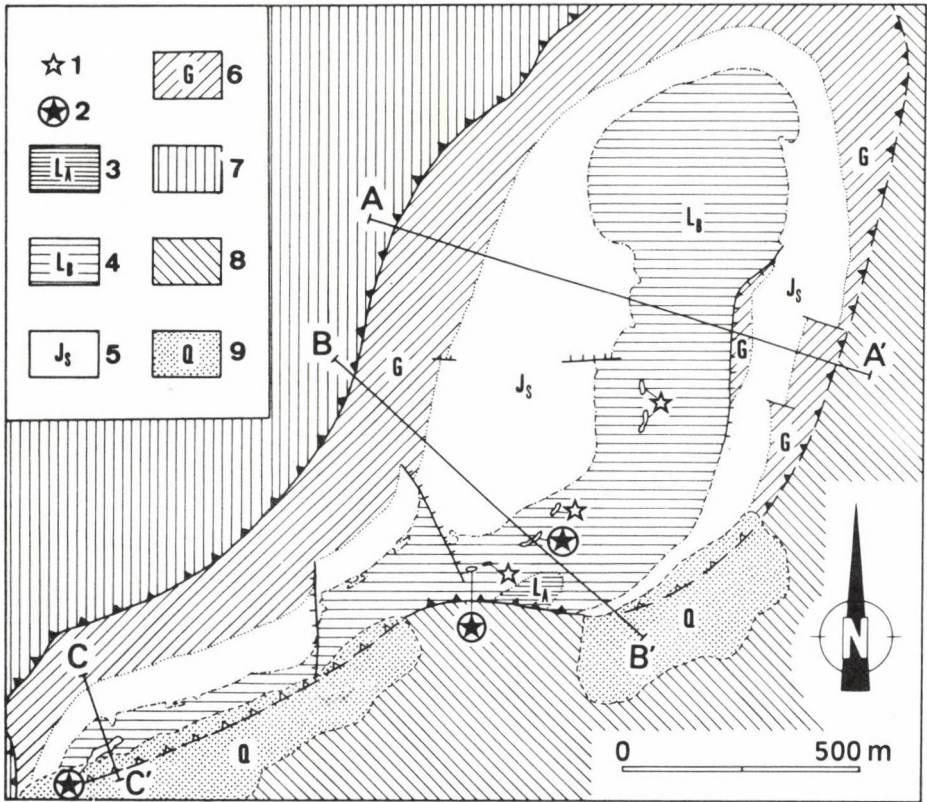
The Sierra de Ponce Unit belongs to the Middle Subbetic and it has a Middle and Late Jurassic sequence composed mainly of pelagic sediments and submarine volcanic rock intercalations, with a Jurassic section in which are abundant the pelagic sediments (marls, limestones) and there are also intercalated submarine volcanic rocks. The Canteras Unit shows a very important stratigraphic gap lacking Middle-Late Liassic and Dogger deposits. The Malm consists of nodular limestones (Upper Ammonitico Rosso Fm.) deposited in a pelagic swell, over shallow platform marine limestones (Gavilán Fm.). According to its typical stratigraphic features and structural position the Canteras Unit belongs to the Internal Subbetic. This unit shows an anticline structure with SE vergence, overthrusting in the same sense over other Cretaceous and Tertiary materials (number 4 in Figure 1) of the Internal Subbetic.

Other Al- and Fe-rich materials outcropping in the Tornajo hill have also been analyzed. They are located 16 km west of the above (see Figs 1 and 3). The Tornajo hill is a block belonging to the tectonic megabreccia of the Crevillente Fault Zone (Smet 1984). It is a major fault zone, extending for hundreds of kilometers subparallel to the axis of the Betic Cordillera. In this tectonic megabreccia numerous blocks float in a matrix of Triassic clays and gypsum. The Jurassic stratigraphy of each of these blocks is usually different in one from the other, being representative of different palaeogeographic domains. It indicates that they were displaced relatively to each other over large distances, as the result of major strike-slip movements along the fault zone. For this reason the attribution of the Tornajo hill to a paleogeographic domain is more problematic, but according to its stratigraphical characteristics could belong to the Internal Subbetic. The Tornajo Jurassic sequence also shows an important stratigraphic gap, lacking Middle-Late Liassic and Dogger deposits. The Callovian and Malm consist of nodular limestones (Upper Ammonitico Rosso Fm.) deposited in pelagic swells, capping Lower Liassic epigenetic dolostones and shallow marine limestones (Gavilán Fm.)

Fig. 1.

Location map of the study area. 1. External Subbetic; 2. Middle Subbetic (Sierra de Ponce Unit); 3. Internal Subbetic (Canteras Unit); 4. Other Cretaceous and Tertiary materials of the Internal Subbetic; 5. Tectonic megabreccia of the Crevillente Fault Zone; 6. Triassic of the Subbetic Units; 7. Tertiary of Espuña-Río Piiego related to Malaguide Units; 8. Internal Zones Malaguide Units; 9. Postorogenic Neogene and Quaternary; 10. Studied outcrops. Inset map: E.Z. (Betic External Zones) and I.Z. (Betic Internal Zones)





Bauxitic materials

Two kinds of alumina-rich rocks have been distinguished: 1) bauxites and bauxitic clays, and 2) collapse breccias with irregular clasts of Lower Liassic limestones and dolostones, and bauxite matrix. Also clayey Al-, Fe-rich materials occurs in the Tornajo hill.

The bauxite bodies and Al-, Fe-rich materials fill karstic cavities in shallow marine limestones and epigenetic dolostones of Early Liassic age (Gavilán Fm.). They have dominantly red, pink or violaceous colours, but brown, yellow and orange colours also occur. Texturally they are mainly composed of a homogeneous matrix (pelitomorphic texture, Bárdossy 1982) but pisolitic, grainy and pseudobrecciate textures are also present. Locally there is parallel lamination, as the only sedimentary structure. The Al-, Fe-rich materials of the Tornajo outcrops show red colour with argillaceous appearance and also locally parallel lamination.

The mineralogical composition was studied by Alias et al. (1972). Boehmite and gibbsite are the alumina minerals present. In the greatest orebody (Cejo de la Grieta) the boehmite is more abundant than the gibbsite. They are always associated with kaolinite, hematites and anatase. Frequently there are reniform or botryoidal concretions of goethite.

With regard to the chemical composition the Shapiro and Brannock (1962) rapid method has been adapted and modified to analyze Al_2O_3 and Fe_2O_3 from bauxitic rock samples with different Fe content (Molina-Diaz et al. 1986–87). The results of these analyses are shown in Table 1. In Zarzadilla de Totana bauxites (Cejo de la Grieta orebody), the total Al_2O_3 and Fe_2O_3 content ranges from 10 to 67, with common values from 40 to 60%. The $\text{Al}_2\text{O}_3/\text{Fe}_2\text{O}_3$ ratio shows often high values, but in some samples Fe_2O_3 is higher than the Al_2O_3 . However, in the Tornajo outcrops, in spite of the bauxitic appearance of the analyzed materials, no real bauxite occurs as the samples have a Al_2O_3 content not higher than 11% and usually with similar amounts of Fe_2O_3 (from 2 to 17%).

All these bauxitic outcrops are of small dimensions; the greatest is the Cejo de la Grieta (5 x 35 m in outcrop) which has been the only handicraft mined bauxite orebody of Southern Spain.

Fig. 2.

Geologic map and cross-sections of the southern part of the Canteras tectonic unit, made from an enlarging copy of the 932-C-12 aerial photograph original scale 1:18000). Note the contact between the 4 and 5 materials, showing karstic morphologies in its western part. 1. Bauxite breccia filling cavities in the Liassic limestones; 2. Bauxite and iron oxides filling karstic cavities; 3. Lower Liassic dolostones; 4. Lower Liassic (Pre-Domerian) white limestones; 5. Pink nodular limestones of Oxfordian–Kimmeridgian age (Ammonitico Rosso Fm.); 6. Lower Cretaceous limestone-marl rhythmite; 7. Jurassic of the Middle Subbetic; 8. Other Cretaceous and Tertiary Subbetic materials (probably Internal Subbetic); 9. Quaternary deposits. (Modified from Vera et al. 1986–87)

Table 1.
Al₂O₃ and Fe₂O₃ content in the studied samples

Sample	Locality	Colour, texture	Al ₂ O ₃ %	Fe ₂ O ₃ %
A-1	M.H.	Iron orebody	2.04	72.90
A-2	M.H.	Yellow; pelitomorphic	18.54	3.36
A-3	M.H.	Pink	39.00	5.40
A-4	M.H.	Greenish	47.48	2.32
A-5	M.H.	Pink; pisolitic	10.42	73.09
A-6	M.H.	Red breccia matrix	1.37	6.59
B-1	C.F.	Violaceous; pelitomorphic	57.29	15.15
B-2	C.F.	Violaceous; pisolitic	57.63	22.89
B-3	C.F.	Pink; pelitomorphic	63.47	11.63
B-4	C.F.	Violaceous; pisolitic	59.38	15.52
C-1	C.G.	Red; pelitomorphic	66.85	2.94
C-2	C.G.	Red; pelitomorphic	61.06	2.30
C-3A1	C.G.	Red; pelitomorphic	43.20	33.12
C-3A2	C.G.	Red; pelitomorphic	65.51	2.31
C-4	C.G.	Red; ooidic	38.90	32.79
C-5	C.G.	Brilliant garnet	48.78	20.64
C-6	C.G.	White with red ribbons	63.18	2.75
C-7A	C.G.	Red; pelitomorphic	24.97	18.15
C-7B	C.G.	White; pelitomorphic	9.89	3.55
C-8	C.G.	Yellow; pseudobrecciated	66.11	5.89
C-14A	C.G.	Yellow; conglomerated;	25.11	29.48
C-14B	C.G.	Reddish brown; pisolitic	23.81	54.83
TO-3	TO.	Pink	0.24	6.59
TO-4	TO.	Brown	0.65	17.43
TO-6	TO.	Red	2.25	1.82
TO-7	TO.	Red	2.98	1.96
TO-8	TO.	Pink; pisolitic	5.37	1.97
TO-9	TO.	Red; arenitic	6.19	3.09
TO-10	TO.	Dark red; arenitic	11.09	3.28
TO-11	TO.	Pink	7.59	3.18
TO-12	TO.	Dark red	7.51	4.52
TO-13	TO.	Yellow	1.84	1.58
TO-14	TO.	Breccia	2.45	2.14
TO-15	TO.	Pink	4.82	2.66
TO-16	TO.	Pink	4.77	5.40
TO-17	TO.	Red	9.79	3.82
TO-18	TO.	Red; conglomerate	7.20	4.67
ZT-54	Can	Violaceous; pelitomorphic	44.40	16.57

Localities:

M.H. – Mina de Hierro orebody (Alias et al., 1972)

C.F. – Waste near to the Cortijo del Francés

C.G. – Cejo de La Grieta orebody

TO. – Tornajo hill

Can. – Pliocene–Quaternary deposit in a limestone quarry

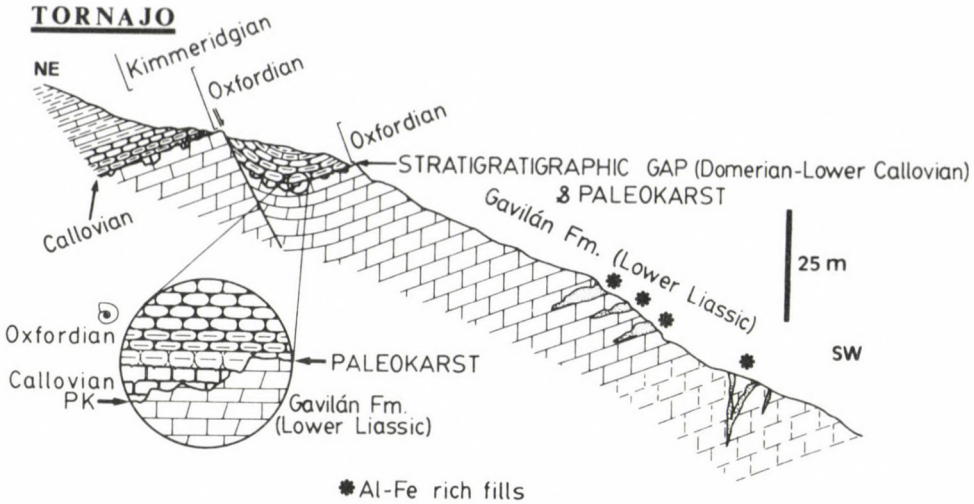


Fig. 3.
Cross-section in the Tornaajo outcrops

Stratigraphic setting of the bauxite orebodies

Figure 2 shows a detailed geologic map of the Zarzadilla de Totana area. In the cross-sections the bauxites appear filling karstic caves below the contact between the overlying pelagic Ammonitico Rosso facies and the underlying shallow platform limestones (Gavilán Fm.). This boundary is an important stratigraphic break of regional extent so that Domerian to Lower Oxfordian deposits are absent (about 40 M.y. are lacking). Special attention was paid to the morphology and associated features of this stratigraphic break to determine the paleokarst surface and to establish the relationship with the bauxitic materials, making detailed maps and schemes of the outcrops and taking a lot of samples. In the majority of the stratigraphic sections it is a paraconformity, but in another places it is a disconformity, and it is possible to observe the paleokarst morphology in cross-section. Fracture-controlled funnel-shaped features of various sizes with locally flat bottoms are interpreted as sinkholes (Fig. 4). Figure 4A shows a vertical section of the main bauxite orebody (Cejo de la Grieta); the bauxites fill a karstic cavity, with irregular geometry but elongated along the bedding. This cavity is more than 5 m wide at right angle to the bedding, and more than 35 m long. Above the bauxite orebody, on the top of the Gavilán Fm., a sinkhole filled in by pelagic Ammonitico Rosso limestones occurs. The sinkhole penetrates 12 m down from the top of the Gavilán Fm., and its maximum observable width is 30 m. The sinkhole-filling shows also slumps, with vergence to the interior of the sinkhole, and collapse breccias. From the observable lower point of this cavity until the bauxite orebody there are 20 m of limestones with Neptunian dikes oblique or perpendicular to bedding (Q type, Wendt 1971; q in Fig. 4A, 4B and 4D), some

Neptunian dikes which are parallel to bedding (S type, Wendt 1971; s in Fig. 4A, 4C and 4D), and breccias with bauxitic matrix filling cavities (b in Fig. 4A and 4D). These features are a distinct evidence of communication between the paleokarstic cavity (sinkhole) and the main bauxite orebody.

The Fig. 4D shows the general morphology of the contact between the liassic limestones and the Ammonitico Rosso pelagic sediments. So, the bauxites and Al-, Fe-rich materials fill seemingly isolated karstic cavities in the Liassic carbonates, but they are vertically related to paleokarst sinkholes and cavities. In the Cejo de la Grieta outcrop no bauxite occurs lower than 35 m below the paleokarst surface. Penetration depth of the karst cavities is considered to be an approximate measure of the amplitude of emergence of the temporary island. The presence of cavities is to be expected in the vadose zones of gravity percolation (James and Choquette 1984), where flat-bottomed cavities are commonly elongate parallel to the water table, or in this case, to the sea level.

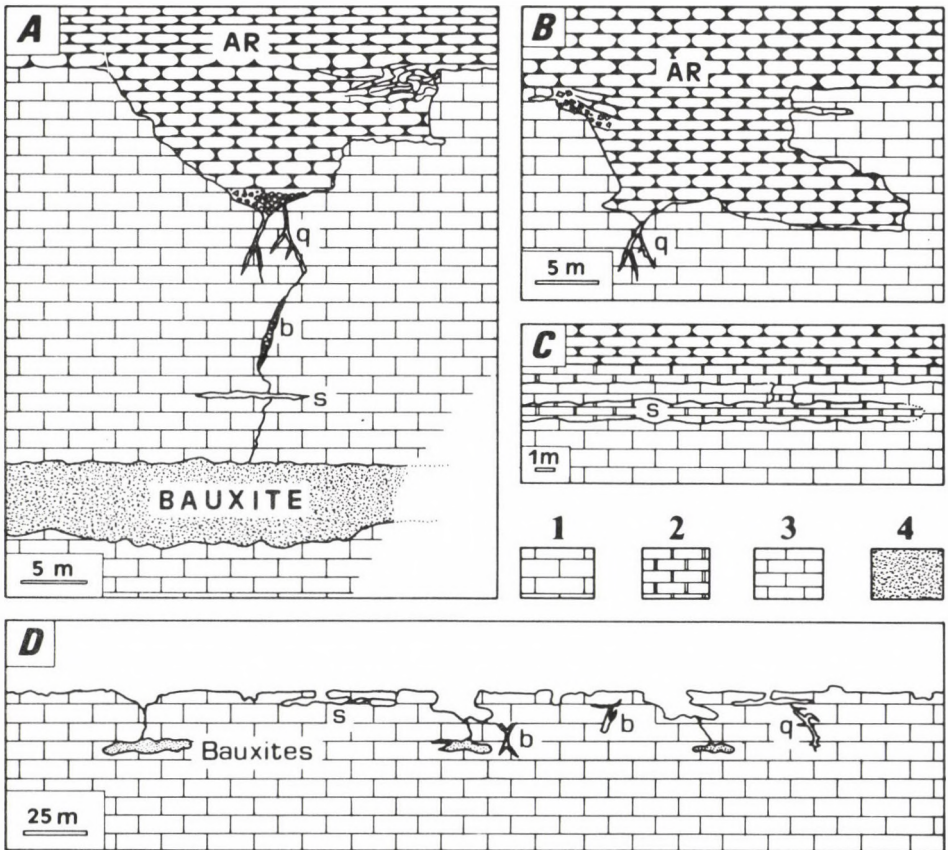


Fig. 4. Morphology of the contact between the Liassic white limestones and the Oxfordian pelagic materials. For explanation see text. Modified from Vera et al. 1986-87)

Origin and paleogeographic significance of the bauxites

We are dealing with karst bauxites coming from the weathering and pedogenesis of Liassic carbonates. The karstification took place between the Carixian and the Oxfordian, probably during Middle Jurassic time. The low Al content of the Liassic limestones and dolostones points out the meteorization of a very great volume of these deposits in carbonate islands up to 150 km far of the continental areas, according to the more recent paleogeographic reconstructions for the Jurassic of the Southern Iberian Margin (Vera et al. 1988, Ruiz-Ortiz et al. 1989). In other Subbetic areas anomalous clay-mineral composition of Upper Liassic pelagic marls, related with pedogenetic processes on nearby carbonate island, have also been recognized (Vera et al. 1989).

Nevertheless the increase of the Al to ore grade could also be due to other processes such as the accumulation of chemically mature aeolian dust (e.g. Maric 1969; D'Argenio 1970; Comer 1974; Taylor and Hughes 1975; Bárdossy et al. 1977; Bárdossy 1982; Brimhall et al. 1988) derived elsewhere from soils, volcanic ash or other volcanic materials. In the Subbetic Zone, basic volcanic rocks occur intercalated in Liassic and, mainly, in Middle Jurassic series deposited in areas paleogeographically adjacent to the pelagic swells. The volcanic events originating these intercalations could have been potential source of volcanic ashes.

With regard to the autochthony or allochthony of the bauxites, we think that they are parautochthonous, according to the proximity between the paleokarstic relief and the bauxitic karstic cavities. The percolation and carriage over short distances from sinkholes down to these cavities was the only transport process.

Figure 5 shows a scheme of the genetic process. In an initial stage, during the Liassic until the Carixian, limestones were deposited in a shallow marine platform (Fig. 5A). Because of the gap between the Carixian and the Middle Oxfordian, we can order the processes occurring in this interval, but we cannot precise the time in which they happened. In the first place faulting along with a drop in sea level caused the isolation of a sedimentary swell and its emergence. This was followed by karstification of the emergent pelagic swell, in an area that might have been a large carbonate island (Fig. 5B). It seems likely that karstification took place mainly above the water table (according to Esteban and Klappa 1983; James and Choquette 1984) under warm and humid conditions. The chemical weathering of the limestones by rain water produced soils (terra rossa), with an alumina enrichment and the liberation of silica, and so bauxitization (Fig. 5C and 5D). A volcanic contribution to the bauxite parent material could exist. In a subsequent submersion stage the soils and superficial deposits were dismantled and the sedimentary filling and paleokarst fossilization began as the sea rose and flooded the pelagic swell at Callovian-Oxfordian times (Fig. 5E and 5F).

An aspect difficult to precise is the exact time in which bauxites were originated. Without doubt it was between the Carixian (about 192 m.y.) and the Middle Oxfordian (about 150 m.y.), but it is possible that the emersion and weathering of the relief were not continuous along this interval. According to the proposed sea

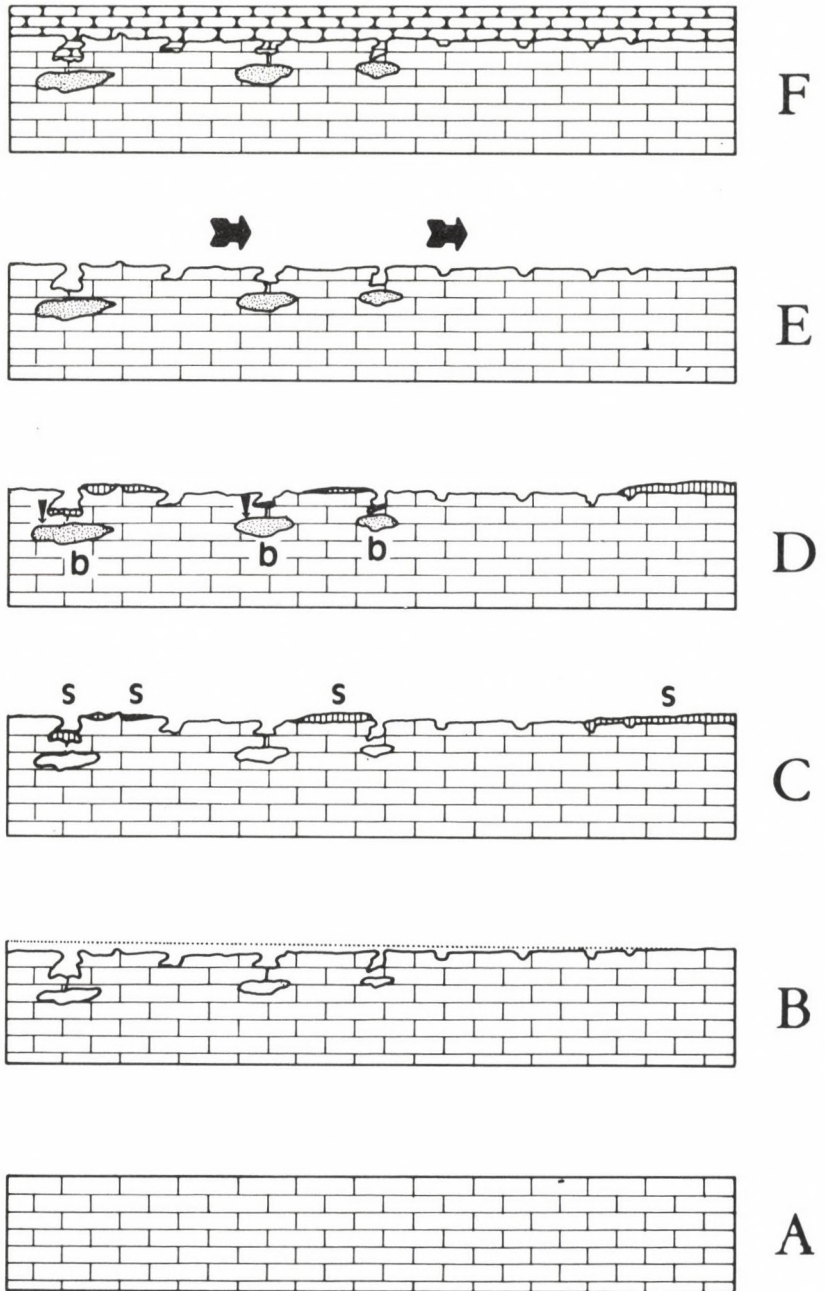


Fig. 5. Genetic sketch of the bauxite formation. For explanation see text. Modified from Vera et al. (1986–87)

level fluctuation curves to the External Zones of the Betic Cordillera (Vera 1988), the times of lowest sea level in the Early and Middle Jurassic, would be the Carixian-Domerian boundary, the Early Aalenian, the Early Bajocian, the Late Bathonian and the Early Callovian, which would be epochs where the karstification and pedogenesis could be maximum. The karstification would be brought about especially in the first phase of lowstand (Early Domerian), immediately after the break of the Liassic carbonate platform. The soil genesis could be continued along the Upper Liassic and Dogger, with a maximum development in the above-mentioned lowstand stages.

These bauxite orebodies are of Mediterranean type (Bárdossy 1982) and they are very similar to those described in other Alpine Mediterranean realms. With regard to the Jurassic bauxites in the Mediterranean belt (Fig. 6) the main karst bauxite regions are those in the Parnassos, Kiona and Helicon Mts. (Hellenids) of Greece (e.g. Papastamatiou 1964, 1965; Bárdossy and Mack 1967; Nia 1968; Valetton et al. 1987) and in the Crna Gora (Montenegro, Yugoslavia) in the Dinarids (e.g. Buric 1966; Grubic 1964, 1975).

There are minor occurrences in Greece on the islands of Euboea (Papastamatiou 1964, 1965; Robert 1971; Guernet and Robert 1973), Skopelos (Papastamatiou 1963) and Amorgos (Marinos 1954), and on the Chalkidike Peninsula (Vardar Zone) (Bárdossy et al. 1973); in Yugoslavia on the Istrian Peninsula (Croatia) near Rovinj (Grubic 1975), on the Hrusika Mts. (Zuzemberk, Slovenia) (Buser and Lukacs 1970), and on Grmec Mts. (SE of Bosanska Krupa) (Jurkovic, 1965); in Switzerland on Dréveneuse (Badoux and De Weisse 1959); in France on Vanoise Massif (Ellemerberger 1955; Goffe and Saliot 1977), on Bedarieux (Languedoc) (Combes et al. 1973) and on the Basque-Bearnoises Pyrenees (Pic de Soudou) (Combes and Peybernes 1987); and in the U.S.S.R. on the Rahow Massif (NE Carpathians) (Denishevich 1958) and on Crimea (Malakovskiy and Lysenko, 1964).

The Jurassic Subbetic bauxites were deposited in pelagic swells temporally emergents. Also in other Alpine domains have been established sedimentation models in which the pelagic swells were locally subaerially exposed, as proposed for instance D'Argenio (1970, 1974), Cousin (1980), Farinacci et al. (1981), D'Argenio and Mindszenty (1987) and Bosellini (1989) in the Apennines, Eastern Alps, Yugoslavia, Greece and so forth. The emersion is mainly documented by paleokarst, bauxite horizons and pronounced unconformities. Eustatic sea level changes and specially rapid tectonic movements are interpreted to have caused a number of platform and pelagic swells to become subaerially exposed. According to Bosellini (1989) these rapid tectonic movements appear to be time-transgressive across an orogenic profile and occurred in different intervals of time span, according to the Tethyan sector involved.

In the proposed model, applicable to other similar Mediterranean Alpine realms, the subaerial exposure surfaces are correlated with hardgrounds and condensed sequences on some pelagic swells (Vera et al. 1988). Karstification took place on the emerged areas while hardgrounds formed in the submerged adjacent areas.

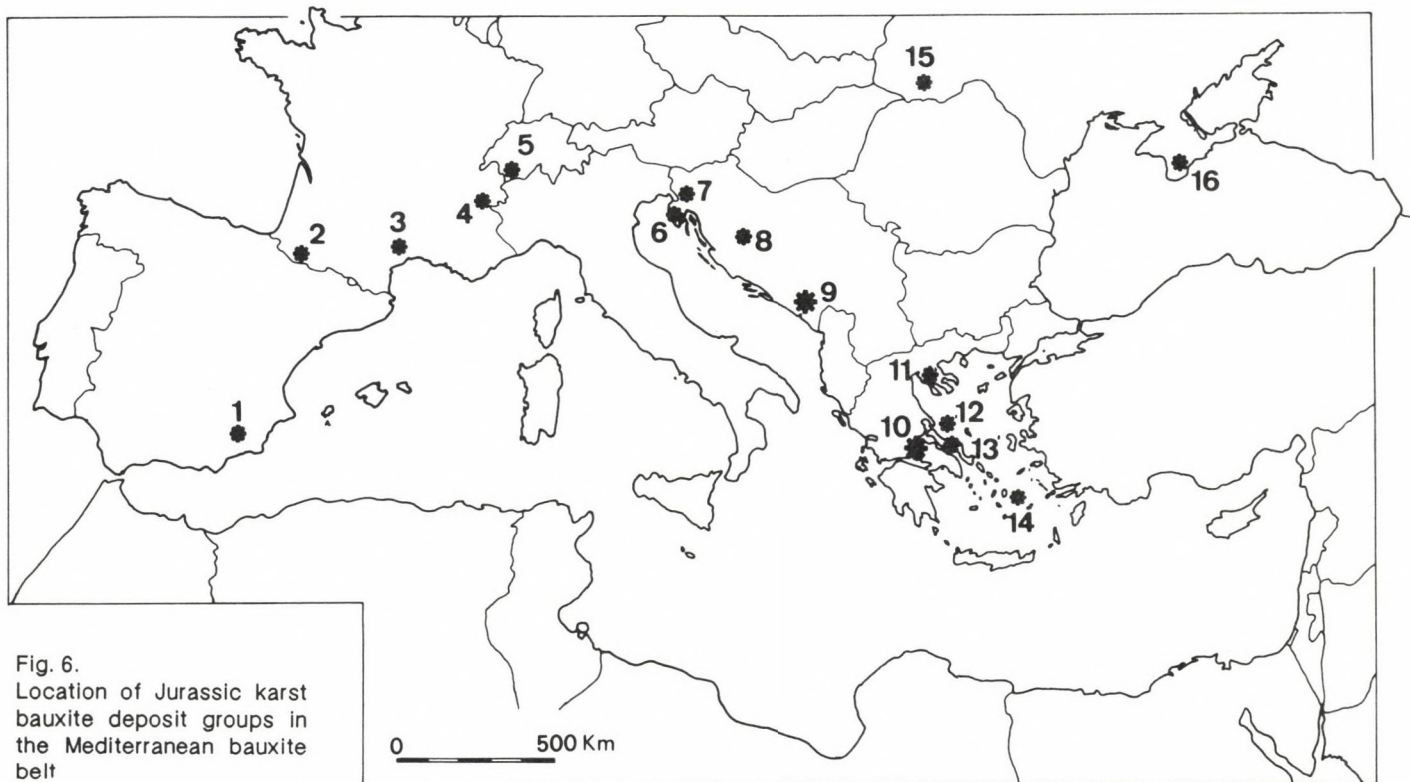


Fig. 6.
Location of Jurassic karst
bauxite deposit groups in
the Mediterranean bauxite
belt

All the bauxitic and non-bauxitic paleokarsts are related to unconformities which resulted from rapid tectonic movements and/or eustatic sea level falls. The subsequent sea level rise caused drowning (starved drowning, in the sense of Bosellini 1989) of the carbonate island and locally the preservation of these karstic bauxites of Mediterranean type.

Summary and conclusions

In the Jurassic of the Subbetic Zone we have recognized several significant stages of emergence and karstification on pelagic swells isolated from any significant terrigenous input. The originated paleokarsts were buried by pelagic sediments.

Bauxites are one of the most convincing evidences of emergence and karstification. Although only one body of bauxite has been mined recently (Cejo de la Grieta in Zarzadilla de Totana, Murcia province), many smaller masses are found near this locality (Vera et al. 1986–87). Two kinds of alumina-rich rocks have been distinguished: 1) bauxites and bauxitic clays and 2) collapse breccias with clasts of Liassic limestones and dolostones, and bauxite matrix. Texturally they are mainly composed of a homogeneous matrix (pelitomorphic texture) but pisolitic and grainy textures also occur. Gibbsite and boehmite are the alumina minerals present and they are always associated with kaolinite and hematites.

The bauxite bodies and Al-, Fe-rich materials fill karstic cavities and caves in shallow marine limestones and epigenetic dolostones of the Lower Liassic (Gavilán Fm.). In the Cejo de la Grieta outcrop no bauxite occurs lower than 35 m below the paleokarst surface and the caves with bauxitic filling are vertically connected along fissures and Neptunian dikes to sinkholes developed on the top of the Gavilán Fm. and covered by Oxfordian red pelagic limestones (Upper Ammonitico Rosso Fm.). Thus karstification took place between the Carixian and the Oxfordian, probably during Middle Jurassic time. The low Al content of the Liassic limestones and dolostones would have required the weathering of a very great volume of these deposits in carbonate islands upto 150 km from the continental areas, according to the more recent paleogeographic reconstructions for the Middle Jurassic of the Southern Iberian Plate Margin. Nevertheless, the increase of Al to oregrade could also be due to other processes such as the accumulation of aeolian dust derived elsewhere from soils, volcanic ash or other volcanic materials. Basic volcanic rocks occurs in the Liassic and Middle Jurassic of the Subbetic Zone in paleogeographically adjacent areas.

In the proposed model, applicable to other similar Mediterranean Alpine realms, the stages of emergence and hardground formation are contemporaneous and spatially related on a given swell (Vera et al. 1988). All the paleokarsts are related to unconformities which resulted from sudden tectonic events and/or eustatic sea level falls. The subsequent sealevel rise caused submergence, paleokarst fossilization and locally the preservation of these karstic bauxites of Mediterranean type.

References

- Alias, L.J., R. Ortiz Silla, M. Rodriguez Gallego 1972: Mineralogia de un yacimiento de bauxita situado al norte de Zarzadilla de Totana Prov. de Murcia). – *Estudios Geologicos*, 28, pp. 209–215.
- Badoux, H.G., De Weisse 1959: Les bauxites siliceuses de Dréveneuse. – *Bull. Soc. Vaudoise Sc. Nat.*, 67, pp. 169–178.
- Bárdossy, Gy. 1982: Karst bauxites, bauxite deposits on carbonate rocks. – *Develop. in Econ. Geol.*, 14. Elsevier. p. 441.
- Bárdossy, Gy., M. Boni, M. Dall 'Aglio, B. D'Argenio, G. Pantó, 1977: Bauxites of Peninsular Italy, Composition, Origin and Geotectonic Significance. – *Monograph Series on Mineral Deposits*, Gebruder Borntraeger, Berlin, 15, pp. 1–61.
- Bárdossy, Gy., E. Mack, 1967: Zur Kenntnis der Bauxite des Parnass-Kona Gebirges. – *Miner. Depos.*, 2, pp. 334–348.
- Bárdossy, Gy., G. Pantó, J. Papastamatiou 1973: Etude mineralogique, pétrographique et geochemique des bauxites du Malm inferieur dans la region de Diastomon (Greece). *Tras. ICSOBA, Zagreb*, 9, pp. 143–149.
- Bosellini, A. 1989: Dynamics of Tethyan carbonate platforms. In: *Controls on Carbonate Platform and Basin Development*. (P.D. Crevello, J.L. Wilson, J.F. Sarg and J.F. Read, Eds). – *Soc. Econ. Paleont. Miner. Spec. Publ.*, 44, pp. 3–13.
- Brimhall, G.H., C.J. Lewis, J.J. Ague, W.E. Dietrich, J. Hampel, T. Teague, P. Rix 1988: Metal enrichment in bauxites by deposition of chemically mature aeolian dust. – *Nature*, 333, pp. 819–823.
- Buric, P. 1966: Geologie des gites de bauxite du Montenegro, Yougoslavie. – *Posebna Izd. Geol. Glasn. Jugosl.*, 8, p. 240
- Buser, S., E. Lukacs 1970: Bauxite in Slovenien. – *MÁFI Évk.*, Budapest, 54, pp. 209–220.
- Combes, P.J. B. Peybernes 1987: Les altérites et les brèches des Pyrénées Basco-Béarnaises liées à l'évolution polyphasée de la marge passive nord-ibérique au Jurassique et au Crétacé inférieur. – *C. R. Acad. Sci. Paris*, 305, pp. 49–54.
- Combes, P.J., G. Glacon, N. Grekoff, J. Medus, J. Sigal, 1973: Etude micropaléontologique d'une argilite associée à la bauxite de Bédarieux (Hérault, France). Nouvelles données sur l'âge de mise en place du mineral. – *C. R. Acad. Sci. Paris, D*, 276, pp. 1669–1672.
- Comer, J.B. 1974: Genesis of Jamaican bauxite. – *Econ. Geol.*, 69, pp. 1251–1264.
- Cousin, M. 1980: Les Rapports Alpes-Dinarides: Le confins de l'Italie et de la Yougoslavie. – *Unpublished Ph. Dissertation, Université de Pierre et Marie Curie, Paris*, p. 517.
- D'Argenio, B. 1970: Central and Southern Italy Cretaceous bauxites. *MÁFI Évk.*, Budapest 54, pp. 221–233.
- D'Argenio, B. 1974: Le piattaforme carbonatiche periadriatiche, Una rassegna di problemi nel quadro geodinamico mesozoico dell'area mediterranea. – *Mem. Soc. Geol. Italiana*, 13, p. 128.
- D'Argenio, B., A. Mindszenty 1988: Cretaceous bauxites in the tectonic framework of the Mediterranean. – *Rend. Soc. Geol. Ital.*, 9 (1986) pp. 257–262.
- Denishevich, A.A. 1958: The bauxites of the Carpathians and their genesis. – In: *Bauxites, their Mineralogy and Genesis*. *Izd. AN SSSR, Moscow*, pp. 347–350.
- Ellemerberger, F. 1955: Bauxites métamorphiques dans le Jurassique de la Vanoise (Savoie). – *Compt. Rend. Somm. Soc. Géol. France*, pp. 29–32.
- Esteban, M., C.F. Klappa 1983: Subaerial exposure environment. In: *Carbonate Depositional Environments*. – P.A. Scholle, D. G. Bebout and C.H. Moore (Eds). – *Am. Ass. Petrol. Geol.*, *Mem.* 33, pp. 1–54.
- Farinacci, S., N. Mariotti, U. Nicosia, G. Pallini, F. Chiavinotto 1981: Jurassic sediments in the Umbro-Marchean Apennines, an alternative model. In: *Proc. Rosso Ammonitico Symposium*, A. Farinacci and S. Elmi (Eds). – *Technoscienza, Roma*. pp. 335–398.

- Goffe, B., P. Saliot 1977: Les associations minéralogiques des roches hyperalumineuses du Dogger de Vanoise. Leur signification dans le métamorphisme régional. – Bull. Soc. Fr. Minér. Cristallogr., 100, pp. 302–309.
- Grubic, A. 1964: Les bauxites de la province dinarique (Yougoslavie). – Bull. Soc. Geol. France, (7), 6, pp. 382–388.
- Grubic, A. 1975: Geology of Yugoslav bauxites. – The Serbian Acad. Sci. and Arts Monographs, v. 44, Section for Natural and Mathematical Sciences, Beograd, p. 181.
- Guernet, C., P. Robert 1973: Sur l'existence de bauxites d'âge jurassique en Eubée (Grèce). – C. R. Acad. Sci. Paris, D, 276, pp. 885–887.
- James, N.P., P.W. Choquette 1984: Diagenesis 9. Limestones. The Meteoric Diagenetic Environment. – Geoscience Canada, 11, pp. 161–194.
- Jurkovic, I. 1965: Lithological types of bauxite in the Suvaja-Solaja region near Bosanska Krupa and their structural elements. Prirodosl. Istraz. Jugosl., Zagreb, 34, pp. 101–109.
- Malakovsky, V.F., N.I. Lysenko 1964: On the discovery of bauxite in the mountainous Crimea. – Litol i Polezn. Iskop., Moscow, 4, pp. 105–108.
- Maric, L. 1969: Relations génétiques entre la terra rossa et les bauxites dans le karst des Dinarides en Yougoslavie. – Bull. Museum National Hist. Natur., Paris, 41, pp. 770–777.
- Marinos, G. 1954: Geological reconnaissance of bauxite on the island of Amorgos. – Inst. for Geol. and Subsurface Res., Report N. 16, Athens, pp. 1–10.
- Molina, J.M., P.A. Ruiz-Ortiz, J.A. Vera 1989: Jurassic karstic bauxites in the Subbetic of Southern Spain. 10th Regional Meet. on Sedim., Budapest, Abstracts, pp. 164–165.
- Molina-Diaz, A., J.M. Molina, P.A. Ruiz-Ortiz, J.A. Vera 1986–87: Técnica de análisis rápido de Al_2O_3 and Fe_2O_3 en rocas bauxíticas. – Acta Geol. Hispánica, 21–22, pp. 593–597.
- Nia, R. 1968: Geologische, petrographische, geochemische Untersuchungen zum Problem der Boehmit-Diaspor-Genese in griechischen Oberkreide-Bauxiten der Parnass-Kiona-Zone. – Thesis, Univ. of Hamburg, p. 133.
- Papastamatiou, J. 1963: Les bauxites de l'île de Skopelos (Sporades du Nord). – Bull. Geol. Soc. Greece, 5, pp. 52–54.
- Papastamatiou, J. 1964: Les gisements de bauxite en Grèce. – Symp. Bauxites, Oxydes et Hydroxydes d'Aluminium, Zagreb, 1–3. X. 1963, 1, pp. 285–293.
- Papastamatiou, J. 1965: Quelques observations sur la genèse des bauxites en Grèce. – Trav. ICSOBA, Zagreb, 1, pp. 3–8.
- Robert, P. 1971: Sur un gisement de bauxite de l'île d'Eudebee (Grèce). – C. R. Acad. Sc. Paris, D, 272, pp. 3228–3330.
- Ruiz-Ortiz, P.A., M.A. Bustillo, J.M. Molina 1989: Radiolarite Sequences of the Subbetic, Betic Cordillera, Southern Spain. In: Siliceous Deposits of the Tethys and Pacific Regions, J.R. Hein and J. Obradovic (Eds). – Springer-Verlag, New York, pp. 107–127.
- Shapiro, L., W.W. Brannock 1962: Rapid analysis of silicate, carbonate and phosphate rocks. – U.S. Geol. Survey Bull., p. 1144-A.
- Smet, M.E.M. 1984: Investigations of the Cevillente Fault Zone and its role in the tectogenesis of the Betic Cordilleras. Southern Spain. – Thesis Univ. Amsterdam, p. 174.
- Taylor, G.R., G. Hughes 1975: Biogenesis of the Rennell bauxite. – Econ. Geol., 70, pp. 542–546.
- Valeton, I., M. Biernamm, R. Reche, F. Rosenberg 1987: Genesis of nickel laterites and bauxites in Greece during Jurassic and Cretaceous and their relation to ultrabasic parent rocks. – Ore Geology Reviews, 2, pp. 359–484.
- Vera, J.A. 1988: Evolución de los sistemas de depósito en el Margen Ibérico de la Cordillera Bética. – Rev. Soc. Geol. España, 1, pp. 373–391.
- Vera, J.A., J.M. Molina, A. Molina-Diaz, P.A. Ruiz-Ortiz 1986–87: Bauxitas kársticas jurásicas en la Zona Subbética Zarzadilla de Totana, prov. de Murcia, sureste de España: Interpretación paleogeográfica. – Acta Geol. Hispánica, 21–22, pp. 351–360.
- Vera, J.A., I. Palomo, M. Ortega-Huertas 1989: Influencia del paleokarst en la mineralogía de arcillas del Lias de Algarinejo (Subbético Medio). – Geogaceta, 6, pp. 16–19.

- Vera, J.A., P.A. Ruiz-Ortiz, M. Garcia-Hernandez, J.M. Molina, 1988: Paleokarst and Related Pelagic Sediments in the Jurassic of the Subbetic Zone, Southern Spain. – In: Paleokarst. N.P. James and P.W. Choquette (Eds). Springer-Verlag New York, pp. 364–384.
- Wendt, J. 1971 : Genese und Fauna submariner sedimentärer Spaltenfüllungen im Mediterraneen Jura. – Paleontog. A., 136, pp. 122–192.

A review of karst bauxites and related paleokarsts in Spain

José Miguel Molina

*Dept. of Stratigraphy and Paleontology
University of Granada, Jaén*

Some of the main characteristics of the Spanish karst bauxites are revised and updated. They are located in four bauxitic regions: 1) the Subbetic Zone in the Betic Cordillera; 2) the Linking Zone between the Catalan Coastal Range and the Iberian Range; 3) the Catalan Coastal Range; and 4) the Pyrenean System (Southern External and Sub-Pyrenean Ranges). Also other two minor occurrences (Portilla de Luna and Haro) are described. A complete updated bibliography about these bauxites is also presented at the end of the article.

Key words: Karst bauxite, main bauxite occurrences in Spain, paleokarst

Introduction

The bauxites in Spain were first recognized by Almera in 1900. He described bauxites in his geological map about the province of Barcelona. They were first identified in Roca Vidal (Montmell Massif, 12 km to the South of La Llacuna).

In the first twenty years of this century new bauxite deposits were reported in the provinces of Barcelona, Tarragona and Lérida (Catalonia) (Faura i Sans 1917, 1918, Boletín Oficial De Minas 1917a, b, c; Calafat, 1917; Fontrodona 1917; Goetz 1917, 1920; Bataller 1919; Faura i Sans and Bataller 1920; Hernandez Sampelayo 1920a, b, c).

Nevertheless, in spite of these works, the bauxite deposits were largely forgotten because of the premature affirmation that our bauxites were not marketable. This research had to be abandoned because they were industrially worthless, especially in competition with the best French bauxites, that covered all the market by that time.

The renewal of the studies on the Spanish bauxites was motivated by the increase in the consumption of aluminium with the Second World War. So Closas Miralles (1942, 1945), Bataller (1943) and Kundelan (1948) published extended accounts about the bauxites in Spain.

The 1950's were a good decade for the Spanish bauxite studies. San Miguel De La Camara (1950, 1954) published two extensive works about the Spanish bauxites, defining the existent paragenesis, the types and the stratigraphic level of these deposits. Also Lapparent (1950) presented a detailed analysis about the stratigraphic location of the Spanish bauxites, he assigned them a Cretaceous age (pre-Senonian) and he included them genetically in the Mediterranean bauxite

Address: J. M. Molina: 23071 Jaén, Universidad de Granada, Facultad de Ciencias,
Experimental de Jaén, Spain

Received: 13 September, 1991

ensemble. Rios and Almela (1950a, b) discovered new bauxite areas in the Southern Pyrenees. Using X-ray diffraction methods Font Tullot (1951) established the characteristic mineralogical associations. Also important in this decade were the works of Cantos (1950), Garcia-Siñeriz (1950), Jungwirth (1951), Sanz (1952) and specially the overview of Closas Miralles (1954, 1957) on the bauxites in the NE of Spain.

In the 1960's Font-Altaba and Closas (1960a, b) described a bauxite deposit on Devonian materials in the NW of Spain (Portilla de Luna, Province of León). Motta and Roch (1962) published interesting observations on the Spanish bauxites and its genetical interpretation. But the most important contributions of this decade were the publications of Combes (1967, 1969) and Combes et al. (1966). In his Doctoral Thesis he presented a useful piece of information on the stratigraphic relation and location, the origin and the paleogeographic significance of the bauxites in the Maestrazgo, Catalán Range and Pyrenees, reconstructing their geological history in comparison with the French bauxites.

In the 1970's Alias et al. (1972) described the mineralogy of bauxites in Zarzadilla de Totana (province of Murcia). Very important was the publication by the Geological and Mining Institute of Spain (I.G.M.E.) of the Metallogenetic Map of Spain and other publications (I.G.M.E., 1972, 1974) with the perspective of the bauxite deposits and their basic characteristics. Caballero et al. (1974) and Ordonez (1977) revised the Spanish bauxite deposits. Mata-Perello and Montoriol-Pous (1975) published the bibliography about the oxides and hydroxides in Catalonia. Galan et al. (1976) studied the mineralogy of bauxitic clays in the NE of the Teruel province (Maestrazgo) and Bárdossy and Fontbote (1977) analyzed the Portilla de Luna deposit aforementioned.

In the 1980's and until now in this decade we can quote the papers of Sebastian Pardo et al. (1985) about the mineralogy and geochemistry of bauxites in Haro (Rioja region), Vera et al. (1986–87, 1990), Molina et al. (1989) and Molina et al. (this volume) concerning to the Jurassic bauxites in the Subbetic, Molina-Diaz et al. (1986–1987) presenting a rapid method for analysis of bauxitic rocks, Blanco et al. (1989) about the pre-Albian weathering that they consider related to the Portilla de Luna bauxites, Molina and Salas (1990) about the Fontdespala deposit in the Linking Zone and La Iglesia and Ordonez (1990) study about the crystallography of kaolinite in bauxite deposits. A compilation of bibliography about bauxites in Spain appears at the end of this article.

After the consideration of this antecedents the purpose of this paper is to review and update some of the most important aspects of the Spanish karst bauxites in the light of this bibliography and with the author own knowledge.

The karst bauxites in Spain are located in four bauxite regions:

- 1) the Subbetic Zone in the Betic Cordillera;
- 2) the Linking Zone between the Catalán Coastal Range and the Iberian Range;
- 3) the Catalán Coastal Range; and
- 4) the Pyrenean System (Southern External and Sub-Pyrenean Ranges) (Fig. 1)

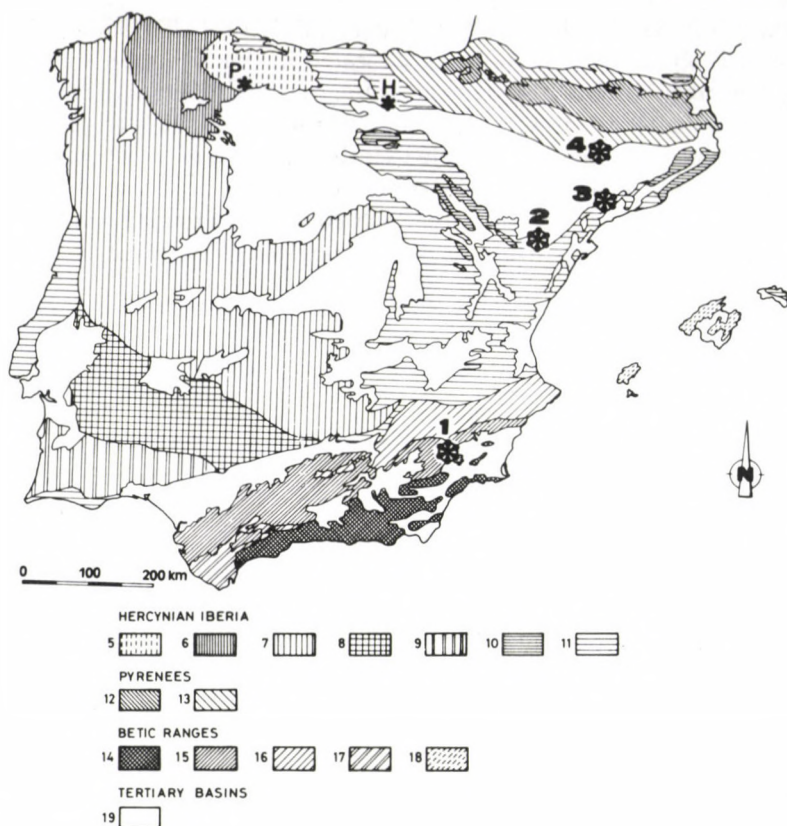


Fig. 1.

Location of the Spanish bauxite regions. 1. Subbetic Zone; 2. Linking Zone; 3. Catalán Coastal Ranges; 4. Pyrenees; 5-11. Hercynian Iberia, 5. Cantabrian Zone; 6. León-W, Asturian zone; 7. Central Iberian Zone; 8. Ossa-Morena Zone; 9. South Portuguese Zone; 10. Paleozoic of Iberian Ranges, Coastal Catalan Range and Menorca; 11. Mesozoic and Paleogene borders of the Iberian Massif; 12-13. Pyrenees, 12. Axial Zone; 13. Subpyrenean Ranges; 14-18. Betic Ranges, 14. Betic Zone; 15. Subbetic Zone, 16. Prebetic Zone; 17. Campo de Gibraltar Units; 18. Mesozoic of the Balearic Island; 19. Tertiary Basins; P-Portilla de Luna; H-Haro

These karstic bauxites belong to the Mediterranean bauxite belt (Combes 1969; Bárdossy 1982; Vera et al. 1986-87).

The main characteristics of these four bauxite regions can be established according to the period of bauxite genesis and accumulation, the age of underlying and overlying beds, the facies of immediate bedrock and cover, bedrock karstification, lithology of bauxites and related sediments, and the structural position.

Other places less important with minor occurrences of bauxites are Portilla de Luna (León) and Haro (Rioja).

The bauxite tonnage in all the Spanish deposits is probably about 62.7×10^6 tonnes of which about 60×10^6 tonnes are located in the NE of Spain (Caballero et al. 1974). The area with the best deposits is the Marginal Sierras in the Southern Pyrenees (Sierra de Montroig and Alos de Balaguer area). This tonnage do not refer to the quantity of bauxite amenable to industrial processing ("ore reserves"), but to the total bulk of bauxitic rocks contained in the deposits. On the other hand is necessary to carry out more research for prospecting bauxites, bauxitic clays and alumina-rich clays in interesting favourable areas (Prebetic Zone and Iberian Ranges specially).

Karst bauxites in the Subbetic Zone

The Subbetic Zone belongs to the External Zones of the Betic Cordillera in the South of Spain. In the Jurassic of the Subbetic Zone we have recognized four significant stages of emergence and karstification (Carixian, Aalenian-Lower Bajocian, Bathonian and Kimmeridgian) on pelagic swells which developed in agreement with times of sealevel fall and marked differential subsidence (Vera 1988; Vera et al. 1988; Garcia-Hernandez et al. 1988; Molina et al. 1990). The originated paleokarst, isolated from any significant terrigenous input, were covered by pelagic sediments mainly of the "Ammonitico Rosso" facies and condensed sequences. The following criteria have been used to recognize paleokarst:

- 1) surface morphologies,
- 2) speleothems,
- 3) collapse breccias,
- 4) laminated continental cavern sediments,
- 5) freshwater phreatic and vadose cements in cavity host rocks,
- 6) some meteoric diagenetic features of the wallrocks,
- 7) geochemical analysis,
- 8) age of pelagic sediments in Neptunian dikes and
- 9) karst bauxites and paleosoils.

These bauxites, one of the most convincing evidences of emergence and karstification, have been studied by Alias et al. (1972), Vera et al. (1986–1987) and Molina et al. (in this volume). This section is necessarily an abstract of this last paper, on which the interested reader can find more information.

Although only one small body of bauxite has been mined recently (Cejo de la Grieta in Zarzadilla de Totana, province of Murcia), many smaller deposits are found near this locality. There are also another studied outcrops of Al- and Fe-rich materials in the Tornajo hill, 16 km west of the above. Two kinds of alumina-rich rocks have been distinguished:

- 1) bauxites and bauxitic clays and
- 2) collapse breccias with clasts of Liassic limestones and dolostones, and bauxite matrix. Texturally they are mainly composed of a homogeneous matrix (pelitomorphic texture) but pisolitic and grainy textures also occur. Gibbsite and

boehmite are the alumina mineral present and they are always associated with kaolinite and hematite.

The bauxite bodies and Al-, Fe-rich materials fill karstic cavities and caves in shallow marine limestones and epigenetic dolostones of the Lower Liassic (Gavilán Fm.). The Jurassic section shows an important stratigraphic gap of regional extent, lacking Late Liassic and Dogger sediments (about 42 M.y.) over the paleokarst surface. In the Cejo de la Grieta outcrop no bauxite occurs lower than 35 m below the paleokarst surface. The caves with bauxitic filling are vertically connected along fissures and Neptunian dikes to sinkholes developed on the top of the Gavilán Fm. and covered by Oxfordian red pelagic limestones (Upper Ammonitico Rosso Fm.). Thus karstification took place between the Carixian and the Oxfordian, probably during Middle Jurassic time. The low Al content of the Liassic limestones and dolostones would have required the weathering of a very great volume of these deposits in carbonate islands upto 150 km from the continental areas, according to the more recent paleogeographic reconstructions for the Middle Jurassic of the southern Iberian plate margin. Nevertheless the increase of Al to ore grade could also be due to other processes such as the accumulation of aeolian dust derived elsewhere from soils, volcanic ash or other volcanic materials. Basic volcanic rocks occur in the Liassic and Middle Jurassic of the Subbetic Zone in paleogeographically adjacent areas.

In the proposed model, applicable to other similar Mediterranean Alpine realms, the subaerial exposure surfaces are correlated with hardgrounds and condensed sequences on some pelagic swells (Vera et al. 1988). All the paleokarsts are related to unconformities which resulted from sudden tectonic events and/or eustatic sea level falls. The subsequent sea level rise caused submergence, paleokarst fossilization and locally the preservation of these karst bauxites of Mediterranean type.

*Karst bauxites in the Linking Zone between the Catalán Coastal Range
and the Iberian Range*

Between the Catalán Coastal Range, dominated by major NE-SW basement faults, and the Iberian Range, dominated by major NW-SE basement faults, there is the Linking Zone where the dominant structural direction is E-W (Guimera, 1988). In the Linking Zone the most important and the best studied bauxite deposits are located in the Nevera de Fuentespalda (Fontdespala in the native Catalán language) in the Teruel province. There also other less important in volume deposits, about 28 km to the NE, in Horta de Sant Joan, Pauls and Prat de Compte (province of Tarragona), and to the W in Beceite, Berge, Cañada de Verich, Foz-Calanda, La Ginebrosa, Peñarroya de Tastavins, Picoso y Valderrobres (province of Teruell).

The Nevera de Fuentespalda deposits can be considered as a representative model of this whole area. The Nevera de Fuentespalda Massif, 2 km to the East of the village of Fuentespalda is composed of Jurassic and Cretaceous rocks with

an anticline structure, surrounded by Tertiary continental materials. These outcrops were previously studied by Combes (1969) and Molina and Salas (1990).

The bauxites, clayey bauxites and bauxitic clays fill lenticular-shaped caves and passage caves that are parallel to the bedding planes. The original cave shapes are modified by abundant collapse breccias, with very characteristic radial fibrous calcite cements. The calcite crystals attain the length of 5 cm forming radial half-spherical, spherical, reniform and rosette-like aggregates. Locally the clasts of these breccias have ferruginous crusts made up of goethite and hematite.

Generally, the bauxite is homogeneous-massive but occurs locally with a heterogeneous-chaotic lithostructure (Bárdossy 1982). In this case blocks of pisoidic bauxite are sharply separated and embedded in softer and more clayey pelitomorphic bauxite. It is a secondary structure generated by subsequent karstification in the bedrock. The mineral composition (gibbsite, kaolinite, hematite, goethite, boehmite diaspore and anatase) was studied by Combes (1969) and Bárdossy (1982, p. 225).

The country rocks are limestones and marly limestones of Upper Oxfordian-Kimmeridgian age (Polpis Fm.; Salas 1987) and locally the uppermost part of the latova Fm. (Mb. Serra de la Creu; Salas 1987) of Middle Oxfordian age. More specifically the Polpis Fm. on the Nevera de Fuentespalda comprises three members: a) the lower member (up to 7 m) is a cyclic alternation of marly limestones and marls; b) the middle member (up to 39 m) consists of limestones with local thickening upward cycles; and c) upper member (up to 16 m) with a very karstified top comprising marly limestones with a local incipient nodular structure and some interbedded dolostone levels. The caves filled with bauxites are located in the lower member or more frequently in the contact between the middle member and lower member. Locally in the bedrock contact there are crystals flowers of gypsum and the country rocks are dolomitized. The paleokarst is buried by the Utrillas sands Fm. (Upper Albian-Cenomanian) and dolomitized limestones of Cenomanian age.

As regards the origin of the bauxite, we agree with the hypothesis of lateritic weathering products as the parent materials. The presence of laterites¹ and their remnants of erosion in paleosoils near these karst bauxite deposits, with very similar textures to the bauxitic clays in the Fuentespalda outcrops, lend support to this idea. About 4 km along to the SE, in the Ports de Beseit area, there are freshwater limestones and lateritic clays (Cantaperdius Fm. of Barremian age; Salas 1987). These materials were deposited in lacustrine environments with periodical subaerial exposures favourable to pedogenetic processes in a tropical climate. The lateritic clays locally contain boehmite (until 7.4% according to Combes 1969) and a mean composition in Al₂O₃ of 34.89% (I.G.M.E. 1974). The comparison between the chemical and mineralogical analysis of these clays and the bauxites shows

1 We use the terms laterite and lateritisation in the sense of Bárdossy (1982, p. 14).

than the change between both needs only a partial desilification and decalcification of the clays.

So the analyzed deposits would be parautochthonous and produced by the washing together, over short distances, of weathering products into local paleodolines and caves of a karstic relief. A longer transport would admit the presence of contaminants (sand, gravel,...) which are not present in the bauxite. The time of transport and fossilization of the karstic paleorelief would be Aptian-Lower Albian given the ages of the parent materials (Cantaperdius Fm.) and the cover materials (Utrillas Fm.).

The other deposits in this bauxitic region are very similar to the Fuentespalda. They are in paleodolines or paleokarstic caves in or in the immediate area below the contact between the Jurassic and Cretaceous materials. The main difference corresponding to the age of the country rocks that in some places (e.g. Horta de Sant Joan) they are limestones and dolostones of Middle Jurassic age (Xelva Fm.).

Karst bauxites in the Catalán Coastal Range

The bauxitic deposits in the Catalán Coastal Range are located in the provinces of Tarragona and Barcelona. There are bauxites in the municipalities of Aiguamurcia, Beliprat, Bisbal del Penedés, Castellví de la Marca, Font-rubi, La Llacuna (Rofes), Montmell (Marmellar), Mediona (Orpinell, Sant Antoni dels Vilats), Santa Maria de Miralles, La Torre de Claramunt, Sant Quintí de Mediona and Santa perpetua de Gaia.

The structure of the Catalán Coastal Range is dominated by longitudinal near-vertical basement faults which trend from NE-SW to ENE-WSW and form a right-stepping, "en echelon" array according to Guimera (1984, 1988).

The bauxite appears on two possible lithostratigraphic units: Lower Muschelkalk (Anisian) or Upper Muschelkalk (Ladinian) limestones and dolomites. More locally in the Montmell area (Roca Vidal) occurs on Upper Jurassic dolostones and limestones. These Triassic carbonates were deposited in shallow ramp environments on a low relief shelf and homoclinal-ramp barrier, locally with buildups (Calvet et al. 1990). It is interesting to notice that in the Lower Muschelkalk unit there are well-developed triassic paleokarsts associated with Pb-Zn-Ba mineralizations (Andreu et al. 1987). The main paleokarst level has a morphology of horizontal cavities from a few centimeters to more than 3 m in height and from a few meters to more than 100 m in length. The cavities are filled by clays and silts, red to brown in colour, with centimetric angular blocks from cave-roof collapse. The surface morphology is smooth to angular. These cavities are interpreted as caves developed in the meteoric phreatic environment.

The Triassic rocks in the Catalan Range have been divided into three tectonosedimentary domains on the basis of regional variations in thickness, facies and stratigraphy (Marzo 1980, Marzo and Calvet 1985, Salvany and Orti 1987; Calvet et al. 1990). The domains for the Muschelkalk are the Gaia-Montseny in the NE, Prades in the central part, and Baix Ebre-Priorat in the SW. The bauxites

appear in the first and third domains and near the boundary with the Linking Zone (Horta de Sant Joan-Pauls area).

The bauxites mainly with conglomeratic and brecciated, and locally also ooidic textures occur filling paleodolines and karstic caves, that can be of large dimensions, for instance in Aiguamurcia, 30 m high and 80 m horizontally. These paleodolines have an important fault control with clear karstified fault surfaces such as the walls of sinkholes. The most important karstification episode of the Triassic materials was before the deposition of the bauxites but later karstification has produced disorganization and brecciation in the bauxitic materials. There also indications of reworking as conglomeratic bauxites and red or white clays with blocks or pebbles of bauxite.

Where it is possible to see the cover rock in Santa María de Mirailles area, for instance, the bauxites are fossilized by the Palaeogene of the eastern Ebro Basin. In its lower part the Palaeogene section is composed by the following units from bottom to top (for instance, Ferrer 1971, Anadon 1978): 1) Mediona Fm. made up predominantly of red clays with abundant carbonated paleosoil levels of continental origin. In this area is inclosed the biostratigraphic unit named "*Bulimus level*" with *Vidaliella gerundensis*. The age of this formation is Upper Thanetian. 2) Orpí Fm. that consist of limestones and dolostones deposited in shallow platform environments, with abundant benthonic foraminifera (*Alveolinids*, *Miliolids*). The age of this formation is Lower-Middle Ilerdian.

It is difficult to establish the ages of the bauxitization and the accumulation because of the great Triassic-Paleocene gap that generally appears, but in close areas to the S and SW of the Mediona-La Llacuna Zone (for instance in Salou, Tarragona, Salomé, Santa Cristina and Garraf) there are Barremian lateritic clays (Cantaperdius Fm., Salas 1987) on dolostones, limestones and marly limestones of Kimmeridgian to Valanginian age, changing the gap between the Kimmeridgian-Barremian in Salou, to the W, and the Valanginian-Barremian in the Garraf Massif, to the E (Salas 1987, Fig. 3). As in the Linking Zone we can consider that these bauxites can be related to these lateritic horizons. Another possibility could be that the parent rocks would be marly and clayey deposits abundant during the Barremian (marls and limestones of Les Artoles Fm.), Lower Aptian (limestones and marls of Xert Fm.), Upper Aptian (marls of Forcall Fm.) or Middle Albian (clays and limestones of Montmell Fm.) all appearing in the S and W of the bauxite outcrops.

In any case the bauxites were originated in the SE versant of the Ebro Massif on the seaside, by the weathering of clayey or marly sediments that are the same age as in the marine section deposited in the close southern sea. Only the continental emerged areas during a sufficiently long time developed bauxites (Aiguamurcia-La Llacuna-Mediona area). On the contrary the nearest sea areas that, after the Hauterivian emergence, were early covered by new marine-coastal-lacustrine sediments not were able to exceed the condition of lateritic clay or more or less weathered marl. Still in the Upper Cretaceous and

the Palaeocene could have reworking of the bauxitic materials shaping the actual lie of the bauxites.

Karst bauxites in the Pyrenean System

The bauxites in the Spanish Pyrenees (province of Lérida) are located in allochthonous thrust sheets in two different areas: 1) Sierras Marginales. The bauxite deposits appear in the municipalities of Alos de Balaguer, Artesa de Segre (Baldomar), Camarasa (Sant Llorenç de Montgai), La Foradada (Rubió d'Agramunt) and Les Avellanes i Santa Linya. 2) Peramola mountains and Intermediate Subunits between the Montsec-Pedraforca and Port del Compte Units. The bauxites are located in the municipalities of Baronia de Rialb (Pallerols), Figols i Alinyà (L'Alzina, Llobera, Les Sorts, Vall de Mig), Josa i Tuixen, La Coma i La Pedra, La Vansa i Fornols (Fornols del Cadi, Montagull, Ossera, Padrinàs, Sant Pere), Peramola and Prat del Compte.

The Sierras Marginales belong to the frontal part of the South Central Pyrenees. They are composed of an imbricate fan thrust system, generally with a little internal deformation by folding. They are bounded to the North and the South by two main thrusts: the Montsec thrust and the floor thrust of the Sierras Marginales over the southern continental Tertiary units. The balanced cross sections shows a shortening of about 11 km between the Montsec thrust and the floor thrust of the Sierras Marginales (Pocovi 1978, Martínez Peña and Pocovi 1988).

In the Sierras Marginales the bauxites are located on Liassic limestones, on grey dolostones of Middle Jurassic age or on white limestones with Kimmeridgian-Lower Tithonian microfossils, and they are covered by alluvial, fluvial and lacustrine clays, marly limestones and sandstones of Upper Santonian age (Souquet 1967) dated by pollen in samples of the Els Combs mines (Saint Mamet). In the Sierra de Boada outcrops (Fuente Foradella, to the South of Alos de Balaguer) it is possible to be more precise in the dating because below the bauxites there are, on Lower Jurassic dolostones, some metres of grey or black clays with lignite, pyrite and gypsum of Bedoulian (Lower Aptian) age (Combes 1969; p. 284).

The Sierras Marginales present a very important stratigraphic gap, with a Jurassic section progressively older to the S by erosion, and a Cretaceous section more and more recent also to the S, the bauxites appear intercalated between these two sections. The Malm exists in the Saint Mamet, Montroig and Sant Jordi Sierras, but was eroded in another more southern (Boada, Os de Balaguer) where the bauxites rest directly on the Dogger black dolostones or even on the Liassic limestones. This arrangement was the result of emergence and erosion of the Jurassic materials during the Neocomian, before the bauxite genesis and deposition.

The Peramola Sierras and Intermediate Subunits in the sense of Caus et al. (1988) are stacked between the Montsec Unit-Pedraforca Zone and the Port del Compte Unit, in the fracture zone of the Segre (Sole-Sugrañes 1978) or Cataluña fault

(Souquet et al. 1977; Sole-Sugrañes and Souquet 1980). This Intermediate Subunits in the contact zone between the allochthonous Montsec Unit and the relative autochthonous of the Port del Compte Unit are equivalent to the Alinyà-Tuixent-La Coma sheets (Ullastre et al. 1987; Ullastre and Masriera 1989).

In the Peramola Sierras and Intermediate Subunits the bauxites are disposed in karstic caves on grey dolostones and white limestones of Middle-Upper Jurassic age and they are covered by Upper Cenomanian limestones with *Prealveolina* (Santa Fé Fm., Mey et al. 1968) and Campanian bioclastic limestones (Bona Fm.; Mey et al. 1968). Locally in the base of the Upper Cretaceous materials also appear sandstone and conglomeratic levels (Adraén Fm.?, Mey et al. 1968).

The bauxites in the Spanish Pyrenees appear in well developed karstic sinkholes and hollows, up to 25 m depth in Les Combs (Saint Mamet), with an important fault control. The bauxites and bauxitic clays have locally intercalations of siliciclastic sandstone and gravels.

The bauxites are red or violaceous with conglomeratic, arenitic or pelitomorphic textures. In some places they present bauxite pebbles rich in iron minerals (hematite or hematite plus goethite). They could be ferricrete crusts ("cuirasses") of eroded lateritic profiles. Their hardness and toughness makes for a preferential iron-enrichment in the course of transport. One of the arguments in their favour is that collomorphic textures of these pebbles much resemble the textures of known lateritic ferricretes. We have seen also good examples of postbauxitic karstification of tectonically inclined limestone beds with venical cracks filled in bauxite on normal fault walls. Also the bauxite appears as fault breccia and there are also striated and highly polished slickensides in the bauxite. Probably according to Petrascheck (1989) these bauxites originally have not been deposited on a "karst senile" but on a "karst embryonal" controlled by faults and fractures.

It is difficult to establish the ages of the episodes of bauxitization and accumulation because the important stratigraphic gap without age dating between the underlying and overlying beds of the bauxites. The bauxitogenic interval would comprise between the Lower Aptian and the Upper Cenomanian according to the shorter hiatus mentioned before and deduced by biostratigraphic data. Nevertheless we are not obliged to consider that in all this long gap the bauxites were in elaboration process, and it is difficult in this case to specify the value of the "infrabauxitic" and "suprabauxitic" gaps. So, we can have non deposition or erosion of the underlying beds, without favorable conditions for the accumulation of the bauxites. Also the overlying protecting beds could not have been deposited immediately after the accumulation of the mineral. But according with Combes (1969) we could admit the genesis of the bauxites during the Upper Aptian-Albian. Even we cannot exclude that the bauxitization would have been continued a longer time after. Combes (1990) considers these bauxites as Languedoc-Provence type with boehmite-gibbsite and boehmite, allochthonous or parallochthonous with non-dominant weathering in situ after the deposition.

Other bauxitic deposits

The Portilla de Luna bauxite deposit is located in the Cantabrian Zone of the Iberian Hercynian Massif. It consists of nests and veins 10 to 20 cm size of white gibbsite and halloysite at and near the contact between Middle Devonian (Eifelian) reef limestones of the Santa Lucia Fm. with the clay shales of contiguous geological formations, more exactly the Upper Member of the La Vid Fm. (Lower Devonian, Emsian) and lower part of the Huergas Fm (Upper Eifelian).

The bauxite Al_2O_3 content varies between 44 to 49 % and it is almost devoid of titanium. The Portilla de Luna deposit was described as a Devonian bauxite by Font-Altaba and Closas (1960) and so it remained a long time as the oldest bauxite in the world (Patterson et al., 1986). After, the analysis of Bárdossy and Fontbote (1970) revealed that the karstification took place clearly after the hercynian orogeny. This deposit was considered by these authors to be the same as at Tulska the product of a secondary bauxitization which took place in the Pliocene and possibly in the Quaternary rather than in the Devonian, so for these authors this deposit is just a rudimentary form of the Tulska deposit.

More recently, according to morphologic and mineralogical arguments Blanco et al. (1987) the bauxites are attributed to Pre-Albian weathering of the hercynian rocks. On affecting silicate rocks the Pre-Albian weathering of clayey materials generally resulted in kaolinization more or less advanced. However in some places on and near the Santa Lucia limestones was possible the genesis of bauxites as result of this weathering.

The small bauxitic deposit near Haro (region of Rioja) is interbedded with siliceous sandstones of Albian age that lay immediately under a calcareous level which occasionally contains thin lignite beds (Sebastian Pardo et al. 1985). The bauxite has a complicated mineralogical composition: anatase, goethite, hematite, pyrite, jarosite, alunite, gibbsite, nordstrandite, halloysite, quartz, feldspar and mica. Here the first occurrence of Nordstrandite in the Iberian Peninsula was described (Sebastian Pardo et al. 1985). The alumina content in the analyzed samples for these authors vary between 8.74 and 54.28%. According to the same authors it is an autochthonous deposit from magmatic or metamorphic parent material (granites, gneisses, quartzites,...)

Summary and conclusions

The karstic bauxite orebodies in Spain are located in four bauxite regions:

- 1) the Subbetic Zone in the Betic Cordillera;
- 2) the Linking Zone between the Catalan Coastal Range and the Iberian Range;
- 3) the Catalan Coastal Range; and
- 4) the Pyrenean System (Southern External and Sub-Pyrenean Ranges). These karstic bauxites belong to the Mediterranean bauxite belt (Combes 1969; Bárdossy 1982; Vera et al. 1986–87).

The main characteristics of these four bauxite regions can be established according to the period of bauxite genesis and accumulation, the age of underlying and overlying beds, the facies of immediate bedrock and cover, bedrock karstification, lithology of bauxites and related sediments, and the structural position. The ages of the underlying beds vary from the Triassic (Muschelkalk facies) in the Catalan Range to the Aptian in the Pyrenees; the ages of the overlying beds from the Oxfordian (Subbetic Zone) to the Paleocene (Catalan Range); and the probable episodes of bauxitization and accumulation from the Middle Jurassic (Subbetic Zone) to the Paleocene (Catalan Range). The bedrocks are shallow marine limestones or epigenetic dolostones that are covered by lacustrine limestones and continental marls and sandstones; locally (Subbetic Zone) the paleokarst is fossilized by shallow pelagic limestones (Ammonitico Rosso Fm.). The karstification is generally strong, the bauxites appearing mainly in karstic caves in the Subbetic and the Linking Zones, and in paleodolines, with an important fault control in the Pyrenees and Catalan Range. Three main bauxitogenic times may be distinguished:

1) Middle Jurassic; 2) Barremian-Aptian, the most important; and 3) Paleocene.

All the bauxites, except for those located in the Catalan Range, are found in allochthonous thrust sheets, with a complex structure, which makes close paleogeographic reconstructions difficult to establish.

Several major problems concerning these bauxites remain unsolved: 1) Autochthony or allochthony degree of these deposits, and which were the parent rocks in the last case, which the source area and which the model of transport and sedimentation. It would be important to study the geochemistry of these bauxites in relation to the paleogeography, particularly the primary distribution and secondary migration of the trace elements. 2) Controls on paleokarst development and relief in the subaerial exposure phases, and differentiation of superimposed bauxitogenic and non-bauxitogenic karstification episodes. 3) Correlation between "bauxitic" and "non-bauxitic" karstification episodes, changes in sea level and local tectonics. It is important to carry out precise paleogeographic reconstructions in these allochthonous terranes with complex tectonic. It could also be interesting to find the possible relationship of "bauxitic" subaerial exposure phases with time intervals, when the amount of atmospheric dust is increased, especially by volcanic events.

References

- Alias Perez, L.R., R. Ortiz Silla, M. Rodriguez Gallego 1972, Mineralogía de un yacimiento de bauxita situado al N. de Zarzadilla de Totana (prov. de Murcia). – *Estudios Geológicos*, 28, pp. 209–215.
- Almera, J. 1900: Mapa Geológico y topográfico de la provincia de Barcelona. Región tercera o del río Foix y la Llacuna. Escala 1:40.000. – Tip. Brossa. Barcelona.
- Anadon, P. 1978: Deslizamientos gravitacionales y depósitos asociados en el Eoceno marino del borde oriental de la Cuenca del Ebro (Sector de Igualada). – *Acta Geol. Hispán.*, XIII, pp. 47–53.

- Anadon, P. 1978: El Paleógeno continental anterior a la transgresión biarriztiense (Eoceno medio) entre los cursos de los ríos Gaiá y Ripoll (provincias de Tarragona y Barcelona). – PhD Thesis, Barcelona University. (Unpublished).
- Andreu, A., F. Calvet, X. Font, X. Viladevall 1987: Las mineralizaciones de Pb–Zn–Ba en el Muschelkalk inferior de los Catalánides. – Cuad. Geol. Ibérica, 11, pp. 779–795.
- Anonimo 1974: Investigación de minerales de bauxita. Fuentespalda (Teruel, Tarragona). Fase previa. – Inst. Geol. Min. España, Colección Info,me. p. 77
- Anonimo 1974: La importancia de las bauxitas españolas y su aplicación en la industria nacional. La industria minera y metalúrgica. – Act. Prof pp. 59–63. I.G.M.E.
- Bárdossy, G. 1982: Karst Bauxites. Bauxite Deposits on Carbonate Rocks. – Dev. in Econ. Geol., 14, Elsevier p. 441.
- Bárdossy, G. and J.M. Fontbote 1977: Observations on the age and origin of the reported bauxite at Portilla de Luna, Spain. – Econ. Geol., 72, pp. 1355–1358.
- Bataller, J.R. 1919: Las bauxitas de Cataluña. Rev. – R. Acad. Ciencias, Madrid, XVIII, pp. 422–470.
- Bataller, J.R. 1921: Nou jaciment de bauxita a Catalunya. – Bul. Inst. Catalana d'Hist. Nat., XXI, p. 152.
- Bataller, J.R. 1943: Las bauxitas del Pirineo de Lérida. – Mem. Real. Acad. Cienc. y Artes de Barcelona, terc. ep., n. 562, v. 27(2), pp. 1–55.
- Blanco, J.A., J.R. Corral Sanchez, S. Sanchez Macias 1989: La alteración prealbense y sus posibilidades mineras en el borde S. de la Cordillera Cantábrica (León y W. de Palencia). – XII Congreso Español de Sedimentología, Bilbao, Simposios, pp. 263–272.
- Boletín Oficial De Minas 1917: Minerales de bauxita en España. Ministerio de Industria y Fomento, Madrid. 5, p. 33.
- Boletín Oficial De Minas 1917: Naturaleza, origen y edad de la formación de la bauxita de la Sierra de la Llacuna (Barcelona). Ministerio de Industria y Fomento, Madrid. 16, pp. 55–58.
- Boletín Oficial De Minas 1917: Yacimientos de bauxita de Barcelona. Ministerio de Industria y Fomento, Madrid. 1, p. 58.
- Caballero, A., F. Menendez Del Valle, J.L. Martín–Vivaldi 1974: Yacimientos españoles de bauxitas y alunitas. – Bol. Geol y Min., LXXXV–1, pp. 32–42.
- Calafat, J. 1917: Sobre los nuevos yacimientos de bauxita españoles. – Bol. Real Soc. Española Hist. Nat., XVII, pp. 415–418.
- Calvet, F., M.E. Tucker, J.M. Henton, 1990: Middle Triassic carbonate ramp systems in the Catalán Basin, northeast Spain, facies, systems tracts, sequences and controls. – Spec. Publ. int. Ass. Sediment., 9, pp. 79–108.
- Cantos, J. 1950: Descubrimiento de una nueva zona bauxitífera en Cataluña. – Ibérica (2ª época), Barcelona, XII (197), pp. 361–363.
- Caus, E., D. Rodes, L. Sole–Sugrañes 1988: Bioestratigrafía y estructura del Cretácico superior de la Vall d'Alinyá (Pirineo oriental, prov. de Lleida). – Acta Geol. Hispánica, 23, pp. 107–118.
- Closas Miralles, J. 1942: Els nous jaciments de bauxita. – Bul. Inst. Cat. Hist. Nat., XXXVII 1937–1949, pp. 22–29.
- Closas Miralles, J. 1945: Criaderos de bauxita y su explotación. – "La Alquimia" C.A. Barcelona. p. 146.
- Closas Miralles, J. 1954: Las bauxitas del NE de España. – XIX Congr. Geol. Internat., Alger, sect. 12, 12, pp. 199–223.
- Closas Miralles, J. 1957: El concepto de "bolsada" en los yacimientos de bauxita. – Homenaje postumo al D. Francisco Padillo Vaquer. Universidad de Barcelona, Facultad de Ciencias, p. 10
- Combes, P.J. 1967: Contribution à l'étude de la genèse des bauxites, Paléo–géographie du Crétacé inférieur et bauxites dans le Maestrazgo nord–oriental (Espagne). – C. R. Acad. Sc. Paris, 264, pp. 703–706.
- Combes, P.J. 1969: Recherches sur la genèse des bauxites dans le Nord–Est de l'Espagne le Languedoc et l'Ariege (France). – Mem. Centre Etudes et Rech. Geol et Hydrogeol., III–IV, Montpellier, p. 342

- Combes, P.J. 1990: Typologie, cadre géodynamique et genèse des bauxites francaises. – *Geodinamica Acta*, 4, pp. 91–109.
- Combes, P.J., G. Glaçon, L. Grambast, 1966: Observations stratigraphiques et paléontologiques sur le Crétacé inférieur du Nord–Est du Maestrazgo (Espagne). *C. R. somm. Soc. Géol. France*, 10, pp. 390–391.
- Faura i Sans, M. 1917: Les bauxites de la Serra de La Llacuna. – *Bull. Inst. Cat. Hist. Nat.*, 17, p. 123.
- Faura i Sans, M. 1918: Naturalesa, origen i edat de formació de les bauxites de la Serra de la Llacuna. – *Bul. Inst. Catalana Hist. Nat.*, XVIII, pp. 49–55.
- Faura i Sans, M. J.R. Bataller, 1920: Les bauxites triasiques de la Catalogne. – *Bull. Soc. Geol. France*, ser. 4, 20, pp. 251–267.
- Ferrer, J. 1971: El Paleoceno y Eoceno del borde sur–oriental de la depresión del Ebro (Cataluña). – *Mém. Suisses de Paléont.*, 90, pp. 70
- Font Tullot, J.M. 1951: Análisis roetgenográficos de algunas bauxitas de la región NE de España. – *Estudios Geol.*, 13, pp. 113–130.
- Font–Altaba, M., M. Closas 1960: A bauxite deposit in the Paleozoic of Leon, Spain. – *Econ. Geol.*, 55, pp. 1285–1290.
- Font–Altaba, M., M.J. Closas 1960: Estudio de un yacimiento de bauxita en el Paleozoico de León. – *Estudios geol.* 16, pp. 157–161.
- Fontrodona, F. 1917: Comunicación oficial de la existencia de criaderos de bauxita en Cataluña. – *Rev. Minera, Madrid*, LXVIII, p. 264.
- Galan, E., F. Lopez Aguayo, S. Aza 1976: Bauxitic clays of NE Teruel (Spain). – *Seventh Conf Clay Mineralogy and Petrology, Karlovy Vary 1976*, pp. 487–497.
- García Siñeriz, J. 1950: Aprovechamiento industrial de las bauxitas de la zona subpirenaica para la producción de óxido de aluminio. – *Imp. Antonio J. Rovira, Artes Gráficas, Barcelona*, p. 21
- García–Hernandez, M., J.R. Mas, J.M. Molina, P.A. Ruiz–Ortiz, J.A. Vera, 1988: Episodio de karstificación en litorales insulares del Jurásico superior (Fm. Ammonitico Rosso, Subbetico Externo, provincia de Córdoba). – *III Coloquio de Estratigrafía y Paleogeografía del Jurásico de España, Logrono, Resúmenes*, pp. 32–35.
- Goetz, R. 1917: La existencia de bauxita en España. – *Rev. Minera, Madrid*, LXVIII, pp. 297–299.
- Goetz, R. 1920: La bauxita de Cataluña. – *Rev. Minera, Madrid*, LXXX, pp. 224–225 and 359–361.
- Guimera J. 1988: Estudi estructural de l'enllaç entre la Serralada Ibèrica i la Serralada Costanera Catalana. – *Ph. Thesis, Barcelona University*, p. 600.
- Guimera, J. 1984: Palaeogene evolution of deformation in the northeastern Iberian Peninsula. – *Geol Mag.*, 12, pp. 413–420.
- Hernandez Sampelayo, P. 1920: Algunas palabras más acerca de las bauxitas de Cataluña. – *Rev. Minera*, LXXI, p. 385.
- Hernandez Sampelayo, P. 1920: Condiciones geológicas de los yacimientos catalanes de bauxitas. – *Bol. Inst. Geol. Espana*, XLI, pp. 8–147.
- Hernandez Sampelayo, P. 1920: Geología y formación de los criaderos catalanes de bauxita. – *Rev. Minera, Madrid*, LXXI, pp. 193–198 and 209–211.
- Iberica 1917: Criaderos de bauxita en Cataluña. – *Rev. Ibérica, Tortosa*, VII (179), p. 355.
- Iberica 1918: Naturaleza, origen y edad de la formación de bauxitas de la Sierra de la Llacuna (Barcelona). – *Rev. Ibérica, Tortosa*, X(241), pp. 114–115.
- Instituto Geológico y Minero De España 1972: Mapa previsor de las mineralizaciones de aluminio. *Mapa Metalogenético de España. Escala 1, 1.500.000. I.G.M.E, Madrid.*
- Instituto Geológico y Minero De España 1974: Estudio previo para la investigación de bauxita en el subsector I, Cataluña, Area 3, La Llacuna (Barcelona y Tarragona). *Colección Informes, I.G.M.E., Madrid.*
- Instituto Geológico y Minero De España 1974: Investigación de minerales de bauxita. Fuentespalda, Teruel. Fase previa. *Colección Informes. Ministerio de Industria*, p. 77
- Instituto Geológico Y Minero De España 1974: Mapa metalogenético de España, E. 1, 200.000. Hojas n. 24 (Berga), n. 34 (Hospitalet), n. 41 (Tortosa) y n. 79 (Murcia). *I.G.M.E, Madrid.*

- Instituto Geológico y Minero De España 1974: Monografía de Rocas Industriales. Bauxita y Laterita. Colección Informes. I.G.M.E., Madrid.
- Jungwirth, J. 1951: Bauxit in Spanien und seine Stellung zu den Bauxiten des "Mittelmeeertypus". – *Montan-Zeitung*, 67(4), pp. 59–64.
- Kundelan, U. 1948: Fabricación de alúmina con materias primas españolas. – *Minería y Metalurgia*, 81, pp. 3–14.
- La Iglesia, A., S. Ordoñez 1989: Cristalinidad de las caolinitas en yacimientos de bauxitas cársticas del NE de España. – *Bol. Soc. Esp. Miner.*, 12, p. 27.
- La Iglesia, A., S. Ordoñez 1990: Cristalinidad de caolinitas en yacimientos de bauxitas cársticas del NE España. – *Bol. Soc. Esp. Miner.* 13, pp. 81–90.
- Lapparent, A.F. de 1950: Niveau stratigraphique des bauxites d'Espagne. – *C. R. Acad. Sc. Paris*, 230, pp. 83–984.
- Marín, A., Galvez Cañero, 1955: Plan de investigación de los yacimientos de bauxita de Peramola (Lérida). – *La Alquimia C.A.-Adaro (Metalogenia)*
- Martínez Peña, M.B., A. Pocovi 1988: El amortiguamiento frontal de la estructura de la cobertera surpirenaica y su relación con el anticlinal de Barbastro–Balaguer. – *Acta Geol. Hispánica*, 23, pp. 81–94.
- Marzo, M. 1980: El Buntsandstein de los Catalánides, Estratigrafía y procesos de sedimentación. – PhD Thesis, Barcelona University, p. 317.
- Marzo, M., F. Calvet 1985: Guía de la excursión al Triásico de los Catalánides. – II. Coloquio de Estratigrafía y Paleogeografía del Pérmico y Triásico de España. La Seo d'Urgell. p. 175.
- Mata-Perello, J.M., J. Montoriol-Pous 1975: Nota referente a la bibliografía sobre los óxidos de Cataluña. – *Acta Geol. Hispán.*, X(3), pp. 89–100.
- Mey, P.H.W., P.J.C., Nagtegaal, K.J. Roberti, J.J.A. Hartvelt, 1968: Lithostratigraphic subdivision of post-hercynian deposits in the south-central Pyrénées, Spain. – *Leidse Geologische Mededelingen*, 41, pp. 22–228.
- Molina, J.M., R. Salas 1990: Mesozoic karstic bauxites in Fontdespala (province of Teruel, Spain), Origin and paleogeography. – Abstracts, IGCP-287 Working Meeting No. 2, Delphi, Greece, pp. 29–30.
- Molina, J.M., J.A. Ruiz-Ortiz, J.A. Vera, (in print, this volume), Jurassic karst bauxites in the Subbetic. Betic Cordillera, Southern Spain.
- Molina, J.M., P.A. Ruiz-Ortiz 1990: Diagnostic features of discontinuities in Mesozoic sedimentary outcrops of the Betic Cordillera (Southern Spain). – 13th International Sedimentological Congress, Nottingham, Abstracts, p. 157.
- Molina, J.M., P.A. Ruiz-Ortiz, J.A. Vera, 1989: Jurassic karstic bauxites in the Subbetic of Southern Spain. – 10th I.A.S. Regional Meet. on Sedim., Budapest, Abstracts, pp. 164–165.
- Molina, J.M., Salas, R., A. Martín-Algarra, J.M. Mata, P.A. Ruiz-Ortiz, J.A. Vera, M. Viladevall 1990: A review of karstic bauxites and related paleokarsts in Spain. – Abstracts, IGCP-287 Working Meeting No. 2, Delphi, Greece, pp. 17–18.
- Molina-Díaz, A., J.M. Molina, P.A. Ruiz-Ortiz, J.A. Vera 1986–1987: Técnica de análisis rápido de Al_2O_3 y Fe_2O_3 en rocas bauxíticas. – *Acta Geol. Hispán.*, 21–22, pp. 593–597.
- Motta, F., E. Roch 1962: Bauxites d'Espagne: observations et interpretations. – *Acta Geologica Hungarica*, VII (2–4), pp. 285–291.
- Ordoñez, S. 1977: Las bauxitas españolas como mena del aluminio. – *Serie Universitaria* 33, Fundación Juan March. p. 64
- Ortiz Silla, R. 1971: Estudio geológico de un sector al N de Zarzadilla de Totana. *Mineralogía y génesis de bauxitas*. – Tesis de Licenciatura, Univ. de Granada. p.192.
- Patterson, S.H., H.F. Kurtz, J.C. Olson, C.L. Neeley 1986: Geology and resources of aluminium. – U. S Geological Survey Professional Paper 1076–D, p. 151
- Petrasccheck, W.E. 1989: The genesis of allochthonous karst-type bauxite deposits of southern Europe. – *Mineral. Deposita*, 24, pp. 77–81.
- Pocovi, A. 1978: Estudio geológico de las Sierras Marginales Catalanas (Prepireneo de Lérida). – PhD Thesis, Barcelona University, p. 218.

- Rios, J.M., A. Almela 1950: Una nueva zona de bauxitas en la provincia de Lérida. – II. Congr. de Ingeniería, I. G. M. E
- Rios, J.M., A. Almela, 1950: Descubrimiento de una nueva zona bauxitífera en Cataluña. – Notas y Com. Inst. Geol Min. España, 20, pp. 179–186.
- Salas, R. 1987: El Malm i el Cretaci inferior entre el Massis de Garraf i la Serra d'Espadà. Anàlisi de conca. – PhD Thesis, Barcelona University, p. 345
- Salvany, J.M., F. Orti, 1987: El Keuper de los Catalánides. – Cuad. Geol. Ibérica, 11, pp. 215–236.
- San Miguel De La Camara, NM 1950: Estudio geológico de los criaderos de bauxita del NE de España. – Imp. Antonio J. Rovira, Ates gráf, Barcelona. p. 35
- San Miguel De La Camara, M. 1954: Geología de las bauxitas españoilas. – R. Soc. Esp. Hist. Nat., t. Extraord. Hom. E Hernández Pacheco, pp. 579–607.
- Sanz, J. 1952: Las bauxitas catalanas. – Rev. Ibérica (2^a época), XVI 273), pp. 41–42.
- Sebastian Pardo, E.M., J. Rodríguez–Gordillo, M. Rodríguez–Gallego, J.D. Martín–Ramos, 1985: Nordstrandita, Al(OH)₃, en las bauxitas de Haro (La Rioja). – Bol. Soc. Española de Mineralogía, 1985, pp. 83–89.
- Sebastian Pardo, E.M., J.D. Martín–Ramos, J.F. Rodríguez–Gordillo, M. Rodríguez–Gallego, E. Perez–Lorente, F. 1985: Mineralogy and geochemistry of bauxites from Haro (La Rioja, Spain). – Abstracts, pp. 301–307.
- Sole–Sugrañes, L. 1978: Gravity and compressive nappes in the Central Southern Pyrenees (Spain). – American Jr. of Sci., 278, pp. 609–637.
- Sole–Sugrañes, L. P. Souquet, 1980: La chaîne alpine des Pyrénées. – Bull. Centr. Rech. Explor. Prod. Elf–Aquitanie. Mem. 3, pp. 157–196.
- Souquet, P. 1967: Le Crétacé sud Pyrénéen en Catalogne, Aragon et Navarre. – PhD Thesis, Toulouse University, p. 514.
- Souquet, P., B. Peybernes, M. Billotte E.J. Debroas 1977: La chaîne alpine des Pyrénées. – Geologie Alpine, 53, pp. 193–216.
- Ullastre, J. A. Masriera 1989: Discusión de algunas apreciaciones estratigráficas relativas al "Cretácico superior de la Vall d'Alinyà" (Pirineo orientai, Lérida). – Acta Geol. Hispánica, 24, pp. 55–58
- Ullastre, J., M. Durand–Delga, A. Masriera 1987: Argumentos para establecer la estructura del sector del pico del Pedraforca a partir del análisis comparativo del Cretácico de este macizo con el de la región de Sallent (Pirineo catalán). – Bol. Geol. y Min. España, 98, pp. 3–22.
- Vera, J.A. 1988: Evolución de los sistemas de depósito en el Margen Ibérico de la Cordillera Bética. – Rev. Soc. Geol. España, 1, pp. 373–391.
- Vera, J.A., J.M. Molina, P.A. Ruiz–Ortiz, 1990: Paleokarsts and bauxites in the Subbetic Zone, Betic Cordillera (Spain). – Abstracts, IGCP–287 Working Meeting No. 2, Delphi, Greece, pp. 23–24.
- Vera, J.A., J.M. Molina, A. Molina–Diaz, P.A. Ruiz–Ortiz 1986–1987: Bauxitas kársticas jurásicas en la Zona Subbética (Zarzadilla de Tótana, prov. Murcia, sureste de España), Interpretación paleogeográfica. – Acta Geol. Hispán., 21–22, pp. 351–360.
- Vera, J.A., P.A. Ruiz–Ortiz, M. Garcia–Hernandez, J.M. Molina 1988: Paleokarst and related sediments in the Jurassic of the Subbetic Zone, Southern Spain. – In: Paleokarst. N.P. James and P.W. Choquette (eds). Springer–Verlag. New York. pp. 364–384.

Les principaux types de gisement et modèles génétiques des bauxites karstiques en France et en Sardaigne

Pierre-Jean Combes

*Université de Montpellier II,
Sciences et Techniques du Languedoc
Géologie des Gîtes minéraux*

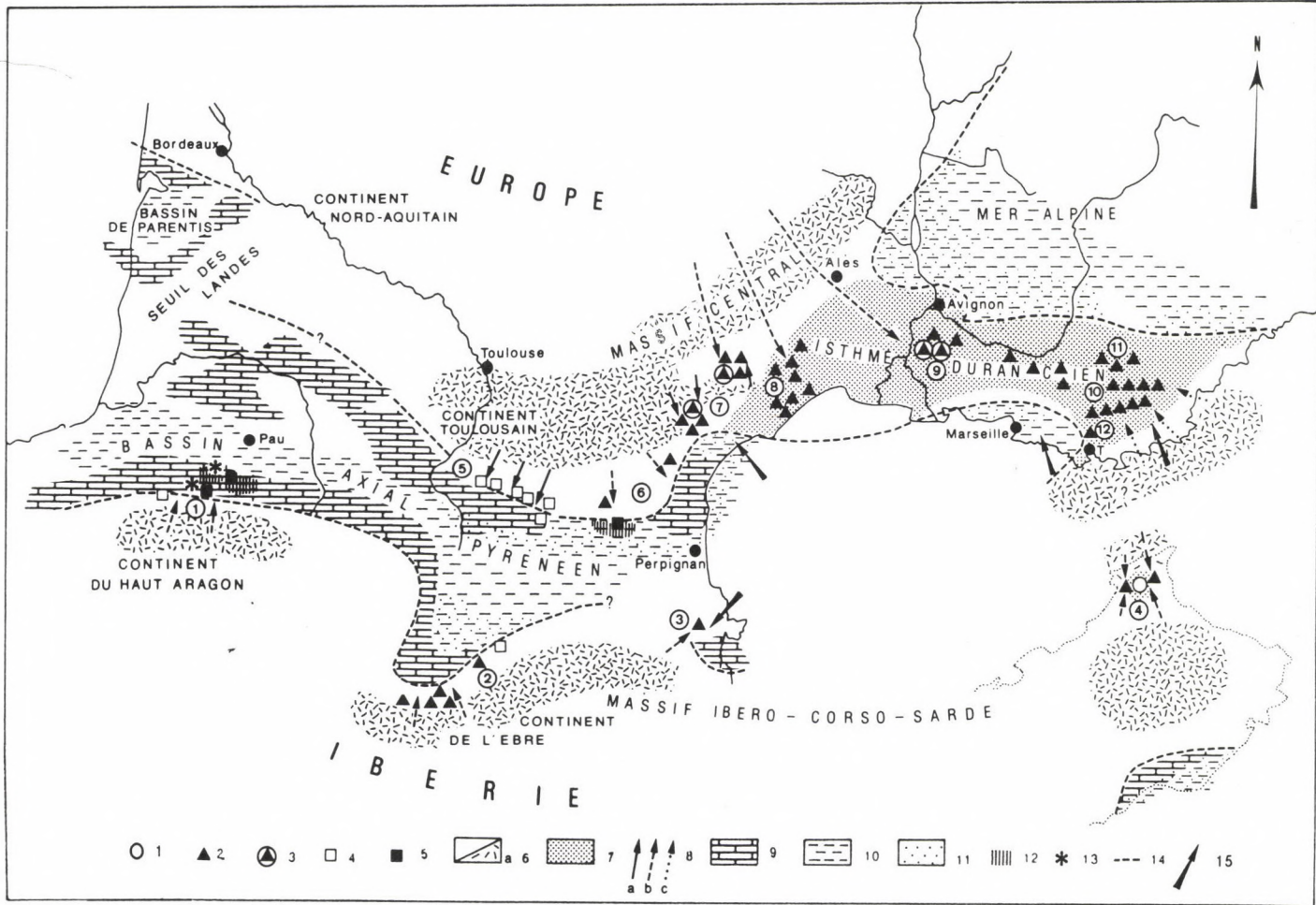
The high-level bauxites of the European and Iberian cratons appear in a relatively long stratigraphic gap during the Early Cretaceous times. As to low-level bauxites on the margins of the Pyrenean axial basin, the stratigraphic gap decreases: these bauxites are incorporated in the Urgonian carbonate platforms. In this stratigraphic and paleogeographic frame, type and origin of deposits reflect the degree of stability which is controlled by tectonic movements and eustatic fluctuations. On the cratons (Sardaigne and Languedoc-Provence types), the bauxites derived generally from the aluminous levels of the post-Hercynian sedimentary cover, which is considered as a mother rock. The types of genesis are controlled by the uplift rate: weak – autochthony with in situ weathering of marls; moderate – parallochthony with vertical and lateral accumulation of marl or argillaceous material on the carbonate substratum during the ferrallitization; significant – residual profiles were eroded and clastic elements deposited in the continental depressions with (relative autochthony or parautochthony) or without (allochthony) extension of the alteration. On the margins (Ariège and Pyrénées occidentales types) the aluminous sediments escaped from the topographical and geochemical traps of the cratons, accumulated and their ferrallitization continued with an eustatic and tectonic control. A synthetic sedimentary model is presented showing all types of deposits with their characteristics from the cratonic high-level (good drainage, oxidant conditions, gibbsite and/or boehmite paragenesis) to the low-level (less oxidant or reducing, with a ground-water close to the land surface, boehmite and/or diasopre paragenesis). In the basins glauconitic marls indicate terrigenous influx from the ferrallitizing areas. The marls in the basins, the Urganian platform carbonates and low-level bauxites correspond to genetic depositional units i.e. systems tracts (*sensu* Vail) caused by eustatic sea level changes.

Key words: Bauxite, uplift rate, tectonic and eustatic control, ferrallitization

Introduction

Dans le Sud de la France et en Sardaigne se rencontrent presque tous les types de gisement des bauxites karstiques ainsi que les principaux modèles pouvant être retenus pour expliquer leur genèse (Fig. 1). La reconstitution d'un paysage synthétique dynamique montre que ces types et modèles génétiques peuvent coexister: leur enchaînement entre l'amont de haut niveau, intracratonique, et l'aval de bas niveau, dans les zones littorales sur les marges stables européenne et ibérique, dépend de la tectonique (valeur du taux de soulèvement) et des fluctuations eustatiques. Le climat ferrallitisant, dans la période examinée, au

Address: Pierre-Jean Combes: Place Eugène Bataillon, 34095 Montpellier Cedex 5, France
Received: 12 September, 1991



Crétacé moyen, est considéré comme stable mais c'est actuellement une simplification, car on n'est pas en mesure de mettre en évidence les variations climatiques qui pourraient éventuellement interférer avec les deux facteurs précédents. Cette approche géodynamique des bauxites karstiques a été présentée dans une étude récente (Combes 1990) dont nous voudrions développer, dans le cadre la 2ème réunion de l'IGCP 287, quelques points essentiels.

I. Principaux types de gisements et modèles génétiques

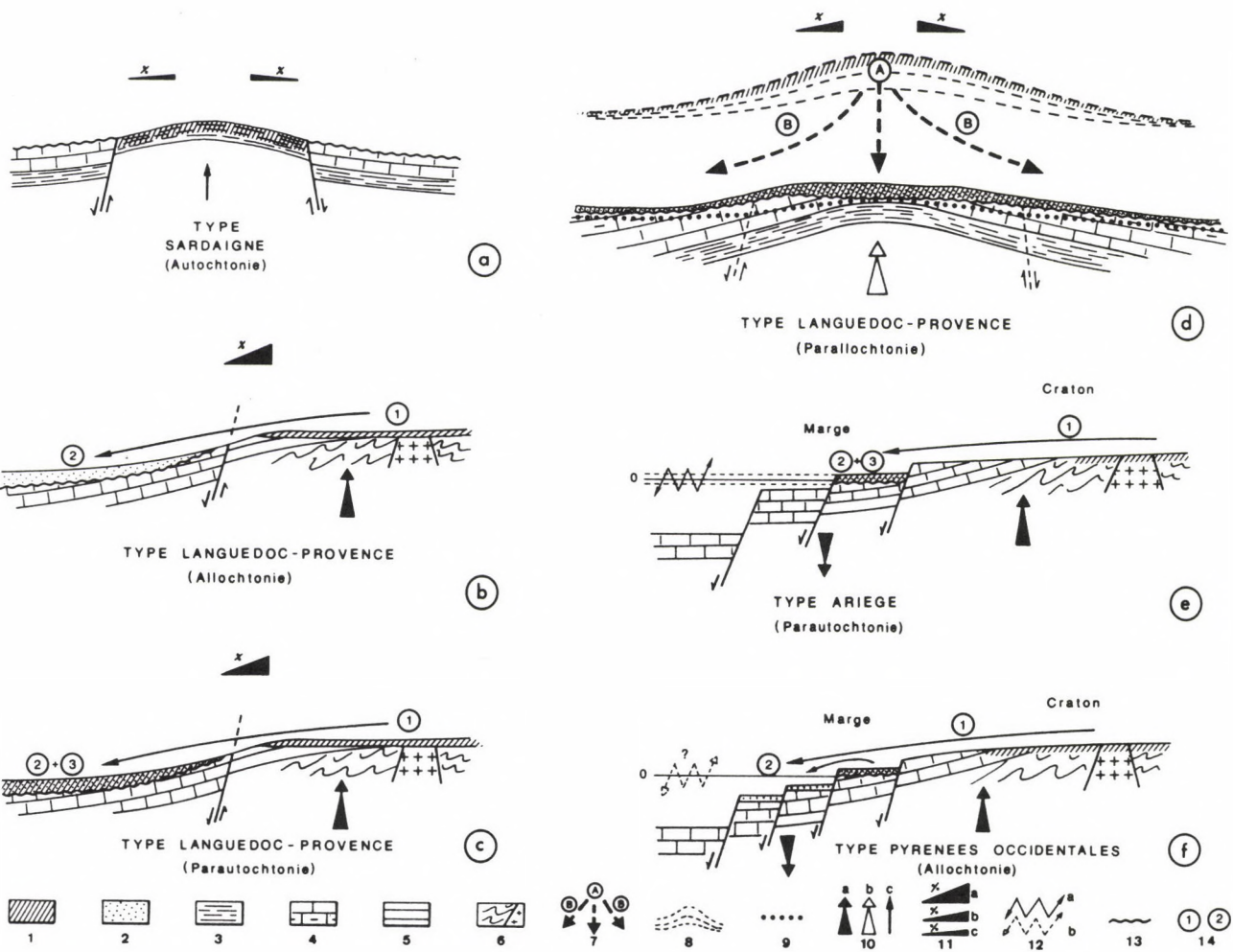
Les gisements peuvent être divisés en 4 types: Sardaigne, Languedoc-Provence, Ariège, Pyrénées occidentales. 4 modèles génétiques sont retenus: autochtonie, parautochtonie (on autochtonie relative), parallochtonie, allochtonie (Fig. 2).

A. - Le type Sardaigne

Développement de l'autochtonie en domaine cratonique (Fig. 2a). Situées sur le craton ibérique (massif ibéro-corso-sarde), les bauxites de Sardaigne (Nurra) ont été étudiées principalement par Pecorini (1956, 1965), Cocco et Pecorini (1959) et plus récemment, à partir de 1979, à l'occasion d'une campagne de prospection qui a permis de découvrir d'importantes réserves (Ceccarini et al. 1984, Sanna et Temussi, 1986; Oggiano et al. 1987). Plusieurs gisements sont détaillés démontrant clairement les conditions de formation. L'un d'entre eux est remarquable et mérite d'être distingué comme "Type Sardaigne" car c'est, jusqu'à maintenant, le cas le plus démonstratif que l'on puisse observer d'altération sur place (autochtonie) de marnes en bauxite. Ce type n'est actuellement pas connu dans les autres régions étudiées.

Fig. 1 ←

Répartition des principaux types de gisements sur les cratons et les marges européenne et ibérique au Crétacé moyen (Paléogéographie, d'après Arnaud-Vanneau et al. 1979). Les gisements et zones paléogéographiques sont indiqués dans leur position actuelle (seule une partie de la Sardaigne est placée en situation anté-dérivée). 1. Bauxite de type Sardaigne à boehmite, autochtone; 2. Bauxite de type Languedoc-Provence à boehmite-gibbsite et boehmite, allochtone ou parallochtone avec poursuite de l'altération sur place non dominante; 3. Même type avec altération sur place importante (parautochtonie); 4. Bauxite de type Ariège, à boehmite-diaspore, parautochtone; 5. Bauxite de type Pyrénées occidentales, à diaspore-chlorite, à dominante allochtone; 6. Domaine continental: a) socle paléozoïque susceptible d'affleurer et d'être ferrallitisé; 7. Domaine continentalisé où les marnes mésozoïques (principalement du Crétacé inférieur) ont pu, après émergence, constituer la roche mère; 8. Apports à partir de l'arrière-pays, (a) démontrés (Bédarieux, St Chinian, Ariège), (b) probables, (c) possibles; 9. Plate-forme carbonatée urgonienne à l'Aptien-Albien; 10. Marnes et marnes gréseuses de bassin à l'Aptien-Albien; 11. Glauconie; 12. Chlorite en croûtes réseau ou disséminée; 13. Bauxite affectée par le métamorphisme pyrénéen; 14. Limite approximative des zones émergées; 15. Secteurs à déplacement tangentiel important à l'Eocène supérieur. Les chiffres indiquent les principaux districts et gisements cités dans le texte: Pyrénées occidentales (1); Sierras marginales (2); Région de Figueras (3); La Nurra (Sardaigne)(4); Ariège (5); Corbières (6); Bédarieux-St Chinian (7); Villeveyrac-Montpellier (8); Les Alpilles (9); région de Brignoles (10); Haut-Var (11); Le Revest (12).



Le gisement que l'on peut prendre comme exemple est le type couche de Graxioleddu au NE d'Olmedo où une marne verdâtre illitique, de faciès purbeckien (Berriasien -Valanginien inférieur), s'altère progressivement en bauxite compacte finement oolithique et pisolithique à boehmite - hématite - goëthite - kaolinite. Le profil d'altération qui peut atteindre 5 m (avec 2 m environ de bonne bauxite à la partie supérieure) a été reconnu par sondages, tranchées et affleurements, sur 24 km². Le toit est représenté par les faciès marins carbonatés coniacien.

L'érosion et karstification du type Sardaigne ont déterminé le passage au type Languedoc - Provence sous forme de couches, lentilles ou poches, sur des murs carbonatés du Jurassique supérieur ou du Valanginien supérieur-Aptien inférieur (faciès urgonien) plus ou moins irréguliers.

Des analogies existent entre les types Sardaigne et Ariège puisqu'il y a également, dans ce dernier, altération sur place de marnes ou argilites avec des profils minéralogiques et géochimiques comparables. Mais des différences paléogéographiques importantes justifient la distinction: dans le type Ariège, marnes et argilites se déposent dans le domaine littoral et sur la plate-forme carbonatée d'une marge; dans le type Sardaigne, les marnes appartiennent à la série lithologique à l'intérieur d'un craton.

La formation du type Sardaigne et son évolution possible en type Languedoc-Provence ont été déterminées par les mouvements tectoniques de la phase autrichienne qui ont permis la formation de plis, le jeu de failles et panneaux soulevés, l'altération des marnes purbeckiennes. L'altération d'autres niveaux alumineux de la série mésozoïque et paléozoïque est également envisagée (Oggiano et al. 1987).

B - Le type Languedoc-Provence

Coexistence de l'allochtonie, parallochtonie et parautochtonie en domaine cratonique

Ce type correspond aux zones cratoniques à évolution relativement longue avec des lacunes stratigraphiques mur/toit importantes. Il est largement représenté côté européen, ibérique et sur l'"Isthme Durancien" (Combes 1990). Les ondulations,

Fig. 2 ←

Schémas les principaux modes de formation des bauxites à substratum carbonaté (= bauxites karstiques) retenus pour la genèse des types Sardaigne, Languedoc-Provence, Ariège et Pyrénées occidentales. Schémas sans échelle. La sédimentation marine synchrone de e et f n'a pas été figurée. 1. Altération sur place (autochtonie); 2. Altérite ou bauxite détritiques; 3. Faciès marneux; 4. Roches carbonatées mésozoïques, a) roche carbonatée argileuse; 5. Permo-Trias à pélites dominantes; 6. Socle paléozoïque sédimentaire, métamorphique et éruptif affecté par la phase hercynienne; 7. Altération sur place et poursuite de l'altération lors de la surimposition karstique dans le substratum carbonaté, (A) déplacement vertical, (B) vertical et latéral; 8. Différents niveaux d'enfoncement; 9. Niveau aquifère; 10. Mouvement vertical fort (a), moyen (b), faible (c); 11. Pente des zones soulevées, forte (a), moyenne (b), faible (c); 12. Rôle de l'eustatisme, démontré (a), possible (b); 13. Paléosurface karstique; 14. Erosion + transport de roches argileuses et d'altérites plus au moins bauxitiques (1), dépôt (2), ferrallitisation (3).

bombements et failles connexes, liés aux mouvements médio-crétacés, ont créé une grande diversité dans les gisements qui justifie les nombreuses hypothèses génétiques proposées par les auteurs et l'impossibilité pour l'une d'elles de les expliquer tous. Trois filières principales peuvent maintenant être retenues.

1. Allochtonie

Le soulèvement de certaines zones permet la ferrallitisation de roches alumineuses en bauxite résiduelle, primaire, dont l'érosion alimente le dépôt de bauxite détritique, secondaire (Fig. 2b). Il s'agit donc d'une bauxite allochtone qui arrive toute faite dans son lieu de dépôt. Elle se caractérise par: des figures de sédimentation (lamination, niveaux conglomératique, granoclassement, galets et clastes bauxitiques, traces de courant etc...); des profils chimico-minéralogiques sans évolution verticale montrant qu'il n'y a pas eu d'altération sur place et dont le tracé irrégulier indique qu'il s'agit de gisements proximaux; des éléments détritiques non bauxitiques (blocs de dolomie ou de calcaire, niveaux gréseux); la présence (mais c'est très rare) de fossiles. Cette origine a été démontrée par certains gisements provençaux (Nicolas 1968) et languedociens (Combes 1969, 1973, 1984). Dans le Languedoc, à Bédarieux et St Chinian, la zone haute nourricière correspondait à l'actuel flanc sud de la Montagne Noire où se situait la bauxite résiduelle. On a montré que la roche mère s'apparente géochimiquement avec les niveaux alumineux de la série paléozoïque ou mésozoïque susceptibles de se trouver soumis à l'altération dès la fin du jurassique dans ce secteur. En Provence et sur les autres zones hautes du Languedoc, la roche mère la plus probable retenue par la plupart des auteurs à la suite de Denizot (1961), correspond aux niveaux marneux du Crétacé inférieur dont l'altération aurait fourni une bauxite résiduelle primaire de type Sardaigne aujourd'hui disparue. La découverte de ce dernier type et son passage latéral effectif, en Sardaigne, à des bauxites détritiques secondaires de type Languedoc-Provence vient étayer solidement cette hypothèse; l'absence de témoins du type Sardaigne en Languedoc-Provence étant vraisemblablement due au développement plus important des mouvements médio-crétacés favorisant la destruction des profils primaires. Parmi les faciès marneux du Crétacé inférieur, ceux de l'Aptien-Albien ont vraisemblablement joué un rôle privilégié sur une partie de l'"Isthme durancien".

2. Autochtonie relative ou parautochtonie

La bauxitisation se produit en deux temps. Dans un premier temps l'altération débute dans un site primaire puis, après érosion-transport-dépôt, se poursuit (deuxième temps) dans un site secondaire. Dans les cas observés, autour de la structure haute de la Montagne Noire méridionale, à St Chinian et Bédarieux, l'altération primaire sur la zone haute n'a guère dépassé le stade kaolinite-hématite-goethite de sorte que l'altération dans le site secondaire est bien évidente (Fig. 2c). On a en effet une évolution verticale des faciès avec des profils minéralogiques et géochimiques indiquant clairement une altération sur place: désilification, augmentation de Fe-Al, forte diminution de la kaolinite et

développement des hydroxydes d'aluminium (Combes 1969, 1973). Par contre, lorsque l'altération primaire est très avancée, l'altération dans le site secondaire est peu apparente et c'est le caractère détritique qui l'emporte. Selon le degré de ferrallitisation atteint en amont dans le site primaire, la trace laissée par l'altération sur place en aval dans le site secondaire sera donc plus ou moins nette et le caractère autochtone ou allochtone pourra varier selon les cas. D'autre part, comme un gisement secondaire peut être à son tour érodé et redéposé ailleurs où l'altération se poursuivra si le climat est favorable, on voit que la notion d'allochtonie et d'autochtonie est très relative et qu'il faut considérer une bauxite comme un élément d'une chaîne évolutive de gisements le long de laquelle se développe l'altération: le caractère autochtone ou allochtone dominant dépendra du degré d'évolution entre l'extrême amont où la ferrallitisation débute (100 % autochtone) et l'extrême aval où arrive un sédiment déjà bauxitisé (100 % allochtone) (Combes 1972, 1984).

Cette genèse en deux temps, que l'on peut démontrer pour certains gisements, avait été retenue comme hypothèse possible par plusieurs auteurs avec un transport restreint d'argiles de décalcification (George 1935; de Weisse 1948, 1949; Bonte 1958) ou de produits alumineux d'altération d'origine plus lointaine (Roch 1956, 1959, 1962). Ces apports lointains sont justifiés par la présence de minéraux lourds, particulièrement le disthène et la staurotite, présents dans la bauxite dans la partie ouest de l'"Isthme durancien" et dont la source se trouve dans le Massif Central méridional (Demangeon 1965, 1969, 1975) où sont connues les isogrades correspondantes (Burg et al. 1984). Bien que l'on ne puisse, dans l'état actuel des reconstructions paléogéographiques et paléostratigraphiques, préciser les modalités de cette relation, la solution la plus simple serait l'établissement d'un système fluvial NS, dès la régression de la fin du jurassique, sur les Grands Causses, leur prolongement méridional vers la Montagne Noire et, au Crétacé Moyen, sur la partie occidentale de l'"Isthme durancien". Cet apport argileux lointain serait venu s'ajouter aux roches mères alumineuses de la série lithologique proprement durancienne (Demangeon 1975).

En Provence, la genèse en deux temps a également été proposée (Valeton, 1966) en faisant intervenir l'érosion de couvertures latéritiques sur les terrains cristallins des Maures-Estérel et la poursuite de l'altération bauxitique après dépôt dans les dépressions de l'"Isthme durancien". Même si la dénudation du socle cristallin au niveau des Maures n'est pas certaine à l'Albien, comme le suggère l'absence, dans les bauxites, de minéraux comme disthène-staurotite abondants dans ce massif, un bombement de sa couverture est probable. On observe en effet une augmentation de l'érosion du mur de la bauxite vers l'Est en se rapprochant des Maures (Masse et Philip 1976; Guieu et Rousset 1978; Laville 1981) où pouvait exister une structure haute, comparable à la Montagne Noire méridionale au Sud du Massif Central, dont les niveaux alumineux de la couverture sédimentaire post-hercynienne auraient pu servir de roche mère pour les altérites primaires. D'autre part, comme on peut l'observer dans la mine maintenant en fin d'exploitation, le gisement du Pas de Recou, le plus proche des Maures, contient

des niveaux détritiques à éléments bauxitiques polygéniques pluricentimétriques, irrégulièrement répartis (Valeton 1966), qui semblent appartenir à des séquences fluvialites plurimétriques, grano-décroissantes, à base ravinante, passant vers le haut à une bauxite fine, pauvre en éléments, bariolée ou flammée, probablement constituée dans la zone de battement d'une paléonappe de plaine alluviale à hydromorphie temporaire. Ces niveaux altérés sur place en bauxite à boehmite à partir d'un matériau détritique à kaolinite-hématite (Valeton 1966), sont comparables, avec une granulométrie plus grossière au Pas de Recou, à la bauxite supérieure de Bédarieux (Combes 1973). Enfin, la présence de quartz rhyolitiques à affinité permienne (Prone et Rousset, 1981) dans des argilites associées aux bauxites est un argument en faveur d'une altération profonde de la couverture des Maures et de l'Estérel.

3. Parallochtonie

Dans cette filière, la dissolution karstique joue un rôle prépondérant sur les bombements de l'"Isthme durancien" (Fig. 2d). Rousset (1969) a montré qu'à partir du dôme varois les marnes de l'Âptien-Albien se sont ferrallitisées en même temps qu'elle s'enfonçaient dans le substratum carbonaté et se déplaçaient latéralement, par colluvionnement et alluvionnement, sur les pentes du dôme jusqu'au niveau hydrostatique où l'évolution s'est arrêtée. Il s'agit donc d'une surimposition verticale et latérale, dans le mur carbonaté, d'une marne ou de tout autre matériau argileux, au cours de sa ferrallitisation. Ce mécanisme, bien analysé par Guendon et Parron (1983) dans les Alpilles, fait apparaître des structures argilo-ferrugineuses, nodulaires, pisolithiques, bréchoïdes, permettant de suivre l'évolution du système verticalement ou latéralement dans des toposéquences reconstituées sur plusieurs centaines de mètres à l'aide d'un grand nombre de sondages. L'apparition de pseudoblocs et pseudogalets bauxitiques est due à la karstification provoquant le démantèlement, par soutirage, d'un profil bauxitique antérieur qui tend à se rétablir dès que le milieu se stabilise. Les traces d'altération sur place sont indiquées par l'évolution verticale des profils pétrographiques, minéralogiques et géochimiques dont les stades les plus évolués se situent à l'aval de la toposéquence. On retrouve donc une chaîne évolutive, déjà observée à propos de l'autochtonie relative mais qui se développe ici d'une manière continue à partir des dômes en faisant jouer enfoncement dans un karst actif et déplacement limité sur les pentes.

Un schéma parallochtoniste comparable, proposé également pour les bauxites provençales (Lajoinie et Laville 1979; Laville, 1981), permet d'expliquer l'accumulation de bauxite sur les dômes ou sur leurs flancs alors que des apports seulement détritiques (allochtonie) devraient rassembler le minéral surtout dans les dépressions. Lorsque la pente des dômes s'accroît, l'érosion peut intervenir et permettre le passage vers l'aval du paysage à des gisements allochtones ou parautochtones si l'altération se poursuit. De même, les travaux de Bonte (1969), appliquant aux bauxites l'évolution morphologique des poches de dissolution de

la craie, mettent en évidence une corrélation étroite entre le fonctionnement des cavités karstiques et l'altération synchrone de sédiments argileux en bauxite.

4. Mode de formation et taux de soulèvement

On voit donc que sur l'"Isthme durancien" et ses dépendances plusieurs scénarios ont pu coexister pour aboutir au type Languedoc-Provence. Cette diversité est due à la relative instabilité tectonique consécutive aux mouvements médio-crétacés dont les soulèvements en panneaux ou dômes, d'importance variable, ont contrôlé l'altération des termes alumineux de la série lithologique et probablement aussi, par leur degré d'intensité, le développement de l'une des filières retenues.

– Les soulèvements importants favoriseraient la formation de gisements parautochtones ou allochtones par dépôt, avec ou sans poursuite de l'altération, en contrebas des dômes sur lesquels se trouvent et sont érodés les gisements primaires (ex. gisements de Bédarieux et St Chinian).

– Les soulèvements modérés détermineraient l'évolution parallochtone contrôlée par les soutirages karstiques et des pentes peu inclinées; les dômes garderaient, en quelque sorte, "leurs" bauxites (ex. les gisements des Alpilles).

– Les faibles soulèvements permettraient la formation et la préservation de profils en place, autochtones, comme le type Sardaigne, le seul absent de l'"Isthme durancien", peut-être parce que les mouvements médio-crétacés y ont été plus accentués qu'en Sardaigne.

Dans ces conditions instables où les différents modes de formation peuvent jouer, on comprend qu'il n'est pas possible d'expliquer tous les gisements de manière univoque comme on a trop souvent essayé de le faire. Des travaux sont encore nécessaires pour reconstituer le cadre paléostrucural au Crétacé moyen, localiser les zones soulevées, les paléofailles et établir, si possible, une relation entre leur degré de fonctionnement et les types de faciès bauxitiques qui en dérivent selon les modèles génétiques à intensité croissante, autochtonie-parallochtonie-parautochtonie-allochtonie, en liaison avec le taux de soulèvement.

C – Le Type Ariège

Parautochtonie à contrôle eustatique dominant sur les gradins proximaux d'une marge stable (Fig. 2e)

Ce type, principalement développé en Ariège où il a été décrit (Combes 1969, 1984; Combes et Peybernès 1981, 1989a et b; Combes et al. 1989), se trouve sur les gradins de la marge européenne, intimement lié aux oscillations de la plate-forme albo-aptienne, à faciès urgonien, transgressive vers le Nord et à déplacement centrifuge par rapport au bassin axial pyrénéen (Fig. 1.). Sur cette bordure littorale à environnement de plate-forme interne ou margino-littoral (lagunes, marais côtiers), les oscillations sont dues au fonctionnement des gradins limités par des failles synsédimentaires et aux fluctuations eustatiques qui jouent un rôle important.

En période de haut niveau marin, se déposent des argilites ferrifères et des marnes provenant de l'érosion de toutes les roches alumineuses plus au moins altérées de l'arrière-pays au Nord, y compris les bauxites résiduelles primaires sur le socle et les types Sardaigne ou Languedoc-Provence qui pouvaient s'y trouver. Les apports terrigènes qui ont échappé à ce piège littoral alimentent vers l'aval la série marneuse du bassin axial pyrénéen. En période de bas niveau marin se produit la ferrallitisation.

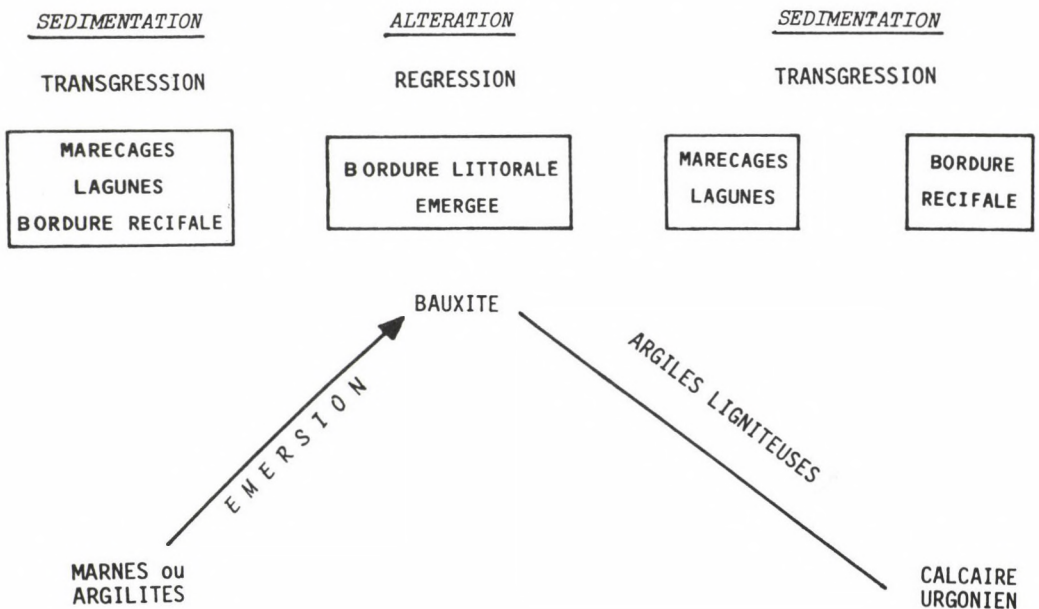
La séquence lithologique bauxitique comprend de bas en haut: argiles plus au moins ligniteuses – calcaire urgonien – bauxite (ou argilite partiellement bauxitisée).

La bauxite provenant de la ferrallitisation des argilites ferrifères ou des marnes préalablement déposées en période de haut niveau, le développement de la séquence bauxitique peut être schématisé comme l'indique le Tabl. 1.

La reconstitution dynamique de la mise en place de cette séquence sur la partie interne de la plate-forme est proposée Fig. 3. en termes de stratigraphie séquentielle en utilisant les cortèges sédimentaires de Vail et al. (1987) appliqués ici à un environnement carbonaté:

– Haut niveau marin (transgression): avancée du domaine margino-littoral (argiles plus ou moins ligniteuses) et de la plate-forme (calcaire urgonien) correspondant à l'Intervalle Transgressif (IT) et au Prisme de Haut Niveau (PHN).

Tabl. 1
Développement de la séquence bauxitique de type Ariège



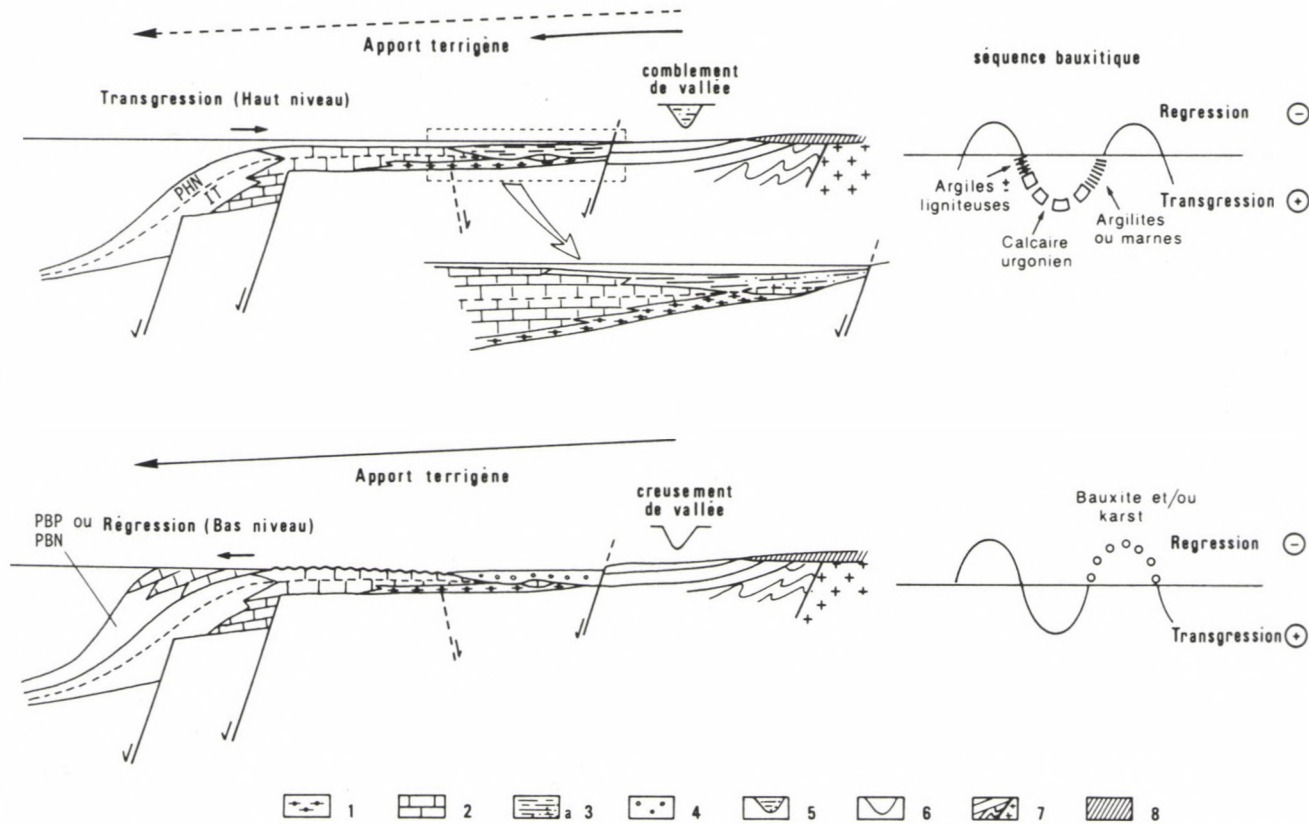


Fig. 3.

Reconstitution dynamique de la séquence bauxitique de type Ariège et essai de corrélation avec les cortèges sédimentaire de Vail et al. (1987). 1. Argiles plus au moins ligniteuses; 2. Calcaire urgonien; 3. Argilites ferrifères ou marnes, a) éléments détritiques; 4. Bauxite; 5. Vallée comblée dans la partie amont; 6. idem, en cours de creusement; 7. Arrière-pays, socle hercynien et couverture post-hercynienne; 8. Altérites et bauxites de l'arrière-pays. Cortèges sédimentaires: IT-Intervalle transgressif; PHN-Prisme de haut niveau; PBN-Prisme de bas niveau; PBP-Prisme de bordure de plate-forme

Dans les parties internes de la plate-forme urgonienne se déposent, de manière discontinue, des sédiments terrigènes (argilites ferrifères à kaolinite-hématite, marnes) roche mère de la bauxite. Sur la bordure externe de la plate-forme, ce cortège sédimentaire passe aux marnes à Ammonites du bassin axial pyrénéen. A ce stade transgressif se situerait le remplissage des vallées, visibles dans la partie amont, creusées antérieurement en période de bas niveau.

– Bas niveau marin (régression): émergence de la plate-forme, bauxitisation des argilites et marnes, karstification et érosion, creusement des vallées qui vont alimenter directement en produit terrigènes la sédimentation marneuse du bassin. Côté externe, constitution d'un Prisme de Bordure de Plate-forme (PBP) avec progradation du calcaire urgonien sur les marnes.

Les oscillations marines peuvent aboutir à la superposition de plusieurs séquences complètes ou non. Les plus simples étant, par exemple, argilite-bauxite, fréquente dans les parties les plus internes de la plate-forme, ou argile \pm ligniteuse-calcaire urgonien dans les moins internes. Elles peuvent être corrélées, à l'aide d'un bon contrôle biostratigraphique, avec les séquences marnes à Ammonites-calcaire urgonien correspondant, en bordure de la plate-forme, aux rétrogradations ou progradations des faciès urgoniens (Combes et Peybernès 1981).

Du point de vue minéralogique et géochimique les niveaux bauxitiques montrent une évolution verticale depuis une argilite ferrifère avec kaolinite (illite, chlorite)-hématite, jusqu'à une bauxite pisolithique à boehmite-diaspore-hématite. Le profil géochimique correspond à une désilification et à un enrichissement en $Al_2O_3-Fe_2O_3$ à partir des argilites qui représentent la roche mère véritable ou, dans certain cas, le premier stade d'altération d'une marne.

L'allochtonie de la roche mère argileuse ou marneuse est claire puisque cette dernière appartient à la série albo-aptienne transgressive sur le substratum jurassique. L'altération s'est produite, dans un deuxième temps, sur des supports différents suivant la position sur la plate-forme carbonatée (Fig. 3). Le type Ariège correspond donc à la parautochtonie, déjà retenue dans le type Languedoc-Provence mais qui se développe ici dans des conditions paléogéographiques spécifiques d'une zone littorale oscillante sur les gradins proximaux d'une marge stable.

D – Le type Pyrénées occidentales (pays Basque, Béarn)

Allochtonie à contrôle tectonique dominant sur les gradins distaux d'une marge stable (Fig. 2f)

Ce type se trouve associé à un système de gradins et de blocs qui constituent, d'une manière symétrique à ceux de l'Ariège (Fig. 1), la marge nord du craton ibérique progressivement submergée par une transgression hétérochrone venue du nord-est (Combes et Peybernès 1987).

Le jeu des gradins détermine le dépôt de produits argileux et d'éléments bauxitiques (pisolithes) qui ont pu, dans certain cas, poursuivre leur altération après le dépôt à la faveur d'oscillations liées au fonctionnement de la marge et

peut-être aussi aux fluctuations eustatiques. Des brèches au mur et au toit accompagnent les failles synsédimentaires limitant les panneaux dont l'enfoncement, vraisemblablement assez brusque, a favorisé la chloritisation diagénétique de la bauxite ou la formation de matrices et de croûtes chloriteuses.

Ces bauxites et altérites dont le caractère détritique est souvent prédominant (stratification, nombreux fragments de pisolithes) sont essentiellement à diaspore-chlorite. Elle se sont déposées et ont évolué en milieu plus réducteur que les bauxites ariégeoises, à un niveau bas peu propice au développement d'altérations importantes (nappe aquifère proche de la surface). Après leur mise en place, les bauxites, rapidement noyées en milieu marin protégé et réducteur, ont pu subir une chloritisation diagénétique.

Dans le paysage sédimentaire, les bauxites basco-béarnaises devaient se situer en position d'extrême bordure littorale en aval du type Ariège de milieu moins réducteur. Les éléments bauxitiques déposés dans cette zone, rendue instable par le fonctionnement de la marge, proviennent de l'érosion des altérites de la paléomarge ibérique ferrallitisée au Sud.

Le type Pyrénées occidentales, bien développé dans les régions basco-béarnaises et, discrètement, au Col de Brézou (Corbières), peut être considéré comme le témoin le plus distal de l'accumulation d'apports bauxitiques d'origine allochtone sur la marge en aval de laquelle se développent les faciès marneux du bassin axial pyrénéen. La manque de données, en partie dû à la faible extension de ce type et à la qualité médiocre des affleurements, ne permet pas, dans l'état actuel des connaissances, d'analyser en terme de stratigraphie séquentielle les gisements et leurs équivalents côté bassin.

II- Le paysage sédimentaire et géodynamique synthétique des bauxites, répartition des principaux types de gisement

En tenant compte du cadre stratigraphique, paléogéographique, paléostructural, de la typologie des gisements et de leur répartition spatiale, nous pouvons rassembler dans un paysage sédimentaire et géodynamique synthétique les principaux types retenus avec leurs caractères essentiels (Fig. 4).

Les types de bauxite s'ordonnent entre un domaine de niveau relativement élevé à l'intérieur du craton ou sur l'"Isthme durancien" et des zones bordières (plaines littorales, plates-formes internes). On retrouve la distinction entre les bauxites de haut niveau associées aux arrière-pays et les bauxites de bas niveau notée dans la nature actuelle ou dans les séries anciennes de nombreuses régions du Monde à propos des bauxites latéritiques (Gordon et al. 1958; Bleackley et Phil 1964; Grubb 1973) ou karstiques (Valeton 1976, 1983a).

Dans le cas des bauxites latéritiques une évolution relativement simple intervient: sur l'arrière-pays et sur les zones hautes se développent des profils de bauxite résiduelle sur des roches de nature variable, l'érosion d'une partie de ces profils alimente le dépôt de sédiments kaoliniques plus ou moins bauxitiques (selon le degré de l'altération antérieure) dans les dépressions ou sur la plaine

côtière. L'altération pourra s'y poursuivre en fonction des conditions locales (oscillations du niveau marin, fluctuation de la nappe aquifère). Le fonctionnement de ce couple amont-aval dépend de l'équilibre érosion-altération lié au taux de soulèvement relatif de l'arrière-pays et des zones hautes (d'origine tectonique ou eustatique) qui peut favoriser la ferrallitisation ou l'érosion et la dispersion des profils résiduels (Samama 1986). A titre d'exemple, en Colombie (Rosas 1976), l'érosion de bauxites de type latéritique intervient lorsque la pente des zones surélevées dépasse 20°; en-dessous, il y a ferrallitisation avec des profils à épaisseur maximum pour des pentes de 5 à 10°.

Dans la partie amont, de haut niveau, du paysage reconstitué (Fig. 4), la situation est plus complexe que pour les bauxites de type latéritique. En effet, la présence de taux de soulèvement variables suivant les points et celle de substratums carbonatés ont comme conséquence la coexistence de plusieurs modes de formation. Dans les zones peu soulevées c'est l'autochtonie qui l'emporte, les bauxites restent sur leurs roches mères comme pour le type Sardaigne. Lorsque les soulèvements sont plus accentués, la parallochtonie se développe avec conjointement altération, enfoncement vertical et déplacement latéral dans le karst de la masse bauxitique qui reste toutefois sur les zones hautes et répartie sur leur flancs. Les zones les plus actives, à soulèvements importants, dispersent leurs bauxites par érosion de profils plus ou moins évolués et accumulation dans les dépression morphologiques de bauxites détritiques (allochtonie) ou d'argilites kaoliniques peu ou pas bauxitiques qui poursuivent sur place leur ferrallitisation (autochtonie relative ou parautochtonie). L'"Isthme durancien", avec le type Languedoc-Provence, illustre bien ces trois dernières filières.

Dans la partie aval, de bas niveau, vont se retrouver, sur les gradins de la marge, les matériaux alumineux issus de l'érosion des roches sédimentaires argileuses de l'arrière-pays ou des altérites du craton qui auront échappé aux pièges morphologiques et géochimiques. Ils vont poursuivre leur altération (parautochtonie) sous le contrôle des oscillations du niveau de base marin liées à l'eustatisme et au jeu des failles synsédimentaires (type Ariège). Sur les derniers gradins (type Pyrénées occidentales), l'instabilité due à l'activité des failles bordières a provoqué le dépôt de brèches et de bauxites détritiques dominantes (allochtonie). Ce piège ultime a probablement été en partie alimenté par l'érosion du type Ariège due au mouvement plus important qu'ailleurs des accidents constituant la marge.

On constate donc que les modes de genèse dans le paysage sédimentaire synthétique dépendent de l'intensité des mouvements tectoniques qui conditionnent la formation sur place, la migration des altérites et la poursuite de leur évolution. Ces mouvements semblent plus sensibles à l'Ouest, le long des marges (failles actives, brèches) dont l'activité a déstabilisé les zones de l'amont permettant aux produits alumineux d'atteindre les ultimes gradins. Le climat étant ferrallitisant en tous points, on peut dire que l'instabilité tectonique a été le facteur essentiel de la formation et de la migration des bauxites dans le paysage sédimentaire. On doit toutefois remarquer que ces mouvements tectoniques ont

été modérés pour permettre à la fois la ferrallitisation et l'érosion ménagée des altérites. Il semble que le fonctionnement des marges passives européenne et ibérique correspond bien à cet état d'équilibre entre altération et érosion, tout au moins jusqu'à l'Albien supérieur (pyrénées) et le Cénomaniens moyen (Provence) où les mouvements se sont accentués avec prédominance de l'érosion (développement des brèches, des grès et des flyschs) et la fin des bauxites.

Du point de vue pétrographique et minéralogique, la relation déjà relevée entre la paléogéographie, les types de faciès et la cote à laquelle se produit l'altération (de Lapparent 1935; Valeton 1965, 1983a; Combes 1969, 1980; Komlóssy 1978; Bárdossy 1982; Combes et Peybernès 1987) apparaît nettement. Les bauxites se répartissent latéralement entre un amont, de haut niveau relatif oxydant, à gibbsite et/ou boehmite et un aval de bas niveau, moins oxydant ou réducteur, à nappe aquifère proche de la surface, aisément submergé en milieu margino-littoral ou de plate-forme interne lors du jeu de la marge et des variations eustatiques, où dominent les paragenèses à boehmite et/ou diaspore, diaspore-chlorite. Tout à fait à l'aval, les marnes du bassin axial pyrénéen, de la bordure de la plate-forme urgonienne et de la mer alpine représentent les apports terrigènes qui ont échappé sur le continent aux pièges du paysage sédimentaire bauxitogène. La néoformation de glauconie, très fréquente dans ces marnes, pourrait correspondre, comme cela a été décrit dans d'autres régions du Monde dont l'arrière-pays émergé est latéritisé (Giresse 1965; Porrenga 1967; Giresse et Odin 1973; Odin 1975; Valeton 1983a et b), aux apports en solution à partir des cratons et des marges en cours de ferrallitisation. Le développement de la glauconie à l'Aptien Supérieur-Albien et jusqu'au Cénomaniens inférieur dans la mer alpine serait donc contemporain de la bauxite et enregistrerait, en domaine marin, la ferrallitisation des territoires émergés. De ce point de vue, les ocres de la région d'Apt et d'Uzès qui proviennent de l'altération de ces faciès glauconieux (Parron et Triat 1976; Triat 1982; Guendon et Parron 1983) durant le Cénomaniens moyen, ne pourraient être considérées comme l'équivalent latéral des bauxites mais seraient dues à une émergence postérieure. Beaucoup reste à faire sur la répartition de la glauconie dans les séries marneuses du Crétacé moyen, sur le développement synchrone de la ferrallitisation et pour déterminer le rôle des facteurs eustatiques, climatiques et tectoniques.

Conclusion

Dans les régions pyrénéennes, en Languedoc, Provence et Sardaigne, les bauxites durant le Barrémien-Aptien-Albien-Cénomaniens inférieur, se mettent en place sur les territoires émergés qui appartiennent aux plaques européenne et ibérique, à leurs marges et à l'"Isthme durancien" assurant une certaine continuité entre les deux dans la partie orientale.

Cette paléogéographie, contrôlée par les mouvements relatifs des deux plaques de part et d'autre du bassin axial pyrénéen, détermine la répartition et la typologie des gisements de bauxite. Sur les plaques, en domaine intracratonique, se forment

des bauxites de haut niveau relatif (types Languedoc-Provence et Sardaigne) durant des lacunes assez longues caractérisant une émerision précoce et un recouvrement tardif. Sur les marges, en bordure des cratons et sur les plates-formes carbonatées urgoniennes, apparaissent des bauxites de bas niveau (types Ariège et Pyrénées occidentales) durant de courtes lacunes, brèves périodes émergées dans une série littorale oscillante.

Le contrôle structural s'exprime également dans le mode de formation. Les mouvements tectoniques, en distension ou compression, liés à la mobilité des plaques, ont provoqué des soulèvements verticaux et le fonctionnement de failles synsédimentaires dont le rôle dans le développement des altérations a été déterminant. Sur les cratons, lorsque les soulèvements sont faibles, les gisements résiduels formés *in situ* (autochtonie) par ferrallitisation de roches mères alumineuses restent sur place comme pour le type Sardaigne sur les marnes du Purbeckien. Lorsque le taux de soulèvement est plus fort (type Languedoc-Provence), les profils résiduels sont détruits et leurs éléments s'accumulent dans les dépressions avec (autochtonie relative ou parautochtonie) ou sans (allochtonie) poursuite de l'altération selon les conditions locales et le degré d'altération atteint dans le site primaire. Un cas intermédiaire apparaît avec les substratums carbonatés. L'altération se développe en effet pendant que la masse en cours de bauxitisation se surimpose dans son propre mur par déplacement vertical et latéral sur les pentes des dômes (parallochtonie). Les roches mères alumineuses les plus fréquemment retenues sont les niveaux marneux de la série mésozoïque et les termes alumineux du socle paléozoïque. Sur les marges, l'enfoncement des gradins limités par des failles actives provoque une certaine instabilité et le dépôt de sédiments argileux ou marneux provenant de l'érosion des roches alumineuses et des altérites intracratonique (types Sardaigne et Languedoc-Provence). Les oscillations du niveau marin, d'origine en grande partie eustatique, permettent, à plusieurs reprises, la ferrallitisation (parautochtonie) de ces sédiments (type Ariège). Sur les derniers gradins, probablement les plus instables, viennent s'accumuler (type Pyrénées occidentales) les produits de l'érosion des bauxites de la marge qui n'ont subi, après leur dépôt, qu'une chloritisation diagénétique (allochtonie dominante).

Ces différents types s'ordonnent dans un paysage sédimentaire synthétique bauxitogène où les soulèvements et jeux de failles de l'arrière-pays conditionnent l'altération et la mise en mouvement des altérites vers les dépressions et vers l'aval où, dernière étape, les apports alumineux ayant échappé aux pièges morphologiques et géochimiques viennent s'accumuler et achever leur évolution. Les paragenèses dans cette migration enregistrent, de l'amont vers l'aval, des conditions de drainage et d'oxydation décroissantes depuis les zones hautes du craton à gibbsite et/ou boehmite jusqu'aux marges de bas niveau à boehmite et/ou diaspore, diaspore-chlorite. Enfin, à l'extrême aval, les marnes glauconieuses des bassins marins synchrones représentent les apports terrigènes en solution et en suspension, issus des territoires émergés en cours de ferrallitisation. Les marnes de bassin, les plate-formes urgoniennes et les bauxites de bas niveau appartiennent

à des unités génétiques de dépôt et sont interprétées en termes de cortèges sédimentaires (sensu Vail) contrôlés par les oscillations eustatiques du niveau marin.

En définitive, dès lors que le climat-facteur essentiel de la géodynamique externe- est ferrallitisant, la genèse des bauxites apparaît sous la dépendance de la géodynamique interne correspondant, dans les régions étudiées, à l'établissement et au fonctionnement des marges européenne et ibérique. L'instabilité tectonique de ces marges et de leur arrière-pays cratonique proche a favorisé le démarrage de la ferrallitisation et l'évolution géochimique d'un manteau d'altérites vers le pôle alumineux jusqu'à son recouvrement par un toit protecteur.

Bibliographie

- Bárdossy, Gy. 1982: Karst Bauxites, Bauxite Deposits on Carbonate Rocks. – Elsevier, Amsterdam, p. 441.
- Bleackley, D., D. Phil 1964: Bauxites and laterites of British Guiana. – Geol. Surv. British Guiana, 34, p. 156.
- Bonte, A. 1958: Réflexions sur l'origine des bauxites et sur l'altération superficielle des calcaires. – C. R. 83e Congr. Soc. Sav., pp. 147–165.
- Bonte, A. 1969: Mise en place et évolution des bauxites sur mur calcaire. – Ann. Inst. Geol. Publ. Hung., 54, 3, pp. 29–49.
- Burg, J.P., A. Leyreloup, J. Marchand, Ph. Matte 1984: Inverted metamorphic zonation and large-scale thrusting in variscan belt: an example in the French Massif Central. – In "Variscan Tectonics of the North Atlantic region". – Geol. Soc., Blackwell Scientific Publ., Hutton and Sanderson, pp. 47–61.
- Ceccarini, C., G. Oggiano, I. Salvatori 1984: Nurra (Sardinia, Italy) bauxite deposit. – In "Bauxite", L. Jacob Ed., A. JI M. E., Soc. Min. Eng., pp. 525–538.
- Cocco, G., G. Pecorini 1959: Osservazione sulle bauxiti della Nurra (Sardegna nord-occidentale). – Atti Acc. Naz. Lincei, 5, pp. 175–214.
- Combes, P. J. 1969 : Recherches sur la genèse des bauxites dans le Nord-Est de l'Espagne, le Languedoc et l'Ariège (France). – Thèse Doct. Etat Univ. Montpellier, Mém. CERGH, 3–4, p. 375.
- Combes, P. J. 1972: Les différents types de bauxites sur substratum carbonaté dans le Languedoc et l'Ariège. Remarques sur la notion d'allochtonie et d'autochtonie. – C. R. Acad. Sc. Paris, 274, D, pp. 1613–1616.
- Combes, P. J. 1973: Etude géologique sur les conditions de mise en place d'une bauxite allochtone à substratum carbonaté: le gisement de Bédarieux (Hérault, France). – I. C. S. O. B. A., 2e Congr. Int. (Nice, 1973), pp. 89–108.
- Combes, P. J. 1980: Source material and sedimentary environment of bauxite formation on a karst topography: some examples. – Int. Ass. Sedim., 1st Europ. Meet. (Bochum, 1980), pp. 140–142.
- Combes, P. J. 1984: Regards sur la géologie des bauxites; aspects récents sur la genèse de quelques gisements à substratum carbonaté. – Bull. Centres Rech. Explor. – Prod. Elf-Aquitaine, 8, 1, pp. 251–274.
- Combes, P. J. 1990: Typologie, cadre géodynamique et genèse des bauxites françaises. – Geodinamica Acta (Paris), 4, 2, pp. 91–109.
- Combes, P. J., B. Peybernès 1981: Le gisement de la Combe de Lé (Pyrénées ariégeoises) en 1981: description, observations et remarques nouvelles sur une bauxite de type Ariège à mise en place polyphasée. – Eclogae Geol. Helv., 74, 3, pp. 587–602.

- Combes, P. J., B. Peybernès 1987: Les altérites et les brèches des Pyrénées Basco-Béarnaises liées à l'évolution polyphasée de la marge passive nord-ibérique au Jurassique et au Crétacé inférieur. – C. R. Acad. Sci. Paris, 305, II., pp. 49–54.
- Combes, P. J., B. Peybernès 1989a: Tectonique albienne dans les gisements de bauxites des Pyrénées ariégeoises (France) en relation avec l'évolution géodynamique de la marge européenne. – C. R. Acad. Sci. Paris, 308, II., pp. 953–959.
- Combes, P. J., B. Peybernès 1989b: Interprétation eustatique des séquences de bauxite de type Ariège dans les Pyrénées Centrales. – *Strata*, 1, 5, pp. 17–19.
- Combes, P. J., B. Peybernès, J. Médus, D. Mongin 1989: Bauxites, horizons à mollusques et palynoflore dans le gisement de Bacqué (Pyrénées ariégeoises): situation sur la marge européenne au Crétacé inférieur, environnement de dépôt, rôle de l'eustatisme. – *Ecolgae Geol. Helv.*, 82/1, pp. 113–131.
- Demangeon, P. 1965: Sur la présence et la signification probable de minéraux du Massif Central dans les bauxites de l'Isthme durancien. – C. R. Acad. Sc. Paris, 261, pp. 2685–2688.
- Demangeon, P. 1969: Sur le matériau initial de la bauxite des gisements occidentaux de l'Isthme durancien. *Ann. Inst. Geol. Publ. hung.*, 54, 3, pp. 387–390.
- Demangeon, P. 1975: A propos du matériel initial des bauxites de l'Isthme durancien. – C. R. Acad. Sc. Paris, 280, D, pp. 237–238.
- Denizot, G. 1961: La composition et la genèse des bauxites de Provence et Languedoc. – *Bull. B. R. G. M.*, 2, pp. 35–46.
- George, P. 1935: La région du Bas-Rhône. – Thèse Lettres, Doct. Etat, Univ. Paris, Baillière et Fils Ed., Paris, p. 691.
- Giresse, P. 1965: Observations sur la présence de "glaucionite" actuelle dans les sédiments ferrugineux peu profonds du bassin gabonais. – C. R. Acad. Sc. Paris, 260, 21, pp. 5597–5600.
- Giresse, P., G.S. Odin 1973: Nature minéralogique et origine des glaucionites du plateau continental du Gabon et du Congo. – *Sedimentology*, 20, pp. 457–488.
- Gordon, M. Jr., J.I. Tracey, M.V. Ellis 1958: Geology of the Arkansas bauxite region. – *U S. Geol. Surv. prof. Pap.*, 299, p. 268.
- Grubb, P. L.C. 1973: Genesis of the Weipa bauxite deposits, N. E. Australia. – *Mineral. Dep.* 6, pp. 265–274.
- Guendon, J.L., C. Parron 1983: Bauxites et ocre crétacées du Sud-Est de la France. Mécanismes de l'altération de roches sédimentaires. – *Trav. Lab. Sc. Terre, Univ. Marseille-Saint Jérôme*, B, 23, p. 142
- Guieu, G., Cl. Rousset 1978: Structures, paléostratigraphie, paléogéographie et genèse des bauxites de Provence. – *Bull. B. R. G. M.*, Fr, II., 4, pp. 311–322.
- Komlóssy, G. 1978: Minéralogie, géochimie et génétique des bauxites du Vietnam du Nord. – *Acta Geol. Acad. Sci. Hung.*, 20, 3–4, pp. 199–244.
- Lajoinie, J.P., P. Laville 1979: Les formations bauxitiques de Provence et du Languedoc. Dimensions et distribution des gisements. – *Mém. B. R. G. M.*, 100, p. 142.
- Lapparent, J. de 1935: Raisons géologiques de la formation des trois hydroxydes d'aluminium naturels. – *Congr. Intern. Mines*, 7, 1, pp. 375–381.
- Laville, P. 1981: La formation bauxitique provençale (France). Séquence des faciès chimiques et paléomorphologie crétacée. – *Chron. Rech. Min.*, 461, p. 51–68.
- Masse, J.P., J. Philip 1976: Paléogéographie et tectonique du Crétacé moyen en Provence. Révision du concept d'isthme durancien. – *Rev. Géogr. phys. Géol. dynam.*, 2, XVIII, 1, pp. 49–66.
- Nicolas, J. 1968: Nouvelles données sur la genèse des bauxites à mur karstique du Sud-Est de la France. – *Miner. Dep.*, 1, 3, pp. 18–33.
- Odin, G.S. 1975: Les glaucionites: constitution, formation, âge. – Thèse Doct. Etat, Univ. Paris VI, p. 245.
- Oggiano, G., G. Sanna, I. Temussi 1987: Caractères géologiques, gîtologiques et géochimiques de la bauxite de la Nurra. In "Groupe Français du Crétacé", – Livret-guide excursion mai 1987 en Sardaigne, pp. 72–124.

- Parron, C., J.M. Triat. 1976: L'ocrification des sables glauconieux albo-cénomaniens du Gard et du Vaucluse. – Bull. Soc. Géol. Fr., 7, XVIII, 1, pp. 21–25.
- Parron, C., J.M. Triat 1977: Nouvelles conceptions sur le Crétacé supérieur du Gard. Répercussions sur la stratigraphie, la paléogéographie et la tectonique de la découverte de trois phases d'altération scontinentales. – Rev. Géogr. phys. Géol. dynam., 2, XIX, 3, pp. 241–250.
- Pecorini, G. 1956: La facies bauxitica del Cretaceo della Nurra. – Rend. Acc. Lincei, 20, pp. 232–239.
- Pecorini, G. 1965: Stratigrafia e distribuzione della bauxiti della Nurra. (Sardegna nord-occidentale). – Symp. Ass. min. Sarda, 1, 86, p. 15.
- Porrenga, D.H. 1967: Glauconite and chamosite as marin depth indicators. – Marine Geology, 5, pp. 495–501.
- Prone, A., Cl. Rousset 1981: Les quartz des rhyolites permiennees comme marqueurs de la rupture paléogéographique médio-crétacé dans le Sud-Est de la France. – Bull. Soc. Géol. Fr., 7, XXIII, 5, pp. 487–492.
- Roch, E. 1956: L'origine alluviale de certaines bauxites du Bas-Languedoc. – C. R. Somm. Soc. Géol. Fr., 6, pp. 218–219.
- Roch, E. 1959: La genèse des bauxites de Provence et du Bas-Languedoc. Ann. Hébert et Haug, – Trav. Lab. Géol. Fac. Sc. Paris, 9, pp. 11–78.
- Roch, E. 1962: A propos des bauxites françaises. – Bull. B. R. G. M., 4, pp. 35–39.
- Rosas, G. H. 1976: Estudio sobre los depositos de bauxita en Cauca y Valle, especialmente el area de Morales y Cahibío. – Bol. Geol. Colombia, 22, 1, pp. 57–84.
- Rousset, Cl. 1969: Le bombement varois; relations entre la bauxitisation au Crétacé moyen, en Provence, et l'évolution originale de la région en régime karstique. – C. R. Acad. Sc. Paris, 268, D, pp. 2331–2334.
- Samama, J.C. 1986: Ore field and continental weathering. – Van Norstrand Reinhold Company p. 326.
- Sanna, G., I. Temussi 1986: La miniera di bauxite di Olmedo. – Industria miner., 6, pp. 7–42.
- Triat, J.M. 1982: Paléoaltération dans le Crétacé supérieur de Provence rhodanienne. – Thèse Doct. Etat., Univ. Marseille; Sciences géol., mém. 68, p. 202.
- Vail, P. R., J.P. Colin, R. Jan Du Chene, J. Kuchly, F. Mediavilla, V. Trifilieff 1987: La stratigraphie séquentielle et son application aux corrélations chronostratigraphiques dans le Jurassique du bassin de Paris. – Bull. Soc. Géol. Fr., 8, III, 7, pp. 1301–1321.
- Valeton, I. 1965: Fazies probleme in südfranzösischen bauxitlagerstätten. – Beitr. Mineral. Petrogr. Dtsch., II, 3, pp. 217–246.
- Valeton, I. 1966: Sur la genèse des gisements de bauxite du Sud-Est de la France. – Bull. Soc. Géol. Fr., 7, VIII, 5, pp. 685–701.
- Valeton, I. 1976: Criteria for autochthonous and allochthonous source material of bauxitic ores on carbonaceous rocks. – Travaux I.C.S.O.B.A., 13, pp. 21–36.
- Valeton, I. (1983a): Palaeoenvironment of lateritic bauxites with vertical and lateral differentiation. – Geol. Soc. Spec. Publ. No. 11, pp. 776–790.
- Valeton, I. (1983b): Klimat Perioden lateritischer Verwitterung und ihr Abbild in den synchronen Sedimentations Räumen. – Z. dt. Geol. Ges., 134, pp. 413–452.
- Weisse, G. de 1948: Les bauxites d'Europe centrale (province dinarique et Hongrie). – Mém. Soc. vaudoise Sc. nat., Lausanne, 9, 1, p. 162.s
- Weisse, G. de 1949: Les bauxites d'Europe central et leur genèse. – Bull. Ass. Suisse Géol. et Ing. Pétrole, 15, 49, pp. 19–28.

Bauxite exploring methods and their results in the Strážovské vrchy Mts., NW Slovakia

František Beleš

Geologický Prieskum, Rožnava

In the Mojtín, Radová-Žiar, Sádočné and Domanižská panva bauxite exploration was carried out between 1983 and 1987. Several geochemical anomalies indicating the presence of bauxite were found by complex geological methods (geophysics, geological mapping, geomorphological and metallometric analysis. These localities will be verified by drilling.

Key words: Bauxite prospection, geophysical methods, Strážovské vrch Mts. NW Slovakia

Introduction

Aluminium production in Czechoslovakia is fully dependent on bauxite import at a continuous rise in prices of this raw material on the world market. With 13 kg of Al per capita, our country is somewhere in the middle of the world primary aluminium consumption. In the forecasts (prognoses) made up to the year of 2000, a 2.75% annual increase doing one third of the minimalized world aluminium consumption rise only has been taken into account. Though considering a rise in the present 65000 t production 2.0 to 2.35 times in the forecasts mentioned above, there still would be a lack of about 2000 even in case of keeping the present import level of this. Nowadays, aluminium production in Žiar nad Hronom still remains an open question. This time it is doubtful, however, whether this aluminium plant being the Al producer in Slovakia will continue in production or not, because there is a hazard of heavy environmental contamination in the Žiarska kotlina Basin.

From the above mentioned it follows that an inevitable estimation of possible partial Al production from local sources is there necessary. That means to do an evaluation and exploration of all the known bauxite occurrences in Slovakia finding new prospective areas or shifting over exploration to some other untraditional Al-bearing raw materials (clays) suitable for industrial production. That is why the so-called "Strážovské vrchy Mts. Project" of bauxite prospection has been on the basis of all the known geological survey works performed in the Mojtín and Pružina regions elaborated.

Address: F. Beleš: Spisska Nova Ves, 60, Rožnava, Czecho-Slovakia

Received: 1 September, 1991

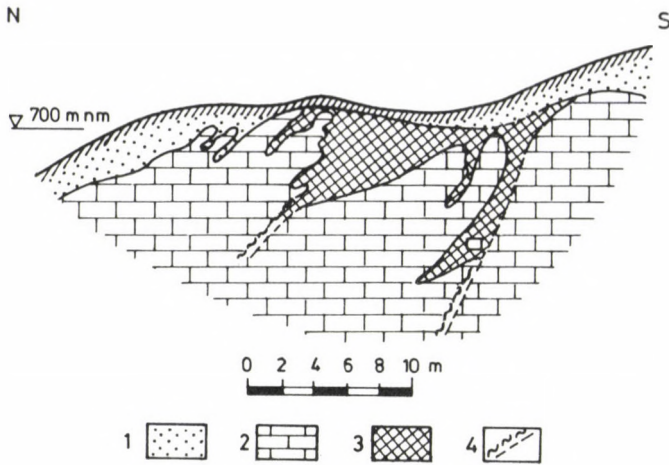


Fig. 2. Section of the Borová bauxite prospect at Mojtín (after I. Čillík, 1965). 1. Débris, slope loam; 2. Triassic limestone and dolomit; 3. Bauxite; 4. Tectonic line

New prospections

The main objective of the project was finding and proving further possible bauxite occurrences in the wider vicinity of the known occurrences (Mojtín, Radová-Žiar and Sádóčné – see Fig. 3) using a complex geological – geochemical – geophysical method to be followed by technical operations for proving the existence of the anomalies found. These technical works would be carried out in the further prospection/exploration phase.

New field activities including geological – geomorphological mapping, geophysics and geochemistry have been performed since 1983 up to 1987. It is the Mojtín site which was first studied by a complex geophysical method in the following modification: Symmetrical Resistivity Profiling (SRP) with Wenner electrode spacing (A 60M 60N 60B), (A 80M 30N 80B), Magnetometry, Gammasspectrometry, Vertical Electric Sounding (VES) with AB up to 200 m and Method of Ultra-Long Waves (ULW). In case of profiling method the measuring interval (step) was 10 m, while in case of VES a 50 m step has been used.

Following this the Radová-Žiar and Sádóčné occurrences have been geoelectrically measures by the following modification: Symmetrical Resistivity Profiling (SRP) with A 80M 20N 80B electrode spacing, Vertical Electric Sounding (VES) with AB electrode spacing up to 300 m. Method of Ultra-Long Waves (ULW), Magnetometry and Gammasspectrometry as well. When performing profiling methods, the measuring interval (step) was 10 m, in case of VES it did 50 m. VES has been carried out in each second profile.

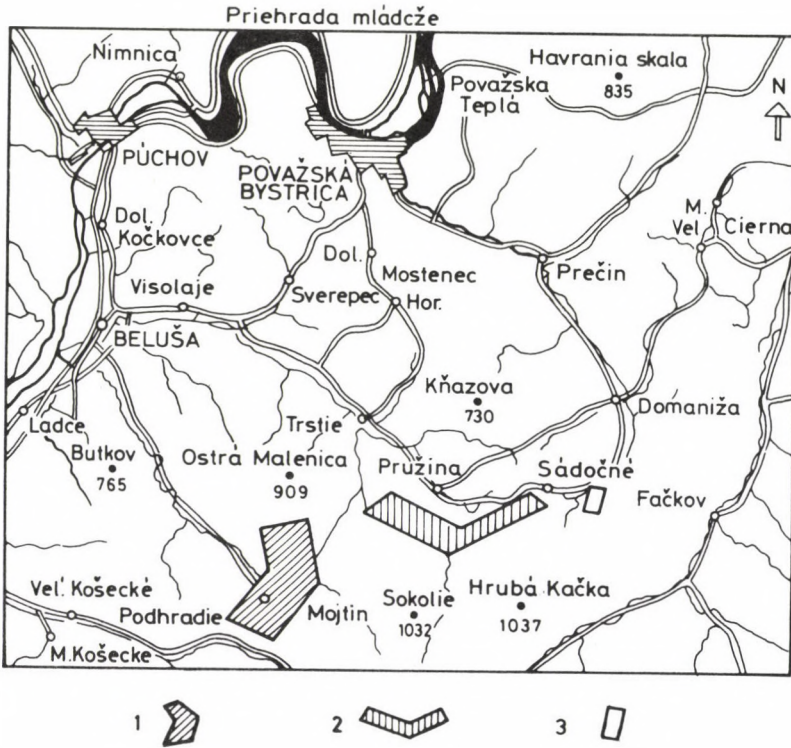


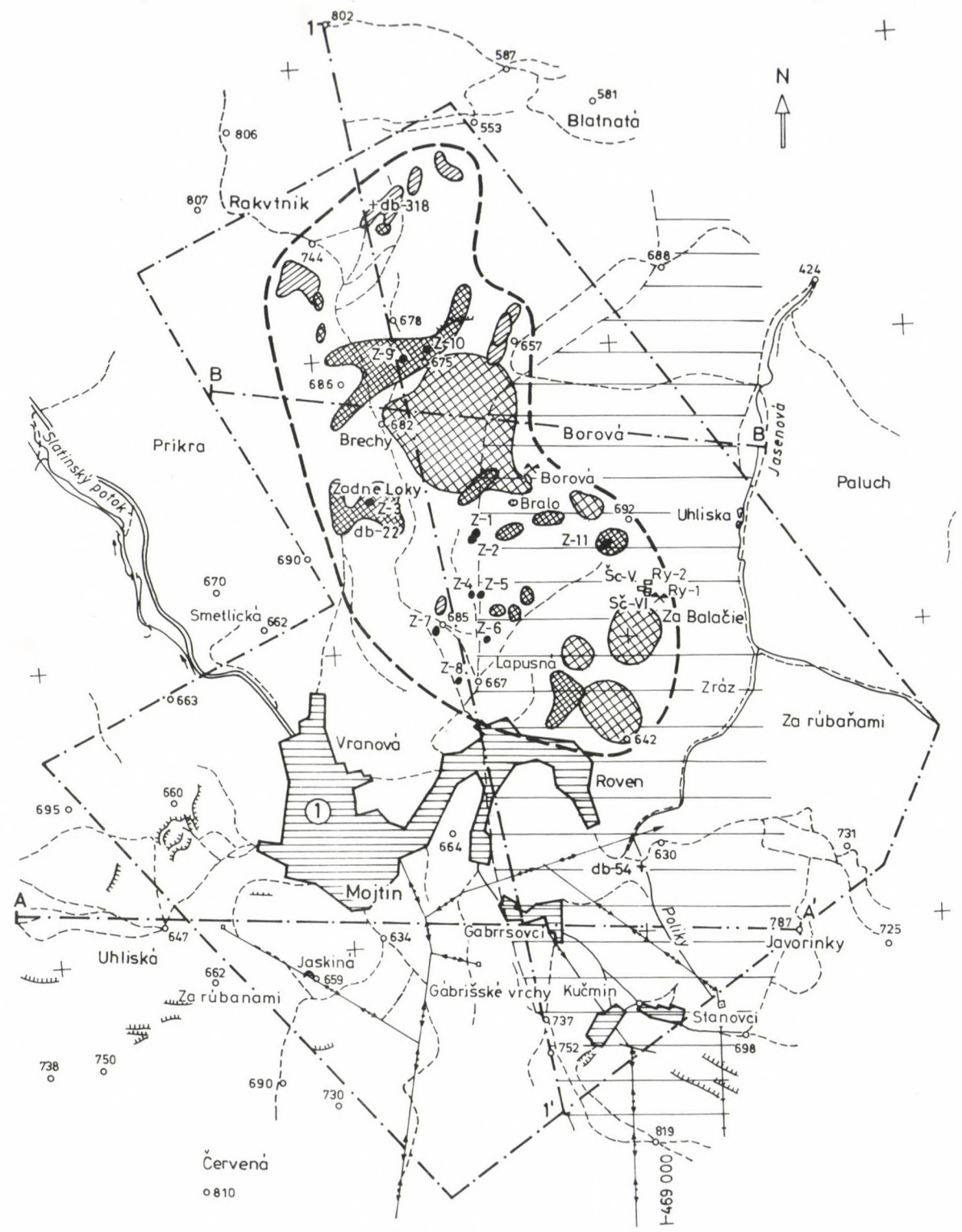
Fig. 3.

Location map showing the exploration areas. 1. The Mojtiín exploration area; 2. the Radovážiar exploration area; 3. The Sádóčné exploration area

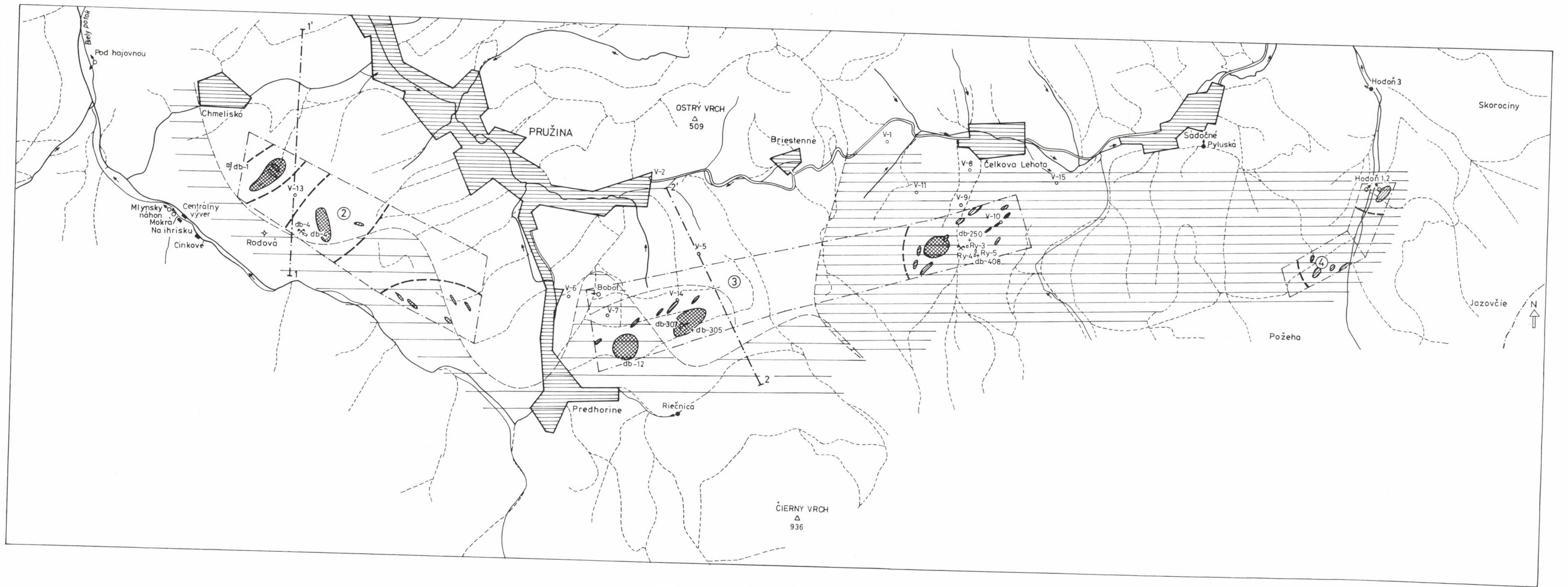
On the basis of the evaluation of individual methods applied they are SRP, VES and ULW which seem to be the most suitable ones from geological structure interpretation and hidden indice prospection point of view.

Contemporaneously with geophysical operations, geochemical works (soil sampling) were experimentally applied for detecting the products of bauxitic rock weathering in soil at the Mojtiín site only one has been realized, too. On the basis of the computer processed results of geochemical soil survey, some increased Ti, B, V and Ga anomalies pointing to the presence of bauxite could have been observed.

In addition to the works mentioned, geological and geomorphological mapping have been in all the sites performed. Geological mapping has been made for finding out and distinguishing late Eocene sediments (conglomerate, breccia, Nummulite limestone) having been preserved in the studied part of the Strážovské vrchy Mts. in form of more or less extensive bodies lying on limestones and dolomites of Middle Triassic age.



- 1
- 2
- 3
- 4
- 5
- 6
- 7
- 8
- 9
- 10
- 11
- 12
- 13
- 14
- 15
- 16



The objective of geomorphological mapping was to encounter and map all the depressions, sinkholes and some other karst phenomena (there was a karst area involved) which could be considered as potential sites of bauxite accumulations supposing that those ones could have been preserved (i.e. not removed from) in such places only where they were covered by younger sediments (conglomerate, breccia) or in some karstic forms (sinkholes, caverns). The subject mapping resulted in geological-geomorphological map compilation at scale of 1 : 10000.

Promising further bauxite prospections

The geological field works carried out proved the existence of several more or less extensive anomalies in the Mojttín, Radová-Ziar and Sádócné sites and may be considered as hidden deposits. There are presumably some bauxite bodies in depth ranging from 20 to 40 m below the surface. Individual anomaly size is rather variable depending likely on the jointing and karstification of the underlying carbonate rocks represented by Wetterstein limestones and partly dolomites. The most extensive anomalies ranging from 30 x 50 m up to 150 x 150 m in the Mojttín site (Fig. 4) have been noticed. In the Sádócné area the anomalies found are varying between 30 x 40 m and 50 x 140 m. The least extensive but most numerous anomalies there are in the Radová-Ziar prospect the largest one covering an area of about 20 x 120 m.

Conclusions

On the basis of geological survey works performed in the sites mentioned, prognostic maps of possible bauxite occurrences showing the areas of promising anomalies limited could have been at a scale of 1 : 10000 compiled.

In Mojttín prospect it is the northern part situated between the Blatná, Rakytník, Zadné Lúky, Lopusná and Borová elevations (Fig. 4) which is considered as the most promising one. For the Radová-Ziar region see Fig. 5 showing the most perspective areas found north of the Radová elevation as well as NE of Predhorie and S of Celková Lehota villages as well. In case of the Sádócné site it is the area extending north of the Pozená elevation which seems to be the most promising one (Fig. 5).

Fig. 4. →

Bauxite occurrences of Mojttín district. 1. The most promising anomalies encountered by geophysical works in the years of 1985 and 86; 2. Old prospects (trenches, pits), natural exposures with bauxite occurrences (1936-1938); 3. Sinkholes; 4. Trenches dug in 1956; 5. Sink; 6. Conspicuous field depressions; 7. Paleogene remnants (conglomerate, breccia, organic limestone); 8. Areas of expected bauxite occurrence where dig and drilling operations will be carried out; 9. The Mojttín-Trstie II. class water source protection zone; 10. The Domaniza II. class water source protection zone; 11. Geological selection; 12. 1, Mojttín site, 2-3, Radová-Ziar site, 4, Sádócné site; 13. Boreholes drilled in the years of 1952 and 53; 14. Spring, adit - not captured; 15. Spring, adit - captures; 16. Cave

Fig. 5. →

Bauxite occurrences of Sádócné district (for legend see Fig. 4)

In conclusion it is necessary to note that special attention should be there paid to the anomalies noticed, further to depressions, sinkholes and Paleogene bodies, which would be proved by drilling, too.

References

- Beleš, F. 1990: Závěrečná správa úlohy Strážovské vrchy – bauxit vyhladávací prieskum. Archív GP, š. p.
- Čillík, I. 1957: Závěrečná správa o vyhladávacom prieskume v roku 1956 – úsek Mojtín
- Maheľ, M. 1962: Vysvetlivky k prehľadnej geologickej mape ČSSR, list Žilina, M = 1 : 20000
- Maheľ, M. et al. 1983: Vysvetlivku ku geologickej mape Strážovských vrchov M = 1 : 50000

The geological setting and facies of bauxite deposits in Hungary, including the conditions of their development

József Knauer, Ágnes Fekete

*Hungarian Geological Survey,
Budapest*

Kálmán Tóth

*Geoprospect Ltd.
Balatonalmádi*

Correlation charts on major bauxite deposits in Hungary are presented. The charts demonstrate the general geological setting and the conditions of the bauxite genesis

Key words: Bauxite, Cretaceous, Eocene, Transdanubian Central Range

In the Transdanubian Central Range (including an area in the left side of river Danube) representing the main bauxite zone in Hungary, a great number of bauxite deposits are known, corresponding to three main bauxite levels, determined by combinations of the overlying and underlying formations. In some younger stratigraphic levels bauxite deposits that were subject to secondary reworking occur, sometimes in considerable amounts but in low grade. The main three levels correspond to the Early Albian, the Early Senonian and the Early Eocene stratigraphic gaps. Gap was particularly long-range in the latter case.

Correlation charts on the major regions (Figs 1, 3, 6 and 8) and some sub-regions (Figs 2, 4, 5, 7 and 9) demonstrate the varied geological setting and facies as first move towards a correlation. Comparative tables of D'Argenio and Mindszenty have also been worked out for a number of typical occurrences (Figs 10 through 14). The bauxite zone in S Transdanubia is presented in similar way (Figs 15 and 16). (The representation of high overlying and deep underlying beds is, in some cases, neglected in the sub-regional charts.)

Publications formerly published by the above authors or others (e.g.: Knauer and Tóth in: Mindszenty et al. 1984; Szantner in: Szantner et al. 1986; Knauer *ibid.*), and some manuscript papers prepared by the Bauxite Prospecting Company in Balatonalmádi, Hungary have also been regarded when working out the charts.

Three examples are given for Upper–Uppermost Albian sequences with hiatus from the Central Range, in which no bauxite deposit is known despite the fact that the hiatus was, indisputably, developed in response to exposure and was accompanied by karstification (Fig. 17).

Addresses: J. Knauer, Á. Fekete: H-1442 Budapest P.O.B. 106, Hungary

K. Tóth: H-8221 Balatonalmádi P.O.B. 31, Hungary

Received: 28 September, 1991

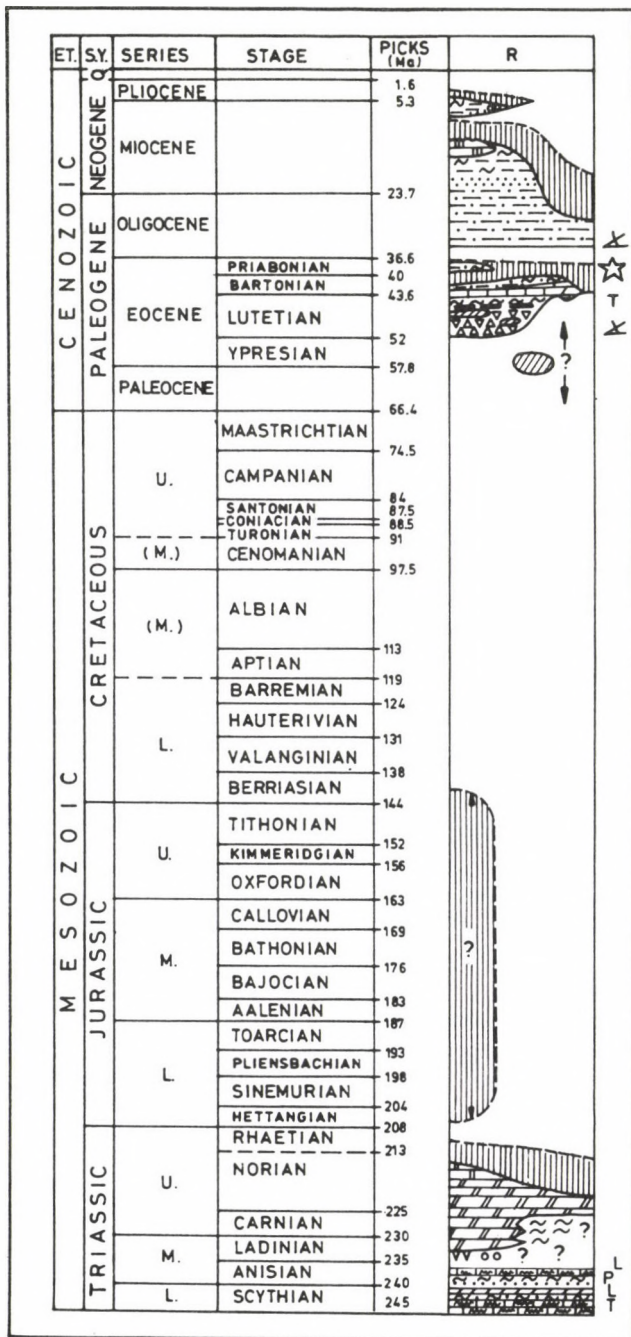


Fig. 1.
Regional correlation chart,
Transdanubian Central
Range (TCR) NE part, SE
side (for the legend see
Fig. 18) (Knauer)

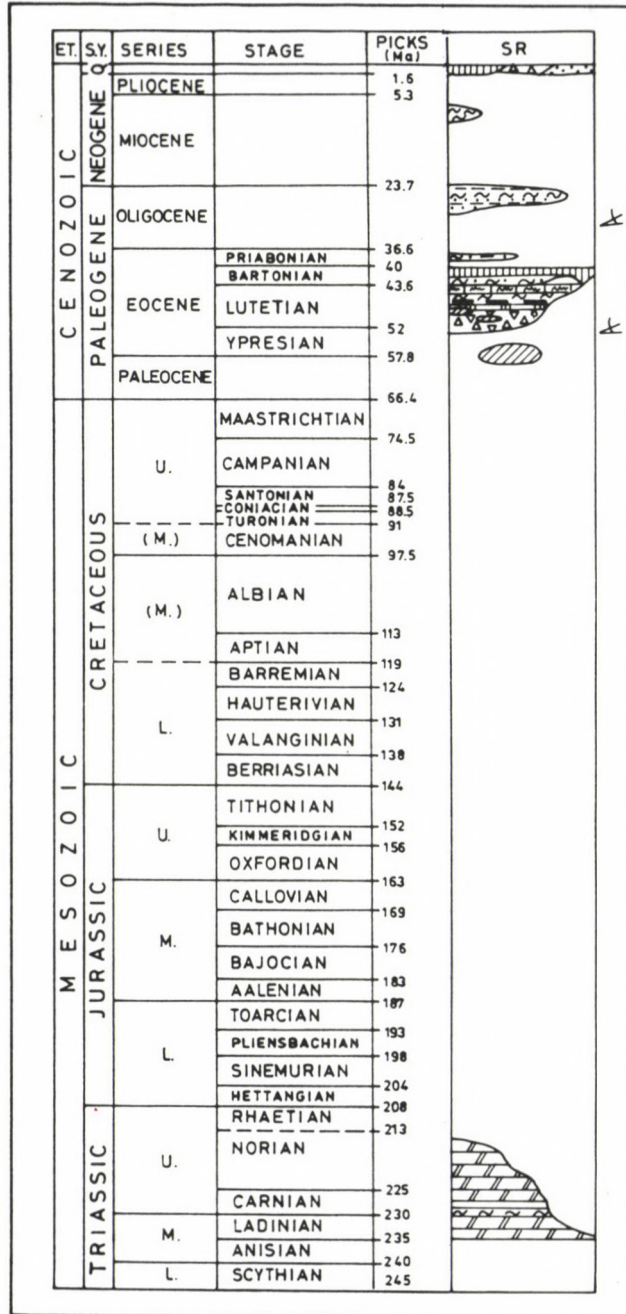


Fig. 2. Subregional (SR) correlation chart, Transdanubian Central Range (TCR) NE part, the Nagyegyháza area (for the legend see Fig. 18) (Tóth)

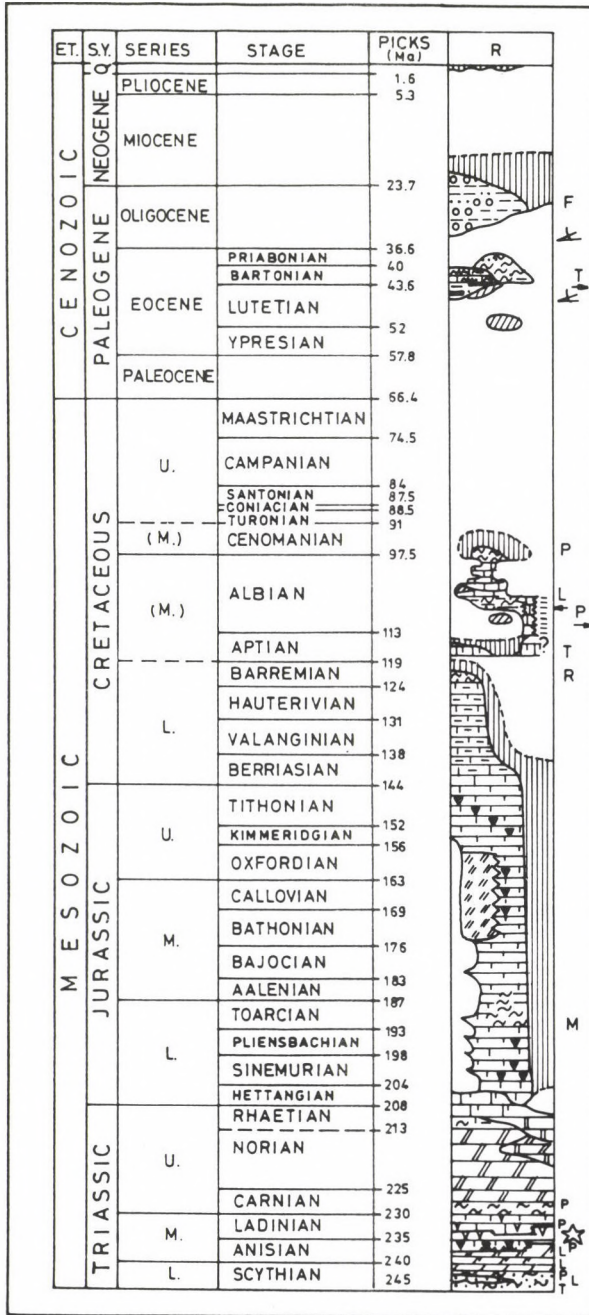


Fig. 3. Regional correlation chart, Transdanubian Central Range (TCR) Central part (for the legend see Fig. 18) (Knauer)

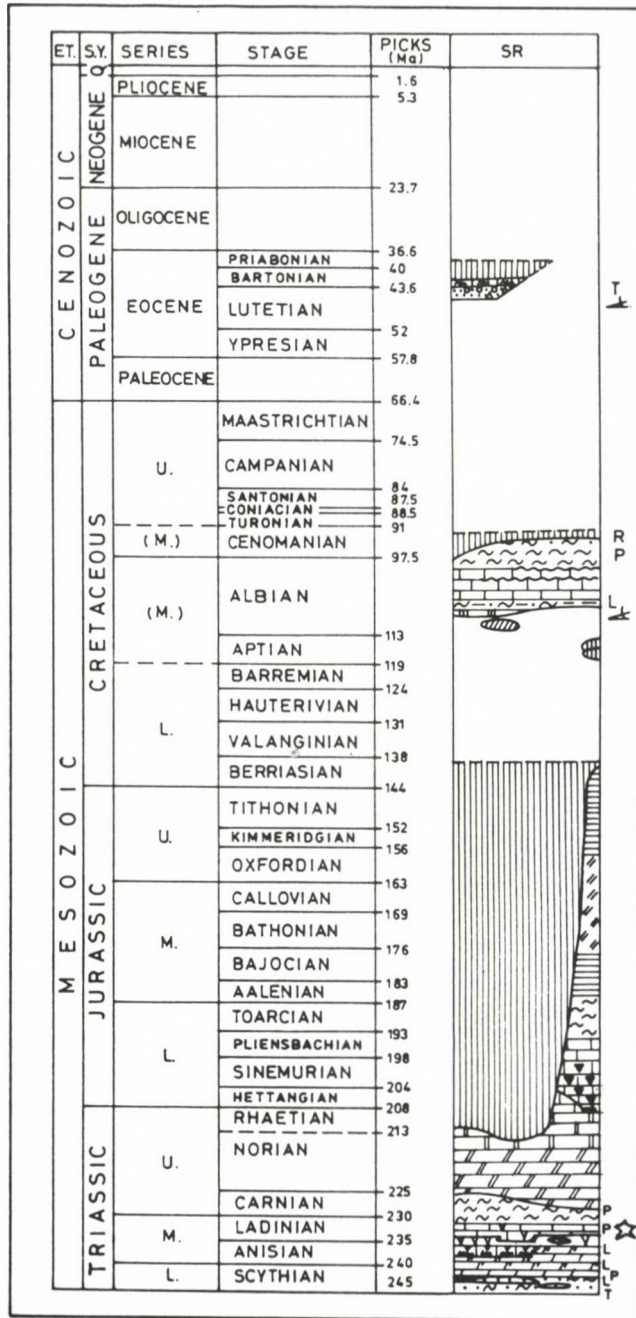


Fig. 4. Subregional (SR) correlation chart, Transdanubian Central Range (TCR) Central part, the Alsópere-Tés area (for the legend see Fig. 18) (Knauer)

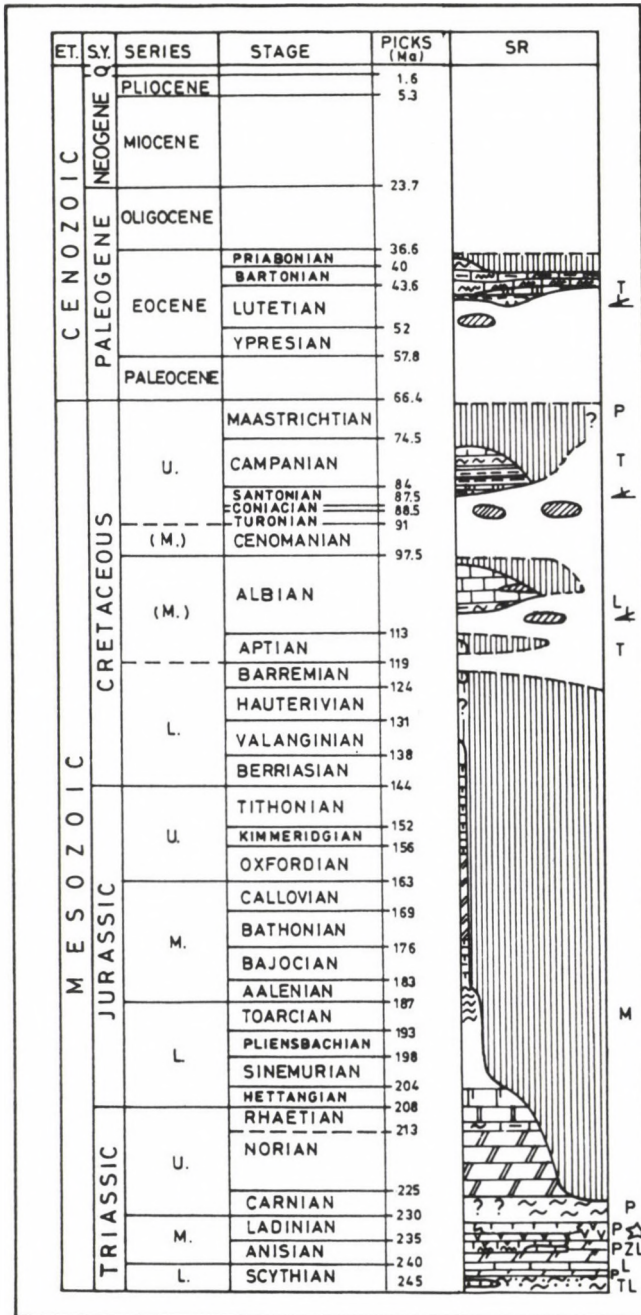


Fig. 5. Subregional (SR) correlation chart, Transdanubian Central Range (TCR) Central part, the central area of the S Bakony Mts. (for the legend see Fig. 18) (Knauer)

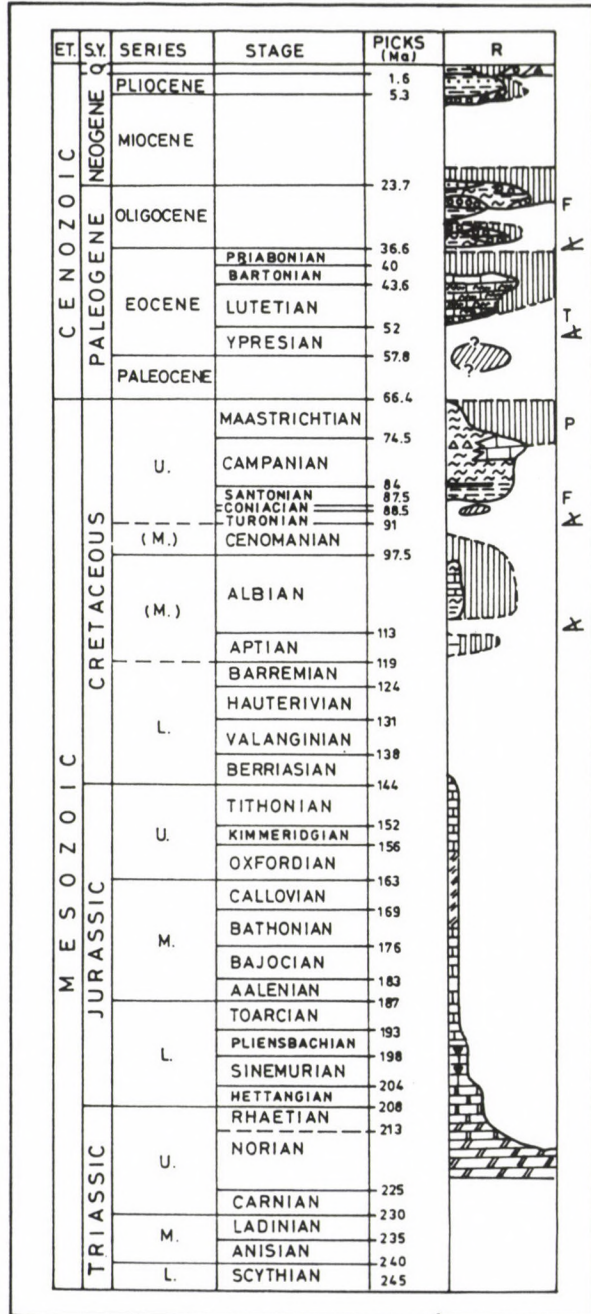


Fig. 6. Regional correlation chart, Transdanubian Central Range (TCR) NW part (for the legend see Fig. 18) (Tóth)

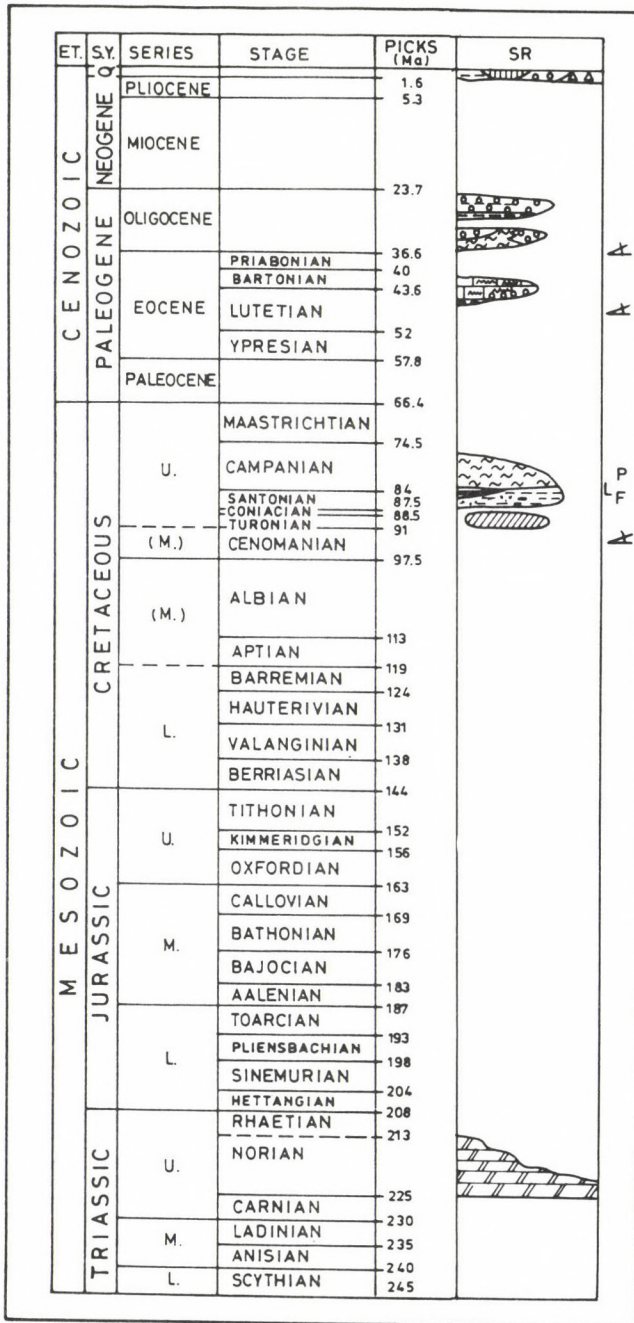


Fig. 7. Subregional correlation chart, Transdanubian Central Range (TCR) NW part, the Iharút area (for the legend see Fig. 18) (Tóth)

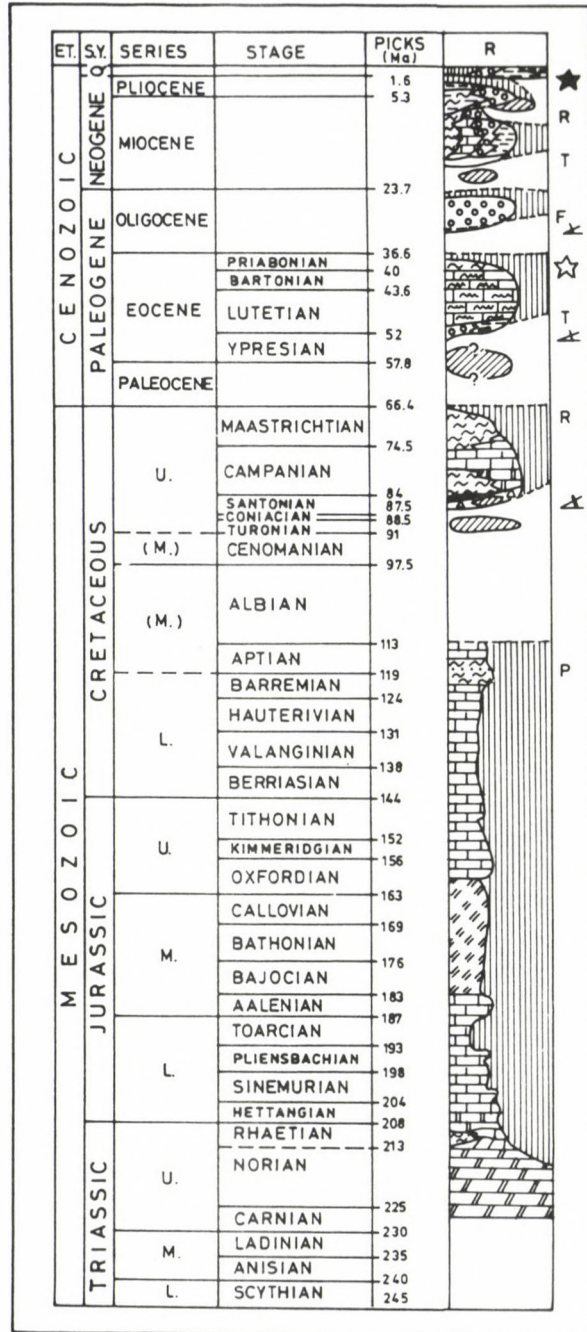


Fig. 8. Regional correlation chart, Transdanubian Central Range (TCR) SW part (for the legend see Fig. 18) (Tóth)

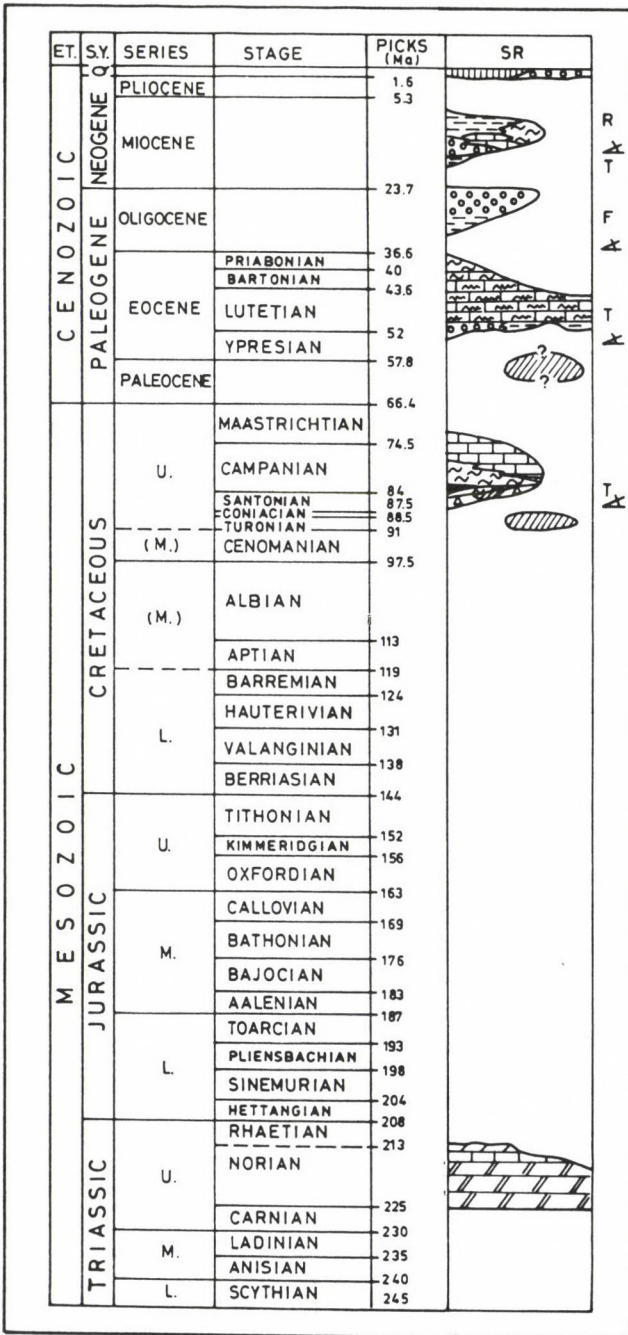


Fig. 9. Subregional correlation chart, Transdanubian Central Range (TCR) SW part, the Nyirád-Nagytárkány area (for the legend see Fig. 18) (Tóth)

TYPE LOCALITY :		CSABPUSZTA	NAGYTÁRKÁNY W.	NYIRÁD
PROCESSES BRINGING ABOUT SUBAERIAL EXPOSURE OF THE CARBONATE SUBSTRATE:		LARAMIAN PHASE	SUBHERZINIAN PHASE	AUSTRIAN TO LARAMIAN PHASE
IMPRINTS IN THE STRATIGRAPHIC RECORD	BAUXITIFEROUS UNCONFORMITY WITH PREVAILING "SURFACE"-KARST			
	NON-BAUXITIC UNCONFORMITY WITH PREVAILING "UNDERGROUND" KARST			
ANGULAR UNCONFORMITY		SLIGHT	MODERATE TO CONSIDERABLE	
ESTIMATED DURATION OF EXPOSURE:		18 MY	26 MY	min. 44 MY
APPARENT STRATIGRAPHIC GAP		MEDIAL	MEDIAL	LARGE
RATE OF REGIONAL SUBSIDENCE		SLOW TO FAST	RATHER FAST	SLOW
CHANGES IN LITHOFACIES OF ASSOCIATED CARBONATES ACROSS THE UNCONFORMITY				
RECORD OF CONTEMPORARY SEA LEVEL CHANGES :				
LITHOFACIES OF ASSOCIATED BAUXITES		DOMINANTLY RED PELITONORPHUS BAUXITE	INT: DIAGENETIC MOSTLY PISOIDIC -DETRITAL KT: Bx sandstone scattered by sand and pebbles in other rocks	NOT RECORDED AS YET
UNDERLYING KARST RELIEF:		SLIGHT	SLIGHT TO HIGH	SLIGHT TO MEDIAL
SUPPOSED SOURCE MATERIAL OF BAUXITES :		PARTLY: CAMPANIAN-MAASTRICHTIAN MARL	?	?
SUPPOSED SOURCE MATERIAL OF NON-BAUXITIC KARST-FILLS				

Fig. 10. Local profiles on SW part of Transdanubian Central Range (for the legend see Fig. 19) (Tóth)

TYPE LOCALITY :		IHARKÚT	IHARKÚT N
PROCESSES BRINGING ABOUT SUBAERIAL EXPOSURE OF THE CARBONATE SUBSTRATE:		SUBHERZINIAN PHASE	SUBHERZINIAN PHASE
IMPRINTS IN THE STRATIGRAPHIC RECORD	BAUXITIFEROUS UNCONFORMITY WITH PREVAILING „SURFACE“-KARST	UPPER 	SANTONIAN 
	NON-BAUXITIC UNCONFORMITY WITH PREVAILING „UNDERGROUND“ KARST	NT NOR	NT NORIAN
ANGULAR UNCONFORMITY		MODERATE	
ESTIMATED DURATION OF EXPOSURE:		26 MY	2 MY
APPARENT STRATIGRAPHIC GAP		MEDIAL	MEDIAL
RATE OF REGIONAL SUBSIDENCE		MODERATE	MODERATE
CHANGES IN LITHOFACIES OF ASSOCIATED CARBONATES ACROSS THE UNCONFORMITY			
RECORD OF CONTEMPORARY SEA LEVEL CHANGES :			
LITHOFACIES OF ASSOCIATED BAUXITES		DIAGENETIC DETRITAL RED BAUXITE	ADMIXTURE OF CARBONATE MATERIAL
UNDERLYING KARST RELIEF :		HIGH	HIGH
SUPPOSED SOURCE MATERIAL OF BAUXITES :			
SUPPOSED SOURCE MATERIAL OF NON-BAUXITIC KARST-FILLS			

Fig. 11. Local profiles on NW part of Transdanubian Central Range (for the legend see Fig. 19) (Tóth)

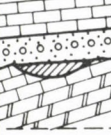
TYPE LOCALITY :		FENYŐFŐ	PORVA	BAKONYOSZLOP
PROCESSES BRINGING ABOUT SUBAERIAL EXPOSURE OF THE CARBONATE SUBSTRATE:		LARAMIAN PHASE ?	AUSTRIAN TO LARAMIAN PHASE	AUSTRIAN TO LARAMIAN PHASE
IMPRINTS IN THE STRATIGRAPHIC RECORD	BAUXITIFEROUS UNCONFORMITY WITH PREVAILING „SURFACE“-KARST			
	NON-BAUXITIC UNCONFORMITY WITH PREVAILING „UNDERGROUND“-KARST			
ANGULAR UNCONFORMITY		MODERATE TO CONSIDERABLE	MODERATE	MODERATE TO CONSIDERABLE
ESTIMATED DURATION OF EXPOSURE:		20 MY	51 MY	51 MY
APPARENT STRATIGRAPHIC GAP		MEDIAL	LARGE	LARGE
RATE OF REGIONAL SUBSIDENCE		RAPID TO MODERATE	RAPID	SLOW TO MODERATE
CHANGES IN LITHOFACIES OF ASSOCIATED CARBONATES ACROSS THE UNCONFORMITY				
RECORD OF CONTEMPORARY SEA LEVEL CHANGES :				
LITHOFACIES OF ASSOCIATED BAUXITES		PELITOMORPHOUS WITH BAUXITE PEBBLES		PELITOMORPHOUS WITH BAUXITE PEBBLES (MORE THAN AT FENYŐFŐ)
UNDERLYING KARST RELIEF:		SLIGHT TO HIGH	SLIGHT TO MEDIAL	SLIGHT TO HIGH
SUPPOSED SOURCE MATERIAL OF BAUXITES :		UNIDENTIFIED OLDER BAUXITE FORMATIONS	NOT RECORDED AS YET	UNIDENTIFIED OLDER BAUXITE FORMATIONS
SUPPOSED SOURCE MATERIAL OF NON-BAUXITIC KARST-FILLS				

Fig. 12. Local profiles on Central part, NW side of Transdanubian Central Range (for the legend see Fig. 19) (Tóth)

TYPE LOCALITY :		ISZKA-SZENTGYÖRGY	MAGYARALMÁS	GANT
PROCESSES BRINGING ABOUT SUBAERIAL EXPOSURE OF THE CARBONATE SUBSTRATE:		NEW KIMMERIAN TO LARAMIAN	NEW KIMMERIAN TO LARAMIAN	AUSTRJAN TO LARAMIAN
IMPRINTS IN THE STRATIGRAPHIC RECORD	BAUXITIFEROUS UNCONFORMITY WITH PREVAILING „SURFACE“-KARST			
	NON-BAUXITIC UNCONFORMITY WITH PREVAILING „UNDERGROUND“ KARST			
ANGULAR UNCONFORMITY		MODERATE	MODERATE	MODERATE
ESTIMATED DURATION OF EXPOSURE:		44 OR 90 MY	44 OR 90 MY	min 44 MY
APPARENT STRATIGRAPHIC GAP		LARGE	LARGE	MEDIAL PROBABLY LARGE
RATE OF REGIONAL SUBSIDENCE		SLOW	RATHER SLOW	SLOW
CHANGES IN LITHOFACIES OF ASSOCIATED CARBONATES ACROSS THE UNCONFORMITY				
RECORD OF CONTEMPORARY SEA LEVEL CHANGES :				
LITHOFACIES OF ASSOCIATED BAUXITES				DIAGENETIC PISOIDIC-DETRITAL
UNDERLYING KARST RELIEF:		MEDIAL	MEDIAL	MEDIAL
SUPPOSED SOURCE MATERIAL OF BAUXITES :				
SUPPOSED SOURCE MATERIAL OF NON-BAUXITIC KARST-FILLS				

Fig. 13. Local profiles on Central part, SE side of Transdanubian Central Range (for the legend see Fig. 19) (Tóth)

TYPE LOCALITY :		NAGYEGYHAZA				
PROCESSES BRINGING ABOUT SUBAERIAL EXPOSURE OF THE CARBONATE SUBSTRATE :		LARANIAN PHASE ?				
IMPRINTS IN THE STRATIGRAPHIC RECORD	BAUXITIFEROUS UNCONFORMITY WITH PREVAILING „SURFACE”-KARST					
	NON-BAUXITIC UNCONFORMITY WITH PREVAILING „UNDERGROUND” KARST					
ANGULAR UNCONFORMITY		MODERATE				
ESTIMATED DURATION OF EXPOSURE :		20 MY AT LEAST				
APPARENT STRATIGRAPHIC GAP		MEDIAL				
RATE OF REGIONAL SUBSIDENCE		RAPID TO SLOW				
CHANGES IN LITHOFACIES OF ASSOCIATED CARBONATES ACROSS THE UNCONFORMITY						
RECORD OF CONTEMPORARY SEA LEVEL CHANGES :						
LITHOFACIES OF ASSOCIATED BAUXITES		DOMINANTLY PELITOMORPHOUS BAUXITE				
UNDERLYING KARST RELIEF :		SLIGHT TO MEDIAL				
SUPPOSED SOURCE MATERIAL OF BAUXITES :						
SUPPOSED SOURCE MATERIAL OF NON-BAUXITIC KARST-FILLS						

Fig. 14. Local profile on NE part, SE side of Transdanubian Central Range (for the legend see Fig. 19) (Tóth)

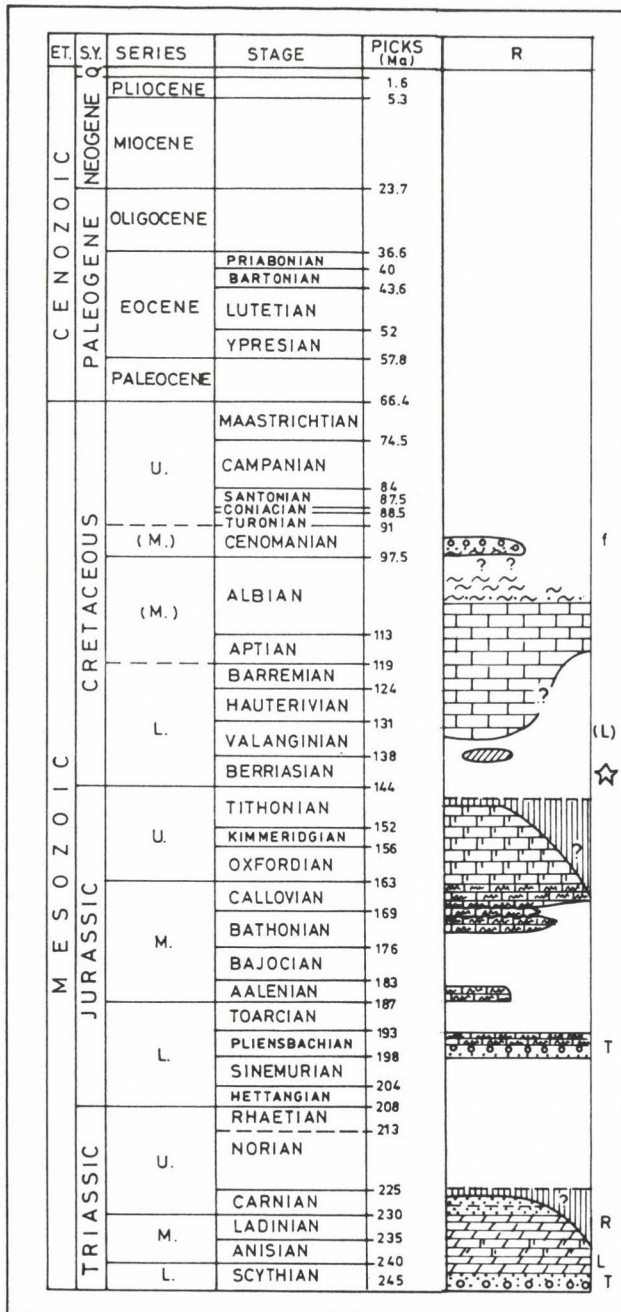


Fig. 15. Regional chart of the S Hungarian bauxite belt (for the legend see Fig. 18) (Fekete)

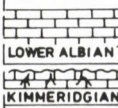
TYPE LOCALITY :		SZARSONLYÓ HILL	TENKES HILL		
PROCESSES BRINGING ABOUT SUBAERIAL EXPOSURE OF THE CARBONATE SUBSTRATE:					
IMPRINTS IN THE STRATIGRAPHIC RECORD	BAUXITIFEROUS UNCONFORMITY WITH PREVAILING „SURFACE“ KARST		NO BAUXITE RECORDED		
	NON-BAUXITIC UNCONFORMITY WITH PREVAILING „UNDERGROUND“ KARST				
ANGULAR UNCONFORMITY		NO	NO OR SLIGHT		
ESTIMATED DURATION OF EXPOSURE:		5-6 MY	35-40 MY		
APPARENT STRATIGRAPHIC GAP		SMALL	LARGE		
RATE OF REGIONAL SUBSIDENCE		NOT RECORDED	NOT RECORDED		
CHANGES IN LITHOFACIES OF ASSOCIATED CARBONATES ACROSS THE UNCONFORMITY		SLIGHT	SLIGHT		
RECORD OF CONTEMPORARY SEA LEVEL CHANGES :		?	?		
LITHOFACIES OF ASSOCIATED BAUXITES		MAINLY OOIDIC	NO BAUXITE		
UNDERLYING KARST RELIEF :		SHALLOW	NOT RECORDED		
SUPPOSED SOURCE MATERIAL OF BAUXITES :		NO DIRECT EVIDENCES			
SUPPOSED SOURCE MATERIAL OF NON-BAUXITIC KARST-FILLS		NO DIRECT EVIDENCES			

Fig. 16. Local profiles of the S Hungarian bauxite belt (for the legend see Fig. 19) (Fekete)

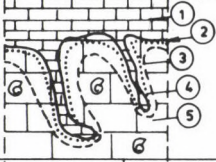
TYPE LOCALITY :		PÉNZESGYŐR SE (TILOS ERDŐ)	ALSÓPERE	BALINKA-MÓR
PROCESSES BRINGING ABOUT SUBAERIAL EXPOSURE OF THE CARBONATE SUBSTRATE:		TECTONICS	TECTONICS	TECTONICS
IMPRINTS IN THE STRATIGRAPHIC RECORD	BAUXITIFEROUS UNCONFORMITY WITH PREVAILING „SURFACE“-KARST			
	NON-BAUXITIC UNCONFORMITY WITH PREVAILING „UNDERGROUND“-KARST			
ANGULAR UNCONFORMITY		NO	NO	NO
ESTIMATED DURATION OF EXPOSURE:		~ 1MY	< 1MY	> 1MY
APPARENT STRATIGRAPHIC GAP		SMALL	VERY SMALL	NOT SO SMALL
RATE OF REGIONAL SUBSIDENCE IN THE NEIGHBOURHOOD		SLOW	VERY SLOW	SLOW TO MODERATE
CHANGES IN LITHOFACIES OF ASSOCIATED CARBONATES ACROSS THE UNCONFORMITY		SLOW (APPEARANCE OF THE FINE DEBRIS OF THE DENUDATED U. ALBIAN LIMESTONE)		
RECORD OF CONTEMPORARY SEA LEVEL CHANGES :				
LITHOFACIES OF ASSOCIATED BAUXITES			NO BAUXITE !	
UNDERLYING KARST RELIEF :		ROCKY	SLIGHT	SLIGHT WITH 3-10 m DEEP KARSTIFIED FISSURES
* DETAIL OF THE LOWER GAP (ALSÓPERE TYPE)				
SOURCE MATERIAL OF NON-BAUXITIC KARST-FILLS		—	—	MATERIAL OF THE NEW SEDIMENTATION (GLAUCONITIC LIMY MARL, LIMESTONE)

Fig. 17.

Non-bauxitic unconformities in the Upper–Uppermost Albian sequence of the central part of the TCR. 1. Grey, Echinodermata debris bearing limestone with glauconite (Zirc Limestone Fm. Gajavölgy Limestone Member); 2. Karstified surface of the Mesterhajag Limestone Member (Zirc Lst. Fm.); 3. Secondarily reduced zone (2 to 10 mm); 4. Oxidated zone (10 to 50 mm); 5. Limestone rich in Annelids, Exogyra and Orbitolina somewhere with other bivalves and gastropods (Kőrisedő Bed of the Mesterhajag M.) 6. Other subunits of the Mesterhajag; M–Orbitolina bearing lmst. (up), small-foram. bearing lmst. (down); 7–8. Pénzeskút Marl Fm.; 8. Villóhegy Bed (nodular marl or calcareous marl abundant in ammonites, echinoidea and gastropods (Knauer)

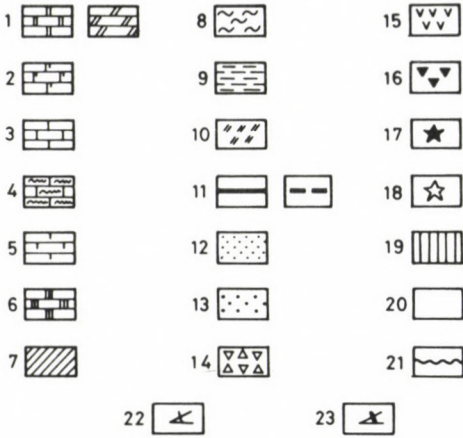


Fig. 18.

Legend for the 1st to 9th and 15th Figures.

1-6. Carbonate rocks; 1. Platform (dominantly or partly loferite) limestone, dolomite, 2. Quasi-platform, 3. Patch- reef, peri-reef and other related rocks, 4. Other shallow-water neritic marine rocks, 5. The rest (marine), 6. Non-marine rocks, 7-16. Other rocks; 7. Bauxite (bauxite bearing formations), 8. Marl, 9. Shale, clay, 10. Radiolarite, 11. Coal bearing formations, paralic, limnic, 12. Sand, sandstone, 13. Pebbles, conglomerate, debris; 15. Tuff; 16. Chert; 17. Volcanism; 18. Distant volcanism; 19. Erosional hiatus; 20. Non-depositional hiatus; 21. Small gap; 22. Low angular unconformity; 23. High angular unconformity; M-mangani-ferous; F-fluvial (fluvio-lacustric); N-near-shore; L-lagoonal; Z-reef and related rocks; T-trans-gressive; R-regressive; P: pelagic; f -Flysh-like

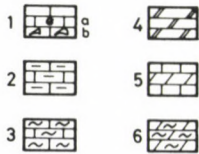


Fig. 19.

Legend for the 10th to 14th and 16th Figures.

1. Limestone, a. Fossil bearing lmst., b. Orbitolina bearing lmst. 2. Argillaceous limestone; 3. Calcareous marl; 4. Dolomite; 5. Dolomitic limestone, calcareous dolomite 6. marly dolomite, for others see Fig. 18. (7 to 9, 12 to 14 and 21)

References

- Mindszenty, A., J. Knauer, F. Szantner 1984: Sedimentological features and the conditions of accumulation of the Iharkút bauxite deposit - *Földtani Közlöny* 114, 1, pp. 19-48.
- Szantner, F., J. Knauer, A. Mindszenty 1986: Bauxitprognózis (The scientific basis and realization of karst bauxite forecast (in Hungarian) pp. 1-467. - Veszprém Committee of Hungarian Academy of Sciences

Application of sedimentological methods to karst bauxites evaluation: the Halimba–Szóc area, Hungary

György Bárdossy
*Hungarian Aluminium Corporation,
Budapest*

Erika Juhász
*Hungarian Geological Institute,
Budapest*

Sedimentological methods were applied by the authors to the study of the Halimba–Szóc bauxite deposits. Mine profiles, borehole samples and thin sections have been evaluated. The main sedimentary facies and their spatial distribution were established. The mode and direction of the bauxite transportation have been determined. The results can be helpful in locating potential high-grade deposits in the area. The methods are suitable for other allochthonous karst bauxite deposits as well.

Key words: Bauxite, exploration, paleogeography, sedimentology

Introduction

Many karst bauxite deposits are of allochthonous and parallochthonous origin (Bárdossy 1982); however, so far sedimentologic methods have been used rarely to their study. To mention are the works of Combes (1972, 1979, 1987, 1990) who first applied these methods for the genetic study of karst bauxite deposits.

In this study we aim to demonstrate the advantages of a sedimentological study in a well explored and partially mined bauxite district of Hungary, where ample information is available on the geometry of the deposits and on their chemical and mineralogical composition.

We developed a new terminology for the description of the sedimentological properties of bauxite in the study area. The nomenclature of Folk (1959) and Dunham (1962) for the classification of carbonate rocks, served as a basis, and was completed by the terminology developed by Mindszenty (1983, 1984) for bauxite textures.

Geological description of the Halimba–Szóc area

The study area is situated in the south-western part of the main bauxite region of Hungary, the Transdanubian Central Range, and it covers about 80 km² (Fig. 1). The area consists of two sedimentary basins separated by a zone of tectonically uplifted Upper Triassic rocks (Fig. 2). The larger, northern basin is the Halimba-Basin, the southern one the Szóc-Basin. Geological observations, some exploration results and laboratory investigations on the bauxite deposits have been published

Addresses: György Bárdossy: H-1387 Budapest, P.O.B. 30, Hungary
Erika Juhász: H-1442 Budapest, P.O.B. 106, Hungary

Received: 14 August, 1991

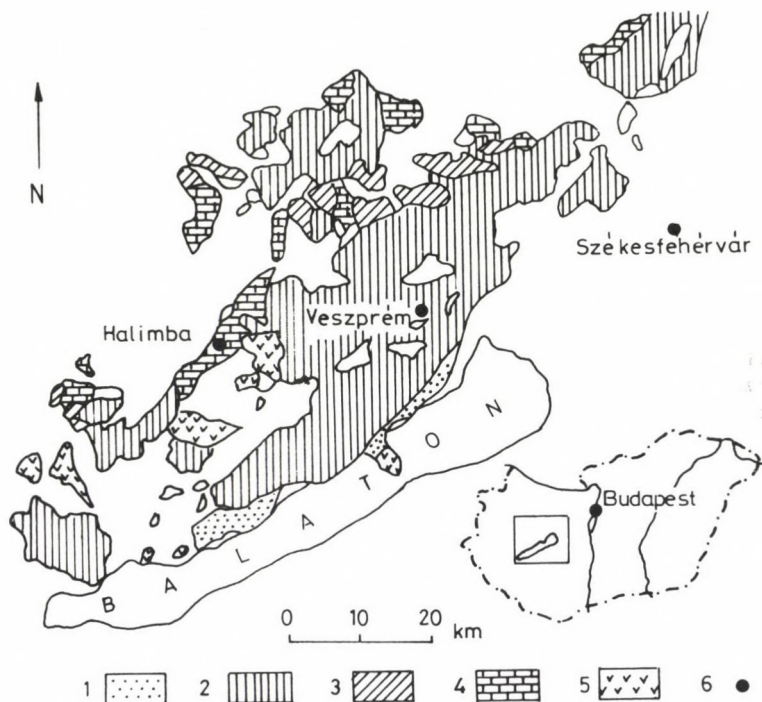


Fig. 1.

Location of the study area. 1. Paleozoic sediments; 2. Triassic to Early Cretaceous sediments; 3. Late Cretaceous sediments; 4. Eocene limestone; 5. Plio-Quaternary basalt; 6. city

by Bárdossy (1957, 1982), Barnabás (1970), Erdélyi (1965), Mindszenty and Gál-Solyomos (1988), Szantner, Knauer and Mindszenty (1986), but no systematic sedimentologic studies were carried out, except the Halimba deposit, evaluated by Juhász (1988, 1989).

A stratiform bauxite deposit occupies the central part of the *Halimba Basin* covering an area of 7 km². The bauxite is underlain by Norian dolostone and by Rhaetian limestone of the "Dachstein" facies. The bauxite is generally 5 to 10 m thick, with a maximum of 35 m in some major karst depressions. The north-western part of the deposit is covered by Senonian sediments consisting of limnic coal measures, marl and coarse conglomerate. The southeastern part of the deposit has a Middle Eocene cover, representing a slow transgression of the epicontinental sea during the Lutetian. The extent of the Senian cover is indicated on Fig. 2.

Along the south-eastern rim of the Halimba Basin ten lenticular bauxite deposits have been explored, called the *Malomvölgy group*. The size of the deposits varies from 0.1 to 0.5 km². The average thickness of the bauxite is less than 10 m, however in local karstic depressions it may reach 15–20 m. The bauxite is underlain by Norian dolostone and it is covered by Middle Eocene clay, lignite, marl and Nummulitic limestone. The Malomvölgy group is separated from the stratiform

Halimba deposit by a zone of 0.5–2 km width, where no bauxite was found between the Triassic and Middle Eocene sediments.

The Szóc Basin is characterized by lenticular deposits, similar in size, shape and stratigraphic position to those of the Malomvölgy area. In the southern part of the Szóc Basin the Eocene cover has been eroded. The remaining bauxite deposits are overlain in this area by Miocene and Pliocene clay and other sediments.

The entire study area has a typical block-faulted structure. The two basins are separated from each other and from the neighbouring Nyirád Basin by major fault

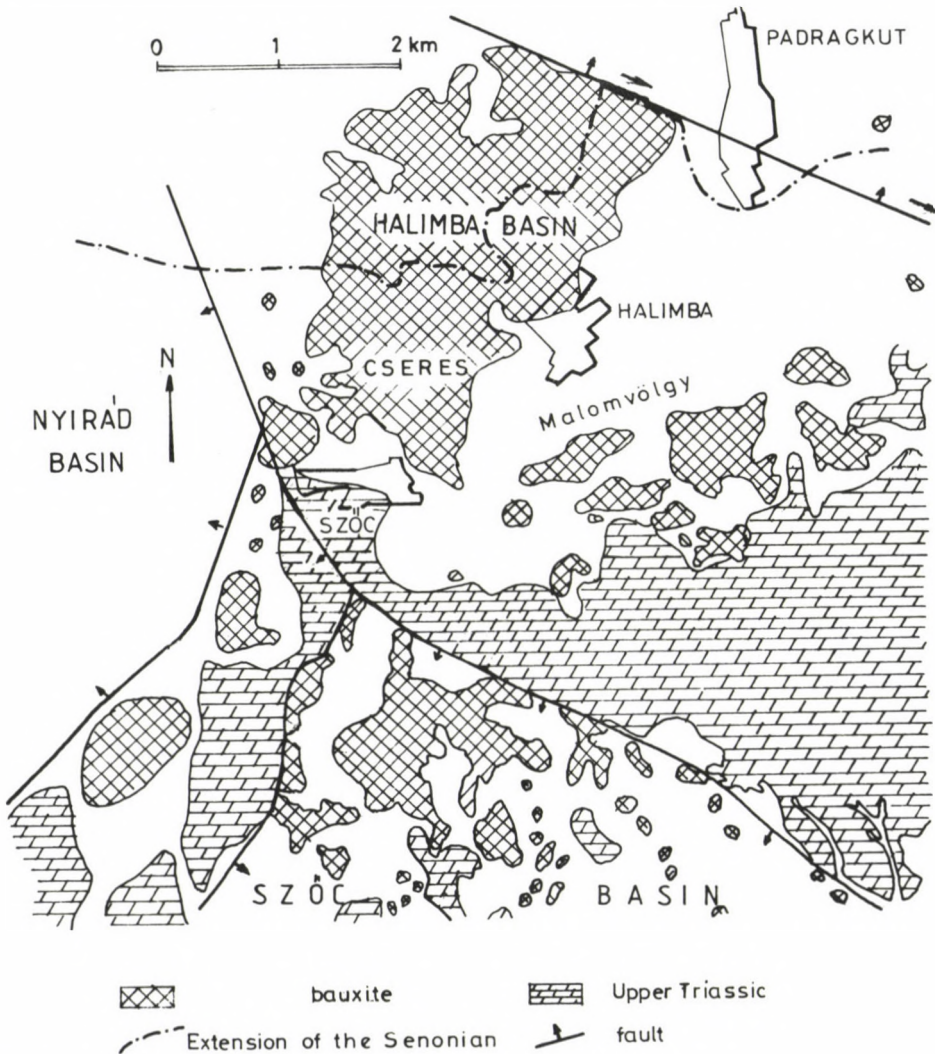


Fig. 2.
Simplified geological map of the Halimba–Szóc area

lines. Minor faults dissect the deposits. Horizontal displacement of kilometre scale has been detected along a fault line bordering the Halimba deposit to the north-east.

The Halimba deposit was formed during the Turonian – Coniacian – Santonian period. On the other hand, the bauxite of the Malomvölgy area and of the Szóc Basin were transported to their present place during the Paleocene and Early Eocene (Bárdossy 1982).

Sampling and methods of investigation

Detailed exploration was carried out in this area since the forties. Several thousand boreholes have been drilled and the bauxite cores have been analyzed for chemical and mineralogical composition by the Bauxite Prospecting Company of the Hungarian Aluminium Corporation. The majority of these data remained unpublished.

The major part of the bauxite deposits has been extracted already by surface and underground mining. At the present time mining activity continues only in the central and northern parts of the Halimba deposit. Systematic sampling, and description of bauxite profiles have been performed by Bárdossy during the entire mining period since 1950. In addition samples taken from exploration boreholes were described. Juhász collected samples from selected exploration boreholes and from the galleries of the present-day Halimba mine.

Altogether we investigated more than 1200 samples macroscopically and in thin sections. Additional chemical, X-ray, thermal and scanning electron microscope studies were carried out on selected samples, and their results were used to complete the sedimentological picture. Finally, the paleoenvironment has been studied, giving us information on the mode, direction and distance of transport; on the depositional properties of the sedimentary basin and on the changes in bauxite quality due to accumulation environment.

The limited extent of this paper prevents us to present our observations and investigations in detail, only the main results and conclusions are presented in the following.

The Senonian bauxite of the Halimba area

At the time of the bauxite formation the Halimba Basin was a karstic alluvial plain, of low relief, corresponding to a mature morphology. The lithological properties, particularly the bedding characteristics of the bauxite refers to a fluvial environment. Within the deposit channel-bar, channel load, flood-plain, flood basin and marsh facies could be distinguished, according to the detailed studies of Juhász (1988).

The sedimentological properties of the Haliba bauxite have been evaluated along profiles across the deposit (Fig. 3).

We conclude that the bauxites has been brought to the Halimba Basin by a river, from a distance of a few tens of kilometres. The source area was situated presumably to the east-southeast of the Halimba Basin. Transportation of bauxite material was followed by deposition of non bauxitic pelitic material, and than by coarse conglomerate. The latter represents the Late Senonian cover of the Halimba bauxite deposit.

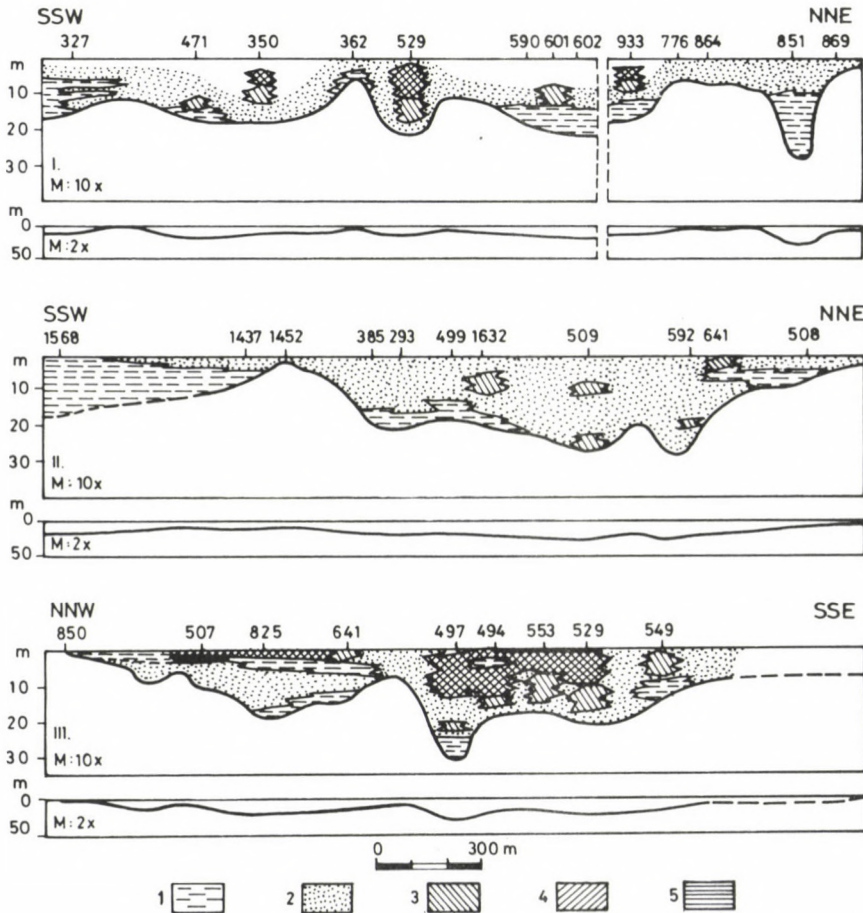


Fig. 3. Halimba deposit. Facies distribution along profiles. 1. Flood-basin facies; 2. Flood-plain facies; 3. Channel-bar facies; 4. Channel-load facies; 5. Marshy facies

Eocene bauxite on the top of the Halimba deposit

During the Paleocene and the Early Eocene parts of the overburden and of the bauxite has been eroded. In low-lying places marshes formed on the bauxite surface. Pollen grains, found in the marshy sediments mark the oldest Eocene in the Transdanubian Central Range (Juhász 1989). This fixed the beginning of the Eocene bauxite accumulation in the Halimba area. The flat-bottom erosion valleys were filled by locally reworked Senonian bauxitic material, mixed with newly formed Eocene bauxite. This bauxite was probably transported by sheet-wash over a short distance – less than 1 km – to its present place. Its occurrence is limited to the south-eastern part of the Halimba deposit and its thickness is generally less than 10 m.

The Malomvölgy bauxite area

The bauxite of the Malomvölgy deposits is unstratified and massive. The main part of the deposits is of aphanitic-intraclastic texture, rarely with few small bauxite clasts (Bárdossy 1982). The upper part of the bauxite profile has been altered by diagenetic and epigenetic processes, producing a bleached or mottled zone 0.5 to 2.0 m thick. Below this horizon, generally at 3–5 m below the top of the deposits, bauxite pebbles, cobbles and even boulders occur in the red aphanitic bauxite. At some places they form a 0.3 to 2.0 m thick layer.

The texture of these bauxite clasts differs essentially from the textures described before from the Halimba area. The bauxite pebbles and boulders consist of densely packed, well rounded and sorted bauxite clasts ("round-grains") of 2 to 5 mm diameter. Rarely bimodal sorting also occurs. Some of the grains have a texture resembling the duricrust of lateritic bauxite profiles. Composite rounded grains also occur, indicating three or more successive events of local reworking. The texture of the boulders is packstone; the matrix being generally well crystallized, gibbsitic. Some boulders are cut by fissures filled with mosaic-calcite, indicating that the clasts have been previously in a vadose diagenetic environment.

The size of the pebbles and boulders varies from 1 to 60 cm in diameter. The largest boulders have been found by us in the south-eastern part of the Malomvölgy area. The size of the boulders quickly diminishes in NW direction. In the northern deposits only a 20–30 cm thick pebbly layer was found with pebbles smaller than 5 cm in diameter. According to the borehole descriptions, no bauxite pebbles were found in the north-western part of this bauxite-area, only aphanitic clayey bauxite and bauxitic clay occurs, as shown on Fig. 4, illustrating typical lithologic profiles observed by us in the open pits.

The highest quality (mainly exploited) bauxite was situated in the south and south-eastern parts of this group of deposits. The alumina content decreases, the silica increases in north-western direction.

The Malomvölgy bauxite differs essentially from the Halimba bauxite, in chemical, mineralogical respects, representing a new and younger bauxite

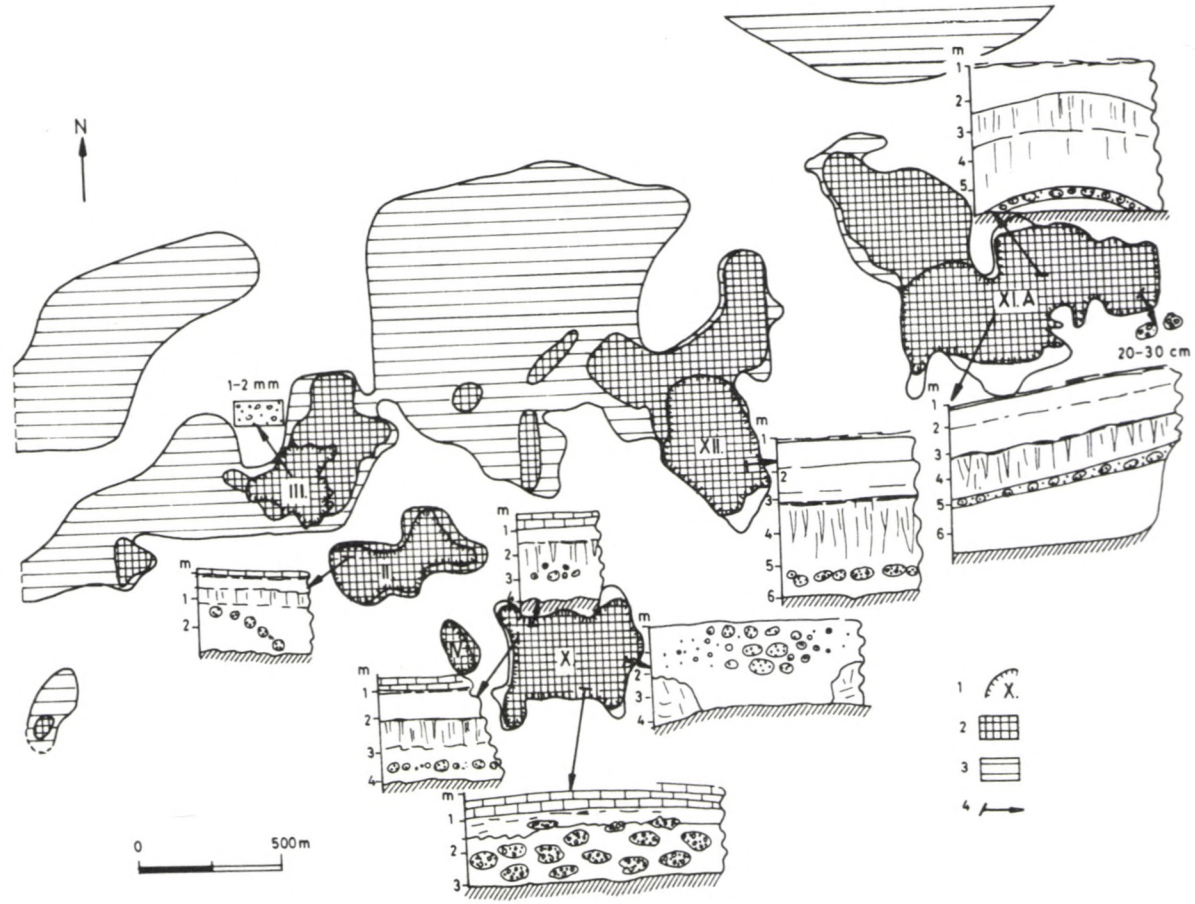


Fig. 4. The Malomvölgy group of deposits. 1. open pits with number; 2. commercial bauxite; 3. clayey bauxite and bauxitic clay; 4. location of the profiles

accumulation (Bárdossy 1982). Its material has been derived in our opinion from the south-east, from a fairly well consolidated older bauxite deposit. At the beginning the loose and fine-grained – mainly clayey – material was washed out and it was transported by "debris flows" to the nearby karstic area. In a second step, more violent, but ephemeral streams transported the rest of the material – partly in the form of coarse clasts – to the Malomvölgy area.

The Szőc bauxite basin

The deposits of the Szőc Basin area are situated to the SSW of the Malomvölgy area, and are of 8–12 m thickness. The bauxite profile is generally similar to that of the Malomvölgy deposits (Bárdossy 1982). The diagenetically and epigenetically altered bauxite zone in the upper part of the profile is found almost in all deposits in 0.5 to 2.0 m thickness. The texture of the bauxite is mainly aphanitic and finely intraclastic; no oolites or pisolites can be observed in it. In the middle part of the profile – about 3–4 m under the top – a layer of clastic bauxite can be observed 30–50 cm in thickness. The bauxite pebbles are less than 30 cm in diameter. Below this layer again aphanitic bauxite can be observed, becoming more and more clayey towards the bottom, and passing into a bauxitic clay. The pebbles are well rounded and they have a packstone texture with well sorted rounded grains of 2 to 5 mm size. The texture of some pebbles resembles the duricrust of lateritic bauxite profiles. The matrix is aphanitic with authigenic gibbsite crystals of more than 10 μm size and small intraclasts. The matrix is more gibbsitic in the central and south-eastern parts of Szőc Basin than at its north-western edge. In our opinion, this is due to differences in the geomorphologic and hydrogeologic position of the deposits at the time of the bauxite accumulation; the central and south-eastern area being more elevated than the north-western one.

Clastic bauxite grains of 0.5 to 2.0 mm size can be observed in the matrix of the pebbly layer. They are of dark red colour and have a high iron content. Such clastic grains are very rare in other parts of the bauxite profile.

The sedimentation of the bauxite in the Szőc Basin was very similar to that of the Malomvölgy area, described above. The average and maximum grain size of the bauxitic clasts however are smaller in the Szőc Basin than in the Malomvölgy area, indicating a relatively more quiet depositional environment.

Conclusions

Our field observations and sedimentological investigations led us to propose a new paleogeographical and sedimentological model for the bauxite accumulation in the study area. Our main conclusions are:

- All bauxite deposits of the Halimba-Szőc area are of allochthonous origin, in contrast to former ideas. Their material derived from erosion of older bauxite deposits possibly of lateritic origin.

– The Senonian covered and the Middle Eocene covered deposits differ not only in the length of the stratigraphic gap between their footwall and overburden,

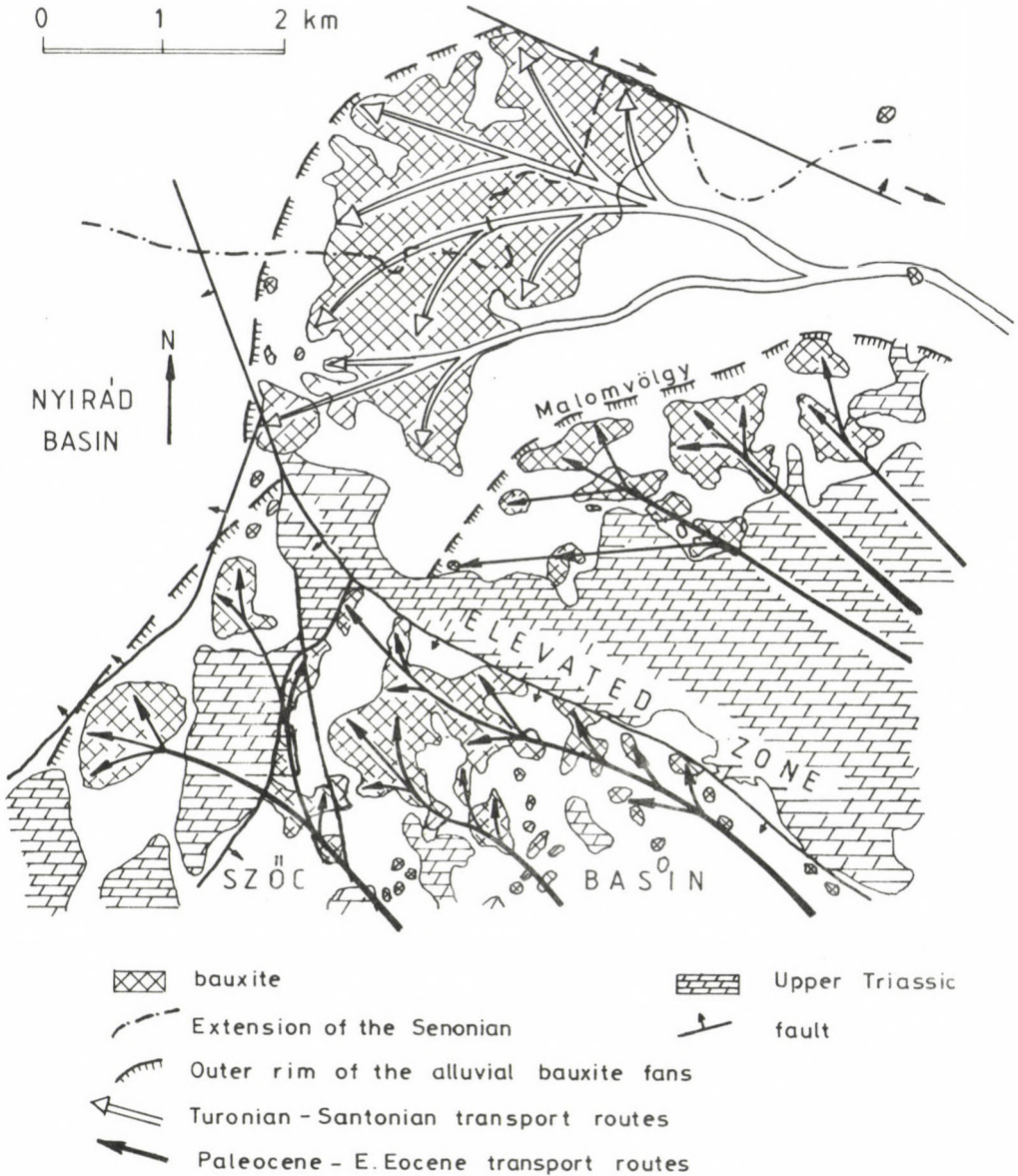


Fig. 5. Reconstruction of the main bauxite transport routes and of the alluvial bauxite fans in the Halimba-Szóc areas. 1. Presumed Turonian-Santonian transport routes; 2. Presumed Paleocene-Early Eocene transport routes; 3. Outer rim of the alluvial bauxite-fans

but they represent in our opinion two different sedimentological phases of bauxite transportation and accumulation.

– The first phase took place during the Turonian–Santonian time leading to the accumulation of a stratiform deposit in the Halimba Basin. The second phase occurred in the Paleocene and Early Eocene and it led to the formation of lenticular deposits in the Malomvölgy area and in the Szóc Basin. The difference in size and geometry of the deposits of the two phases is related to differences in the mode of transportation of the bauxite and in slightly differing paleomorphological conditions.

– The deposits of the two bauxite-forming periods are laterally separated by a barren zone of 0.5 to 2.0 km width. Another barren zone of 1 to 6 km width separates the Halimba–Szóc deposits from those of the Nyírád bauxite district, situated to the west of this area (Fig. 5).

– Sedimentological evidence indicates that the mode and the direction of transportation was different in the two bauxite-forming phases. During the first phase the bauxite was transported by river to the deposition area. This assumption has been confirmed by recognition of channel-bar, channel-load, flood-plain, and flood-basin facies in the Halimba deposit. During the second phase presumably first fine-grained clayey-bauxitic mud and fine clasts were brought into the karst area by several, more or less parallel debris flows. It was followed by deposition of coarse bauxite pebbles and boulders, transported by violent ephemeral streams. Bauxite transportation ended with fine grained bauxitic mud, deposition which was followed by the formation of marshes in local depressions.

– The bauxitic sediment accumulated during both phases in the form of large alluvial fans, pinching out along convex arcuate lines, as illustrated in Fig. 5. The presumed main transport axes are also indicated on the map.

– It is a common feature for both phases that only fine clayey bauxite and bauxitic clay reached the outer rim of the fans. The highest grade bauxite accumulated in the central and inner parts of the fans, along high energy zones, with maximum transport energy.

– An ESE–WNW main transport direction can be suggested for the central and northern part of the Halimba deposit. For the southern part of the deposit – called Cseres – a south-westward directed branch of the main river is presumed.

– It is very likely that the bauxite was brought into the Malomvölgy area by three or four, more or less parallel SE–NW directed periodic streams (Fig. 5). The highest energy transport occurred in the southern part of the area, as indicated by the large bauxite boulders of the Malomvölgy X. deposit.

– A similar mode of transport has been recognized for the deposits of the Szóc Basin. However it must have been a lower energy flow, as indicated by the smaller size of the bauxite clasts. The main direction here again was SE–NW and it occurred presumably along three main transport routes (Fig. 5).

– There is a marked difference in the form of the bauxite fan of the two areas: the Szóc fan is more elongated in SE–NW direction – its length is about 4 km, whereas the Malomvölgy fan is only less than 2 km wide.

– The two areas were separated at the time of the bauxite transportation by an elevated zone of Triassic dolostones. This hill or cliff still existed when both bauxite areas were submerged by the Middle Eocene sea. Large – up to 50 cm – dolostone boulders, embedded in the Eocene limestone confirm this idea.

– In contrast to the stratiform Halimba deposit, the bauxite of the Malomvölgy and Szóc fans did not form a continuous sheet, it only filled flat-bottom paleovalleys and more or less isolated karstic depressions. The reasons for this difference are not completely clear, presumably a more elevated and accentuated karst morphology was the main controlling factor.

– The alluvial bauxite fan has been covered almost immediately by Late Senonian sediments in the Halimba Basin, allowing no time for an *in situ* bauxitization. Our sedimentological investigations indicate that in the Malomvölgy and Szóc areas the transgression was not so immediate. The climate being favourable, (Bárdossy 1982) an *in situ* continuation of the bauxitisation is very likely. However, this process did not change considerably the composition of the bauxitic sediment. This could be concluded from the study of a large number of chemical bauxite profiles, showing only few gradual vertical changes of the chemical components, typical for autochthonous bauxite deposits. On the other hand, strong diagenetic chemical alterations affected the top part of the deposits under the influence of their marshy cover e.g. part of their initial iron content has been leached, the other part being transformed into pyrite or marcasite. In places where the Eocene overburden has been entirely eroded or thinned to less than 10 meters, epigenetic oxidation of the reduced pyrite-bearing bauxite occurred, with the formation of secondary sulphate minerals and secondary iron crusts and concretions. These diagenetic and epigenetic processes often conceal the initial sedimentary textures and structures in the top part of the deposits.

– The new sedimentological model outlined above has also practical consequences for bauxite exploration and mining in the given area. E.g. The optimum zone of high-grade bauxite could be located in all the three alluvial bauxite-fans. Furthermore there is little or no hope to find new commercial bauxite deposits along the outer rim of the fans or outside the fans.

References

- Bárdossy, Gy. 1957: Der Bauxit der Umgebung von Szőc und Nyirád. – Jahrbuch der Ungarischen Geologischen Anstalt. Vol. XLVI. fasc. 3, pp. 433–454 Budapest
- Bárdossy, Gy. 1982: Karst Bauxites. Bauxite Deposits on Carbonate Rocks. – Elsevier Scientific Publ. Co. Amterdam – Oxford – New York. p. 441.
- Barnabás, K. 1970: Die vergleichende Untersuchung der charakteristischen Bauxitlagerstätten des Mittelgebirges von Dunántúl. – Jahrbuch der Ungarischen Geologischen Anstalt. Vol. LIV. fasc. 3, pp. 69–93 Budapest
- Combes, P.J. 1972: Les différents types de bauxite sur substratum carbonaté dans le Languedoc et l'Ariège. – C. R. Acad. Sci. Paris t, 274. pp. 1613–1616
- Combes, P.J. 1979: Observations sédimentologiques, paléogéographiques, minéralogiques et géochimiques sur les bauxites du deuxième horizon dans la zone du Parnasse, Grèce. – Bull. Soc. Géol. France. t. XXI, pp. 485–494.
- Combes, P.J. 1987: Les bauxites du sud de la France: schéma de synthèse, relations avec les marges Iberique et Européenne au Crétacé moyen. – lier Congrès Français de Sédimentologie. pp. 110–111. Paris.
- Combes, P.J. 1990: Typologie, cadre géodynamique et genèse des bauxites françaises. – Geodinamica Acta, 4. 2, pp. 91–109. Paris.
- Dunham, R.J. 1962: Classification of carbonate rocks according to depositional texture. – Mem. Am. Assoc. Petrol. Geol. Tulsa. 1, pp. 108–121.
- Erdélyi, M. 1965: Geological studies in the Halimba Basin. – Acta Geologica Hung. IX, pp. 339–362. Budapest.
- Folk, R.L. 1959: Practical classification of limestones. – Am. Assoc. Petrol. Geol. Bull. V. 43, pp. 1–38.
- Juhász, E. 1988. Sedimentological features of the Halimba bauxite and paleogeographic reconstruction. – Acta Geologica Hung. 31, pp. 111–136. Budapest.
- Juhász, E. 1989: Joint occurrence of Late Cretaceous and Eocene bauxite beds at Halimba, Transdanubia, Hungary. – MÁFI Évi Jel. 1987-ről, pp. 179–188. Budapest.
- Mindszenty, A. 1983: Some bauxitic textures and their genetic interpretation. – Geologický Zborník – Geologica Carpathica 34, pp. 665–674. Bratislava.
- Mindszenty, A. 1984: The lithology of some Hungarian bauxites. A contribution to the paleogeographic reconstruction. – Acta Geologica Hung. 27, pp. 441–455. Budapest.
- Mindszenty, A., K. Gál-Solymos 1988: Geological significance of the extraclasts of the Halimba bauxite deposit. – Annual Report Hung. Geol. Inst. of 1986, pp. 451–467. Budapest
- Szantner, F., J. Knauer, A. Mindszenty 1986: Prognosis of bauxite (in Hungarian). – Committe of Hungarian Academy of Sciences p. 472. Veszprém

Tectonic and eustatic control of bauxite formation in the Transdanubian Central Range (Hungary)

János Haas

*Academical Research Group, Dept. of Geology
Eötvös Loránd University of Sciences, Budapest*

A significant part of factors control the karst-bauxite formation is connected with transgressive-regressive (T–R) facies cycles. An analysis of the role of tectonically vs. eustatically controlled T–R cycles in the bauxite genesis was carried out in the Transdanubian Central Range's classical bauxite area.

The primary bauxite deposits are connected with 2nd order unconformities and they are covered by 2nd order facies cycles. These "productive" unconformities are tectonically controlled.

Key words: Karst-bauxite, cyclicity, tectonics, eustacy, Transdanubian Central Range, Mesozoicum

Introduction

Formation of karst-bauxite deposits is controlled by paleogeographic factors determining their accumulation and preservation in time and space. A significant part of the controlling factors is connected with transgressive–regressive (T–R) cycles (Haas 1984). The aim of the present paper is to analyze the role of tectonically and/or eustatically controlled T–R cycles in bauxite formation and to illustrate it by case stories from the classical karst-bauxite area of the Transdanubian Central Range (TCR).

Paleogeographic conditions

The overall paleogeographic conditions of karst-bauxite formation were described in detail in Bárdossy's comprehensive works (1977, 1982) These can be summarised as follows (see: Fig. 1):

1. Lateritic weathering – it requires

- subaerial exposure of the potential parent rocks
- suitable climate (tropical with alternation of wet and dry seasons, mean annual temperature 24° C, precipitation 1200 mm/y)
- appropriate topography (peneplane plateau)

2. Transport of weathering products and accumulation on the karstic substrate.

Necessary conditions are:

- significant surface extension of rocks suitable for karstification
- appropriate conditions for karstification (climate, physiography, tectonically controlled potential channel ways for water)

Address: János Haas: 1088 Budapest, Múzeum krt 4/a, Hungary

Received: 04 October, 1991

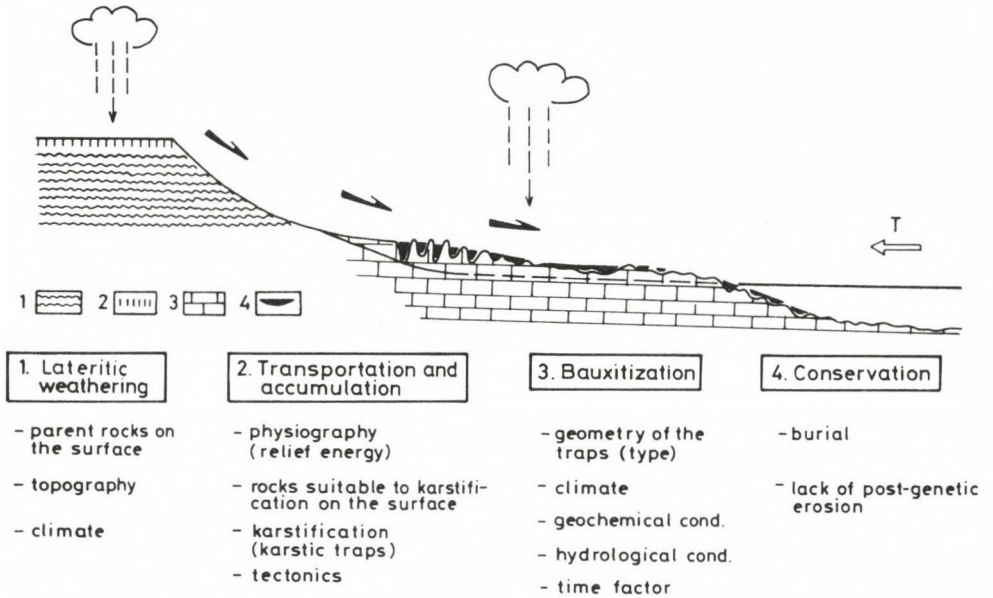


Fig. 1. Paleogeographic schema of the Mediterranean karst-bauxite formation. 1. Parent rocks; 2. Weathering crust; 3 Carbonate rocks; 4. Bauxite deposits; T-Transgression

- formation of tectonic grabens and/or karstic traps
- physiography suitable for transport of the weathering products from the source area to the karst area
- 3. Bauxitization (continuation of the bauxitization process in the karst traps) and bauxite diagenesis. Important factors are:
 - geometry of the traps (genetic type)
 - local geochemical conditions (pH, Eh, etc.)
 - hydrological conditions (distance from karstic water table, permeability of the basement rocks, etc.)
 - climate
 - time factor (duration of suitable conditions for bauxitization)
- 4. Preservation of bauxite deposits requires
 - post-depositional covering (in the same T-R cycle)
 - lack of post-depositional/post-lithification erosion (during the subsequent cycles)

Cyclic evolution model

In the background of conditions listed above there are only few common factors of critical importance. One of them is the climate which plays a decisive role in the processes of lateritization, bauxitization and karstification.

Another group of the conditions can be connected with T-R cycles. Bauxites are terrestrial sedimentary rocks which have been formed in certain sedimentary

environments i.e. facies zones. Consequently bauxite facies can be fitted into the cyclic tectonic-sedimentary evolution model. According to Walther's law they have migrated together with the surrounding facies belts during relative sea level changes. Within an idealized T-R cycle the position of facies zones being connection with the bauxite genesis are shown by Fig. 2.

Changes in the bauxite-genetic conditions during an idealized T-R cycle were described by Haas (1984). Main points are below:

1. Bauxitization, transportation and accumulation of the weathering products took place during the low sea-level period of a T-R cycle

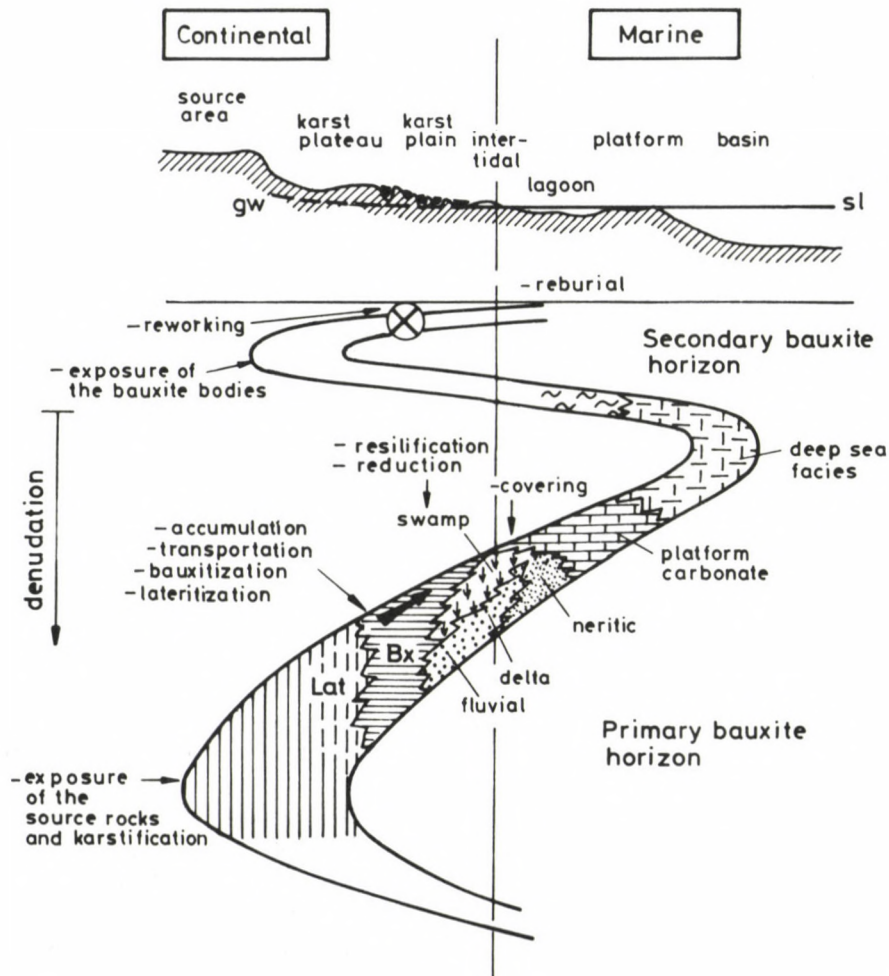


Fig. 2. Karst-bauxite genetic processes within an idealized T-R facies cycle

2. The amplitude of the relative sea level drop controls lateral extension of source area, measure of erosion, type and rate of weathering and type, rate and depth of karstification.

3. In the late phase of the low sea level period as well as at the beginning of the next relative sea level rise large continental (karst) areas can approach the base level and accumulation of the weathered material may begin in the tectonic grabens, erosional depressions as well as in the karstic traps. The altitude of depositional areas relative to the actual sea level controls the drainage and consequently the leaching pattern, the bauxitization as well as early to shallow burial diagenesis.

4. During transgressions bauxite deposits become either covered or destroyed. Conditions are suitable for their preservation only if the cover is deposited in a low energy environment (e.g. alluvial plain, swamp, lake, lagoon). If bauxite accumulation areas shift into a high energy zone (e.g. rocky coast, reef front) this is obviously not very suitable from the point of view of the preservation of the bauxite.

5. In the late phase of the transgression period the elevated karst plateaus become also flooded and transformed into carbonate platforms as a rule. Consequently the possibility of bauxite formation/accumulation comes to an end in the given T-R cycle.

Based on considerations listed above relationships between karst bauxite genesis and the long-term (2nd order) T-R cycles seems to be plausible. Amplitude of relative sea level changes in these cases is 10^1 – 10^2 m.

However high frequency cyclicity can also play some role in bauxite genesis. It may cause intermittent accumulation and changing conditions during bauxitization and early diagenesis and occasionally it may influence the development of the cover, too.

Relative sea level changes are controlled by eustatic, tectonic and sedimentological factors. The question is which one of these factors is the critical in any given case. To answer this question a detailed evolution analysis of the area is necessary.

Application of the cycle model for the TCR bauxites

The TCR is one of the classical areas of Mediterranean-type karst bauxites where deposits of commercial importance are known in three primary genetic horizons from the Mid-Cretaceous to early Tertiary times.

In early stages of the Alpine evolution the TCR structural unit was a segment of the Tethyan divergent continental margin and was situated between the Southern Alps and the Eastern Alps (Kázmér and Kovács 1985, Balla 1988, Haas et al. 1990). It reached its present-day position as a consequence of large-scale microplate reorganization in the Late Cretaceous–Early Tertiary convergent period.

Major phases of this evolution are as follows (Fig. 3):

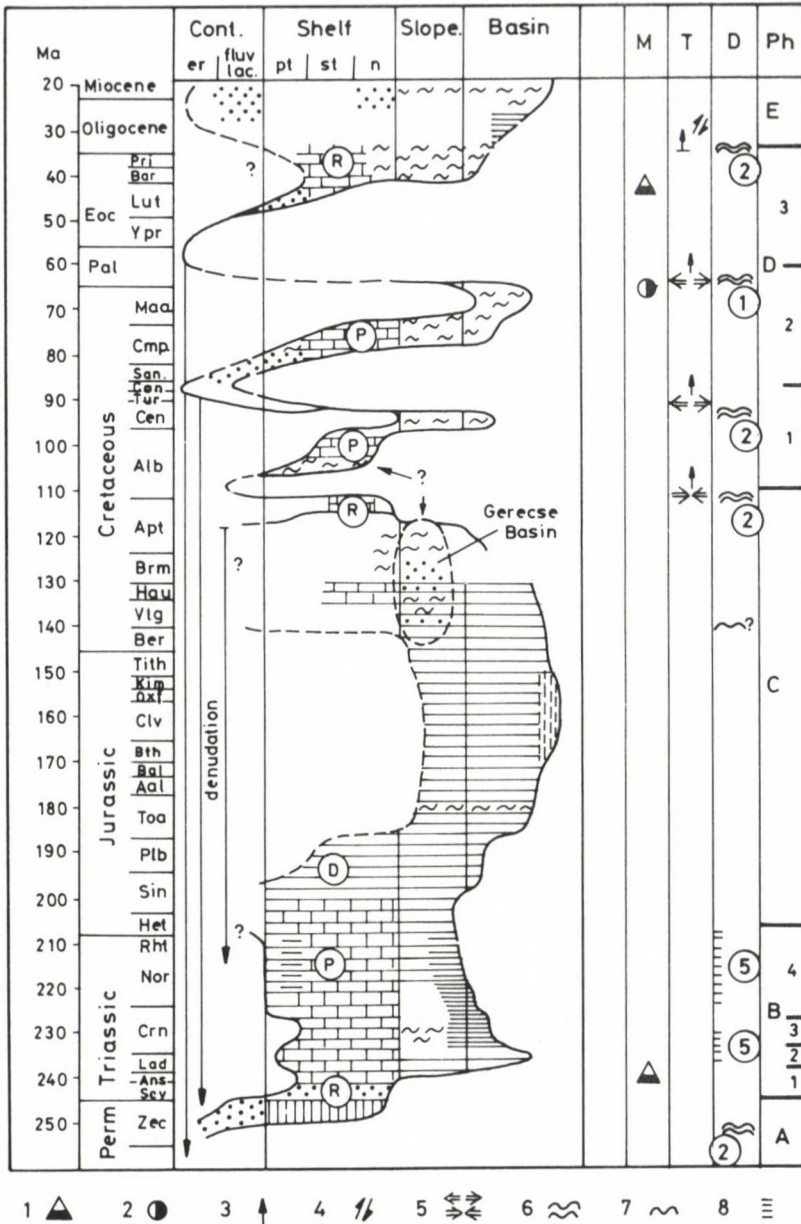


Fig. 3. Schema of Alpine evolution in the Transdanubian Central Range. M – magmatism; T – tectonism; D – disconformities; Ph – evolution phases; 1. intermedier volcanism; 2. Alkaline dykes; 3. Postorogenic subsidence; 4. Large scale strike-slip displacement; 5. Orogenic phase; 6. Regional unconformity (2nd order); 7. Local unconformity; 8. unconformities at the base of high frequency cycles (5th order)

I. Divergent-margin phase

A) Initial continental rifting (P)

B) Shelf evolution (T)

- 1. siliciclastic – carbonate ramp phase (T₁) – 3rd order cycles without subaerial exposure
- 2. first carbonate platforms and their tectonic segmentation (failed rift) – volcanism (T₂)
- 3. carbonate banks and basins with argillaceous and carbonate sedimentation (Carnian) – 3rd order T–R cycles controlled the extension of the banks
- 4. major carbonate platform evolution (Late Carnian–Earliest Jurassic) Short-term (4th and 5th order) unconformity bounded cycles (Lofer cycles Milankovitch frequency band) Intraformational paleokarst features, paleosoil layers and vadose fabrics were formed in the short term subaerial periods.

C) Rifting phase (J–K₁) Platform segmentation, drowning, sea-mount-graben structure, general deepeningII. Convergent margin phase (K₂–M₁)

A) Orogenic events (Aptian/Albian, Turonian, Paleocene) overall emersions, long-term subaerial exposure (2nd order unconformities) – bauxite formation, post-orogenic subsidence – 2nd order T–R supercycles (covering sequence)

B) Large scale lateral displacement of the TCR (E₃–M₁)

Based on the analysis of the Alpine evolution of the TCR unit we can conclude that:

1) In the divergent margin phase conditions of karst bauxite formation could hardly be fulfilled due to lack of subaerial gaps or very short-term subaerial periods (10⁰–10¹ ka).

2) In the convergent margin phase long-term emersion periods existed when conditions favourable for bauxite formation could develop.

A diagram of the latter phase (Mid-Cretaceous to Mid-Eocene) is shown in Fig 4. demonstrating the tectonic events, the elevation and subsidence periods, and the eustatic sea level curve (after Haq et al. 1987). The diagram suggests that the three primary bauxitiferous horizons of the TCR are in correspond very well with the main orogenic events (Aptian/Albian–Austrian phase; Turonian - Subhercynian phase; and Paleocene–Laramian phase). They are controlled by 2nd order unconformities (gap range=4–22 Ma) and covered by 2nd order T–R supercycles (range=10–23 Ma). Thus stratigraphic position of the primary bauxite formations was controlled predominantly by orogenic processes: the pre-orogenic and synorogenic uplift on one hand and the post-orogenic subsidence on the other. The eustatic sea level curve does not seem to correlate with the bauxite formation periods although sea level oscillation could influence the genetic processes during the transgression periods.

The possible influence 3rd order and high frequency sea level oscillations on bauxite genesis is demonstrated by the Senonian evolution model (Figs 5 and 6). During the continental period sea level changes were important controlling factors of weathering, erosion and transportation of the weathered material, and of accumulation and early diagenesis. It is highly probable that the changing

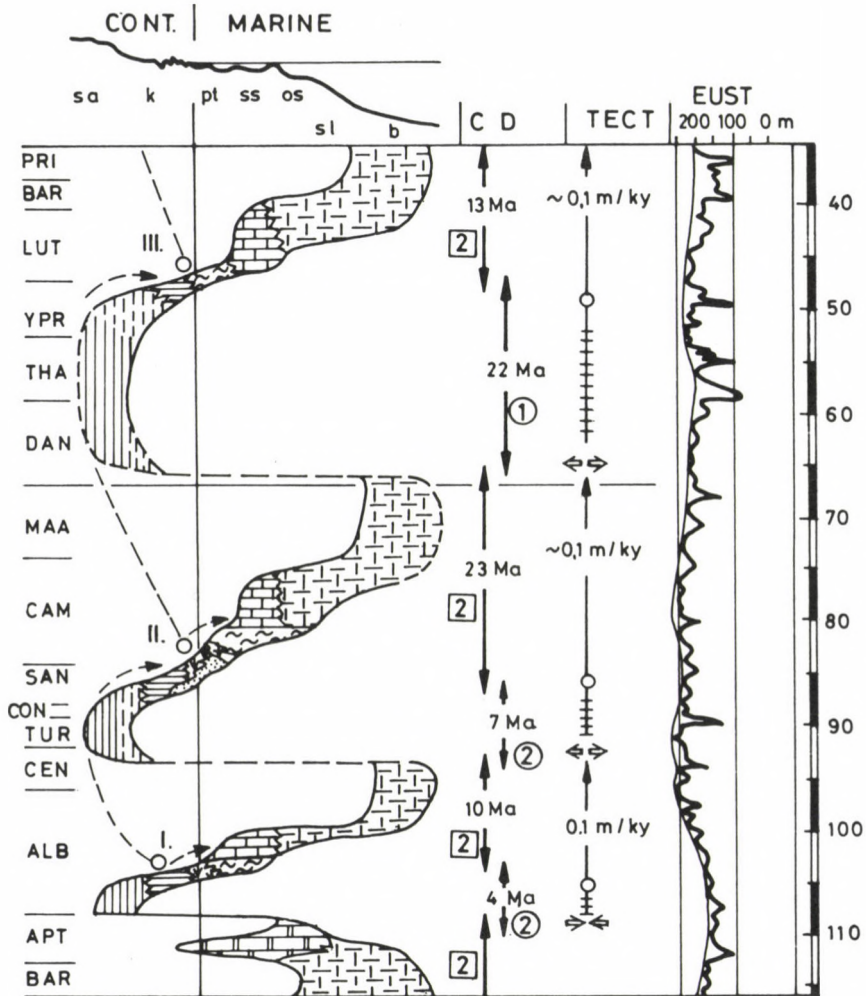


Fig. 4. Second order facies cycles and tectonism in the TCR and the global eustatic curve (after Haq et al. 1987). Sa - Source area; k - Karst plateau; pt - Peritidal zone; ss - Shallow shelf; os - Open shelf; sl - Slope; b - Basin. Symbols are the same as in Fig. 2. C - Range and order of facies cycles; D - Range and order of unconformities; TECT - Tectonism: 1. Uplift; 2. Orogenic event; 3. Post-orogenic subsidence (subsidence rate)

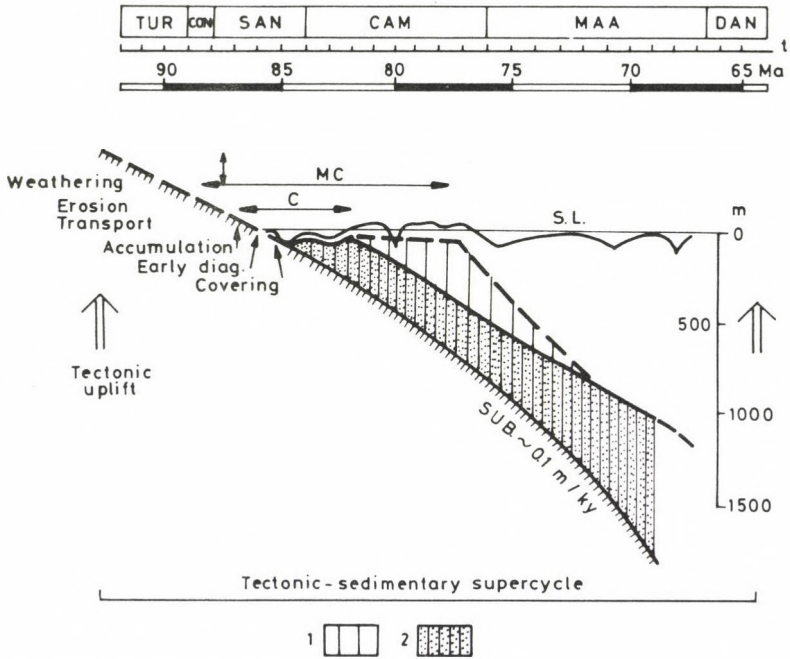


Fig. 5. Subsidence, sediment accumulation, sea-level diagram of the Senonian cycle in the TCR. MC – Record of 3rd order sea-level oscillation; C – Record of 4th, 5th order sea-level oscillation; S.L. – Sea-level; SUB – Subsidence (subsidence rate); 1. Carbonate platform; 2. Basin facies

conditions are recorded by the bauxite profiles, however, identification and correlation of these changes may prove to be extremely difficult.

In the transgression period due to the regional subsidence topographic highs became flooded and carbonate platforms formed on them. High frequency sea level drops could result in short-term subaerial exposures in this environment but these short periods were not sufficient for the bauxite formation although local reworking/redeposition may have taken place.

Conclusions

1. Karst bauxites like other continental facies can be fit into a cyclic evolution model.
2. Facies zones (paleoenvironments) of critical importance in bauxite genesis are as follows:
 - continental source areas
 - available exposed karst surface

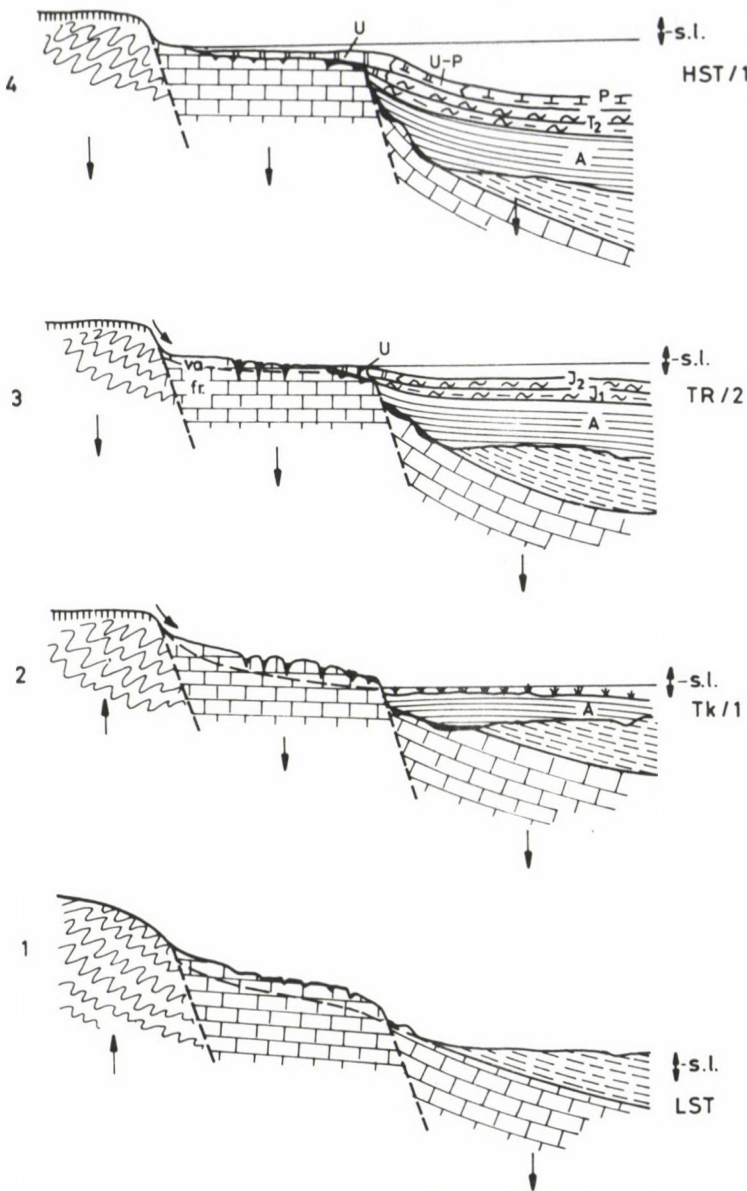


Fig. 6.

Basin evolution and sediment accumulation in the TCR in the early part of the Senonian facies cycle. 1. Lowstand period (Turonian-Coniacian); 2. Early part of the transgression period (Santonian); 3. Late part of the transgression period (Early Campanian); 4. Early part of the high stand period (Late Campanian); A – coal-bearing formation (Ajka Coal F.); J₁ – Brackish water neritic marl (Jákó Marl F. lower member); J₂ – Normal marine neritic marl (Jákó Marl F. upper member); K – Rudist limestone (Ugod Limestone F.); P – Deep water marl (Polányi Marl F.); U-P – Platform-basin transitional facies; s.l. – 4th–5th order sea-level oscillation; va – Vadose zone; fr – Freatic zone

– continental or marine environments for the deposition of the cover.

3. In the TCR (an example for a deformed margin) the primary bauxite formations are connected with 2nd order unconformities and bauxite horizons are covered by 2nd order T-R supercycles.

4. Productive bauxitiferous unconformities are tectonically controlled (orogeny related uplifts).

5. The role of 3rd to 5th order (predominantly eustatically controlled) cyclicity in the bauxite genesis is also detectable. It can influence processes of weathering, transportation, bauxitization and early diagenesis.

References

- Balla, Z. 1988: Clockwise paleomagnetic rotations in the Alps in the light of the structural pattern of the Transdanubian Range (Hungary). – *Tectonophysics*, 145, pp. 277–292.
- Bárdossy, Gy. 1977: Karsztbauxitok. – Akadémiai Kiadó, Budapest, p. 413.
- Bárdossy, Gy. 1982: Karst bauxites. Bauxite Deposits on Carbonate Rocks. – *Developments in Economic Geology*, 14, pp. 1–441, Elsevier.
- Haas, J. 1984: Paleogeographic and geochronologic circumstances of bauxite generation in Hungary. – *Acta Geol. Hung.*, 27, 1–2, pp. 23–39.
- Haas, J., G. Császár, S. Kovács, A. Vörös 1990: Evolution of the Western part of the Tethys as reflected by the geological formations of Hungary. – *Acta Geod. Geoph. Mont. Hung.*, 25, 3–4, pp. 325–344.
- Haq, B.U., J. Hardenbohl, P. Vail 1987: Chronology of fluctuating sea level since the Triassic. – *Sciences*, 235, pp. 1156–1167.
- Kázmér, M., S. Kovács 1985: Permian–Paleogene paleogeography along the Eastern part of the Insubric-Periadriatic lineament system: Evidence for continental escape of Bakony-Drauzug Unit. – *Acta Geol. Hung.*, 28, 1–2, pp. 71–84.

Geoexplorer – the development of a knowledge-based consultation system for supergene deposits

Markus Wagner, Karsten Fischer,
Klaus Germann

Institute of Economic Geology – TU Berlin

Junfeng Luo,
Wolfdietrich Skala

Institute of Mathematical Geology – FU Berlin

Some existing expert systems such as PROSPECTOR have been designed mainly for the purpose of regional resource assessment or for mineral deposit prospecting. The development of a knowledge-based system that supports exploration and assessment of supergene deposits (laterite and bauxite) is the main goal of a scientific project. This system, GEOEXPLORER, should not only deal with the problems of searching for mineral deposits, but it should also cover the evaluation of the spatial occurrence as well as the deposit appraisal. This publication provides an overlook of the development of GEOEXPLORER.

Key words: GEOEXPLORER, supergene deposit, laterite, bauxite

Introduction

GEOEXPLORER is a knowledge-based computer system being designed to support exploration and resource assessment of supergene ore-deposits, which is the main goal of a long-term project financed by the DFG (German Research Foundation). It is being developed by an interdisciplinary team of scientists at the Institute of Economic Geology in co-operation with the Institutes of Mathematical Geology and Computer Sciences.

Modern prospecting and exploration of mineral deposits may be considered as sequential processes, which can be divided into different stages. At each stage, conclusions and decisions must be made according to the relevant geological information and available data in order to finally verify the maximum profit of the economic mineral deposit under study.

To support this probabilistic approach, many statistical methods have been applied for such practical purposes as prognosis of frequencies of occurrence or identification of prospective areas since the mid-sixties. "Geostatistics" and "Quantitative Resource Evaluation" have hence become keywords in mineral exploration. The methods of knowledge-based or expert systems (XPS) show another way to provide an aid as an exploration assistant.

One of the obvious advantages of expert systems towards conventional statistics is that descriptive or genetic geological models can easily be formalized and used

Addresses: M. Wagner, K. Fischer, K. Germann: D-1000 Berlin 12, Ernst-Reuter Platz 1. Germany
J. Luo, W. Skala: D-1000 Berlin 46, Malteserstr. 74-100. Germany

Received: 14 August, 1991

for mineral exploration. Besides, the built-in knowledge base allows a transfer of the application from one area to another without taking care of the training area definition, which is indispensable when applying statistical models (Luo 1990).

The basic architecture of expert systems

An expert system is a computer software, which uses Artificial Intelligence (AI) methods to solve problems and give advice simulating a human expert. Unlike conventional programs, it can manipulate knowledge and "fuzzy" information as well as numeric data, and explain to the user why certain information is required, how it is processed and a decision is reached.

To avoid misunderstandings, it should be stressed that it is only human knowledge which is restored in an expert system. On principle, knowledge-based systems "reproduce" a human expert by making his knowledge available to a computer and by disposing it to a non-expert in this domain. The five principle components of such a system are:

- The knowledge base or stored expertise supplied by specialists in the specific problem domain.
- The inference engine incorporating the problem solving mechanism.
- The user interface which provides the working environment.
- The explanation module allowing the systems supervision.
- The knowledge acquisition program to keep the system's knowledge base up-to-date.

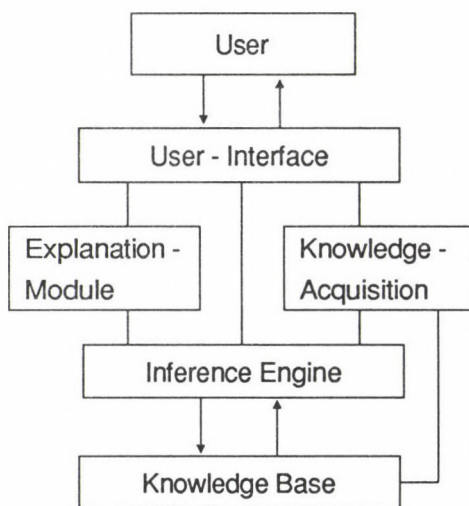


Fig. 1.
The basic architecture of an expert system

During a consultation with a knowledge-based system, the user poses a problem through the interface to the inference engine, which scans the knowledge base for relevant information, processes it, and finally provides a response.

In addition to requesting information when needed and providing conclusions, the system will give reasons why it needs information and explain how it reaches a decision. Therefore a fourth component, the explanation module is needed. This transparency allows the user to monitor the path of the consulting session and to modify the appropriate parameters if a change in the process is desired. These explanatory system statements are necessary for the user to supervise his automatic colleague and

to give him confidence in the program's answers.

As the advices and conclusions reached by an expert system can only be as good as its knowledge base, that is to say its input-information, this data needs a regular maintenance or update provided by the fifth module, the knowledge acquisition program. The five components and their interaction are shown in Fig. 1.

Expert systems in mineral exploration

Expert systems have proven to be most effective when applied to specific, well defined problems, as demonstrated by their use in oil exploration. In the mineral industry expert systems are used primarily at the processing phase. Yet, only few have been developed for exploration, although their potential as consultants with total recall is likely to be realized in the near future.

The first attempt of applying AI-methods to mineral exploration has been done by PROSPECTOR, an expert system which addresses the most general exploration concept: a given set of observations in a specified region leads to the determination of the mineral potential of this area. The original PROSPECTOR was developed at the SRI International in co-operation with the United States Geological Survey between 1974 and 1983 (Hart et al. 1978). It was credited with locating an extension of a molybdenum deposit, which had eluded experienced geologists. The work on the project continued at the U.S. Geological Survey, which in 1984 presented the muPROSPECTOR. Patterned after the original system, it was implemented on the IBM PC¹ (McCammon 1986).

Unlike PROSPECTOR, GEOEXPLORER should not only deal with the problems of searching for and of prospect assessment, but should also meet requirements for evaluating their spatial occurrences as well as estimating their economic values. Besides, an interface to an external data base is taken into account, too. The system's development is divided into two main phases:

The development of a prototype – in order to reach this goal within a justifiable time span, the system's knowledge base will represent just one single type among all supergene deposits, the bauxite deposits. One reason for this choice is that bauxite deposits show definitive regularities, as for instance the geographic distribution of the main bauxite provinces (Bárdossy 1989). Anyhow it is planned to compile geologic models of various weathering deposits, such as Ni-, Mn-, Au- and REE-laterites as well as phosphates and kaolinities, in a later stage of development. Therefore the system's architecture must be able to handle the incorporation of different models in its knowledge base.

The primary task of this first phase is to define the paleoclimatic and paleogeographic rules, the paleomorphologic and hydrogeologic settings,

1 The use of trade names in this publication is for identification purposes only and does not imply endorsement by the T.U. Berlin.

tectono-stratigraphic domains and parent rock types, which control the occurrence of bauxite deposits. Furthermore such indices as geophysical and geochemical indicators, soil or plant types, which might indicate an occurrence of bauxite, have to be taken into account.

Consequently GEOEXPLORER should be able to estimate the likelihood of occurrence of a bauxite deposit, whether it is buried or surficial, whether karstic or lateritic, in the area under research.

The completion to the final version – during the second phase the prototype should be expanded and completed to its final version, as under the systems support, it should not only be possible to achieve the first stage of exploration, the local approach towards the ore deposit, like already performed by the prototype, but also be able to estimate economic values of a bauxite deposit according to such criteria as grade and tonnage.

Starting the development

One of the questions to start with, when developing a knowledge based system is: Who might be the potential users of the product? Two groups of users with totally different demands and requirements result from this consideration. These are:

Exploration companies or exploration departments of the Aluminium Industry companies. In this case the system should support the exploration work according to economic criteria and finally render the possibility of profitable mining. Although this group of users is lacking such an expert system which for instance could be of great use in risk analyses, its realization at a University Institute is more than uncertain. One of the main complicating factors is, that exploration work and results of the companies are, for business reasons, generally considered confidential.

Geological surveys of developing countries. The local geologists might not have detailed domain knowledge or no access to essential literature to make themselves acquainted with the topic.

Here, the system would show its educative characteristics. If desired, basic information on supergene deposits will be provided to the user. In a consultation, the answers given by the geologist to questions asked by the program will be matched with the information in the knowledge base and compared with geologic models of a possible bauxite deposit occurring in the area under investigation. In this case, the systems capacity would be able to handle the challenges of the early prospecting stage in an exploration campaign. Two reasons, why such a user might consult GEOEXPLORER are thinkable:

The country, for what reasons ever, wants to discover the lacking mineral resource on its national territory.

Samples, randomly taken during a former mapping campaign, turn out to be enriched with free alumina hydrate, although until now, no occurrence of bauxite has been registered in this area.

The proceeding of the system will be completely different in those two cases.

In the first case it will try to estimate the possibility of occurrence by checking whether, or to what extent the geologic premises for chemical weathering are fulfilled in the selected region; having reached a positive answer, the system investigates furthermore.

In the second case the system chooses another path in order to manage the local approach. It might be wished by the user to discover a rather small mineable bauxite deposit within a vast laterized area. Therefore GEOEXPLORER will start to observe direct or indirect indicators, such as weathering minerals, weathering crusts or typical sedimentary facies accompanying bauxite deposits (Valeton 1983). Besides it will concentrate on the lithology, as under favorable conditions the entire surface might laterize, but economic bauxite deposits will, like in Brazil, form only above the outcrops of certain parent rocks, for instance alkaline ring structures (Bárdossy 1983).

Figure 2 represents the global knowledge and inference network of regional-geological data disposable to GEOEXPLORER in the first stage of exploration.

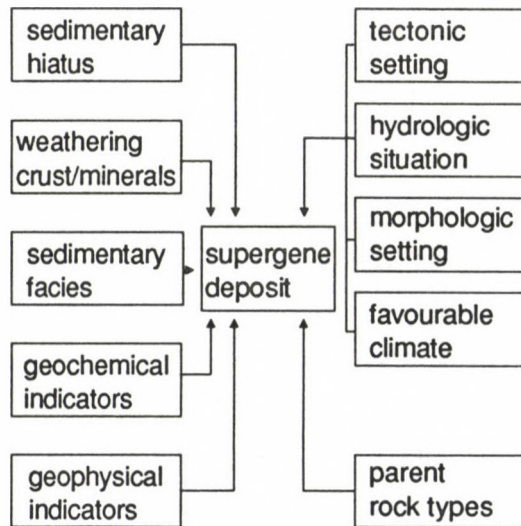


Fig. 2. Relevant geologic indicators and premises in the first prospection stage

Geexplorer's architecture

Figure 3 shows the flowchart of a consultation process for exploring bauxite deposits via GEOEXPLORER. This process covers practically all the main stages of an exploration campaign. The extent, however, all tasks can be accomplished, depends on the input-information supplied by the user. We should emphasize here that the end-user is expected to be a trained geologist, not a layman.

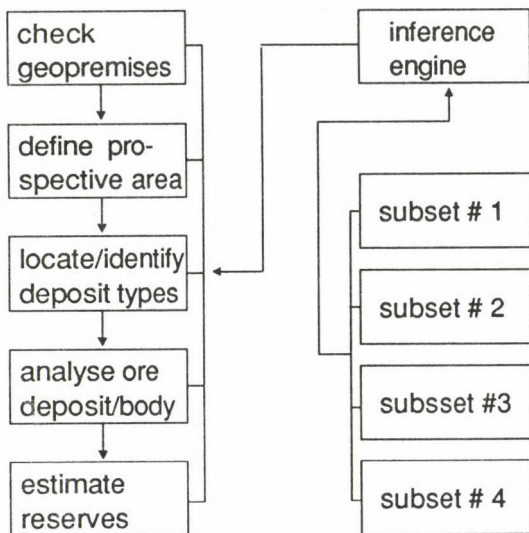


Fig. 3.
The flowchart of GEOEXPLORER

GEOEXPLORER cannot make direct observations and must therefore depend upon the skill of the user in this regard. Being due to its integrated destinations, the built-in knowledge base of GEOEXPLORER has to be designed consisting of four subsets.

Subset # 1 comprises mainly such basic geologic facts and rules as rock or mineral types and their classification, geologic ages, that is to say geologic premises and indicators for supergene deposits.

Subset # 2 deals with the known weathering deposit models and a classification of them. The knowledge about these deposit models has to be formalized in a way of frame representation. The important slots are such features as parent rock types, components of the ore, geochemical and geophysical indicators, general shape of the ore body, age of mineralization as well as paleogeographic position.

Subset # 3 contains the spatial features of supergene deposits. As for e.g. weathering profiles and models which describe the spatial distribution and extension of deposit regions or belts (Bárdossy 1983).

Subset # 4 is to be designed to store criteria which describe the economic value of the deposit.

Knowledge acquisition

For GEOEXPLORER to make use of the models mentioned above, the relevant information must be stored in the computer in a form different from ordinary prose or textbook descriptions. Instead a model must be highly structured so that the system can draw inferences by examining the parts of the model and relations among them. During the first stage of the project this means to derive relevant facts and rules on the genesis, exploration and appraisal of bauxite deposits and

combine them to an inference net. This can be achieved either by the study of literature or by interviewing domain experts. Since the commencement of the GEOEXPLORER – project in February 1990, we already had the opportunity to interview Prof. Bárdossy, the former chief geologist of the Hungarian Aluminium Corporation, and Prof. Valetton, the senior expert in supergene deposit research, about this topic. Further interviews are planned.

In those semi-structured interviews it is aspired to fathom the proceedings of the expert posed a concrete problem. Experts tend to solve domain problems by intuition. This means, they don't visualize all the facts and rules they make use of in a problem solving process. We might say, the expert acts unconscious, in contrast to a layman who recapitulates all disposable facts and examines their relevance and validity when solving a problem. But exactly those features guarantee the experts efficiency and accuracy. To illustrate the difference between an expert and a layman it may be compared to the one between a knowledge based system and a conventional data base.

When interviewing specialists we must try to solve this problem of "unconsciousness", because exactly those decision patterns and thoughts are the theme of our interest. After all, the system's "brain" should work in a similar mode.

Current status and future plans

GEOEXPLORER is in a rather early experimental stage. The fact-rule sets are still being constructed, although fragments of them are already implemented in the PROLOG programming language, a language specially designed for AI applications. PROLOG embodies the concept of declarative or descriptive programming. Different types of knowledge representation and the use of shells are still to be tested. A shell can be defined as a pre-developed core around which an expert system can be constructed by adding domain-specific information. Although an expert system integrated in a shell may be less run-time efficient than one designed using a programming language like PROLOG or LISP, a suitable shell speeds up developing and allows rapid prototyping – an important feature when the project capacities are for the time being restricted to 3 men years.

Like most new technologies, expert systems have occasionally failed, usually when they were used with unrealistic expectations. An expert system should be considered an assistant, not a substitute, for a human worker. In many cases, the main benefit of its consultation will be to alert the geologist to unsuspected possibilities. Yet, when properly applied, the expert system can enhance the ability of the specialist and raise the level of his work above his potential capability. However, in contrast to the oil industry, mine explorationists have been very slow in accepting this recent computer technology, although many aspects of mineral exploration are ideally suited to it. The first significant successes of expert systems in mineral exploration are likely to result from applications dealing with specific, clearly defined problems of narrow scope like monitoring and optimising the operation of exploration instruments, planning a geochemical or geophysical

survey or defining a metallogenic area from soil geochemistry. Moreover, expert systems will gain popularity as "intelligent" geological references and for tutoring in exploration techniques, an aspect of particular interest to developing countries.

Acknowledgements

Thanks are expressed to the German Research Foundation (DFG) for funding the GEOEXPLORER research project. We are indebted to Prof. G. Bárdossy and Prof. I. Valetton for their useful suggestions and friendly support.

References

- Bárdossy, Gy. 1989: A review of worldwide bauxite reserves, and their mining and economic importance. – *Erzmetall*, 42, 4, pp. 172–177.
- Bárdossy, Gy. 1983: A comparison of the main lateritic bauxite regions of our globe. in: *Lateritisation Processes*. – Proceedings of the II International Seminar (Melfi A. J. and Carvalho A. ed.), São Paulo - Brazil, pp. 15–51.
- Hart, P. E., R.O. Duda, M.T. Einaudi 1978: PROSPECTOR – A Computer-Based Consultation System for Mineral Exploration. – *Mathematical Geology*, 10, 5, pp. 589–610.
- Luo, J. 1990: Statistical mineral prediction without defining a training area. – *Mathematical Geology*, 22, 3, pp. 235–239
- McCammon, R. B. 1986: The muPROSPECTOR mineral consultant system, a microcomputer-based expert system for regional mineral resources evaluation. – *U.S. Geol. Survey Bulletin* 1687, Denver – Colorado, p. 35 .
- Valetton, I. 1983: Klimaperioden lateritischer Verwitterung und ihr Abbild in den synchronen Sedimentationsräumen. – *Zeitschrift der deutschen geol. Gesellschaft*, Hannover Germany, pp. 413–452.

GUIDELINES FOR AUTHORS

Acta Geologica Hungarica is an English-language quarterly publishing papers on geological topics (geochemistry, mineralogy, petrology, paleontology, stratigraphy, tectonics, economic geology, regional geology, applied geology). Along with papers on outstanding scientific achievements and on the main lines of geological research in Hungary, reports on workshops of geological research, on major scientific meetings, and on contributions to international research projects will be accepted.

Manuscripts are to be sent to the Editorial Office for refereeing, editing, and translation into English.

A clear, careful and unequivocal formulation of the papers, lucidity of style and the use of uniform nomenclature adopted in Hungary are basic requirements. It is convenient to subdivide the text of the papers into sections under subheadings.

Form of manuscript

The paper complete with abstract, figures, captions, tables and bibliography should not exceed 25 pages (25 double-spaced lines with a 3 cm margin on both sides).

The first page should include:

- the title of the paper
- the name of the author(s)
- the name of the institution and city where the work was done
- an abstract of not more than 200 words
- a list of five to ten keywords
- a footnote with the name and postal address of the author(s)

The SI (System International) should be used for all units of measurements.

References

In text citations the author's name and the year of publication should be given. The reference list, which follows the text, should be typed double-spaced, arranged alphabetically, and should not be numbered. For the preferred sequence and punctuation of authors' names see the examples below.

The author's name is followed by the year of publication in parentheses, the title of the paper or book (individual words in English titles of papers should have lower case initials, those of books upper case ones). Paper titles are followed by periodical titles, a comma, volume number, and inclusive page numbers. For books the publisher and the place of publication should be given.

Examples:

Bruckle, L. H. (1982): Late Cenozoic planktonic diatom zones from the eastern equatorial Pacific. *Nova Hedwigia*, Belh., **39**, 217-246.

Surdam, R. C., H. P. Eugster (1976): Mineral reaction in the sedimentary deposits of the Lake Magadi region, Kenya. *Geol. Soc. Amer. Bull.*, **87**, 1739-1752.

Perelman, A. J. (1976): *Geochemistry of Epigenesis*. Plenum Press, New York, Amsterdam.

Figures and tables

Figures and tables should be referred to in the text and their approximate place indicated on the margin.

Figures should be clear line drawings (suitable for being redrawn without consulting the author) or good-quality black-and-white photographic prints. The author's name, title of the paper, and figure number (arabic) should be indicated with a soft pencil on the back of each figure. Figure captions should be listed at the end of the manuscript. They should be as concise as possible.

Tables should be typed on separate sheets with the number (roman) and a brief title at the top. Horizontal lines should be omitted.

Proofs and reprints

The authors will be sent a set of galley and page proofs each. These should be proofread and returned to the Editorial Office within a week of receipt. Fifty reprints are supplied free of charge, additional reprints may be ordered.

307216

Acta Geologica Hungarica

VOLUME 34 NUMBER 4, 1991

EDITOR

J. FÜLÖP

EDITOR-IN-CHIEF

J. HAAS

EDITORIAL BOARD

**G. CSÁSZÁR, G. HÁMOR, F. HORVÁTH,
T. KECSKEMÉTI, GY. PANTÓ, T. SZEDERKÉNYI,
Á. KRIVÁN-HORVÁTH (Co-ordinating Editor)**



Akadémiai Kiadó, Budapest

ACTA GEOL. HUNG. 34(4) 271-443 (1991) HU ISSN 0236-5278

ACTA GEOLOGICA

A QUARTERLY OF THE HUNGARIAN ACADEMY OF SCIENCES

Acta Geologica publishes original reports of studies in geology, crystallography, mineralogy, petrography, geochemistry and paleontology.

Acta Geologica is published in yearly volumes of four issues by

AKADÉMIAI KIADÓ

Publishing House of the Hungarian Academy of Sciences
H-1117 Budapest, Prielle Kornélia u. 19–35.

Manuscripts and editorial correspondence should be addressed to

Acta Geologica

H-1363 Budapest, P.O. Box 24

Subscription information

Orders should be addressed to

AKADÉMIAI KIADÓ

H-1519 Budapest, P.O. Box 245

Acta Geologica Hungarica is abstracted/indexed in Bibliographie des Sciences de la Terre, Biological Abstracts, Chemical Abstracts, Chemie-Information, Hydro-Index, Mineralogical Abstracts



TETHYAN BAUXITES

IGCP 287

Part II

Contents

Bauxites and related paleokarst in Southern Italy, Sicily and Sardinia <i>L. Simone, G. Carannante, B. D'Argenio, D. Ruberti, A. Mindszenty</i>	273
Bauxite deposits of Yugoslavia – The state of the Art <i>B. Šinkovec, K. Šakač</i> .	307
Contribution to the geochemistry of Hungarian karst bauxites and the allochthony/ autochthony problem <i>Z. Maksimovic, A. Mindszenty,</i> <i>Gy. Pantó</i>	317
Bauxites in Albania <i>V. Kici, L. Peza, D. Skhupi, A. Xhomo</i>	335
Bauxite deposits and Senonian formations in Hungary (Palynological analysis) <i>Á. Siegl-Farkas</i>	345
Stratigraphical position of the bauxite deposits in the Pădurea Craiului Mountains (Northern Apuseni Mountains) <i>S. Bordea, G. Mantea</i>	351
Petrography and Sedimentology of the Cretaceous Continental Complex of the Eastern Hățeg Basin (South Carpathians – Romania) <i>J. Becze-Deák</i>	377
Concentrations of rare earth in Greek bauxites <i>M. Laskou</i>	395
Remarks on the genesis and ore-dressing of the alluvial bauxite occurrences of Parnass–Ghiona–Elikon (Greece) <i>A. Vgenopoulos,</i> <i>K. Daskalakis</i>	405
Mineralogical and geochemical correlation between the different Tethyan bauxitic types <i>A. Vgenopoulos</i>	409
Bauxite deposits related to the Tethyan Basins in Iran <i>M. Sharifi Nourian,</i> <i>F. Rahimzadeh, M. Ehsanbakhsh</i>	413
Main geological feature of "Sedimentary" bauxites deposits in China <i>W. Liancheng, Z. Naixian</i>	427
Mineralogy and geochemistry of bauxite in Yang Quan Area, Shan Xi Province (China) <i>Z. Naixian, W. Liancheng, M. Yuguang</i>	437
Forthcoming Events	445

Bauxites and related paleokarst in Southern Italy, Sicily and Sardinia

Lucia Simone, Gabriele Carannante, Andrea Mindszenty,
Bruno D'Argenio, Daniela Ruberti,

*Dipartimento di scienze della Terra
del Università di Napoli, Napoli*

*Eötvös Loránd University of Sciences
Department of Applied Geology, Budapest*

A brief summarization of general geological and stratigraphical setting and genetical characteristics of bauxite deposits and related paleokarst in Peninsular Italy, Sicily and Sardinia is presented. The most important features and data are demonstrated in maps, diagrams and tables.

Key words: Bauxite, paleokarst, Jurassic, Cretaceous, Southern Italy, Sicily, Sardinia

Introduction

Bauxites (partly also of economic interest) occur in Peninsular Italy, Sicily and Sardinia. Mining activity formerly concentrated to Apulia and the Southern Appennines has been shifted to Sardinia during the past 15 years or so (Fig. 1). Beyond their economic importance, however, bauxites receive more and more attention also in Italy, because of the paleogeographic information they offer to the sedimentary geologist.

The study of paleokarst phenomena in general and those associated with bauxites in particular dates back to the early sixties in Italy. The first description of the intricate phreatic-lens related cavity system partly filled by bauxite in the Campo Sauro area (Matese Mts) Appennines was given by D'Argenio (1967) and was followed by detailed analysis of other bauxite-filled paleokarst occurrences by Carannante et al. (1974). An updated revision of all previous data with a tentative synthesis was published recently by Carannante et al. (1991).

As to bauxites, the first economy-oriented systematic accounts on the bauxites of Campania, the Abruzzi and Apulia were published in the late sixties by De Weisse (1973), Crescenti-Vighi (1964, 1970), followed by the first paleogeographic reconstructions by D'Argenio (1969) and an annotated bibliography by Boni (1972). A monograph on South-Central Italy bauxites summarizing all the previous data and including substantial new observations and analytical results was published by Bárdossy et al. in 1977.

Detailed work on the bauxites Sardinia began in as a result of intense exploration activity on the Island. Up-to-date stratigraphical and general geological data were published by Sanna-Temussi (1968) and Cherchi et al. (1978). Combes (1990) pointed

Address: L. Simone, G. Carannante, B. D'Argenio, D. Ruberti: Largo S. Marcellino 10 80 138 Napoli, Italy

A. Mindszenty: H-1088 Budapest, Múzeum krt. 4/a, Hungary

Received: 24 November, 1991.

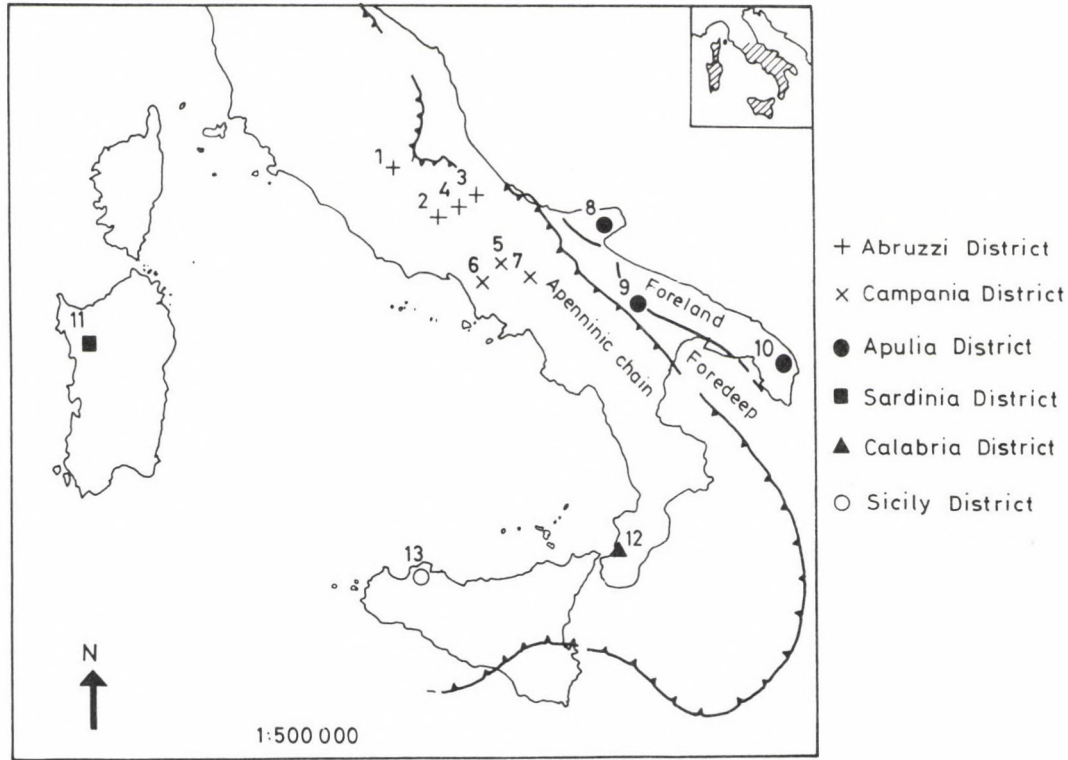


Fig. 1
 Bauxites of Southern Italy, Sardinia and Sicily. Locality map. 1–4. Abruzzi district; 1. M. Velino–Ocre Mountains; 2. Marsica Mts; 3. Maiella Mts; 4. Morrone Mts; 5–7. Campanian district; 5. Matese Mts; 6. M. Maggiore; 7. M. Camposauro; 8–10. Apulia district; 8. Gargano peninsula; 9. Northern Murge; 10. Salento; 11. Nurra; 12. Palizzi; 13. Gallo

out the close genetic relationship between the bauxites of Sardinia and Languedoc-Provence in France.

Minor bauxite indications were reported recently from Sicily by Ferla-Bommarito (1989) and from Calabria by Bouillin et al. (1985).

A lithology and morphofacies oriented review of earlier data with additional new observations on Southern Italian bauxites permitted to update the earlier reconstructions and to fit the bauxites of Peninsular Italy and Sardinia into the tectonic framework of the Mediterranean (D'Argenio and Mindszenty 1987, 1991 and D'Argenio et al. 1987).

As to stratigraphy: after the first concise work of Crescenti and Vighi no systematic revision of the bauxitic and non-bauxitic paleokarst horizons of the South-Central Appennines was undertaken. Occasional new data were published from Apulia (Luperto-Sinni and Masse 1982) and from the Abruzzi Campania region (Chiocchini et al. 1989 and Ruberti 1991), where the revision is still underway. The stratigraphic position of the Sardinian bauxite was established lately by Cherchi et al. (1985) and does not require updating at the moment.

Bauxites of Peninsular Italy

All bauxites of the Peninsula are of Cretaceous age. They occur in stratigraphic gaps interrupting cyclic shallow-water carbonate sequences in the extensive Abruzzi-Campania-Lucania (Figs 2-6, Tables 1-12) and the Apulia carbonate platform domains. The apparent time-span encompassed by the main bauxite horizon platform domains. The apparent time-span encompassed by the main bauxite horizon (with deposits of potentially economic value) varies. At most it covers about two stages: bauxites filling the maximum stratigraphic gap are underlain by Albian strata and are covered by Turonian/Senonian sediments (e.g.

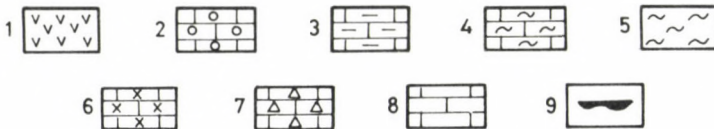


Fig. 2

Key for the figures. 1. calcareous tufa (Miocene); 2. grainstones with pectinids (Lower Miocene of Abruzzi Region), limestones, subordinately marls, with brachiopods, madreporaires, foraminifera, coralline, algae, echinoids, bivalvia (Lower Miocene of Calabria Region); 3. organic limestones with foraminifera, rudists, echinoids, red algae (Upper Cretaceous); 4. muddy limestones alternating with liferitic and/or stromatolitic limestones (Upper Cretaceous); 5. pelagic marls with glauconitic nodules (Upper Cretaceous of Sardinia Region); 6. bioclastic limestones with pelecypod fauna (Cenomanian); 7. limestones with black lithoclasts (Middle-Upper Cretaceous); 8. bioclastic limestones ("Urgonian" type in Sardinia Region) (Lower Cretaceous; Upper Triassic-Lower Jurassic in Calabria and Sicily Regions); 9. bauxites

Regia Piana, Matese). At other places the gap is considerably smaller: bauxites in the Maggiore Mts underlain by Uppermost Albian are covered by the Lower Cenomanian. Remarkably enough, at places where the gap reaches its minimum, higher up, at the base of the Senonian often a second "subsidiary" bauxite horizon can be observed which, however, becomes covered very rapidly, still within the Lower Senonian. Areal distribution of the two bauxite horizons suggests that at least in the Matese Mts they do reflect the slightly tilted (updomed?) morphology of the substrate, around the highest elevated parts of which the lacuna lasted much longer than it did around the low-level, peripheral areas which, however, after a brief period of submergence became re-exposed again.

Bauxite deposits of Apulia seem to be slightly younger than the Turonian–Senonian covered bauxites of the Matese Mts Maggiore group (Figs 7–10, Tables 13–16). They occur in a somewhat smaller stratigraphic gap between Cenomanian and Senonian strata. Also they are anomalous from the point of view of the bauxite-filled karst morphology. Unlike any other Southern Italian bauxites, the bauxite-filled dolinae of the Murge area are unusually deep (40 m) and display a clear tectonic control with elongated karstic "canyons" consisting of coalescent E–W or NNW–SSE oriented sinkholes (D'Argenio et al. 1988, Luperto-Sinni et al. 1991), suggesting that subaerial exposure and bauxite formation was facilitated here by a more pronounced (tectonically controlled) local uplift (updoming?) than in the Matese Mts Maggiore area.

The only indication of bauxite in Calabria (Figs 16, 17, Table 19) is associated with a small outcrop of intensely karstified/brecciated Upper Jurassic limestones at the base of the Oligo-Miocene clastic Palizzi Formation. Because of the apparently large stratigraphic gap it is very difficult to say whether the bauxite, filling a small karstic pocket of the Jurassic limestone, is itself Upper Jurassic/Lower Cretaceous or perhaps – like all the other bauxite occurrences of the Peninsula – rather Upper Cretaceous. Minerologically it is different from those of the Matese Mts Maggiore group, because in addition to boehmite it contains also diaspore (Bouillin et al. 1985). Based on their relationship to the enclosing rocks and the general geological make-up of the area they occur in, they are considered to be analogues of the bauxites of Sardinia rather than of those known from the Peninsula.

Bauxite deposits of *Sardinia* occur at a regional unconformity developed on the surface of Neocomian to Albian limestones and are covered by a Senonian transgression succession (Figs 11–15, Tables 17, 18). They fill a tectonically controlled shallow karst relief, display a variegated lithology often with clear signs of transportation. Both by lithology and by their relationship to their bedrock and cover they are strikingly similar to the bauxite deposits of Languedoc and Provence in France (Combes 1990; Cherchi et al. 1985).

Unlike all other Italian bauxites (which invariably occur at subaerial exposure surfaces related to some regional unconformity/disconformity), the only bauxite deposit of *Sicily* occurs at a local paleokarst developed on the surface of an uplifted block of probably rather limited extension (Figs 18, 19, Table 20). Whether the

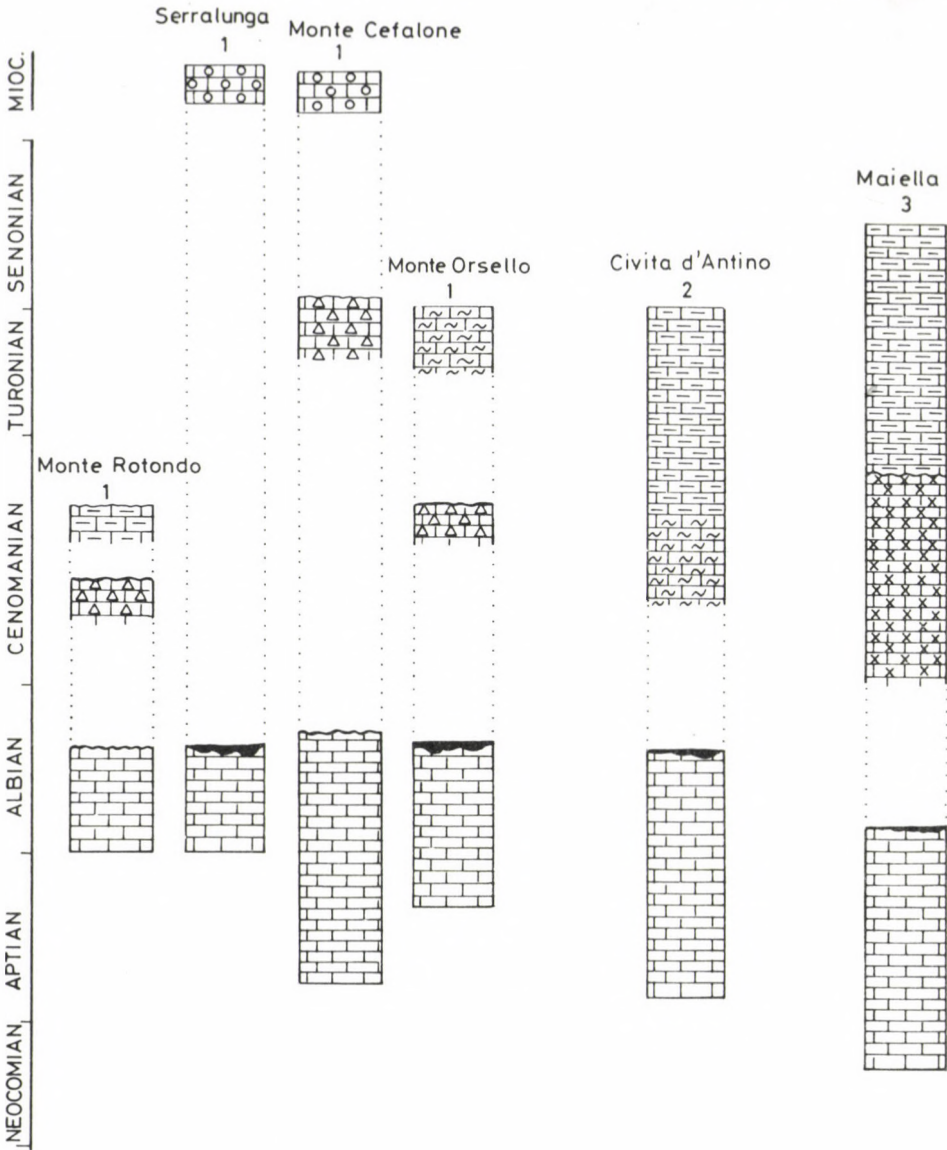


Fig. 3
Bauxites of Southern Italy (Abruzzi district) Stratigraphic columns. (Numbers indicate localities shown on Fig. 1. For legend see Fig. 2)

disconformity (which locally resulted in exposure) was of regional importance is not yet settled. There are some observations which suggest that the disconformity was regional, but extension-related and therefore subaerial exposure and bauxitization could take place locally at the margins of the subsiding tilted blocks only. (Di Stefano and Mindszenty in prep). If so, these bauxites may be analogues to those described by Molina et al. (1988, 1991) from the Subbetic Zone of Spain.

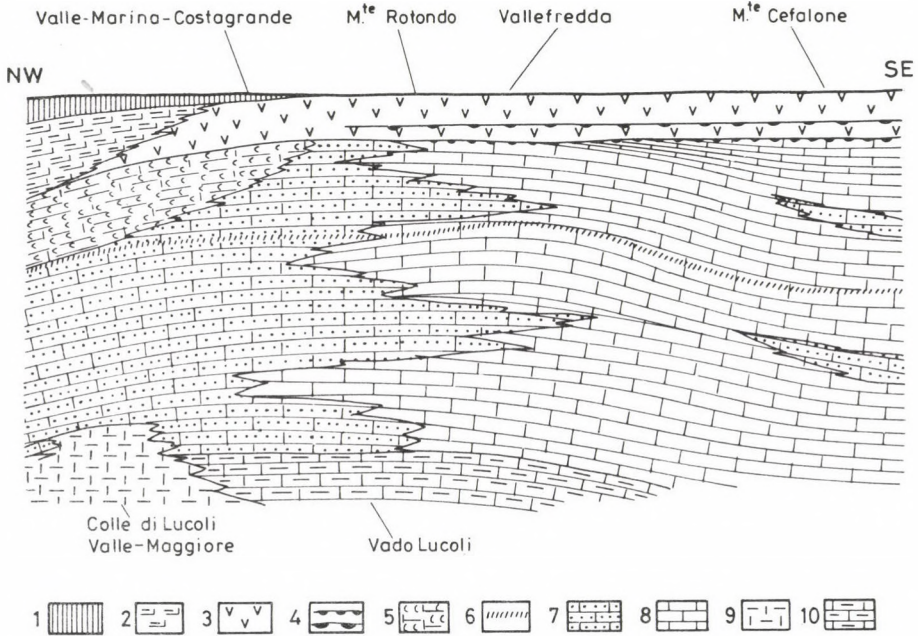


Fig. 4

Schematic diagram showing stratigraphic relationship in the Abruzzi bauxite district (after Bosif and Manfredini 1969). 1. Eocene; 2. Cenomanian-Maastrichtian transitional complex (with probable lacunae) 3. Mid-Cenomanian-Lower Turonian; 4. bauxite horizons; 5. Albian: Colle Raponaglia Formation; 6. top of *Salpingoporella dinarica* beds (Aptian/Albian boundary); 7. Neocomian-Albian: predominantly sparry microfacies; 8. Neocomian-Albian (Lower Cenomanian at Mts Cefalone): predominantly micritic microfacies; 9. Malm-Neocomian: bioherms; 10. Malm: biostroms, vertical exaggeration: 4X.

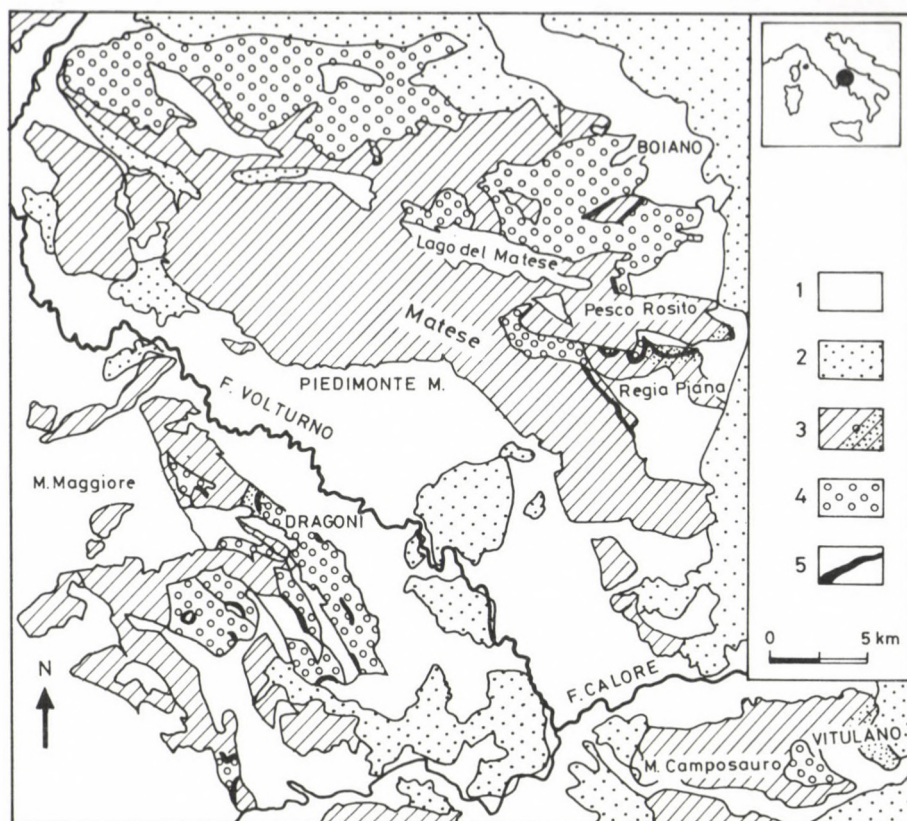


Table 1
Italy, Abruzzi district, Monti D'Ocre

1. Angular unconformity	Disconformity
2. Estimated duration of exposure	Not reported
3. Apparent stratigraphic gap	Albian pp. -Middle/Upper Cenomanian
4. Rate of regional subsidence	Not reported
5. Changes in lithofacies across unconformity	From lagoonal to open shelf
6. Record of contemporary sea-level changes	
7. Bedrock petrography and age	Calcareous bioclastic wackestone/packstone, Lower Aptian
8. Cover petrography	Calcareous bioclastic grainstones/packstones
9. Age of cover	Uppermost Cenomanian
10. Lithofacies of associated bauxite	Not reported
11. Underlying karst relief	Gentle
12. Supposed source material of bauxite	Volcanic and minor other windblown dust
13. Supposed source material of non bx. karst fills	Remnants of the partially dissolved sediments + crystal silt + lms. clasts
14. Lithology, size and shape of bx. deposit	Deep sink holes up to more than 10 m deep
15. Bauxite texture	Pelitimorphous-intraclastic-oolitic
16. Bauxite structure	Massive
17. Chemical composition of bauxite (%)	50-55/6-11, Fe ₂ O ₃ : 18-23, TiO ₂ : 2.5-2.9, P ₂ O ₅ : 0.05-0.1
18. Mineral composition of bauxite	Boehmite, kaolinite, montmorillonite, >>Geothite
19. Accessory minerals of bauxite	Monazite
20. Trace elements in the bauxite (ppm)	Pb: 28-144, Zn: 11-99, Cu: 7-166, Sr: 40-139, Li: 6-178, U: 1-7

Fig. 5 ←

Schematic geologic map of the Matese – M. Maggiore – Camposauro area. 1. fluvial-lacustrine, alluvial and volcanic deposits, Quaternary; 2. siliciclastic and carbonate deposits, Tertiary; 3. rudstid-bearing neritic carbonate deposits, sometimes resedimented, Upper Cretaceous; 4. dolomites and dolomitic limestones, platform limestones, Upper Triassic–Lower Cretaceous, a. deeply karstified Lower Cretaceous limestones; 5. bauxites

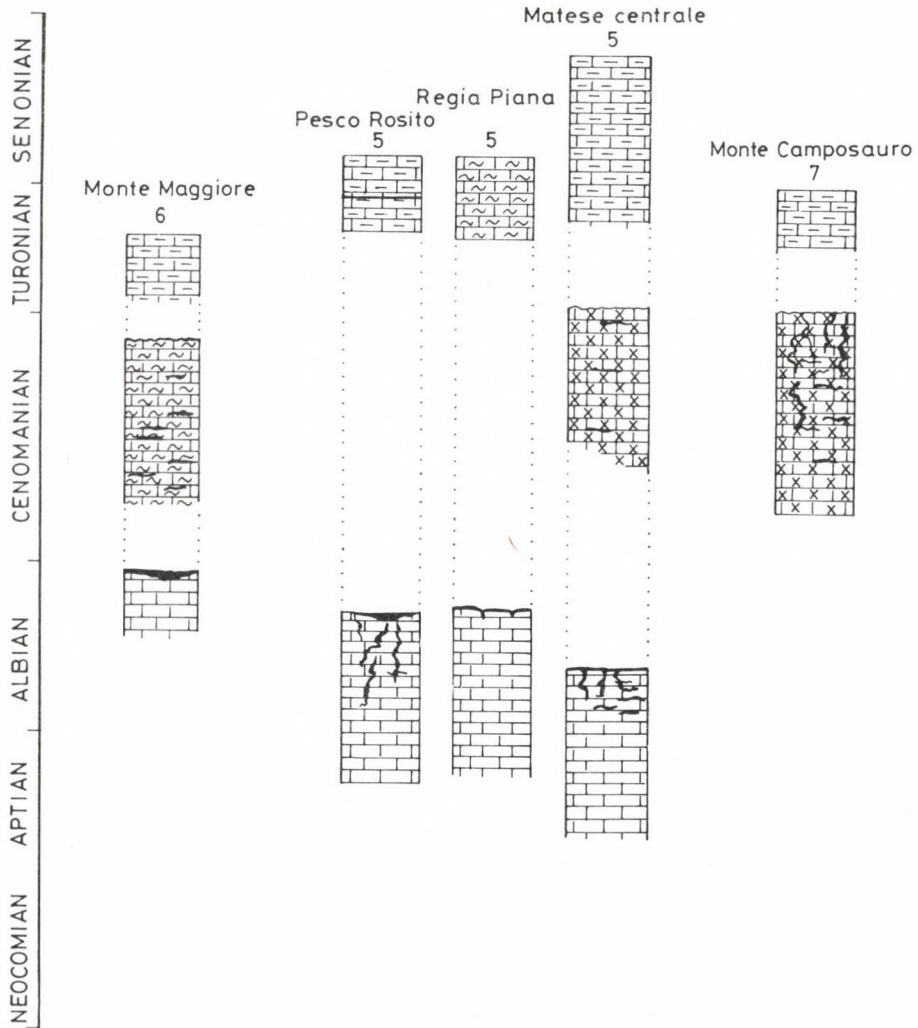


Fig. 6

Bauxites of Southern Italy (Campanian district). Stratigraphic columns. (Numbers indicate localities shown on Fig. 1. For legend see Fig. 2)

Table 2
Italy, Abruzzi district, Maiella

1. Angular unconformity	Disconformity
2. Estimated duration of exposure	Not reported (10 My)
3. Apparent stratigraphic gap	Albian–Middle Cenomanian
4. Rate of regional subsidence	Not reported
5. Changes in lithofacies across unconformity	From lagoonal to open shelf with variable circulation
6. Record of contemporary sea-level changes	Calcareous bioclastic wackestone/packstone, Upper Aptian–Lower Albian
7. Bedrock petrography and age	Calcareous bioclastic packstone/grainstones Upper Cenomanian
8. Cover petrography	Not reported
9. Age of cover	Gentle
10. Lithofacies of associated bauxite	Volcanic and other minor windblown dust
11. Underlying karst relief	Remnants of the partially dissolved sediments + crystal silt. + lms. clasts
12. Supposed source material of bauxite	Discontinuous horizon (lenses and pockets)
13. Supposed source material of non bx. karst fills	Oolitic/conglomeratic
14. Lithology, size and shape of bx. deposit	Massive
15. Bauxite texture	No data
16. Bauxite structure	Boehmite, kaolinite, hematite > goethite, an., siderite
17. Chemical composition of bauxite (%)	No data
18. Mineral composition of bauxite	No data
19. Accessory minerals of bauxite	No data
20. Trace elements in the bauxite (ppm)	No data

Table 3
Italy, Abruzzi district, Marsica

1. Angular unconformity	Disconformity
2. Estimated duration of exposure	Not reported (<10 My)
3. Apparent stratigraphic gap	Albian pp.–Middle/Upper Cenomanian
4. Rate of regional subsidence	Not reported
5. Changes in lithofacies across unconformity	From lagoonal to open shelf
6. Record of contemporary sea-level changes	Calcareous bioclastic wackestone/packstone. Lower–Middle Albian
7. Bedrock petrography and age	Calcareous bioclastic packstone/grainstones Uppermost Cenomanian
8. Cover petrography	Not reported
9. Age of cover	Gentle to middle karst
10. Lithofacies of associated bauxite	Volcanic and minor other windblown dust
11. Underlying karst relief	Remnants of the partially dissolved sediments + crystal silt + lms. clasts
12. Supposed source material of bauxite	Sink holes (up to more than 8 m deep)
13. Supposed source material of non bx. karst fills	Conglomeratic/oolitic/intraclastic
14. Lithology, size and shape of bx deposit	Massive
15. Bauxite texture	47–52/5–10, Fe ₂ O ₃ : 18–24, TiO ₂ : 3.0–3.5
16. Bauxite structure	Boehmite, kaolinite, hematite, calcite, an., magnetite-maghemite
17. Chemical composition of bauxite (%)	No data
18. Mineral composition of bauxite	No data
19. Accessory minerals of bauxite	No data
20. Trace elements in the bauxite (ppm)	No data

Table 4
Texture characteristics of bauxites from the Abruzzi district

	1	2	3	4	5	6	7	8	9	10
<i>Maiella Mt.</i>										
<i>(Caramanico)</i>										
Oolitic arenitic bx	1/2	15–20	50–60 –	0–5	15–20	11	–	yellow red		3
Oolitic-conglomeratic bx.	1/4	20–25	35–50 –	0–5	20–35	15	–	red yellow		3, 4
Oolitic limy bx.	1/4	15–20	50–60 –	–	10–15	9	10–15	dark red, ocre		1, 2
<i>Monti d'Ocre</i>										
<i>(Campo Felice)</i>										
Arenitic-pelitimorphic bx.	3/10	35–55	5–25 –	5	30–45	10	–	dark red > red > light red		19, 20, 21, 22, 26
Arenitic-conglomeratic-oolitic bx.	3/10	15–40	20–25 –	30–40	0–5	12	0–15	light red > red		1, 6, 7, 8, 10
Arenitic bx.	2/10	25/35	1–20 –	5–10	35–45	10	–	violet red > red		9, 11, 17, 23, 24
Pelitimorphic bauxitic clay "Green clay"	1/10 tr	40–65 80–100	10–20 – – –	2–10	5–15	3	–	yellow, red, violet green > grey		2, 15, 27, 28, 13, 14
Oolitic bx.	1/10	15–20	50–70 –	–	10–15	–	–	dark red		16
<i>Marsica Mt.</i>										
<i>(M. Turchio)</i>										
Conglomeratic-oidic bx.	4/10	35–40	25–30 –	–	25–35	13	–	light red > white		4, 5, 6,
Oolitic arenitic bx	2/10	35–40	35–40 –	0–5	20–25	9	–	dark red > yellow red, yellow		1, 3, 2
Oolitic bx.	2/10	20–30	50–60 –	0–5	10–15	5	–	red, yellow		2
Pelitimorphic-oolitic-arenitic bx.	1/10	40–50	20–30 –	–	15–20	8	–	mottled, red		7
Pelitimorphic-oolitic clayey bx.	1/10	50–60	20–25 –	0–5	5–10	5	–	mottled		8

Symbols: 1. proportions of textures, 2. authigenic groundmass (%), 3. ooides (%), 4. detrital mineral grain (%), 5. secondary segregations and older texture elements (%), 6. detrital bx. grains (%), 7. maximal diameter of detrital bx. grains (mm), 8. secondary calcite segregations (%), 9. colour, 10. samples No.

Table 5
Mineralogy of bauxites from Abruzzi district

1	2	3	4	5	6	7	8	9	10	11	12	13	14	15	16	17	18	19	20	21	22	23	24	25	26	27	28	29	30	31		
<i>Abruzzi district</i>																																
										<i>Monti d'Ocre</i>											<i>Campo Felice deposit (Orsello)</i>											
5.	-	-	-	3.0	-	-	2.0	-	5.0	0.4	4.6	9.3	-	-	-	-	-	-	-	-	-	74.2	1.0	0.1	tr.	-	-	0.2	2	10		
4.	-	1.2	-	0.9	-	-	0.8	-	1.1	0.2	1.0	0.2	-	-	-	-	-	-	-	-	-	93.2	0.9	0.2	tr.	-	-	0.1	n.d.	12		
3.	-	1.4	-	0.8	-	-	10.1	-	-	0.1	2.2	-	-	-	-	-	-	-	-	-	-	84.6	-	0.2	0.1	-	-	0.2	-	4		
30.	-	1.8	-	12.1	-	-	12.7	-	12.2	-	1.1	0.3	-	-	-	-	-	-	-	-	-	57.5	-	0.8	0.3	-	-	0.8	n.d.	10		
2.	-	24.1	-	7.2	-	-	22.2	-	-	0.5	9.4	2.1	-	-	-	-	-	-	-	-	-	29.9	-	2.1	0.8	-	-	2	1	5		
1.	-	58.4	-	6.3	-	-	7.4	-	-	-	0.2	18.1	-	-	-	-	-	-	-	-	-	5.2	-	2.2	0.6	-	-	2	3	n.d.		
27.	-	63.5	0.4	11.7	-	-	12.9	-	-	0.3	5.7	-	-	-	-	-	-	0.3	-	-	-	0.9	-	2.1	0.8	-	-	1.0	-	10		
26.	-	70.4	-	10.5	-	-	-	-	-	0.3	3.0	11.2	-	-	-	-	-	-	-	-	-	-	-	2.6	0.6	-	-	1.0	3	13		
8.	0.3	70.8	-	4.3	-	-	-	-	-	-	-	20.8	-	-	-	-	-	-	-	-	-	-	-	1.9	0.5	-	-	1.1	2-3	-		
7.	-	63.5	-	7.7	-	-	-	-	-	tr	0.4	24.2	-	-	-	-	-	-	-	-	-	-	-	1.7	0.6	-	-	1.1	2-3	n.d.		
9.	-	50.3	-	18.7	-	-	-	-	-	-	-	27.0	-	-	-	-	-	-	-	-	-	-	-	2.0	0.5	-	-	1.1	3	-		
20.	-	54.0	-	12.4	-	-	7.0	-	-	-	-	21.1	-	-	-	-	-	-	-	-	-	-	0.4	0.4	2.1	0.6	-	-	1.0	3	-	
22.	-	57.0	-	10.7	-	-	5.0	-	-	-	1.5	21.2	-	-	-	-	-	-	-	-	-	0.3	-	2.2	0.6	-	-	1.1	2-3	8		
21.	-	69.0	-	7.8	-	-	-	-	-	-	-	19.0	-	-	-	-	-	-	-	-	-	-	-	2.0	0.7	-	-	1.1	3	-		
19.	-	40.7	-	27.4	-	-	8.2	-	-	-	-	19.3	-	-	-	-	-	-	-	-	-	0.5	-	2.0	0.6	-	-	1.0	2	-		
17.	tr.	51.0	-	15.7	-	-	-	-	-	-	-	29.2	-	-	-	-	-	-	-	-	-	-	0.3	-	2.0	0.5	-	-	1.0	2-3	-	
16.	-	66.8	-	15.0	-	-	-	-	-	-	-	14.0	-	-	-	-	-	-	-	-	-	-	-	2.2	0.6	-	-	1.0	2-3	-		
16/1	-	77.1	-	15.9	tr.	-	-	-	-	-	-	1.2	-	-	-	-	-	-	-	-	0.4	-	0.4	-	3.0	0.8	-	-	0.9	2-3	-	
15.	-	48.6	-	30.8	-	-	-	-	-	-	-	16.0	-	-	-	-	-	-	-	-	-	0.5	-	2.1	0.5	-	-	1.1	3	-		
10.	-	47.9	-	18.7	-	-	-	-	5.1	-	-	21.7	2.0	-	-	-	-	-	-	-	-	0.6	-	2.0	0.5	-	-	1.1	3	-		
11.	-	53.7	-	21.1	-	-	9.0	-	-	-	-	9.6	1.5	-	-	-	-	-	-	-	-	0.3	0.4	0.4	-	2.1	0.5	-	-	1.1	1-2	-
14.	-	22.7	-	33.1	-	-	28.1	-	9.5	-	-	2.0	-	-	-	-	-	-	-	-	-	0.4	-	1.4	-	1.0	0.4	-	-	1.0	1	-
32.	-	-	-	20.1	-	-	68.1	4.3	-	-	-	-	-	-	-	-	-	-	-	-	-	1.2	-	4.1	-	1.0	tr.	-	-	0.8	-	-
31.	-	-	-	10.9	-	-	57.3	5.2	-	-	-	-	-	-	-	-	-	-	-	-	-	0.3	-	24.9	-	0.3	0.3	-	-	0.4	-	-
25.	0.5	65.4	0.5	8.5	-	-	-	-	-	0.4	9.8	11.4	-	-	-	-	-	-	-	-	-	-	-	-	1.8	0.3	-	-	1.0	4	14	
24.	-	52.2	-	10.1	-	-	-	-	-	-	-	22.6	-	-	-	-	-	-	-	-	-	-	0.5	10.8	-	1.9	0.5	-	-	1.0	3	-
23.	-	59.	-	9.9	-	-	3.0	-	-	-	tr.	23.7	-	-	-	-	-	-	-	-	-	-	-	-	1.8	0.4	-	-	1.0	4	-	
<i>Abruzzi district</i>																																
										<i>Monti d'Ocre</i>											<i>Cava il Nibbio deposit</i>											
13.	-	54.2	-	19.0	-	-	3.1	-	-	-	-	19.7	0.5	-	-	-	-	-	-	-	-	-	-	0.2	1.5	0.3	-	-	1.1	3-4	-	
<i>Abruzzi district</i>																																
										<i>Monti Marsica</i>											<i>Leccie nei Marsi deposit</i>											
11.	-	57.3	-	7.1	-	-	-	-	-	-	-	19.3	3.1	-	-	-	-	-	-	-	-	-	-	9.6	-	1.7	0.4	-	-	1.1	2	-
<i>Abruzzi district</i>																																
										<i>Monti Marsica</i>											<i>Monte Turchio deposit</i>											
10.	-	68.3	-	6.0	-	-	1.2	-	-	-	-	19.5	0.8	-	-	-	-	-	-	-	-	0.2	-	-	-	2.1	0.6	-	-	1.1	4	-
<i>Abruzzi district</i>																																
										<i>Monte del Morrone</i>											<i>Pacenro south deposit</i>											
1.	-	22.2	-	24.4	-	-	-	-	-	-	-	0.6	37.0	-	-	-	-	-	-	-	-	-	-	-	-	-	-	-	-	-	-	-
<i>Abruzzi district</i>																																
										<i>Monte Maiella</i>											<i>West. slope deposit</i>											
2.	-	59.5	-	7.5	-	-	-	-	-	-	-	1.0	26.2	-	-	-	-	-	-	-	-	0.8	-	-	-	2.2	0.6	-	-	1.2	4	n.d.

Symbols: 1. sample No; 2. diaspore; 3 boehmite; 4 gibbsite; 5. metahalloysite; 6. kaolinite; 7. chlorite diokt.; 8. chlorite triokt.; 9. illite, hydromuscovite; 10. montmorillonite; 11. mixed-layer clay minerals; 12. quartz; 13. goethite; 14. haematite; 15. magnetite, maghemite; 16. pyrite, marcasite; 17. fibroferrite; 18. melanterite; 19. gypsum; 20. alunite; 21. siderite, oligonite; 22. rodochrosite; 23. calcite; 24. ankerite, dolomite; 25. anatase; 26. rutile; 27. psilomelane; 28. todorokite, 29. absorbed water above 100 °C; 30. Al₂O₃ substitution in haematite; 31. AlOOH substitution in goethite; tr - traces; nd - not determinable because of small quantity; * - mixture of glaukonite and illite with predominance of glaukonite

Table 6
Italy, Campania district, Monte Maggiore

1. Angular unconformity	No or not well evident
2. Estimated duration of exposure	? (< 10 My)
3. Apparent stratigraphic gap	Uppermost Albian–Lower Cenomanian
4. Rate of regional subsidence	?
5. Changes in lithofacies across unconformity	From lagoonal to restricted lagoonal/peritidal
6. Record of contemporary sea-level changes	
7. Bedrock petrography and age	Calcareous bioclastic wackestone/packstone, Upper Albian
8. Cover petrography	Bioclastic wackestones cyclically alternating with dolomitized laminites
9. Age of cover	Middle Cenomanian
10. Lithofacies of associated bauxite	Vadose (main horizon), phreatic (upper horizon)
11. Underlying karst relief	Gentle
12. Supposed source material of bauxite	Volcanic dust
13. Supposed source material of non bx. karst fills	Remnants of the partially dissolved sediments + crystal silt
14. Lithology, size and shape of bx. deposit	From few to 50 cm level with local development of dolina (6–10 m thick)
15. Bauxite texture	Mainly oolitic packstones
16. Bauxite structure	Massive
17. Chemical composition of bauxite (%)	50–55/4–9, Fe ₂ O ₃ : 22–28; TiO ₂ : 2.2–2.6; P ₂ O ₅ : 0.05–0.1
18. Mineral composition of bauxite	Boehmite, kaolinite (montmorillonite, illite) Goethite, an
19. Accessory minerals of bauxite	no data
20. Trace elements in the bauxite (ppm)	Pb: 35–165; Cu: 11–260; Co: 11–90, Ni: 88–220; Cr: 190–260; Mn: 970–1700

Table 7
Italy, Campania district, Regia Piana

1. Angular unconformity	Disconformity
2. Estimated duration of exposure	Not reported (≤ 10 My)
3. Apparent stratigraphic gap	Albian pp. –Turonian pp.
4. Rate of regional subsidence	Not reported
5. Changes in lithofacies across unconformity	From lagoonal to open shelf
6. Record of contemporary sea-level changes	
7. Bedrock petrography and age	Calcareous bioclastic wackestone/packstone, Albian
8. Cover petrography	Calcareous bioclastic packstone/grainstones
9. Age of cover	Uppermost Turonian–Senonian
10. Lithofacies of associated bauxite	Saturated (phreatic) passing to oxidized clasts in matrix of saturated bauxite
11. Underlying karst relief	Gentle
12. Supposed source material of bauxite	Volcanic and other minor windblown dust
13. Supposed source material of non bx. karst fills	Remnants of the partially dissolved sediments + crystal silt
14. Lithology, size and shape of bx. deposit	Discontinuous pockets few meters in diameter, up to 2 m deep
15. Bauxite texture	Oolitic packstone to clastic floatstone in matrix of oolitic packstones
16. Bauxite structure	Massive with a clear erosional surface between the above lithotypes
17. Chemical composition of bauxite (%)	No data
18. Mineral composition of bauxite	Boehmite (di), kaolinite, goethite, py., an.
19. Accessory minerals of bauxite	No data
20. Trace elements in the bauxite (ppm)	Pb: 11–86; Cu: 3–10; Co: 0–15; Ni: 70–120; Cr: 160–290; Mn: 250–840; Y: 0–55; La: 0–70; Sr: 52–200; B: 0–32

Table 8
Italy, Campanian district, Pesco Rosito

1. Angular unconformity	Disconformity
2. Estimated duration of exposure	Not reported (< 10 My)
3. Apparent stratigraphic gap	Albian pp.–Turonian pp.
4. Rate of regional subsidence	Not reported
5. Changes in lithofacies across unconformity	From lagoonal to open shelf
6. Record of contemporary sea-level changes	
7. Bedrock petrography and age	Calcareous bioclastic wackestone/packstone, Albian
8. Cover petrography	Calcareous bioclastic grainstones
9. Age of cover	Uppermost Turonian–Senonian
10. Lithofacies of associated bauxite	Transported in vadose regime
11. Underlying karst relief	Mainly fracture controlled
12. Supposed source material of bauxite	Volcanic and minor other windblown dust
13. Supposed source material of non bx. karst fills	Remnants of the partially dissolved sediments + crystal silt + lms. clasts
14. Lithology, size and shape of b.x deposit	Discontinuous lense, up to 1 m thick
15. Bauxite texture	Clastic floatstones in matrix of oolitic packstones
16. Bauxite structure	Massive
17. Chemical composition of bauxite (%)	No data
18. Mineral composition of bauxite	No representative data (Boehmite, kaolinite, hematite)
19. Accessory minerals of bauxite	No data
20. Trace elements in the bauxite (ppm)	No data

Table 9
Italy, Campanian district, Matese centrale

1. Angular unconformity	Disconformity
2. Estimated duration of exposure	Not reported (< 10 My)
3. Apparent stratigraphic gap	Upper Albian–Middle/Upper Cenomanian
4. Rate of regional subsidence	Not reported
5. Changes in lithofacies across unconformity	From lagoonal to open shelf with variable circulation
6. Record of contemporary sea-level changes	
7. Bedrock petrography and age	Calcareous bioclastic wackestone/packstone, Lower Albian
8. Cover petrography	Calcareous bioclastic packstone/grainstones
9. Age of cover	Upper Cenomanian
10. Lithofacies of associated bauxite	Transported
11. Underlying karst relief	Gentle
12. Supposed source material of bauxite	Volcanic and other minor windblown dust
13. Supposed source material of non bx. karst fills	Remnants of the partially dissolved sediments + crystal silt + lms. clasts
14. Lithology, size and shape of bx. deposit	Discontinuous horizon (pockets, up to 0.5 m deep)
15. Bauxite texture	Clastic floatstones in matrix of oolitic packstones
16. Bauxite structure	Massive
17. Chemical composition of bauxite (%)	No data
18. Mineral composition of bauxite	No data
19. Accessory minerals of bauxite	No data
20. Trace elements in the bauxite (ppm)	No data

Table 10
Italy, Campania district, Camposauro

1. Angular unconformity	Disconformity
2. Estimated duration of exposure	Not reported (<10 My)
3. Apparent stratigraphic gap	Upper Cenomanian–Lower Turonian
4. Rate of regional subsidence	Not reported
5. Changes in lithofacies across unconformity	From variable circulation to higher energy open shelf
6. Record of contemporary sea-level changes	
7. Bedrock petrography and age	Calcareous bioclastic packstone, Cenomanian
8. Cover petrography	Calcareous bioclastic packstone/grainstones
9. Age of cover	Upper Turonian
10. Lithofacies of associated bauxite	Transported (originally vadose)
11. Underlying karst relief	Fracture controlled hypogean karst
12. Supposed source material of bauxite	Volcanic and other minor windblown dust
13. Supposed source material of non bx. karst fills	Remnants of the partially dissolved sediments + crystal silt + lms. clasts
14. Lithology, size and shape of bx deposit	Filling of hypogean karst cavities
15. Bauxite texture	Clastic floatstones
16. Bauxite structure	Filling structures
17. Chemical composition of bauxite (%)	No data
18. Mineral composition of bauxite	No data
19. Accessory minerals of bauxite	No data
20. Trace elements in the bauxite (ppm)	No data

Table 11
Texture characteristics of bauxites from the Campania district

	1	2	3	4	5	6	7	8	9	10
<i>Matese Mt.</i>										
<i>(Regia Piana)</i>										
Oolitic bx.	2/3	20–30	60–70	–	–	5–10	2	–	ocre > violet-red	2
Oolitic- onglomeratic bx	1/3	5–35	30–70	–	0–10	20–35	25	–	violet-red > ocre >> mottled > grey	1
<i>M. Maggiore</i>										
<i>Mt (Dragoni)</i>										
Arenitic-oolitic bx.	1/2	20–40	10–40	–	0–5	10–50	4	–	red,	1, 2, 3, 4, 6, 9, 13
Oolitic bx.	1/8	20–40	55–65	–	–	10–20	3	–	dark red red > light red > yellow	7
Oolitic limy bx.	1/8	20–30	40–50	–	–	10–25	5	5–20	brickled. light red	10
Pelitimorphic bauxitic clay	1/8	70–80	20–30	5–10	–	–	–	–	ocre	5, 8
Pelitimorphic- oolitic bx.	1/8	50–60	20–25	–	0–5	15–20	–	–	light red- yellow	15

Symbols: 1. proportions of textures, 2. authigenic groundmass (%), 3. ooides (%), 4. detrital mineral grain (%), 5. secondary segregations and older texture elements (%), 6. detrital bx. grains (%), 7. maximal diameter of detrital bx. grains (mm), 8. secondary calcite segregations (%), 9. colour, 10. samples No.

Table 12
Mineralogy of bauxites from Campania district

	1	2	3	4	5	6	7	8	9	10	11	12	13	14	15	16	17	18	18	20	21	22	23	24	25	26	27	28	29	30	31	
<i>Campania district, Monte Maggiore, Castello Dragoni deposit</i>																																
11.	-	0.8	-	-	1.3	-	-	1.0	0.5	-	-	0.4	0.3	-	-	-	-	-	-	-	-	-	94.8	-	0.1	-	0.4	-	0.2	n.d.	10	
5.	-	6.7	-	-	19.3	-	-	27.5	16.8	-	8.7	11.2	-	-	-	-	-	-	-	-	-	-	5.0	-	2.4	0.7	-	-	1.4	-	14	
8.	-	2.7	1.3	-	10.3	-	-	56.9	9.5	-	4.0	8.7	-	-	-	-	-	-	-	-	-	-	2.3	-	1.9	0.7	-	-	1.4	-	13	
10.	-	52.5	-	-	3.0	-	-	-	-	-	-	1.7	18.4	-	-	-	-	-	-	-	-	-	20.8	-	1.4	0.5	-	-	1.4	2	15	
9.	-	69.7	-	-	3.9	-	-	-	-	-	-	0.3	16.5	-	-	-	-	-	-	-	-	-	5.3	-	1.9	0.7	-	-	1.4	2	14	
7.	-	68.0	-	-	3.4	-	-	-	-	-	-	5.1	18.9	-	-	-	-	-	-	-	-	-	0.3	-	2.0	0.6	-	-	1.4	2	18	
1.	-	50.9	-	-	15.7	-	-	-	-	-	-	1.4	28.4	-	-	-	-	-	-	-	0.2	-	-	-	1.5	0.4	-	-	1.4	2	17	
2.	-	57.0	-	-	2.1	-	-	-	-	-	-	1.7	35.3	-	-	-	-	-	-	-	-	-	-	-	1.6	0.6	-	-	1.4	3	20	
3.	-	55.6	-	-	13.5	-	-	-	-	-	-	1.6	24.6	-	-	-	-	-	-	-	0.4	-	-	-	2.2	0.4	-	-	1.4	2	11	
4.	-	65.7	-	-	5.3	-	-	-	-	-	-	0.4	22.8	1.7	-	-	-	-	-	-	-	-	-	-	1.9	0.5	-	-	1.4	2	17	
6.	-	65.6	-	-	11.6	-	-	-	-	-	-	0.4	18.1	-	-	-	-	-	-	-	-	-	-	-	2.0	0.5	-	-	1.4	2	17	
13.	-	60.9	-	-	13.8	-	-	-	-	-	-	0.4	20.7	-	-	-	-	-	-	-	-	-	-	-	-	1.9	0.6	-	-	1.4	2	11
12.	-	51.3	-	-	8.0	-	-	-	-	-	-	0.6	10.7	-	-	-	-	-	-	-	-	-	25.6	-	1.6	0.5	-	-	1.4	2	13	
14.	-	0.9	-	-	3.0	-	-	2.6	-	-	-	0.7	0.7	-	-	-	-	-	-	-	-	-	90.4	-	0.2	-	1.0	-	0.4	1-2	20	
<i>Campania district, Monti Matese, Regia Piana deposit</i>																																
1.	0.2	60.3	-	-	27.5	-	-	-	-	-	-	2.3	-	-	-	3.0	1.1	0.4	-	-	0.5	-	-	2.5	0.6	-	-	1.1	-	n d.		
8.	-	63.6	-	-	24.3	-	-	-	-	-	-	4.9	1.6	-	-	-	-	-	-	-	-	-	0.2	2.8	0.8	-	-	1.4	3-4	7		
<i>Campania district, Monti Matese, Cusano Mutri deposit</i>																																
9A.	0.6	62.3	2.3	-	10.8	-	-	-	-	-	-	-	-	-	15.2	-	-	1.0	2.8	-	-	-	-	-	2.5	0.7	-	-	1.4	-	-	
9B.	-	74.1	-	-	9.3	-	-	-	-	-	-	10.8	0.5	-	-	-	-	-	-	-	-	-	-	-	-	2.7	0.8	-	-	1.4	n d.	11

Symbols: 1. sample No; 2. diaspro; 3 boehmite; 4 gibbsite; 5. metahalloysite; 6. kaolinite; 7. chlorite diokt.; 8. chlorite triokt.; 9. illite, hydromuscovite; 10. montmorillonite; 11. mixed-layer clay minerals; 12. quartz; 13. goethite; 14. haematite; 15. magnetite, maghemite; 16. pyrite, marcasite; 17. fibroferrite; 18. melanterite; 19. gypsum; 20. alunite; 21. siderite, oligonite; 22. rodochrosite; 23. calcite; 24. ankerite, dolomite; 25. anatase; 26. rutile; 27. psilomelane; 28. todorokite, 29. absorbed water above 100 °C; 30. Al₂O₃ substitution in haematite; 31. AlOOH substitution in goethite; tr - traces; nd - not determinable because of small quantity; * - mixture of glaukonite and illite with predominance of glaukonite

Apulia

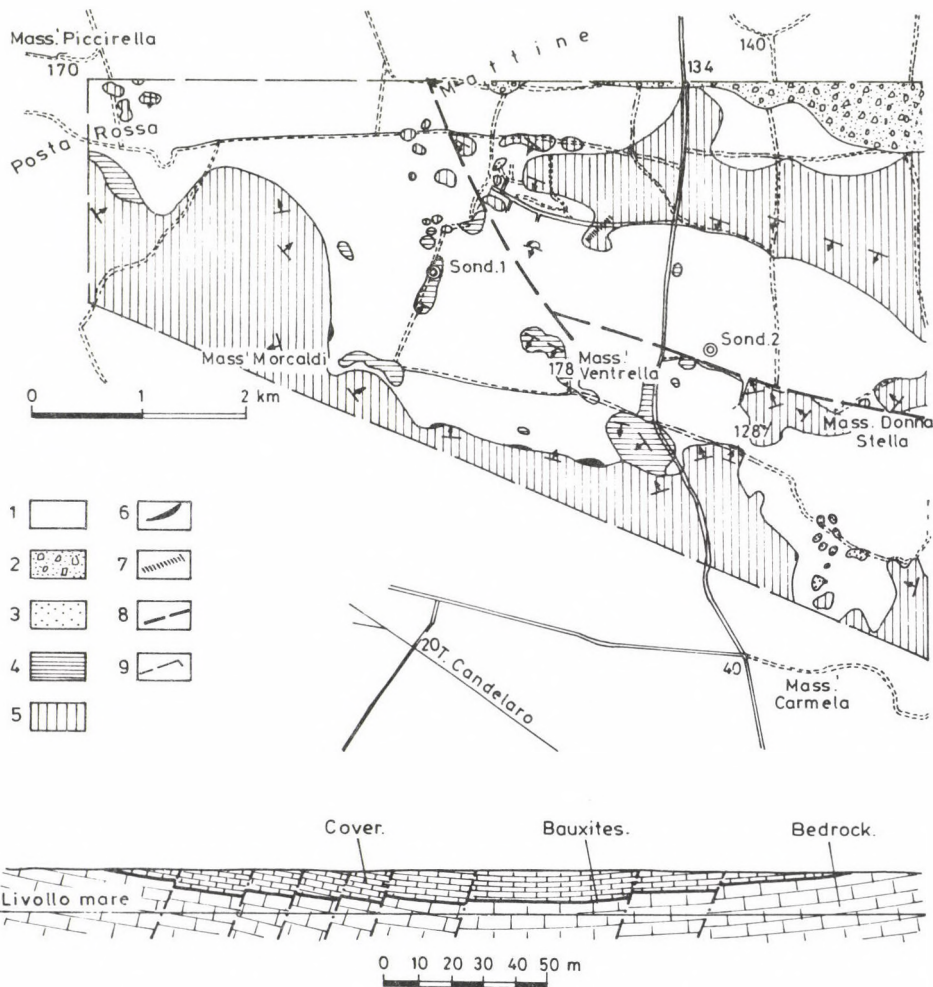


Fig. 7
Schematic geologic map of the S. Giovanni Rotondo Area (Gargano). 1-2. continental deposits, Quaternary; 3. calcarenites ("pietra leccese" Auct.), Miocene; 4. limestones and marls, Upper Cretaceous (Senonian?); 5. limestones (calcarenites), Lower Cretaceous-Cenomanian; 6. bauxites; 7. Mattine sequence; 8. faults; 9. area limits

Fig. 8.†
Locality map of the S. Egidio Area (Gargano). a) 1. lacustrine shales, Quaternary; 2. calcarenites ("pietra leccese" Auct.); 3. limestones and marls (Upper Cretaceous); 4. calcarenites. Lower Cretaceous-Cenomanian. 5. bauxites 6. bedrock limestones, Lower-Middle Cretaceous. b) 1. lacustrine shales, Quaternary; 2. calcarenites, Miocene; 3. shale, Miocene; 4. cover limestones, Upper Cretaceous; 5. bauxites; 6. bedrock limestones, Lower-Middle Cretaceous; (by Crescenti and Vighi 1964, modified)

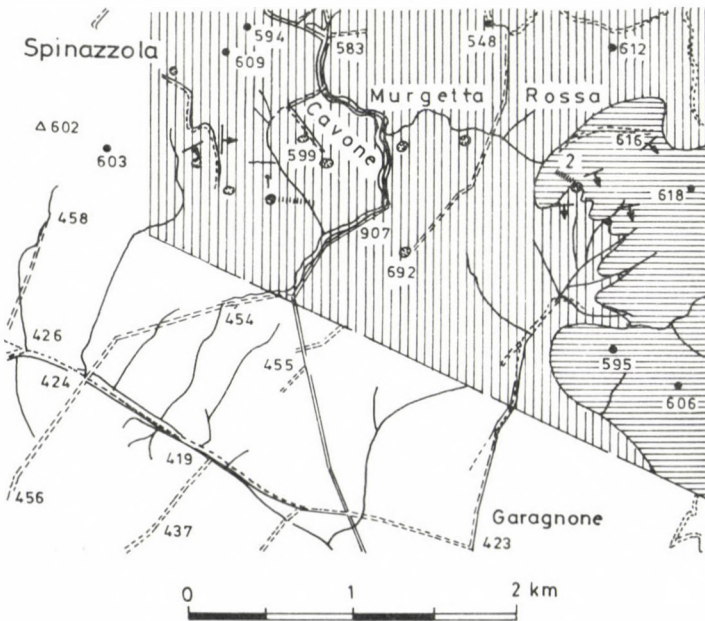
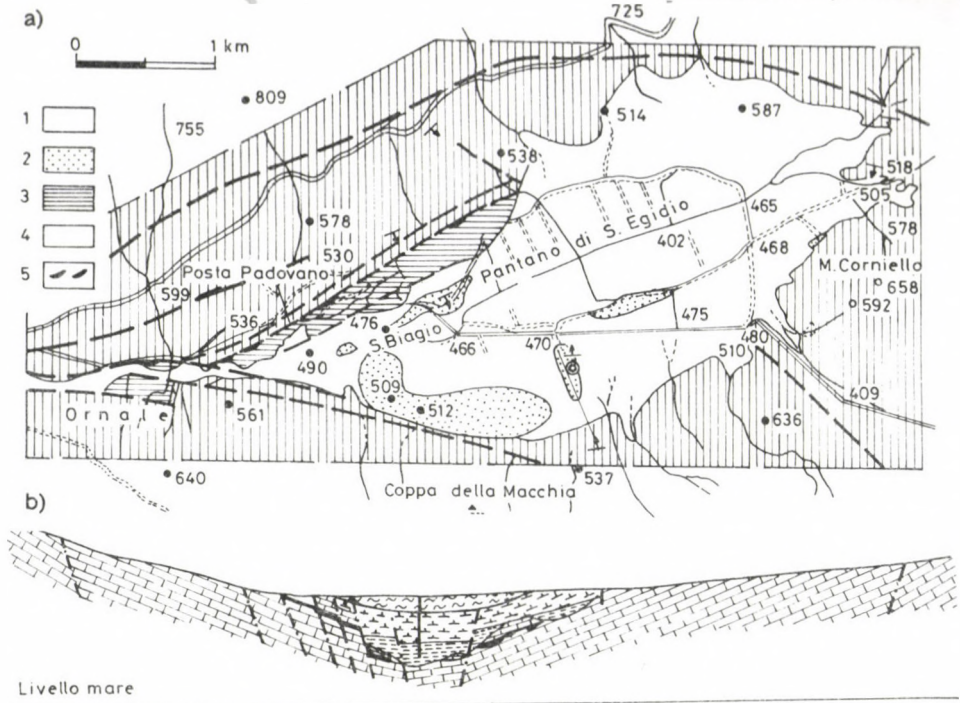


Fig. 9
 Schematic geologic map of the Spinazzola area. 1. Upper Cretaceous limestones; 2. Lower Cretaceous limestones (calcarinites); 3. bauxites; 4. bauxite pockets; 5. stratigraphic series: 1) Cavone, 2) Murgetta Rossa (Crescenti and Vighi 1964, modified)

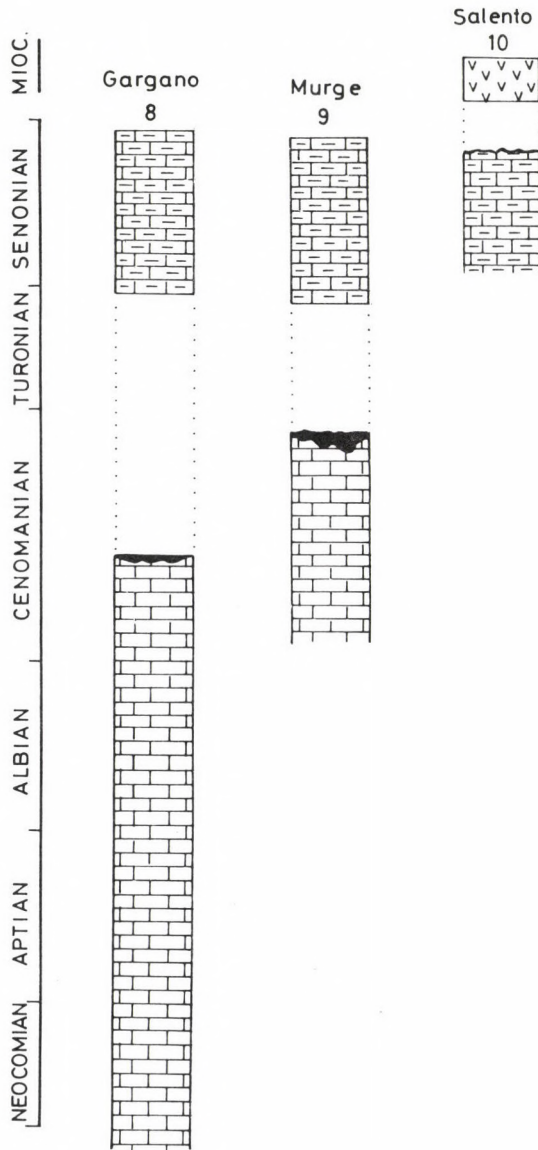


Fig. 10
Bauxites of Southern Italy (Apulia district) Stratigraphic columns. (Numbers indicate localities shown on Fig. 1. For legend see Fig. 2)

Table 13
Italy, Apulia district, Gargano

1. Angular unconformity	Low angle unconformity
2. Estimated duration of exposure	Not reported (< 10 My)
3. Apparent stratigraphic gap	Cenomanian–Turonian
4. Rate of regional subsidence	Not reported
5. Changes in lithofacies across unconformity	No substantial changes
6. Record of contemporary sea-level changes	
7. Bedrock petrography and age	Calcareous bioclastic wackestone/packstone, Albian
8. Cover petrography	Calcareous mudstone/wackestone
9. Age of cover	Senonian
10. Lithofacies of associated bauxite	Vadose
11. Underlying karst relief	Medium depth doline type
12. Supposed source material of bauxite	Volcanic and other minor windblow dust
13. Supposed source material of non bx. karst fills	No data
14. Lithology, size and shape of bx. deposit	Lense shaped doline fills up to more than 10 m thick
15. Bauxite texture	Oolitic packstone. (see also tables)
16. Bauxite structure	Massive
17. Chemical composition of bauxite (%)	46–52/5–10, Fe ₂ O ₃ :17–22; TiO ₂ :3.2–3.8; P ₂ O ₅ : 0.05–0.5
18. Mineral composition of bauxite	Boehmite, Kaolinite, Hematite > Goethite, An, Calcite
19. Accessory minerals of bauxite	No Data
20. Trace elements in the bauxite (ppm)	Pb: 17–79; Zn: 5–9; Cu: 7–12; Sr: 80–199; Li: 0.7–4; U: 0.5–17

Table 14
Italy, Apulia district, Spinazzola

1. Angular unconformity	Low angle unconformity
2. Estimated duration of exposure	Not reported (< 10 My)
3. Apparent stratigraphic gap	Cenomanian pp.–Turonian pp.
4. Rate of regional subsidence	Not reported
5. Changes in lithofacies across unconformity	From lagoonal to open lagoon
6. Record of contemporary sea-level changes	
7. Bedrock petrography and age	Calcareous bioclastic wackestone/packstones, Cenomanian
8. Cover petrography	Calcareous bioclastic packstone
9. Age of cover	Senonian
10. Lithofacies of associated bauxite	Vadose
11. Underlying karst relief	Deep canyon (more than 40 m deep)
12. Supposed source material of bauxite	Volcanic and other minor windblow dust
13. Supposed source material of non bx. karst fills	No data
14. Lithology, size and shape of bx. deposit	Deep canyon fill shape
15. Bauxite texture	Oolitic packstone
16. Bauxite structure	Massive
17. Chemical composition of bauxite (%)	46–51/5–10, Fe ₂ O ₃ : 16–22; TiO ₂ : 3.5–4.08; P ₂ O ₅ : 0.05–0.1
18. Mineral composition of bauxite	Boehmite > gibbsite, kaolinite, hematite, goethite, an. (calcite)
19. Accessory minerals of bauxite	zircon, serpentine, garnet, quartz, mica
20. Trace elements in the bauxite (ppm)	Pb: 17–144; Zn: 11–99; Cu: 7–166; Sr: 40–199; Li: 6–198; U: 1–7;

Table 15
Mineralogy of bauxites from Apulia district (from Bárdossy et al. 1975)

Actia Geologica Hungaria

	1	2	3	4	5	6	7	8	9	10	11	12	13	14	15	16	17	18	19	20	21	22	23	24	25	26	27	28	29	30	31				
<i>Apulia district</i>	<i>G Gargano Peninsula</i>					<i>San Giovanni Rotondo deposit</i>																													
23	-	4.6	-	-	6.5	-	-	-	-	-	-	-	0.7	-	-	-	-	-	-	-	-	-	-	86.6	-	0.5	0.1	-	-	0.7	-	nd.			
22	-	2.4	-	-	12.5	-	-	-	-	-	-	-	2.7	-	-	-	-	-	-	-	-	-	80.2	-	0.9	0.1	-	-	0.8	-	nd.				
21	-	4.6	-	-	6.5	-	-	-	-	-	-	-	0.3	-	-	-	-	-	-	-	-	-	86.6	-	0.7	0.1	-	-	0.8	-	nd.				
20	-	2.5	-	-	14.2	-	-	-	-	-	-	-	3.4	-	-	-	-	-	-	-	-	-	77.1	-	1.2	0.2	-	-	1.0	-	10				
19	-	4.9	-	-	15.8	-	-	-	-	-	-	-	3.3	-	-	-	-	-	-	-	-	-	73.0	-	1.3	0.2	-	-	1.1	-	13				
18	-	19.5	-	-	2.1	-	-	-	-	-	-	-	0.9	2.0	-	-	-	-	-	-	-	-	72.7	-	1.0	0.2	-	-	1.2	2	16				
17	-	37.9	-	-	2.5	-	-	-	-	-	-	-	1.5	8.7	-	-	-	-	-	-	-	-	44.7	-	2.1	0.5	-	-	1.7	2-3	20				
16	-	41.6	-	-	3.2	-	-	-	-	-	-	-	3.0	12.3	-	-	-	-	-	-	-	-	35.0	-	2.1	0.6	-	-	1.8	2-3	25				
15	-	38.9	0.8	-	5.1	-	-	-	-	-	-	-	1.0	17.4	-	-	-	-	-	-	-	-	31.7	-	2.2	0.8	-	-	1.7	4	nd.				
14	-	55.5	-	-	5.0	-	-	-	-	-	-	-	4.9	12.9	-	-	-	-	-	-	-	-	16.1	-	2.7	0.7	-	-	1.7	2-3	28				
13	-	67.1	-	-	3.0	-	-	-	-	-	-	-	3.0	21.5	-	-	-	-	-	-	-	-	-	-	-	2.7	0.7	-	-	1.6	4	28			
12	-	55.2	0.9	-	13.8	-	-	-	-	-	-	-	0.6	23.8	-	-	-	-	-	-	-	-	-	-	-	2.8	0.9	-	-	1.6	3	29			
11	-	54.5	0.6	-	15.1	-	-	-	-	-	-	-	1.6	22.8	-	-	-	-	-	-	-	-	-	-	-	2.6	0.8	-	-	1.6	4	32			
10	-	62.6	0.8	-	11.6	-	-	-	-	-	-	-	1.2	18.2	-	-	-	-	-	-	-	-	-	-	-	2.6	1.0	-	-	1.6	4	28			
9	-	51.2	0.6	-	22.0	-	-	-	-	-	-	-	5.8	14.9	-	-	-	-	-	-	-	-	-	-	-	2.9	0.6	-	-	1.6	4-5	30			
8	-	23.7	-	-	36.8	-	-	-	-	-	-	-	4.4	27.7	-	-	-	-	-	-	-	-	-	-	-	5.2	0.2	-	-	1.6	3	18			
7	-	47.4	2.4	-	21.3	-	-	-	-	-	-	-	2.0	21.6	-	-	-	-	-	-	-	-	-	-	-	2.7	0.6	-	-	1.6	4	12			
6	-	49.4	-	-	17.6	-	-	-	-	-	-	-	1.6	25.0	-	-	-	-	-	-	-	0.4	-	-	-	3.3	0.7	-	-	1.6	3	17			
5	0.2	18.1	2.3	-	58.8	-	-	-	-	-	-	-	1.8	13.3	-	-	-	-	-	-	-	0.7	-	-	-	2.4	0.4	-	-	1.6	3	17			
2	-	22.5	-	-	52.1	-	-	-	-	-	-	-	4.0	16.2	-	-	-	-	-	-	-	-	-	-	-	2.6	0.7	-	-	1.5	3-4	14			
1	-	9.4	-	-	64.5	-	-	-	4.0	-	-	-	-	15.5	-	-	-	-	-	-	-	-	-	-	-	2.0	0.3	-	-	1.4	3	-			
3	-	16.3	-	-	59.1	1.7	-	-	-	-	-	-	3.9	5.7	-	-	-	-	-	-	-	-	-	8.5	-	2.4	0.4	-	-	1.6	2-3	14			
<i>Apulia district</i>	<i>Murge Spinazzola deposit</i>																																		
17	-	27.9	1.6	-	45.8	-	-	-	-	-	-	-	9.2	7.0	1.6	-	-	-	-	-	-	-	-	-	-	4.6	0.4	-	-	1.5	1	19			
13	-	-	-	-	74.9	-	-	-	-	-	-	-	19.5	-	-	-	-	-	-	-	-	-	-	2.3	-	1.3	0.1	-	-	1.5	-	9			
15	-	51.2	-	-	15.9	-	-	-	-	-	-	-	15.3	11.5	-	-	-	-	-	-	-	-	-	-	-	3.3	0.4	-	-	1.5	3	14			
12	-	5.9	-	-	12.7	-	-	-	-	-	-	-	6.0	2.2	-	-	-	-	-	-	-	-	64.7	-	1.2	tr.	-	5.4	1.5	1-2	8				
23	-	30.1	-	-	42.2	-	-	-	-	-	-	-	4.4	17.1	-	-	-	-	-	-	-	-	-	-	-	3.8	0.2	-	-	1.7	4	17			
22	-	24.5	1.9	9.9	39.0	-	-	-	-	-	-	-	-	18.7	1.5	-	-	-	-	-	-	-	-	-	-	2.2	0.3	-	-	1.5	4	-			
21	-	51.0	-	-	18.4	-	-	-	-	-	-	-	-	24.3	-	-	-	-	-	-	-	-	-	-	-	4.0	0.3	-	-	1.5	3	-			
20	-	37.0	-	-	36.5	-	-	-	-	-	-	-	-	19.7	-	-	-	-	-	-	-	0.4	-	-	-	4.2	0.2	-	-	1.5	3	-			
19	-	31.1	-	-	35.0	-	-	-	-	-	-	-	2.1	25.6	0.3	-	-	-	-	-	-	-	-	-	-	3.6	0.3	-	-	1.5	4-5	18			
18A	-	63.2	1.3	-	5.2	-	-	-	-	-	-	-	19.8	3.5	-	-	-	-	-	-	-	-	-	-	-	4.5	0.6	-	-	1.5	2	18			
18B	-	65.2	2.4	-	5.6	-	-	-	-	-	-	-	0.6	18.8	-	-	-	-	-	-	-	-	-	0.8	-	4.1	0.6	-	-	1.5	2-3	18-20			
9	-	61.0	-	-	13.2	-	-	-	-	-	-	-	0.5	18.7	-	-	-	-	-	-	-	-	-	-	-	4.1	0.6	-	-	1.5	4-5	19			
8	-	50.8	-	-	12.2	-	-	-	-	-	-	-	3.3	27.3	-	-	-	-	-	-	-	-	0.3	-	-	3.8	0.5	-	-	1.4	2	17			
7	-	17.5	-	-	60.7	-	-	-	-	-	-	-	2.0	14.4	-	-	-	-	-	-	-	-	-	-	-	3.2	0.2	-	-	1.5	2	15			
6	-	49.0	-	-	19.8	-	-	-	-	-	-	-	-	23.9	-	-	-	-	-	-	-	-	-	-	-	4.2	0.3	-	-	1.8	2	-			
5	-	47.7	-	-	17.3	-	-	-	-	-	-	-	13.7	14.8	-	-	-	-	-	-	-	-	-	-	-	4.1	0.4	-	-	1.6	2	16			
4	-	26.7	-	-	36.3	-	-	-	-	-	-	-	12.2	18.8	-	-	-	-	-	-	-	-	-	-	-	3.8	0.2	-	-	1.5	2	16			
3	-	6.2	-	-	63.3	-	-	-	-	-	-	-	11.2	14.1	-	-	-	-	-	-	-	-	-	-	-	3.0	0.2	-	-	1.5	2	11			
2B	-	2.0	-	-	55.2	0.9	-	13.9	-	-	-	-	10.7	13.3	-	-	-	-	-	-	-	-	-	-	-	1.8	0.4	-	-	1.4	3	9			
2A	-	0.6	-	-	63.7	-	-	12.5	-	-	-	-	13.3	5.4	-	-	-	-	-	-	-	-	-	-	-	2.5	0.1	-	-	1.5	2-3	10			
11	-	3.7	-	-	71.5	6.1	-	-	-	-	-	-	6.9	7.9	-	-	-	-	-	-	-	-	-	-	-	1.8	0.2	-	-	1.5	2	11			
<i>Apulia district</i>	<i>Salento Peninsula</i>					<i>Monte Vergine deposit</i>																													
1	-	61.0	3.0	-	3.6	-	-	-	-	-	-	-	6.5	21.7	-	-	-	-	-	-	-	-	-	-	-	1.6	0.6	-	-	1.6	3	25			

292 L. Simone et al.

Table 16
Texture characteristics of bauxites from Apulia district

	1	2	3	4	5	6	7	8	9	10
<i>Spinazzola</i>										
Oolitic-pelito- morphic bx.	1/2	35-70	15-55	-	0-5	10-25	10	-	red, dark red >yellow	9, 15, 19, 20,21, 22, 23
Oolitic bx.	1/4	20-35	50-60	-	0-5	10-20	11	-	red>yellow> dark red	6, 8, 18
Pelitimorphic bauxitic clay	1/8	60-95	0-10	-	0-20	0-10	0.5	0-5	yellow>red> mottled	2, 2b, 37, 11, 14
Pelitimorphic arenitic bx	1/16	40-45	35-40	-	0-3	20-35	1	-	dark red> yellow	5
Pelitimorphic oolitic clayey bx.	1/32	60-65	20-25	-	5-10	5-15	2	-	mottled>yellow	4
Oolitic bauxitic clay	1/32	30-35	60-65	0.1	-	0-10	-	-	yellow, ocre	13
<i>Gargano (S. Giovanni Rotondo)</i>										
Oolitic -pelito- morphic bx	4/10	40-55	35-45	-	0-5	5-15	7	0-5	red>> yellow	1, 2, 6, 9, 10, 15
Oolitic-arenitic bx.	2/10	35-40	30-40	-	0-5	20-25	15	0-5	red>mottled	7, 11, 13, 14
Pelitimorphic oolitic-clayey bx.	2/10	60-65	20-30	-	-	10-15	2	0-5	red, dark red	5, 8, 12
Oolitic-limy bx.	1/10	25-35	40-55	-	-	10-15	10	10-15	red-ocre	4, 16, 17
Pelitimorphic bauxitic clay	1/10	65-70	10-15	-	5	-	-	10-15	yellow>red	3

Symbols: 1. proportions of textures, 2. authigenic groundmass (%), 3. ooides (%), 4. detrital mineral grain (%), 5. secondary segregations and older texture elements (%), 6. detrital bx. grains (%), 7. maximal diameter of detrital bx. grains (mm), 8. secondary calcite segregations (%), 9. colour, 10. samples No.

Symbols for Table 15: 1. sample No; 2. diaspore; 3 boehmite; 4 gibbsite; 5. metahalloysite; 6. kaolinite; 7. chlorite diokt.; 8. chlorite triokt.; 9. illite, hydromuscovite; 10. montmorillonite; 11. mixed-layer clay minerals; 12. quartz; 13. goethite; 14. haematite; 15. magnetite, maghemite; 16. pyrite, marcasite; 17. fibroferrite; 18. melanterite; 19. gypsum; 20. alunite; 21. siderite, oligonite; 22. rodochrosite; 23. calcite; 24. ankerite, dolomite; 25. anatase; 26. rutile; 27. psilomelane; 28. todorokite, 29. absorbed water above 100 °C; 30. Al₂O₃ substitution in haematite; 31. AlOOH substitution in goethite; tr - traces; nd - not determinable because of small quantity; * - mixture of glaukonite and illite with predominance of glaukonite

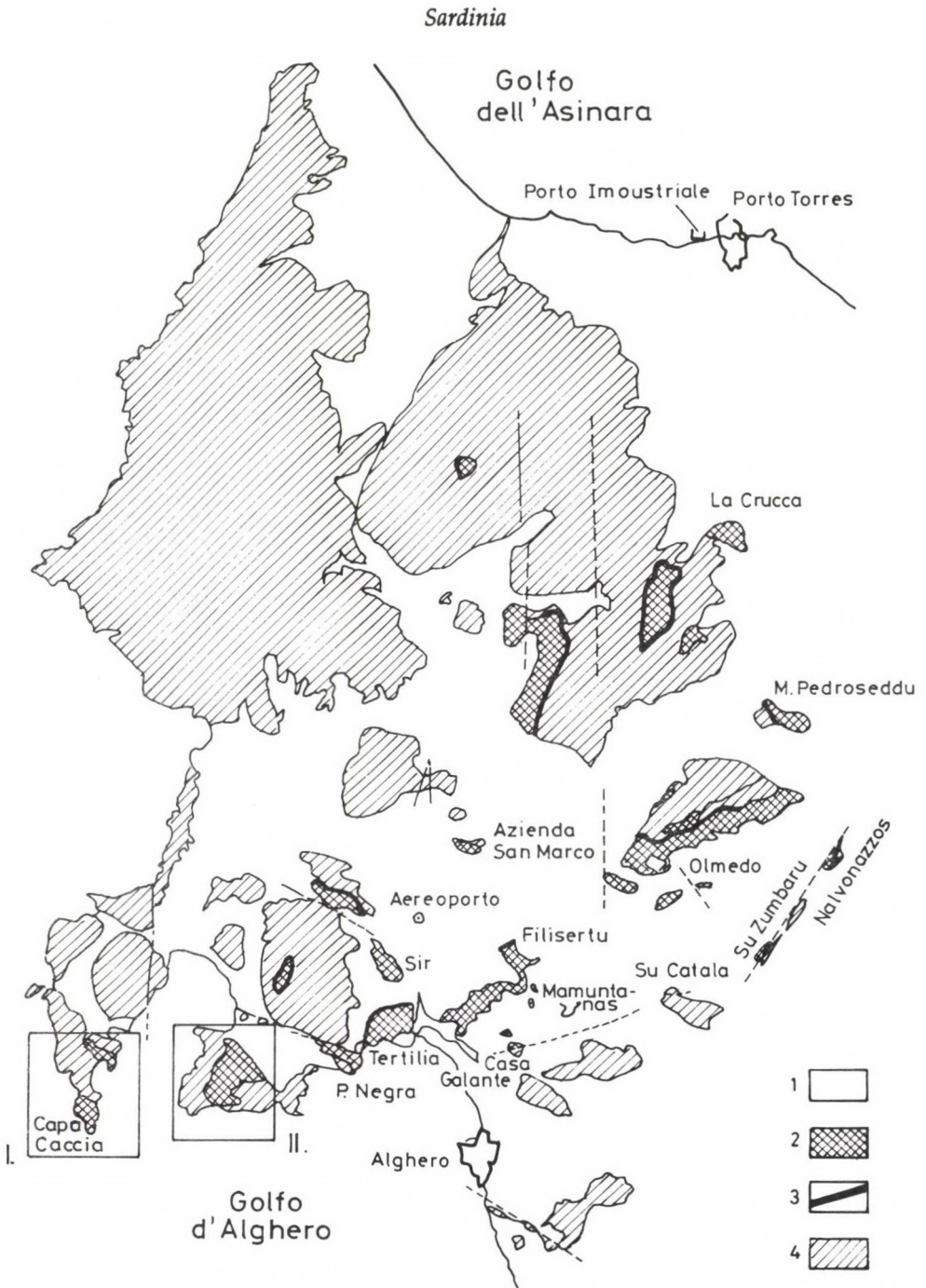


Fig. 11
 Schematic map of the bauxite outcrops of the Nurra-Olmedo area. 1. Pre-Cretaceous Formations; 2. bauxite-cover, Upper Cretaceous; 3. bauxite; 4. bedrock (by Sanna and Temussi 1986, redrawn)

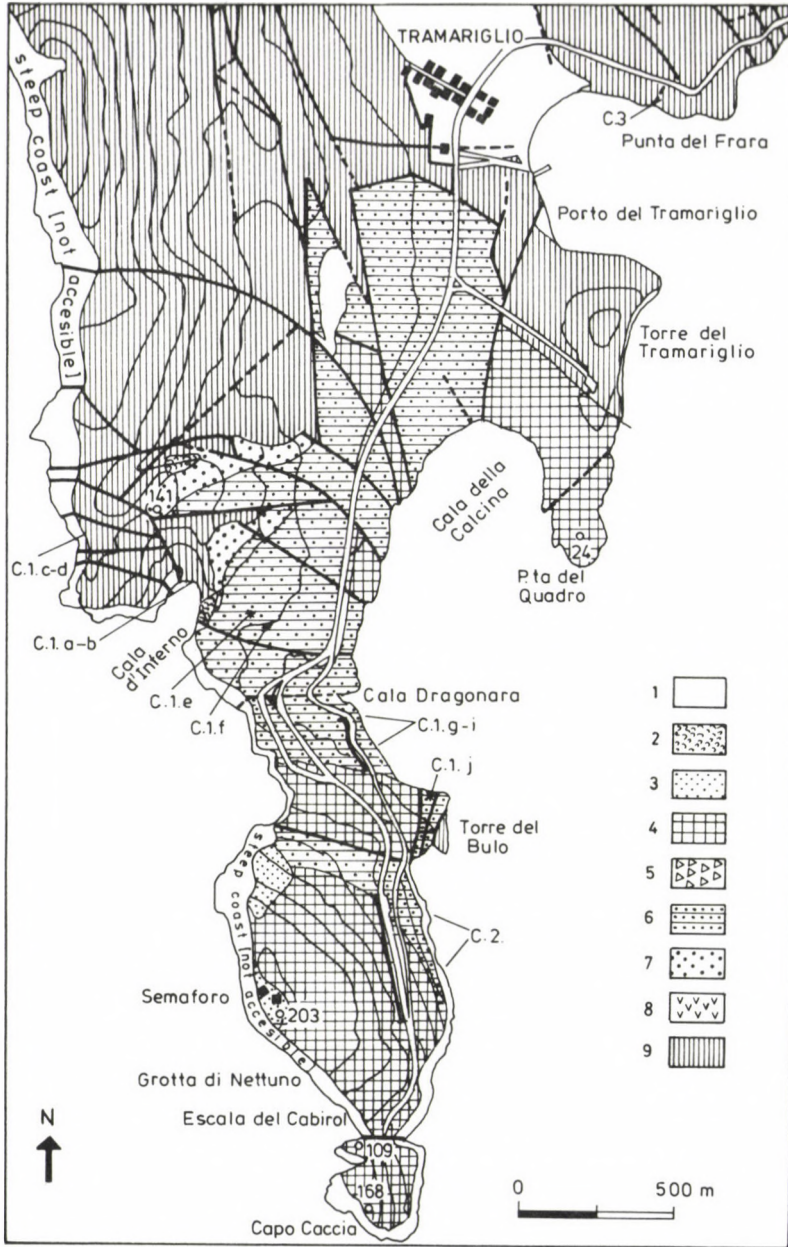


Fig. 12
 Geologic map of Capo Caccia area. 1. alluvial deposits; 2. lithified debris; 3. fossil dunes; 4. Coniacian–Santonian; 5. Munieria-limestone (Cenomanian?); 6. Urgonian (Hauterivian–Lower Aptian); 7. Urgonian (Valanginian); 8. Purbeckian; 9. Jurassic

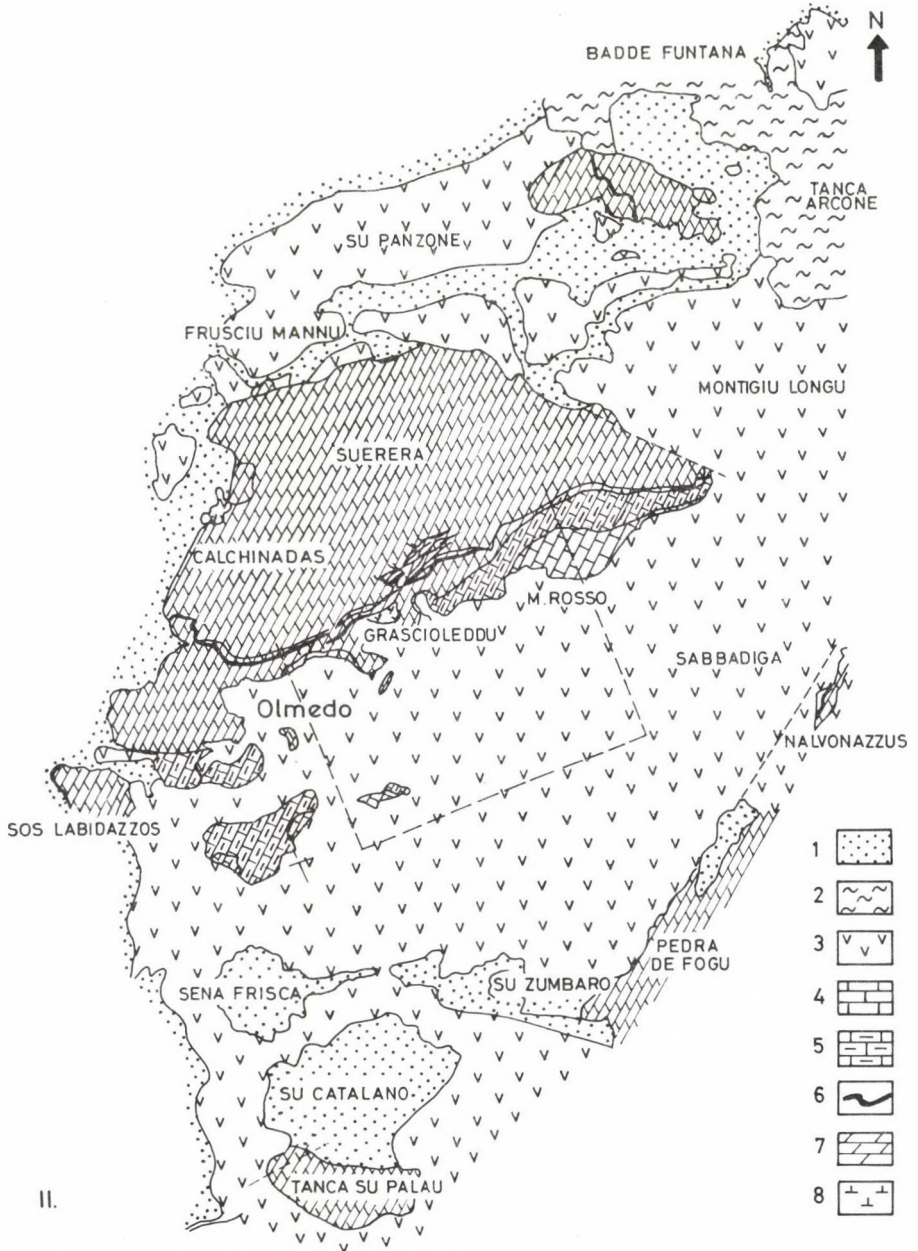


Fig. 13
 Geologic map of Olmedo area. 1. alluvial deposits; 2. marls and calcareous marls, Miocene; 3. Volcanic deposits, Oligo-Miocene; 4. Hippurites limestones, Upper Cretaceous; 5. glauconitic limestones alternating with marls, Upper Cretaceous; 6. bauxites; 7. limestones and dolomitic limestones; 8. green marls and calcareous marls, Lower Cretaceous

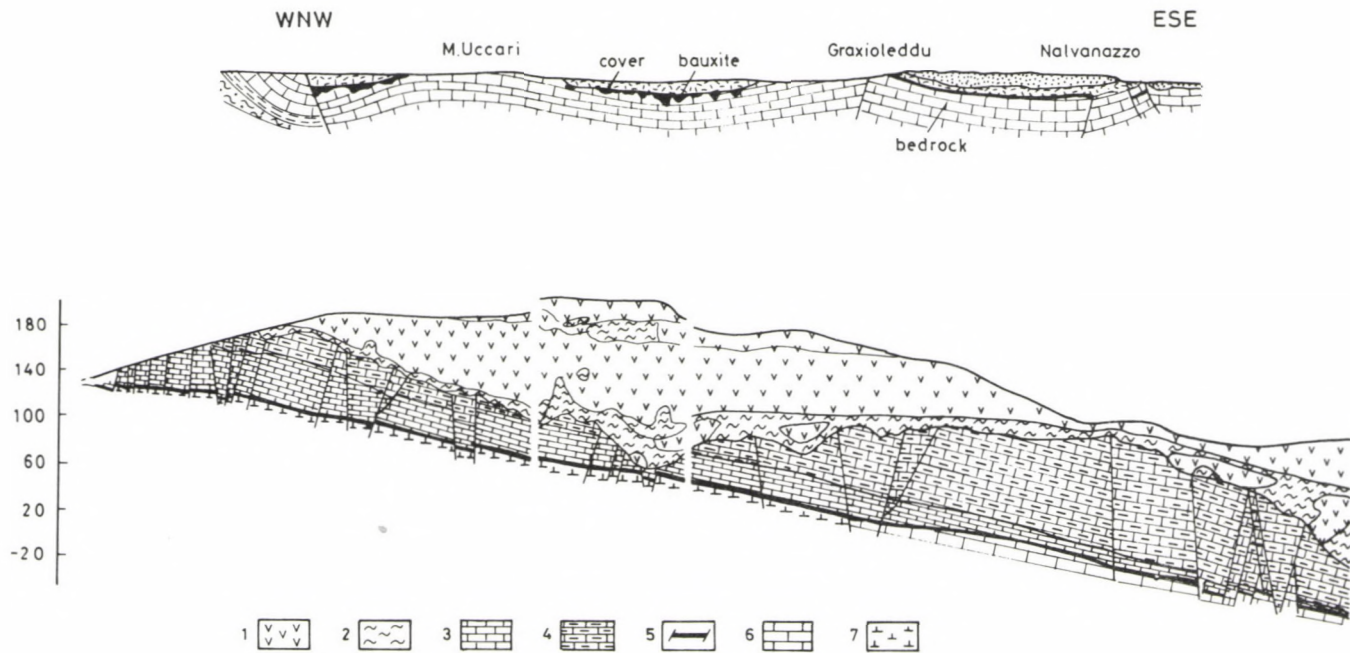


Fig. 14

Schematic geologic profile of the Olmedo area. 1. volcanic deposits, Oligo-Miocene; 2. shales; 3. Hippurites limestone, Upper Cretaceous; 4. glauconitic limestones alternating with marls, Upper Cretaceous; 5. bauxites; 6. limestones and dolomitic limestones, Lower Cretaceous; 7. green marls and calcareous marls, Lower Cretaceous (By Haehnel, 1983, modified)

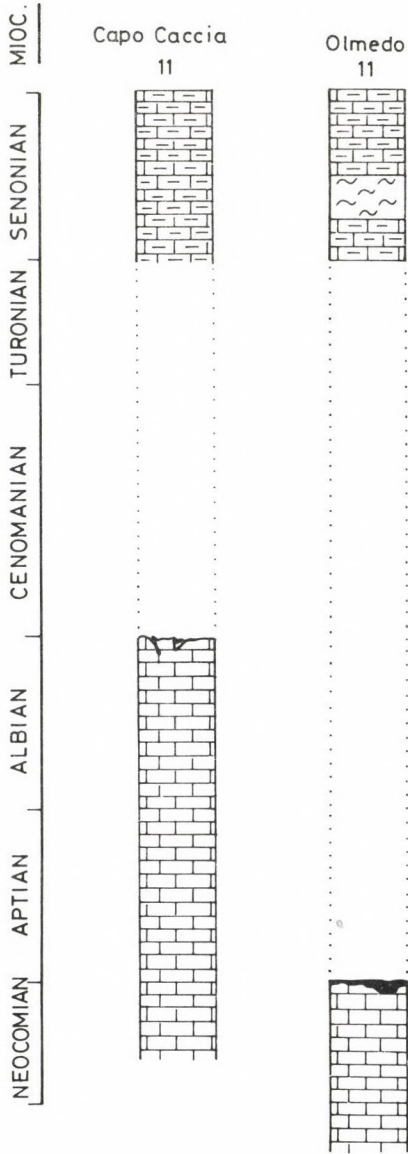


Fig. 15
Bauxites of Sardinia. Stratigraphic columns.
(Numbers indicate localities shown on
Fig. 1. For legend see Fig. 2)

Table 17
Italy, Sardinia district, Capo Cacca

1. Angular unconformity	Low to high angle
2. Estimated duration of exposure	Not reported (≤ 10 My)
3. Apparent stratigraphic gap	Variable (Barremian–Lower Aptian, to Lowermost Senonian)
4. Rate of regional subsidence	Not reported
5. Changes in lithofacies across unconformity	No substantial changes
6. Record of contemporary sea-level changes	
7. Bedrock petrography and age	Calcareous bioclastic grainstone, not younger than Lower Aptian
8. Cover petrography	Calcareous bioclastic grainstones
9. Age of cover	Lower Senonian
10. Lithofacies of associated bauxite	Transported clasts
11. Underlying karst relief	Mainly fracture controlled
12. Supposed source material of bauxite	Bauxitization of clayey intervals ("Purbekian") parautochthon–autochthon
13. Supposed source material of non bx. karst fills	Limestone clasts
14. Lithology, size and shape of bx. deposit	Lensoïd with basal fracture network
15. Bauxite texture	Floatstones
16. Bauxite structure	fissure fills?
17. Chemical composition of bauxite	No data
18. Mineral composition of bauxite (%)	No data
19. Accessory minerals of bauxite	No data
20. Trace elements in the bauxite (ppm)	No data

Table 18
Italy, Sardinia district, Olmedo

1. Angular unconformity	Disconformity
2. Estimated duration of exposure	Not reported (?)
3. Apparent stratigraphic gap	Variable (Lower Valanginian–Barremian, to Lower Senonian)
4. Rate of regional subsidence	Not reported
5. Changes in lithofacies across unconformity	No substantial changes
6. Record of contemporary sea-level changes	Not reported
7. Bedrock petrography and age	Calcareous bioclastic grainstones, not younger than Barremian
8. Cover petrography	Calcareous bioclastic grainstones
9. Age of cover	Lower Senonian
10. Lithofacies of associated bauxite	varied (vadose to semiphreatic)
11. Underlying karst relief	Medium karst topography
12. Supposed source material of bauxite	Bauxitization of clayey intervals ("Purbekian") parautochthon–autochthon
13. Supposed source material of non bx. karst fills	Limestone clasts
14. Lithology, size and shape of bx. deposit	Lensoïd and lense shaped doline fills
15. Bauxite texture	Floatstones passing to oolitic and clastic (conglomeratic)
16. Bauxite structure	Massive
17. Chemical composition of bauxite	See Sanna and Temussi 1986
18. Mineral composition of bauxite (%)	See Sanna and Temussi 1986
19. Accessory minerals of bauxite	See Sanna and Temussi 1986
20. Trace elements in the bauxite (ppm)	See Sanna and Temussi 1986

Calabria

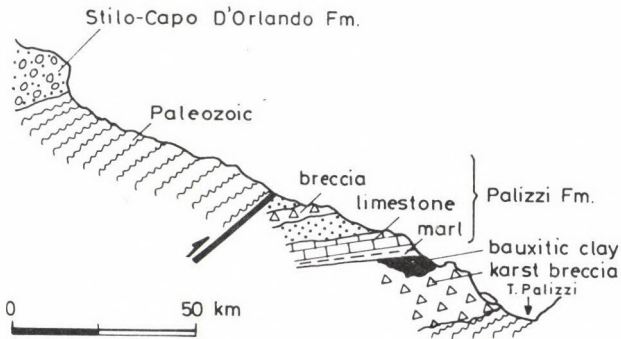
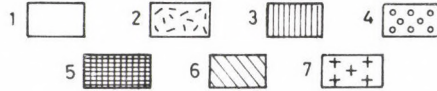
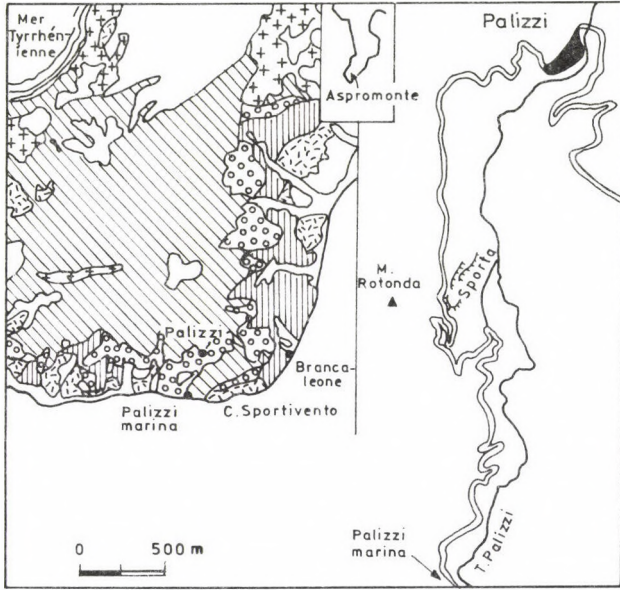


Fig. 16
 Locality map and profile of the Aspromonte bauxite outcrop. 1. Pleistocene–Recent; 2. Pliocene; 3. variegated clay; 4. Stilo–Capo D’Orlando Fm.; 5. Jurassic; 6. metamorphic complex; 7. granodiorite

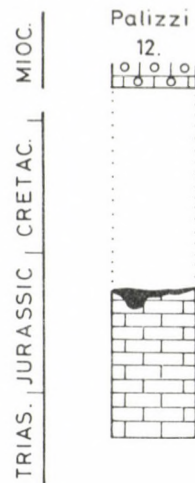


Fig. 17
Bauxites of Southern Italy (Calabria). Stratigraphic column. (Number indicates locality shown on Fig. 1. For legend see Fig. 2)

Table 19
Italy, Calabria district, Palizzi (Aspromonte)

1. Angular unconformity	?
2. Estimated duration of exposure	impossible to estimate
3. Apparent stratigraphic gap	Malm/ Oligo-Miocene
4. Rate of regional subsidence	
5. Changes in lithofacies across unconformity	major
6. Record of contemporary sea-level changes	
7. Bedrock petrography and age	Malmian shallow-water limestone
8. Cover petrography	Calcareous marl, lignitiferous marl
9. Age of cover	Oligomiocene
10. Lithofacies of associated bauxite	No data
11. Underlying karst relief	No data
12. Supposed source material of bauxite	No data
13. Supposed source material of non bx. karst fills	
14. Lithology, size and shape of bx. deposit	erosion remnants in small karstic pockets
15. Bauxite texture	No data
16. Bauxite structure	No data
17. Chemical composition of bauxite	
18. Mineral composition of bauxite	boehmite, diaspore, kaolinite
19. Accessory minerals of bauxite	No data
20. Trace elements in the bauxite	No data

Sicily

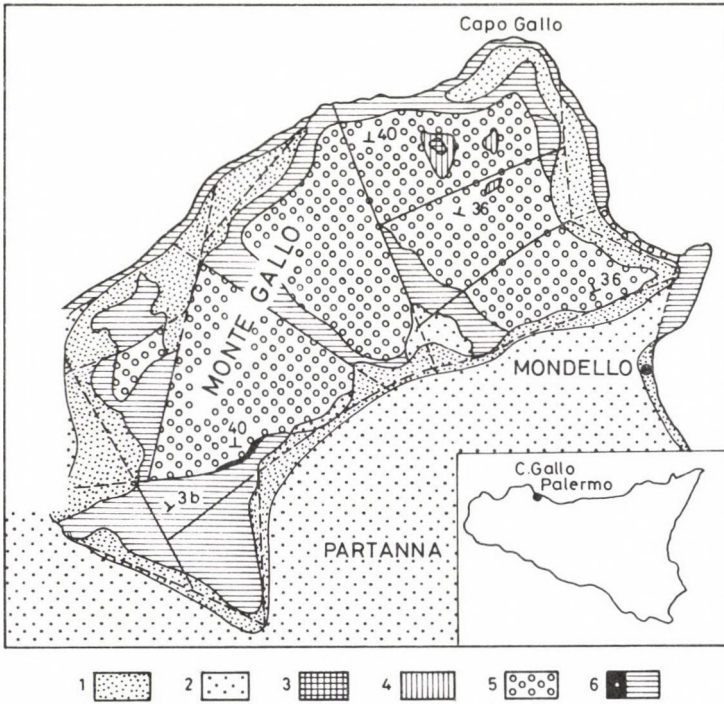


Fig. 18
 Geological map of the Monte Gallo area (Palermo, Sicily).
 1–2. continental deposit, Quaternary; 3. "Scaglia"-like limestones, Eocene; 4. Rudists limestones, Upper cretaceous; 5. lagoonal limestones, Malm–Lower Cretaceous; 6. bauxites (a) Dolostones and dolomitic limestones (b). Upper Trias–Lower Lias (by Bommarito 1981, modified)

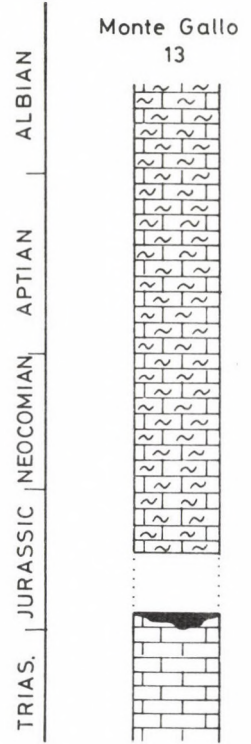


Fig. 19
 Stratigraphic column of the bauxite of Sicily.
 (Number indicates locality shown on Fig. 1. For legend see Fig. 2)

Table 20
Italy, Sicily district, Monte Gallo

1. Angular unconformity	Disconformity
2. Estimated duration of exposure	? (> 10 My)
3. Apparent stratigraphic gap	Norian to Liassic? Oxfordian
4. Rate of regional subsidence	
5. Changes in lithofacies across unconformity	minor
6. Record of contemporary sea-level changes	yes
7. Bedrock petrography and age	Norian to Liassic cyclic (loferitic) shallow-water carbonate
8. Cover petrography	shallow-water carbonates (back-reef lagoon)
9. Age of cover	? Oxfordian
10. Lithofacies of associated bauxite	Vadose >> semi-phreatic
11. Underlying karst relief	
12. Supposed source material of bauxite	? wind-blown dust (partly of basaltic volcanic origin)
13. Supposed source material of non bx. karst fills	
14. Lithology, size and shape of bx. deposit	discontinuous layers small-scale pockets
15. Bauxite texture	pelitomorphic with scattered round grains and primitive ooids (floatstone)
16. Bauxite structure	Massive
17. Chemical composition of bauxite (%)	28-30/37-40, Fe ₂ O ₃ : 9-20; TiO ₂ : 1.7-2.2; P ₂ O ₅ : 0.05-0.1
18. Mineral composition of bauxite	Boehmite, kaolinite illite, hematite, an.
19. Accessory minerals of bauxite	
20. Trace elements in the bauxite (ppm)	Pb: 125-160; Cu: 43-57; Zn: 228-444; Li: 660-998; B: 182-192; Co: 179-226; Ni: 155-216; Cr: 135-161; Y: 43-53 (280 in ooids); La: 25-40; Sr: 130-216

References

- Bárdossy, Gy., M. Boni, M. Dall'Aglio, B. D'Argenio, Gy. Pantó 1977: Bauxites of Peninsular Italy. Composition, origin and geotectonic significance. – Monograph Series on Mineral Deposits, 15, p. 61, Gerbruder Borntraeger, Berlin–Stuttgart.
- Bommarito, Ferla 1988: Bauxiti nella Piattaforma Carbonatica Panormide di Monte Gallo (Palermo). – Boll. Soc. Geol. It., 107, pp. 597–591.
- Boni, M. 1972: Bauxiti dell'Italia centrale, meridionale e della Sardegna (Bibliografia ragionata). – Da: "L'industria Mineraria", anno XXIII, fascicoli di Ottobre e Novembre.
- Bosi, C., M. Manfredini 1967: Osservazioni geologiche nella zona di Campo Felice (L'Aquila). – Mem. Soc. Geol. It., 6, pp. 246–267.
- Bouillin, J.P. et al. 1985: Transgression de l'Oligocène inférieur (formation de Palizzi) sur un karst à remplissage bauxitique dans les zones internes calabropéloriatines (Italie). – C. R. Acad. Sc. Paris, 301, 11, 6.
- Carannante, G., B. D'Argenio, B. Dello Iacovo, V. Ferreri, A. Mindszenty, L. Simone 1988: Carsismo cretatico in Campania. Elementi analitici. Atti del 74^o. – Congr. Naz. Soc. Geol. It., A90–A100, Sorrento.
- Carannante, G., B. D'Argenio, V. Ferreri, A. Mindszenty, L. Simone 1988: Facies e ambienti carbonatici nell'intervallo Cretacico–Miocene dell'Appennino Campano. Fasi tardive nella evoluzine di un dominio di piattaforma tra emersioni ripetute ed annegamento (Matese, Camposauro, Monte Maggiore). – 74^o Congr. Naz. Soc. Geol. It., Sorrento, Excursion guide.
- Carannante, G., B. D'Argenio, V. Ferreri, L. Simone 1987: Cretaceous paleokarst of the Campania Appennines: from early diagenetic to late fillings stages. A case history. – Rend. Soc. Geol. It., pp. 251–256.
- Carannante, G., B. D'Argenio, B. Dello Iacovo, V. Ferreri, A. Mindszenty, L. Simone 1991: Studi sul carsismo cretatico dell'Appennino Campano. – Mem. Soc. Geol. It. (in press).
- Carannante, G., Ferreri, L. Simone 1974: Le cavità paleocarsiche cretatiche di Dragoni (Campania). – Boll. Soc. Natur. in Napoli, 83, pp. 51–161.
- Cherchi, A. 1985: Micropaleontological researches in Sardinia. – Guidebook. 19th European Micropaleontological Colloquium, Sardinia.
- Cherci, A. et al. 1987: Excursion dans le Cretace de la Sardaigne nordoccidentale. – In Cherci A. (ed): "Excursion en Sardaigne", Livret guide.
- Chiocchini, M., A. Mancinelli, A. Romano '1989: The gaps in the Middle-Upper Cretaceous series of the Southern Appennines (Abruzzi and Campania Regions). – Geobios, mémoire special, 11, pp. 133–149.
- Crescenti, U., S. Sartoni 1963: Sintesi biostratigraphica del Mesozoico dell'Italia meridionale. – Mem. Soc. Geol. It., 4, 2, pp. 685–692.
- Crescenti, U., L. Vighi 1970: Risultati delle ricerche eseguite sulle formazioni bauxitiche cretatiche del Casertano e del Matese, in Campanian. – Mem. Soc. Geol. It., 9, pp. 401–434.
- Crescenti, U., L. Vighi 1964: Caratteristiche, geni e stratigrafia dei depositi bauxitici cretacei del Gargano e delle Murge; cenni argille con pisoliti del Salento (Pugliae). – Boll. Soc. Geol. It., 83, pp. 285–338.
- D'Argenio, B. 1963: Una transgressione del Cretacico superiore nell'Appennino Campano. – Mem. Soc. Geol. It., 4, p. 52.
- D'Argenio, B. 1967: Geologia del Gruppo del Taburno–Camposauro (Appennino Campano). – Atti Acc. SC. Fis. e Matem. di Napoli, 6, pp. 32–218.
- D'Argenio, B. 1969: Central and Southern Italy Cretaceous bauxites stratigraphy and paleogeography. – Ann. Inst. Geol. Publ. Hung. Budapest, 54, pp. 221–233.
- D'Argenio, B. 1974: Le piattaforme carbonatiche periadriatiche. Una rassegna di problemi nel quadro geodinamico mesozoico dell'area mediterranea. – Mem. Soc. Geol. It., 13.
- D'Argenio, B., A. Mindszenty, Gy. Bárdossy, E. Juhász, M. Boni 1987: Bauxites of Southern Italy revisited. – Rend. Soc. Geol. It., 9, 2, pp. 263–268.

- D'Argenio, B., A. Mindszenty 1987: Cretaceous bauxites in the tectonic framework of the Mediterranean. – *Rend. Soc. Geol. It.*, 9, pp. 257–262.
- D'Argenio, B., A. Mindszenty 1991: Karst bauxites at regional unconformities and geotectonic correlation in the cretaceous of the Mediterranean. – *Boll. Soc. Geol. It.* (in press).
- D'Argenio, B., A. Mindszenty, Gy. Bárdossy, E. Juhász, M. Boni 1987: Bauxites of Southern Italy revisited. – *Rend. Soc. Geol. It.*, 9, pp. 263–268.
- D'Argenio, B., E. Luperto Sinni, A. Mindszenty, G. Richetti 1988: Da Ponte dell'Impiso a Corato. – In Cocco, E., B. D'Argenio (eds.): *L'Appennino Campano-Lucano nel Quadro Geologico dell'Italia Meridionale*. – 74^o Congr. Naz. Soc. Geol. Ita., pp. 215–225.
- De Weisse, G. 1973: Quelques considerations sur les bauxites des Abruzzes et sur la presence du cuire dans un gisement. – *ICSOBA 3rd Congr. Internat. Nice*, pp. 63–71.
- Luperto Sinni, E., A. Reina, R. Santarcangelo 1991: Bauxite deposits near Spinazzola (Murge Baresi, Southern Italy). – *Field Symp. on Tethyan Cretaceous Formations and Related Mineral Resources. IGCP. Project 262 Tirana, Albania, Abstracts*.
- Luperto Sinni, E. J.P. Masse 1982: Contributo della Paleoeologia alla paleogeografia della parte meridionale della piattaforma Apula nel Cretacico inferiore. – *Geologica Rom.*, 21, pp. 859–877.
- Ruberti, D. 1991: Il Cretacico in facies di piattaforma carbonatica del Matese. *Studi stratigrafici e sedimentologici*. – Tesi di dottorato inedita. Roma.
- Sanna, G., I. Temussi 1986: La miniera di bauxite di olmedo. – *Da: "L'industria mineraria"*, 6,
- Sartoni, S., M.L. Colalongo 1964: Sul Cretacico dei dintori di Caiazzo (Caserta). – *Mem. Soc. Geol. It.*, 4, 1/2, pp. 1–18.
- Sartoni, S., V. Crescenti 1962: Ricerche biostratigrafiche sul Mesozoico dell'Appennino Meridionale. – *Giorn. Geologica*, 29, pp. 161–388, Bologna.

Bauxite deposits of Yugoslavia – The state of the Art

Boris Šinkovec
RGN Fakultet, Zagreb

Kresimir Šakać
Prirodoslovni Muzej, Zagreb

Bauxites occur in many stratigraphic horizons in Yugoslavia, from the Triassic to the Tertiary. Distribution of the bauxitiferous horizons and stratigraphic position of the bauxite deposits are displayed in maps and diagrams

Key words: Bauxite, Mesozoicum, Tertiary, Dinarids

*Introduction**

Bauxites occur in several stratigraphic gaps interrupting shallow water carbonate successions of the External Dinarids.

The oldest known deposits are those occurring in the Dinaric High Zone in Triassic successions of Slovenia, Croatia, Bosnia and Montenegro. Best studied of them are those of Vrace and Lika where the bauxite fills a shallow karst relief formed on the surface of Anisian–Ladinian (?) limestones and is covered by Carnian (?) conglomerates, tuffitic sandstones, clays and dolomites. The subaerial exposure phases they are associated with, is generally assigned to the "Idrijan" tectogenetic phase which brought about extensive differential uplift in several sectors of the Dinarids.

Jurassic bauxites, disconformably intercalated within Malmian shallow water carbonates are known from Slovenia, Istria, Bosnia and Montenegro. Depending on the degree of karstic erosion they are underlain by Kimmeridgean to Norian limestones and dolomites and are covered by Kimmeridgean limestones.

Some of the bauxite deposits of Montenegro and Bosnia are covered by Lower Cretaceous (Neocomian) sediments. In Montenegro these are disconformably underlain by Upper Triassic to Kimmeridgean limestones, in Bosnia by Titonian to Valanginian limestones suggesting an independent Lower Cretaceous bauxite horizon within the area of the Dinaric High Karst.

Most of the economy grade bauxite deposits of Yugoslavia were formed in Cretaceous times. Middle Cretaceous bauxites, filling a moderately dissected karst relief on the surface of Middle Triassic shallow water carbonates and covered by

* Introductory text written by A. Mindszenty

Address: B. Šinkovec: Pierotti jeva 6, 41000 Zagreb, Croatia
K. Šakać: Demetrova 2, 41000 Zagreb, Croatia

Received: 15 December, 1991.

Albian to Cenomanian sands, marls, clays and limestones, are known from the internal margins of the External Dinarids (Vlasenica) only.

More in the External Zones but still within the area of the Dinaric High Karst, younger Cenomanian–Turonian to Senonian bauxites occur at several localities in Montenegro, Bosnia and to a lesser extent in Kosovo–Metohija. According to the age of their bedrock and cover they record two separate brief subaerial exposure phases probably unrelated to each other. The first one occurs between the Neocomian and the Cenomanian (and is probably contemporaneous with the Vlasenica bauxite). After this gap carbonate-platform sedimentation is restored without any major facies change. The second subaerial exposure phase is restricted to a short gap between the Turonian and the Santonian to Maastrichtian, however, the cover sequence suggests that major changes of the sedimentary regime took place right after the deposition of bauxites: the cover consists of breccias, limestones and higher up by flysh-type sediments.

In Paleogene times a pronounced shift of bauxite formation can be observed from the internal towards the more external zones of the External Dinarids. Almost all bauxite deposits of the Adriatic carbonate platform were formed in the Early to the Late Paleogene. There are two separate stratigraphic gaps, both of them associated with economy-grade bauxites. The older one occurs between the Senonian and the Paleocene (sometimes depending on the degree of erosion underneath, bedrocks as old as Albian were also described from below the Paleocene-covered bauxites). The younger gap occurs between Upper Cretaceous to Lower Eocene and Upper Lutetian strata. Much like in the case of the Cretaceous bauxites also here the older gap reflects no major changes of the sedimentary regime in association with the bauxitiferous disconformity, whereas in the younger gap bauxites fill a tectonically controlled relief with moderate to large angular unconformity, and the cover sequence displays a major facies changes as compared with the underlying bedrock formations.

Redeposited bauxites are mentioned with Oligocene and Miocene cover as well, from both the Adriatic and the Dinaric platform. Whether and to what an extent these youngest bauxites are the results of Oligocene and/or Miocene bauxitization processes is questionable and would require more detailed investigations.

Table 1
Upper Triassic bauxites

1. Angular unconformity	No
2. Estimated duration of exposure	4-10 My
3. Apparent stratigraphic gap	Small to moderate
4. Rate of regional subsidence	Does not change across the unconformity
5. Changes in lithofacies across unconformity	Major change
6. Record of contemporary sea-level changes	No direct record
7. Bedrock petrography and age	Limestones, Ladinian, rarely Anisian
8. Cover petrography	Conglomerates, tuffitic sandstones, clays, dolomites
9. Age of cover	Carnian, 228 My
10. Lithofacies of associated bauxite	Shallow
11. Underlying karst relief	Mostly Middle Triassic marl and pyroclastics
12. Supposed source material of bauxite	Mostly Middle Triassic marl and pyroclastics
13. Supposed source material of non bx. karst fills	
14. Lithology, size and shape of bx. deposit	Very heterogeneous: kaolinitic clays, bauxitic clays, clayey bauxites, bauxites, conglomerates
15. Bauxite texture	Mostly oolitic, also pseudoporphyric, pelitomorphic
16. Bauxite structure	Massive, sporadically bedded or schistic (Mazin deposit)
17. Chemical composition of bauxite (%)	Al ₂ O ₃ : 45-53, SiO ₂ : 8-23, Fe ₂ O ₃ : 15-23, L.i.: 12
18. Mineral composition of bauxite	Boehmite, diaspore, kaolinite, hematite, pyrophyllite (Mazin deposit)
19. Accessory minerals of bauxite	Very rare: zircon, tourmaline, corundum, garnet
20. Trace elements in the bauxite (ppm)	Zr: 430, Cr: 150; V: 290; Ni: 29; Co: 10; Cu: 6 ΣREE: 777

Table 2
Malm bauxites

1. Angular unconformity	No or weak
2. Estimated duration of exposure	3-? My
3. Apparent stratigraphic gap	Small to large
4. Rate of regional subsidence	Does not change across the unconformity
5. Changes in lithofacies across unconformity	Essentially unchanged
6. Record of contemporary sea-level changes	No direct record
7. Bedrock petrography and age	Limestones and dolomites. Norian to Kimmeridgian
8. Cover petrography	Limestones
9. Age of cover	Tithonian, 138 My
10. Lithofacies of associated bauxite	Shallow to variegated
11. Underlying karst relief	Carbonate residue (?), windblow dust (?), aluminosilicate rocks (?)
12. Supposed source material of bauxite	-
13. Supposed source material of non bx. karst fills	
14. Lithology, size and shape of bx. deposit	Homogeneous, middle to large, lenses and layers
15. Bauxite texture	Detrital, pelitomorphic
16. Bauxite structure	Massive
17. Chemical composition of bauxite (%)	Al ₂ O ₃ : 44-58, SiO ₂ : 3-18, Fe ₂ O ₃ : 16-23, L.i.: 12-14
18. Mineral composition of bauxite	Boehmite, kaolinite, hematite
19. Accessory minerals of bauxite	Very rare
20. Trace elements in the bauxite (ppm)	Ni: 155-240; Co: 25-40; Cr: 180-30; V: 300; Zr: 450; Cu: 50-80; ΣREE: 600; B: 110; Zn: 424; Pb: 117

Table 3/1
Lower Cretaceous bauxites

1. Angular unconformity	Weak
2. Estimated duration of exposure	10 My
3. Apparent stratigraphic gap	Moderate
4. Rate of regional subsidence	Does not change across the unconformity
5. Changes in lithofacies across unconformity	Essentially unchanged
6. Record of contemporary sea-level changes	No direct record
7. Bedrock petrography and age	Limestones, Kimmeridgian
8. Cover petrography	Limestones
9. Age of cover	Neocomian, 120 My
10. Lithofacies of associated bauxite	
11. Underlying karst relief	Shallow
12. Supposed source material of bauxite	Carbonate residue (?), windblown dust (?)
13. Supposed source material of non bx. karst fills	Carbonate residue (?), windblown dust (?)
14. Lithology, size and shape of bx. deposit	Homogeneous, small lenses
15. Bauxite texture	Pelitomorphic
16. Bauxite structure	Massive
17. Chemical composition of bauxite (%)	Al ₂ O ₃ : 39, SiO ₂ : 23, Fe ₂ O ₃ : 22, L.i.: 12
18. Mineral composition of bauxite	Kaolinite, boehmite, goethite, hematite
19. Accessory minerals of bauxite	?
20. Trace elements in the bauxite (ppm)	V: 500; Zr: 250; Ni: 2670; Cr: 100

Table 3/2
Late Lower Cretaceous bauxites

1. Angular unconformity	Large
2. Estimated duration of exposure	?
3. Apparent stratigraphic gap	Large
4. Rate of regional subsidence	May dramatically change across the unconformity
5. Changes in lithofacies across unconformity	Major change
6. Record of contemporary sea-level changes	-
7. Bedrock petrography and age	Carbonate beds, Middle Triassic
8. Cover petrography	Sands, marles, clays, limestones
9. Age of cover	Albian-Cenomanian, 90-100 My
10. Lithofacies of associated bauxite	-
11. Underlying karst relief	Variegated
12. Supposed source material of bauxite	From different igneous, metamorphic and sedimentary rocks
13. Supposed source material of non bx. karst fills	-
14. Lithology, size and shape of bx. deposit	Homogeneous, orebodies are small to big, in form of lenses or big nests
15. Bauxite texture	Detrital and pelitomorphic
16. Bauxite structure	Massive
17. Chemical composition of bauxite (%)	Al ₂ O ₃ : 53.10, SiO ₂ : 5.75, Fe ₂ O ₃ : 5.452, L.i.: 1.852
18. Mineral composition of bauxite	Boehmite, hematite, kaolinite
19. Accessory minerals of bauxite	Rare: zircon, epidote, zoisite, amphibolite, rutile, tourmaline, chlorite, garnet, anatase
20. Trace elements in the bauxite (ppm)	Ni: 477; Zr: 431; Cr: 409; V: 201; Y: 145; Zn: 112; B: 95; Nb: 91; Pb: 69; Cu: 67; La: 97



Fig. 1

A D R I A T I C U M

QUATERNARY	HOLOCENE	CALABRIAN	0-0.01	
	PLEISTOCENE	PIACENZIAN	1.6	
NEOGENE	PLIOCENE	ZANCLEAN	3.4	
		MESSINIAN	5.3	
			6.5	
	MIOCENE	TORTONIAN	11.2	
		SERRAVALLIAN	15.1	
OLIGOCENE	CHATTIAN	16.6		
	RUPELIAN	21.8		
	BURDIGALIAN	22.7		
PALEOGENE	Eocene	Ypresian	23.6	
		Lutetian	34.6	
		Thanetian	40.0	
	Oligocene	Bartonian	43.6	
		Priabonian	57.0	
	Paleocene	Unnamed	57.8	
		Unnamed	60.6	
		Danian	63.6	
	CRETACEOUS	LATE	Maastrichtian	66.4
			Campanian	74.5
Santonian			86.0	
Coniacian			87.5	
Turonian			91.5	
EARLY		Albian	97.5	
		Aptian	113	
		Barremian	119	
		Hauterivian	124	
MIDDLE		Berriasian	131	
		Berriasian	138	
		Tithonian	144	
		Kimmeridgian	152	
		Oxfordian	156	
JURASSIC	Callovian	163		
	Bathonian	169		
	Bajocian	176		
	Aalenian	183		
	Toarcian	187		
	Pliensbachian	193		
TRIASSIC	Sinemurian	204		
	Hettangian	208		
	Norian	223		
	Carnian	230		
	Ladinian	235		
EARLY	Anisian	240		
	Scythian	245		

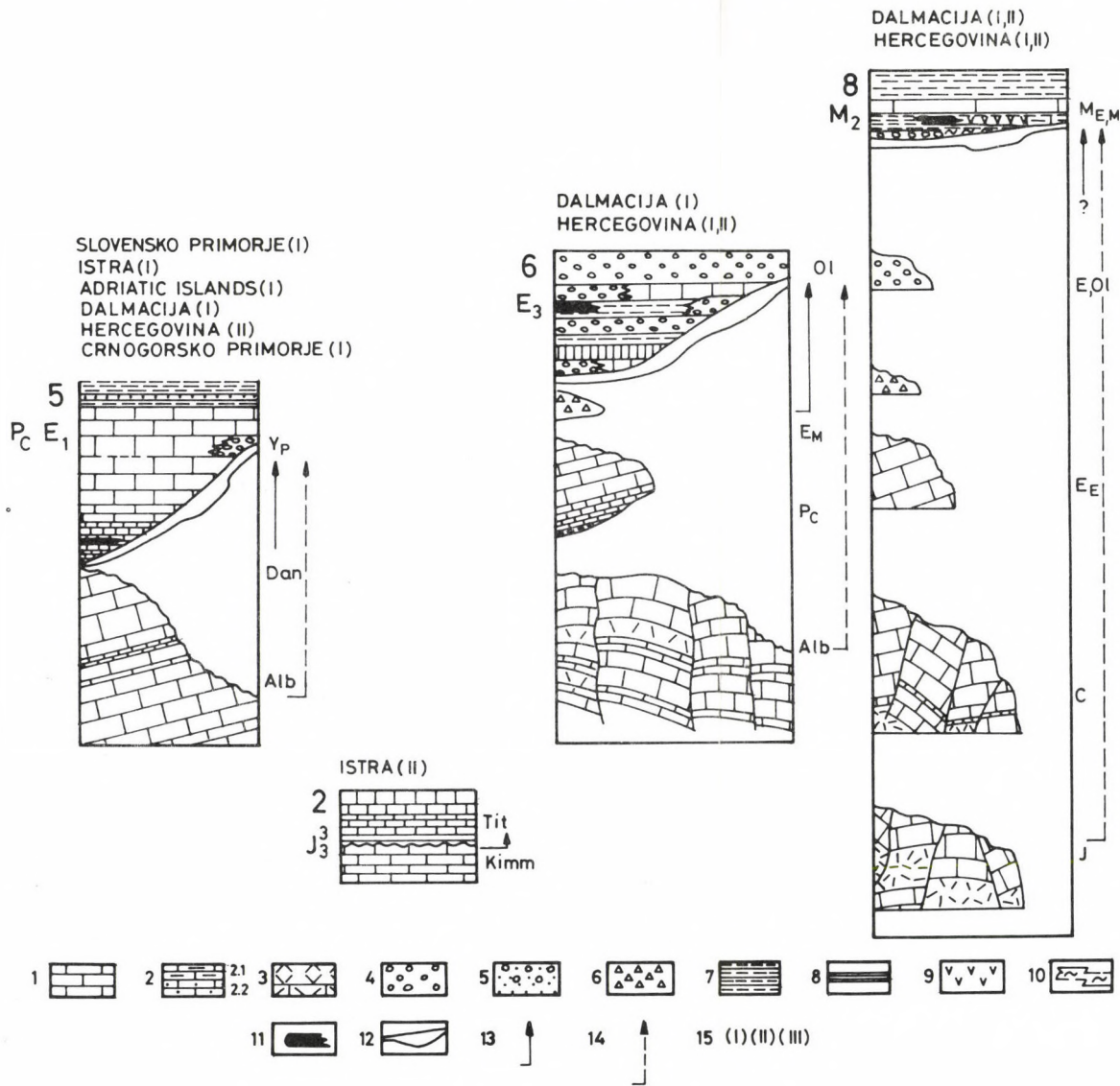


Fig. 2

D I N A R I C U M

YUGOSLAVIA

TERTIARY	NEOGENE	PLIOCENE	CALENZIAN	0.01	
			PIACENZIAN	1.6	
			ZANCLEAN	3.4	
			MESSINIAN	5.3	
				6.5	
		MIOCENE	L	TORTONIAN	
			H	SERRAVALLIAN	11.2
				LAMBHIAN	15.1
			E	BURDIGALIAN	16.6
				AQUITANIAN	21.8
PALEOGENE	OLIGOCENE	L	CHATTEAN	30.0	
		E	RUPELIAN	34.6	
			PRIABONIAN	40.0	
			BARTONIAN	42.6	
		M	LUTETIAN	57.0	
	Eocene	E	YPRESIAN	57.8	
			THANETIAN	60.6	
			UNNAMED	63.6	
				66.4	
			DANIAN	66.4	

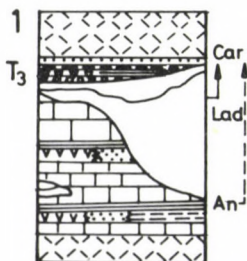
CRETACEOUS	LATE	HAASTRICHTIAN	66.4
		CAMPANIAN	74.5
		SANTONIAN	84.0
		CONIACIAN	87.5
		TURONIAN	88.5
	EARLY	ALBIAN	91
		APTIAN	97.5
		BARREMIAN	113
		HAUTERIVIAN	119
		VALANGINIAN	124
JURASSIC	LATE	BERRIASIAN	131
		TITHONIAN	138
		KIMMERIDGIAN	144
		OXFORDIAN	152
		CALLOVIAN	156
	MIDDLE	BATHONIAN	163
		BAJOCIAN	168
		AALENIAN	176
		TOARCIAN	183
		PLIENSCHACHIAN	187
EARLY	Sinemurian	193	
	Hettangian	198	
		204	
		208	
		208	
TRIASSIC	LATE	NORIAN	223
		CARNIAN	230
		LADINIAN	235
	EARLY	ANISIAN	240
		SCYTHIAN	245

N

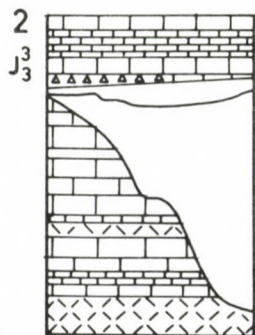
C

L

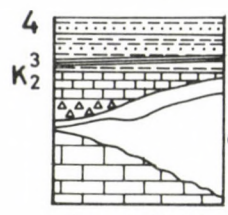
A



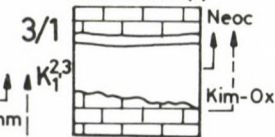
SLOVENIJA (I)
BOSNA W (I,II)
HERCEGOVINA E (I)
CRNA GORA (II,III)



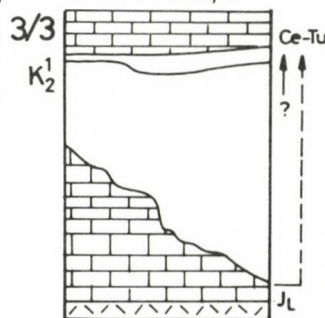
SLOVENIJA SE (I)
KORDUN (I)
BOSNA W (II)
KOSOVO (II)



DALMACIJA (I)



CRNA GORA (I,II)



BOSNA W (II)
KORDUN (I)
HERCEGOVINA (I)

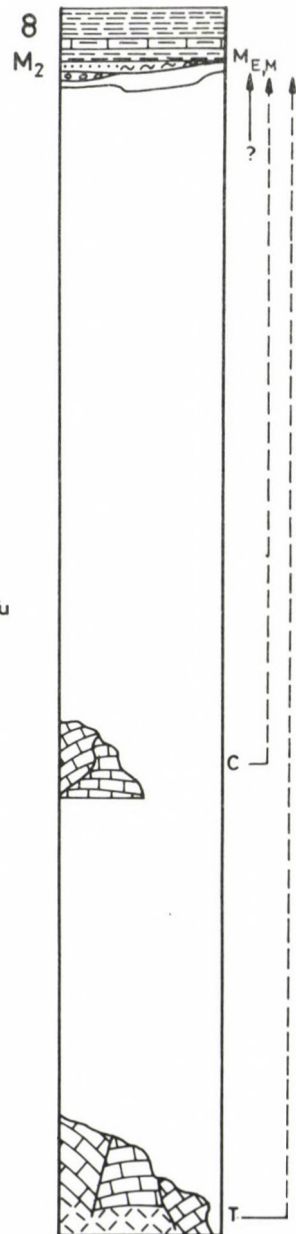


Fig. 3

YUGOSLAVIA

KARPATHO-BALKAN ARCH

SUPRADINARICUM

PERIOD	SUBPERIOD	AGE		METER	
		LOWER	UPPER		
TERTIARY	NEOGENE	PLIOCENE	CA L A B R I T A N	0.01	
			P I A C E N Z I A N	1.6	
			Z A N C L E A N	3.4	
		MIOCENE	L	H E S S I A N	5.3
				T O R T O N I A N	6.5
			M	S E R R A V A L L I A N	11.2
				L A N G H I A N	15.1
				B U R D I G A L I A N	16.6
			E	A Q U I T A N I A N	21.8
					22.7
	PALEOGENE	OLIGOCENE	L C H A T T I A N	30.0	
			E R U P E L I A N	34.6	
		Eocene	L P R I A B O N I A N	40.0	
			B A R T O N I A N	43.6	
			L U T E T I A N	57.0	
		PALEOCENE	E	Y P R E S I A N	57.8
					60.6
			L	S E L A N I A N	63.6
				U N N A M E D	66.4
D A N I A N					
CRETACEOUS	LATE	H A A S T R I C H T I A N	66.4		
		C A M P A N I A N	74.5		
		S A N T O N I A N	84.0		
		C O N I A C I A N	87.5		
		T U R O N I A N	88.5		
	EARLY	NEOCENIAN	C E N O M A N I A N	91	
				97.5	
			A L B I A N	113	
			A P T I A N	119	
			B A R R E M I A N	124	
		MIOCENIAN	H A U T E R I A N	131	
			V A L A N G I A N	138	
			B E R R I A S I A N	144	
			T I T H O N I A N	152	
			K I M M E R I D G I A N	156	
JURASSIC	LATE	O X F O R D I A N	163		
		C A L L O V I A N	169		
	MIDDLE	B A T H O N I A N	176		
		B A J O C I A N	183		
		A A L E N I A N	187		
	EARLY	P L I E N S B A C H I A N	193		
		S I N E M U R I A N	198		
		H E T T A N G I A N	204		
			208		
			223		
TRIASSIC	LATE	N O R I A N	223		
		C A R N I A N	230		
	MIDDLE	L A D I N I A N	235		
		A N I S I A N	240		
		S C Y T H I A N	245		

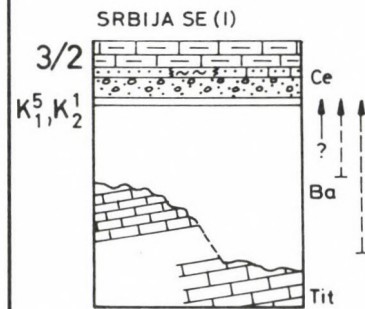
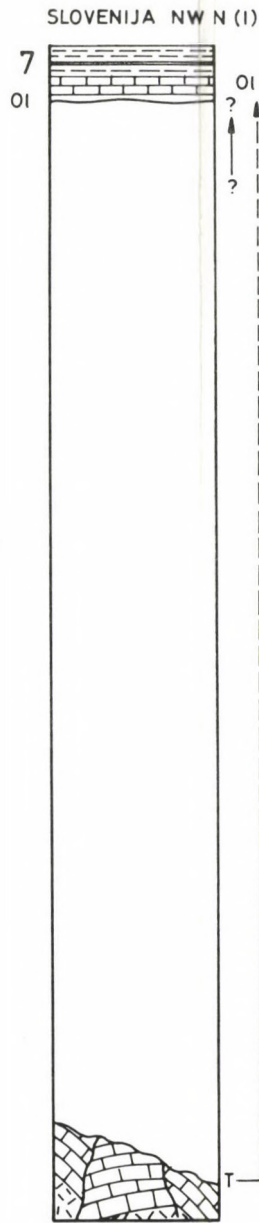
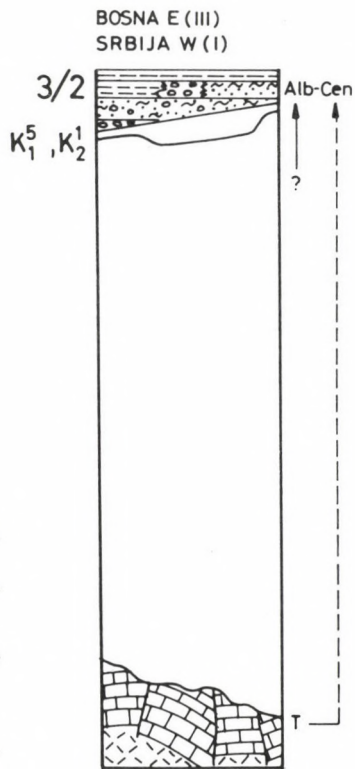


Fig. 4

N
C
L
A

Table 3/3
Early Upper Cretaceous

1. Angular unconformity	Weak
2. Estimated duration of exposure	4-? My
3. Apparent stratigraphic gap	Moderate to large
4. Rate of regional subsidence	Does not change across the unconformity
5. Changes in lithofacies across unconformity	Essentially unchange
6. Record of contemporary sea-level changes	-
7. Bedrock petrography and age	Limestones, Jurassic-Late Cretaceous
8. Cover petrography	Limestones
9. Age of cover	Cenomanian-Turonian, 90-95 My
10. Lithofacies of associated bauxite	-
11. Underlying karst relief	Moderate
12. Supposed source material of bauxite	?
13. Supposed source material of non bx. karst fills	
14. Lithology, size and shape of bx. deposit	Heterogeneous, white clay and white clayey bauxite, red bauxite, ore bodies are small to moderate, lenses and layers
15. Bauxite texture	Detrital and pelitomorphic
16. Bauxite structure	Massive
17. Chemical composition of bauxite (%)	Al ₂ O ₃ : 33-67, SiO ₂ : 5-38, Fe ₂ O ₃ : 2-25, L.i.:13-15
18. Mineral composition of bauxite	Kaolinite, boehmite, goethite, hematite
19. Accessory minerals of bauxite	Piroxene, amphibole, zircon, garnet
20. Trace elements in the bauxite (ppm)	Zr: 287; V: 218; Cr: 214; Ni: 136; Li: 90; Ba: 50; Sc: 28; Y: 24

Table 4
Senonian Bauxites

1. Angular unconformity	No or weak
2. Estimated duration of exposure	4-25 My
3. Apparent stratigraphic gap	Moderate
4. Rate of regional subsidence	Does not change across the unconformity
5. Changes in lithofacies across unconformity	Major change
6. Record of contemporary sea-level changes	No direct record
7. Bedrock petrography and age	Limestones, Albanian, to Cenomanian, Turonian
8. Cover petrography	Breccias, limestones, flush
9. Age of cover	Santonian-Maastrichtian 86-65 My
10. Lithofacies of associated bauxite	
11. Underlying karst relief	Shallow/moderate
12. Supposed source material of bauxite	Carbonate residue (?), windblown dust (?)
13. Supposed source material of non bx. karst fills	-
14. Lithology, size and shape of bx. deposit	Homogeneous, small to moderate, lenses and layers
15. Bauxite texture	Oolitic
16. Bauxite structure	Massive
17. Chemical composition of bauxite (%)	Al ₂ O ₃ : 58-72, SiO ₂ : 1.2-5, Fe ₂ O ₃ : 6-22, L.i.:12-14
18. Mineral composition of bauxite	Boehmite (diaspore), hematite, goethite
19. Accessory minerals of bauxite	Very rare
20. Trace elements in the bauxite (ppm)	Ni: 175; Co: 18; Cr: 560; V: 360; Zr: 480; Cu: 26; ΣREE: 575 (Kordun) Ni: 1082; Co: 112; Cr: 3860; V: 430; Zr:539; Cu: 25; Nb: 106; Y: 74; Pb: 78; La: 65 (Kosovo)

Table 5
Early Paleogene bauxites

1. Angular unconformity	Weak
2. Estimated duration of exposure	2–18 My
3. Apparent stratigraphic gap	Small to moderate
4. Rate of regional subsidence	Does not change across the unconformity
5. Changes in lithofacies across unconformity	Minor changes
6. Record of contemporary sea-level changes	?
7. Bedrock petrography and age	Limestones, Upper Cretaceous, rarely Albian
8. Cover petrography	Limestones, clayey limestones
9. Age of cover	Paleocene–Early Eocene, 63–45 My
10. Lithofacies of associated bauxite	
11. Underlying karst relief	Moderate
12. Supposed source material of bauxite	Mostly carbonate residue
13. Supposed source material of non bx. karst fills	–
14. Lithology, size and shape of bx deposit	Homogeneous, orebodies are small, rarely moderate which were formed by filling of sinkholes
15. Bauxite texture	Oolitic
16. Bauxite structure	Massive
17. Chemical composition of bauxite (%)	Al ₂ O ₃ : 52–602, SiO ₂ : 1–6, Fe ₂ O ₃ : 17–24, L.i.: 13–16
18. Mineral composition of bauxite	Boehmite (gibbsite), hematite, goethite, kaolinite
19. Accessory minerals of bauxite	Very rare: zircon, tourmaline, staurolite, anatase, garnet, corundum
20. Trace elements in the bauxite (ppm)	Ni: 210–440; Co: 20–30; Cr: 480–1200; V: 490–960; Zr: 480; Cu: 40–55; Ga: 90; Pb: 112; Zn: 210; Y: 170; Mo: 20; ΣREE (Istra): 573

Table 6
Late Paleogene bauxites

1. Angular unconformity	Large
2. Estimated duration of exposure	2–12 My
3. Apparent stratigraphic gap	Small to large
4. Rate of regional subsidence	May dramatically change across the unconformity
5. Changes in lithofacies across unconformity	Major change
6. Record of contemporary sea-level changes	?
7. Bedrock petrography and age	Limestones, locally carbonate breccias, Upper Cretaceous, Lower Eocene
8. Cover petrography	Conglomerates, marles, limestones
9. Age of cover	Upper Lutetian–Lower Rupelian, 40–30 My
10. Lithofacies of associated bauxite	
11. Underlying karst relief	Variegated, sometimes very deep
12. Supposed source material of bauxite	Eolian material of volcanic and terrigenous origin and carbonate residue
13. Supposed source material of non bx. karst fills	–
14. Lithology, size and shape of bx. deposit	Homogeneous, orebodies differ in size and shape, they are in form of lenses or big nests
15. Bauxite texture	Mostly detrital
16. Bauxite structure	Massive
17. Chemical composition of bauxite (%)	Al ₂ O ₃ : 45–52, SiO ₂ : 4–10, Fe ₂ O ₃ : 17–25, L.i.: 17–25
18. Mineral composition of bauxite	Gibbsite, boehmite, (g:b = 1.5–10: 1), hematite, kaolinite
19. Accessory minerals of bauxite	Frequent and various: zircon, tourmaline, rutile, garnet, kyanite, staurolite, andalusite
20. Trace elements in the bauxite (ppm)	Ni: 300–750; Co: 30–80; Cr: 550–1400; V: 500–1400; Zr: 460; Cu: 30–200; Ga: 85; Pb: 110; Zn: 450; Y: 100; Mo: 20–180; ΣREE: 568

Table 7
Oligocene bauxites

1. Angular unconformity	Large
2. Estimated duration of exposure	?
3. Apparent stratigraphic gap	Large
4. Rate of regional subsidence	May dramatically change across the unconformity
5. Changes in lithofacies across unconformity	Major change
6. Record of contemporary sea-level changes	
7. Bedrock petrography and age	Limestones, Middle and Late Triassic
8. Cover petrography	Limestones, marles
9. Age of cover	Oligocene, 27 My
10. Lithofacies of associated bauxite	
11. Underlying karst relief	Variegated
12. Supposed source material of bauxite	Mostly tuff (?)
13. Supposed source material of non bx. karst fills	-
14. Lithology, size and shape of bx. deposit	Homogeneous, orebodies are small, in form of lenses
15. Bauxite texture	Detrital
16. Bauxite structure	Massive, sporadically slaty (schisty)
17. Chemical composition of bauxite (%)	Al ₂ O ₃ : 45-65, SiO ₂ : 2-18, Fe ₂ O ₃ : 15-24, L.i.: 12-14
18. Mineral composition of bauxite	Diaspore, chlorite, kaolinite, goethite
19. Accessory minerals of bauxite	?
20. Trace elements in the bauxite (ppm)	?

Table 8
Miocene bauxites

1. Angular unconformity	Large
2. Estimated duration of exposure	9-10 My (?)
3. Apparent stratigraphic gap	Moderate to large
4. Rate of regional subsidence	May dramatically change across the unconformity
5. Changes in lithofacies across unconformity	Major change
6. Record of contemporary sea-level changes	-
7. Bedrock petrography and age	Carbonate beds, Jurassic (rare), Cretaceous (dominantly), Eocene
8. Cover petrography	Marles and clayey limestones
9. Age of cover	Middle Miocene, 15 My
10. Lithofacies of associated bauxite	
11. Underlying karst relief	Variegated
12. Supposed source material of bauxite	Eolian material of volcanic and terrigenous origin and (in some area) also redeposited Paleogene bauxites
13. Supposed source material of non bx. karst fills	-
14. Lithology, size and shape of bx. deposit	Homogeneous, orebodies differ in size, in form of lenses
15. Bauxite texture	Detrital and pelitomorphic
16. Bauxite structure	Massive
17. Chemical composition of bauxite (%)	Al ₂ O ₃ : 38-45, SiO ₂ : 12-25, Fe ₂ O ₃ : 13-20, L.i.: 18-22
18. Mineral composition of bauxite	Gibbsite (\pm boehmite), kaolinite, hematite, goethite
19. Accessory minerals of bauxite	Similar to Late Paleogene bauxites
20. Trace elements in the bauxite	Ni: 110-450; Co: 5-70; Cr: 170-900; V: 250-950; Zr: 380-780; Cu: 15-110; Ga: 90; Pb: 77; Zu: 380; Y: 70; Mo: 15; Σ REE: 583

Fig. 1→

Distribution of the bauxite-bearing horizons in Yugoslavia. 1. Upper Triassic bauxites; 2. Malm bauxites; 3. Lower Cretaceous bauxites; 4 Late Lower Cretaceous Bauxites; 5. Early Upper Cretaceous bauxites, 6. Senonian bauxites; 7. Early paleogene bauxites; 8. Late Paleogene bauxites; 9. Oligocene bauxites; 10. Miocene bauxites; A-Adriaticum; D-Dinaricum; S-Supradinaricum; SM-Serbo-Macedonian Massif; KB-Karpatho-Balkan arch

Fig. 2→

Stratigraphic position of the bauxite of Adriaticum. 1. Limestone; 2.1. Clayey limestone; 2.2. Sandy limestone; 3. Dolomite; 4. Conglomerate; 5. Sandy Conglomerate; 6. Breccia; 7. Marl; 8. Shale; 9. Tuff; 10. Clay; 11. Coal; 12. Bauxite; 13. Estimate duration of exposure; 14. Apparent stratigraphical gap; 15. Size of bauxite deposit: I. Small, II. Medium, III. Big

Fig. 3→

Stratigraphic position of the bauxite of Dinaricum (for legend see Fig. 2)

Fig. 4→

Stratigraphic position of the bauxite of Supradinaricum (for legend see Fig. 2)

References

- Crnićki, J. 1978: Structure controlled bauxite deposits of Dalmatia. – 4th Intern. Congr. of ICSOBA Athens Vol. I, pp. 114–129.
- Grubić, A. 1970: Les bauxites en Yougoslavie. – Ann. Inst. Geol. Publ. Hung., 54, 3, pp. 195–208.
- Jurković, I. K. Šakać 1964: Stratigraphical, paragenetical and genetical characteristics of the bauxites in Yugoslavia. – Symp. ICSOBA, Zagreb, I, pp. 253–263.
- Maksimović, Z. 1968: Distribution of trace elements in bauxite deposits of Hercegovina, Yugoslavia. Travaux ICSOBA 5, Zagreb, pp. 63–70.
- Maksimović, Z. 1977: Fossil weathering crusts in Yugoslavia and some geological problems. – Bull. Acad. Serbe Sci., 15, pp. 119–130.
- Maksimović, Z., B. Scavnicar, A. Dangic 1983: The origin of karstic bauxites from the Vlasenica area, Yugoslavia. – Travaux ICSOBA 13 (18), Zagreb, pp. 29–38.
- Radoičić, R. 1987: Bauxites of the Internal Dinarids: Stratigraphy and facies of bedrock and cover (Bosnia–Metohija sector). – Rend. Soc. Geol. It., 9, pp. 277–280.
- Šinkovec, B. 1970: Geology of the Triassic bauxites of Lika, Yugoslavia. – Acta Geol. VII (Prirod. istr. 39), Zagreb, pp. 5–58.
- Šinkovec, B. 1971: Geological features and origin of Vrace bauxite deposit, Croatia. – II Intern. Symp. ICSOBA, Budapest, II, pp. 39–52.
- Šinkovec, B. 1973: The origin of Early paleogene bauxites of Istria, Yugoslavia. 3^{eme} Cong. Intern. ICSOBA, Nice, pp. 151–164.
- Šinkovec, B. 1986: Bauxite texture as an indicator of bauxite deposits formation. – Travaux ICSOBA 16–17 "1985/87" pp. 217–223.
- Šušnjara, A., B. Ščavničar 1978: Heavy minerals as provenance indices of Tertiary bauxites in Dalmatia (Yugoslavia). – 4th Intern. Congr. ICSOBA, Athens, 2., pp. 822–836.
- Trubelja, F., J. Papeš 1983: Bauxites of Central Bosnia (the surrounding region of Jajce). – Travaux ICSOBA 13 (18), Zagreb, pp. 39–50.

Contribution to the geochemistry of Hungarian karst bauxites and the allochthony/autochthony problem

Zoran Maksimović

University of Beograd, Department of Mineralogy, Crystallography, Petrology and Geochemistry, Beograd

Andrea Mindszenty

Eötvös Loránd University of Sciences Department of Applied Geology, Budapest

György Pantó

Hungarian Academy of Sciences Laboratory for Geochemical Research Budapest

Studies based on systematic trace element analysis of bauxite profiles in Hungary provide useful information on the allochthony/autochthony problem. Some of the studied deposits show total allochthony or total autochthony, but the majority of them have got intermediate characters.

Key words: Bauxite, paleokarst, paleosol, sedimentology, trace elements, paleogeography, Cretaceous, Eocene, Transdanubian Central Range, Villány Mts

Introduction

Allochthony versus autochthony

The problem of allochthony and autochthony is one of the oldest controversies in karstbauxite geology. Because of the colloidal grain size of their major mineral constituents, bauxites were considered to be chemical precipitates at first. Later on, when more and more attention was paid to their lithology, clastic textures became recognized and those displaying clearly conglomeratic textures and large scale bedding were qualified as "resedimented" as opposed to those being more homogeneous and therefore considered as having been formed "in situ". With the advent of "microsedimentology" it became clear soon that even the most homogeneous-looking bauxites may contain microclasts and exhibit "sedimentary" structures on the micro-scale. Komlóssy (1968) and Bonte (1969) proposed that this microclastic texture was the "sine qua non" of bauxite formation on the karst terrain, because the endorheic drainage of the karst provides for repeated local transport and redeposition of the weathering products on the irregular surface. Bonte suggested the term "parautochthony" to designate this local (sometimes

Addresses: Z. Maksimović: Djusina 7, 11000 Beograd, Serbia

Gy. Pantó: H-1112 Budapest, Budaörsi út, 45 Hungary

A. Mindszenty: H-1088 Budapest, Múzeum krt. 4/a, Hungary

Received: 16 December, 1991.

only cm to dm scale) transport. The term was rapidly accepted and has been used by geologists working in bauxite geology ever since then.

However, the original definition of allochthony, parautochthony and autochthony having been based mainly on genetic criteria, to qualify a deposit as parautochthonous or allochthonous has remained a matter of taste as a result of which the reliability of data acquired in the past twenty years is rather questionable. The attempts of Combes (1984, 1990a); Valetton (1990, 1991); Bárdossy (1982); Mindszenty et al. (1989); Bárdossy et al. (1990) finally resulted in the establishment of a new more precise definition now already supported by textural/structural criteria as well.

According to their scheme *allochthony* means that the sediment was bauxitized elsewhere and was deposited on its present place after considerable fluvial or mass-movement type transport (the order of magnitude of transport is supposed to have been several hundreds of meters or even kilometers); *autochthony*, on the other hand, means that the "prebauxitic" material was bauxitized in situ as a result of processes similar to ferrallitization proper, interrupted or not by recurrent small-scale (cm to dm) mechanical transport (called parautochthonous redeposition) resulted/accompanied by sheet-wash, soil-creep, little slumps or other small-scale mass-movement on the dissected karst terrain. *Autochthony* therefore does not necessarily mean that the prebauxitic material is itself exclusively autochthonous (e.g. dissolution residue of the bedrock). On the contrary: in most cases we have the evidence of the prebauxitic material brought to the karst terrain by wind or by other (fluvial or areal) means of transport.

Clear distinction is not always possible and along with the careful study of the bauxite itself may require also other pertinent geological information to be taken into consideration.

Autochthony is thought to be indicated texturally by in situ segregational and accretional ooids (the outermost crusts of which show a gradual transition towards the surrounding matrix). Matrix and ooids/intraclasts are essentially of the same geochemical facies. Non-spherical grains are mainly intraclasts in this group. In the case of mudstone-type pelitomorphous bauxites autochthony can not be recognized on the basis of texture alone. Autochthony on the large scale is reflected by the regular grade pattern of the deposits (best grades occurring normally above the deepest holes in the bottom of the bauxite-filled sinkholes, providing for optimum drainage and therefore for optimum bauxitization) (Nia 1967; Valetton 1976; Bárdossy 1982; Südi 1981; Mindszenty et al. 1989).

Allochthony, on the other hand, is shown by a generally high diversity of ooids/pisoids and clastic grains (which all have abrupt contacts toward the enclosing matrix); the presence of bauxite pebbles and by the capriciously changing grade of the ore within the deposits. Very frequently the geochemical facies of ooids/pisoids is markedly different from that of the matrix. Among non-spherical grains frequently also non-bauxitic extraclasts occur in this group. Grade pattern is irregular within the deposit: large-scale (cross)-stratification, graded bedding, etc. may be apparent both on the macroscopic and microscopic scale.

Parautochthony or "allochtonie relatif" (sensu Combes 1990) is characterized by an apparently clastic texture (with abundant intraclasts), however, with clear signs of in situ texture-forming as well (faint accretion-rims around intraclasts, etc.) and often with regular, karstmorphology-related grade pattern. There may or may not be a difference between the geochemical facies of matrix and grains. Stratification – if any – occurs on the microscopical scale only.

As pointed out lately by Combes and Valetton, allochthony, autochthony and parautochthony are not absolute categories. To qualify a given deposit needs careful studies and it is always the predominant characters on the basis of which we may decide whether the bauxite is allochthonous rather than just parautochthonous. Within one and the same deposit there may be parts exhibiting clear signs of autochthony alternating with undoubtedly allochthonous parts. Recognition of the areal distribution of predominantly allochthonous and autochthonous lithotypes may in fact help to understand the sometimes not at all simple story recorded by a given deposit. Also it has to be born in mind that between "autochtonie absolue" and "allochtonie absolue" there is a wide range of possibilities to have deposits the formation of which was controlled by (even repeated) phases of "true" allochthonous transport succeeded by "in situ" geochemical changes trying to conceal the sedimentary structures previously formed. The ratio between allochthony or autochthony related textures and structures is therefore essentially the measure of the intensity of in situ geochemical processes having affected the bauxite after its final deposition.

Geochemical criteria of autochthony/allochthony

Geochemistry being so important in the course of bauxite formation we propose that geochemical data in general and trace element geochemistry in particular be used as a criterion when trying to establish the predominantly allochthonous or autochthonous nature of a deposit.

Geochemical studies clearly indicate that most of the "in situ" deposits display a downward enrichment, culminating in a marked concentration at the base of a particular group of "mobile" trace elements. This progressive enrichment of Ni, Co, Cu, Y, La–Lu, Be, Li, Mo, Zn, Mn, Pb and Ba towards the bottom has been observed in numerous karst bauxite deposits of Greece, Yugoslavia and Southern France (Combes 1969; Maksimović and Papastamatiou 1973; Caillère et al. 1976; Maksimović 1976a; Maksimović and Roaldset 1976; Maksimović and De Weisse 1979; Maksimović and Pantó 1980, 1983, 1985, 1989, 1991). Identical trace element patterns exist in the Miocene–Pliocene karstic bauxites of Jamaica, which are not covered by sediments and are probably still in the process of formation (Maksimović 1978). One example of this is shown by Fig. 1.

On the basis of the geochemical evidence, Maksimović (1976a, 1979) demonstrated that these trace element patterns, shown by nearly all karstic bauxites formed in situ, are syngenetic and have developed contemporaneously with the bauxitisation of argillaceous material accumulated in the karstic depressions. The enrichment of "mobile" trace elements in the lowermost parts of

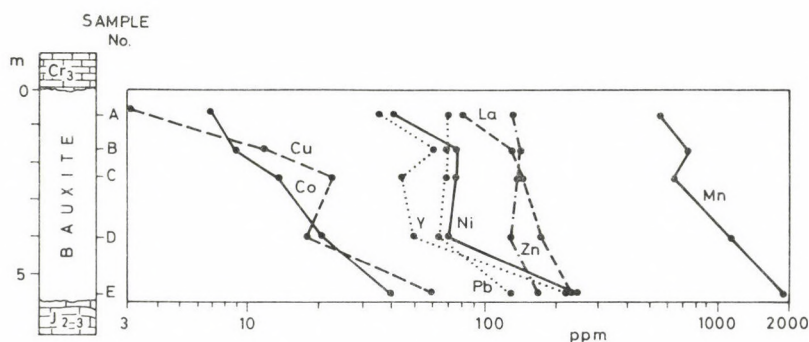


Fig. 1
Trace element distribution along the vertical profile of an autochthonous deposit (after Maksimović and De Weisse 1979)

karst bauxites is essentially attributed to the role that the carbonate footwall played as pH-barrier for solutions that percolated downwards during the bauxitization process. In numerous deposits, as a result of high concentration of "mobile" trace elements, authigenic minerals of REE's, nickel, manganese and copper have been formed above the footwall (Maksimović 1988).

Erosion, transport and redeposition of karstic bauxites may result in the degradation and finally, in the total destruction of the primary trace element distribution patterns. Therefore we think that geochemical criteria could efficiently be used to distinguish karst bauxites formed in situ from those having been redeposited after a previous stage of bauxitization (Maksimović 1988). They also offer the possibility to assess the degree of allochthony/autochthony of any given karst bauxite deposit.

Hungary, being one of the "classical" bauxite-countries of the Mediterranean region, offers a good opportunity to test this hypothesis, the more, so that systematic lithology-oriented study of its several bauxite horizons has already provided a framework into which the geochemical data can easily be fitted and petrological and geochemical results can be cross-checked.

Geological backgrounds

Bauxite deposits of Hungary

The oldest bauxite deposits of Hungary are those occurring at the Jurassic/Cretaceous boundary in the Villány Mts (South Hungary). A brief subaerial exposure phase interrupting an otherwise continuous shallow-water carbonate sequence resulted in karstification of Upper Jurassic (Malm, Lombardia arachnoidea zone) limestones and the deposition of argillaceous bauxites filling the irregularities of the shallow karst relief. The coverbeds being of Early Cretaceous age (Valanginian according to Bodrogi, Lobitzer, Knauer, pers. com.),

there is a general agreement about the subaerial exposure phase having had a duration of cca. 1 to 2 million years around the Jurassic/Cretaceous boundary. There is no appreciable angular unconformity between bauxite its bedrock and cover, so subaerial exposure was probably brought about by the interplay of eustasy and some very gentle intraplate-stress induced crustal deformation as suggested lately by D'Argenio and Mindszenty (1990) for other "conformable" bauxites of the Mediterranean.

All the major, economically significant bauxite deposits of Hungary occur in the Transdanubian Central Range (TCR) and are confined to the Triassic/Senonian, Triassic/Eocene and Senonian/Eocene contacts (Fig. 2). Additional uneconomic reserves are known from the base of the Albian and redeposited bauxites or partly eroded remnants of one or the other of the major horizons, resting on Triassic rocks and covered by various younger formations of Oligocene to Pleistocene age are also abundant.

Although the age of the individual deposits has been disputed, nowadays it is generally agreed that there are three bauxitiferous stratigraphic horizons (Fig. 3):

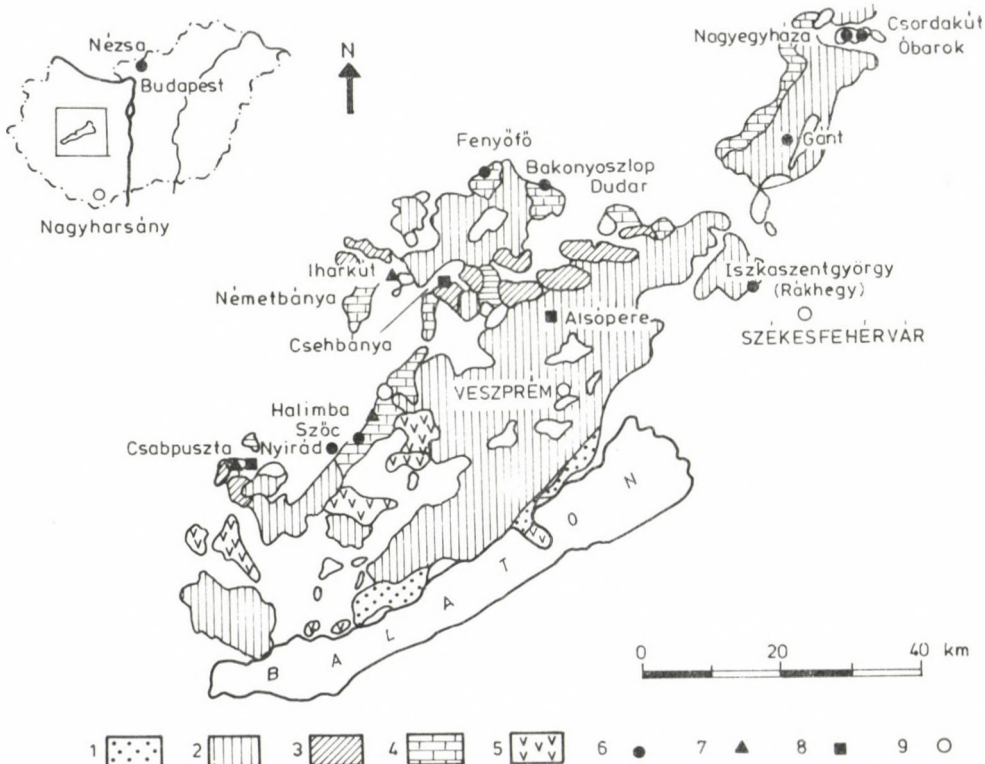


Fig. 2
Major bauxite deposits of the Transdanubian Central Range 1. Paleozoic; 2. Triassic–Jurassic–Lower Cretaceous; 3. Upper Cretaceous; 4. Eocene; 5. neovolcanics; 6. Eocene bauxite; 7. Senonian bauxite; 8. Albian bauxite; 9. Neocomian bauxite

- Pre-Albian/Aptian
- Turonian/Senonian and
- Paleocene/Eocene

Each of these horizons can be correlated with distinct tectonic phases of the Alpine orogeny which brought about subaerial exposure and karst denudation of the Mesozoic carbonate terrain and led to the accumulation of bauxites. Those deposits covered by Albian strata we correlate with the Austrian phase; the Turonian/Senonian ones with the Pre-Gosau phase and the Paleocene/Eocene bauxites with the Laramian phase.

Deposits belonging to the lowermost (Pre-Albian) horizon are known from the base of the Albian Munieria marl (Tés Clay-Marl Formation). They are mostly thin,

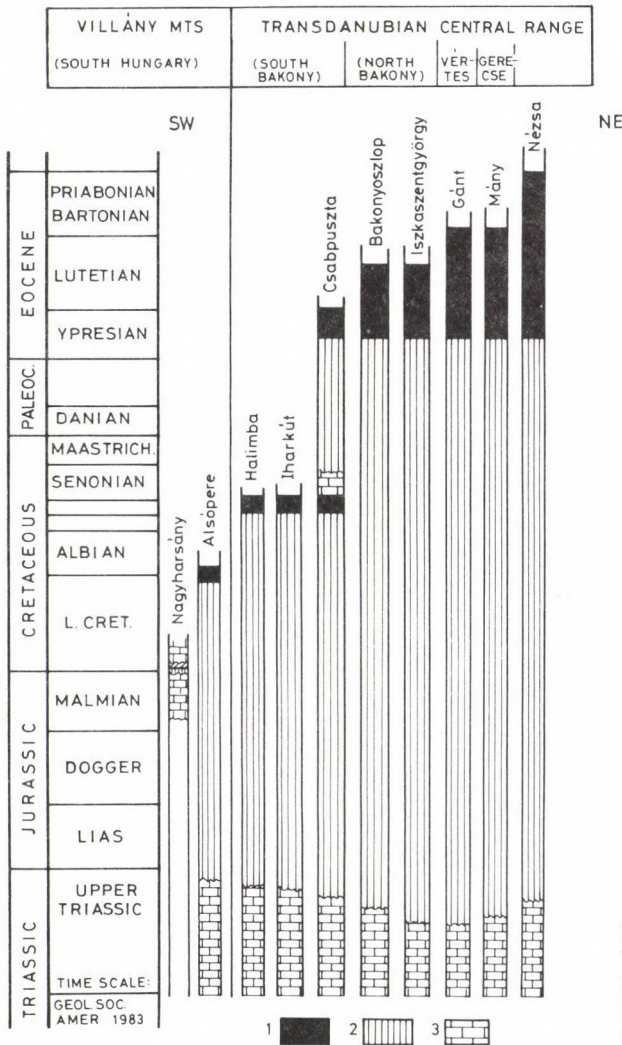


Fig. 3
The stratigraphic position of bauxites in Hungary. 1. emersion; 2. supposed erosional hiatus; 3. bedrock

blanket-like deposits, overlying a shallow karst topography on the surface of the Upper Triassic Dachstein Limestone. Their lithology (cobbles and pebbles of rather diverse (oolitic, intraclastic) texture, colour, size and hardness; embedded in a usually pale yellowish, kaolinitiferous bauxitic matrix) suggests that they are eroded and redeposited remnants of some "vadose" deposits. Vestiges of "vadose" deposits were in fact penetrated by boreholes near the village of Csehánya (dark-red, hematite-rich, oolitic bauxite, filling karstic cavities in Jurassic limestone). Areally, the known Pre-Albian/Albian bauxites are concentrated to the central part of the TCR (vicinity of the villages of Alsópere, Olaszfalu and Tés in the Northern Bakony and few scattered occurrences near Padragkút in the south).

Deposits of the second ("main", Turonian/Senonian) horizon, though much more widespread, are still confined essentially to the central part of the TCR (localities of Halimba and Csabpuszta in the Southern Bakony and Iharkút in the Northern Bakony). They rest on a deeply karstified Upper Triassic carbonate substratum, filling the "hollows" of a mature, prevailing surface-paleo-karst morphology which implies a strong tectonic control (elongate karst forms arranged parallel to the principal tectonic directions of the Bakony (NNW-SSE; NE-SW)). Depending on their positions as related to the paleo-base-level of erosion they may fill canyons, deep sinkholes, i.e. dolines or large shallow "uvala"- or "polje"-like karstic forms. Accordingly, their lithofacies may reflect either highly-oxidizing (vadose) conditions coupled with a considerable autochthony (*sensu* Bonte) in deep sinkholes or dolines; or less oxidizing (phreatic) environments sometimes with striking allochthony (mostly in shallow poljes or uvalas). Oolitic-pisolitic litho-types invariably prevail in deposits of the Turonian/Senonian bauxite horizon.

Evidence for underground cavity-type karstification associated with the bauxitic episode is scarce – at least at the level of deposits currently under development. Only from a few boreholes there were reported narrowing-down, funnel-shaped karst forms and fissure-fillings far beneath the level of economic mining.

Primary cover of the deposits of this second horizon is either a thick fine-grained siliciclastic fluvial (deltaic) sequence of Upper Senonian age (Iharkút) and/or a limnic-to-paralic lignitiferous sequence (Halimba), likewise Upper Senonian. In the southern extremes of the Bakony (Nyirád, Csabpuszta) also various facies of the Upper Senonian Pachyodont patch-reefs serve as immediate cover of the Turonian/Senonian bauxites. The lithofacies of the coverbeds apparently reflects the underlying erosional relief produced by tectonically controlled karst-planation processes during the preceding denudation period.

Bauxite deposits of the third ("upper", Paleocene/Eocene) horizon are known (1) from the contact of Cr₃/E₂ in areas where Post-Senonian denudation exposed the surface of the Pachyodont-limestone, and (2) from the T₃/E₂ contact where Pre-Middle Eocene denudation reached down to the Triassic basement.

Deposits of type (1) are restricted to the Southern Bakony whereas type (2) is the most widespread bauxite formation of the TCR with deposits spread from Sümeg in the south to Nagyegyháza and Pilisszántó to the north.

In group (1) the bauxite fills shallow irregular karstic "depressions" of no particular or only slight tectonic control. It is soft, friable, highly porous and apparently less consolidated than the material of any of the older deposits. It is predominantly of pelitomorphic/intraclastic texture sometimes with roundgrains, pseudo-oids and pebbles but never with true ooids or pisoids.

On the basis of thorough lithofacies studies it is assumed that the deposition of bauxite in this period took place mostly in a vadose to semi-vadose environment. At places, however, this vadose character of the ore is severely "camouflaged" in the topmost part of the deposits by a strong phreatic overprint (pyritization, etc.) obviously connected with the gradual upraisal of the groundwater table at the beginning of the Eocene transgression. At some places, underlying, at other places substituting this stagnant-water facies, products of a paleosol-forming episode can be recognized on the top of the deposits. The paleosols are essentially pedogenetically altered bauxites (with well-developed cambic horizon as opposed to the geochemically non-stratified, quasi-oxic bulk of the deposit). They suggest that climatic conditions and/or drainage must have undergone some (probably deteriorating) changes towards the end of the accumulation of the bauxite.

The deposits of group (2) show rather high facies diversity: along with apparently autochthonous vadose to semi-vadose lithofacies, striking allochthony and phreatic/semiphreatic facies may occur, in fact, allochthony is much more widespread than either in the case of the Senonian or in the case of group (1) Eocene bauxites. As to the underlying relief, it has to be pointed out, that in most cases group (2) Eocene bauxites fill shallow to medium-depth asymmetric half-graben-like structures, the bottom of which shows medium to low karst relief. At several occurrences pelitomorph and coarse clastic lithotypes occur together. Sometimes coarse clastics (consisting of moderately sorted bauxite pebbles) form layers/lenticular bodies alternating with the pelitomorph bulk of the deposits (Gánt); sometimes they are localized to the uppermost part of the bauxitic complex (Nagyegyháza).

The cover-beds show an even greater facies diversity than the bauxite itself. Paleosols; fluvial deposits (sandy-pebbly alluvium); lacustrine sediments (freshwater limestones/marls); limnic to paralic coal seams; various kinds of lagoonal deposits (from the restricted to the open-circulation shelf-lagoon environment) may occur as the immediate cover of the bauxite. Like in the case of the Senonian horizon, also here the facies-pattern, of the Eocene coverbeds at any given area is a function of the underlying, partly bauxite-filled erosional relief.

The increase of facies diversity of both bauxite and cover, the morphology of the deposits and the increased frequency of transportation phenomena within the bauxite all point to some syndepositional tectonic event(s), presumably connected to strike-slip motions having affected the territory of TCR during Early to Middle Eocene times as supposed by Báldi and Báldi-Beke (1985), Kázmér (1984) and others.

Of the Eocene bauxites group (1) deposits are supposed to be older in the sense of having been buried by the Eocene transgression as early as the uppermost

Cuisian (Kopek et al. 1965; Szantner et al. 1986) whereas group (2) deposits, covered by Lutetian strata younging from SW to the NE, are considered to be somewhat younger. (It should be noted that all arguments regarding the age of group (2) deposits are, however, necessarily indirect because there are no fossils in the bauxites and the apparent stratigraphic gap is rather wide (T₃/E₂). Investigations to elaborate a micromineralogy-based correlation was attempted by Mindszenty et al. (1991), the amount of knowledge, however, does not allow firm conclusions as yet!)

Systematic lithofacies studies of bauxites with the aim of an eventual paleomorphological reconstruction for the bauxitiferous horizons of Hungary are under way. Though far from complete, preliminary results already permit some general statements, summarized below:

Lower Cretaceous horizon

Mineralogy and morphofacies of the Lower Cretaceous bauxite in South Hungary suggest that deposition took place in a close-to-groundwater position resulting in "semi-phreatic" rather than strictly "vadose" diagenetic (and perhaps also depositional) environment, as a consequence of which the bauxite is often paleocoloured with a yellowish to greenish tint. Large-scale redeposition seems to be unlikely: no coarse grained lithologies, stratification or grading could be observed in any of the exposures. Though sedimentological data are scarce (Dudich and Mindszenty 1985; Nagy 1989) the homogeneous oolitic wackestone/packstone texture of the bauxite points also to in situ evolution of the sediment rather than to large-scale allochthony. This is in fairly good accordance with the general geological situation: brief stratigraphic gap, shallow karst relief formed on a quiet carbonate platform and showing no signs of any major orogeny-related tectonics.

Mid Cretaceous horizon

Information is scarce and indirect (a few samples from long-ago abandoned old mines, and some more recent boreholes; profiles and borehole logs in old exploration reports). The few evidence, however, shows that the majority of the bauxite which "survived" all post-Albian denudation periods was allochthonous i.e. deposited after some shorter or longer transport in a phreatic to semi-phreatic environment (probably close to the base level of erosion). The texture of the bauxite pebbles, however, indicated that adjoining this low-level terrain there must have been some higher elevated areas as well, where accumulation of bauxites under vadose conditions was taking place. Part of these vadose deposits were eroded off and redeposited still during the Pre-Albian subaerial exposure phase whereas the rest probably fell victim to erosion later on.

Upper Cretaceous horizon

Lithofacies and morphology of the two Senonian deposits investigated in details (Iharkút and Halimba) are strikingly different suggesting that the erosional relief

brought about by the Austrian phase must have been rather diverse. Along with dissected high-level karst-terrains with deep sinkholes filled by "vadose" bauxites showing a considerable degree of autochthony (like Iharkút), there were also large depressions close to the base level of erosion, where the eroded material of higher elevated deposits accumulated under semi-vadose conditions (like Halimba). Transportation of bauxite to these low-level areas took place by ephemeral water-courses as it was shown by Juhász (1988), whereas in high-level terrains a gradual change of the hydrography, from a predominantly ephemeral fluvial system during the early stages of karstplanation to an essentially endorheic, sheetwash-dominated drainage pattern on the mature surface with ephemeral water-courses gaining ground again in the senile stage was postulated by Mindszenty (1983).

A common though not yet fully understood feature of all Cretaceous bauxites in the TCR is the predominance of oolitic/pisolitic textures (as opposed to the pelitomorphic/intraclastic character of their younger Eocene counterparts).

Paleocene/Eocene horizon

As it was pointed out in the introduction the age of the deposits considered as Paleocene/Eocene is merely an inference to which there is but one exception (Csabpuszta, in the Southern Bakony, where the bauxite occurs at the contact of Cretaceous and Eocene strata). The rest of the so-called "Eocene" bauxites is underlain by Triassic and covered by Eocene. By lithofacies they indicate a low-to-medium karst relief not very far from, but still above the karstic water table (vadose to semi-vadose lithofacies!) during the early stages of the Paleocene/Eocene bauxitization period. Parts of this karst relief, however, got dissected later on, probably quite abruptly, leading to intense erosion, transport and redeposition of large amounts of previously formed bauxite in low-level areas under phreatic to semi-phreatic conditions (e.g. conglomeratic bauxites at Gánt or Csordakút).

Geochemistry of Hungarian karst bauxites

Sampling and analytical procedure

130 samples were collected from 12 Hungarian bauxite deposits of various age and lithology (Fig. 2) along vertical profiles from hanging wall to footwall. In this way samples collected represent the whole profile of a deposit, avoiding depletion or enrichment of trace elements in some levels biasing the comparison. Most of the analysed profiles can be taken as representatives of the average trace element content of the deposits sampled. Exceptions are only those deposits where only 1 to 2 samples were available for the analysis (see below).

Trace elements were determined by emission spectrographic technique using a high-dispersion grating + prism spectrograph Model EST-1 (Maksimović 1976b). Burning was undertaken in a controlled atmosphere (Ar + O) with Ge as internal standard. The overall precision of the method was $\pm 10\%$. The accuracy of the

analysis was monitored by including international geochemical reference samples in the analytical program (USGS G-1, USGS W-1, ZGI-TB, ZGI-KH, Flanagan 1973, BX-N and DT-N, De La Roche-Govindaraju 1973). Detection limit is given in Table 1.

Results and discussion

Results are presented in the form of average trace element contents in Table 1. Deposits are listed according to age: Lower Cretaceous: Nagyharsány; Middle Cretaceous: Csehbánya; Upper Cretaceous: Iharkút, Németbánya, Halimba; Eocene: Nézsa, Csordakút, Obarok, Gánt, Dudar, Szóc, Nyirád.

The observed values for Nyirád, Halimba, Szóc and Gánt were comparable to those published by Dudich (1972).

The two samples analysed from the Middle Cretaceous bauxite horizon were considered as non-representative* and therefore omitted from Table 2 where all results are summarized for bauxites of various age. General trends seen in this Table and to be pointed out are: (a) an increase of Cr, V and Zn in bauxites from the Early Cretaceous to the Eocene and (b) a decrease of Y and La in the same direction with the highest concentrations observed in the Lower Cretaceous bauxites of Nagyharsány. Whether or not this reflects a temporal/spacial variation in the supposed non-carbonatic source terrains for the areas compared cannot be decided on the basis of geochemistry alone.

Variations of the "mobile" trace elements with depth were also observed in some of the deposits studied (Figs 4, 5, 6 cf. with Fig. 1)

The *Nagyharsány deposit* is characterized by a concentration of the "mobile" trace elements at the footwall (Fig. 4). Rare earth elements are especially concentrated giving rise to the formation of authigenic bastnaesite (Bárdossy and Pantó 1973; Maksimovic and Pantó 1983). The trace element pattern indicates that for the major part of the deposit intense bauxitization took place in situ in the present place of the sediment. Therefore we may consider this case as "autochthonie absolue". Direct geological evidence from the bauxite was not highly informative. The general geological setting reflects a very flat paleomorphology indirectly suggesting that the chances of large-scale transport/redeposition were minor. The Nagyharsány bauxite deposit is the oldest deposit in Hungary and belongs to the "Tisza" tectonic unit supposed to have belonged to the Northern (European) margin of Tethys in Lower Cretaceous times (Géczy 1973; Márton 1981; Royden and Horváth 1988). This may partly explain the anomalous rare earth element content of the bauxite as compared with all the other samples collected from the Transdanubian Central Range belonging to the "Pelso Unit". This latter, lying North of the Balaton-Darnó tectonic lineament, shows a distinct Southern Tethyan (African) affiliation and apparently not only had a different source terrain but also its geodynamic history must have been different from that of the Tisza Unit (Channel et al. 1979; Royden and Horváth 1988 and others). One of the possible

* were collected most probably from the lowermost part of the deposit exposed by boreholes only

Table 1
Trace elements in some Hungarian bauxite deposits (ppm)

	Cretaceous						Eocene						
	Lower		Middle	Upper			N. Hungary	Gerecse Mts.		N. Bakony	Vértes Mts.	South Bakony	
	S. Hungary	Nagy-harsány	Cseh-bánya ¹⁾	Iharkút	Német-bánya	Halimba		Nézsa	Csordakút	Óbarok	Dudar	Gánt	Nyírad
B	3	75	47	96	97	49	28	37	23	*	28	69	59
Be	1	8.3	6.8	7.7	5	6.5	2.4	1.9	*	2.2	2.7	4.3	6.1
Ga	2	39	28	20	19	33	38	23	15	16	24	34	43
Cr	1	148	210	123	130	218	255	316	210	133	219	207	216
V	3	142	325	300	163	410	222	567	550	103	318	483	511
Nb	32	93	56	73	56	61	76	71	50	*	54	73	69
Mo	1	12	*	3	*	8	*	*	13	*	*	10	17
Ni	1	164	208	160	115	172	103	74	110	111	163	204	155
Co	1	17	27	12	8	21	23	14	18	10	20	23	14
Cu	1	19	43	48	31	30	26	43	52	19	44	49	36
Zr	10	148	*	102	36	113	317	359	440	*	476	286	183
Mn	1	968	5000	1414	710	1400	2336	446	450	1170	1143	1114	1145
Zr	10	312	680	257	223	220	290	254	270	213	182	212	202
Sn	3	11	*	4	*	9	13	13	5	*	11	6	12
Sc	2	21	49	17	17	21	28	27	15	28	21	17	21
Y	3	158	98	139	81	55	42	33	32	100	60	68	41
La	10	123	98	74	75	73	36	67	68	48	57	100	57
Sr	3	116	67	485	530	108	193	545	160	223	291	200	152
Pb	3	75	173	69	62	110	65	100	86	15	89	123	100
Ba	3	6	117	16	13	7	58	175	135	71	39	13	29
n		17	2	14	9	23	12	4	1	2	21	15	10

Symbols: S – detection limit (ppm); * – below detection limit; ¹⁾ – the only samples accessible but not representative; n – number of samples

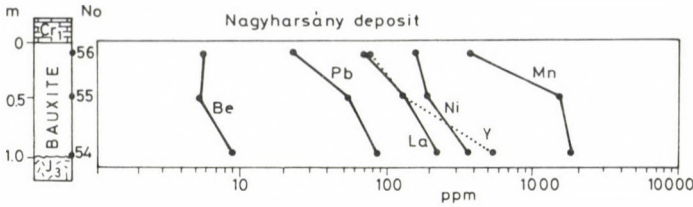


Fig. 4 Trace element distribution along the vertical profile of the Nagyharsány deposit (Indicative of "autochtonie absolue")

Table 2

Average trace element contents of Hungarian bauxite deposits (ppm) belonging to different stratigraphic horizons

	South Hungary	Transdanubian Central Range	
	Lower Cretaceous ¹	Upper Cretaceous ²	Eocene ³
B	75	73	42
Be	8.3	6.6	3.4
Ga	39	26	31
Cr	148	171	226
V	142	327	380
Nb	93	64	60
Mo	12	1.1	5
Ni	164	157	152
Co	17	16	19
Cu	19	36	39
Zn	148	94	340
Mn	968	1298	1304
Zr	312	232	219
Sn	11	1.3	9
Sc	21	19	22
Y	158	88	55
La	123	74	57
Sr	116	310	242
Pb	75	88	92
Ba	6	11	45
n	17	46	65

1) Nagyharsány; 2) Iharkút, Németbánya, Halimba; 3) Nézsa, Csordakút, Óbarok, Nyirád, Szóc, Gánt, Dudar

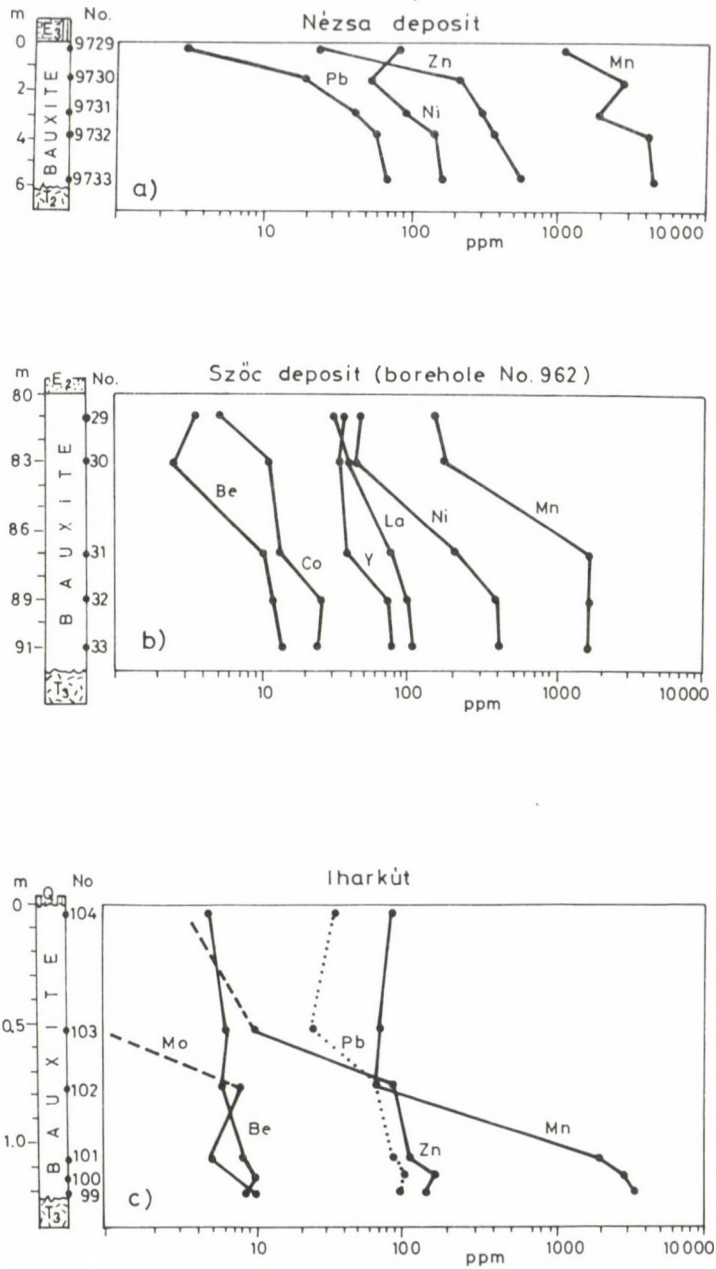


Fig. 6 Trace element distribution along the vertical profile at Nézsza (a), Szöc (b), Iharkút (c)

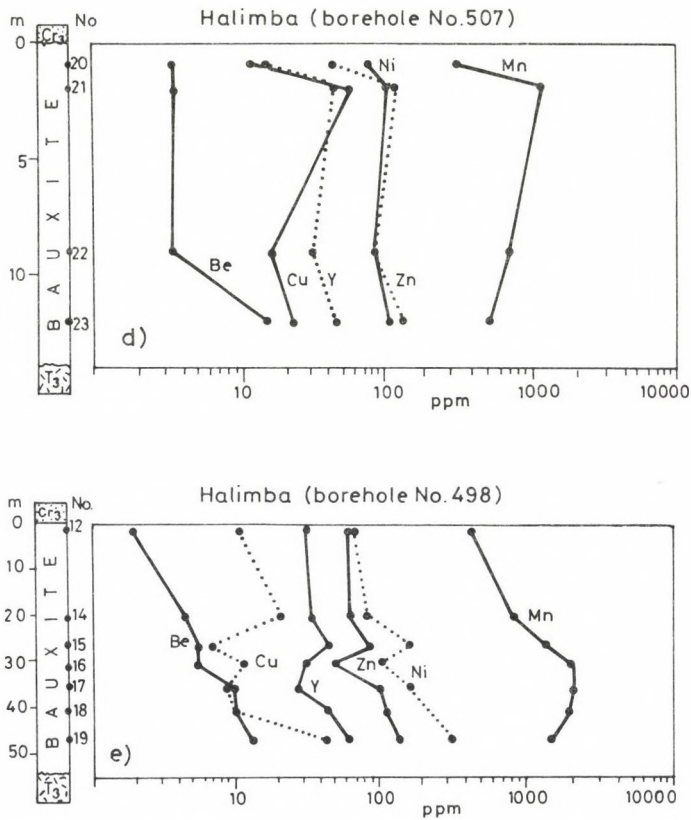


Fig. 6 Trace element distribution along the vertical profile at Halimba (d, e)

Conclusions

This study demonstrates that systematic trace element analyses of representative vertical profiles of bauxite deposits may provide useful information relevant to the allochthony/autochthony problem. The studied Hungarian bauxite deposits are good examples for that conclusion. Some of them are extremes, with total allochthony (Gánt) or total autochthony (Nagyharsány). The majority of the studied deposits, however, shows intermediate characters, suggesting various degrees of allochthony/autochthony. We think therefore, that in addition to sedimentological study, geochemical criteria could be very useful in estimating the degree of "in situ" geochemical changes in karst bauxites.

References

- Báldi, T., M. Báldi-Beke 1985: The evolution of the Hungarian Paleogene basins. – *Acta Geol. Hung.*, 28, 1–2, pp. 5–28.
- Bárdossy, Gy., Gy. Pantó 1973: Trace mineral and element investigation in bauxites by electron probe. – 3^{ème} Congress ICSOBA, Nice, pp. 47–53.
- Bárdossy, Gy. 1982: Karst bauxites. Bauxite deposits on carbonate rocks. – Elsevier–Akad. Kiadó, pp. 1–144. Budapest
- Bárdossy, Gy., I. Valetton, Gy. Komlóssy, P.J. Combes, A. Mindszenty, J. Knauer 1990: Discussion on the problems of allochthony and autochthony. – *Newsletter 2, IGCP–287*, pp. 8–13.
- Bonte, A 1969: Mise en place et evolution des bauxites sur mur calcaire. – *Ann. Inst. Geol. Publ. Hung.*, 54, 3, pp. 29–49.
- Caillère, S., Z. Maksimović, Th. Pobeguín 1976: Les éléments en trace dans quelques bauxites karstiques de l'Ariege et du Var. – *Travaux ISCOBA 13*. pp. 233–252, Zagreb.
- Channel, J.T., B. D'Argenio, F. Horváth 1979: Adria, the African promontory in Mesozoic Mediterranean Paleogeography. – *Earth Sci. Reviews*, 15. pp. 213–292.
- Combes, P.J. 1969: Recherches sur la genese des bauxites dans le Nord-Est de l'Espagne, le Languedoc et l'Ariege (France). – *Université Montpellier, Mém. CERGH III–IV*, pp. 1–342.
- Combes, P.J. 1984: Regards sur la geologie des bauxites; aspects recents sur la genese de quelques gisements a substratum carbonate. – *Bull. Centres Rech. Explor. Prod. Elf Aquitaine*, 8, 1, pp. 251–274.
- Combes, P.J. 1990: Typologie, cadre geodynamique et genese des bauxites françaises. – *Geodynamica Acta (Paris)*, 4, 2, pp. 91–109.
- D'Argenio, B., A. Mindszenty 1991: Karst bauxites at regional unconformities and geotectonic correlation in the Mediterranean. – *Bull. Geol. Soc. It.*, 110, pp. 85–92.
- De la Roche, N., K. Govindaraju 1973: Étalons de référence pour l'analyse de la bauxite et du disthène. – 3^{ème} Congress ICSOBA, Nice, pp. 367–381.
- Dudich, E. 1972: Beiträge zum geochemischen Verteilung der Spurenelementgehalte der Karstbauxite von Ungarn, Rumänien, Bulgarien und Jugoslawien. – *IXth Congress Carpatho-Balkan Geol. Assoc.*, 4, pp. 47–55.
- Dudich, E., A. Mindszenty 1985: Contribution to the comparative geochemistry and petrology of bauxites in the Villány Mts. (SE Transdanubia, Hungary) and in the Padurea Craiului Bihar Mts area (W. Transylvania, Romania). – *Bull. Geol. Soc. Hung.*, 114, 1, pp. 118.
- Flanagan, F.J. 1973: 1972 values for international geochemical reference samples. – *Geochim. Cosmochim. Acta*, 37, pp. 1189–1200.
- Géczy, B. 1973: Plate Tectonics and paleogeography in the East-Mediterranean Mesozoic. – *Acta Geol. Hung.*, 17, pp. 421–428.
- Juhász, E. 1988: Sedimentological features of the Halimba bauxite and paleogeographic reconstruction. – *Acta Geol. Hung.*, 31, 1–2, pp. 111–136.
- Kázmér, M. 1984: Continental escape of the Bakony–Drauzug unit in the Paleogene. – *Ált. Földt. Szemle* 20, pp. 55–102, (in hungarian, with English abstract).
- Kázmér, M., S. Kovács 1985: Permian–Paleogene Paleogeography along the Eastern Part of the Insubric–Periadriatic Lineament System: Evidence for Continental Escape of the Bakony–Drauzug Unit. – *Acta Geol. Hung.*, 28, 1–2, pp. 71–84.
- Komlóssy, Gy. 1967: Contribution a la connaissance de la genese des bauxites hongroises. – *Acta Geol. Hung.*, 20, 3–4, pp. 199–244.
- Kopek, G., E. Dudich, T. Kecskeméti 1965: Stratigraphische Probleme des Eozens im Transdanubischen Mittelgebirge Ungarns. – *Acta Geol. Acad. Sci. Hung.*, 9, pp. 411–420.
- Maksimović, Z. 1976a: Genesis of some Mediterranean karstic bauxite deposits. – *Travaux ICSOBA 13*, pp. 1–14, Zagreb.
- Maksimović, Z. 1976b: Trace elements in some Yugoslav bauxite deposits and their significance. – 4th Yugoslav Symp. Explor. Bauxites Hercegnovi. pp. 29–33 (in Serbian with English abstract)

- Maksimović, Z. 1978: Nickel in karstic environment: in bauxites and in karstic nickel deposits. – Bull. du BRGM (sect. II) 3, pp. 173–183.
- Maksimović, Z. 1979: Geochemical study of the Marmara bauxite deposit. Implication for the genesis of brindleyite. – *Travaux ICSOBA*, 15, pp. 109–120, Zagreb.
- Maksimović, Z. 1988: Geochemical criteria to differentiate karstbauxites formed in situ from redeposited bauxites. – *Geoloski glasnik. Posebno izdanje, Titograd*, 6, pp. 93–101 (in Serbian with English abstract).
- Maksimović, Z., G. De Weisse 1979: Geochemical study of an overturned bauxite deposit in Les Codouls (S. France). – *Travaux ICSOBA*, 15, pp. 109–120, Zagreb.
- Maksimović, Z., Gy. Pantó 1987: The occurrence and genesis of the hydroxyl-bastnaesites from Montenegro, Yugoslavia. – *Bull. Acad. Serb. Sci. Arts*, 27, pp. 15–20, Beograd.
- Maksimović, Z., Gy. Pantó 1991: Contribution to the geochemistry of the rare earth elements in the karstic bauxite deposits of Yugoslavia and Greece. – In: Pavich, M.J. (Ed.): *Weathering and Soils, Geoderma*, 51, pp. 93–109.
- Maksimović, Z., Gy. Pantó 1980: Bastnaesite- (La) and monazite- (Nd) a new variety of monazite from Marmara bauxite deposit (Greece). – *Bull. Acad. Serb. Sci. Arts*, 20, pp. 35–42, Beograd.
- Maksimović, Z. – Gy. Pantó 1985: Hydroxyl-bastnaesite- (Nd), a new mineral from Montenegro, Yugoslavia. – *Miner. Magazine* 49, pp. 717–720.
- Maksimović, Z., J. Papastamatiou 1973: Distribution d'oligoéléments dans les gisements de bauxite de la Grèce centrale. 3^{ème} Congrès ICSOBA, Nice, pp. 33–46.
- Maksimović, Z., E. Roaldset 1976: Lanthanide elements in some Mediterranean karstic bauxite deposits. – *Travaux ICSOBA*, 13, pp. 199–220, Zagreb.
- Maksimović, Z., Gy. Pantó 1983: Mineralogy of Yttrium and Lanthanide elements in karstic bauxite deposits. – *Travaux. ICSOBA* 18, pp. 191–200, Zagreb.
- Márton, P., 1981: Tectonic implications of paleomagnetic data for the Carpatho-Pannonian region. – *Earth. Evol. Sci.*, 1, pp. 257–264.
- Mindszenty, A 1983: Late Senonian morphological evolution of the Iharkút karst area as reconstructs on the basis of sedimentological features of the bauxite. – *Travaux ICSOBA*, 13, (18) pp. 61–72.
- Mindszenty, A., A. Horváth, A. Szóts 1989: Karst bauxites in the Transdanubian Midmountains. – In Császár (Ed.) *Excursion Guidebook*, 10th Regional meeting, IAS. Budapest, pp. 11–48.
- Mindszenty, A., K. Gál-Solymos, A. Csordás Tith, I. Imre, Gy. Felvári, A.W. Ruttner, T. Böröczky, J. Knauer 1991: Extraclasts from Cretaceous/Tertiary Bauxites of the Transdanubian Central Range and the Northern Calcareous Alps. Preliminary Results and Tentative Geological Interpretation. – *Jubiläumsschrift 20 Jahre Geol. Zusammenarbeit Österreich-Ungarn* (Eds: H. Lobitzer, G. Császár) Teil I. pp. 309–345.
- Nagy, S. 1989: Sedimentological study of the Nagyharsány bauxite deposit. Diploma work, Eötvös L. University, Dept. Mineralogy (manuscript, in Hungarian) Budapest.
- Nia, R. 1967: Geologische, Petrographische, geochemische Untersuchungen zum Problem der Boehmit-Diaspor Genese in griechischen Oberkreide-bauxiten der Parnass-Ghiona Zone. Diss. Erlang. Doktorgr. Univ. pp. 1–133, Hamburg.
- Royden, L.H., F. Horváth 1988: The Pannonian Basin. – *AAPG. Mem.* 45, pp. 1–394.
- Südi, E. 1981: Comparative sedimentological study of the Iharkút-IX and Németsbánya-XI bauxite deposits (Nort Bakony, Hungary). – Diploma work, Eötvös L. Univ. dept. Mineralogy, pp. 1–53 (manuscript, in Hungarian).
- Szantner, F., J. Knauer, A. Mindszenty 1986: Bauxite prognosis – Veszprém Committee of Hungarian Academy of Sciences, pp. 1–472 (in Hungarian with English abstract).
- Valeton, I. 1976: Criteria for autochthonous and allochthonous source material of bauxitic ores on carbonaceous rocks. – *Travaux ICSOBA*, 13, pp. 21–36.
- Valeton, I. 1991: Processes of allochthony and autochthony in bauxites on carbonate platforms of the Mediterranean area. *Mineral Wealth*, 71. Athens pp. 13–28.

Bauxites in Albania

Vangjel Kici, Luftulla Peza,
Defrin Skhupi, Abedin Xhomo
Geological Institute, Tirana

A short review of the Albanian bauxites is presented. In the Albanides deposits occur in different stratigraphic levels from Upper Triassic to Middle Miocene. The characteristic features and most important data of tyhe bauxitiferous horizons are summarized in tables and stratigraphic columns.

Key words: Bauxite, Mesozoicum, Tertiary, Albanides

Introduction

The Albanides are divided into two parts by the Shkodër-Pejë transversal: Southern and Northern Albanids. The following zones can be distinguished in the Southern Albanides (the northern continuation of Hellenides) from the west to the east, based on the paleogeographic development: Sazani zone (Preapulian zone in Italy and Paksos in Greece), Ionian zone, Kruja zone (Gavrovo in Greece and Dalmatian zone in Yugoslavia), Krasta-Cukali zone (Pindos zone in Greece and Budva zone in Yugoslavia), Mirdita zone (Subpelagonian zone in Greece and Serbian zone in Yugoslavia) and Korabi zone (Pelagonian zone in Greece and Golia zone in Yugoslavia) (Fig. 1).

In addition to the Kruja and Krasta-Cukali zones, also the Albanian Alps zone with two subzones, Malësi e Madhe (High Karst) and Valbona (Prekarstic subzone), respectively, Kelmendi zone (Bosniac zone) and Gashi zone (Durmitor zone) are distinguished in the northern Albanides. To the northwest they continue as the Dinarides.

Bauxites in the Albanides occur in the Kruja, Albanian Alps and Mirdita zones. They are localized at different stratigraphic levels, from Upper Triassic to Middle Miocene. Those situated between Santonian–Campanian limestones and Middle Eocene terrigene deposits (Mirdita zone) and those between Upper Senonian limestones and Middle Miocene ones (Kruja zone) are widespread and they are most important ones. Bauxites occurring between the Ladinian and Upper Triassic limestones (Albanian Alps zone) and those between the Triassic and Cenomanian–Turonian limestones (Mirdita zone) are also fairly important. The bauxites of these two horizons have been studied in more details.

The bauxite horizon of the Albanides can be characterized as follows:

Addresses: V. Kici, L. Peza, D. Skhupi, A. Xhomo: Instituti i Kerkemeve Gjeologjike Bll. Vasil Shanto
Tirana, Albania

Received: 25 November, 1991.

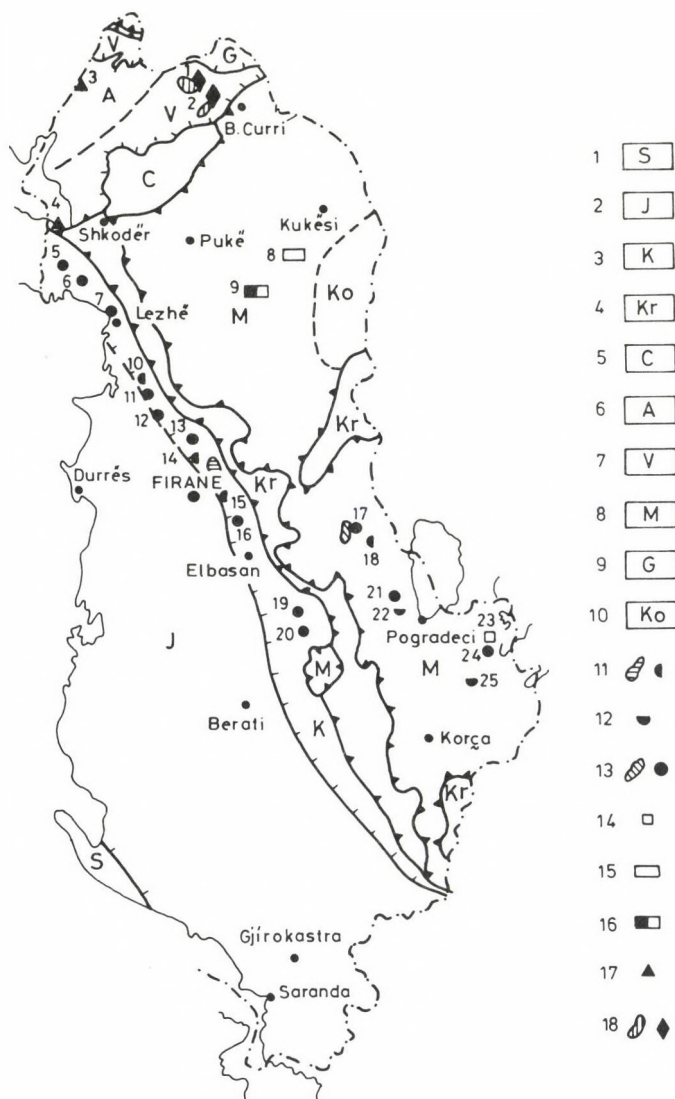


Fig. 1
Tectonic scheme of Albanides with distribution of the bauxitic horizons. 1. Sazani Zone; 2. Ioniane Zone; 3. Kruja Zone; 4, 5. Krasta-Cukali Zone; (4. Krasta Subzone, 5. Cukali Subzone); 6. M.e. Madhe Subzone; 7. Valbona Subzone; 8. Mirdita Zone; 9. Gashi zone; 10. Korabi Zone; 11. Miocene bauxites, 12. Oligocene bauxites; 13. Eocene bauxites, 14. Senonian bauxites; 15. Cenomanian bauxites; 16. Lower Cretaceous bauxites; 17. Tithonian bauxites; 18. Upper Triassic bauxites

Bauxite horizons of the Albanides

Bauxites between Ladinian and Upper Triassic

They occur in the Albanian Alps zone (Fig. 2). The ore bodies are situated on the karstified surface of Ladinian limestones and dolomites and are covered by Carnian limestones with *Clypeina besici*. They are lenticular or stratiform 1–2 m thick (to 5 m rarely), and, more seldom, they fill 20–30 m deep sinkholes, as in the Valbona valley (Prozhmë). The ore-bodies consist mainly of diasporitic bauxites and more seldom of boehmitic ones.

Changes and transitions from bauxite to argillaceous bauxite and bauxitic clays or from bauxite to bauxitic breccias can often be observed. Sometimes bauxites are completely absent to texture, they are pelitic-oolitic, whereas their structure is massive. Reddish colour is predominant but, sometimes greyish bauxites, also occur.

Generally, they are conformably intercalated between the Ladinian and Carnian carbonates. It is only Tarabosh (Vidhgarë) where they are associated with an observable unconformity.

Bauxitic clays between the Kimmeridgian and Tithonian

They occur only in the restricted sector of the Malësi e Madhe subzone near the state bordered with Yugoslavia. Along strike they pass into conglomeratic limestones and, sometimes, completely disappear. They are rest on the unkarstified surface of the Kimmeridgian limestones and are conformably overlain by limestones and dolomites with *Clypeina jurassica* (Tithonian). The 1–12–15 m thick reddish bauxitic clays may contain conglomerate layers with limestone pebbles and, more seldom ostracodal and charophytic limestones as well. The bauxite is of oolitic texture.

Bauxites between the Neocomian and Barremian–Aptian

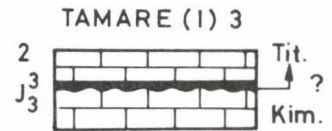
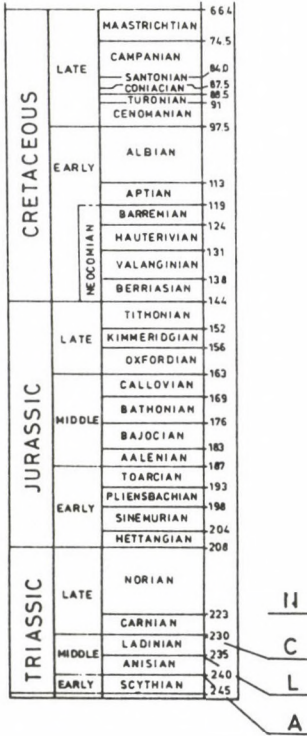
They occur in the Krej Lurë region (northern sectors of the Mirdita zone) (Fig. 3) and have a limited extension. The ore-bodies rest on the undulate surface of brecciated limestones. The breccia is cemented by biomicrite and contains Berriasian–Valanginian calpionellids. The karst is weakly developed. The reddish bauxite bodies are very rich in iron (25–30 % Fe_2O_3). Major minerals are boehmite (35–40 %), gibbsite (15–25 %) and kaolinite (10–15 %). They are stratiform or lens shaped, about 2 m thick, and are covered by the Barremian–Aptian conglomeratic limestones. The bauxite is pelitic and oolitic in texture.

Bauxites between the Upper Triassic and Cenomanian–Turonian

They are encountered only the Vrini i Arnit deposit (southeast of the town Kukësi) (Fig. 3) in the northern sectors of the Mirdita zone. The lenticular to stratiform bauxite bodies and those filling deep sinkholes unconformably rest on the intensely karstified surface of the Upper Triassic–Liassic limestones. The reddish iron-rich bauxite of good quality often occurs at the bottom, whereas the

argillic and conglomeratic and brecciated bauxite are confirmed to the upper parts of the deposits. The ore-bodies are covered by a thin sheet of mottled clayey and sandy intercalations, which upwards pass into the Cenomanian-Turonian limestones. Major minerals are: boehmite, hematite and kaolinite.

ALBANIAN ALPS ZONE



VALBONE (I-II) 1
LUGU I THIUT (I-II), 2
VIDHGARE (I), 4

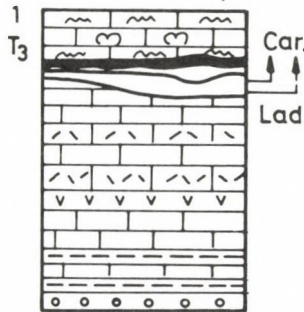
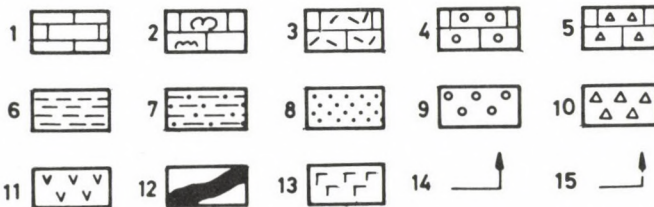


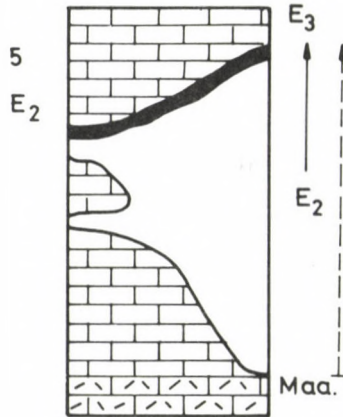
Fig. 2
Stratigraphic position of the Bauxite of Albania, Albanian Alps Zone
1. limestones; 2. limestones with megalodonts and stromatolitic limestones; 3. dolomites; 4. conglomeratic limestones; 5. brecciated limestones; 6. clay; 7. siltstone; 8. sandstone; 9. conglomerates; 10. breccia; 11. tuff; 12. bauxite; 13. Lower Jurassic rocks
14. estimated duration of exposure; 15. apparent stratigraphic gap; size of bauxite deposits: I. very small; II. small; III. moderate



KRUJA ZONE

QUATERNARY	PLIOCENE	CALABRIAN	0-01		
			1.6		
TERTIARY	PALEOGENE	Eocene	3.4		
			Oligocene	5.3	
				6.5	
			Miocene	11.2	
				15.1	
16.6					
TERTIARY	PALEOGENE	Oligocene	21.8		
			22.7		
		Eocene	34.6		
			40.0		
			43.6		
		Paleocene	57.0		
			57.8		
		CRETACEOUS	EARLY	Maastrichtian	66.4
					74.5
				Cenomanian	84.0
87.5					
89.5					
Albian	91				
	97.5				
	MIDDLE			113	
				119	
				124	
131					
138					
JURASSIC	MIDDLE	Tithonian	144		
			152		
		Kimmeridgian	156		
			163		
		Oxfordian	169		
			176		
		Early	183		
			187		
		TRIASSIC	LATE	Toarcian	193
					198
Pliensbachian	204				
	208				

KAKARIQ (I) 5,6,7
 MAKARESH (I) 11,12
 DAJTI (I) 13,16
 TERVOLI (I) 19,20



DAJTI (III) 15
 MALI BJESHIT (II) 14
 SKUNJEL (I) 10

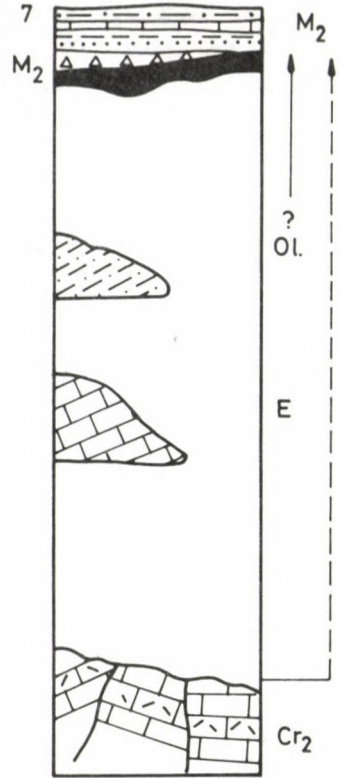


Fig. 3
 Stratigraphic position of the Bauxite of Albania, Kruja Zone
 (For legend see Fig. 2)

Bauxites between the Upper Triassic and Senonian

They are of limited extension in the Mali i Thatë (northeast of Korça), in the southern sectors of the Mirdita zone. The lenticular bauxite bodies and deeper sinkhole filling are all unconformably overlying the Upper Triassic–Liassic dolomites and limestones. In some cases, their thickness reaches 13 m. They have pelitic and oolitic texture and massive structure. Sometimes boehmite and sometimes hematite are prevalent (29–44 % Fe_2O_3 ; 11–35 % Al_2O_3). The bauxite is concordantly covered by Santonian–Campanian conglomeratic limestones with rudists.

Middle Eocene bauxites

They occur in the Kruja zone (Fig. 4) only and are situated on the slightly karstified surface of Maastrichtian and younger including Lower Lutetian dolomites and limestones.

The bauxite – fills cavities or more seldom small (0.2–3 m deep) dolinas – is of pelitic, oolitic to pisolitic texture and of massive, more seldom brecciated structure. In general, the Eocene bauxites are rich in iron. Major minerals are boehmite, kaolinite and hematite, in the reddish and pyrite in the grey-coloured lithotypes. Economically they are not very significant.

The bauxite bodies are covered by Upper Lutetian limestones.

Bauxites between the Senonian and Eocene or Oligocene

In the Mirdita zone, Eocene bauxites occur in southern Albania only. At Mali i Thatë they rest on the karstified surface of the Upper Triassic–Liassic limestones. The ore bodies are of cavity filling or lenticular shape with capriciously changing thickness (reaching up to 23 m). They are pelitic-oolitic in texture and massive in structure. Hematite (to 44 % Fe_2O_3) and boehmite are their prevalent mineral constituents.

In Dardhë (Librazhd), Çervenakë (Progradec) the Eocene bauxites occur on the karstified surface of Santonian–Campanian limestones. The bauxite bodies are essentially cavity-fillings or lenses (to 15 m thick). As to texture they are pelitic, oolitic and/or brecciated and show a massive structure. Major minerals are boehmite, hematite and kaolinite. The bauxite is generally reddish and, more seldom, greyish. The latter lithotypes contain also pyrite.

The Eocene bauxites are everywhere covered by terrigenous or carbonate deposits of the Upper Middle Eocene. Due to subsequent erosion they are often exposed on the surface.

In Zemblak (Korçë) and Saselisht, in the southern continuation of Çervenaka occurrence bauxites occur on the karstified surface of Santonian–Campanian limestones and are covered by terrigenous molasse deposits (sandstones and conglomerates) of Rupelian age. Between bedrock and cover there is an observable unconformity in this case. The bauxites look the same as those in Çerveneka. It

PERIOD	EPOCH	STAGE	AGE (Ma)
TERTIARY	PALEOGENE	ZANCLIAN	5.3
		HESSELIAN	6.5
		TORTONIAN	11.2
		SERRAVALLIAN	15.1
		LANGHIAN	16.6
	Eocene	BURDIGALIAN	21.8
		AQUITANIAN	22.7
		CHATTIAN	30.0
		RUPELIAN	34.6
		PRIABONIAN	40.0
CRETACEOUS	LATE	BARTONIAN	43.6
		LUTETIAN	57.0
		YPRESIAN	57.8
		THANETIAN	60.6
		UNNAMED	63.6
	EARLY	DANIAN	66.4
		MAASTRICHTIAN	74.5
		CAMPANIAN	84.0
		SANTONIAN	87.5
		CONIACIAN	91
JURASSIC	MIDDLE	TURONIAN	97.5
		CENOMANIAN	113
		ALBIAN	119
		APTIAN	124
		BARREMIAN	131
	EARLY	HAUTERIVIAN	138
		VALANGINIAN	144
		TITHONIAN	152
		RIMMERDGIAN	156
		OXFORDIAN	163
TRIASSIC	MIDDLE	CALLOVIAN	169
		BATHONIAN	176
		BAJOCIAN	183
	EARLY	AALENIAN	187
		TOARCICAN	193
LATE	PLIENSCHACHIAN	198	
	SINEURIAN	204	
	MEISSNERIAN	208	
	NORIAN	223	
	CARNIAN	230	
MIDDLE	LADINIAN	235	
	ANISIAN	240	
	SCYTHIAN	245	

MIRDITA ZONE

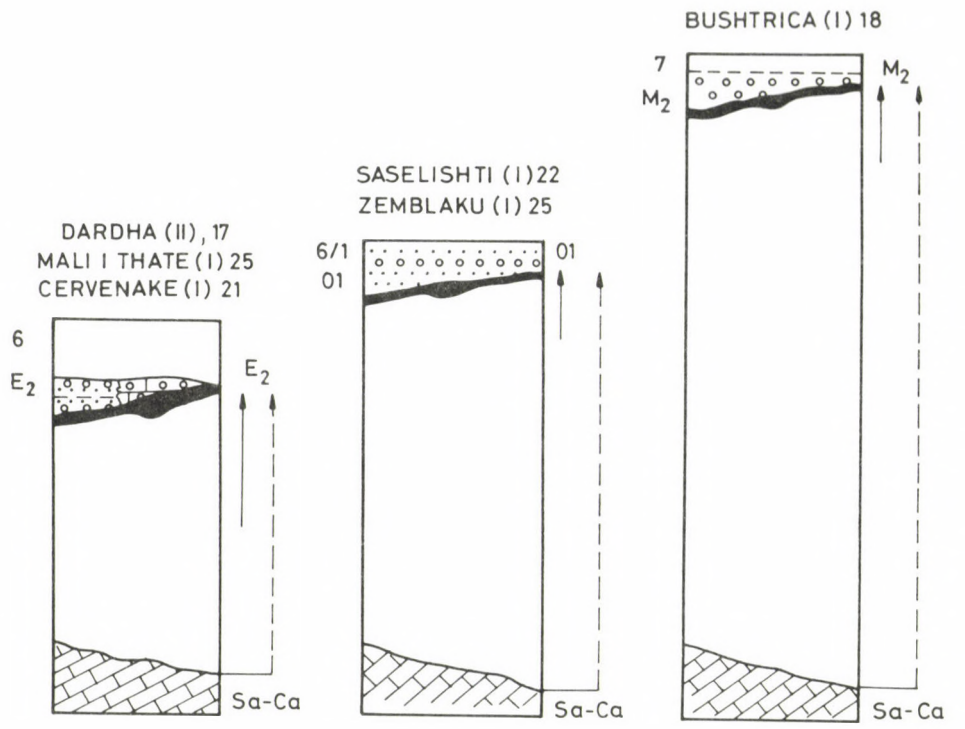
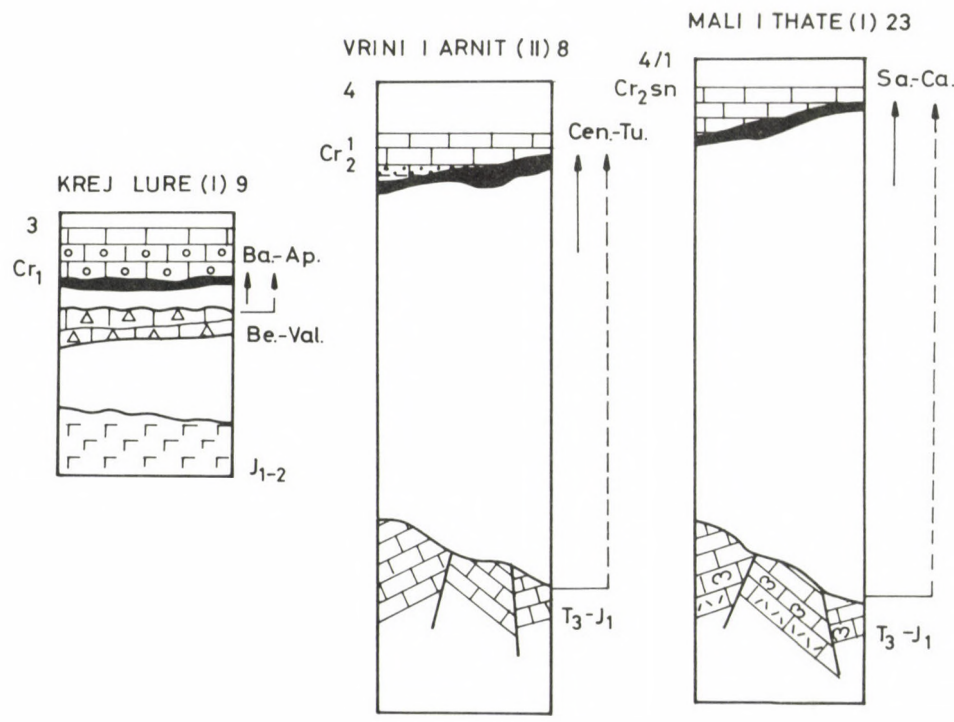


Fig. 4 Stratigraphic position of the Bauxite of Albania, Mirdita Zone (For legend see Fig. 2)

is possible that they represent the same level (the Eocene one) here covered not by the uppermost Lutetian transgression but by the Oligocene one. The main minerals are boehmite, hematite and kaolinite.

Miocene bauxites

They are widespread mainly in the Kruja zone. Small outcrops were described also from the Mirdita zone.

In the Kruja zone, Middle Miocene bauxites occur in the Dajti anticline, in the Milot-Tirana sector. They unconformably occur on the highly dissected karstified surface of the Campanian-Maastrichtian limestones. The lenticular stratiform bauxite bodies are of 20-104 m thick and are composed either of reddish bauxite with hematite or of greyish bauxites with pyrite and bauxitic clays. Boehmite, gibbsite and kaolinite could be distinguished in the "clay" fraction. The largest bauxite reserves of our country is concentrated mostly in the Dajti deposit (10 million tons) belonging to this particular type.

Bauxites are concordantly covered by terrigenous-carbonate deposits, mostly of Middle Miocene (Serravalian?) age (carbonate breccias). As a result of erosion very often they are exposed on the surface.

A very small outcrop of the Miocene bauxite horizons occurs in the Mirdita zone (in the Bushtrice sectors). It is unconformably underlain by Santonian-Campanian limestones and is covered by reddish terrigenous-molasse Librazhdi Formation Middle Miocene (Serravalian?) in age.

Table 1
Upper Triassic bauxites (Albanian Alps zones)

1. Angular unconformity	No
2. Estimated duration of exposure	2-7 My
3. Apparent stratigraphic gap	Small
4. Rate of regional subsidence	Does not change across the unconformity
5. Changes in lithofacies across unconformity	Major change
6. Record of contemporary sea-level changes	-
7. Bedrock petrography and age	Limestones and dolomites, Ladinian
8. Cover petrography	Limestones
9. Age of cover	Carnian
10. Lithofacies of associated bauxite	-
11. Underlying karst relief	Shallow
12. Supposed source material of bauxite	Mainly different volcanite piroclastice rocks and limestones of different ages
13. Supposed source material of non bx. karst fills	Mainly different volcanite piroclastics rocks and limestones of different ages
14. Lithology, size and shape of bx. deposit	Heterogeneous: bauxites, clayey bauxites, bauxitic clays, orebodies are small to moderate, layered and lenses ore big nests
15. Bauxite texture	Oolitic - pelitomorphic
16. Bauxite structure	Massive, sporadically bedded
17. Chemical composition of bauxite	Al ₂ O ₃ : 48-57 %, SiO ₂ : 6-20 %; Fe ₂ O ₃ : 11-18 %
18. Mineral composition of bauxite	Diaspore, boehmite, hematite, kaolinite, pyrite, chlorite
19. Accessory minerals of bauxite	Rare: Zircon, rutile, tourmaline, corundum
20. Trace elements in the bauxite	-

Table 2
Malm bauxites (Albanian Alps zone Malesia Madehe s/z)

1. Angular unconformity	No
2. Estimated duration of exposure	0.5–1 My
3. Apparent stratigraphic gap	Small
4. Rate of regional subsidence	Does not change across the unconformity
5. Changes in lithofacies across unconformity	Essentially unchanged
6. Record of contemporary sea-level changes	–
7. Bedrock petrography and age	Limestones, Kimmeridgian
8. Cover petrography	Limestones
9. Age of cover	Tithonian, 138 My
10. Lithofacies of associated bauxite	–
11. Underlying karst relief	Shallow to variegated
12. Supposed source material of bauxite	Alumosilicate rocks, limestones
13. Supposed source material of non bx. karst fills	–
14. Lithology, size and shape of bx. deposit	Very heterogenous: clayey bauxites, bauxitic clays, conglomerates, carbonate breccias, small lenses
15. Bauxite texture	Oolitic – pelitomorph
16. Bauxite structure	Bedded or schistic
17. Chemical composition of bauxite	Al ₂ O ₃ : 35–40 %, SiO ₂ : 27–40 %; Fe ₂ O ₃ : 3–6 %
18. Mineral composition of bauxite	–
19. Accessory minerals of bauxite	–
20. Trace elements in the bauxite	–

Table 3
Lower Cretaceous bauxites (Mirdita zone)

1. Angular unconformity	No
2. Estimated duration of exposure	5–10 My
3. Apparent stratigraphic gap	Moderate
4. Rate of regional subsidence	Does not change across the unconformity
5. Changes in lithofacies across unconformity	Major changes
6. Record of contemporary sea-level changes	No direct record
7. Bedrock petrography and age	Brecciated limestones, Berriasian–Valanginian
8. Cover petrography	Conglomerates and conglomeratic limestones
9. Age of cover	Barremian–Aptian, 140–120 My
10. Lithofacies of associated bauxite	–
11. Underlying karst relief	Variiegated
12. Supposed source material of bauxite	Alteration of the magmatic, intermediate, basic ultrabasic and metamorphic rocks
13. Supposed source material of non bx. karst fills	Alteration of the magmatic, intermediate, basic ultrabasic and metamorphic rocks
14. Lithology, size and shape of bx. deposit	Heterogeneous: clayey bauxites, bauxitic clays, small lenses
15. Bauxite texture	Pelitomorph
16. Bauxite structure	Massive
17. Chemical composition of bauxite	Al ₂ O ₃ : 39.1–46.6%, SiO ₂ : 13–16.4 %; Fe ₂ O ₃ : 23–27 %
18. Mineral composition of bauxite	Boehmite, hematite, gibbsite, goethite, kaolinite
19. Accessory minerals of bauxite	Rutile, zircon, chromite, pyroxene, granate
20. Trace elements in the bauxite	–

Table 4
Early Upper Cretaceous bauxites (Mirdita zone)

1. Angular unconformity	Large
2. Estimated duration of exposure	10–12, My
3. Apparent stratigraphic gap	Large
4. Rate of regional subsidence	–
5. Changes in lithofacies across unconformity	Major change
6. Record of contemporary sea-level changes	–
7. Bedrock petrography and age	Limestones, Middle Upper, Triassic, 240–220 My
8. Cover petrography	Limestones
9. Age of cover	Turonian, 90 My and Cenomanian
10. Lithofacies of associated bauxite	–
11. Underlying karst relief	Shallow to variegated or Santonian–Campanian, 94–74 My
12. Supposed source material of bauxite	Alteration of the magmatic, intermediate-acid, basic ultrabasic and metamorphic rocks
13. Supposed source material of non bx. karst fills	Alteration of the magmatic, intermediate-acid, basic ultrabasic and metamorphic rocks
14. Lithology, size and shape of bx. deposit	Heterogeneous bauxites, clayey bauxites, bauxitic clays, small to moderate lenses
15. Bauxite texture	Pelitomorphic and oolitic
16. Bauxite structure	Massive
17. Chemical composition of bauxite	Al ₂ O ₃ : 43.06–47.47%, SiO ₂ : 11.45–15.3%; Fe ₂ O ₃ : 25–26 %
18. Mineral composition of bauxite	Boehmite, hematite, kaolinite
19. Accessory minerals of bauxite	Rutile, zircon, chromite, tourmaline, chlorite
20. Trace elements in the bauxite (%)	Zr: 0.01, Cr: 0.01–0.05, V: 0.01–0.05, Ni: 0.07–0.08, Co: 0.02–0.05, Cu: 0.001–0.003

Table 5
Middle Eocene bauxite (Kruja zone)

1. Angular unconformity	No or weak
2. Estimated duration of exposure	2–12 My
3. Apparent stratigraphic gap	Small to moderate
4. Rate of regional subsidence	May change across the unconformity
5. Changes in lithofacies across unconformity	Major change
6. Record of contemporary sea-level changes	–
7. Bedrock petrography and age	Limestones and dolomites, Maastrichtian–Lower Lutetian
8. Cover petrography	Limestones
9. Age of cover	Upper Lutetian–Priabonian (43–40 My)
10. Lithofacies of associated bauxite	–
11. Underlying karst relief	Shallow
12. Supposed source material of bauxite	Mainly of the magmatic, intermediate-acid, basic and ultrabasic rocks. Less the redeposition of the Cretaceous bauxites.
13. Supposed source material of non bx. karst fills	Mainly of the magmatic, intermediate-acid, basic and ultrabasic rocks. Less the redeposition of the Cretaceous bauxites.
14. Lithology, size and shape of bx. deposit	Homogeneous, orebodies different in size and shape, they are in form of nests or lenses
15. Bauxite texture	Oolitic and pelitomorphic, detrital
16. Bauxite structure	Massive bedded
17. Chemical composition of bauxite	Al ₂ O ₃ : 31–45%, SiO ₂ : 10–13%; Fe ₂ O ₃ : 11–24%, Li.: 13.4%
18. Mineral composition of bauxite	Boehmite, kaolinite, hematite, gibbsite, chlorite
19. Accessory minerals of bauxite	Zircon, rutile, tourmaline, chromite, pyroxene, barite, granate
20. Trace elements in the bauxite (%)	Cr: 0.015–0.02, V: 0.005, Ni: 0.05, Co: 0.003, Cu: 0.002

Table 6
Middle Eocene and Oligocene bauxites (Mirdita zone)

1. Angular unconformity	Large
2. Estimated duration of exposure	10–20 My
3. Apparent stratigraphic gap	Moderate to large
4. Rate of regional subsidence	May change across the unconformity
5. Changes in lithofacies across unconformity	Major change
6. Record of contemporary sea-level changes	No direct record
7. Bedrock petrography and age	Limestones, Upper Triassic and Santonian–Campanian
8. Cover petrography	Sandstones
9. Age of cover	Upper Lutetian (43 My) or Rupelian (30 My)
10. Lithofacies of associated bauxite	–
11. Underlying karst relief	Variegated, sometimes deep
12. Supposed source material of bauxite	Mainly of the magmatic, intermediate–acid, basic and ultrabasic rocks. Less the redeposition of the Cretaceous bauxites
13. Supposed source material of non bx. karst fills	Mainly of the magmatic, intermediate–acid, basic and ultrabasic rocks. Less the redeposition of the Cretaceous bauxites
14. Lithology, size and shape of bx. deposit	Heterogeneous; orebodies are small rarely moderate which formed by filling of sinkholes
15. Bauxite texture	Pelitomorph and pelitomorph–oolitic
16. Bauxite structure	Massive
17. Chemical composition of bauxite	Al ₂ O ₃ : 47–54%, SiO ₂ : 2.7–12%; Fe ₂ O ₃ : 23–27%, Li.: 12.2 %
18. Mineral composition of bauxite	Boehmite, hematite, kaolinite, gibbsite, chlorite
19. Accessory minerals of bauxite	Zirkon, chromite, rutile, spinell, pyroxene, tourmaline
20. Trace elements in the bauxite (%)	Zr: 0.01, Cr: 0.01–0.03, V: 0.005–0.01, Ni: 0.01–0.05, Co: 0.001–0.005, Cu: 0.003–0.005

Table 7
Miocene bauxites (Kruja zone and Mirdita zone)

1. Angular unconformity	Large
2. Estimated duration of exposure	5–10 My
3. Apparent stratigraphic gap	Moderate to large
4. Rate of regional subsidence	Show dramatically change across the unconformity
5. Changes in lithofacies across unconformity	Major change
6. Record of contemporary sea-level changes	–
7. Bedrock petrography and age	Carbonate beds (Limestones and dolomites), Campanian, Maastrichtian
8. Cover petrography	Breccias, conglomerates, sands
9. Age of cover	Middle Miocene (Serravalian) 15 My
10. Lithofacies of associated bauxite	–
11. Underlying karst relief	Variegated, sometimes very deep
12. Supposed source material of bauxite	By the magmatic, intermediate–acid, basic and ultrabasic rocks and by the redeposition of the Cretaceous and Paleogene bauxites
13. Supposed source material of non bx. karst fills	By the magmatic, intermediate–acid, basic and ultrabasic rocks and by the redeposition of the Cretaceous and Paleogene bauxites
14. Lithology, size and shape of bx. deposit	Heterogenous
15. Bauxite texture	Pelitomorph–oolitic
16. Bauxite structure	Massive and bedded
17. Chemical composition of bauxite (%)	Al ₂ O ₃ : 37–49%, SiO ₂ : 6–16%; Fe ₂ O ₃ : 17–24%, Li.: 14.5–19%
18. Mineral composition of bauxite	Boehmite, gibbsite, hematite, kaolinite
19. Accessory minerals of bauxite	Chromite, zircon, rutile, amphibole, pyroxene, granate, chlorite
20. Trace elements in the bauxite (%)	Zr: 0.06–0.12, Cr: 0.01–0.03, V: 0.01–0.03, Ni: 0.02–0.05, Co: 0.003–0.005, Cu: 0.002–0.005

Bauxite deposits and Senonian formations in Hungary (Palynological analysis)

Ágnes Siegl-Farkas

Hungarian Geological Survey, Budapest

In the Transdanubian Central Range Senonian formations may occur both in the footwall and in the hanging wall of bauxites of different ages.

According to palynological investigations sedimentation lasted from the Upper Santonian till the Upper Maastrichtian. Based on palynostratigraphy this period has been divided into 8 dominance zones and within them 8 dominance subzones.

During the Upper Cretaceous the NW coast of the Tethys belonged to the tropical-subtropical Mediterranean region of the Normapolles phytogeographical province.

Key words: Transdanubian Central Range, Senonian, palynostratigraphy, bauxite

Introduction

In the *Transdanubian Central Range* the *Senonian* sedimentation started in the *Santonian* following the *Pregosauian–Subhercynian* orogenic phase and came to an end in the *Maastrichtian*. *Senonian* sequences are underlain by older *Mesozoic* formations, mainly *Upper Triassic* karstified carbonates

This continuous sequence representing a transgressional sedimentary cycle can be subdivided to the following evolutionary phases as well as lithostratigraphical units (Fig. 1).

Succession begins with the fluvio-lacustrine then marshy-boggy, coaly, clayey-coaly sandy layers of the *Ajka Coal Formation*. The alluvial sandy gravelly

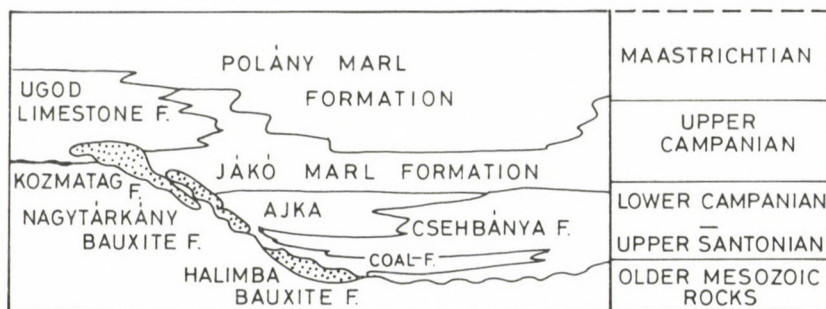


Fig. 1

Simplified section to illustrate relationships between bauxite and Senonian hanging wall formations (after J. Haas and E. Jocha-Edelényi 1980)

Address: Á. Siegl-Farkas: H-1442 Budapest P.O.B. 106, Hungary

Received: 30 September, 1991.

CHRONO - STRATIGRAPHY		LITHOSTRATIGRAPHY	PALYNOZONATION		TIME IN M. YEARS	
						CENTRAL RANGE TYPE
MAASTRICHTIAN	UPPER	POLÁNY MARL FORMATION	bakonyensis - praesubhercynicus		3.0	
	LOWER		Pseudopapillopollis Semioculopollis	devecserensis		5.0
		sahi				
CAMPANIAN	UPPER	UGOD LIMST. F.	bajtai - lenneri		1.5	
	LOWER		JAKÓ MARL FORM.	triangularis spatiosus		3.0
SANTONIAN	UPPER	AJKA COAL FORM.		Hungaropollis	Hungaropollis - Krutzschipollis	
	LOWER		oculus - oculoglomeratus			
		triangularis - Oculopollis				
CONIACIAN	UPPER	CSEHÉBÁNYA FORMATION	zaklinskaiaeglobosus	Oculopollis - Hungaropollis		2.8
	LOWER			Oculopollis - Triatriopollenites		
		Oculopollis - Brecolpites				
TURONIAN	UPPER	KÖZMATAG FORMATION	Oculopollis - Trilobosporites		1.0	
	LOWER		Oculopollis - Complexiopollis		1.2	
		HALIMBA B. F.			1.4	
			NAGYTÁRKÁNY B. F.			1.9
				1.9		

Fig. 2 Palynostratigraphy of the Senonian hanging wall formations of bauxite in the Central Range

variegated clay facies of the *Csehbánya Formation* in some places may fully substitute the *Ajka Coal Formation*. The transgressive *Jákó Marl Formation* consisting of clayey and marly layers may be intercalated with the rudistid *Ugod Limestone Formation* deposited on carbonate platforms.

The closing member of the Senonian sequence is the pelagic *Polány Marl Formation* of wide extension. It consists of calcareous marl and silty, sandy marl and in the lower part authigenic breccia interbeds.

According to palynological investigations depositional process of the Senonian formations lasted from the *Late Santonian* till the *Late Maastrichtian*. Based on palynostratigraphy this period can be divided into 8 assemblage or dominance zones and within them 8 dominance subzones (Góczán 1964, 1973; Siegl-Farkas 1983, 1986, 1989; Góczán and Siegl-Farkas 1990) (Fig. 2).

In certain areas of the *Transdanubian Central Range* bauxites have been deposited in the karstic depressions of the Triassic carbonates in the basement of the aforementioned Senonian formations.

These bauxites can be connected to the reductive covering formations. However, in some cases bauxites were formed just before the covering in other cases they were reworked from the earlier deposits (Fig. 3).

The *Senonian formations* may be both the *footwall* and the *hanging wall* of the bauxites of different ages.

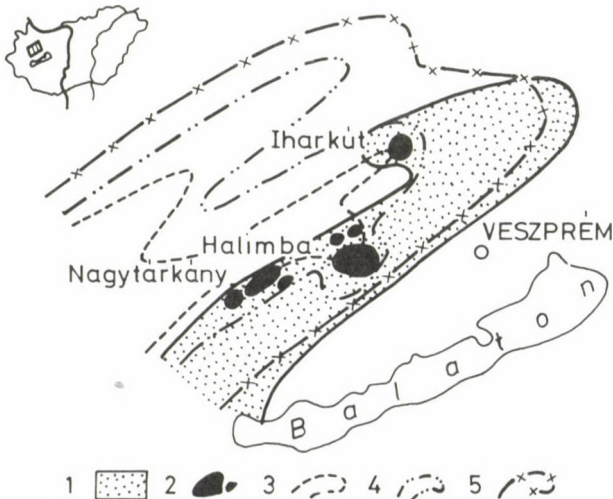


Fig. 3
Paleogeographic circumstances of bauxite formations in the Central Range during the Senonian transgression cycle. 1. bauxite accumulation area; 2. bauxite deposits; 3. Santonian shoreline; 4. Early Campanian shoreline; 5. Late Campanian shoreline

Bauxite formations of the Senonian bauxite horizon

The autochthonous-parautochthonous *Nagytárkány Bauxite Formation* is covered either by the *Csehbánya Formations* or the *Jákó Marl*, or rarely the *Ajka Coal* or the *Ugod Limestone Formation*.

The *Halimba Bauxite Formation* is covered by the *Ajka Coal Formation*. Accumulation of the bauxite material took place under alluvial, swampy and lacustrine conditions (Juhász 1988).

The *Kozmatag Formation* contains clasts from the nearby *Nagytárkány Bauxite Formation* and from the pre-Senonian (mainly Triassic) bedrocks too. The terrestrial clastic material was deposited in shallow marine environment together with bioclasts of rudists and other molluscs (Gellai and Ludas 1983). The cover is either the *Ajka Coal* or *Jákó Marl*, or the *Ugod Limestone Formation*.

Thus it can be concluded that any of formations of the Senonian transgressional sequence may be the cover of the Senonian bauxite horizon, except the *Polány Marl Formation*.

Since fossils are very scarcely or completely lacking in the bauxites, their age can be determined only on the basis of their original/primary cover.

Senonian covering formations either of freshwater (fluvial, lacustrine, swampy) or of marine origin can be equally characterized by sporomorph associations. Classifying the covering formations into palynological zones we can obtain the most probable age of the covering process of the bauxite deposits.

In the most common case bauxites were covered by the *Ajka Coal*, or the *Csehbánya Formation* or the *Jákó Marl Formation*. These formations can be classified into the Upper Santonian *Oculopollis – Trilobosporites* or the Lower Campanian *Zaklinskiaie – Globosus* and *Hungaropollis Dominance-Zones*.

Some of the bauxite deposits are covered by the *Jákó Marl* or the *Ugod Limestone Formations*. These belong to the upper part of the *Hungaropollis Dominance-Zone* and to the Upper Campanian *triangularis – spatiosus* – or *bajtai – lenneri Assemblage-Zones*.

These areas were more elevated in this period, than the areas where sedimentation under reduction conditions was started earlier.

However, it is possible that bauxite accumulation continued in these areas even during this period in the local depressions (karstic traps).

It is important to note that the oldest, Upper Santonian *Oculopollis – Complexiopollis Dominance-Zone* have not been found so far in the covering sequences of the bauxite formations. This oldest dominance zone has been known so far only from the areas of the early depressions *Sümeg (Sp.-1.)*, borehole and *Gyepükaján (Gy.-9.)*, borehole. It suggests that in more elevated areas of the Central Range bauxite accumulation took place during this period.

It should be mentioned a *new data* concerning the age of the accumulation of the *Halimba Bauxite Formation*. Based on the sporomorph association determined from a recently exposed coaly layer in the footwall we assume that the period of bauxite accumulation should be put between the *Middle Albian Crassipollis dekae*

Oppel Zone (Juhász 1979) and the Upper Santonian *Oculopollis* – *Trilobosporites* Dominance-Zone.

The Ugod Limestone Formation is exceptional among the Senonian formations since it can be both cover and footwall of bauxite deposits.

The Ugod Limestone Formation can be classified into the *triangularis* – *spatiosus* and *bajtai* – *lenneri* Assemblage-Zones, respectively. However if it has acted as bauxite footwall, the Polány Marl Formation deposited during the Maastrichtian *Pseudopapillopollis*- *Semioculopollis*- and *bakonyensis* – *praesughercynicus* Assemblage-Zones must have been denuded before the Early Eocene.

Paleoenvironmental conclusions

In the Transdanubian Central Range the footwalls of the Senonian bauxites are karstified Upper Triassic formations as a rule but in some areas Early Jurassic or Middle Cretaceous carbonates occur too.

Denudation of these formations took place most probably in the Turonian – Coniacian ages. During the Late Cretaceous the sedimentary basin of the Central Range belonged to the Mediterranean region of the Normapolles phytogeographical province. At the end of the Cenomanian as well as beginning of the Turonian the angiosperm Normapolles genera were suddenly spreaded over the NW coast of the Tethys of tropical subtropical climate. First representatives of the Normapolles were found in the formations of the Upper Santonian *Oculopollis* – *Complexiopollis* Dominance-Zone in the Central Range.

The fact that these forms were present on the slopes of karstic platforms already in an earlier phase of the Late Cretaceous is proved by their mass occurrence in the early reductive sediments.

In the marshy-boggy areas in addition to the mainly tree-shaped Normapolles genera, a rich brushwood vegetation was characteristic. Gymnosperms can only scarcely be found. Whereas on the continent the Normapolles vegetation was the predominant, the sea was rich in floral microplanktons.

The extremely rainy tropical – subtropical climate was favourable for bauxite formations became cooler only at the end of the Maastrichtian (Góczán 1964). Until this time climatic conditions may have been suitable for the bauxite generation.

References

- Császár, G. et al. 1990: Terrestrial and shallow-marine Cretaceous clastics. – Cretaceous Research. In press.
- D'Argenio, B., A. Mindszenty 1987: Cretaceous bauxites in the tectonic framework of the Mediterranean. – Rend. Soc. Geol. It., 9 (1986) pp. 256–262.
- Góczán, F. 1964: Stratigraphic palynology of the Hungarian Upper Cretaceous. – Acta Geologica, 8, 1–4, pp. 229–264.
- Góczán, F. 1973: Oberkretazische Kohlenbildung in Ungarn im lichte der Palynologie. – Proc. of the III. International Palyn. Conf. 1971. Moscow. The Palynology of Cenophytic, Publ. Off. "Nauka", pp. 28–35.
- Góczán, F., Á. Siegl-Farkas 1990: Palynostratigraphical zonation of Senonian sediments in Hungary. – Review of Paleobotany and Palynology, 66, pp. 361–377.
- Gellai, M., F. Ludas 1983: Adatok az Ugodi Mészkö Formáció és a Jákói Marga Formáció bázisrétegeinek megismeréséhez. (New data on the basal strata of the Ugod Limestones Formation and of the Jákó Marl Formation). – Földt. Közl., 113, 2, pp. 147–162.
- Haas, J. 1984: Paleogeographic and geochronologic circumstances of bauxite generation in Hungary. – Acta Geol. Hung., 27, 1–2, pp. 23–39.
- Haas, J., E. Jocha-Edelényi 1980: A Dunántúli-középhegység bauxitföldtani térképe. Felső-kréta bauxitszint (Bauxite geological map of the Transdanubian Mid-Mountains. The Upper Cretaceous bauxite horizon). – MÁFI
- Juhász, E. 1988: A Halimbai Bauxit felhalmozódásának története litológiai és üledékföldtani jellegei alapján. (History of accumulation of the Halimba Bauxite on the basis of its lithological and sedimentological features). – C. Sc. theses (in Hungarian).
- Juhász, M. 1979: A dunántúli alsó-és középsőkréta palynológiája. (Palynology of the Lower and Middle Cretaceous of Transdanubia). – C. Sc. theses (in Hungarian).
- Károly, Gy. et al. 1970: Stratigraphic horizons of the footwall and hanging-wall formations of bauxite deposits in Hungary. – Ann. Inst. Geol. Publ. Hung., 54, 3, pp. 95–107.
- Mindszenty, A., B. D'Argenio 1987: Bauxites of the Northern Calcareous Alps and the Transdanubian Central Range: A comparative estimate. – Rend. Soc. Geol. It., 9 (1986) pp. 269–276.
- Siegl-Farkas, Á. 1983: Palynology of the Senonian Formations at Magyarpolány. – Őslénytani viták (Discussiones Palaeontologicae), 29, pp. 59–69.
- Siegl-Farkas, Á. 1986: Palynostratigraphy of the Senonian from borehole Bácsalmás-1 (S Great Hungarian Plain). – MÁFI Évi Jel. az 1984. évről, pp. 429–459.
- Siegl-Farkas, Á. 1989: Palynostratigraphical boundary between the Santonian–Campanian and the Campanian–Maastrichtian in Hungary. – XIV. Congress CBGA, Sofia, pp. 775–778.
- Szantner, F. et al. 1986: Bauxitprognózis. A karsztbauxitok prognózisának tudományos alapjai és gyakorlati megvalósítása (Bauxite prognostics. Scientific bases and practical realization of karst bauxite prognostics). – Veszprém Committee of Hungarian Academy of Sciences.

Stratigraphical position of the bauxite deposits in the Pădurea Craiului Mountains (Northern Apuseni Mountains)

Sever Bordea, Gheorg Mantea

Geological and Geophysical Institute, Bucarest

The bauxite deposits of the Padurea Craiului Mountains (NW Romania) are exclusively trapped in the calcareous rocks forming the Bihor Platform. These rocks, mostly attributed to the Late Jurassic, belong to the Bihor Unit and the Vălani Nappe. This latter forms the base of the Codru Nappe system.

We give a lithologic, biostratigraphic and structural description of the footwall and hanging wall of the bauxites. The footwall is made up entirely of Late Jurassic carbonates. As a result of the Late-Kimmerian movements (corresponding to the "Wealdian event") the Pădurea Craiului Mountains was uplifted above sea level and was carved by paleokarst. This karst formed the traps for the bauxite minerals.

The Early Cretaceous rocks forming the cover of the bauxite are equally constituted by carbonates. They were deposited in a lacustrine, then marine environment. The marine formations were formed in a back-reef facies.

Key words: Bauxite, Late Jurassic, Bihor Unit, Vălani Nappe, Codru Nappe system

Introduction

The bauxite deposits of Romania are located in some of the structural units which build up the Apuseni Mountains, i.e. in the Bihor Unit (Padurea Craiului Mts and Vladeasa-Bihor Mts) and in the Vălani Nappe member of the Codru Nappes System, moreover the Southern Carpathians; in the Pui-Ohaba-Ponor zone of the Getic Domain (Fig. 1).

The Apuseni Mountains which comprise the Padurea Craiului Mts as well belong as a whole to the internids. Their main structure forming orogeny took place during the Upper Cretaceous. In contrast to other segments of the Carpathian arc, that is to the East Carpathians and to the Southern Carpathians, these mountains are fringing as an the Transylvanian Depression to the west.

The majority of the bauxite deposits is bound to the Bihor unit while some of them appear in the sequence of the Vălani Nappe.

The bauxite occurrences of Pădurea Craiului Mountains have been known since the early 20th century, but detailed study of them had been performed in the last 25 years.

Address: S. Bordea, G. Mantea: Str. Caransebes 1. Sector 1 Cod. 78344 Bucuresti-32, Rumania

Received: 1 September, 1991.

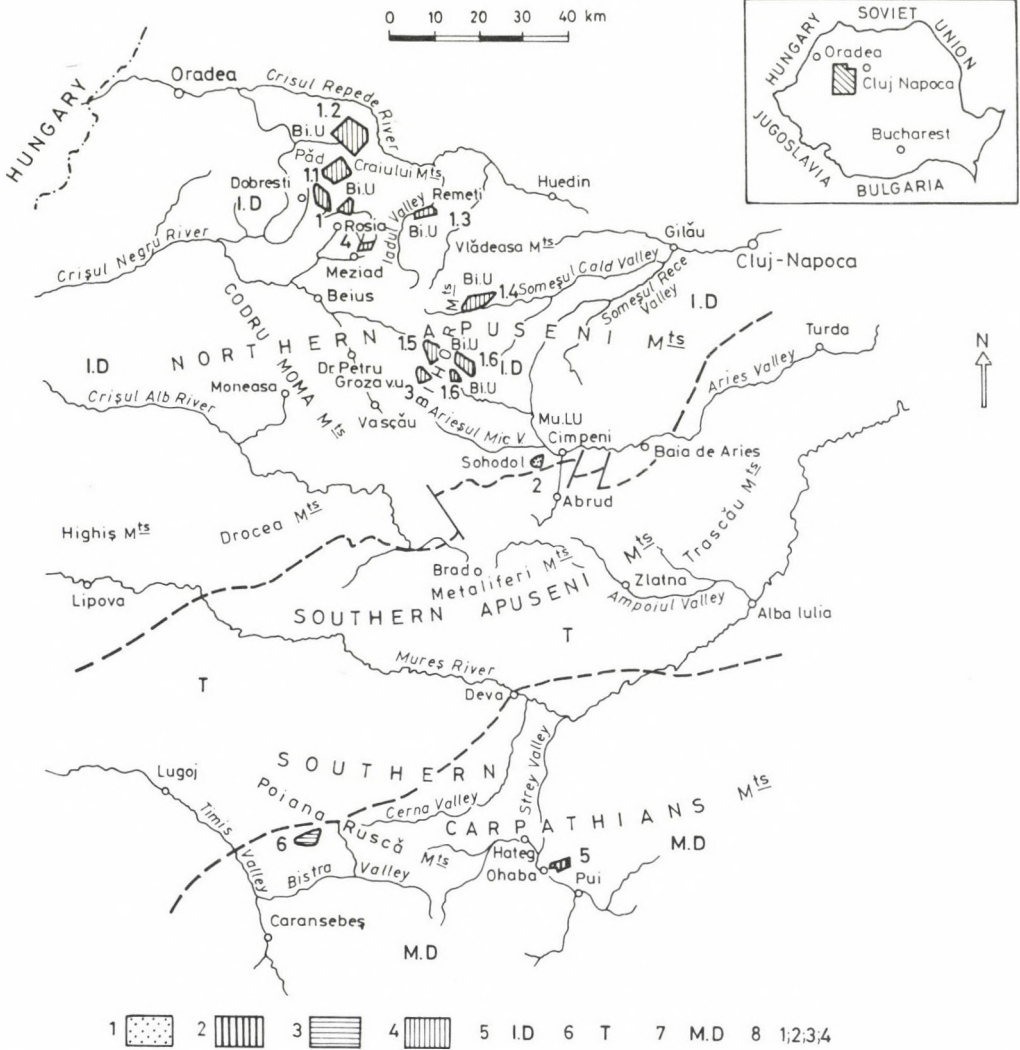


Fig. 1
 Distribution of the bauxite-bearing horizons in Romania. 1. Neocomian bauxites; 2. Lower Cretaceous (Albian?) bauxites; 3. Albian bauxites; 4. Santonian bauxites; I.D. – Internal Dacides; Bi. U. – Bihor Unit; V – Văłani Nappe; MuL – Muncelu Lupsa Nappe); T – Transylvanides; M.D. – Median Dacides

With the exception of Pătrulius and Iosof (1974) and Dragastan et al. (1988) the researchers put all bauxites in the Neocomian (Sanovici et al. 1976; Bordea 1987; Mantea 1985; Dragastan et al. 1982). According to the opinion of Patrulius, besides the Neocomian bauxites, known from the surface, from boreholes and from mining

in operations as well, it is possible to find other bauxite horizons too an intra-Tithonian one and an intra-Barremian one. According to the opinion of Dragastan et al. (1988) the first generation of bauxites appears in the Tithonian, while the last one occurs between Barremian limestones forming their bedrock and the Bedoulian Gugu Breccia in their hanging wall. It is very important to mention that both of the authors are paleontologists and their opinion is necessary to be taken with certain reserve.

In the Bihor unit, the bedrocks of the bauxite deposits show differences from south to north. To illustrate these changes of facies we present three stratigraphical columns (Fig. 2, columns S, C, N) showing the lithological, biostratigraphical and structural characteristics of the rocks constituting the bedrock sequence and the cover of the bauxites. The establishment of these stratigraphical columns is based on surface investigations correlated with data obtained from boreholes and mines.

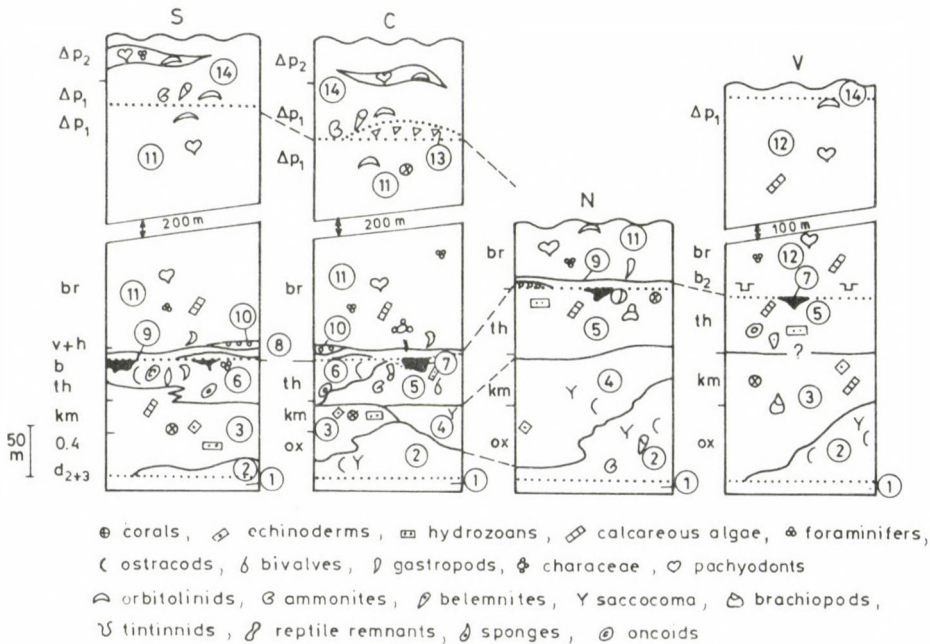


Fig. 2. Stratigraphical columns of the Bihor Unit (S – southern part; C – central part, N – northern part) and the Vălni Nappe (V). 1. Pre Middle-Callovia formations; 2. Vad Lm.; 3. Farcu Lm.; 4. Gălășeni Lm.; 5. Cornet Lm.; 6. Albioara Lm.; 7. bauxites; 8. Rivularia theodori-bearing micrites; 9. Characeae-bearing Lm.; 10. Tiny gastropods-bearing Lm.; 11. Pachyodonts-bearing lower Lm.; 12. Pachyodont-bearing Lm.; 13. Gugu breccia; 14. Ecleja Fm.

Bauxite deposits of the Pădurea Craiului Mts

In the Pădurea Craiului Mountains the bauxite deposits are located in three main areas in its southern part, in the central and in the northern part.

Southern part

The southern part, comprises the Lunca Sprice-Răcas, Sclavu (Fig. 3); Pleș-Vida and Roșia-Albioara zones, where the bauxite deposits are in stage of exploitation today. The stratigraphic succession for all these zones is represented in Fig. 2, column S.

The lowermost stratigraphic horizon of the bedrock complex is represented by the Vad Limestone. This formation can be found in the northern limb of the zone (Albioara) only where it appears in restricted areas having reduced thickness (10 m); southwards the Vad Limestone is missing (see the drillings which do not meet this limestone) and it is substituted by the Farcu Limestone.

The Vad Limestone of the Albioara zone is represented by pelmicrite-packstone type texture with small oncoids and seldom glauconite grains. It is dark coloured, well stratified limestone which contains fragments of echinoderms and small bivalves. This limestone is of Middle Callovian–Oxfordian age and represents lagoonal sedimentation.

The thickness of the Farcu Limestone, well developed in the south of the Pădurea Craiului Mts is about 35–60 m. It is neither overlain by the Albioara Limestone nor covered directly by bauxites. This fact suggests that the denudation at the end of Jurassic was strong that sometimes the Albioara Limestone has been entirely removed.

The Farcu Limestone is a perireefal limestone built up by colonial organisms. It is massive, light coloured, medium-grained, similar to the Stramberg facies. As to its microfacies, pelsparites (grainstones) containing sparse bioclasts and biomicrites (calcarenites) of packstone and wackestone type are characteristic. The fossil content is represented by remnants of echinoderms (*Plegiocidaris cervicalis*), solitary and colonial corals, incorporated frequently in patch-reefs, incrustant (Spongiomorfidae) or branchy hydrozoans, shells of bivalves, nerineids, bryozoans, brachiopods, foraminifers, calcareous algae (*Salpingoporella pygmaea*, *Cayeuxia* sp. etc.). Usually, the transition between this type of limestone and the upper member (Albioara Limestone) is gradual, even lateral transitions can be found too (Fig. 2, column S). The Farcu Limestone is of Middle Callovian–Tithonian age.

The Albioara Limestone has a considerable extension. It covers the whole southern part of the Pădurea Craiului. It is build up by dark gray limestones of micrite, pelmicrite, calcarenite, of (mudstone, packstone and wackestone) texture. The presence of oncoids amounting sometimes up to 40% of the mass of the rock is the main characteristic of this limestone. Networks of *Bacinella*, or bivalve fragments in the core of the oncoids are common. The Albioara Limestone is well-stratified and contains foraminifers (*Parurgonia caeliensis*, *textulariids*),

INTERNAL DACIDES
NORTHERN APUSENI M^{ts} - BIHOR UNIT

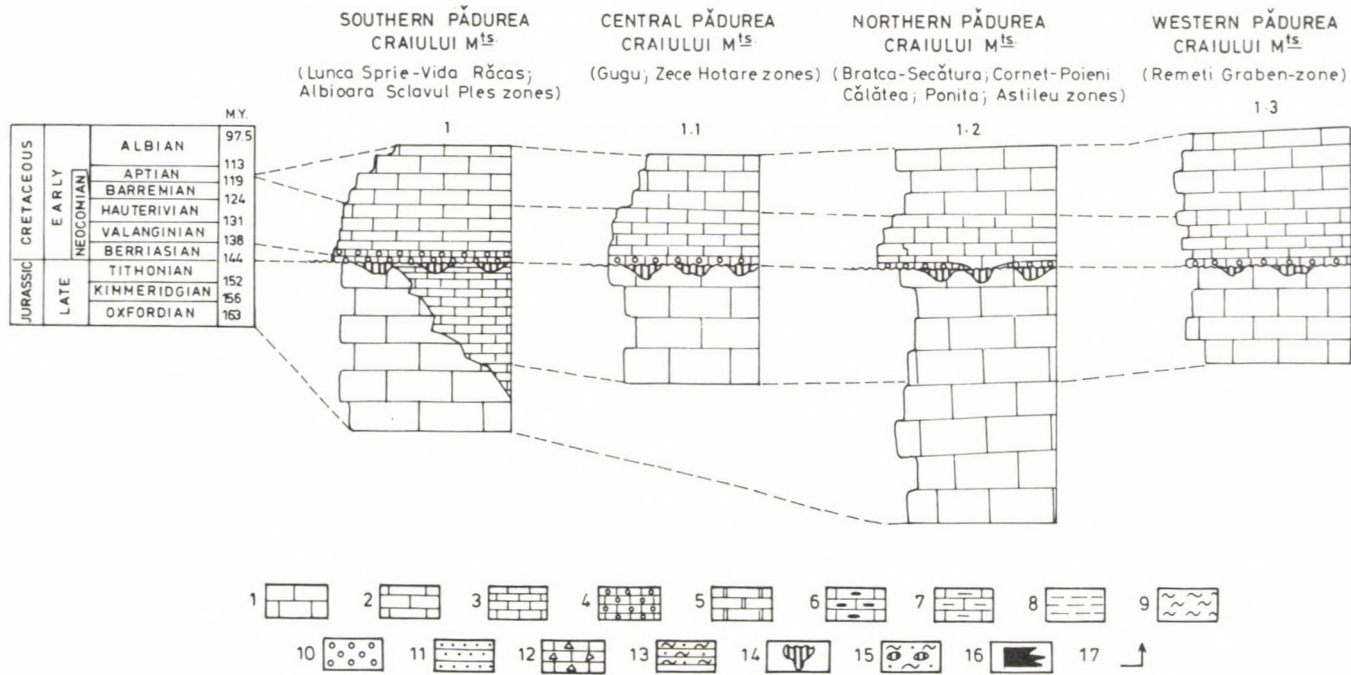


Fig. 3
Stratigraphic position of the bauxite deposits of Rumania, Internal Dacides, Northern Apuseni Mt.-Bihor Unit. 1. reefal limestones; 2. limestones of back-reef facies; 3. stratified limestones ("lagoon facies"); 4. limestones of lacustrine facies; 5. dolomites and calcareous dolomites; 6. siliceous components-bearing limestones; 7. marly limestones; 8. marls; 9. shales; 10. conglomerates; 11. sandstones; 12. calcareous breccias; 13. shaly-sandy flysch alternating with wildflysch episodes; 14. bauxite bodies; 15. detrito-chemical-bauxitiferous formation; 16. coals; 17. estimated duration of exposure

II. INTERNAL DACIDES
 VLĂDEASA - BIHOR M^{ts}, BIHOR UNIT

SOUTHERN BIHOR M^{ts}.
 MUNCELU LUPȘA NAPPE

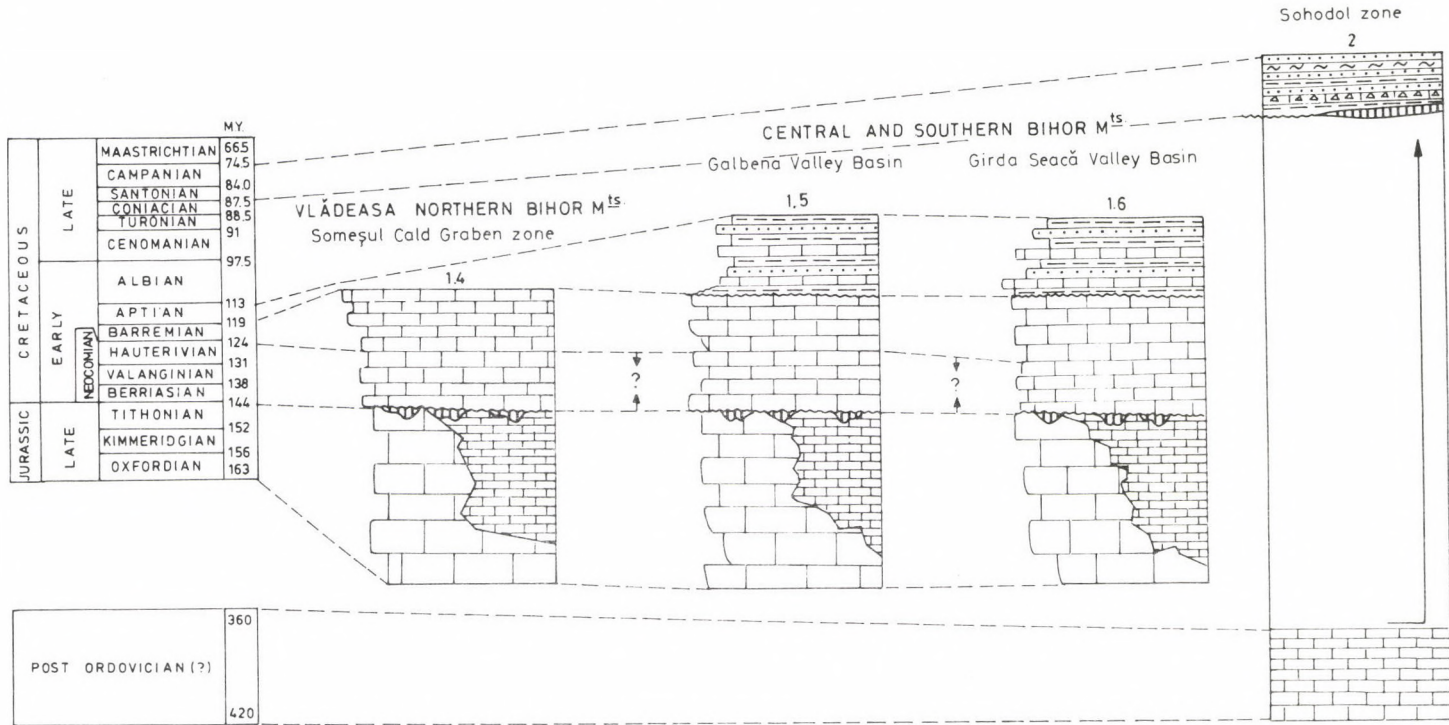


Fig. 4
 Stratigraphic position of the bauxite deposits of Rumania, Internal Dacides Vlădeasa-Bihor Mts, Bihor Unit. (For legend see Fig. 3)

ostracods, richly ornamented gastropods (*Nerinea* sp.), calcareous algae (*Conicospirulina basiliensis*, *Salpingoporella pygmaea*) etc.. Based on the occurrence of *Salpingoporella grudii* and *Heteroporella ancii* found in the lower part of the Albioara Limestone it can be put into the Kimmeridgian (Dragastan et al. 1988), whereas the upper part of it can be placed in the Tithonian stage. The microfacies of the Albioara Limestone indicates a low-energy lagoon facies. The thickness of Albioara Limestone is estimated as being between 35 and 70 m.

The bauxites appear at the base of the Cretaceous cycle. At the end of the Jurassic the New Kimmerian movements led to the emersion of the territory comprising the Bihor Carbonate Platform. This platform has been affected by positive eustatic movements as well as disjunctive accidents. On the surface of the Upper Jurassic paleokarst bauxite deposits have been formed. The bauxites are mainly of diasporic-hematitic, rarely boehmitic composition, they are massive and red in colour. Formed by special influence of Laramian magmatites, sometimes black bauxites appear as well. The bauxite lenses have 10–150 m in diameter and 5 m in thickness. The stratigraphic interval during which the bauxite deposits have been accumulated is Lower Berriasian age. The bauxites are covered discontinuously by *Rivularia theodori*-bearing micritic limestones (Dragastan et al. 1988) which are assigned to Valanginian stage.

The Characeae-bearing limestone is the first member of the hanging wall series of the bauxites. It consists of dark grey micrites and pelmicrites (mudstone and packstone) containing small gastropods and ostracods and Charophytae (*Atopochara trivalvi*, *Porochara* sp. etc). The limestone member of 1–4 m thickness represents a lacustrine facies. It is considered of Hauterivian (Dragastan et al. 1967; Ianovici et al. 1976) or Lower Barremian age (Dragastan et al. 1988).

The Characeae-bearing limestone is overlain discontinuously by limestone beds containing tiny gastropods representing brackish-water facies of Lower Cretaceous age. The thickness of this member is 2–4 m.

The Pachyodont-bearing limestone member constitutes the bulk of the hanging wall series the bauxite deposits. This Urgonian limestone of back-reef facies consists of light coloured, stratified micrites and pelmicrites of packstone type, dismicrites characterized by fenestral laminoid fabrics, and rarely calcarenites. In the upper part of sequence bioclastic calcarenites of wackestone type appear. They contain small biohermes of pachyodonts (*Requena minor* is abundant in some places), hydrozoans, gastropods, foraminifers (miliolids, textulariids, etc.), calcareous algae (*Salpingoporella dinarica*, *S. genevensis*, etc.). The thickness of the Pachyodont-bearing limestone member is between 150–500 m. Its age is Hauterivian?–Barremian–Lowest Bedoulian.

The Ecleja Formation consists mainly of dark-grey to blackish marls and argillaceous marls, having numerous thick intercalations (up to 100 m) of grey to dark-grey limestone with textures of intrapelmicrite, grainstone, biocalcarenites of wackestone type, and contains numerous pachyodonts and miliolids associated with calcareous algae.

The Ecleja Formation overlies transgressively the Pachyodont-bearing limestone (Patrulius et al. 1982) and can be assigned to the Bedoulian–Gargasian? interval due to its fossil content (ammonites, belemnites, orbitolinids).

Central Part

The central part of the Pădurea Craiului Mountains includes important commercial bauxite deposits: Zece Hotare, Cornet, Poenita and Poeni (Fig. 3). The stratigraphic succession of these zones is presented in Fig. 2, column C.

The Vad Limestone is similar to its correspondent in the southern part of the Pădurea Craiului Mountains. This facies contains dark grey micrites, pelmicrites and seldom calcarenites. The presence of siliceous components was observed at different levels. This limestone, with a poor fossil content (*Saccocoma* sp., ostracods) has a thickness up to 60 m. The Vad Limestone belongs stratigraphically to the Upper Callovian–Kimmeridgian.

The Gălăşeni Limestone (Oxfordian–Kimmeridgian) is light-grey coloured with bad stratification. Siliceous components are common. The microfacies of Gălăşeni Limestone represented by micrites, pelmicrites, pelsparites and calcarenites containing *Saccocoma* fragments, ostracods and foraminifers. This limestone is considered to represent a coeval facies of the Vad Limestone in its lower part and of the Farcu Limestone in its upper part.

The Farcu Limestone (Oxfordian–Kimmeridgian) is a massive reefal limestone. Its common characteristics are described in Fig. 2, column S. The thickness of this limestone is about 50 m. In the central part of Pădurea Craiului Mts., the main members in the footwall of the bauxite deposits are the Albioara Limestone and the Cornet Limestone. The latter covers or laterally substitutes the first one.

The Cornet Limestone is a typical representant of the Stramberg facies. It is light coloured, massive, and the presence of patch-reef features is remarkable. The Cornet Limestone has bioclastic texture with coarse grains and a fine matrix (packstone), with scanty sparitic cement. From biostratigraphical point of view corals, hydrozoans (*Ellipsactinia*), sponges, echinoderms (*Plegiocidaris cervicalis*, *P. blumenbachi*), bivalves, gastropods, bryozoans (*Neopleura*), plenty of brachiopods, few ammonites (*Neoglochiceras pseudocharachteis*) and calcareous algae (*Clypeina jurassica*) are worth to mention. The ammonite found at the base of a bauxite lens indicates a Lower–Middle Tithonian age. Without taking into account the large-scale denudation, many researchers thought that the upper part of the Cornet Limestone belongs to the Middle Tithonian. Based on this erroneous idea they put forward a hypothesis on the existence of an intra-Tithonian bauxite horizon.

The first deposits of the Cretaceous cycle are represented by the bauxites which have the same stratigraphic position like those in the southern part of Pădurea Craiului. In the Cornet zone the following succession of bauxite generations can be distinguished (Patrulius et al. 1979): a) massive arenitic-detrital, stratified bauxite which is under exploitation today; b) pelitomorphous or detrital, stratified bauxite which fills lateral cavities formed subsequent to the massive bauxite, and

contains reptile remnants (Thelessosauridae, Coelosauridae, Carnosauridae and Iguanodontidae (Jurcsák, in Patručius et al. 1979)). The presence of the reptile bones indicates the existence of a plain karst and a tropical climate.

The *Rivularia theodori*-bearing micritic limestone, the *Characeae*-bearing limestone and the tiny gastropod-bearing limestone members have the same characteristics as those described in the southern part of the Pădurea Craiului Mountains. The pachyodont-bearing limestone is well developed. In the Ponita zone it has a thickness of 400 m. In the lower part of the sequence micrites with fenestral laminoid fabrics appear (Patručius et al. 1977); in the middle part of it the limestones are relatively coarse-grained and contain Codiacean algae (*Boueina*), Dasycladacean algae (*Salpingoporella genevensis*, *Cylindroporella* sp.), foraminifers (*Trocholina alpina*, miliolids, lituolidae) corals, brachiopods, gastropods, crinoids. The upper part of this limestone is built up by calcarenites and calcirudites of grainstone type. It contains orbitolinids (*Palorbitolina*, *Orbitolinopsis*), miliolids, corals, gastropods, pachyodonts, echinoderms and calcareous algae (*Salpingoporella genevensis*).

The pachyodont-bearing limestone alternates with the Gugu Breccia and is overlain transgressively by it. It is built up by Barremian limestone clasts and blocks of *Characeae*-bearing limestone, Tithonian limestone of Cornet type and bauxite. The diameter of these clasts is variable (3–100 cm). The Gugu Breccia may reach the thickness about 10 m. Stratigraphically it belongs to the Bedoulian substage.

The Ecleja Formation contains mainly dark-grey marls, limy marls and grey to blackish packstone occurring in intercalations. At the base of this formation ammonites and belemnites have been found indicating its Upper Bedoulian–Gargasian age. The Ecleja Formation overlies unconformably and transgressively either the pachyodont-bearing limestone (at different levels), or the Gugu Breccia. The thickness of this formation is 20 m in the east and 600 m in the west.

Northern part

The northern part of the Pădurea Craiului Mts. comprises the Ana and Secatura zones, where the bauxite deposits are under exploitation today (Fig. 3). The stratigraphic successions of these zones are presented in Fig. 2, column N.

The Vad Limestone occupying extensive areas, in this part of the mountains reaches maximum 120 m in thickness. At the base of this formation, marly limestones appear, succeeded by light-grey limestones with rare ferriferous ooids and siliceous nodules. These limestones contain a rich fauna of in Oxfordian ammonites. The middle part of the succession is built up by dark micrites and pelmicrites. Silicious components are common. They contain *Tubiphytes* sp., *Saccocoma* sp. In the upper part of the Vad Limestone dark-grey pelmicrites and pelsparites of packstone type are predominant containing *Saccocoma* sp., ostracods, belemnites, echinoderm remnants. The age of the Vad Limestone is Middle Callovian–Kimmeridgian.

The Gălăşeni Limestone has a thickness between 40 and 130 m. It overlies and substitutes a part of the Vad Limestone (see Fig. 2, column N). The Gălăşeni Limestone is stratified light grey, sometimes with siliceous components. Characteristic microfacies are by pelmicrites, pelsparites with small oncoids, micrites and even calcarenites. In the central part of the sequence *Saccocoma* sp., ostracods and foraminifers are frequent. The Gălăşeni Limestone belongs to the Oxfordian–Kimmeridgian.

The last Upper Jurassic member, the Cornet Limestone is similar to that which occurs in the central part of the Pădurea Craiului Mts. In the upper part of this limestone the abundance of *Clypeina jurassica* and *Actinoporella podolica* is to be mentioned. The bauxites and the Characeae-bearing limestone present the same characteristics and stratigraphic position as their correspondents elsewhere in the Pădurea Craiului. The tiny gastropods-bearing limestone can be found only sporadically.

The pachyodont-bearing limestone has been removed almost completely by erosion; it shows common features with its correspondent in the central part of the Pădurea Craiului Mountains.

Vălani Nappe

This structural unit belongs to the Codru Nappes System which has been defined by Patruşiu (1971) in the central and southern part of the Pădurea Craiului Mts. Its excellent outcrops appear in two tectonic windows (Peştera and Meziad) in the Strîmtura Valley (Rosia zone) (Fig. 5).

Referring to the synthetical stratigraphical column (Fig. 2, column V) some similarities between the Bihor Unit and the Vălani Nappe are obvious. The bedrock of the bauxite deposits is the Gresten Formation which is overlain by Saccocoma-bearing grey to dark-grey well stratified pelsparites and pelmicrites of packstone type reaching thickness of 35 m. This limestone can be considered as a possible equivalent of the Vad Limestone. Its fossil content is represented by foraminifers, ostracods, echinoderm fragments. Saccocoma fragments can be found in the upper part. In the Strîmtura Valley these limestones are substituted gradually by reefal, massive, white–light-grey bioclastic limestones of 30–180 m thick with biomicrite, pelmicrite and calcarenite (wackestone). They have the same texture and fossil content as Farcu and Cornet Limestones. The age of the bauxites is probably Lower Berriasian because the Lower Cretaceous marine carbonate sequence begins with Calpionellidae-bearing dismicrites and pelmicrites representing the Berriasian substage near Cabesti (G. Pop, verbal communication). The main characteristics of these bauxites were described by Papiu et al. (1981).

The Early Cretaceous limestones in the hanging wall of the bauxite deposits are represented only by the pachyodont-bearing limestone member. It has a thickness of about 200 m and belongs to the Berriasian–Middle Bedoulian substages. At the base of the Cretaceous succession the absence of the Characeae-bearing limestone and of the tiny gastropods-bearing limestone members are worth to mention.

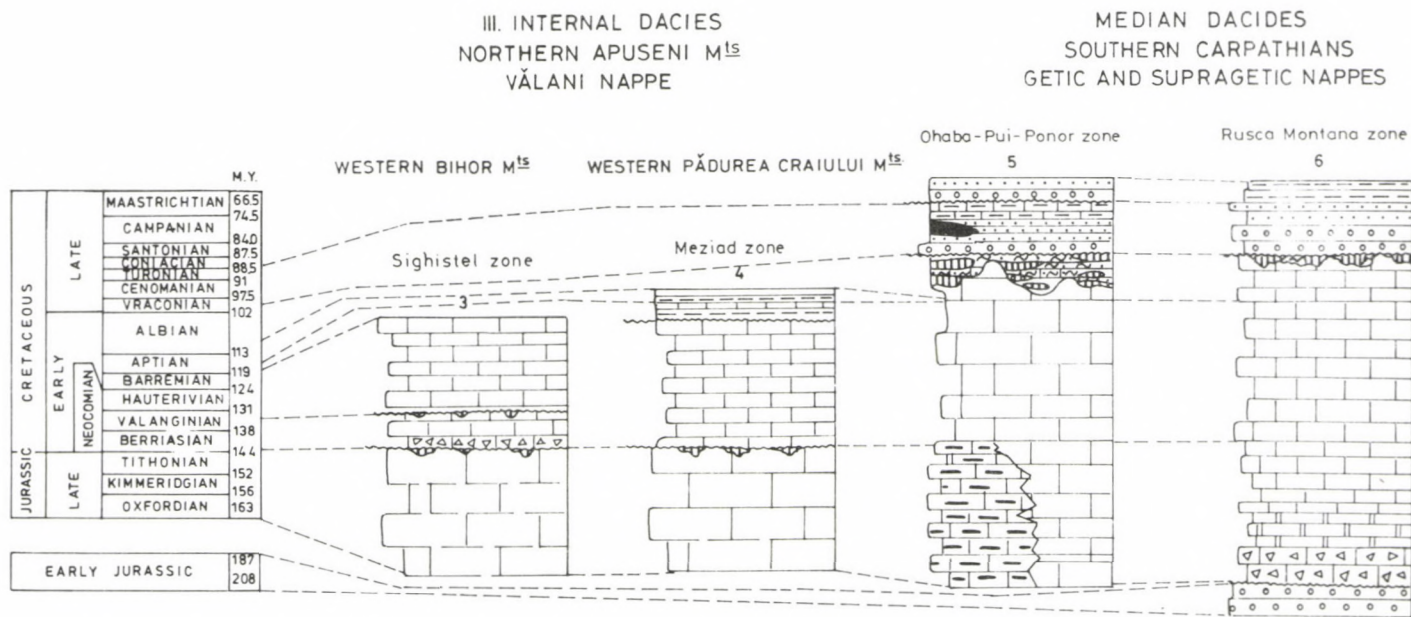


Fig. 5
Stratigraphic position of the bauxite deposits of Rumania, Internal Dacides, Northern Apuseni Mts, Văłani Nappe and Median Dacides, Southern Carpathians Getic and Supragetic nappes. (For legend see Fig. 3)

The pachyodont-bearing limestone has the same lithological biostratigraphical and structural characteristics as in other parts of the Pădurea Craiului Mts.

The Ecleja Formation represents the detrital equivalent of its correspondent in the central part of Pădurea Craiului.

Conclusions

In the Bihor Unit and the southern part of the Pădurea Mts, the Upper Callovian–Kimmeridgian carbonate deposits forming the footwall of bauxite ores are developed in reefal facies; in the central part this facies is replaced by a deep water one (Vad Limestone). With exception of the southern margin where the reefal facies appears again; in the northern part of the Pădurea Craiului Mts only the deep water facies occurs except of excepting some regions where the upper part of the Kimmeridgian is represented by a reefal facies. This fact reflects an effect of the sedimentological evolution of the Bihor Carbonate Platform. At the beginning of the Tithonian in the southern part of the Pădurea Craiului Mts a lagoon was formed (Albioara Limestone), which in the central and northern zones passes into typical reefal facies – the Stramberg facies (Cornet Limestone).

Subsequent to the uplift of the Bihor Carbonate Platform and the formation of bauxites the sedimentogenetic processes were controlled by slow subsidence and transgression. At the beginning of the Cretaceous cycle lacustrine facies (*Rivularia theodori*-bearing micrites and Characeae-bearing limestone) and then a brackish facies (tiny gastropods-bearing limestone) appeared. During the Barremian the sea covered entirely the Bihor Carbonate Platform and backreef facies developed. In the Bedoulian the evolution of this platform came to an end and neritic-pelagic facies (Ecleja Fm.) became stable in the whole region.

In the Vălani Nappe the reefal facies became widespread except the western areas where the facies characteristic of the Vad Limestone were preserved in the Upper Callovian–Lower Kimmeridgian interval too. In the Tithonian only a reefal facies (Cornet Limestone – of Stramberg type) was developed. After the bauxite accumulation the sedimentogenesis started directly with a basinal facies (Calpionellidae-bearing limestones) and succeeded by a back-reef type marine facies.

The carbonate formations which constitute the footwall of the bauxites belong to the upper part of the Upper Tithonian *Clypeina jurassica* biozone.

The oldest formations belonging to the hanging wall of the bauxites represent the Berriasian both in the Bihor Unit and in the Vălani Nappe.

Due to an intensive erosion at the end of the Upper Jurassic, the bauxites rest on diverse Upper Jurassic lithostratigraphical units (Vad Lm., Gălășeni Lm., Farcu Lm., Albioara Lm., Cornet Lm.).

In the central part of the Pădurea Craiului Mts several successive bauxite types can be identified which have been formed during the Berriasian.

Table 1

Bauxite ores of the Southern Padurea Craiului Mountains (Lunca Sprie-Vida-Răcaș zones; Albioara-Sclavul Pleș zones)

1. Geotectonic location at the time of bauxite accumulation	Northern (European) margin of Tethyan realm; Internal Dacides, Bihor Unit
2. Processes bringing a subaerial exposure of the carbonatic substratum	Eustatic > tectonic control
3. Imprints in the stratigraphic record	Weak to moderate; moderate to large bauxitiferous unconformity with prevailing paleokarst; weak non-bauxitic unconformity between bedrock and cover
4. Estimated duration of exposure	3-5 My
5. Apparent stratigraphic gap	Small to moderate
6. Rate of regional subsidence	Moderate
7. Changes in lithofacies of associated rocks across the unconformity	Clearly changes
8. Lithofacies of associated bauxites	Autochthonous
9. Underlying karst relief	Shallow moderate; moderate to high
10. Supposed source material of bauxites	Crystalline rocks of the Gilau Massif
11. Supposed source material of non-bauxitic karst fills	Lower Jurassic detritic rocks - Bihor Unit; Quaternary deposits
12. Lithology, size and shape of bauxite deposits	Homogeneous, ore bodies are small to moderate, in form as lenses of Aston or Caguanes type
13. Bauxite texture	Mostly ooidic, rarely pelitomorphic
14. Bauxite structure	Massive
15. Chemical composition of bauxites (%)	Al ₂ O ₃ : 61-64; SiO ₂ : 2.6-3.2; Fe ₂ O ₃ + FeO: 21.5-22; TiO ₂ : 2.5-3.1
16. Mineral composition of bauxites (%)	Diaspore: 62-68; Boehmite: less than 5; Hematite: 18-22; Kaolinite: 5-7.5; Goethite: 3-6; Leptochlorite: less than 1
17. Accessory minerals from bauxites (%)	Magnetite: less than 1; Anatase: 2.4-3.1
18. Trace elements in the bauxites (ppm.)	No data
19. Type of ore; age	Karst bauxites, residuale; Lower Berriasian
20. Bedrock petrography, main biostratigraphical data, age	Limestones; corals hydrozoans, echinoderms (<i>Plegiocidaris cervicalis</i>), gastropods, foraminifers, calcareous algae (<i>Clypeina jurassica</i> , <i>Salpingoporella pygmaea</i>), ostracods, bivalves; Oxfordian-Tithonian
21. Cover petrography, main biostratigraphical data, age	Limestones, characeae, ostracods, gastropods, bivalves (<i>Requenia minor</i>), corals, foraminifers (miliolids, orbitolinids), calcareous algae (<i>Salpingoporella dinarica</i> , <i>S. genevensis</i> , <i>Actinoporella podolica</i> etc.); Lower Valanginian-Lower Aptian

Table 1.1
Bauxite ores of the Central Pădurea Craiului Mountains (Gugu; Zece Hotare zones)

1. Geotectonic location at the time of bauxite accumulation	Northern (European) margin of the Tethyan realm; Internal Dacides – Bihor Unit
2. Processes bringing a subaerial exposure of the carbonatic substratum	Eustatic > tectonic control; tectonic control
3. Imprints in the stratigraphic record	Weak-moderate to large bauxitiferous unconformity with prevailing paleokarst; weak non-bauxitic unconformity between bedrock and cover
4. Estimated duration of exposure	3–5 My
5. Apparent stratigraphic gap	Small to moderate
6. Rate of regional subsidence	Moderate
7. Changes in lithofacies of associated rocks across the unconformity	Clearly changes
8. Lithofacies of associated bauxites	Autochthonous
9. Underlying karst relief	Shallow moderate; moderate to high
10. Supposed source material of bauxites	Crystalline rocks of the Gilau Massif
11. Supposed source material of non-bauxitic karst fills	Lower Jurassic detritic rocks; Aptian detritic rocks (Ecleja Formation); Quaternary deposits
12. Lithology, size and shape of bauxite deposits	Homogeneous, ore bodies are small to moderate, in form as lenses of Aston or Caguanes type
13. Bauxite texture	Mostly ooidic, rarely pelitomorphitic
14. Bauxite structure	Massive
15. Chemical composition of bauxites (%)	Al ₂ O ₃ : 51.4–68.5; SiO ₂ : 2.0–8.75; Fe ₂ O ₃ + FeO: 7.7–30.8; TiO ₂ : about 3
16. Mineral composition of bauxites (%)	Diaspore: up to 67; Boehmite: up to 76; Hematite: 1.5–29.5; Kaolinite: 4–17; Goethite: less than 8; Magnetite: less than 1; Leptochlorite: less than 17
17. Accessory minerals from bauxites (%)	Anatase: about 3
18. Trace elements in the bauxites (ppm)	No data
19. Type of ore; age	Karst bauxites, residuale; Lower Berriasian
20. Bedrock petrography, main biostratigraphical data, age	Reefal limestones (of Stramberg facies); corals hydrozoans, calcareous sponges, echinoderms (<i>Plegiocidaris cervicalis</i> , <i>P. blumenbachi</i> , <i>Rhabdocidaris cepeoides</i> , <i>Balanocrinus subteres</i> etc.) gastropods, bivalves, bryozoans, belemnites, calcareous algae (<i>Clypeina jurassica</i>); Tithonian
21. Cover petrography, main biostratigraphical data, age	Limestones; characeae, ostracods, gastropods, foraminifers (Miliolids, orbitolinids), calcareous algae (<i>Salpingoporella dinarica</i> , <i>S. genevensis</i> etc.); Lower Valanginian–Lower Aptian

Table 1.2

Northern Pădurea Craiului Mountains (Bratca–Secătura zone; Cornet–Poieni zone; Călășea zone; Ponjta zone; Aștileu zone)

1. Geotectonic location at the time of bauxite accumulation	Northern margin (European) of the Tethyan realm; Internal Dacides–Bihor Unit
2. Processes bringing a subaerial exposure of the carbonatic substratum	Eustatic > tectonic control; tectonic control
3. Imprints in the stratigraphic record	Weak-moderate to large bauxitiferous unconformity with prevailing paleokarst; moderate non-bauxitic unconformity between bedrock and cover
4. Estimated duration of exposure	3–5 My
5. Apparent stratigraphic gap	Small to moderate
6. Rate of regional subsidence	Moderate
7. Changes in lithofacies of associated rocks across the unconformity	Clearly changes
8. Lithofacies of associated bauxites	Autochthonous
9. Underlying karst relief	Shallow moderate; moderate to high
10. Supposed source material of bauxites	Crystalline rocks of the Gilau Massif
11. Supposed source material of non-bauxitic karst fills	Lower Jurassic detritic rocks; Quaternary deposits
12. Lithology, size and shape of bauxite deposits	Homogeneous, ore bodies are generally moderate, in form as lenses of Aston or Caguanes type
13. Bauxite texture	Mostly ooidic, rarely pelitomorphitic
14. Bauxite structure	Massive
15. Cemical composition of bauxites (%)	Al ₂ O ₃ : 50–61; SiO ₂ : 2.6–9.2; Fe ₂ O ₃ : 15–28; TiO ₂ : 2.5–3
16. Mineral composition of bauxites (%)	Diaspore: 52–78; Boehmite: 8.5–9; Hematite: 6–30; Kaolinite: 4–18; Goethite: 0.13–12.7
17. Accessory minerals from bauxites (%)	Anatase: 2.5–3.8; Magnetite: less than 1
18. Trace elements in the bauxites (ppm)	Ga: 31–65; Sn: 8.5–26; Ni: 130–370; Co: 20–89; Cr: 286–1000; V: 222–360; Sr: 46–262; Nb: 60; Be: 9–18; Cu: 1000–1300; Zn: 201; Ba: 33; Li: 61; Zr: 800; Mg: 1111; Mn: 731
19. Type of ore; age	Karst bauxites residuale; Lower Berriasian
20. Bedrock petrography, main biostratigraphical data, age	Limestones; bivalves, corals, echinoderms (<i>Plegiocidaris cervicalis</i> , <i>P. blumenbachi</i> etc.), gastropods, brachiopods, ammonites (<i>Neoglochiceras pseudocarachteis</i> etc.), belemnites, calcareous algae: <i>Clypeina jurassica</i> ; Oxfordian–Tithonian
21. Cover petrography, main biostratigraphical data, age	Limestones: characeae, ostracods, gastropods, corals, foraminifers (miliolods, orbitolids), calcareous algae (<i>Salpingoporella dinarica</i> , <i>S. genevensis</i> , <i>Actinoporella podolica</i> etc.); Lower Valanginian–Lower Aptian

Table 1.3
Eastern Pădurea Craiului Mountains (Remeti Graben zone)

1. Geotectonic location at the time of bauxite accumulation	Northern (European) margin of the Tethyan realm; Internal Dacides, Bihor Unit
2. Processes bringing a subaerial exposure of the carbonatic substratum	Eustatic > tectonic control; tectonic control
3. Imprints in the stratigraphic record	Weak to moderate bauxitiferous unconformity with prevailing paleokarst; weak to moderate non-bauxitic unconformity between bedrock and cover
4. Estimated duration of exposure	3–5 Ma
5. Apparent stratigraphic gap	Small to moderate
6. Rate of regional subsidence	Moderate
7. Changes in lithofacies of associated rocks across the unconformity	Clearly changes
8. Lithofacies of associated bauxites	Autochthonous
9. Underlying karst relief	Shallow moderate; moderate to high
10. Supposed source material of bauxites	Crystalline rocks of the Gilau Massif
11. Supposed source material of non-bauxitic karst fills	Lower Jurassic detritic rocks; Quaternary deposits
12. Lithology, size and shape of bauxite deposits	Homogeneous, partially thermal- meta- morphosed, ore bodies are small to moderate, in form as lenses of Aston or Caganues type
13. Bauxite texture	Mostly ooidic
14. Bauxite structure	Massive
15. Chemical composition of bauxites (%)	Al ₂ O ₃ : 45.2–55.1; SiO ₂ : 1.1–7.02 Fe ₂ O ₃ : 20–38; FeO: 1.7–7.5; TiO ₂ : 2.5
16. Mineral composition of bauxites (%)	Diaspore: 50–52; Hematite: 14–36; Kaolinite: 1.6–8; Leptochlorite: 1.6–8;
17. Accessory minerals from bauxites (%)	Anatase: 2.7–3; Magnetite: less than 1
18. Trace elements in the bauxites (ppm)	No data
19. Type of ore; age	Karst bauxites, residuale; Lower Berriasian
20. Bedrock petrography, main biostratigraphical data, age	Limestones; bivalves, gastropods, calcareous sponges, hydrozoans, corals, echinoderms, foraminifers (<i>Trocholina alpina</i> , <i>T. elongata</i> etc.), calcareous algae (<i>Macroporella pygmaea</i> , <i>Cayeuxia moldavica</i> , <i>C. curdistanensis</i>); Tithonian
21. Cover petrography, main biostratigraphical data, age	Limestones: characeae, ostracods, bivalves, gastropods, brachiopods, corals, hydrozoans, foraminifers (miliolids, orbitolinids), calcareous algae (<i>Salpingoporella dinarica</i> , <i>S. turgida</i> , <i>Macroporella verticilata</i> , <i>Clypeina solkani</i> , <i>Bouetia hochsteteri</i>); Lower Valanginian–Lower Aptian

Table 1.4

Bauxite ores of the Vlădasa–Northern Bihor Mts (Someșul Cald Graben zone)

1. Geotectonic location at the time of bauxite accumulation	Northern (European) margin of the Tethyan realm; Internal Dacides, Bihor Unit
2. Processes bringing a subaerial exposure of the carbonatic substratum	Eustatic > tectonic control; tectonic control
3. Imprints in the stratigraphic record	Weak to moderate; moderate to large bauxitiferous unconformity with prevailing paleokarst; weak to moderate non-bauxitic unconformity between bedrock and cover
4. Estimated duration of exposure	3–4 My
5. Apparent stratigraphic gap	Small to moderate
6. Rate of regional subsidence	Moderate
7. Changes in lithofacies of associated rocks across the unconformity	Clearly changes
8. Lithofacies of associated bauxites	Autochthonous
9. Underlying karst relief	Shallow to moderate; moderate to high
10. Supposed source material of bauxites	Crystalline rocks of the Gilau Massif
11. Supposed source material of non-bauxitic karst fills	Silurian, Permian and Triassic detritic rocks – Codru Nappes; Lower Jurassic detritic rocks – Bihor Unit; Quaternary deposits
12. Lithology, size and shape of bauxite deposits	Homogeneous, ore bodies are small to moderate in forms as lenses of Aston or Caguanes type
13. Bauxite texture	Oooidic
14. Bauxite structure	Massive
15. Chemical composition of bauxites (%)	Al ₂ O ₃ : 48.3–55.4; SiO ₂ : 1.3–9.4 Fe ₂ O ₃ : 13.9–26.6; FeO: 0.4–7.8; TiO ₂ : 2.1–3.1
16. Mineral composition of bauxites (%)	Diaspore: 62–68; Hematite: 3.1–26.5; Kaolinite: 0.4–13.2; Goethite: 4.5–24.4
17. Accessory minerals from bauxites (%)	Magnetite: less than 1; Anatase: 2.1–3.1
18. Trace elements in the bauxites (in p.p.m.)	Ni: 116; Co: 18; Cr: 266; V: 350; Sc: 48; Nb: 61; Ga: 61; Sn: 17; Zr: 1463; Be: 7; Cu: 30; Pb: 77; Ba: 52; Sr: 30; Li: 103
19. Type of ore; age	Karst bauxites, residuale; Lower Berriasian
20. Bedrock petrography, main biostratigraphical data, age	Limestones: bivalves, gastropods (Nerineids), brachiopods, echinoderms (<i>Plegiocidaris cervicalis</i>), corals, calcareous sponges, encrusting (Spongiomorphides) or branching (<i>Cladocoropsis</i>) hydrozoans, foraminifers, calcareous algae (<i>Clypeina jurassica</i> , <i>Salpingoporella pygmaea</i>); Oxfordian–Tithonian
21. Cover petrography, main biostratigraphical data, age	Limestones: bivalves, gastropods, bryozoans, calcareous sponges, foraminifers (<i>Orbitolinopsis kiliani</i> , <i>O. simplex</i> , <i>O. lenticularis</i> , <i>O. (Mesorbitolina) lotzei</i> , calcareous algae (<i>Salpingoporella dinarica</i> , <i>S. genevensis</i>); Lower Valanginian– Lower Aptian

Table 1.5
Bauxite ores of the Central Bihar Mts (Galbena Valley Basin)

1. Geotectonic location at the time of bauxite accumulation	Northern (European) margin of the Tethyan realm, Internal Dacides–Bihar Unit
2. Processes bringing a subaerial exposure of the carbonatic substratum	Eustatic > tectonic control; tectonic control
3. Imprints in the stratigraphic record	Weak to moderate; moderate to large bauxitiferous unconformity with prevailing paleokarst; weak to moderate non-bauxitic unconformity between bedrock and cover
4. Estimated duration of exposure	3–4 My
5. Apparent stratigraphic gap	Small to moderate
6. Rate of regional subsidence	Moderate
7. Changes in lithofacies of associated rocks across the unconformity	Clearly changes
8. Lithofacies of associated bauxites	Autochthonous
9. Underlying karst relief	Shallow to moderate; moderate to high
10. Supposed source material of bauxites	Crystalline rocks of the Gilau Massif
11. Supposed source material of non-bauxitic karst fills	Lower Jurassic detritic rocks Bihar Unit; Berriasian, Valanginian, Hauterivian, lower part of Barremian limestones developed under a basinal facies from western Bihar Mts., Quaternary deposits
12. Lithology, size and shape of bauxite deposits	Homogeneous, partially thermic-metamorphosed, ore bodies are small to moderate, in form as lenses of Aston or Caguanes type
13. Bauxite texture	Mostly ooidic; pelitomorphic
14. Bauxite structure	Massive
15. Chemical composition of bauxites (%)	Al ₂ O ₃ : 40.2–61.3; SiO ₂ : 1.05–8.66 Fe ₂ O ₃ : 14.02–43.5; FeO: 0.3–5.5 TiO ₂ : 2.2–3.8
16. Mineral composition of bauxites (%)	Diaspore: 45.7–64.3; Hematite: 2.0–29.6; Kaolinite: 2.5–10.8; Goethite: 8.2–42.3
17. Accessory minerals from bauxites (%)	Anatase: 2.2–3.1; Chlorite: 0.9–15.7; Pyrite: 0.1–0.2
18. Trace elements in the bauxites (ppm)	Ni: 119.5; Co: 19.1; Cr: 322; V: 410; Sc: 45; Nb: 75; Zr: 715; Be: 7; Ga: 46; Sn: 8.8; Mn: 365; Ba: 38; Sr: 14; Pb: 82 Li: 44
19. Type of ore; age	Karst bauxites, residual; Lower Berriasian
20. Bedrock petrography, main biostratigraphical data, age	Limestones, marls, sandstones: bivalves, gastropods, brachiopods, corals, hydrozoans, bryozoans, calcareous sponges, echinoderms (<i>Plectocidaris cervicalis</i>), foraminifers, calcareous algae (<i>Clypeina jurassica</i> , <i>Salpingoporella pygmaea</i>); Oxfordian–Tithonian
21. Cover petrography, main biostratigraphical data, age	Limestones of Urgonian facies, carbonatic breccias associated with bauxitiferous elements – including bauxite lenses, bauxitiferous clays etc. – filling karst cavities; bivalves (<i>Requena minor</i>), gastropods, foraminifers (miliolids, orbitolinids – <i>Paleorbitolina lenticularis</i> , <i>Orbitolina conulus</i> , <i>Orbitolinopsis capuensis</i>), calcareous algae (<i>Salpingoporella dinarica</i> , <i>S. muelhbergii</i> , <i>S. genevensis</i> , <i>Cayeuxia allioti</i> , <i>C. athanasiui</i> , <i>Clypeina solkani</i> , <i>Bacinella irregularis</i>), ammonites (<i>Chelonicerus cornuillianus</i>); Barremian–Aptian

Table 1.6
Bauxite ores of the Southern Bihor Mts (Girda Seaca Valley Basin)

1. Geotectonic location at the time of bauxite accumulation	Northern (European) margin of the Tethyan realm, Internal Dacides, Bihor Unit
2. Processes bringing a subaerial exposure of the carbonatic substratum	Eustatic > tectonic control; tectonic control
3. Imprints in the stratigraphic record	Weak to moderate, moderate to large bauxitiferous unconformity with prevailing paleokarst; weak to moderate non-bauxitic unconformity between bedrock and cover
4. Estimated duration of exposure	3–4 My
5. Apparent stratigraphic gap	Small to moderate
6. Rate of regional subsidence	Moderate
7. Changes in lithofacies of associated rocks across the unconformity	Clearly changes
8. Lithofacies of associated bauxites	Autochthonous
9. Underlying karst relief	Shallow to moderate; moderate to high
10. Supposed source material of bauxites	Crystalline rocks of the Gilau Massif
11. Supposed source material of non-bauxitic karst fills	Lower Jurassic detritic rocks – Bihor Unit; Berriasian, Valanginian, Hauterivian, lower part of Barremian limestones developed under in a basinal facies from western Bihor Mts. – Valani Nappe, Quaternary deposits
12. Lithology, size and shape of bauxite deposits	Homogeneous, ore bodies are small to moderate, in form as lenses of Aston or Caguanes type
13. Bauxite texture	Mostly ooidic
14. Bauxite structure	Massive
15. Chemical composition of bauxites (%)	Al ₂ O ₃ : 47.32–76.59; SiO ₂ : 1.05–10.15; Fe ₂ O ₃ : 1.5–22.8 ; FeO: 0.5–8; TiO ₂ : 2.1–3.9
16. Mineral composition of bauxites (%)	Diaspore: 49.2–90.0; Hematite: 1.2–22.8; Kaolinite: 1–14; Goethite: 2.0–13
17. Accessory minerals from bauxites (%)	Anatase: 2.2–4.6; Chlorite: 1.5–17.8
18. Trace elements in the bauxites (ppm)	Ni: 70; Co: 14.3; Cr: 444; V: 437; Sc: 45; Nb: 52; Zr: 861; Be: 5.5; Ga: 53; Sn: 25; Mn: 290; Ba: 62; Sr: 52; Pb: 103; Cu: 10; Li: 20.8
19. Type of ore; age	Karst bauxites, residual; Lower Berriasian
20. Bedrock petrography, main biostratigraphical data, age	Limestones: bivalves, gastropods, crinoids, brachiopods, corals, hydrozoans, bryozoans, foraminifers (<i>Trocholina alpina</i>), calcareous sponges, calcareous algae (<i>Clypeina jurassica</i> , <i>Salpingoporella pygmaea</i> etc.); Oxfordian–Tithonian
21. Cover petrography, main biostratigraphical data, age	Limestones of Urgonian facies, carbonatic breccias associated with bauxitiferous elements – including bauxite lenses, bauxitic clay etc. – filling karst cavities, bivalves (<i>Requienia minor</i>), gastropods, bryozoans, echionderms, hydrozoans (<i>Chaetetopsis favret</i>), foraminifers (miliolids, trocholines, nodosariids, orbitolinids), calcareous algae (<i>Salpingoporella meliae</i> , <i>S. genevensis</i> , <i>S. dinarica</i> , <i>Cayeuxia ellioti</i> , <i>Bacinella irregularis</i>); the presence of Calpionellidae-bearing carbonatic breccias probably refer to relict formations belonging to a pelagic-planktonic, basinal facies which have been transported from the western part of the Bihor Mts. as consequences of post orogenic movements during the Neocomian interval; Barremian–Lower Aptian

Table 2
Bauxite ores of the southern Bihar Mts (Sohodol zone)

1. Geotectonic location at the time of bauxite accumulation	Northern (European) margin of the Tethyan realm; Internal Dacides Muncel Lupsa Nappe
2. Processes bringing a subaerial exposure of the carbonatic substratum	Eustatic and tectonic control
3. Imprints in the stratigraphic record	Weak to moderate bauxitiferous unconformity with paleokarst; moderate to large non-bauxitic unconformity between bedrock and cover
4. Estimated duration of exposure	Large
5. Apparent stratigraphic gap	
6. Rate of regional subsidence	No; No to weak (for bedrock); moderate to large (for cover)
7. Changes in lithofacies of associated rocks across the unconformity	Major changes
8. Lithofacies of associated bauxites	Allochthonous
9. Underlying karst relief	Shallow; shallow to moderate
10. Supposed source material of bauxites	Crystalline rocks of the Gilau Massif
11. Supposed source material of non-bauxitic karst fills	Crystalline rocks of the Muncel Series; Late Cretaceous deposits; Quaternary deposits
12. Lithology, size and shape of bauxite deposits	Heterogeneous bauxites included into a detrito-chemical bauxitiferous formation; the bauxites appear in form of lenses or often presenting stratiform tendencies at contact with the bedrock
13. Bauxite texture	Ooidic; pelitomorphic, shaly
14. Bauxite structure	Massive; stratified bauxites
15. Chemical composition of bauxites (%)	Al ₂ O ₃ : 33–57; SiO ₂ : 2.5–12; Fe ₂ O ₃ + FeO: 11–26; TiO ₂ : 1.8–2.8 ; CaO: 0.45–28; MgO: 0.15–1.4
16. Mineral composition of bauxites (%)	Boehmite: 45.7–49; Diaspore: 0.76–5.3; Hematite + Goethite: 6–23; Kaolinite: 7–30
17. Accessory minerals from bauxites (%)	Very rare
18. Trace elements in the bauxites (ppm)	Ni: 56–208; Co: 10.5–184; Cr: 57–260; V: 198–302; Mr 840—more than 1000; Be: 7.5–16.5; Zr: 520–940; Sn: 21–50; Cu: less than 4–90; Pb: 58–325; Ga: 41–99; Ba: 20–290; Li: 88–6600; Sr: 274—more than 1000
19. Type of ore; age	Karst bauxites, residuale allochthonous detrito-chemical bauxites; Santonian
20. Bedrock petrography, main biostratigraphical data, age	Marbles; paleontological and paleo-floral content: no evidences; Post-Ordovician
21. Cover petrography, main biostratigraphical data, age	Marls, bioherms-bearing marls and sandy marls, seldom calcareous breccias of Gosau facies; shaly-sandy flysh alternating with wildflysh episods; bivalves (numerous species of <i>Inoceramus</i> , <i>Hippurites</i> , etc.), gastropods, corals, foraminifers (<i>Globotruncana marginata</i> , <i>G. iapparanti iapparanti</i> , <i>G. iapparante tricarinata</i> , <i>G. stuarti</i> , <i>G. fornicata</i> etc.); Santonian–Campanian

Table 3
Bauxite ores of the western Bihor Mts (Sighistel zone)

1. Geotectonic location at the time of bauxite accumulation	Northern (European) margin of the Tethyan realm; Internal Dacides Valani Nappe
2. Processes bringing a subaerial exposure of the carbonatic substratum	Eustatic > tectonic control
3. Imprints in the stratigraphic record	Weak to moderate
4. Estimated duration of exposure	14 My
5. Apparent stratigraphic gap	Weak to moderate
6. Rate of regional subsidence	Moderate
7. Changes in lithofacies of associated rocks across the unconformity	Clearly changes
8. Lithofacies of associated bauxites	Autochthonous
9. Underlying karst relief	Shallow to moderate; moderate to high
10. Supposed source material of bauxites	Crystalline rocks of the Gilau Massif
11. Supposed source material of non-bauxitic karst fills	Permian Lower Triassic, Lower Jurassic detritic rocks –Valani Nappe; Permian. Lower Triassic detritic rocks – Arieseni Nappe, Quaternary deposits
12. Lithology, size and shape of bauxite deposits	Homogeneous, ore bodies are small to moderate, in form as lenses of Aston or Caguanes type
13. Bauxite texture	Mostly ooidic; pelitomorph
14. Bauxite structure	Massive
15. Chemical composition of bauxites (%)	Al ₂ O ₃ 53.7–75; SiO ₂ : 3.3–8.6; Fe ₂ O ₃ : 12.7–25.5; TiO ₂ 3.6–4.3; CaO: 1.7–11.2
16. Mineral composition of bauxites (%)	Diaspore: 50–55; Hematite: 15–25; Goethite: less than 10
17. Accessory minerals from bauxites (%)	Very rare
18. Trace elements in the bauxites (ppm)	No data
19. Type of ore; age	Karst bauxites, residual; Lower Berriasian
20. Bedrock petrography, main biostratigraphical data, age	Limestones, calcareous breccias; bivalves, hydrozoans (<i>Ellipsactinia caprensis</i>), corals, gastropods, echinids, foraminifers (<i>Trocholina gr. alpina</i>), calpionells (<i>Calpionella alpina</i> , <i>Remainella cf. cadisciana</i> , <i>Calpionellopsis simplex</i> , <i>Remaniella dadayi</i> , <i>Tintinnopsella carpathica</i>), calcareous algae (<i>Clypeina jurassica</i> , <i>Cayeuxia moldavica</i> , <i>Actinoporella podolica</i> , <i>Salpingoporella pygmaea</i> , <i>S. johnsoni</i>); Oxfordian–Lower Valanginia.
21. Cover petrography, main biostratigraphical data, age	Limestones: bivalves (pachyodonts), corals, foraminifers (miliolids), echinids, calcareous algae; Barremian–Lower Aptian

Table 4
Bauxite ores of the southern Pădurea Craiului Mts (Meziad zone)

1. Geotectonic location at the time of bauxite accumulation	Northern (European) margin of the Tethyan realm; Internal Dacides, Valani Nappe
2. Processes bringing a subaerial exposure of the carbonatic substratum	Eustatic > tectonic control; tectonic control
3. Imprints in the stratigraphic record	Weak to moderate bauxitiferous unconformity with prevailing paleokarst weak, non-bauxitic unconformity between bedrock and cover
4. Estimated duration of exposure	4–6 My
5. Apparent stratigraphic gap	Small to moderate
6. Rate of regional subsidence	Moderate
7. Changes in lithofacies of associated rocks across the unconformity	Clearly changes
8. Lithofacies of associated bauxites	Autochthonous
9. Underlying karst relief	Shallow to moderate
10. Supposed source material of bauxites	Crystalline rocks of the Gilau Massif
11. Supposed source material of non-bauxitic karst fills	Triassic, Lower Jurassic rocks–Valani Nappe; Permian detritic rocks; Neogene and Quaternary deposits
12. Lithology, size and shape of bauxite deposits	Homogeneous, ore bodies are small to moderate, in form as lenses of Aston or Caguanes type
13. Bauxite texture	Mostly ooidic, rarely pelitomorph
14. Bauxite structure	Massive
15. Chemical composition of bauxites (%)	Al ₂ O ₃ 62.3; SiO ₂ : 5.05; Fe ₂ O ₃ : 18.25; FeO: 27.7 TiO ₂ : 2.05
16. Mineral composition of bauxites (%)	Diaspore: 63.9; Hematite: 9.7; Kaolinite: 9.3; Goethite: 11.4
17. Accessory minerals from bauxites (%)	Anatase: 2.6; Chlorite: 7.3
18. Trace elements in the bauxites (ppm)	Ni: 11; Co: 19; Cr: 372; V: 303; Sc: 46; Nb: 70; Ga: 50; Sn: 8; Zr: 664; Be: 8.4; Cu: 27; Pb: 95; Ba: 28; Sr: 33; Li: 65
19. Type of ore; age	Karst bauxites, residuale; Lower Berriasian
20. Bedrock petrography, main biostratigraphical data, age	Limestones: bivalves, gastropods, echinoderms, brachiopods, corals, hydrozoans, foraminifers, calcareous algae (<i>Clypeina jurassica</i>); Kimmeridgian–Tithonian
21. Cover petrography, main biostratigraphical data, age	Limestones, marls, sandstones: bivalves, (<i>Requenia minor</i>) gastropods, foraminifers (miliolids, orbitolinids), tintinnoids; Lower Valanginian–Aptian

Table 5 ↓
Bauxite ores of the Ohaba–Pui–ponor Zone Poiana Ruscă Mountains

1. Geotectonic location at the time of bauxite accumulation	Northern (European) margin of the Tethyan realm; Median Dacides–Getic and Supragetic Nappes
2. Processes bringing a subaerial exposure of the carbonatic substratum	Eustatic > tectonic control; tectonic control
3. Imprints in the stratigraphic record	Weak to moderate bauxitiferous unconformity with paleokarst; moderate to large non-bauxitic unconformity between bedrock and cover
4. Estimated duration of exposure	15–17 My
5. Apparent stratigraphic gap	Moderate
6. Rate of regional subsidence	Weak to moderate (for bedrock); moderate to large (for cover)
7. Changes in lithofacies of associated rocks across the unconformity	Major changes
8. Lithofacies of associated bauxites	Autochthonous; allochthonous
9. Underlying karst relief	Shallow, shallow to moderate or even to large
10. Supposed source material of bauxites	Crystalline rocks of the Sebes Series (Getic Nappe) – Southern Carpathians
11. Supposed source material of non-bauxitic karst fills	Crystalline rocks of the Sebes Series, Permian conglomerates and sandstones, Lower Jurassic conglomerates and sandstones of Gresten facies, Late Cretaceous detritic rocks; Neogene and Quaternary deposits
12. Lithology, size and shape of bauxite deposits	Detrito-chemical bauxitiferous formation which consists of bauxites, bauxitiferous–ferruginous shales, red conglomerates sandstones and argillaceous schists; allochthonous bauxites as detrito-chemical bauxitiferous formation have about 50 m in thickness and can be found as a layer; sometimes bauxite orebodies appear included into the detrito-chemical bauxitiferous formation assigned to post-Bedoulian–ante-Vraconian interval, they are small to moderate and have a shape as lenses of Aston on Caguanes type; they are settled predominantly in the intermediary zone of the analogous formations with large bauxite deposits of Gánt (Hungary), of Early Cretaceous bauxites of Provence (South of France), Arrière etc.
13. Bauxite texture	Ooidic; pelitomorphous, schistose
14. Bauxite structure	Massive; stratified bauxites
15. Chemical composition of bauxites (%)	Al ₂ O ₃ : 28.73–54.83; SiO ₂ : 0.62–40.99; Fe ₂ O ₃ : 5.6–35; FeO: 0.6–1.5; TiO ₂ : 1.10–5.12
16. Mineral composition of bauxites (%)	Boehmite: 49.9–64.4; Hematite: 15.36–33.21; Kaolinite: 1.38–17.4; Goethite: 3.35–12.72 (for bauxites); Boehmite: 0.33–22.52; Hematite: 5.74–18.98; Kaolinite: 47.59–75.75; Goethite: 1.95–7.27 (for bauxitiferous argillaceous rocks)
17. Accessory minerals from bauxites (%)	Chlorite: 1.24–2.71; Anatase: 2.45–4 (for bauxites); Chlorite: 1.42–3.23; Anatase: 1.11–2.87 (for bauxitiferous argillaceous rocks)
18. Trace elements in the bauxites (ppm)	Ni: 35–270; Co: 4–74; Cr: 102–425; V: 80–460; Mn: 81–1000; Be: 3.6–10.3; Zr: 255–1050; Sn: 4.4–11; Cu: 4–115; Pb: 50–150; Ga: 22–60; Ba: 11–470; L: 6–1050; Sr: 138–910; Ca: 100–4000; Mg: 180–2900
19. Type of ore; age	Karst bauxite, residuale; Albian
20. Bedrock petrography, main biostratigraphical data, age	Limestones, ammonites (<i>Perisphinctes</i> sp., <i>Lamellaphynchus</i> c.f. <i>zitteli</i> etc.), belemnites (<i>Belemnites pistiliformis</i>), Tintinnidae, radiolarians (<i>Sphaerellaria</i> , <i>Nassellaria</i>)?, gastropods, <i>Calpionella alpina</i> , <i>Saccocoma</i> sp., corals (<i>Heliostraea</i> cf. <i>lifolensis</i> , <i>Aplosmilium nuda</i> , <i>A. thurmanii</i> , <i>Kladophilium ramea</i>) – Stramberg facies; bivalves (<i>Requienia ammonia</i> , <i>Toucasia carinata</i> etc.), calcareous sponges, hydrozoans, foraminifers, calcareous algae (<i>Clypeina parvissima</i> , <i>Mercierella dacica</i> , <i>Cayeuxia anae</i> , <i>C. moldavica</i>); Late Jurassic – Bedoulian
21. Cover petrography, main biostratigraphical data, age	Conglomerates, sandstones, shales, sometimes coal intercalations containing plant remnants, teeth remnants of scleractinians (Vraconian–Lower Cenomanian); marls, sandy shales (Middle Cenomanian); sandy-argillaceous series (Upper Cenomanian–Middle Turonian); ammonites (<i>Mantelliceras mantelli</i> , <i>Acanthoceras rhotomagense</i> , <i>A. Mantelli</i> etc.) corals (<i>Aulosmilium cuneiformis</i> , <i>Trochomilium complanata</i>), bivalves (<i>Exogyra columba</i> , <i>E. conica</i> , <i>Modyola polygena</i>), gastropods (<i>Nerinea incavata</i> , <i>N. parva</i>), foraminifers (<i>Rotaliopora appeninica</i> , <i>Praeglobotruncana stephani</i>) Vraconian–Middle Turonian

Table 6
Bauxite ores of the Poiana Rușica Mountains (The Rusca Montana Basin)

1. Geotectonic location at the time of bauxite accumulation	Northern (Europeana) margin of the Tethyan realm: Median Dacides – Getic Nappe, the western part of South Carpathians
2. Processes bringing a subaerial exposure of the carbonatic substratum	Eustatic and tectonic control; tectonic control; thermal metamorphic control
3. Imprints in the stratigraphic record	Weak to moderate bauxitiferous unconformity with paleokarst; moderate to large non-bauxitic unconformity between bedrock and cover
4. Estimated duration of exposure	24–30 My
5. Apparent stratigraphic gap	Moderate to large
6. Rate of regional subsidence	Weak to moderate (for bedrock); moderate to large (for cover)
7. Changes in lithofacies of associated rocks across the unconformity	Major changes
8. Lithofacies of associated bauxites	Autochthonous; allochthonous
9. Underlying karst relief	Shallow; shallow to moderate
10. Supposed source material of bauxites	Crystalline rocks of the Sebes series (Getic nappe) – Southern Carpathians
11. Supposed source material of non-bauxitic karst fills	Lower Jurassic detritic rocks; Late Cretaceous detritic rocks; Quaternary deposits
12. Lithology, size and shape of bauxite deposits	Heterogeneous detrito-chemical bauxitiferous formation (massive bauxite passing at the upper part to shaly one with detrital material); metamorphosed bauxites; bauxite ore bodies are small to moderate, in form as lenses of Aston or Caguanes type
13. Bauxite texture	Mostly ooidic; pelitomorphic (difficult to be recognized due to the thermal metamorphism)
14. Bauxite structure	Massive; stratified bauxites
15. Chemical composition of bauxites (%)	Al ₂ O ₃ : 45.4–63.5; SiO ₂ : 1.0–12.68; Fe ₂ O ₃ : 18.4–23.40; TiO ₂ : 2–3.3
16. Mineral composition of bauxite (%)	Diaspore: 37–59; Boehmite: 0–9; Hematite: 0–8; Kaolinite: 0–5; Goethite: 0–8; Corundum: 0–33
17. Accessory minerals from bauxites (%)	Chlorite: 5–36; Rutile+Anatase: 2.4–3.3; Pyrite: 0.1–25.9;
18. Trace elements in the bauxites (ppm)	Ni: 125–475; Co: 23–52; Cr: 230–290; V: 500–630; Se: 43–62; Mn: 780–1300; Nb: 37–65; Zr: 530–700; Be: 4.6–9; Sn: 6–11; Ga: 42–58; Cu: 52–175; Pb: 20–225; Ba: 24–1000; Sr: 28–155; Li: 34–400
19. Type of ore; age	Karst bauxites, residuales; Albian (?)
20. Bedrock petrography, main biostratigraphical data, age	Limestones: corals (<i>Cladocora humilis</i> , <i>Calamophyllia compressa</i> etc.), ostracods, hydrozoans (<i>Cladocoropsis mirabilis</i>), calcareous algae (<i>Cayeuxia pia</i> , <i>Thaumatoporella parvovesciculofera</i> , <i>Bacinella irregularis</i> , <i>Lithocodium aggregatum</i> , <i>Phychoporida lobatum</i> , <i>Labyrinthina</i> sp., <i>Parurgonia</i> sp., <i>Nodophtalmidium jurassicum</i> , <i>Pseudocyclammica lituus</i> , <i>Kilianina rahonensis</i> , <i>Kurnubia palastiniensis</i> etc.); Late Jurassic–Early Cretaceous (?)
21. Cover petrography, main biostratigraphical data, age	Conglomerates, calcareous sandstones; bivalves (<i>Exogyra columba</i> , E. cf. <i>squamata servitensis</i> , E. cf. <i>marmeti</i> , <i>Cyprina</i> sp.), ammonites as <i>Calycoceras boulei</i> ; Cenomanian; sandy limy marls, tuffitic calcareous sandstones, basic tuffites, marls, siliceous rocks as intercalations, allodapic limestones; foraminifers (<i>Rotalipora</i> gr. <i>appenninica</i> , <i>Praeglobotruncana stephani</i> , <i>Pithonella ovalis</i> , <i>P. sphaerica</i> , <i>Globotruncana</i> gr. <i>lapparenti</i> , corallinaceae (<i>Paraphyllum amphiroaeforme</i> , <i>Hemiphyllum atacicum</i> , <i>Archaelitothamnium cretaceum</i> , <i>Peysonella antiqua</i>); frequently appear flysh and wildfish sequences; Turonian–Coniacian(?)

Up to now in the Pădurea Craiului Mts, we have no evidences for primary Barremian or Aptian bauxites. The numerous exploratory boreholes did not penetrate such intra-Barremian or Aptian bauxite deposits;

The New-Kimmerian orogenic phase caused relative sea level changes and faults which affected the formations of the footwall; subsequently the Austrian movements formed the structure of the Pădurea Craiului Mts.

References

- Bordea, S., J. Bordea 1987: Note préliminaire sur la présence des orbitolinidés primitifs du calcaire d'Albioara (au sud de Pădurea Craiului, Monts Apuseni). – D.S. Inst. Geol. Geofiz., 72–73, pp. 45–53, Bucuresti.
- Cibotaru, T., T. Brustur 1980: Contribution à la connaissance de la géologie de la zone Meziad (Monts Padurea Craiului) avec considérations spéciales sur la bauxite. – Rev. Roum. de Géologie, Géophysique et Géographie, 24, București.
- Dragastan, O., D. Istocestu, M. Diaconu 1967: Etude du niveau á Charophytes d'âges Crétacé inférieur des Monts Padurea Craiului (Roumanie). – Rev. Micropal., 9, pp. 23–28, Paris.
- Dragastan, O., M. Coman, E. Stiuică 1988: Bauxite-bearing formations and facies in the Padurea Craiului and Bihor Mountains (Northern Apuseni). – Rev. Roum. Géol. Géophys, Géogr, Géologie, 32, pp. 67–81, Bucuresti.
- Ianovici, V., M. Borcoș, M. Bleahu, D. Patrulius, M. Lupu., R. Dimitrescu, H. Savu 1976: Geologia Muntilor Apuseni. – Ed. Acad. R. S. R. pp. 163–166, București.
- Mantea, Gh. 1985: Geological studies in the upper basin of the Somesul Cald Valley and the Valea Seaca Valley region – Bihor-Vlădeasa Mountains. – An. Inst. Geol. Geofiz., 66, pp. 1–89, Bucuresti.
- Papiu, C.V., Gh. Mantea, V. Iosof, Fl. Popescu, C. Udrescu, V. Neacșu 1981: L'étude chimico-minéralogique des bauxites de la région de Meziad (sud de Massif de Padurea Craiului). – D.S. Inst. Geol. Geofiz., 68, pp. 131–150, Bucuresti.
- Patrulius, D. 1971: Unitatea de Valani: un nou element structural al pînzelor de Codru (Muntii Apuseni). – D.S. Inst. Geol., LVII, 5, pp. 155–171, Bucuresti.
- Patrulius, D., V. Iosof 1974: Nota asupra a doua noi tipuri de bauxite din Muntii Apuseni. – D.S. Inst. Geol (Zăcăminte), 60, pp. 61–64, Bucuresti.
- Patrulius, D., S. Bordea, J. Bordea, Gh. Mantea, E. Avram, A. Baltreș 1977: Report of the Institute of Geology and Geophysics, Bucuresti.
- Patrulius, D., F. Marinescu, A. Baltreș, S. Radan, Al. Madeșan, L. Artin, C. Rifaat, T. Jurcsák 1979: Report, Archives of the Institute Geology and Geophysics, Bucuresti.
- Patrulius, D., S. Bordea, E. Avram 1982: La brèche de Gugu –un exemple de contrôle tectonique de la sédimentation sur une plate-forme carbonatée barremo-bedoulienne (Pădurea Craiului – Monts Apuseni). – D.S. Inst. Geol. Geofiz., 66, 4, pp. 109–117, Bucuresti.

Petrography and Sedimentology of the Cretaceous Continental Complex of the Eastern Hațeg Basin (South Carpathians – Romania)

Judit Becze-Deák

*Post-Graduate Soil Science
State University, Gent*

Genetical conclusions related to the bauxite bearing continental complex of Gargasian–Albian age, located on the Mesozoic paleokarst of the Hațeg Basin (South Carpathians) are presented. This continental complex consists of a red-russet pelitic (bauxite bearing) complex overlain by an arenitic (red and grey sandstone) formation. The contact between the two is clearcut sometimes erosional. The paper presents the results of textural, chemical and mineralogical studies carried out in order to understand the conditions of formation of the continental complex.

Key words: Bauxite, paleokarst, sediment petrography, geochemistry, Middle Cretaceous, Hațeg Basin, South Carpathians

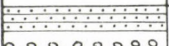
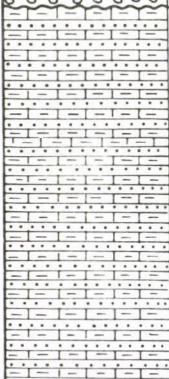
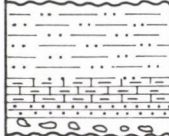
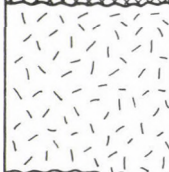
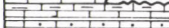
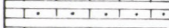
Introduction

The continental complex of the SW part of Sebes Mountains is underlain by Lower Aptian limestones and covered by an Upper Cretaceous (Vraconian) sequence. Accordingly it is generally considered to be Gargasian and/or Albian in age (Grigorescu et al. 1990). Details of lithology and areal distribution of the various lithotypes are shown in Fig. 1. The lower part of this continental complex consists of red-russet pelitic (bauxite bearing) sediments passing into a red-brownish and grey arenitic (sandstones and microconglomerats) formation upwards. The contact between these two members is rather sharp sometimes with erosional features to be observed. In the majority of the area the continental complex is exposed on the surface, however, around Varnita it is covered by 270 meters of younger Upper Cretaceous sediments. Maximum thickness of the continental complex is 60 m. It forms a discontinuous layer the lower surface of which follows the morphology of the underlying Mesozoic limestones. The parameters of continental formations are very variable from 40/30 (Varnita) to 500/20 (Murgoi) and 800/150–200 (Comarnic–Poieni) (Papiu et al. 1971).

Chemical and mineralogical analyses show a rather particular lithological variation within the pelitic formation: argillaceous rocks occur along the periphery of the basin and at the bottom and the top of the formation, whereas bauxites preferably occur at the center. Mineralogical analyses show that compositional

Address: J. Becze-Deák: Str Fundatura Maghiara 6B, Ghorgheni 4200, jud Harghita, Romania

Received: 23 October, 1991.

Lithological column	Thickness (m)	Age	Lithological description	Sedimentary environment
	50	Upper Maastrichtian	Sandstones, Conglomerates	Litoral
	500 700	Campanian-Maastrichtian	Alternation of marls and sandstones (Flysh)	Marin
	20-50	Santonian Upper-Campanian	Marls and sandstone (Flysh)	Marin
	150 200	Coniacian	Limestones Sandstones Conglomerates	Subsident litoral
	200 250	Cenomanian-Lower Coniacian	Sandy clay Marls Sandstones Conglomerates	External shelf Internal shelf Litoral
	50	Upper-Albian-Lower Cenom.	Sandstones, Conglomerates	Lacustrin
	60	Albian	Pelitic (bauxite bearing) and arenitic	Continental
	300	Lower Cretaceous (till lower Aptian)	Urgonian type limestones	Shelf
	100 125	Tithonian - Upper Oxfordian	a.) Limestones with cherts b.) Recifal limestones	a) Marin (pelagic) b) shelf
	30	Upper Collovian - Lower Oxf.	Limestones and marls	Marin (Pelagic)
	40-50	Lower and Middle Collovian	Compact sandy limestones	Marin
	30-50	Aalenian Bathonian	Sandstones and sandy limestones	Marin (Shallow)
	100 125	Lias	Sandstones with coaly lenses Conglomerates	Continental (Grester facies)
	100 125	Lower Permian	Red-beds* type sandstone Coarser conglomerates	Continental
		Precambrian	Micashists, Paragneises	

changes are gradual (Figs 2–6). The argillaceous members of the complex are of pelitic grain-size, red to russet or sometimes white in colour. Free alumina is few or absent in them, their clay-mineral is almost exclusively kaolinite. Bauxites (s. s.) are red to russet in colour, their free alumina content is as high as 49.9–64.41% (mainly in the form of boehmite) accompanied by lesser amounts of kaolinite (17.47%). The thickness of the bauxitic horizon is variable (from 0.2–0.5 m till to 15 m), maximum thickness was observed in Comarnic Poieni where it reached 25 m (Fig. 7), (Papiu et al. 1971).

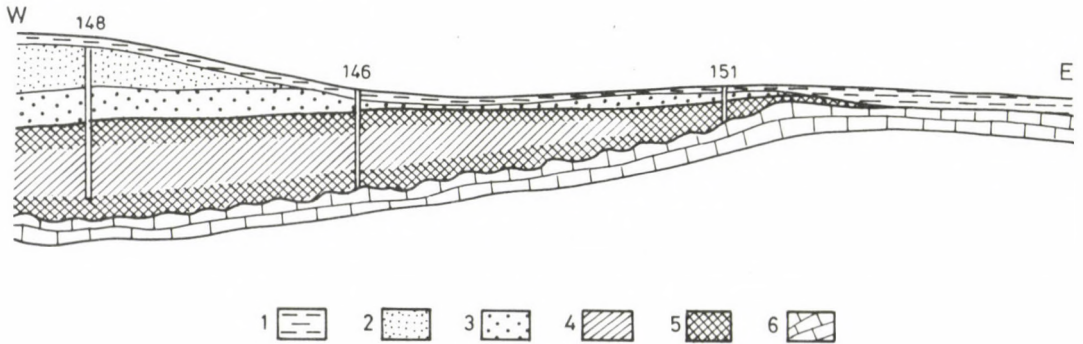


Fig. 2
Comarnic lens (after Papiu et al. 1971). 1. Quaternary caly; 2. Vraconian sandstone; 3. Albian red bauxite; 4. kaolinitic bauxite; 5. bauxite; 6. limestone (Barr.–Aptian)

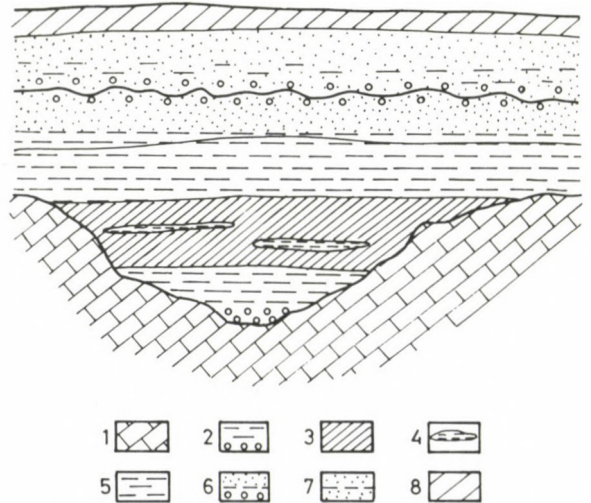


Fig. 3
Murgoi lens (after Papiu et al. 1971). 1. limestones; 2. argillaceous horizon; 3. bauxitic horizon; 4. argillaceous insertions; 5. argillaceous horizon; 6. Vraconian sandstones; 7. arenitic formation (Albian); 8. Quaternary deposits

Fig. 1 ←
Schematic lithological column of Eastern Hațeg Basin

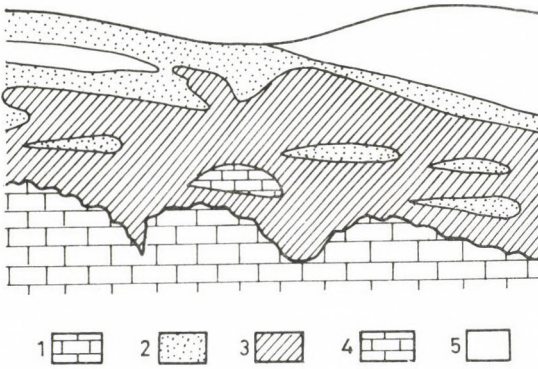
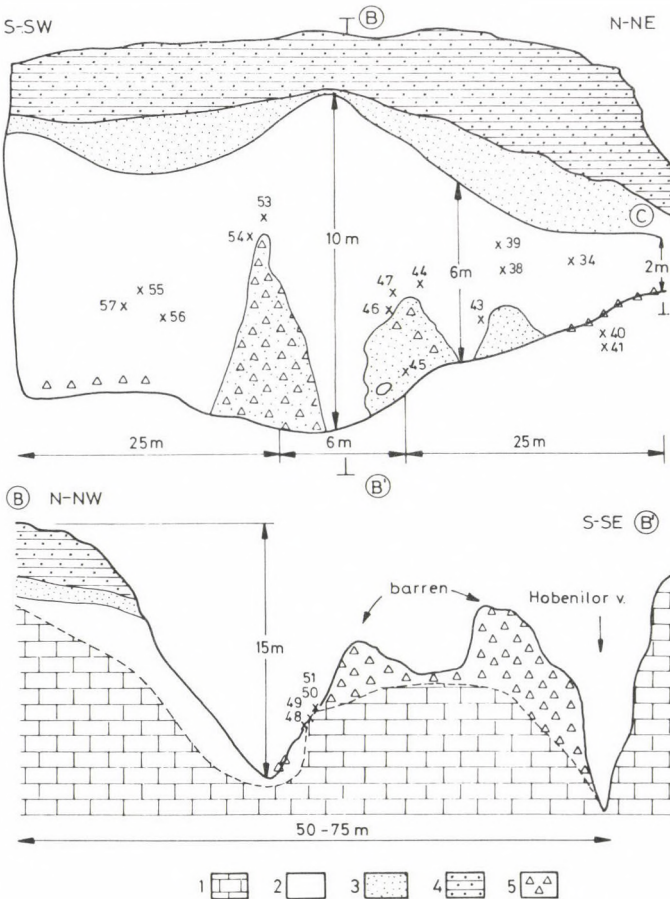


Fig. 4
Varnita lens (Igheabului)(after Stilla (1970). 1. limestones (Barr.-Aptian); 2. arenitic formation (Albian); 3. bauxite (Albian); 4. limestone fragments; 5. Vraconian sandstones



Figs 5,6
Profiles of the Comarnic lens. 1. limestone; 2. bauxite-bearing formation; 3. grey sandstone; 4. red sandstone; 5. debris

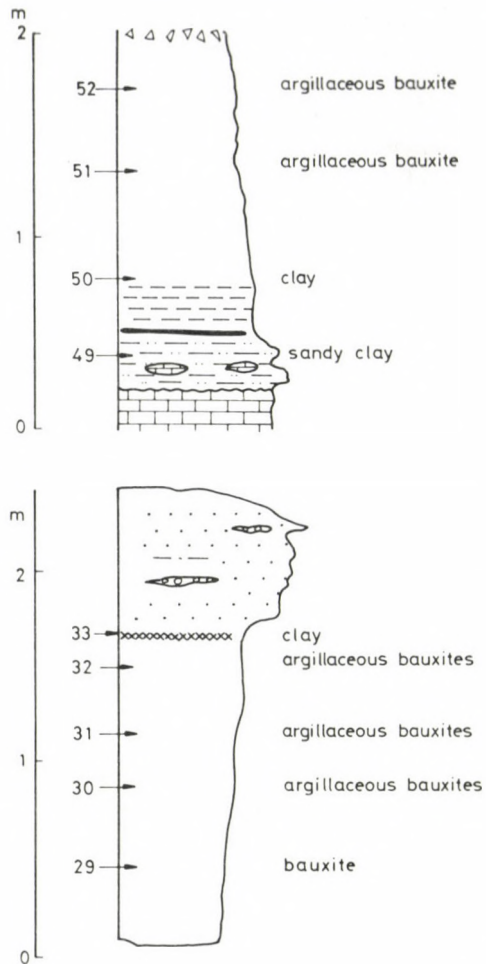


Fig. 7
Lithological columns for Comarnic lens

Bauxite petrography

On the macroscopic scale the *bauxite bearing formation* is represented by lenticular bodies of homogeneous red-russet colour, locally with deferrification-patches it does not show any apparent sign of large-scale transport. It is only the subangular, less-than centimeter-size, iron rich intraclasts which suggest a possible paraautochthon transport. Generally all the components of the bauxite bearing formation are of the same hardness and they show no visible stratification. Hematite when presents usually increases the specific weight of argillaceous rocks so that they may be similar to the component bauxite bearing formation. However,

due to increased amounts of kaolinite and goethite clays often present brown-yellow to whitish colour as well. In this formation local deferrification accompanied by the presence of kaolinite frequently occurs either along fissures or randomly as irregular patches. On the broken surface sometimes finely disseminated, or mm size "porphyric" pyrite aggregates can be observed. In these cases the surrounding surface is always friable and pale. Sometimes in the center of 2–3 cm size deferrification patches pyritized root remnants could be detected. The *arenitic formation* is made up by sandstones and irregular microconglomeratic intercalations, however without any regular internal stratification.

Predominant colour of these rocks is red but tints of grey and greenish grey are also common. Colour changes are always very irregular. In the case of Comarnic Poeni deposit the bauxite bearing formation is overlain by a predominantly grey coloured sandstone locally with traces of coal as well (Figs 8, 9, 10).

As to mineralogy main components are boehmite, kaolinite, hematite and anatase and though in various amounts they are present both in the argillaceous rocks and the bauxites. In addition to this important amounts of muscovite were observed particularly in the argillaceous rocks. The mineralogical composition of the bauxite bearing formation is shown by Tables 1 and 2. Microscopical study of the thin sections indicated a pelitomorphous, iron rich matrix for the bauxite bearing formation, sometimes with scattered subangular intraclasts. They are hematite-rich, opaque occasionally dissected by kaolinite filled syneresis-cracks. Extraclasts identified are muscovite, biotite, zircon, rutile, turmalin. Muscovite and biotite could be observed only rarely in the bauxite samples, however, they

Table 1
Limits of variation of mineralogical composition for bauxite-bearing formation from Eastern Hăţeg Basin (after Papiu et al. 1971)

Minerals	Limit of variation (%)
Boehmite	0.33–64.41
Kaolinit	1.38–74.94
Dickit	12.98–89.20
Chlorit	1.42–2.71
Muscovit	3.06–8.08
Hematit	5.74–33.21
Goethit	1.95–7.27
Hidrated iron oxides	1.85–11.72
Anatase	1.22–5.41
Pyrite	0.20–7.63

are much abundant (especially muscovite) in the clays. Alteration of muscovite into kaolinite could also be observed. Intermediate stages of this alteration are marked by decolouration and swelling of the muscovite flakes; accompanied by fading of the colours of birefringence. In the uppermost argillaceous horizon vermiform kaolinite replacing muscovite could be observed. Sometimes the matrix is affected by deferrification. The presence of recrystallized kaolinite and disseminated pyrite are characteristic of this process. Kaolinite may fill fissures or for globular aggregates. The presence of pyrite sometimes indicate the remains of rootlets of up to 2 cm size. In the deferrificated zones

Table 2
Mineralogical composition of samples collected from Comarnic and Bordu Rosu Lenses

Nr.	Smp	Locality	Bx. min. B	Clay minerals			Iron minerals		Other minerals					IH	Observations	
				K	I	Ch	H	G	A	Q	F	C	Sd			
1.	13a	Bordu-Rosu		84			16		?						0.97	bauxitic clay
2.	13b1	"		87		±	13		?						1.12	"
3.	13b2	"		92		2	4		?						1.00	"
4.	13b3	"		89		±	11		?						0.97	"
5.	13'	"		+		+										limestone
6.	13'	"		+												limestone
7.	20bc	"		90		±	10		?							bauxitic clay
8.	25	Comarnic-Poeni	56	21		+	20		3							bauxite
9.	27	"	47	25		4	22		3							argillaceous bx.
10.	29	"	56	16		5	24		?							bauxite
11.	30	"	52	24		6	8		?							argillaceous bx.
12.	31	"	55	27		5	12		3							argillaceous bx.
13.	32	"	59	30			8		3						0.87	argillaceous bx.
14.	33	"	2	62	31		5		?							arenitic clay
15.	36	"		37	25				?	24	2	8	4			matrix of sandstone
16.	36	"		40	29				?	17	3		11			"
17.	37	"		39	31				?	28	2					"
18.	38	"	50	16		5	28		3							iron rich bx.
19.	39	"	71	±		+	26		3							iron rich bx.
20.	43	"	69	+		7	21		4							bauxite
21.	44	"	73			5	20		4							bauxite
22.	45	"	57	14		6	20		3							bauxite
23.	46	"	66	+		8	23		4							bauxite
24.	48	"		±	±										>95	limestone
25.	49	"		38	38		+	24	?							arenitic clay
26.	50	"		91		3	4	4	?						1.73	clay
27.	51	"	43	42		3	11		3							argillaceous bx.
28.	52	"	47	36		+	17		?							argillaceous bx.
29.	53	"	74			±	21		5							bauxite
30.	54	"	73	15		6	3		4							bauxite
31.	57	"	80	+		?	20		?							bauxite
32.	-	"	66				31		3							iron rich bx.
33.	-	"	18	32	22	4	25		?							bauxitic clay
34.	-	"	53	33		4	8		4						1.00	argillaceous bx.

Symbols: B - boehmite, K - kaolinite, I - muscovite, Ch - chlorite, H - hematite, G - goethite, A - anatase, Q - quartz, F - feldspar, C - calcite, Sd - siderite, IH - Hinckley crystallinity index

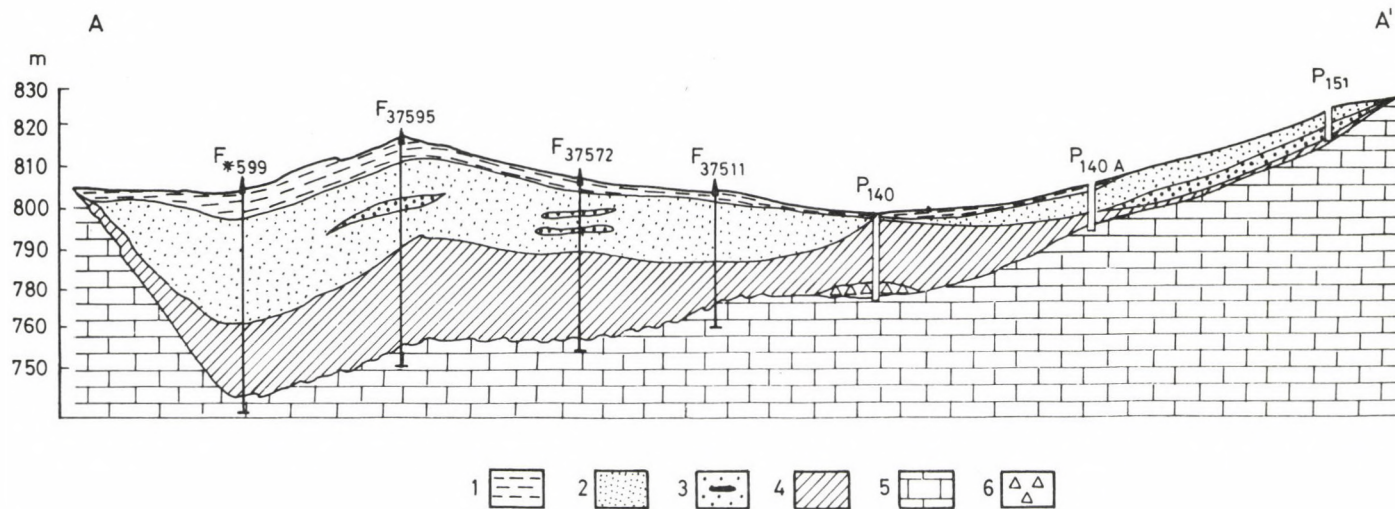


Fig. 8
 Geological Profiles of Comarnic lens. 1. Quaternary red clay; 2. Albian red sandstone; 3. Albian grey sandstone with coaly lenses; 4. Albian bauxite-bearing formation; 5. Urgonian limestones; 6. debris

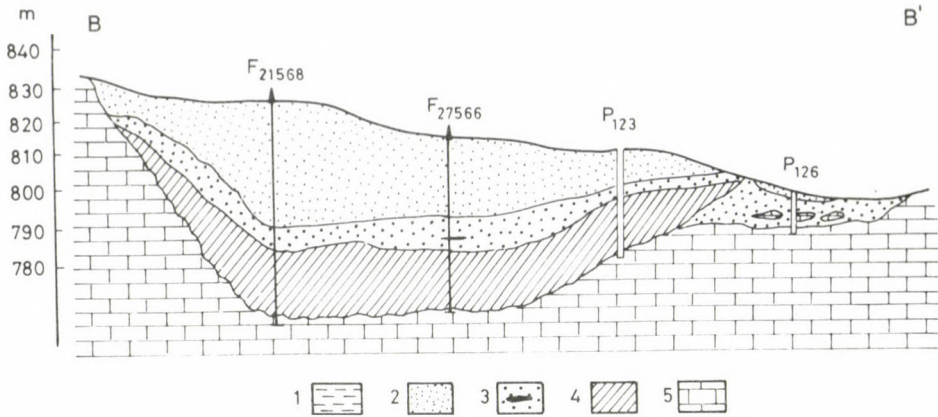


Fig. 9
Geological Profiles of Comarnic lens. (For legend see Fig. 8)

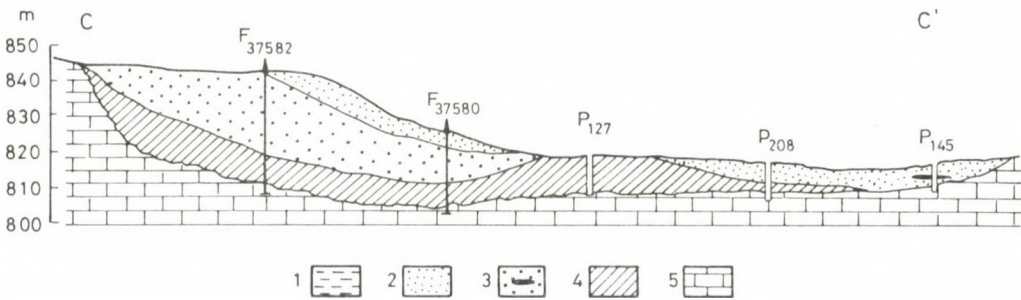


Fig. 10
Geological Profiles of Comarnic lens. (For legend see Fig. 8)

sometimes the presence of chlorite could also be observed. As to the mineralogy of the arenitic formation, X-ray analyses of the matrix suggest an argillaceous material consisting predominantly of kaolinite and of anatase (Table 3). No free alumina is present in the arenites. The red sandstones matrix are rich in hematite and always contain some goethite. As to their clay minerals the grey, greenish-grey sandstones are identical to the red ones only, they are much poorer in hematite. Sorting is generally in the sandstones. Sandgrains are quartz, feldspar, muscovite and biotite. The undulous extinctions of quartz point to its metamorphic origin. Muscovite and biotite give the bulk of the detrital components and they show

different stages of alteration to kaolinite and chlorite, respectively. The feldspar group is represented by microcline and subangular to angular plagioclase. The moderate quantity of quartz (less than 50%) as opposed to the abundance of muscovite, biotite, feldspars, and accessories is an indication of the low degree of maturity of the arenitic group (Table 4). Lithoclasts are mainly quartzites and/or quartz feldspar bearing crystalline rock fragments. As to grain-size the arenitic formation qualifies as a microconglomeratic sandstone, the mineralogy and the nature of the matrix of which shows that it consists of lithic graywackes (Fig. 11).

Table 3
Mineralogical composition of the matrix of sandstone (After Papiu et al. 1971)

Minerals	H-180	H-20	H-25a	H-25b
Kaolinite	55.5	58.1	30.1	82.2
Dickite	25.5	15.3	39.4	4.8
Leptochlorite	–	5.7	4.5	–
Hematite	11.4	18.6	18.5	10.1
Goethite	5.3	–	4.8	–
Anatase	2.6	2.3	2.7	2.9

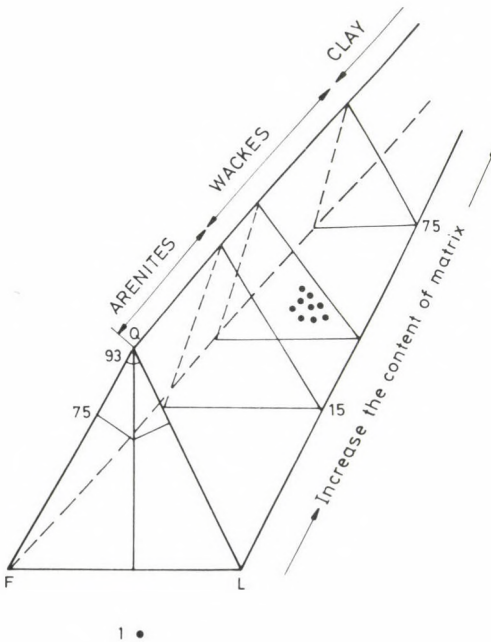


Fig. 11
The Pettijohn diagram for classification the arenitic formation. 1. The samples from arenitic formation

Table 4
Mineralogical composition of epiclastic formation

Minerals	Grey, H-25b (average%)	Red, H-25a (average %)	Red, H-20 (average %)	Grey greenish. H 35 (average %)
Quartz	34.78	37.00	47.50	± 30
Microcline	6.99	2.20	-	rare
Biotite	6.16	-	-	± 10 -15
Biotite (+chloritized)	13.16	9.80	13.00	± 0.5- 1
Muscovite-sericite	26.03	17.30	11.00	34
Argillaceous hematitic matrix	-	32.00	27.00	-
Argillaceous leptochloritic matrix	8.00	-	-	20
Other detrital components	4.88	1.70	1.50	±

Geochemistry

Chemical analyses of the continental complex of the Eastern Hațeg Basin are presented in Tables 5 and 6. For the *bauxite bearing formation* the most important observation is that variations of the alumina content are minor and that the decrease of the percentages of boehmite is generally accompanied by an increase in kaolinite. There is no free silica in the ore, all the silica content is bound to kaolinite. Accordingly there is no K₂O in bauxites whereas the non-bauxitic, argillaceous members of the sequence do contain also K indicating the presence of muscovite. Almost all the iron content is in oxidized form. Fe (II) could not be detected in the free-alumina-rich bauxites from Murgoi, however, it is always present in clayey bauxites; containing leptochlorites and rarely also siderite (Murgoi, Pades, Comarnic) and pyrite (Comarnic, Pades). TiO₂ is present in the form of anatase and correlates very well with the iron and free alumina content of the

Elements	Limit of variation (average %)
SiO ₂	0.62-40.99
Al ₂ O ₃	28.60-54.83
Fe ₂ O ₃	7.83-35.10
FeO	0 - 4.51
MgO	0.02- 0.47
CaO	0.06- 0.88
Na ₂ O	0.08- 0.43
K ₂ O	trace- 0.94
TiO ₂	1.20- 5.21
MnO	0.01- 0.53
P ₂ O ₅	0- 0.35
S	0- 0.22
CO ₂	0- 2.76
H ₂ O	22.28-13.48

Table 5
Limits of variation of chemical composition for bauxite bearing formation from Hațeg area (After Papiu et al. 1971)

Table 6
Chemical composition of arenitic formation (After Papiu et al. 1971)

Elements	H-180	H-20	H-25a	H25b
SiO ₂	45.89	47.04	52.30	70.57
Al ₂ O ₃	25.10	26.28	22.69	17.10
Fe ₂ O ₃	7.97	10.48	7.71	2.10
FeO	0.77	1.94	1.80	0.48
MgO	2.00	0.28	0.70	1.20
CaO	0.94	1.13	1.32	0.60
Na ₂ O	3.12	0.13	0.29	0.30
K ₂ O	0.27	3.01	4.63	3.14
TiO ₂	2.28	1.28	0.95	0.65
MnO	0.08	0.15	0.14	0.09
P ₂ O ₅	0.04	0.12	0.15	0.11
S	0.30	trace	0.12	0.05
CO ₂	–	–	–	–
H ₂ O	10.70	8.39	6.96	4.06
Total	99.87	99.62	98.97	99.30

Table 7
Limits of variation of minor elements
for Hațeg Basin (After Cotulbea 1982)

Elements	Content (ppm)
Cr	3–5
Ni	30–170
Co	3–45
Mo	100
Pb	25–80
Zn	100
Bi, Sn, In	3–10
W	<30
Cu	<100
Cd	<30
Au	<0.3
Sb	<30
As	<100
Ge	<5

ore. Na₂O could be observed in the matrix only. Trace elements content is presented in Table 7. When platted on Schroll's diagram (Fig. 12) bauxites from the Hațeg Basin fall to an area overlapping with both the lateritic and the karst bauxite fields. Chemical analyses from the arenitic formation are presented in Table 7. The most interesting feature is the fluctuation of TiO₂ (0.65–1.28%). Very probably only a part of this fluctuation originates in the detrital fraction, part of it certainly reflects TiO₂ variations in the argillaceous matrix (anatase), like in the case of the bauxite bearing formation. Minimum TiO₂ figures were observed in grey, deferificated lithologies (Papiu et al. 1971).

The average content of the major elements for the Comarnic Poeni bauxite lens are presented in Table 8. Statistical analyses for the simple frequency distribution of the average alumina and silica contents show an unimodal repartition for alumina with a definite primary enrichment and a bimodal repartition for silica with a secondary enrichment (Figs 13, 14).

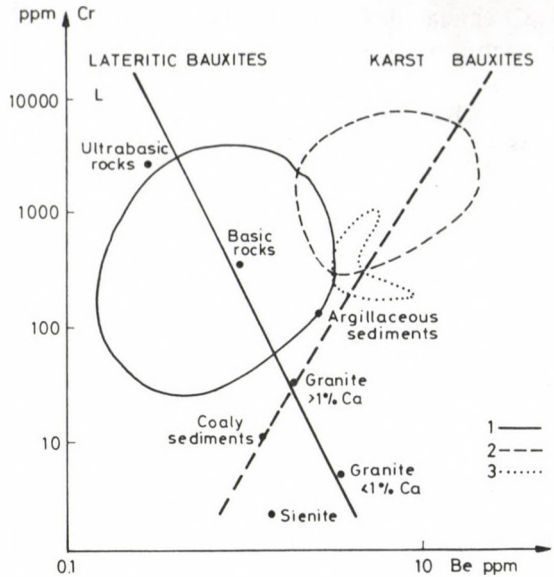


Fig. 12
Schroll diagram for bauxites from Hatég Basin. 1. lateritic bauxites, Europa; 2. karst bauxites, Europa; 3. bauxites from Hatég Basin

Discussion

The study of variation of the thickness of the bauxitic levels at Comarnic indicates that bauxite is thickest always where the underlying paleokarst is deepest. The average distribution of alumina and silica is rather irregular, and shows no firm correlation with the paleokarst relief. The only systematic variation can be observed in the NW-SE direction where the average content of silica decreases above the deepest parts the paleokarst relief.

The homogeneous and massif appearance of the bauxite bearing formation and the pelithomorphous texture of all the bauxitic members suggest that initially all bauxite levels of this formation formed one single sediment body. In accordance with this the transitions between clay, bauxitic clay, clayey bauxite are always gradual within the bauxitiferous complex.

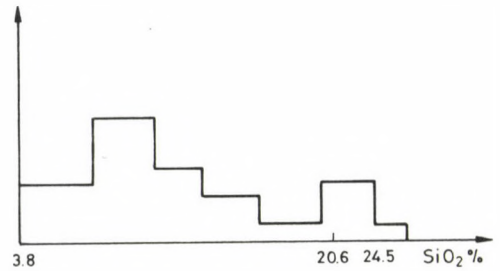


Fig. 13
Simple frequency distribution for average silica content for Comarnic lens

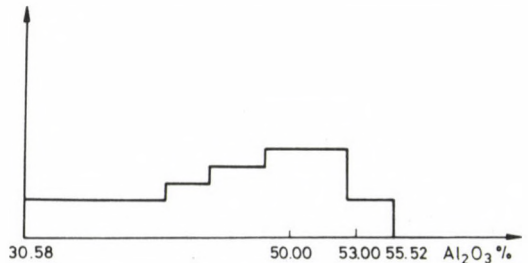


Fig. 14
Simple frequency distribution for average alumina content for Comarnic lens

The geochemical features can be best explained by plotting the data into Schroll's diagram (Fig. 12) in which all figures of Hateg bauxite basin occur in a field overlapping with that of both the karstic and lateritic bauxites. The presence of tourmaline, rutile and zircon grains in all bauxite levels is another argument for the initially considerable "homogeneity" of the "prebauxitic" sediment. It was most probably a silty (may be arenitic) iron-rich (hematitic-kaolinitic) clay washed onto the carbonate surface by areal waterflows. The silty/arenitic character is suggested by the presence of the "extraclasts" mentioned above. Under the conditions of tropical climate this argillaceous rock was apparently submitted to lateritic alteration. Along with the climate also the presence of the carbonate substrate on the other hand.

The role of the carbonate substrate is important for two reasons: by its morphology

- it plays the role of the "trap" for the accumulation of the initial argillaceous sediment and protects it from erosion
- it provides for the necessary physico-chemical conditions of bauxitizations.

The "trap" role was given by the paleorelief characterized by the presence of large morphological depressions. The size and scale of the bauxite bodies points to the existence of large polje-like karst forms. In the case of the Comarnic deposit within the large "polje" there are local topographic "highs" and "lows". The "lows" are coincident with the maximum thickness of the bauxitic horizon (Fig. 1). In the Murgoi zone the paleorelief consists of smaller scale vertical walled sinkholes (Papiu et al. 1971). This paleomorphology probably corresponds to the mature stage of a "tower karst" morphology. In nature tower karst areas bauxitization generally comes to an end and when the increase of relief energy in the backgrounds results, in the increase of fluvial erosion triggering the deposition of coarser grained clastic sediments rather than just fine-grained chemical weathering products (Szantner et al. 1986). The physico-chemical conditions offered by the presence of the karstic substrate include good drainage and favourable Eh and pH for bauxitization. Good drainage was provided by the karstic channelways and the positions of the site accumulation relative to the karst-water level (the base level of erosion) controlled the Eh and pH of the depositional environment. The morphology of the paleodepressions, characterized by large areal extension with rather gentle "highs" and "lows" suggests a shallow karst relief close to the base level of erosion. Also the boehmitic-hematitic association indicates also weakly oxygenated environment characterized by moderate drainage. Also the pH conditions: the observations of tropical areas show that as compared to the pH of rain water varying between 3.3 to 6.5, the pH of the karst-waters is characterized by values between 8 to 8.4 and at the karstic surface the "abrasion pH" reaches values of 9 to 9.6 (Szantner et al. 1986). These values are favorable for the dissolution and removal of silica and the enrichment of alumina, iron and titanium and may suggest that in the Hateg basin bauxites formed by in situ bauxitization of argillaceous sediments, deposited on the karst surface (Szantner et al. 1986).

The possibility of transformation of kaolinite into boehmite under conditions of sluggish drainage, low alkalinity and the presence of Ca^{2+} ions was demonstrated by Heydeman (1966); Keller, Wescott and Bledsoe (1954); Pedro and Bernier (1966), in (Bárdossy 1977). One of the problems could be the general impermeability of argillaceous sediments. But according to latest research (Bárdossy and Aleva 1990) the presence of silt or fine sand size particles in argillaceous sediments considerably increases the permeability. The possibility of circulation within bauxitic sediments is also generally admitted as long as the bauxite is unconsolidated. One of the problems which requires further research is the presence of muscovite or transformation of muscovite into boehmite a very alkaline environment was demonstrated (Janovici et al. 1979), this possibility is not a satisfactory answer. The enrichment of muscovite, however, may also be considered simply as a result of the changing composition of the fine grained sediment arriving onto the karst terrain.

It is suggested that under favourable climatic conditions bauxitization of argillaceous sediments by processes similar to lateritization, but with the special influence of the karstic substrate is a possibility to reckon with. In lateritic profiles (Bárdossy et al. 1990) the direction of mineral alteration is a downward directed process. Water, enriched in dissolved silica is evacuated by the karstic system. In the Hateg Basin deepest parts of the relief apparently offered the best channelways for drainage, this is why the deepest points coincide with the thickest bauxite levels (Fig. 1). An argument for this supposition may be the observation, according to which recent karst springs are able to transport hundreds of tons of dissolved silica, annually like e.g. the karst spring of Divulje (Yugoslavia) (Bárdossy 1977). Lateritization of argillaceous sediments may have resulted in the transition from argillaceous rocks to bauxites through several intermediate stages. In the lower part of the sediment the percolating water was enriched in silica giving rise to the formation of the argillaceous layer underneath the bauxite. The local permeability of the sediments and the specific karstic drainage system may explain the exceptions to the general scheme outlined above (argillaceous intercalations in bauxitic horizons: decrease of thickness or total absence of argillaceous horizons) and also the irregular variation of the average alumina and silica content within bauxitic horizons.

The alternation of wet and dry seasons probably account for the parautochthonous redeposition of the sediment, which resulted in the formation of the intraclasts, described above. The relative mobility of the sediments could be brought about also by karstification simultaneous with the bauxitization. Postdepositional karstification is shown by angular bauxite fragments found in the lower argillaceous horizon at Murgoi (Papiu et al. 1971) and also by dissolved limestone fragments observed during the field work.

The contact between the bauxite bearing and the arenitic formation indicates that before the deposition of the latter the bauxite bearing formation became more or less consolidated. The structural characters of the arenitic formation – with the frequent lateral grain size variations, the absence of stratification, – all suggest

that it was transported by a torrential system. The mineralogical composition (the immature character, the presence of feldspars) indicate a dry climate and a high rate of sedimentation. Extraclasts (e.g. quartz, muscovite, biotite and feldspars and particularly litoclasts of quartzite and crystalline rocks) give ample information about the source area. The hematitic argillaceous matrix with anatase but without free alumina suggests that the arenitic formation is probably closely related to the argillaceous sediments below. The consanguin character is indicated by the presence of the same accessory minerals, too. The geochemical facies of deposition and the diagenetic evolution of this sediment was variable, as suggested by the variation of red (hematitic) and grey-greenish (goethitic with chlorite) sandstones. In the Comarnic deposit where borehole information proved the predominance of chlorite and the presence of coal an oxygen-poor primary depositional environment (most probably a swamp) can be envisaged. The swamp was apparently a consequence of the relatively low permeability of the sediments underneath.

The source area for the continental complex, as shown by its mineralogical composition, was most probably mesometamorphic terrain (pragneises, micashists, quartzites) of the boarder surroundings. The increase of the volume of the clastic complex from SE to NW and its fan-like disposition suggest that the source area was situated to the NW of the basin. It is suggested that the pelitic and arenitic sediments represent different stages of the alteration of the adjacent crystalline massif and the alteration products were probably transported by surface water flows to the karst surface. The grain size of the argillaceous sediments suggests a rather low transport energy.

The effect of tectonic movements: according to its stratigraphic position the continental complex of Hațeg is a consequence of the so-called Mesocretaceous (Austrian) tectogenetic phase, which resulted in the overthrusting of the Getic and Supragetic Nappes (Sandulescu 1984). Synchronously with this evolution the Getic carbonate platform was uplifted, exposed and karstified. From the Vraconian on relief energy in the backgrounds had been increased to such an extent, that the karst became covered first by the continental complex and then by marine sediments. It is possible that the uplift of the carbonate platform was associated with the formation of a peripheral bulge in the front of the advancing Supragetic Nappes – similar to what was described by Desrochers and James from the Early Paleozoic of Quebec, Canada (Desrochers and Noel 1985). To prove this, however, it would obviously need more detailed tectonic mapping of the area. The tectonic movements resulted also in the fracturation of the exposed karstic platform. The fractured zones were particularly favourable for karstification and later on as a consequence also for bauxitization. This could clearly be observed in the case of the Comarnic deposit the orientation of which corresponds very well to that of the Liton fault. Also the other deep-karst zones are aligned parallel the same direction (Fig. 1).

Diagenetical evolution: after having been covered the bauxite bearing formation was subject to diagenetic transformations. The most important transformations

are to percolating silica rich, reducing waters which determined the deferrification processes; the alteration of muscovite into kaolinite; the recrystallization of kaolinite aggregates surrounding decayed plant remnants and (locally) pyritization. The vermiform kaolinite aggregates point to a transformations under acid conditions (Papiu et al. 1971).

Conclusions

The bauxites of the Eastern Hateg Basin are karst bauxites from the point of view of their substrate, but genetically they could be classified as belonging to the *Ariege* type, of Bárdossy because they were formed apparently by typical in situ lateritization processes. Such bauxites were described by Combes from France (Combes 1969). Economically they are of no great interest of (medium-grade high-silica, high-iron bauxites). Variations of grade within the deposit are irregular without macroscopically observable transitions between the argillaceous and the bauxitic horizons, which make any grade-prediction an illusory.

Acknowledgement

I wish to thank to dr. A. Mindszenty (from the Budapest ELTE University) for her help in introducing me in bauxite sedimentology. I also thank to dr. S. Radan (from the Roumanian Geological Research Institute), who helped me with the XRD analyses. At the same time I wish to thank to Professors dr. N. Anastasiu and C. Fabian (from the University of Bucharest) for their advices during my work.

References

- Bárdossy, Gy., G.J.J. Aleva 1990: Lateritic bauxites. – Akadémiai Kiadó, Budapest.
- Bárdossy, Gy. 1977: Karsztbauxitok. – Akadémiai Kiadó, Budapest
- Combes, P.J. 1969: Observations et interpretations nouvelles sour les bauxites de l'Ariege. – Ann. Inst. Geol. Publ. Hung. LIV, 3. pp.
- Desrochers, A., J.P. Noel 1985: Early Paleozoic Surface and Subsurface Paleokarst. Middle Ordovician Carbonates, Mignan Islands, Quebec. – Unpubl. Ph.D. thesis, Memorial of Univ. New Founland.
- Grigorescu, D., E. Avram, N. Anastasiu, Gr. Pop 1990: International symposium of non marine Cretaceous formations from Roumania. – Inst. of Geology, Romania
- Ianovici, V., V. Stiopol, E. Constantinescu 1979: Mineralogie. – Ed. didactica si pedagogica pp. 562–566.
- Jacota, Gr., S. Minzatu, Al. Cocis, E. Tanasuica 1970: Raport geologic asupra lucrarilor de explorare geologice din zona SE a regiunii Ohaba-Ponor. – Arh. I.G.G. Bucuresti, 3,
- Papiu, V.C., S. Minzatu, N. Iosof 1971: Acatuirea chimico-mineralogica a formatiunilor bauxitifere den bazinul Hateg. – D.S. Inst Geol., Bucurest, LVII, 2, pp.
- Sandulescu, 1984: Geotectonica Romaniei. – Ed. Tech. Bucuresti pp. 209–224.
- Stilla, A. 1977: Bauxitele de la Ohaba-Ponor. – D.S. Inst Geol., Bucuresti, LXIV. pp.
- Szantner, F., J. Knauer, A. Mindszenty 1986: Bauxitprognózis. – Veszprém Committee of Hungarian Academy of Sciences. (in Hungarian). Veszprém, pp. 60–65.

Concentrations of rare earths in Greek bauxites

Magda Laskou

University of Athens, Department of Geology

Bauxite samples collected from the Pelagonian, Subpelagonian, Gavrovo–Tripolitsa, Vardar and Parnassa–Ghiona zones were analyzed for major and trace elements, including rare elements (REE), using X-ray fluorescence and ICP/MS methods. Also, the mineralogical composition of the bauxite ores was determined by a combination of microscopic, XRD and DTA examinations.

The total REE content ranges from 147 to 560 ppm, the average being 325. The concentration of REE are characterized by the following order: Ce, La, Nd, Pr, Sm, Gd, Dy, Er, Y, Eu, Ho, Tb, Lu, Tm. A statistical analysis indicates a strong mutual relationship among all the REE. Cerium is the dominant element and accounts for about 42% of the REE. Lanthanum content is high, too. Thus Ce and La contents seems to regulate the bulk concentration of Σ REE. The rare earth elements are correlated directly with iron. Bauxite samples with a low Fe₂O₃ content show a low REE content, too. It seems likely that the REE content and distribution have been strongly influenced by diagenesis.

Relationship between the REE content in the studied bauxites and their age and also their geological position is evident.

Key words: Greece, bauxite, trace elements, rare elements

Introduction

The Greek bauxite deposits are included in the Mediterranean karst bauxite belt. They are hosted within carbonate rocks and has been created during four different geological ages.

Detailed investigations of bauxite deposits of various iron content, which are found in the eastern, central or western part of Greece were made by many investigators.

The studied bauxite samples were collected from bauxite deposits that belong to different geographical districts, different geological zones of various age, in order to obtain a detailed view of possible trends. The samples were collected from the Amorgos (Marmarenia), Atalandi (Anthochori), Glifa (Petalada), Nafpactos (Klokova), Parnasse–Ghiona, Pilos (Kordella), Smerna (Kaifa), Skopelos (Panormo) and also Chalkidiki peninsula (Petalona).

For the purpose to evaluate the rare elements distribution in Greek bauxites and to compare their compositions available from other places and also to study the physicochemical conditions of bauxite formation, the mineralogical composition and major and trace elements, including rare elements (REE), were determined.

Address: M. Laskou: Panestimiopolis, Ano Ilisia Gr–157 01 Athens, Greece

Received: 2 October, 1991.

General geological setting

The analyzed bauxite samples were collected from karstic deposits and occurrences belonging to various geotectonic zones of Greece (Fig. 1).

Detailed description of the geology of the studied deposits were presented by many investigators: Papastamatiou et al. (1940); Marinos (1954); Aronis (1955); Aubuin et al. (1958); Kiskyras (1972); 1983, Marinos (1958); Papastamatiou (1960, 1963); Celet (1962); Marinos et al. (1962); Tataris (1963); Maratos (1967); Aubuin (1970); Ferriere (1977); Fytrolakis and Papanikolaou (1981); Christaras (1986); Valetou et al. (1987) and others.

In the present study only a short review of geological setting of the studied deposits is presented. The studied bauxite deposits from the area of Atalandi (Subpelagonian zone) belong to the lower bauxite horizon. On the basis of geological and paleontological data on the carbonates hosted bauxite occurrences at the areas of Glifa and Skopelos (all in Pelagonian zone) they are also considered



Fig. 1
Sketch map showing the tectonic zones of Greece (Aubuin 1958) and the localities of the studied bauxite ores

to belong to the lower bauxite horizon. Recent geological study of the Amorgos Island revealed that at the Krikela area within neritic limestones of Upper Cretaceous–Middle Eocene age, bauxite deposits were found. The analyzed bauxite sample from Parnasse–Ghiona geotectonic zone belong to the third bauxite horizon. The bauxite ores from the Chalkidiki peninsula (Katsika area), which belong to the Vardar zone are overlain by Upper Cretaceous limestones and underlain by limestone of probably Low Cretaceous–Upper Jurassic age. Regarding the bauxite occurrences in the western Greece, they are of Eocene age and besides their small thickness they are widespread within limestones of the Gavrovo zone.

Analytical methods

All the selected samples have been prepared for analysis and study by crushing and grinding to pass 200 mesh ASTM sieve.

Mineralogical studies included 1) identification of the minerals by X-ray diffraction methods, 2) and by techniques of thermal analysis, 3) examinations, using petrographic or reflecting microscope. For the X-ray diffraction investigations a Philips PW 1010 apparatus and Cu $K\alpha$ radiation have been used in the University of Athens. Thermal analysis has been carried out using Derivatograph D–1500 with Thermo–Gas–Titrimetric equipment of the Hungarian Optical Works, in the University of Athens (J. Paulik and F. Paulik 1981, Paulik et al. 1982).

Chemical analyses for major and trace elements of the selected samples were done by X-ray fluorescence methods following the method of Brown et al. (1973), using a Philips PW 1450 apparatus, in the University of Manchester, England. Determinations of the rare elements were made by ICP/MS method. The analytic work was done in X-ray Assay Laboratories, Canada.

Mineralogical composition

Detailed investigations of bauxites from the areas of Atalandi, Glifa and Skopelos were made by Laskou (1981) and Laskou et al. (1983). The present study includes also samples collected from the areas of Amorgos, Chalkidiki, Parnasse, Nafpactos, Pilos and Smerna (Fig. 1).

The minerals can be grouped as follows: diaspore, boehmite (aluminium oxides and hydroxides), hematite, goethite, chromite (iron oxides and hydroxides), anatase, rutile, ilmenorutile (titanium oxides and hydroxides), chloritoid, kaolinite, halloysite, chamosite, clinochlorite, paragonite, illite (silicates), alunite (sulphates).

Thus diaspore or boehmite is the principal aluminium mineral in all these areas except Skopelos which is characterized by an abundance of chloritoid or illite (Table 1). In addition the presence of fine grained sulphates and chromite in bauxite from the area of Skopelos is common.

The samples of Skopelos are metamorphised. These deposits have been affected by a low grade metamorphism.

Table 1
Mineralogical composition of bauxite ores from Greece

Samples	Location	Geo-tectonic zone	Mineralogical composition
N.R-2	Nafpactos	G	dia. + goeth. + anat. + hem.
SM. PM-1	Smerna	G	dia. + hem. + anat.
PKORD-1	Pilos	G	boeh. + goeth. + anat. + hem. + cham.
A. MARM-III ₂	Amorgos	Pl	dia. + hem. + ilm. + rut. + kao. + goeth. + kao. gibbs. + ill
CH.K-2	Chalkidi	V	anat. + cham. + dia. + hem. + goeth. + rut. + ser.
P.B-3	Parnasse	Pk	anat. + dia. + goeth. + hem. + rut.
ANTH.-4D	Atalandi	Sb	boeh. + hem. + anat. + goeth.
G.T-6	Glifa	Pl	dia. + ilm. + anat. + rut. + ill. + goeth. + hall.
S.P.-8	Skopelos	Pl	chld. + hem. + dia. + rut. + alun. + chromite + gibb. + kao. + parag.
S.P.-1	Skopelos	Pl	ill. + ser. + sap. + cham. + hem. + anat. + rut. + alun. + chrom. + dia.

Representation of data

An earlier published information on chemical composition (major and trace elements) from the areas of Atalandi, Glifa and Skopelos was given by Laskou (1931), Laskou, F. Paulik, J. Paulik (1983). It was followed a summarization on platinum group elements (PGE) plus gold by Laskou and Economou (1990).

A representative analyses of samples from all the localities (Table 2) revealed that chemical composition of these bauxite deposits are various. According to the enrichment of the Fe₂O₃ in the bauxite samples, red bauxite samples and low iron bauxite samples were distinguished. The samples from Skopelos are both red or green coloured. Also, based on the chromium and nickel content three groups can be distinguished: a) bauxites which are characterized by a relatively low Cr and Ni contents, b) bauxites which are characterized by high Cr and low Ni, c) bauxitic laterites from Skopelos Island with high Cr and Ni contents (Table 2).

It is obvious that on the basis of all major oxides as well as Cr and Ni the Skopelos samples (Table 2) resemble to bauxitic laterites of Locris area (Valeton et al. 1987). In addition the Skopelos samples show as high as 3.7 wt. % Na₂O and relatively a high copper content (about 400 ppm Cu).

The concentrations of REE in parts per million in the analyzed bauxitic samples are given in Table 3. The values of Σ REE (Σ LREE/ Σ HREE) (where Σ LREE is the sum of the abundance of La, Ce, Pr, Nd, Sm and Eu and Σ HREE is the sum of the

Table 2
Chemical composition of bauxite ores from Greece

Wt %	1	2	3	4	5	6	7	8	9	10
SiO ₂	3.17	5.65	7.22	6.06	1.50	11.56	38.03	331.75	0.71	20.1
Al ₂ O ₃	53.66	48.39	59.81	54.80	59.40	65.14	35.32	34.34	58.1	46.3
Fe ₂ O ₃	25.11	28.37	12.93	22.42	24.34	4.22	10.69	21.87	26.9	16.2
MnO	0.05	0.02	0.09	0.05	0.04	0.17	0.25	0.22	0.02	0.02
MgO	0.08	0.06	0.09	0.09	0.12	0.10	2.39	0.75	0.26	1.18
K ₂ O	0.27	0.55	0.21	0.19	0.10	1.11	0.98	0.10	0.01	1.54
Na ₂ O	0.00	0.04	0.00	0.87	0.44	1.08	3.69	3.14	0.01	0.31
TiO ₂	3.11	3.00	4.01	3.60	2.42	4.03	2.63	1.96	2.87	2.10
CaO	0.09	0.10	0.11	0.11	0.98	-	0.06	0.06	0.05	0.75
P ₂ O ₅	0.08	0.06	0.05	0.07	0.05	0.00	0.00	0.00	0.06	0.12
L.I.	14.43	13.50	15.15	11.21	11.55	12.64	6.12	5.60	11.1	11.5
ppm										
Nb	100	90	100	80	100	120	50	50	80	50
Zr	750	700	680	550	660	1160	430	390	680	470
Sr	404	225	308	32	150	60	80	50	10	65
Zn	210	274	130	350	-	30	120	140	60	510
Cu	50	115	70	4	90	90	430	400	10	10
Ni	445	600	570	200	410	90	2350	1880	250	120
Cr	3090	1835	2923	480	460	440	1820	1740	1180	230
V	590	510	380	100	190	740	420	470	280	155
Ba	30	50	40	70	110	-	-	-	180	240
Sc	20	30	20	60	75	50	50	50	30	23

Symbols: 1. Nafpactos, 2. Smerna, 3. Pilos, 4. Amorgos, 5. Atalandi, 6. Glifa, 7, 8. Skopelos, 9. Parnasse-Ghiona, 10. Chalkidi

Table 3
Rare element concentration in bauxite ores from Greece

Element	1	2	3	4	5	6	7	8	9	10
Y	59	9	17	34	46	14	39	22	51	61
La	119	47.9	45.1	117	89.9	18.7	47.6	53.3	15.8	88.7
Ce	176	69.7	71.5	239	222	71.8	110	86.6	221	173
Pr	18	8.4	9.1	23.4	18.3	5	12	10.3	4.4	17.8
Nd	63.1	27.0	29.8	98.3	69	20	52.9	39.9	17.3	69.7
Sm	9.4	3.0	3.5	14.2	12.6	3.8	13.4	7.1	4.4	12.9
Eu	2.3	0.55	0.82	2.7	2.78	1.05	3.29	2.35	1.38	3.57
Gd	9.3	1.8	2.6	9.8	11.60	2.8	12.5	6.8	4.1	9.8
Tb	1.4	0.2	0.4	1.3	1.8	0.4	1.9	0.9	1.9	1.5
Dy	8.7	1.6	2.9	7.2	10.7	3.1	10.6	5.5	6.6	10.9
Ho	1.82	0.36	0.66	1.53	2.12	0.68	1.98	0.91	1.82	2.61
Er	5.3	0.9	1.9	4.7	6.3	1.9	5.3	2.3	5.3	7.8
Tm	0.6	0.1	0.2	0.6	0.8	0.2	0.6	0.1	1.0	1.2
Yb	4.7	1.2	2.5	5.4	5.8	2.8	4.6	1.5	5.7	7.6
Lu	0.69	0.22	0.42	0.85	0.85	0.46	0.64	0.24	0.79	1.04
REE	479.31	171.93	188.4	559.98	500.55	146.69	316.31	239.80	342.28	469.12
La/Lu	172.5	217.7	107.4	137.6	105.8	40.7	74.4	222.1	20	85.29
ΣLREE	387.8	156.55	159.8	494.6	414.6	120.35	239.19	199.55	264.28	365.67
ΣHREE	91.52	15.38	28.58	65.38	85.97	26.34	77.12	40.25	27	42.45
ΣLREE										
ΣHREE	4.24	10.18	5.59	7.57	4.82	4.57	3.1	4.96	9.79	8.61
Tb/Yb	1.89	1.87	1.51	1.19	1.30	0.9	0.9	1.34	0.33	0.20
La/Yb	25.3	39.9	18.04	21.66	15.5	6.68	10.34	35.5	2.77	11.67
La/Nd	1.88	1.77	1.51	1.19	1.30	0.94	0.90	1.34	0.91	1.27
La/Sm	12.66	15.97	12.89	8.24	7.13	4.92	3.55	7.5	3.59	6.88
Ce/La	1.48	1.46	1.59	2.04	2.47	3.80	2.31	1.6	1399	1.95
Eu/Sm	0.24	0.18	0.23	0.19	0.22	0.28	0.24	0.33	0.31	0.28

Symbols: for numbers see Table 2; * ΣLREE = La + Ce + Pr + Nd + Sm + Eu, **ΣHREE = Gd + Tb + Dy + Ho + Er + Tm + Yb + Lu

abundance of Gd, Tb, Dy, Ho, Er, Tm, Yb and Lu) and also the ratios Tb/Yb, La/Yb, La/Nd, La/Sm, Ce/La, Eu/Sm and the variation in the ratio of light REE to heavy REE (3.1 to 10.18) is given in the Table 3, too.

Generally the total REE content vary from one deposit to the other and ranges from 147 ppm to 560 ppm. The average value of the red bauxite samples with high iron content is 387 ppm. The content in grey sample, from Glifa deposit, with low iron content is 147 ppm and the average value of the bauxitic samples from Skopelos with intermediate iron content is 278 ppm.

In the analyzed samples Ce is the dominant rare element and accounts for about 42% of the Σ REE. Generally Ce and La contents seems to control the bulk concentrations of Σ REE.

Also the chondrite rare elements concentrations used to normalize the sample data. These data are plotted in a logarithm scale versus a linear scale of atomic number (Fig. 2). In this figure it is seen that the REE-patterns vary with a marked enrichment in light REE as compared to the heavy ones. The larger depletion for Tm and Tb is obvious. Also the bauxite samples show a low Eu content compared with the other REE which are pronounced by the more or less negative anomalies presented in the chondrite-normalized REE distribution patterns of the samples. Positive anomalies for Ce, Pr, Sm and Gd were found in some samples. It seems likely that the above differences are not correlated with the degree of metamorphism since they are observed in bauxite occurrences of low or without metamorphism.

The calculations of the correlation coefficients (r) between the rare elements emphasize a strong mutual relationship among all the Σ REE. Generally, the rare earth (Σ REE) show a positive correlation with Fe_2O_3 ($r = 0.47$), CaO ($r = 0.49$), P_2O_5 (0.52), Zn ($r = 0.58$) and negative correlation with V ($r = -0.68$) and MnO ($r = -0.45$).

The higher Σ LREE/ Σ HREE ratio in the green sample of Skopelos may indicate that Σ HREE removed in preference to Σ LREE in accordance with the concentration of Fe_2O_3 . Regarding the heavy REE in the same sample the decrease is progressively more intense from Gd to Lu. Y and Sm are also more decreased than the other LREE but La is enriched in the green sample from Skopelos.

In the case of the Glifa deposit, the iron was strongly leached out and the REE were also strongly depleted.

Discussion

Given that the HREE are preferentially removed under alkaline and weakly alkaline conditions (Goldschmidt 1958, Vlasov 1966, Rakama and Sahama 1968) and that differification is attributed to the alkalinity of the environment "caused by the presence of limestones" (Kiskyras 1983), it seems likely that bauxites with lower REE concentrations and lower iron content (Tables 2, 3) may have formed by a process of partial leaching of iron. Thus, the differences in the distribution of the REE among samples from the area of Skopelos, reflect the different removal of the absorbed REE under acid to alkaline conditions.

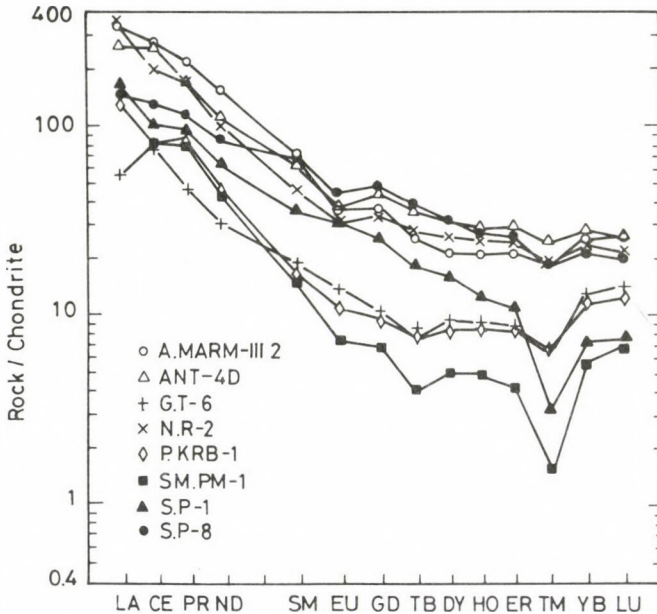


Fig. 2
Chondrite normalized REE
patterns in bauxite from
Greece.

The Glifa bauxite samples which are strongly iron depleted are also strongly depleted in Σ REE (LREE \sim 120 ppm, HREE \sim 26 ppm). Such a difference may suggest that an acidic or interchanging environment rather than alkaline–earkly alkaline was responsible for the composition of the Glifa samples.

Thus, generally the characteristic differences of Σ REE distribution in intermediate in Fe_2O_3 bauxitic laterites from Skopelos and the lowest concentrations of REE in white bauxite samples from Glifa, clearly shown that these were not formed under the same conditions as the red ones.

Finally, the geochemistry and diagenetic changes in Eh–pH seems directly applicable to the explanation of the REE-patterns (Fig. 2), but in accordance with the concentration of initial REE content in the parent rocks and the ground water, too.

Also it is seen that the REE abundances in bauxitic samples of the third bauxite horizon are considerable higher than those in the other horizons.

Conclusions

1. The (Σ REE / Σ HREE) ratio varies intensively from one deposit to the other and from one sample to the other inside the same deposit, too.

2. In the studied bauxites, the lowest REE contents are obtained from samples with the lowest Fe_2O_3 content. In general the available data suggest the concentrations of REE are affected by diagenesis.

3. The behaviour of LREE or HREE is a good diagnostic factor for the determination of the environment (Eh-pH) of bauxite formation.

4. The variation of the REE concentrations in bauxitic samples from b1, b3 and b4 bauxite horizon showed that the average of Σ REE; in b1 and b4 horizons are lower than that of the b3 horizon.

Acknowledgements

The author is particularly grateful to Prof. M. Economou for the helpful discussions and the constructive comments.

References

- Aronis, G. 1955: Geographical distribution, geological placing and aspects on the genesis of the Greek bauxite. – Bull. of the Geol. Soc. of Greece, II, pp. 55–79.
- Aubuïn, J., J.H. Brunn, P. Celet, 1958: Les massifs du Klokova et Varasova (Akarnanies). – Ann. Geol. P. Hell., IX, 6, pp. 256–259.
- Aubuïn, J., M. Bonneau, P. Celet, J. Charvet, B. Clement, J. Degardin, J. Dercourt, J. Ferriere, J. Fleury, C. Guernet, H. Maillot, J. Mania, J. Mansy, J. Terry, F. Theibault, P. Tsollias, J. Verriez 1970: Contribution à la geologies Hellenides: le Gavrovo, le Pinde et la zone ophiolitique subpélagonienne. – Ann. Soc. Geol. 4, pp. 277–306.
- Brown, C., D. Hughes, J. Esson 1973: New X–R–F data retrieval techniques and their application to U.S.G.S. Sranard rocks. – Chem. Geol. Amsterdam, II, pp. 223–229.
- Celet, P. 1962: Contribution à l'étude géologique du Parnasse–Ghiona et d'une partie des regions meridionales de la Grece continentale. – Ann. Geol. Pays Hell., 13, p. 446.
- Christaras, B. 1986: La chamosite, un composant des bauxites du mont Katsika, Chalcidique, Greece. – Bull. Geol. Soc. Greece, XXI, pp. 9–14.
- Ferriere, J. 1977: Le secteur meridional di massif metamorphique de Thessalie le massif du Pelion et ses environs. – VIth Colloquium on the geology of Aegean Region. Proceedings, I, pp. 291–309
- Fytrolakis, N., D. Papanikolaou, A. Panagopulos 1981: Stratigraphy and structure of Amorgos Island, Aegean sea. – Annl. geol., XXX, 2, pp. 455–472.
- Goldschmidts, V. M. 1958: Geochemistry. – Oxford University Press.
- Kiskyras, D. 1972: Geotectonic zones in Greece. – Bull. of the Geol. Soc. of Greece, IX, 2, pp. 93–110.
- Kiskyras, D. 1983: About the favourable conditions for the bauxite deferrification and the problem of the white bauxites in Greece. – Leaching and diffusion in rocks and their weathering products. Theophrastus Publications, pp. 441–469, Athens.
- Laskou, M. 1981: Mineralogy, Geochemistry and Genesis of some karst type bauxite deposits from eastern greece. – Ph. D. Thesis, Athens.
- Laskou, M., M. Econoou 1990: Platinum group elements and gold concentrations in Greek bauxites. – Geol. Balcanica, 21, 2, pp. 65–77.
- Laskou, M., F. Paulik, J. Paulik 1983: Contribution to the knowledge of bauxite deposits in the Locrida, Greece. – Travaux. 13, 18, pp. 72–84.
- Maratos, G., K. Rigopoulos, A. Athanasiou 1967: Two geological maps of Atalandi and Elatia. – Inst. Geol. Subsurf. Res. Athens.
- Marinos, G. 1954: Geological Reconnaissance of Bauxite on the Island of Amorgos. – Inst. Geol. Subsurface Res. Athens. Geological Reconnaissance, 16, p. 10.
- Marinos, G., M. Reichel 1958: The fossiliferous permian in Eastern Continental Greece and Euboea. – Inst. Geol. Miner. Exploration. The Geology of Greece. 8. p. 16.
- Marinos, G., J. Anastopoulos, G. Maratos, N. Melidonis, B. Andronopoulos 1962: Geological map of Almiros. – Inst. Geol. Subsurf. Res. Athens.

- Papastamatiou, I. 1960: La géologie de la région montagneuse du Parnasse-Ghiona-Oeta. – Extr. Bull. Soc. Geol. France 7e. 2, pp. 398–409.
- Papastamatiou, J. 1963: Les bauxites de l'île de Skopelos (Sporades du Nord), – Bull. Geol. Soc. Greece 5, pp. 52–74.
- Papastamatiou, J., G. Marinos 1940: Untersuchungen über den Geologischen Ban der Nord-Sporaden. – Prakt. Acad. of Athens, 15, pp. 344–346.
- Paulik, J., F. Paulik 1981: Simultaneous thermoanalytical examination by means of the derivatograph, in Wilson's Comprehensive Analytical Chemistry, Amsterdam.
- Paulik, J., F. Paulik, M. Arnold 1982: Influence of the Special Experimental Conditions Established by Quasi-Isothermal Quasi-Isobaric Thermogravimetric Technique on the Kinetics and Mechanism of Thermal Decomposition Reactions. – Journal of Therm. Analysis, 25, pp. 327–340.
- Rakama, K., Th. Sahama 1968: Geochemistry. – The Univ. of Chicago Press.
- Tataris, A. 1968: The Middle Eocene Bauxites of the Tripolitza Zone and the Tectonic Events within the Eocene. – Bull. of the Geological Soc. of Greece, V, 2, pp. 36–58.
- Valeton, I., M. Biermann, R. Reche, F. Rosenberg 1987: Genesis of nickel laterites and bauxites in Greece during the Jurassic and Cretaceous and their relation to ultrabasic parent rocks. – Ore Geology Reviews, 2, pp. 359–404.
- Vlasov, K. 1966: Geochemistry of Rare Elements. – Israel Program for Scientific Translations Ltd., I, p. 688. Jerusalem, Israel.

Remarks on the genesis and ore-dressing of the alluvial bauxite occurrences of Parnass–Ghiona–Elikon (Greece)

Andreas Vgenopoulos

*National Technical University
Department of Mining and Metallurgical
Engineering, Athens*

K. Daskalakis

*Ethnikis Amynis
Athens*

Introduction

The alluvial bauxites which are abundant in the Parnass–Ghiona zone are product of weathering of initial bauxite deposits. The grain size of 80% bauxite is 70 μm . The disintegration of the binding material of the bauxite is due to rainwater and to temperature changes (day/night) which bring about contraction and expansion at the material. Thus separation of diaspor-boehmite takes place due to their great solubility in the prevailing low pH environment and diaspor-boehmite are transported by rainwater and are widely distributed. In contrast kaolinite and partly hematite which are less soluble in low pH remain in place with the result to have a high content of SiO_2 in alluvial bauxite and which can reach 36–40%.

In the alluvial bauxites of the mentioned occurrences it has been found that the non-altered, coarse grained parts of the bauxite maintain their initial mineralogical composition, in contrast the altered portions show changes in their mineralogical composition, we have an increase in silica and kaolinite also the initial diaspor is changed to a semi-amorphous material and a great portion is changed into gibbsite. Haematite is altered to goethite.

A typical Granulometric analysis of an Alluvial Bauxite is shown in Table 1.

Comparable changes have been determined in the B3 bauxitic horizon, in which case too, the fine grained parts contain a greater portion of SiO_2 and CaO and a smaller content of Al_2O_3 as compared with coarse grained parts.

In this case only a material transfer took place due to structural destruction, but no mineralogical change was observed.

On the basis of the above observations a number of crushings and sievings have been carried out in a number of bauxite occurrences with an aim to determine whether we have "release" of minerals.

Addresses: A. Vgenopoulos: National Technical University, 42, Patission Str. 106 82 Athens, Greece

K. Daskalakis: Ethnikis Amynis 1, 155 69, Papagou, Athens, Greece

Received: 12 December, 1991.

Table 1

The material originates from the third bauxitic horizon and passed through jaw-crusher exit opening of 45 mm. The sieving was executed by means of water.

Granulation, mm			SiO ₂				Al ₂ O ₃				CaO			
	%	Cum. weight	%	Metal units	Recovery	Cum. recovery	%	Metal units	Recovery	Cum. recovery	%	Metal units	Recovery	Cum. recovery
+63	2.3	2.3	1.44	3.312	1.4	1.4	62.6	143.98	2.5	2.5	0.2	0.46	0.36	0.36
63-45	9.9	12.2	0.9	8.91	3.78	5.18	61.9	612.8	10.6	13.1	0.3	2.97	2.38	2.74
45-31.5	14.1	25.3	0.4	5.64	2.39	7.57	61.8	871.3	15.7	28.27	0.3	4.23	3.4	6.114
31.5-22.4	11.1	37.4	0.4	4.44	1.88	9.45	60.5	671.5	11.69	39.96	0.3	3.33	2.67	8.81
22.4-11.2	21	58.4	0.7	14.7	6.23	15.68	60.3	1266.3	22.4	62.0	0.5	10.5	8.44	17.25
11.2-3.0	22	80.4	0.7	15.4	6.53	22.21	59.8	1315.6	22.89	84.89	0.5	11	8.84	26.09
3.9-1.0	8.0	88.4	3.1	24.8	10.52	32.73	56.0	448	7.8	92.69	0.9	7.2	5.78	31.87
1.0-0.5	2.9	91.4	6.6	19.14	8.12	40.85	53.2	154.2	2.68	95.37	3.1	8.99	7.22	39.09
0.5-0.00	8.6	100	16.2	139.3	59.12	100	30.2	259.7	4.52	100	8.8	75.68	60.85	100
	100		2.3	235.6	100	-	57.4	5743.4	100	-	1.2	124.3	100	-

The results of a representative test are shown in Table 1. The crushing has been made in jaw-crusher and the sieving with the help of water.

The results of these tests show that we have an enrichment of SiO_2 and CaO in the fine grained parts in comparison to the coarse grained in which, in contrast, we have an enrichment of Al_2O_3 .

Table 1. further shows that from the bauxite with an initial composition of Al_2O_3 : 57.4%, SiO_2 : 2.3% and CaO : 1.2% if the fraction – 0.5 mm is removed (which represents 8.6%) then the remaining will have the following composition: Al_2O_3 : 59.89%, SiO_2 : 1.02%, CaO : 0.51%.

In support of these tests microscopic observations showed that for grain-size below 60 μm there is a release of 100%. For the grain-size – 200 μm there is a corresponding release of 90% and for the grain size – 500 μm the release is 80%.

The fact that, during, this analysis, a structural destruction, as well as, a high release of Al_2O_3 was observed in – 100 micron part may conclude new methods of bauxite enrichment giving new aspects concerning the commerciality of Hellenic bauxites.

References

- Daskalakis, K., I. Mészáros, G. Rezessy, Z. Szóvényi, L. Szabadváry 1984–85: Travaux, Vols. 14–15.
Vgenopoulos, A.G. 1989: The Significance of paragenesis in Bauxites. – Theophrastus Publ. Athens,
In Book of weathering products Deposits. Vol. II.

Mineralogical and geochemical correlation between the different Tethyan bauxitic types

Andreas Vgenopoulos

National Technical University

Dept. of Mining and Metallurgical Engineering

Section of Geological Sciences, Athens

Introduction

The different mineralogical and chemical composition of the bauxites of the various horizons of the Tethys is connected mainly to the conditions of the bauxite formation or the conditions having prevailed after the bauxite formation (see Vgenopoulos 1984, 1985, 1986, 1987, 1989).

In order to understand all the bauxitic deposits of the Tethys, the presentation of all data in a table could facilitate the comparison and the interpretation of the differences which exist between them.

On this basis, in this work data from bauxites from Greece and Hungary are presented in tables which could be completed or revised according to the suggestions which will be made during the IGCP-287 meeting. Compare Tables 1 and 2.

Address: A. Vgenopoulos: National Technical University, 42, Patission Str. 106 82 Athens, Greece

Received: 12 December, 1991.

Akadémiai Kiadó, Budapest

Table 1
Geological situation and mineralogical composition of important Greek and Hungarian bauxites

	Location	Hanging wall	Minerals	Footwall
Greek bauxites	Florina b6	Tertiary	Gibb., boeh., he., goeth., kaol., an., (mu., tu., gy., fsp)	Triassic
	Pylos Klokova b5	Campanian	Pylos: boeh., goeth., goeth., an., chl Klokova: d, goet., an., kaol	Lutecian
	Euboea b4	Santonian- Campanian	D., he., ru., an., kaol., chl.	Upper Cretaceous
	Central Greece Parnas-Ghiona- Helicon, Kalidromon b3 alluvial	Surface	Unweathered: d., he., goeth., an. Weathered: gibb., q., kaol., an.	Upper Cretaceous
	b3	Upper Cretaceous	D., he., goeth., an.	Lower-Middle Cretaceous
	b2	Lower, Middle Cretaceous	Boehm., he., (d), goeth., an.	Upper Jurassic
	b1	Upper Jurassic	D., he., goeth., an., ru., (boehm)	Upper Triassic- Middle Jurassic
Hungarian bauxites	Csabpuszta	Middle Eocene	Gibb., boehm., he., goeth., an.	Cretaceous
	Gánt	Eocene	Boehm., gibb., goeth., chl., an., Upper Triassic	
	Iharkút	Cretaceous	Gibb., kaol., boehm., goeth., an. or boehm., gibb., he., an.	Triassic

Symbols: d. - diaspor, boehm. - boehmite, gibb. - gibbsite, he. - hematite, goeth. - goethite, an. - anatase, ru. - rutile, kaol. - kaolinite, q. - quartz, chl. - chlorite, mu. - muscovite, tu. - tourmaline, gy. - gypsum, fsp. - feldspars

Table 2
Chemical composition of various bauxitic horizons from Greece and Hungary

	b1	b2	b3	b4	b5	b6	Gánt	Iharkút	Csabpuszta
SiO ₂	1.8-12	1.2-8	1.7-7	1-2	1.5-10	15-30	10.5	5.8	3
Al ₂ O ₃	46-71	43-71	50-80	45-55	49-70	32-47	49.2	52.6	56
Fe ₂ O ₃	7-33	17-15	15-30	30-32	11-15*	16-18	20.5	23.6	23
					14-24**				
CaO	0.1-0.4	0.08-0.18	0.03-0.3	25-33	0.06-0.15	0.03-1	-	-	-
TiO ₂	0.7-3.0	0.8-2.6	1.8-2.9	2.8-3.2	2.3-3	1.2-2.3	2.8	2.3	2.6
H ₂ O	12-14	11.3-12.4	10-14	9-11	11-16	19-30	16.4	15.3	13.8

* Pylos, ** Klokova

References

- Ekonomopoulou, N., A. Vgenopoulos 1985: Mineralogical and Chemical Study of the Clokova (Aetoloakarnania) and Pylos (Messinia) Bauxites (in Greek). – Mineral Wealth Bd. 39.
- Ekonomopoulou-Kyriokopolou, N. 1991: A Comparative Geochemical and Mineralogical Study of Central Greece's bauxite horizons. (Diss. in Greek). – National Technical University. Dept. of Mining and Metallurgical Engineering, Section of Geological Sciences, Athens.
- Vgenopoulos, A.G. 1983: Tertiary gibbsitic bauxite from Florina N. Greece, Conclusions concerning the Genesis and possibilities of its industrial use, Habil. – Nat. Techn. Univ., Dept. of Mining and Metallurgical Engineering, Section of Geological Sciences, Athens.
- Vgenopoulos, A.G. 1984: Boehmit- bzw. Diasporgenese in Bauxiten in Abhängigkeit vom Redoxgleichgewicht. – Chem. Erde 43/84.
- Vgenopoulos, A.G. 1986: Some additional data about the genesis of boehmite resp. diaspore in the bauxitic outcrops of Kallidromon mountain in Central Greece. – Travaux 16–17, 2986/1988.
- Vgenopoulos, A.G. 1989: The significance of Paragenesis in Bauxites. – Theophrastus Publ. Athens, in Book of Weathering Products Deposits Vol. II.

Bauxite deposits related to the Tethyan Basins in Iran

M. Sharifi Nourian

F. Rahimzadeh, M. Ehsanbakhsh

Geological Survey of Iran, Tehran

Basic information on karst-bauxite deposits of Iran is presented. Upper Cretaceous bauxites are known in the Zagros Mts. Permian, Triassic and/or Lower Jurassic horizons were discovered in Central Iran. Permian and Jurassic bauxites were found in the Elborz Mts.

Key words: Bauxite, Upper Paleozoicum, Mesozoicum, Zagros Mts., Elborz Mts., Central Iran

Introduction

The political boundaries of Iran enclose a short section of the orogenic belt between the Arabian–African Unit in the South and the Asian block in the North.

The territory of Iran represents the continuation of the Alpine–Himalayan orogenic belt, of several thousand kms long extending from Europe through Yugoslavia, the Aegean sea, Turkey, Iraq, Iran, Afghanistan, the Hindukush Mts, the Pamir and Himalaya Mts., as far as the Brahmaputra river valley in India. In Iran there is the prolongation of the large Mediterranean bauxite province with geosynclinal type bauxite in France, Hungary, Yugoslavia, Greece and Turkey.

Bauxite occurrences in Iran were first mentioned in the work of Walther and Kursten (1958), which was a body of diasporite in Bulubulu at Kerman.

In 1966 bauxite prospection started by the Geological Survey of Iran. Samimi (1966) discovered bauxite in Middle Cretaceous Bangestan Limestone Group.

The Yazd bauxite occurrence was discovered by Valleh (1966), described by De Weisse (1967). The Dopolan deposits in High Zagros Mts was discovered by M. Sharifi Nourian (1967). The Semirrom clay deposit was discovered by Sharifi and Movahed (1966). The refractory clay of Robat-e-Khan (Tabas area) was discovered by Samimi, Sharifi and Ghasemipor (1970). Investigation of Sar-e-Fariab deposit was carried out by Strojexport–Geoindustria (Czechoslovakia) in 1976.

Explorations of Alumiran Co. were followed by Iran Bauxite Exploration Project (1982). Systematic exploration of bauxite by present project is as follows.

Abgarm area (Central Iran); preliminary exploration stage including: geophysical prospecting and exploratory tunnel drilling.

Yazd and Bukan area, geological prospections (preliminary stage) including sampling, trenching and chemical analysis of samples (Fig. 1).

Address: M. Sharifi Nourian, F. Rahimzadeh, M. Ehsanbakhsh: Geological Survey of Iran
P.O.Box 13185–1494 Tehran, Iran

Received: 15 December, 1991.

In all above-mentioned regions geological maps are prepared or scheduled to prepare (scale: 1 : 20 000 and 1 : 50 000).

All of present matters are based on previous works, but we need much more data to reply questions about paleogeography, sedimentology and alumosilicate deposition history.



Fig. 1
 Distribution of high alumina materials in Iran. 1. pre-Liassic bauxite; 2. pre-Liassic bauxite and clay; 3. pre-Liassic clay; 4. Cretaceous Bauxite; 5. Cretaceous clay; 6. capital

Geographic distribution, stratigraphic setting and mineralogical features of clay and bauxite deposits of Iran are shown in Table 1 (Fig. 2).

Based on stratigraphic situation of Iranian bauxites, the territory of Iran was divided to three main parts.

A. Zagros Mts.: In this area hiatus starts in the Cenomanian–Turonian. The Semirom bauxites and clays and the Sar-e-Fariab bauxite deposit occur in this hiatus. Bauxitic materials are covered by Santonian shale and argillaceous limestone (Figs 3, 4).

B. Central Iran: two or more (even 5) bauxitic horizons were discovered. These horizons are Triassic or Permian/Triassic and Liassic age, respectively.

C. Elborz Mts.: In this region one or two distinct bauxitic horizons are present. The first horizon belongs to the Carboniferous?–Permian hiatus. The second is Jurassic age (Sirjan belt–Bukan area)(Fig. 5).

Table 1
Information chart for some of the alumosilicate deposits of Iran

Area	Region	Age	Mineralogy	Bedrock	Cover	Description
Kuh-e-Nor	Zagros Mts.	Cenomanian–Turonian	boehmite hematite kaolinite	carbonate	carbonate	Samimi (1973)
Bukan	Sanandaj-Sirjan Belt	Upper Permian and Jurassic	diaspore hematite	carbonate	carbonate	Samimi (1971)
Do-Polan	Zagros Mts.	Permotriassic	diaspore boehmite alunite	carbonate	carbonate	Samimi and Sharifi (1969)
Mahabad	Sanandaj-Sirjan Belt	Permian	diaspore chamozite	carbonate	carbonate	Samimi (1963)
Semirom	Zagros Mts.	Turonian	kaolinite	carbonate	carbonate	Sharifi and Movahed (1967)
Yazd	Central Iran	Permian	diaspore anatase hematite	dolomite	shale	Sluiter (1967)
Kerman	Central Iran	Rhaetian	diaspore	dolomite	shale	Taghizadeh (1969)
Sar-e-Fariab	Zagros Mts.	Cenomanian–Turonian	boehmite kaolinite	carbonate	carbonate	Strojexport-Geoindustria Corp. (1972)

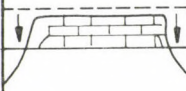
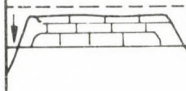
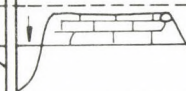
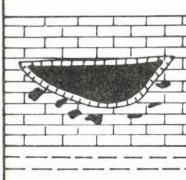
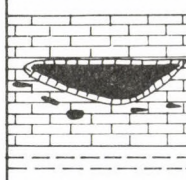
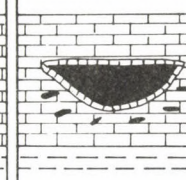
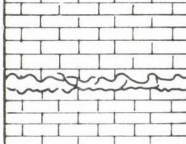
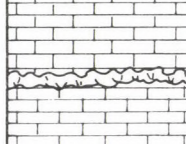
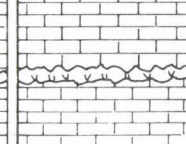
TYPE LOCALITY :		Zagros Mount.	Elborz Mount.	Central Iran
PROCESSES BRINGING ABOUT SUBAREAL EXPOSURE OF THE CARBONATE SUBSTRATE :				
		Sea level drop	Sea level drop	Sea level drop
IMPRINT ON STRATIGRAPHIC RECORD	BAUXITIFEROUS UNCONFORMITY WITH PREVAILINGLY SURFACE - KARST :			
	NON-BAUXITIC UNCONFORMITY WITH PREVAILINGLY UNDERGROUND KARST			
ANGULAR UNCONFORMITY :		NO	NO	NO
ESTIMATED DURATION OF EXPOSURE :		6-10 MY.	?	10 MY.
APPARENT STRATIGRAPHIC GAP :		Small	Small	Intermediate
RATE OF REGIONAL SUBSIDENCE :		Does not change across the unconformity	May change across the unconformity	Does not change across the unconformity
CHANGE IN LITHOFACIES OF ASSOCIATED CARBONATE AGROSS THE UNCONFORMITY :		Minor change ?	Major change	Major change
RECORD CONTEMPORARY SEA LEVEL CHANGES :		Direct evidence of oscillations in adjoining shallow water carbonate area	Only major sea level changes recorded	Only major sea level changes recorded
LITHOFACIES OF ASSOCIATED BAUXITE :		Rather homogenous prevailingly autoch./parautoch.	Heterogenous autoch./alloch.	Rather homogenous prevailingly autoch./parautoch.
UNDERLAYING KARST RELIEF :		Shallow	Shallow	Shallow
SUPPOSED SOURCE MATERIAL OF BAUXITE :		Carbonate residue	Dolomite residue	Carbonate residue
SUPPOSED SOURCE MATERIAL OF NON-BAUXITIC KARST FILLS		Carbonate residue	Dolomite residue	Carbonate residue

Fig. 2
Bauxitic materials and paleokarsts in Iran

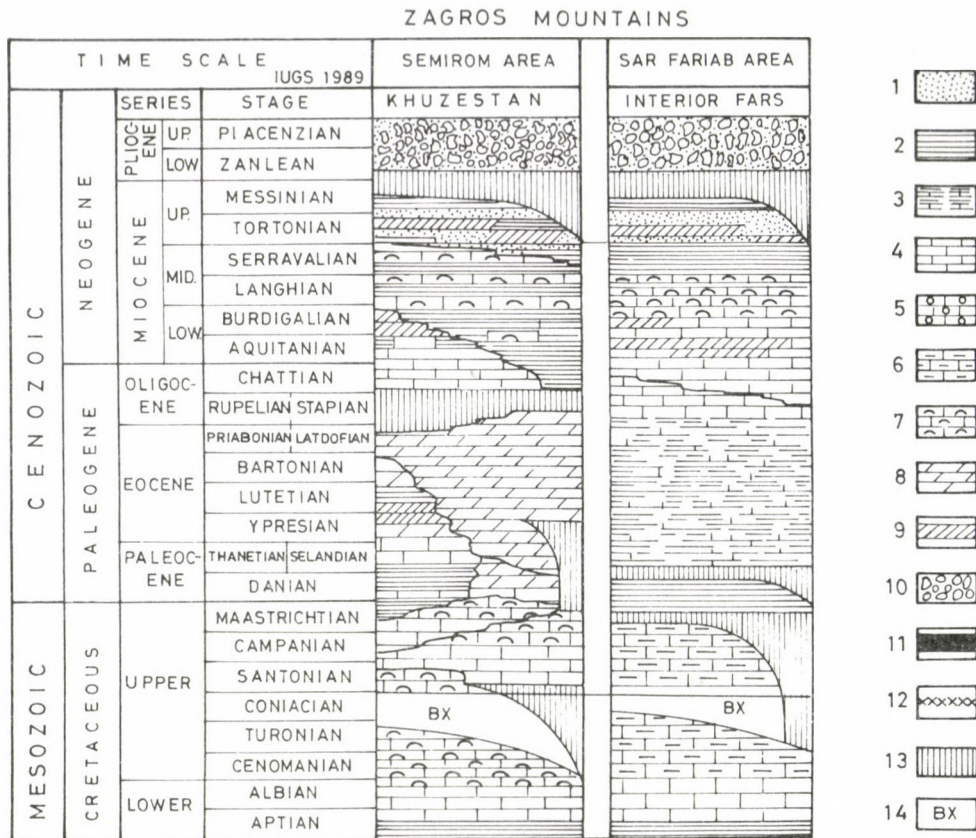
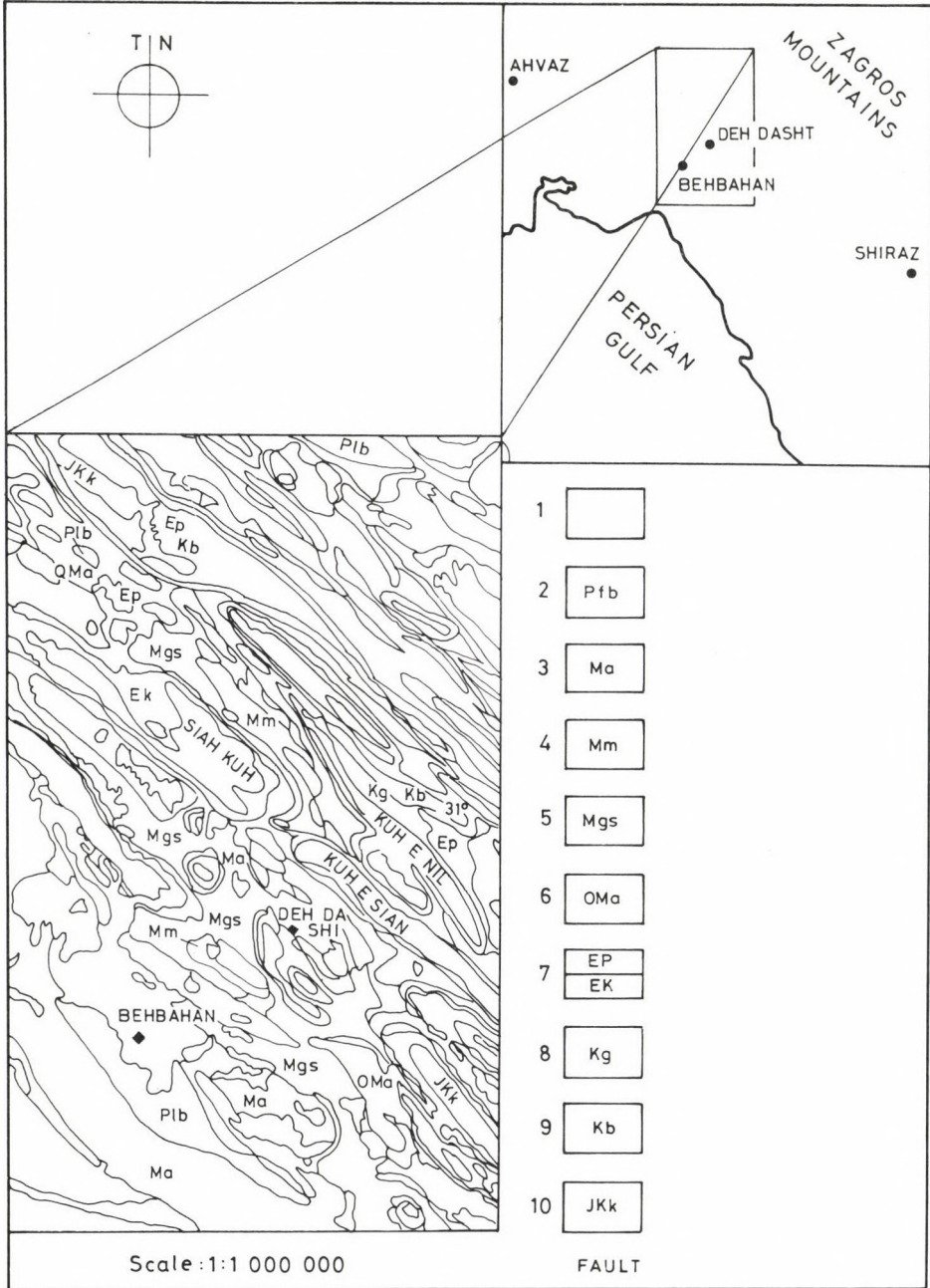


Fig. 3
The preliminary geohistory logs for Iranian bauxitic material deposits, Zagros Mountains. 1. sandstone; 2. shale; 3. calcareous shale; 4. limestone; 5. oolitic limestone; 6. argillaceous limestone; 7. shaly limestone; 8. dolomite; 9. gypsum; 10. conglomerate; 11. coal; 12. massive igneous rock; 13. erosional hiatus; 14. bauxitic material genesis and related hiatus

Fig. 4 →
Geological map of Zagros Mountains. 1. Quaternary; 2. Pliocene, Bakhtyari Fm.; 3. Miocene, Agha Jari Fm.; 4. Miocene, Mishan Fm.; 5. Miocene, Gachsaran Fm.; 6. Oligocene-Miocene, Asmari Fm.; 7. Eocene, Pabeh Fm., Eocene-Cretaceous; 8. Cretaceous, Gurpi Fm.; 9. Cretaceous, Bangestan Group; 10. Jurassic-Cretaceous, Khami Group



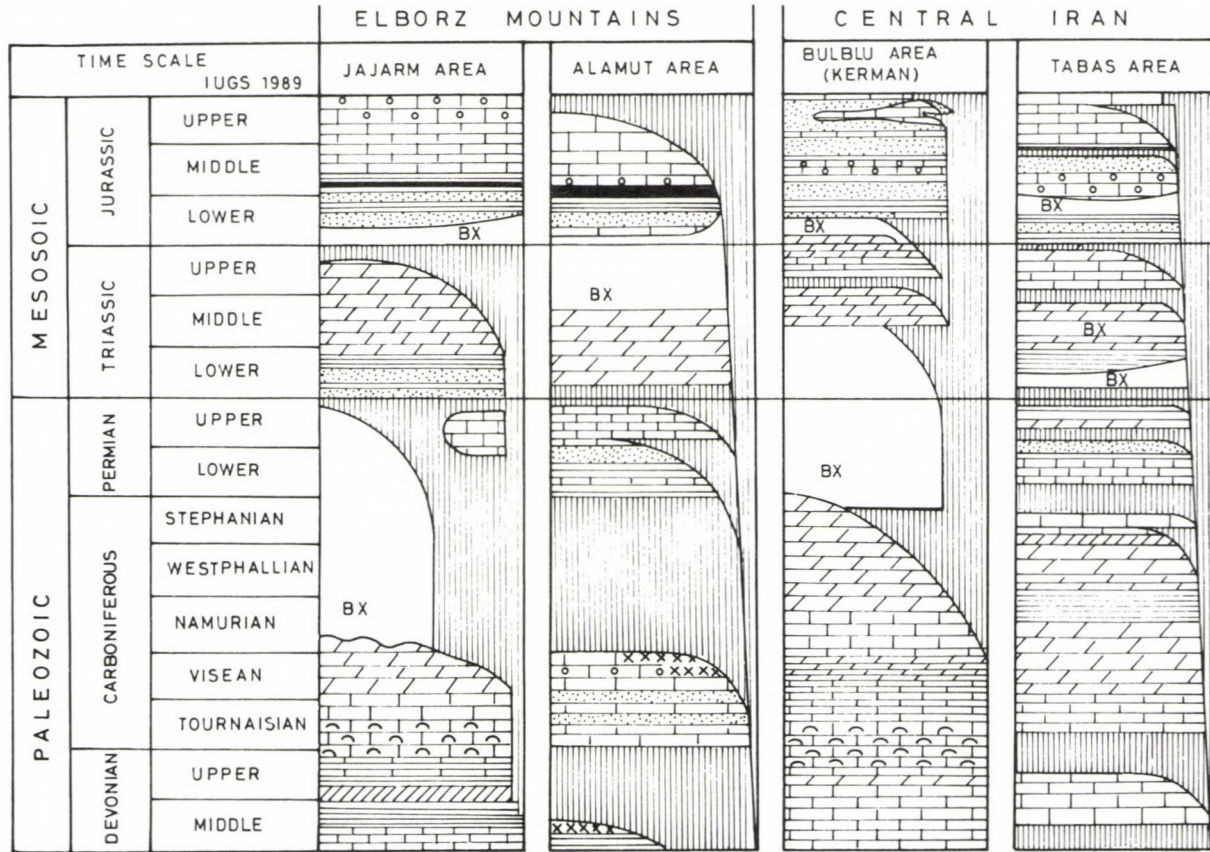


Fig. 5 The preliminary geohistory logs for Iranian bauxitic material deposits, Elborz Mountains and Central Iran. (For legend see Fig. 3)

Description of bauxite areas

The Sar-e-Fariab deposits

The region is situated in the High Zagros. It is a NW–SE trending range in the western part of Iran. Its Mesozoic–Cenozoic epicontinental sequence is a part of the sedimentary wedge of the NE part of the Arabian platform was folded during the Plio-Quaternary orogenic phase. Sar-e-Fariab is located at the boundary of the Khouzestan and Ckohluyeh provinces.

The origination of the bauxite deposits in the area is related to the hiatus between the Upper Cretaceous Sarvak and Ilam Formations.

The lateral extension of the bauxite horizon vary from 8–12 km, and average thickness is 1–2 m.

The bauxite bodies, are found in shallow karstic depressions of the underlying Sarvak Formation. They are lenticular and show an irregular zonation.

The bauxites were likely formed in situ by bauxitization of clayey shallow-water sediments under tropical climate.

From mineralogical viewpoint, the Sar-e-Fariab bauxites are monohydrates (boehmitic to boehmitic–kaolinitic), diaspore is secondary to accessory and gibbsite is scarce.

Geological setting: Area is located in the strongly folded subzone of the Zagros Mts. Four anticlinal units are found in this territory, namely Kuh-e-Nil, Mandon, Kuh-e-Delof and Kuh-e-Siah. Shear thrust and shifts are very common.

The folding structures usually manifest very well recognizable SW vergency, with steep, often structurally more complex SW flanks. Slight epirogenic movements were taking place. Faults and joint systems were formed

Lithology: Bedrock: thick bedded massive rudist limestone. Bauxite: boehmite-type. Cover: well bedded, grey and light grey, white, fine-grained argillaceous limestone, of deep water facies..

Biostratigraphy: Bedrock: *Peneroplis planatus*, *Rhipidionina-Casertana-Castro*, *Neoendothyra Appennica-castro*, Miliolitic foraminifers, mainly *Spiroloculina* sp., *Quinqueloculina* div. sp., Bauxite: No any fossils. Cover: Miliolid Foraminifera are predominant, mainly *Quinqueloculina*, *Minouxia* sp., *Rotalia* sp., *Ammobaculites* sp., *Dicyclina* sp., *Valvulammina* sp.

Age: Bedrock: Lower Cretaceous (top bed rock: Lower Turonian). Cover: Upper Cretaceous, (base of cover: Lower Santonian). Bauxite accumulation: Lower Turonian?

Bauxite petrology: The bauxite is pisolitic. Both, size and percentage of pisoles increase toward the center of the deposits. Marginal part of bauxite bodies are lighter. The bauxite matrix is very fine grained. Basic textural elements occurring in the matrix are ooids and pisoids which are spherical or oval. Larger pisoids often manifest radial and/or concentric inner jointing which usually filled with kaolinite.

Mineralogy: The principal aluminium bearing mineral is boehmite. Diaspore and gibbsite are accessories and rare. Other minerals are the kaolinite group, calcite, goethite, hematite, limonite.

Geochemistry: Chemical analysis are reported from several localities. Three representative analyses are as follow:

L.O.I.	SiO ₂	Al ₂ O ₃	Fe ₂ O ₃	TiO ₂	CaO	MgO	P ₂ O ₅	Na ₂ O	K ₂ O	MnO
12.95	5.06	61.41	18.40	1.95	0.10	0.07	0.18	0.02	0.02,	0.02
13.50	7.00	59.90	15.70	2.59	0.21	0.15	0.13	0.02	0.04	0.05
13.45	10.04	57.84	14.91	2.49	0.10	0.23	0.01	0.03	0.04	0.03

Genetic model: A genetic model is offered by Duda (1979). Briefly, this model states; "after sedimentation of Sarvak Limestone Formation in the neritic environment, epirogeny and sea regression produced shallow karst. Lake and lagoon sedimentation of clayey sediments was followed by regression, tropical climate and bauxitization. Some of this bauxite eroded after genesis and covered by sedimentation of Ilam (cover) due to sea transgression. Orogeny and erosion exposed the bauxite outcrops". This model is not unique. Some other theories were also offered for bauxite genesis.

Exploration: Regional geological maps (in a scale 1 : 1 000 000 and local maps in a scale 1 : 10000) are available. Magnetic and geoelectric geophysical methods have been used for the bauxite exploration in the Sar-e-Fariab region. All the bauxite bodies have manifested in anomalies from 8 to 150 gamma.

Reserves: Drilling works and samplings for calculation of reserves have been done. The reserves of the Sar-e-Fariab area are 759,087 tons in C2 category and are not sufficient for the industrial scale exploration and an alumina plant construction.

Jajarm deposit

The region is situated in the Eastern Elborz. It is a NW-SE trending range in the northeastern part of Iran. Its Mesozoic epicontinental sequence is a part of the Mesozoic sedimentary cycle. Elborz Mountains was folded during the Late Alpien orogenic phase. Jajarm area is located in the Khorasan Province. The origination of the bauxite deposits in the area is related to the hiatus between the Upper Triassic Elika and Shemshalk Formations.

The lateral extension of bauxite horizon is 12 km, average thickness is 8-10 m, the bauxite bodies are found in shallow karst depressions of the underlying Elika Formation. They are layered-type deposits. The bauxites were formed in situ by lateritization of clay shallow water sediment under tropical climate.

From mineralogical point of view, the Jajarm bauxites are trihydrates (diaspore, boehmite). Kaolinite and chamosite are secondary to accessory minerals.

Geological setting: The area is located in the southernmost part of a structural unit built up by several anticlines and synclines with general trend of ENE and

WSW. A thrust fault of 70 km long with NE to SW trend has effected the north limb of the Zoo anticline (where the bauxite zone is situated).

Lithology: Bedrock: thick bedded dolomite of 200 m thickness. Bauxite: diasporitic-type. Cover: coal-bearing shale and sandstone of shallow lagoonal facies

Age: Bedrock: Upper Triassic, bauxite: Triassic–Jurassic. cover: ?

Bauxite petrology: The bauxite is fine grain to oolitic. Pisolites occur very rarely. Within the deposits 3 rock-types can be distinguished: hard diasporic bauxite, clayey bauxite and kaolinite. The texture of the hard bauxite is oolitic to pisolitic. Maximum grain size is 2 cm. The pisolites are generally spherical or oval.

Mineralogy: The main Al-bearing mineral is the diaspore, whereas gibbsite is the secondary Al-mineral. Chamosite is the main silicate mineral. Other minerals are goethite and hematite and anatase.

Geochemistry: Based on chemical analysis of different samples, the average percentage as follows

L.O.I.	SiO ₂	Al ₂ O ₃	Fe ₂ O ₃	TiO ₂
7.13–13.32	4.0–14.3	41.3–69.2	2.0–31.2	2.3–5.7

Reserves: 19000kt (C2 = R3 category). On this basis an alumina plant is expected to be constructed.

Exploration: Geological maps on the region namely North Central Iran Koh-e-Kurkhud Quadrangle (scale 1 : 250000) and some detailed maps about the localities are available. Three geological sections (total length of 6200 meters) 26 trenches, boreholes (12 km) and geoelectric measurements were carried out.

Yazd area

The region is located in a NE–SW trending range in Central Iran. Its Upper Paleozoic and Mesozoic epicontinental sequence is a part of the of Upper Paleozoic – Mesozoic sedimentary cycle. The Central Iran mountains were folded during the Late Kimmerian orogenic phase. Dorbid is located at Yazd Province. The bauxite deposits in the area are related to the hiatus between Permian and Upper Triassic formations.

The lateral extension of the bauxite horizon is more than 10 km, average thickness is 2 to 4 meters, the bauxite bodies are found in shallow karst depressions of the underlying Permian formation. They are lenticular-shape deposits. The bauxites were likely originated by in situ lateritization–bauxitization of clay (residual soils postulated by Sluiter et al.) in tropical climate. From mineralogical point of view, the Yazd bauxites are trihydrate-type (diaspore, boehmite). Their clay minerals are chamosite, illite. Kaolinite is subordinate to accessory minerals.

Geological setting: The area is located in a rather strongly folded region, which has complicated structure. It seems to be likely that an overturn anticline is the major structural element with internal (secondary) folding.

The contrast in the lithological properties between the thick bedded footwall dolomites and the almost friable shales of the hanging wall caused various dislocations along their contact surface.

Lithology: Bedrock: well-bedded crystalline dolomite and marly dolomite. Bauxite: diasporic. Cover: originally dark-grey or black shale but due to weathering light-grey, white and red, respectively. Shallow lagoonal facies.

Biostratigraphy: Bedrock and bauxite: unfossiliferous. Cover: plant fossils (*Equisetum* sp.) and Lamellibranchs (*Pleuromya Unioites*, *Modiola*).

Age: Bedrock: Upper Permian, cover: Upper Triassic (Rhaetian).

Bauxite petrology: The bauxite is fine grain to pisolitic very rarely with concretions. Al-content increases towards the top of the bauxitic horizon.

Mineralogy: The main Al-bearing mineral is the diaspore, although boehmite is also occur. Chamosite is the main silica mineral. Other minerals are goethite-hematite, limonite, sometimes kaolinite.

Geochemistry: Results of chemical analyses of different samples (average percentage) are as follows

SiO ₂	Al ₂ O ₃	Fe ₂ O ₃	TiO ₂
1.2-14	41.1-58.2	3-36.2	4-7.2

Exploration: Geological maps of North Central Iran (scale: 1 : 1000000) and of the Ardakan Quadrangle area (scale: 1 : 250000) and maps of the bauxitic area (scale 1 : 50000 and 1 : 2000) are available.

Two geological sections (total length of 1800 m – 20 samples). 115 trenches (295 bauxite samples) 12 cuts (81 samples) and an exploratory tunnel of 5 meters long were carried out.

Reserves: According to geological reserve estimations (in class D), the workable reserves of NE Yazd are 2 million tons.

Do-Polan Area

The Do-Polan clayey bauxite deposit is located in Bakhtiari Province in the High Zagros. The bedrocks were deformed by the Hercynian and pre-Hercynian orogenic phases, and they were folded by the Alpien-Himalayan orogenic phases.

The deposits are sandwiched between carbonate rocks. Tops of bauxite bodies are smooth but their bottoms are irregular.

From mineralogical viewpoint, bauxite boulders are diasporic. Boehmite has been found in some samples. The clay minerals are represented by some illite. No chamosite has been detected. Amount of hematite and goethite is roughly equal anatase and rutile are present.

The kaolinite deposit is assumed to lie at, or close to the Permian-Triassic boundary. Near the top of the deposit there is a discontinuous layer of varying thickness (max 2 m), containing high percentage of bauxite boulders in a kaolinitic matrix. The boulders consist of a very hard light-grey finely pisolitic bauxite. Their Al-content may reach as high value as 73%.

Dariush Dam Deposits

The Dariush Dam Deposit (75 km to the North of Shiraz) is situated in the Zagros Mts. These deposits are lenticular similar to the Sar-e-Fariab, but much more scattered and noncommercial. Their main importance is that they help to outline the region of Cretaceous emersion and bauxitization.

Mineralogically, bauxites are purely diasporic. In contrast with the Sar-e-Fariab bauxite deposits kaolinite is accompanied by chamosite. Goethite is markedly subordinate to hematite. Along with anatase, some rutile was also detected.

Semirom Area

The region is situated in the High Zagros, 28 kms to the Southwest of Semirom. Altitude is about 2300 m.

The deposit is correlatable with Sar-e-Fariab bauxites. It was formed from clay deposits related to the hiatus between the Upper Cretaceous Sarvak and Ilam Formations.

The deposit is a ferruginous clay bed of large extent and up to 11 m thick. 5 million tons extractable reserves is proven.

Ferruginous clay contains minor amount of hematite, anatase, boehmite and traces of quartz.

Near the kaolinite deposit in Tang-e-Ashkgerd, Kuh-e-Hosseini, Kuh-e-Gartang, 13 bauxitic pockets are present. These bauxite pockets are diasporic. Some boehmite and anatase is present too.

At the top, hard pistachio-green pisolitic bauxite cover the hard liver red pisolitic bauxite pockets.

Abgarm Area

The region is located in the Central Iran zone, in a NW–SE trending range in the northwestern part of Iran. It belongs to the Upper Paleozoic and Mesozoic epicontinental sequence. The Central Iran mountains were folded during the Late Kimmerian orogenic phase. Abgarm is located in the Zangan Province. The bauxite deposits in the area are related to two horizons: Upper Permian limestone and the base of Lias.

The length of bauxite exposures is about 17 km. The maximum thickness is 10 m. As to the bauxite bodies they are situated on the karstified surface of the underlying Ruteh Formation in the case of the first horizon. As for the second horizon the bedrock is the Elika Formation. From mineralogical point of view, the Abgarm bauxites are diasporic-type. Kaolinite and chamosite are secondary to accessory minerals.

Bukan Area

The region is located in Western Elborz Mts. in a NW–SE trending range in the northwestern part of Iran. Bauxites belong to the Upper Paleozoic and Mesozoic epicontinental sequence.

Elborz Mountains was folded during Late Alpine orogenic phase. Bukan is located in the western Azarbaijan Province. The bauxite deposits in the area is related to two horizons: Upper Permian limestone and the base of Lias.

The length of bauxite exposures are over 40 km. The maximum thickness of the deposit is 10 meters.

The bauxite bodies are found in the shallow karst depressions of the underlying Ruteh and Elika Formations. They are layered-type deposits.

Mineralogically, the Bukan bauxites are diasporic. Boehmite, kaolinite and chamosite are secondary to accessory minerals.

Siahroudbar Area

The region is located in the eastern part of the NW-SE trending range in the northeastern region of Iran. It is in correspondence with the Mesozoic epicontinental sequence. Siahroudbar is located in the eastern part of the Mazandaran Province. The bauxite deposits in the area appeared at the base of Lias. The length of bauxite exposure is over 20 kms, whereas the maximum thickness of the deposit is about 10 m. The bauxite bodies are found in shallow karst depressions of the underlying Elika Formation. They are layered-type deposits.

From mineralogical point of view, the Siahroudbar bauxites are diasporic. Kaolinite and chamosite are secondary to accessory minerals.

References

- De Weisse, G. 1967: Gisement de bauxite d'Iran. - Alusuisse Internal report of Geological Survey of Iran (G.S.I.) Zurich
- Samimi N.M. 1968: Bauxite investigation in Mahabad Area North West Iran. - G.S.I. Internal report, Tehran
- Samimi, M. 1971 Bauxite investigation in Bukan Area. - G.S.I. Internal report, Tehran
- Sharifi, M. 1967: Discover of bauxite deposit in Do Polan (S. W. ISFN). - G.S.I. Internal report, Tehran
- Sharifi, M., A.M. Movahed 1967: Cretaceous refractory clay of Semirrom Area (Zagros Mountains) - G.S.I. Internal report, Tehran
- Sharifi, M., M. Samimi 1969: A study of Do Polan laterite and bauxite horizon in Bakhtiari Area. - G.S.I. Internal report, Tehran
- Sluiter, W.J. 1968: Report on the bauxite deposits. N.E. of Yazd. - G.S.I. Internal report, Tehran
- Stojexport-Geoindustrial 1979: Iran Cretaceous bauxite Sar-e-Fariab Area. - G.S.I. Internal report, Tehran
- Stojexport-Geoindustrial 1984: Cretaceous bauxite of the Zagros Mountains, Iran. - G.S.I. Internal report, Tehran

Main geological feature of "Sedimentary" bauxites deposits in China

Wang Liancheng, Zhang Naixian

Institute of Geology, Academia Sinica

Stratigraphic setting, mineralogy, geochemistry texture and structure of the "sedimentary" bauxite in China is presented. Genetic processes: weathering, transportation, deposition and diagenesis are also discussed.

Key words: Bauxite, paleokarst, diagenesis, Permian, Carboniferous, China

Introduction

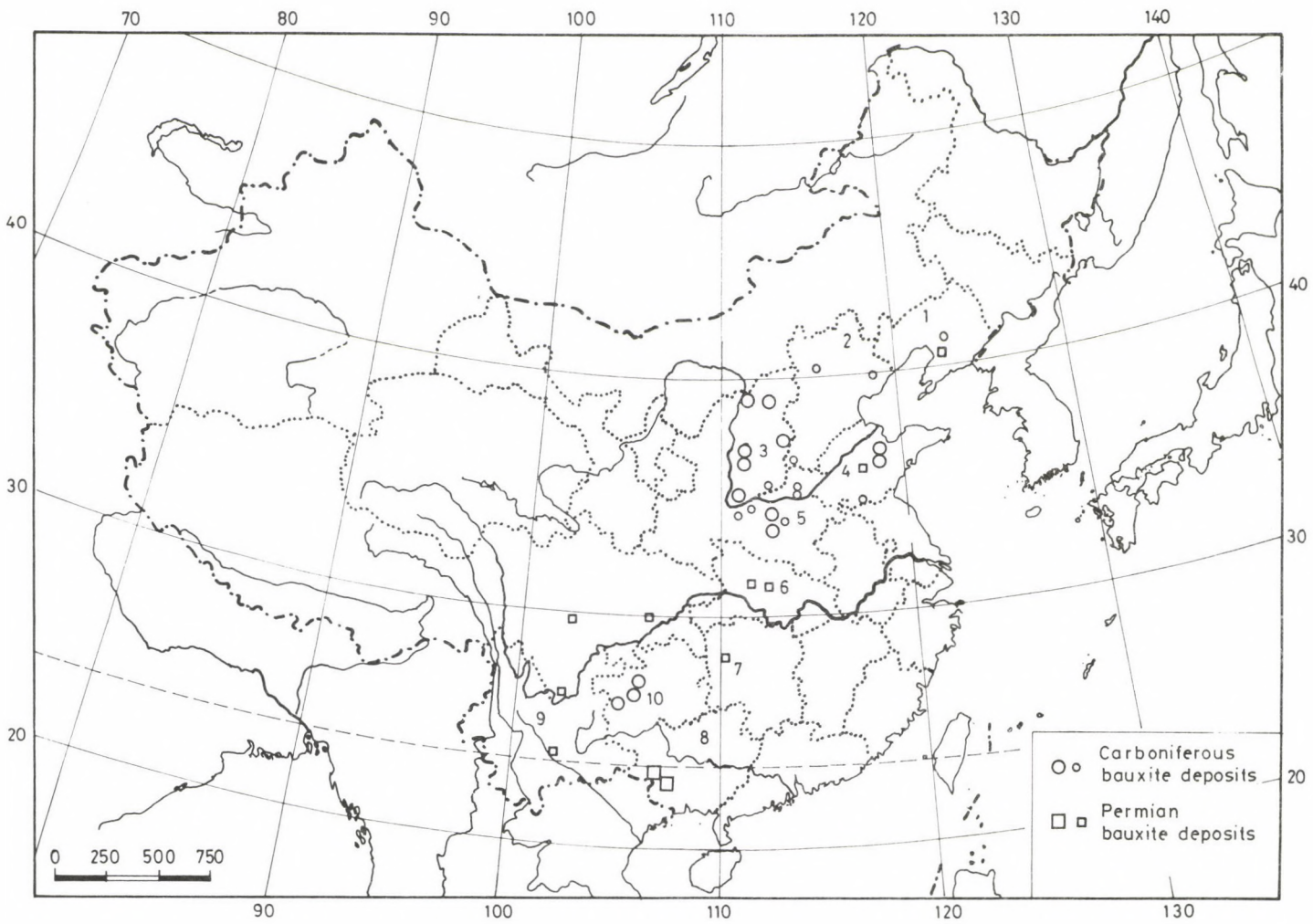
The bauxite deposits are of extensive distribution in China. They can be divided into three genetic types, i.e. laterite type, accumulate type and sedimentary type. *Laterite type* bauxite found only in Zhang Po, Fujian province and Peng Lai, Hainan province. All of them were formed in Quaternary and result from weathering of basalt bodies. "Accumulate" type bauxite (karst bauxite) distributed in Yunnan province and Guangxi autonomous region in south-western China. They all accumulated in some karst depressions from the nearby sedimentary bauxite deposits. Both types of bauxite deposits are small in scale and confine in distribution. The third type, "*sedimentary*" bauxites are the most important from the economic point of view. Most bauxite resources in China belong to this group (over 90% of total bauxite reserves of China). They occur in northern and south-western China including Shandong, Shanxi, Henan, Guizhou Province and Guangxi autonomous region. Some occurrences are known also from Hebei, Liaoning, Yunnan, Sichuan, Hunan and Hubei province (Fig. 1).

Stratigraphy

All "sedimentary" bauxite deposits in China were formed in Permo-Carboniferous. A great majority of them occurs as disconformity related deposits overlying erosional surfaces of shallow water carbonate successions of Cambrian or Ordovician age. Only a few smaller bauxite deposits are found on the surface of silicate rocks (e.g. basalts). In northern China, the main minerogenetic epoch of bauxite deposits is clearly the Carboniferous even though as a result of a diachronous transgression a slight time difference of the immediate cover is observable in the different districts. Deposits are younger in the SW than in the

Addresses: W. Liancheng, Z. Naixian: Beijing 100029, P.O.Box 634, China

Received: 18 October, 1991.



NE (Fig. 2). In south-western China, sedimentary bauxite deposits are mainly of Permian age whereas in the middle part of Guizhou province they are supposed to have formed in Middle-Early Carboniferous times. There are two main types of rocks having served as the substratum of the bauxite-bearing complex: (1) Carbonate rocks with a concavo-convex karstic/erosional surface. A majority of bauxite deposits including the greatest ones occurs on such surfaces (2). Silicate rocks sedimentary or igneous including sandstone – shale series or basalts. Deposits associated with them are of smaller scale and occur only at a few places in Shandong, Hunan and Liaoning province.

As to the karst-related occurrences, vertical profiles of the bauxite-bearing series is rather uniform everywhere (Figs 3, 4). They generally can be divided into three main parts: the *lower part* consists of Fe–Al rich claystones including lenses and

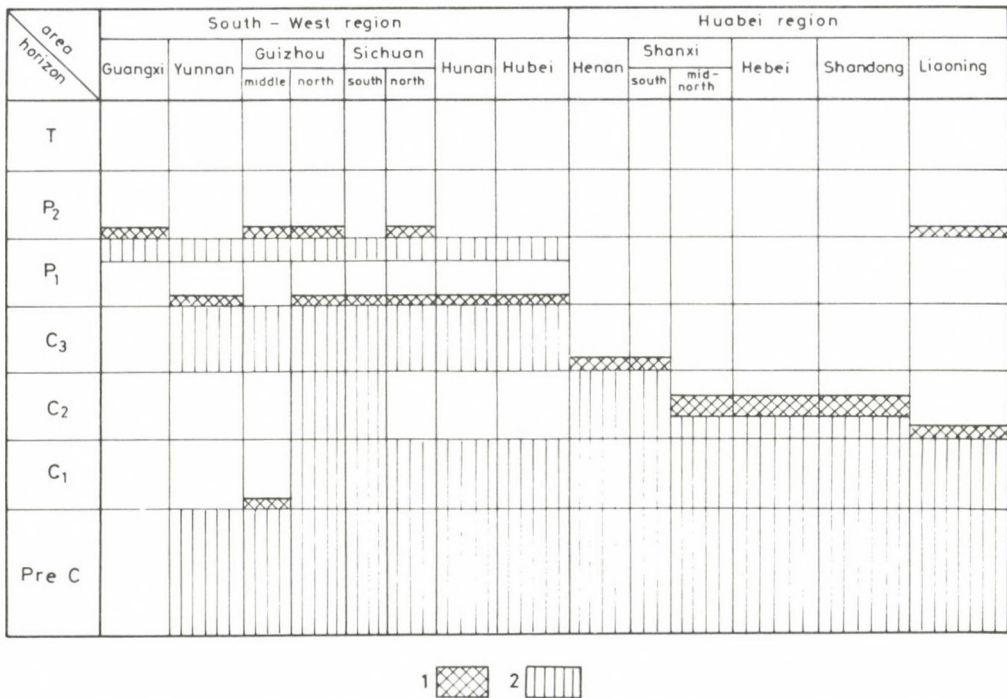


Fig. 2
Regional distribution sketch of sedimentary bauxite horizons in China. 1. bauxite; 2. underlying sedimentary strata

Fig. 1 ←
Distribution sketch of "sedimentary" bauxite deposits in China. Liaoning province; 2. Hebei province; 3. Shanxi province; 4. Shandong province; 5. Henan province; 6. Hubei province; 7. Hunan province; 8. Guanxi autonomous region; 9. Yunnan province; 10. Guizhou province; 11. Sichuan province

Age	thickness (M)	Columnar Pattern	lithological characters
C ₃	Superstratum bauxite-bearing series	2-5	neritic limestone With fusulinid fossils a few of sandstone shale in lowest part
		0.5-15	gray, gray-black-silt shale, carbonaceous shale With thin coal seam and plant fossils some clay bands lower part
		1-6	light-dark gray bauxite some clay intercalations in lower part
		1-5	gray, gray-black Fe-bearing clayrock a lot of irregular nested hematite limonite or siderite and pyrite
O ₂			gray massive limestone with intercalated some shale beds

Fig. 3
Columnar sketch of bauxite-bearing series of rocks in Western Henan province

Age	thickness (M)	Columnar Pattern	lithological characters
C ₂	Bauxite bearing series	super-stratum	flaggy limestone with chert concretions and brachiopoda fossils above than present carbonaceous and calc shale
		7-8	Clay bands clay-siltstone fine sandstone Carbonaceous shale intercalate coal seams some scour surfaces top
		5-7	bauxite include alumina-bearing clayrock and ferruginous clayrock
		0-5	ferallitic clayrock include lenticular or lested limonite hematite and a few of pyrite
O ₂	630-820		light gray massive or elastic limestone

Fig. 4
Columnar sketch of bauxite-bearing series of rocks in Yang Quan district, Shanxi province

concretions of hematite, limonite, goethite and so on. In some profiles, especially in the south-western region abundant pyrite, siderite and/or chamosite was found in this lower part. The middle part of the profile is generally the one containing the oregrade bauxite in about 1 to 6 m thickness. Sometimes intercalated clay beds occur in them. The *upper part* consists of silty-shale, carbonaceous shale with thin coal seams and is about 0,5 to 15 m thick. In some areas, this part is substituted by siltstones or sandstones.

Mineral composition

Sedimentary bauxite ores consists of Al-minerals, Fe-minerals, clay minerals, Ti-minerals and accessory detrital grains. Various mineral components are listed in Table 1. Zhang Naixian et al. (1985) studied mineralogy of bauxite in Gongxian county, Henan province. Of the Al-minerals, diaspore is major component, whereas boehmite and gibbsite are less abundant (general < 5 %). This is a general feature of sedimentary bauxites in China. Diaspore appears mainly as micro-crystalline grains, the diameter of which is about 5 μm . Their color is greyish-white or light yellowish-brown. This fine-grained diaspore is present both in the matrix and in the pisoids and ooids. Another generation of (much coarser grained) diaspore was also observed as bright tabular or columnar crystals scattered around in the matrix of ore-grade bauxites. The grain-size of these large diaspore about 0.2 x 0.3 mm (Plate 1). Under the electron microscope, diaspore appears as foliate or tabular crystals. Sometimes aggregates consisting of oriented crystallites are also present.

Of the clay minerals, kaolinite is the major component. A large part of kaolinite is very probably of "inherited" clastic origin. Its grain-size is about 5 μm . It appears as white, light yellow-brown colored, foliate or flaky grains often partially replaced by diaspore. Other clay minerals present are illite, chlorite, chamosite, pyrophyllite, montmorillonite, dickite. Dickite appears as micro hexagonal flakes. They are regularly arranged into polysynthetic aggregates and often replace diaspores in late diagenetic stage (Plate 1).

Table 1
Mineral composition of sedimentary bauxite in China

Major component	Secondary component	Rare component
Diaspore	Boehmite, Illite, Dickite,	Feldspar, Zircon, Monazite,
Kaolinite	Hematite, Goethite, Pyrite, Siderite, Chamosite, Chlorite, Pyrauxite, Montmorillonite, Quartz, Muscovite, Gibbsite, Anatase, Allophane, Calcedony	Calcite, Rutile, Titanite, Tourmaline, Leucocene, Epidote

Main Fe-minerals are hematite, goethite, siderite pyrite and so on. Their percentage in ore grade bauxite is very much varied. Usually, the total content of Fe-minerals mainly (hematite and goethite) is less than 5%. But in some cases especially in some of the bauxite deposits of south-western China, the amount of Fe-minerals may reach as well 25% and also there is more pyrite, siderite and chamosite there. Of the clastic (detrital) minerals, besides kaolinite rare muscovite flakes, quartz, feldspar, zircon, monazite, rutile and tourmaline has to be mentioned. They are supposed to have had some acidic parent rocks as a source (cf. Zhang Naixian et al. in this volume).

Chemical composition

Chemical composition of bauxite ores of two typical minig areas presented in Tables 2 and 3. We can see that sedimentary bauxites in China compare very well with the majority of bauxite deposits of other countries in the world. They are rather high in Al_2O_3 and SiO_2 and apart from some exceptions relatively poor in Fe_2O_3 . In a few of the deposits otherwise ore-grade bauxites are anomalously rich in S. Accordingly the economic classification of bauxites in China is as follows: (1) Low-Fe, Low-S-diaspore ore: the ore is white or light grey in color, consists mainly of diaspore, kaolinite some hematite. Average chemical composition is Al_2O_3 60–70%, SiO_2 6–15%, Fe_2O_3 7%. (2) High-Fe-diaspore ore: it contains more hematite and is brown colored. Average chemical composition is Al_2O_3 50–60%, SiO_2 3.5–18.8%, Fe_2O_3 10–20%. (3) High-S diaspore ore: The ore is dark colored. It contains large amounts of pyrite. Average chemical composition: Al_2O_3 50–60%, SiO_2 5–15%, Fe_2O_3 contents is varied, S-content may be as high as 7%. Correlation between Al_2O_3 and TiO_2 is positive.

Table 2
Chemical analysis of bauxite ores of Yang Quan area

Sample	Al_2O_3	SiO_2	TiO_2	Fe_2O_3	CaO	MgO	K ₂ O	Na ₂ O	LOI	Total
Gray compact bauxite ore	73.83	5.48	4.21	1.40	0.43	0.18	0.03	0.02	14.44	99.57
Yellow-brown compact bauxite ore	71.37	1.50	3.00	8.44	0.43	0.53	0.03	0.03	14.59	99.92
Gray pisolitic-oolitic bauxite ore	70.02	8.92	3.00	0.72	0.49	0.67	0.03	0.02	14.49	98.36
Gray fine-grained bauxite ore	60.24	20.25	2.10	2.07	0.37	0.04	0.03	0.02	14.08	99.20
Gray coarse-grained bauxite ore	61.63	17.88	1.75	5.82	0.37	0.13	0.050	0.07	14.40	99.55

Table 3
Chemical analysis of bauxite ores in Henan province

Composition	Lowest content %	Highest content %	Ordinary content %
Al ₂ O ₃	40	82.82	65-75
SiO ₂	< 0.5	22.00	5-15
Fe ₂ O ₃	0.5	29.19	2-4
TiO ₂	1.38	5.58	2.5-3.5
CaO	0.02	2.65	0.2-0.4
MgO	trace	1.29	0.02-0.3
K ₂ O	0.05	4.65	< 1
Na ₂ O	trace	0.95	0.07-0.4
S	0.115	13.44	0.1-0.5
LOI	11	15	13-14

Texture and structure

There are three main textural types recognized in sedimentary bauxites in China: 1) *Compact texture*. It consist of microcrystalline, cryptocrystalline or colloidal-size grains. It looks to be isotropic under the microscope (Plate 1). In some of these lithotypes, even though obscures, a few clastic, pisolitic or oolitic textural components can also be seen. We think that these may have been alteration products of originally clastic or pisolitic-oolitic textures. 2) *Pisolitic-oolitic texture*. It consists of microcrystalline-cryptocrystalline matrix and scattered embedded pisolites and ooides in it (Plate 1). Pisoids and ooids possess clear concentricly layered structure with concentric and also occasionally radial craks. The matrix: ooids pisoids ratio varies, sometimes embedded textural elements are exclusively ooids sometimes pisoids. More frequently, however, pisolids and ooids are mixed at various proportions. The amount of pisoids and ooids as related to the matrix may be as high as 40 to 50%. 3) *Clastic texture*. It consists of a microcrystalline matrix and bauxite fragments embedded in it. Ratio of matrix to clasts may be as high as 50%. Size and shape (sphericity) of the fragments varies: they may occur as angular or sub-rounded grains (Plate 1). Sometimes larger clastic fragments may enclose smaller ones together with pisoids and ooids as well (bauxite "pebbles"). This indicates that before final deposition several stages of transportation may have occurred. A part of the fragments are clearly intraclasts (elongate angular grains). The structures of the bauxite is generally massive though also laminated and stalactitic structure do occur. Most common is the massive structure. The components of massive ores are arranged randomly as a result of which the ores looks like a massive block. In laminated ores the arrangement of minerals and other components is oriented and this laminated structure is expressed also on the macro-scale by alternating color and grain size. The lamination appears generally as parallel, wavy or (locally) as funnel-filling curved planes (Plate 2).

"Stalactite-shaped" structures consist of colloidal materials. They may occur either as smooth or as irregularly curved surfaces (Plate 2).

Formation and genesis of sedimentary bauxites of China

The genesis of sedimentary bauxites is traditionally a controversial problem in China. Liao Shifan (1986) suggested that sedimentary bauxites formed originally as laterites and later on when flooded by sea water or lake water they formed low-grade bauxites. Subsequent emersion and interaction with surface waters were invoked to explain their alteration and the observed lithological features. Liu Changling (1988) attributed the genesis of sedimentary bauxites to allochthonous processes. According to him weathering products formed elsewhere were transported and deposited as clastic sediments into water-filled basins. We think that the formation of sedimentary bauxites in China is a more complex process than that. It can be divided into at least four stages: 1) Formation of a palaeoerosion surface and the related lateritic weathering crust. 2) Transportation and deposition of the weathering products. 3) Diagenesis. 4) Epigenesis.

Palaeoerosion surface and lateritic weathering crust

There is a rather long range sedimentary gap in the Paleozoic of northern and south-western China. Extensive areas built up of Cambrian–Ordovician carbonate rocks became exposed probably during the Devonian–Carboniferous times and underwent an erosion as a result of which a peneplaned (at places rather dissected) karst surface was formed. Laterally adjoining this karstified surface old crystalline rocks rich in Fe, Al, Si were also exposed – among them metamorphosed mafics and ultramafics. There is a general agreement about China having been situated in the tropical belt for most of Carboniferous and Permian times. As a result of extensive lateritic weathering exposed non-carbonate rocks underwent considerable desilication and Fe and Al became relatively concentrated. The Fe–Al rich weathering crust thus formed may have served later on as the source material for the formation of bauxites.

Transportation and deposition of weathering products

In mid to late Carboniferous times Huabei and south-western China underwent a gradual large-scale transgression. The extensive peneplaned erosion surface was overridden by the sea. Higher elevated parts of the relief (mainly those built up of old crystalline rocks) still remained exposed for some time. "Epeiric sea" zones, estuaries, paralic lakes and swamps adjoining the still exposed land became suitable centers of deposition. Various surface water courses and mud flows may have transported and deposited the weathering products as mechanically suspended or colloidal load from the old landsurface into these basins. Coarse or finer clastic sediments were apparently deposited from linear water courses in shallow nearshore areas of the "epicontinental" realm. Sediments carried by mud flows accumulated in massive deposits without visible bedding. Finer grained

materials, on the other hand, when deposited in calm water bodies (ponds, ephemeral lakes?) may exhibit well-preserved laminations. It is supposed that the depositional process was longlasting enough to (?indirectly) record eustatic changes of sea-level. While emergence above the water surface sediments became scoured and subject to dewatering and desiccation. The semi-consolidated material may have been broken up by occasional water flows to form intraclasts which then became deposited again. The phenomenon of larger pebbles often containing smaller clasts indicated that the process of erosion-deposition was repeated ("parautochthonous transport").

Diagenesis

Diagenesis began after final deposition of the sediments. Under their own load they began to be compacted. Meanwhile, owing to bacterial chemical processes, some of the original minerals such as some clastic clay minerals, gibbsite, Fe-minerals and Ti-minerals were decomposed and reprecipitated. New minerals such as microcrystalline diaspore, some of boehmite, anatase, hematite and goethite were formed. Mobilization and reprecipitation of Fe, Al materials may have resulted in the formation of some of the pisoids ooids and concretions. Then, at places where the ground water table was raised and conditions changed in reducing environment, pyrite, siderite and chamosite were formed. Large diaspore crystals in the matrix and in pisolids and ooids were formed in late diagenetic stages. In addition also dickite replaced diaspore in some of the ooides or pisolites.

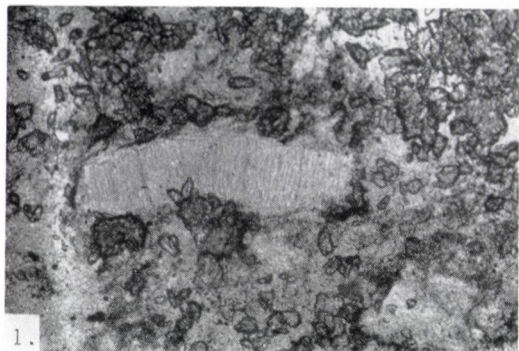
Epigenesis

It is known that in the majority of the cases sedimentary bauxite deposits are overlain by carbonaceous claystones and coal seams. It indicates that the environment at that time changed from that of a swamp. In the case of those deposits accumulated in a near-shore marine environment the swamp with its temporary exposure phase resulted in "epigenetic" changes. Interaction with downward percolating temporarily oxidizing waters resulted in the alteration of early pyrite into limonite. On the surface of some bauxites the formation of a tarnish and an enrichment in Al can be observed. Some Al-minerals were decomposed and reprecipitated as gibbsite or alumogel in joints, cracks and holes. Part of the kaolinite has been altered to illite.** Similar alteration observed in Permian phreatic bauxites of N. Vietnam were ascribed to recent oxidation by Mindszenty and Bérczi (1982). The swampy environment may rather be responsible for the reducing conditions during syndiagenesis in an apparently paralic swamp (The Editor).

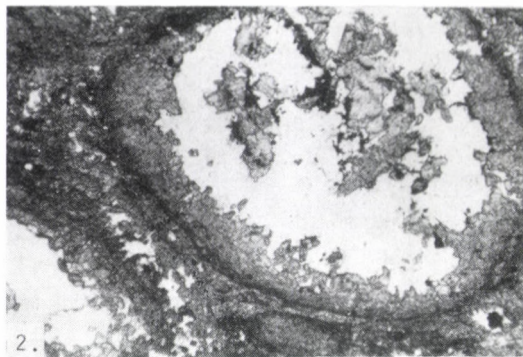
References

- Naixian., Z., J. Surong 1985: Petrographic and Mineralogical Characteristics of Bauxite and Series of Ore-Bearing in Gongxian County, Henan Province. – *Scientia Geologica Sinica*, 4, pp. 170–179.
- Shifan, L. 1986: The Genesis of Bauxite and the Sedimentary Process of Its Ore Deposit in China. – *Acta Sedimentologica Sinica*, 4, pp. 1–8.
- Changling, L. 1988: Geological Feature and Genesis of carboniferous Bauxite in China. – *Acta Sedimentologica Sinica*, 6, pp. 3–10.

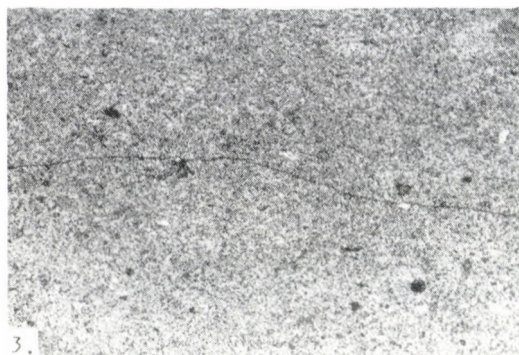
PLATE 1



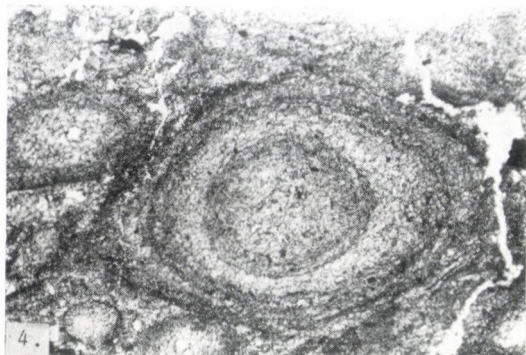
1. Coarse diasporic crystal. $\times 210$



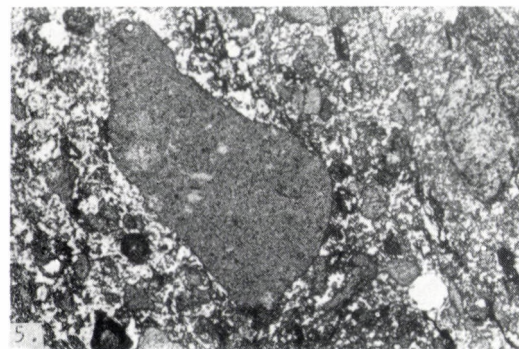
2. Dickites replace diasporic in pisolites or oolites. $\times 66$



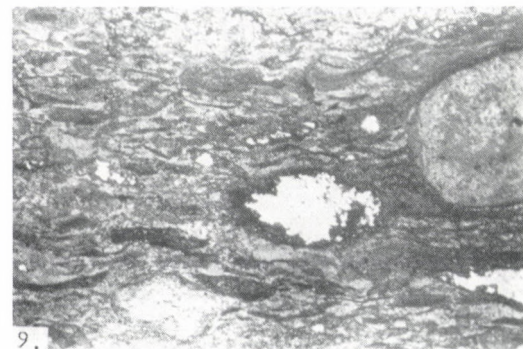
3. Compact texture. $\times 66$



4. Pisolitic-oolitic texture. $\times 66$



5. Clastic texture. $\times 66$

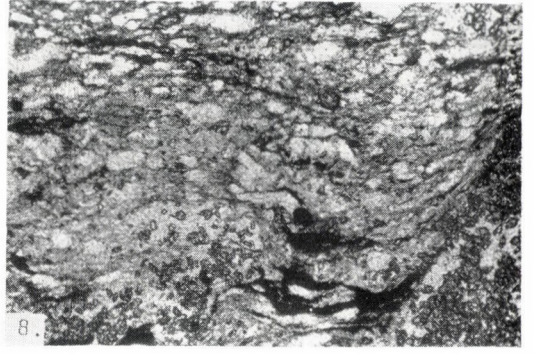


6. Parallel laminated structure. $\times 66$

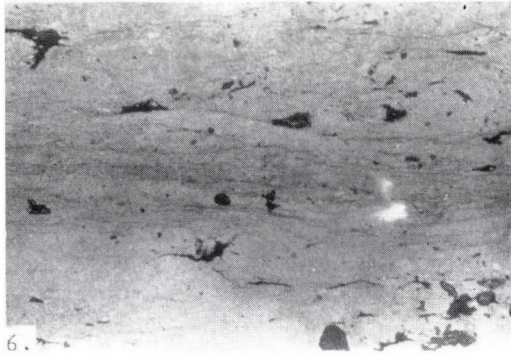
PLATE 2



7. Wavy laminated structure. $\times 66$



8. Funnel laminated structure. $\times 66$



9. Stalactitic structure. $\times 66$

Mineralogy and geochemistry of bauxite in Yang Quan Area, Shan Xi Province (China)

Zhang Naixian, Wang Liancheng

Ma Yuguang

Institute of Geology, Academia Sinica

Mineralogy and geochemistry of economy grade deposits in the Yang Quan area are discussed. Deposits are underlain by karstified Mid-Ordovician limestones. Bauxites and the covering series are mid-Carboniferous in age. In the mineral assemblage diaspore is always present, kaolinite, dickite and halloysite also occur. Data on chemical composition and trace elements are presented

Key words: Bauxite, mineralogy, geochemistry, diaspore, clay-minerals, trace elements, Yang Quan area, Shai Xi Province

Introduction

The Yang Quan area is located in the eastern part of Shan Xi province. It is one of the most important bauxite districts in China. Up to now, 24 economy-grade bauxite occurrences were found in this area. Total reserve amount to 220 million tons. The deposits occur in a district of over 50 km long and about 6 km wide striking from northern Yu xian to southern Xiyang county. Along the eastern and north-eastern side of this bauxite zone a few tens of kms from the known bauxite deposits Pre-Ordovician metamorphics and epimetamorphics are exposed and considered as the possible source materials of the bauxite-bearing series.

All the bauxite deposits in this area are of the sedimentary type, associated with an eroded/karstified unconformity surface formed on mid-Ordovician limestones. The contact between bauxite and its bedrock is very clear, rugged and rough. There are no traces of weathering to be seen on the underlying limestone. The bauxite-bearing series is of mid-Carboniferous age and can be divided into three parts: The lower part consists of brown, gray or variegated ferruginous clay stones with lenticular, nest-like or concretionary hematite or limonite ore bodies embedded in them. The thickness of this lower units is 0 to 5 ms. The middle part consists of gray or brown bauxite exhibiting pisolitic-oolitic or compact texture and sometimes striped structure. The relationship of these different lithotypes is irregular: they are lenticular and often show gradual transition to each other. The thickness of this middle part of the bauxite complex is about 5 to 7 m; the upper part consists of greyish-black clayey sandstones, claystones, carbonaceous shale and coal seams including abundant plant fossils. The thickness is about 7 to 8 m.

Address: Zhang Naixian, Wang Liancheng, Ma Yuguang: Beijing 100029 P.O.Box 634, China

Received: 14 October, 1991.

The strata directly overlying the bauxite-bearing series are composed of light grey neritic limestones and sandstones, shales and coal seams. The limestones are rich in brachiopods and fusulinids.

Mineralogy

As to mineralogy all bauxites of northern China are rather similar to each other (Naixian et al. 1985, 1987). In the Yang Quan area, though the mineral assemblages found the upper, middle and lower parts of the bauxite-bearing series are different, diaspore and clay minerals are always present as the main mineral components exception is the iron mineral assemblage of the lower part. In the followings we shall describe mainly diaspore and some special clay minerals.

Diaspore

Diaspore is almost the only Al-mineral in the bauxite-bearing series. In ore-grade bauxites the diaspore content may reach 70 to 90 percent, with only subordinated amounts of kaolinite and accessories as illite, dickite, halloysite, pyrophyllite, hematite, anatase, rutile, zircon, tourmaline, feldspar and quartz. In the claystone overlying the bauxite, kaolinite and other clay minerals are predominant with only smaller amounts of diaspore accompanying it (usually < 10 %).

Microscopic study showed that diaspore appears as microgranular, planar or platy aggregates. Most of the fine crypto-crystalline diaspore and probably some of the coarse crystals as well were formed in late diagenetic stages. XRD characters are: $d_{110} = 3.97 \text{ \AA}$, $d_{130} = 2.55 \text{ \AA}$, $d_{140} = 2.07 \text{ \AA}$ (Fig. 1a). DTA curves showed that a

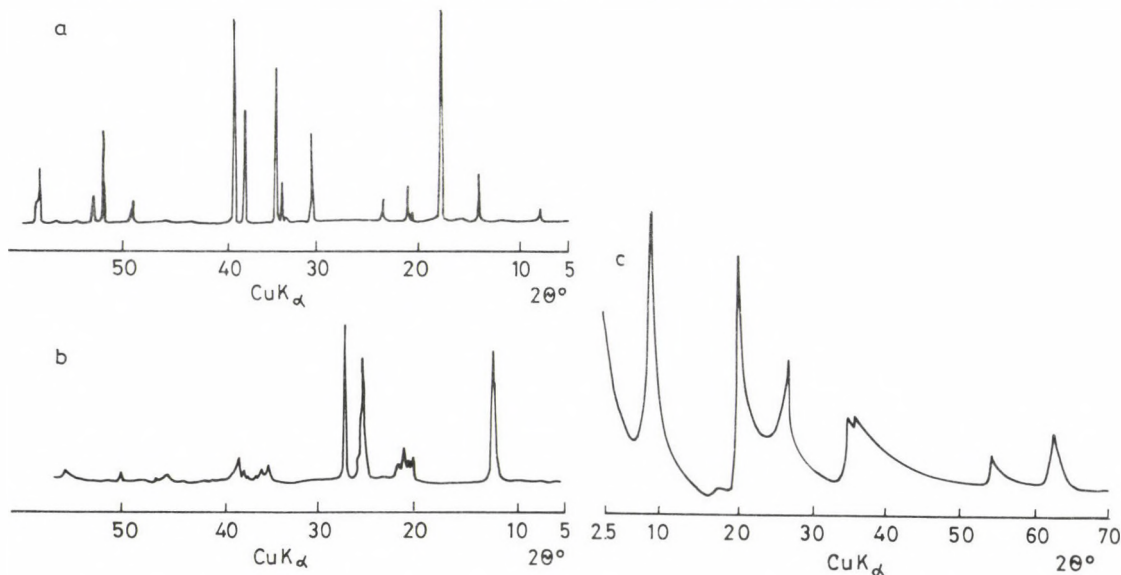


Fig. 1
XRD patterns. a) Diaspore; b) Kaolinite; c) Halloysite

large endothermic peak (due to loss of inherent moisture) begins at 450°C with the largest values occurring between 550 and 560°C and ending at 650°C. After that, there is no change up to 1000°C (Fig. 2a). This shows that the dewatering product is an α - Al_2O_3 . Special bands on the infrared spectrum occurred at 2115 cm^{-1} , 1980 cm^{-1} , 1080 cm^{-1} and 750 cm^{-1} (Fig. 3a).

SEM research showed well-crystallized columnar, lamellar and platy crystalline aggregates (Plate 1).

Kaolinite

Kaolinite is "omnipresent" in all the bauxite-bearing series. In ore-grade bauxites, it is the most important "associated" mineral, whereas in the claystones it is the major constituent. Shape and crystallinity of kaolinite is different in the different horizons.

X-ray diffraction patterns, differential thermal curves and the infrared absorption spectrum of kaolinites studied are shown in Figs 1b, 2b and 3b.

Kaolinites appear mainly as microgranular aggregates (Plate 1), well crystallized planar aggregates (Plate 1) or lamellar aggregates (Plate 1). Less frequently also coarse grained vermicular kaolinite crystals were also observed (Plate 2) in the more kaolinite-rich rocks varieties. In ore-grade bauxites the kaolinite associated

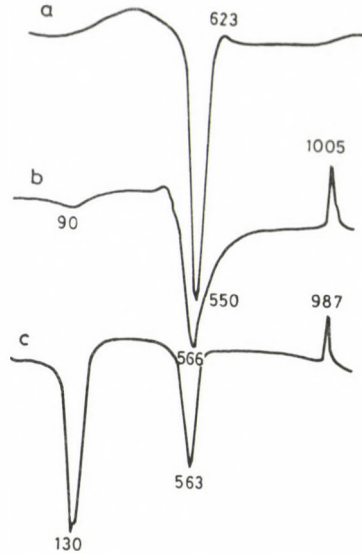


Fig. 2
DTA curves. a) Diaspore; b) Kaolinite;
c) Halloysite

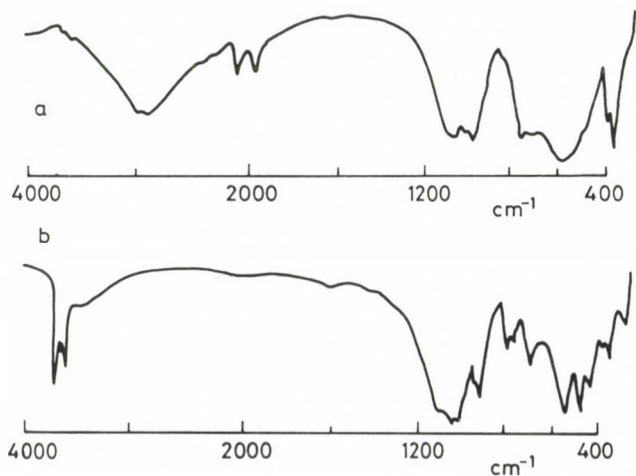


Fig. 3
IR spectrum. a) Diaspore;
b) Kaolinite

with diaspore is predominantly microgranular with only a few coarse platy kaolinite crystals scattered around. We think that the majority of kaolinite especially the planar and the coarse vermicular crystals are of detrital origin, whereas the microgranular aggregates are the products of diagenetic processes.

Dickite

Pisolites and ooides in ore-grade pisolitic-oolitic bauxites consist of grey microcrystalline diaspore. Apparently part of the diaspore replaced by dickite in late diagenetic stages and therefore pisolites and ooides affected by this "dickitization" became white in color.

SEM studies showed that dickite appears as a well-oriented schistose aggregate (Plate 3). The three special reflections used to identify on the X-ray diffraction pattern were: $d_{001} = 7.10 \text{ \AA}$, $d_{004} = 3.56 \text{ \AA}$, $d_{020} = 2.32 \text{ \AA}$. On the DTA curve, there is a strong endothermic peak at 688°C caused by loss of OH from the crystal structure. The obvious exothermic peak at 998°C is interpreted as product of phase transition of dickite. Characteristic absorption bands of the infrared absorption spectrum were observed at 3700 cm^{-1} , 3645 cm^{-1} , 3615 cm^{-1} , 1158 cm^{-1} , 1035 cm^{-1} , 1000 cm^{-1} , 910 cm^{-1} and so on. The three OH shock absorption bands (3700 cm^{-1} , 3645 cm^{-1} and 3615 cm^{-1}) show without doubt that the mineral is not kaolinite.

Halloysite

Halloysite appears in irregular fault-related veinlets in tectonically affected zones. It is pure white, fine and smooth. SEM research indicated that it appears as fine fibrous and tubular aggregates (Plate 2). X-ray diffraction special reflections

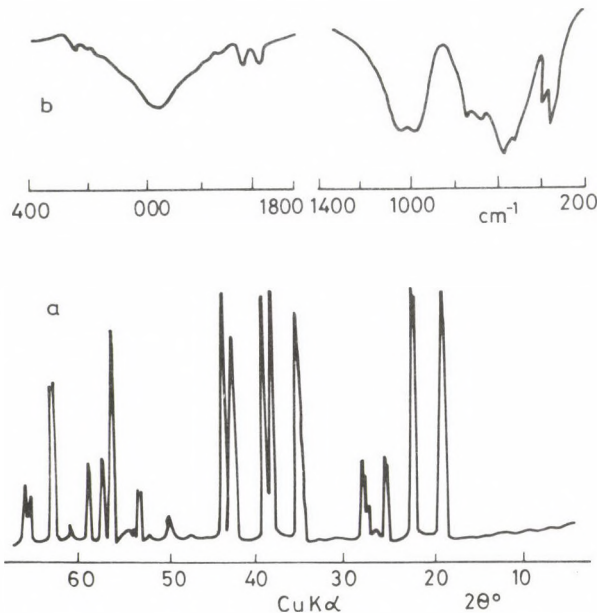


Fig. 4
XRD pattern and IR spectrum
of dickite. a) XRD; b) IR

used to identify it were $d_{001} = 9.97 \text{ \AA}$, $d_{02} = 4.41 \text{ \AA}$, $d_{003} = 3.33 \text{ \AA}$, $d_{060} = 1.48 \text{ \AA}$ (Fig. 4a). The infrared spectrum is shown by Fig. 4b.

In addition, small amounts of other clay minerals such as chlorite, pyrophyllite etc. were also found both in ore-grade bauxites and in other clay-rich rocks of the bauxite complex. In the bauxite they are always close associated with diaspore and kaolinite.

Geochemistry

Chemical composition and trace element contents are shown by Tables 1 and 2. The samples were collected from the Tai Hushi and Bai Jiazhuang deposits of the Yang Quan area. Sequential numbering of samples 1–4 in Table 1 represents sampling from bottom to top. Chemical constituents in Table 1 showed that bauxite deposits in this area are rather rich in SiO_2 and poor Fe_2O_3 . As to the relationship of the main components to each other: Al_2O_3 shows a positive correlation with TiO_2 and negative correlation with Fe_2O_3 like in all the bauxite deposits of northern China (Zhang et al. 1987).

Many authors (Özlü 1983; Laskou et al. 1983; Arp 1985; Valetton et al. 1987) have studied the trace element contents in bauxites with the aim of locating source areas or at least source rocks. Characteristic trace elements analysed from the Yang Quan bauxite complex are shown in Table 2. The amount of lithophile elements such as Pb, Zn, Zr, La, Y and so on are close to or higher than the average figures for ordinary "sialic" rocks and/or sedimentary rocks. V content is equal to that of

Table 1
Chemical composition of bauxites from Yang Quan Area

No.	Samples	Chemical analysis (%)									
		SiO_2	TiO_2	Al_2O_3	Fe_2O_3	MnO	CaO	MgO	K_2O	Na_2O	P_2O_5
Y ¹⁴	Ferruginous clay	43.89	2.00	33.22	4.46	0.003	0.18	0.28	1.29	0.46	0.21
Y ¹³	Clay rock	43.14	1.95	36.02	1.09	0.002	0.19	0.30	1.25	0.46	0.22
Y ¹²	Kaolinitic rock	45.33	1.60	38.56	1.13	0.002	0.11	0.09	0.40	0.42	0.22
Y ¹¹	Clay rock	44.43	1.69	34.97	1.19	0.003	0.23	0.50	3.27	0.54	0.20
Y ¹⁰	Ferruginous clay	38.69	1.97	32.23	11.68	0.024	0.21	0.20	0.68	0.44	0.22
Y ⁹	Ferruginous clay	17.62	0.56	14.19	47.9	0.056	0.91	0.19	0.30	0.44	0.23
Y ⁸	Bauxite	43.89	2.54	40.88	1.38	0.007	0.30	0.20	0.69	0.79	0.26
Y ⁷	Bauxite	7.88	3.32	74.48	0.83	0.004	0.16	0.05	0.31	0.49	0.32
Y ⁶	Bauxite	10.59	4.28	69.93	0.79	0.003	0.05	0.01	0.60	0.40	0.35
Y ⁵	Bauxite	28.29	2.48	49.42	3.97	0.013	0.19	0.21	1.38	0.43	0.39
Y ⁴	Bauxite	33.27	2.14	43.58	3.49	0.0033	0.19	0.32	0.193	0.46	0.36
Y ³	Bauxite	30.98	2.33	47.39	1.66	0.013	0.24	0.50	3.33	0.46	0.40
Y ²	Ferruginous clay	18.38	2.66	17.69	38.95	0.014	4.12	0.59	1.42	0.44	0.34
Y ¹	Limestone (O_2)	1.46	0.039	0.91	0.53	0.024	52.16	0.31	0.29	0.36	0.046

Table 2
Trace element contents of bauxites from Yang Quan Area

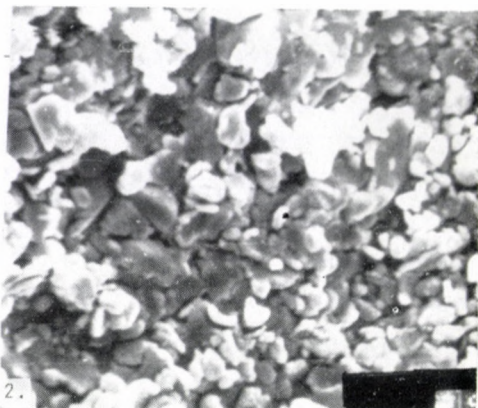
No.	Trace elements (ppm)																
	Ba	Sr	Cr	Ni	Co	V	Cu	Pb	Zn	Be	Nb	Zr	Sc	Y	Yb	La	Ce
Y ¹⁴	269.0	118.3	86.7	41.7	23.3	169.8	41.6	18.4	77.2	1.4	26.5	452.1	11.4	20.7	1.5	72.1	76.4
Y ¹³	316.3	205.5	95.8	53.2	22.6	125.8	37.1	18.0	87.0	1.7	31.0	438.1	11.4	47.7	2.1	63.2	93.7
Y ¹²	212.5	83.8	118.5	23.7	17.4	129.4	36.8	18.4	92.3	1.4	26.7	370.2	10.0	19.7	1.3	38.9	62.3
Y ¹¹	501.4	171.0	107.9	36.6	20.2	198.3	45.0	18.3	83.4	1.8	34.4	366.2	14.3	48.5	2.4	67.6	116.7
Y ¹⁰	197.4	113.4	150.0	63.1	67.9	166.2	70.8	18.0	89.6	1.9	43.5	456.1	17.1	55.8	3.0	84.9	122.8
Y ⁹	415.3	101.4	258.1	245.9	116.6	435.1	103.3	23.0	143.8	2.5	30.2	959.5	65.6	128.5	5.3	82.2	81.3
Y ⁸	367.9	205.8	162.4	42.5	30.6	212.5	59.2	23.1	98.5	2.8	64.0	705.8	16.4	32.0	2.4	71.6	188.5
Y ⁷	171.8	32.7	183.3	19.5	24.9	205.6	61.2	31.4	157.2	2.7	54.3	953.3	14.3	38.0	3.5	19.2	40.8
Y ⁶	224.9	212.1	218.1	20.2	31.8	247.0	74.6	30.6	79.5	3.5	69.9	1371.0	18.3	51.6	5.1	74.4	164.0
Y ⁵	338.2	586.7	153.6	62.2	27.1	273.0	66.2	25.0	89.6	3.0	97.0	878.1	23.7	89.0	8.0	279.8	412.3
Y ⁴	386.0	599.8	138.3	54.3	23.3	268.8	61.2	23.2	92.1	2.3	65.0	641.7	17.0	78.7	7.2	206.3	361.0
Y ³	501.9	656.6	159.0	53.6	33.8	395.8	55.2	25.0	114.1	3.4	75.8	681.4	23.7	216.6	13.0	167.1	413.2
Y ²	348.4	312.4	126.6	91.4	41.5	160.1	178.2	21.4	123.4	4.1	96.7	827.3	38.5	410.9	28.7	210.5	355.1
Y ¹	149.2	142.2	49.1	17.3	7.8	23.6	32.6	3.5	82.8	1.8	51.2	44.9	8.9	31.0	s2.1	43.8	160.9



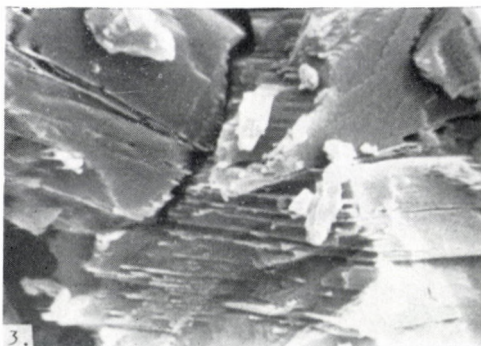
PLATE 1



1. Well-crystallized columnar diasporite.
× 5000



2. Lamellar crystals of diasporite. × 5000



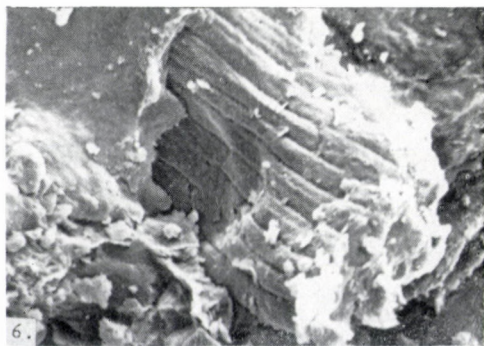
3. Platy crystallites of diasporite. × 3000



4. Microgranular kaolinite. × 10 000

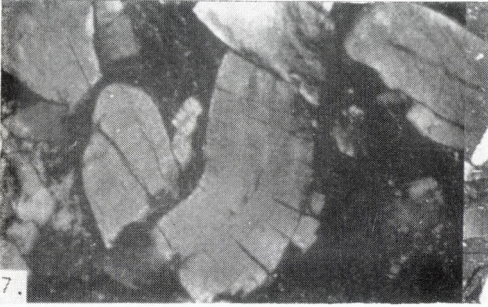


5. Well-crystallized platy kaolinite. × 8000



6. Lamellar kaolinite. × 440

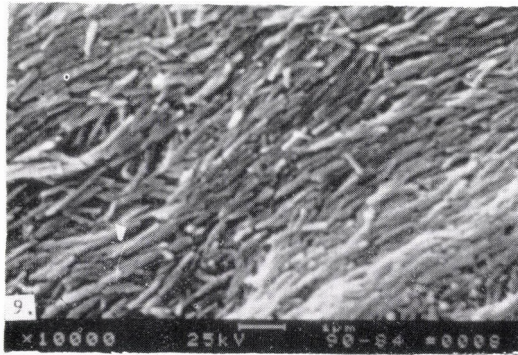
PLATE 2



7. Coarse vermicular kaolinite. $\times 37$



8. Dickite crystals. $\times 10\ 000$



9. Fine fibrous halloysite. $\times 10\ 000$

the sedimentary average. The amount of siderophile elements like Cr, Ni, Co, Cu is, however, considerably higher than average and is close to the figure considered to be characteristic of mafic rocks. This indicates that the geology of the source area must have been rather complex i.e. built up of various types of mafic and "sialic" rocks, because the geochemical characteristics of the bauxite-bearing series are in good agreement with that of the supposed eastern source area. We suggest that the source material of bauxites and bauxitiferous rocks of Yang Quan arrived from the east and originated partly in the old metamorphic complex partly in lower-grade metamorphic sedimentary rocks exposed to subaerial erosion.

References

- Arp, T. 1985: Geologische kartierung des gebietes un tithronion im kallidromengebirge, mittelgriechenland und petrographische bearbeitung des karst bauxites (b1). – Thesis, Univ. of Hamburg, Hamburg, p. 213.
- Laskou, M., F. Paulik, J. Paulik 1983: Contribution to the knowledge of Bauxite deposits in the locria, Greece. – 5th Int. Congress ICSOBA, Zagreb, pp. 73–84.
- Özlü, N. 1983: Trace element content of karst bauxites and their parent rocks in the mediterranean belt. – *Mineral deposits*, 18, pp. 469–476.
- Valeton, M., R. Biermann, Reche, F. Rosenberg 1987: *Ore geology reviews*, 2, pp. 359–404. Elsevier Science Publishers B.V., Amsterdam. Printed in the Netherlands.
- Naixian, Z., J. Surong 1985: Petrographic and mineralogical characteristics of bauxite and series of ore-bearing in Gongxian county, Henan province. – *Scientia Geologica Sinica*, 2, pp. 170–179.
- Naixian, Z., T. Katsutoshi 1987: Petrological and mineralogical characteristics of bauxite deposits in China. – *Rep. Fac. Sci., Kagoshima Univ. of Japan*, 20, pp. 13–33.

Forthcoming Events

ZEOLITE '93

The 4th International Conference on the Occurrence, Properties, and Utilization of Natural Zeolites

Boise, Idaho – June 20–27, 1993

In addition to poster presentations, the conference will include symposia with invited speakers on:

- Mineralogy and New Occurrences;
- Geosynthesis and Stability, Isotopic Studies;
- Presence in Petroleum Reservoirs;
- Adsorption, Catalytic and Ion-Exchange Properties;
- Water and Wastewater Treatment;
- Radioactive Fallout Treatment and Nuclear Waste Containment;
- Heavy Metal Removal;
- Animal Nutrition;
- Agronomic and Horticultural Applications;
- Production and Marketing;
- Building and Construction Uses.

An all-participant mid-week field trip is included and an optional 3-day post-conference field trip is offered.

Conference Information:

E.A. Mumpton
Department of the Earth Sciences
SUNY-College at Brockport
Brockport, Ny 14420
Phone: 716-395-2334
Fax: 716-395-2416

Technical Program:

J.R. Boles
Department of Geological Sciences
University of California
Santa Barbara, Ca 93106
Phone: 805-893-3719
Fax: 805-893-2314

PRINTED IN HUNGARY
Akadémiai Kiadó és Nyomda Vállalat,
Budapest

ACTA GEOLOGICA HUNGARICA

EDITOR

J. Fülöp

Volume 34

Akadémiai Kiadó és Nyomda Vállalat,
Budapest 1991

ACTA GEOLOGICA HUNGARICA

Vol. 34

Contents

Numbers 1–2

Triassic paleogeography and Cimmerian orogeny in SE Bulgaria and on the adjacent territories. <i>Petar M. Gochev</i>	3
Triassic carbonate platform of the Drina–Ivajnica element (Dinarides). <i>Mara M. Dimitrijević, Milorad D. Dimitrijević</i>	15
Middle Miocene mangrove vegetation in Hungary. <i>Esther Nagy, József Kókay</i>	45
Lithostratigraphical and sedimentological framework of the Pannonian (s. l.) sedimentary sequence in the Hungarian Plain (Alföld), Eastern Hungary. <i>Györgyi Juhász</i>	53
Biostratigraphic revision of the Middle Pontian (Late Neogene) Battonya Sequence, Pannonian basin (Hungary). <i>Imre Magyar</i>	73
Diagenesis and low-temperature metamorphism in a tectonic link between the Dinarides and the Western Carpathians: the basement of the Igal (Central Hungarian) Unit. <i>P. Árkai, Cs. Lantai, I. Fórizs, Gy. Lelkes-Felvári</i>	81
K–Ar dating of the Perelik volcanic massif (Central Rhodopes, Bulgaria). <i>Zoltán Pécskay, Kadosa Balogh, Alexandra Harkovska</i>	101
Studies on chromite and its significance in the Lower and Middle Cretaceous of the Tatabánya Basin and Vértes Foreground. <i>Klára Vaskó-Dávid</i>	111
The heavy mineral content and mineralogical maturity of the Cenozoic psammites in Hungary. <i>Edit Thamó-Bozsó</i>	127
Genetics of garnets from andesites of the Karancs Mountains. <i>Csaba Lantai</i>	133

Book reviews

Chaline, J.: Paleontology of Vertebrates. <i>Miklós Monostori</i>	155
Hellmut Grabert: Der Amazonas – Geschichte und Probleme eines Strombietes zwischen Pazifik und Atlantik. <i>Ottó Tomschey</i>	156
Hartmut Heinrichs – Albert Günter Hermann: Praktikum der Analytischen Geochemie. <i>Iláikó Vidra</i>	157

Number 3

Tethyan Bauxites. <i>The state of the Art</i>	161
Jurassic karst bauxites in the Subbetic, Betic Cordillera, Southern Spain. <i>J. M. Molina, P. A. Ruiz-Ortiz, J. A. Vera</i>	163
A review of karst bauxites and related paleokarsts in Spain. <i>J. M. Molina</i>	179
Les principaux types de gisement et modeles genetiques des bauxites karstiques en France en Sardaigne. <i>P. J. Combes</i>	191
Bauxite exploring methods and their results in the Strázovské vrchy Mts., NW Slovakia. <i>F. Beleš</i>	215
The geological setting and facies of bauxite deposits in Hungary, including the conditions of their development. <i>J. Knauer, Á. Fekete, K. Tóth</i>	223

Application of sedimentological methods to karst bauxites evaluation: the Halimba-Szóc area, Hungary. Gy. Bárdossy, E. Juhász	243
Tectonic and eustatic control of bauxite formation in the Transdanubian Central Range (Hungary). J. Haas	255
Geoexplorer – the development of a knowledge-based consultation system for supergene deposits. M. Wagner, K. Fischer, K. Germann, J. Luo, W. Skala	265

Number 4

Bauxites and related paleokarst in Southern Italy, Sicily and Sardinia L. Simone, G. Carranante, B. D'Argenio, D. Ruberti, A. Mindszenty	273
Bauxite deposits of Yugoslavia – The state of the Art B. Šinkovec, K. Šakač	307
Contribution to the geochemistry of Hungarian karst bauxites and the allochthony/ autochthony problem Z. Maksimović, A. Mindszenty, Gy. Pantó	317
Bauxites in Albania V. Kici, L. Peza, D. Skhupi, A. Xhomo	335
Bauxite deposits and Senonian formations in Hungary (Palynological analysis) Á. Siegl-Farkas	345
Stratigraphical position of the bauxite deposits in the Pădurea Craiului Mountains (Northern Apuseni Mountains) S. Bordea, G. Mantea	351
Petrography and Sedimentology of the Cretaceous Continental Complex of the Eastern Hațeg Basin (South Carpathians – Romania) J. Becze-Deák	377
Concentrations of rare earth in Greek bauxites M. Laskou	395
Remarks on the genesis and ore-dressing of the alluvial bauxite occurrences of Parnass-Ghiona-Elikon (Greece) A. Vgenopoulos, K. Daskalakis	405
Mineralogical and geochemical correlation between the different Tethyan bauxitic types A. Vgenopoulos	409
Bauxite deposits related to the Tethyan Basins in Iran M. Sharifi Nourian, F. Rahimzadeh, M. Ehsanbakhsh	413
Main geological feature of "Sedimentary" bauxites deposits in China W. Liancheng, Z. Naixian	427
Mineralogy and geochemistry of bauxite in Yang Quan Area, Shan Xi Province (China) Z. Naixian, W. Liancheng, M. Yuguang	437
Forthcoming Events	445

GUIDELINES FOR AUTHORS

Acta Geologica Hungarica is an English-language quarterly publishing papers on geological topics (geochemistry, mineralogy, petrology, paleontology, stratigraphy, tectonics, economic geology, regional geology, applied geology). Along with papers on outstanding scientific achievements and on the main lines of geological research in Hungary, reports on workshops of geological research, on major scientific meetings, and on contributions to international research projects will be accepted.

Manuscripts are to be sent to the Editorial Office for refereeing, editing, and translation into English.

A clear, careful and unequivocal formulation of the papers, lucidity of style and the use of uniform nomenclature adopted in Hungary are basic requirements. It is convenient to subdivide the text of the papers into sections under subheadings.

Form of manuscript

The paper complete with abstract, figures, captions, tables and bibliography should not exceed 25 pages (25 double-spaced lines with a 3 cm margin on both sides).

The first page should include:

- the title of the paper
- the name of the author(s)
- the name of the institution and city where the work was done
- an abstract of not more than 200 words
- a list of five to ten keywords
- a footnote with the name and postal address of the author(s)

The SI (System International) should be used for all units of measurements.

References

In text citations the author's name and the year of publication should be given. The reference list, which follows the text, should be typed double-spaced, arranged alphabetically, and should not be numbered. For the preferred sequence and punctuation of authors' names see the examples below.

The author's name is followed by the year of publication in parentheses, the title of the paper or book (individual words in English titles of papers should have lower case initials, those of books upper case ones). Paper titles are followed by periodical titles, a comma, volume number, and inclusive page numbers. For books the publisher and the place of publication should be given.

Examples:

Bruckle, L. H. (1982): Late Cenozoic planktonic diatom zones from the eastern equatorial Pacific. *Nova Hedwigia*, Belh., **39**, 217–246.

Surdam, R. C., H. P. Eugster (1976): Mineral reaction in the sedimentary deposits of the Lake Magadi region, Kenya. *Geol. Soc. Amer. Bull.*, **87**, 1739–1752.

Perelman, A. J. (1976): *Geochemistry of Epigenesis*. Plenum Press, New York, Amsterdam.

Figures and tables

Figures and tables should be referred to in the text and their approximate place indicated on the margin.

Figures should be clear line drawings (suitable for being redrawn without consulting the author) or good-quality black-and-white photographic prints. The author's name, title of the paper, and figure number (arabic) should be indicated with a soft pencil on the back of each figure. Figure captions should be listed at the end of the manuscript. They should be as concise as possible.

Tables should be typed on separate sheets with the number (roman) and a brief title at the top. Horizontal lines should be omitted.

Proofs and reprints

The authors will be sent a set of galley and page proofs each. These should be proofread and returned to the Editorial Office within a week of receipt. Fifty reprints are supplied free of charge, additional reprints may be ordered.

Index: 26.010